FACULTY OF SCIENCES

CONDENSED MATTER PHYSICS, CRISTALOGRAPHY AND MINERALOGY DEPARTMENT

DOCTORAL THESIS

POLYOLEFIN BASED CELLULAR MATERIALS. DEVELOPMENT OF NEW PRODUCTION ROUTES AND OPTIMIZATION OF BARRIER AND MECHANICAL PROPERTIES BY THE ADDITION OF NANOCLAYS

This dissertation is submitted in partial fulfillment of the requirements for the degree of Doctor of Philosophy in Physics by Javier Escudero Arconada to the University of Valladolid

Supervisor:
Miguel Ángel Rodríguez Pérez

October 2015

A mis padres,
por absolutamente todo.

El principio de la Sabiduría es el temor de Dios
Proverbios 9:10

Hay que observar que, en cierto sentido,
toda ciencia y todo pensamiento humano
es una forma de juego
J. Bronowski

Agradecimientos

Muchas veces soñé con que llegase el momento de escritura de estas palabras e incluso en ocasiones albergué serias dudas de que finalmente fuera a llegar. Es un momento bonito, en el que se ponen las cartas sobre la mesa, boca arriba, y en el que uno se da cuenta de que si tengo la mano ganadora de la partida no es gracias a mi, sino fundamentalmente a mucha otra gente que ha caminado junto a mi. Es un momento de sinceridad y de hacer justicia.

En primer lugar quisiera agradecer la consecución de este doctorado al Prof. Dr. Miguel Ángel Rodríguez Pérez. Sin sus enseñanzas, ejemplo y paciencia no hubiera sido posible estar hoy escribiendo estas páginas.

Creo haber tenido una etapa doctoral bastante completa. Ello es consecuencia por una parte de la consecución de una beca para la Formación del Profesorado Universitario (FPU) concedida por el Ministerio de Educación y Ciencia. Gracias a esta beca pude impartir docencia, experiencia muy enriquecedora y de la cual también aprendí mucho. También pude realizar las dos estancias en centros de investigación extranjeros, experiencias no solo científicas sino fundamentalmente personales, con fuerte influencia en la persona que soy hoy. En este sentido no puedo más que agradecer la oportunidad que se me brindó.

Por otra parte me vi involucrado de primera mano en el desarrollo de un Proyecto Europeo denominado Nancore con la participación de empresas privadas y entidades académicas de todo Europa. Tuve la oportunidad de participar no solo en la parte científica sino en todas las reuniones de seguimiento y gestión que se llevaron a cabo a lo largo del proyecto. Lecciones que van más allá de lo académico y que me han servido en etapas posteriores. De este ámbito quiero tener un recuerdo especial hacia las investigadoras de la Universidad de Lovaina, Oksana Shishkina y Larissa Gorbatikh, mencionables tanto en lo técnico como en lo cercano, y a los representantes de la empresa italiana Azimut Benetti, Carlo Ighina y Matteo Lasa de cuya forma italiana de hacer las cosas creo que un español puede aprender. En general todo el desarrollo del Proyecto Europeo y sus integrantes son una de las experiencias vitales que difícilmente podré olvidar. Creo además que como grupo de investigación hicimos un papel muy aceptable.

Previo al comienzo de mi tesis doctoral, pero casi como parte de ella, pude disfrutar de una estancia de investigación en el Helmholtz Zentrum Berlin. Vivir en un piso alquilado en Berlín durante dos meses fue la primera experiencia de independencia que tuve. Todo en paralelo con la primera experiencia investigadora fuerte que viví bajo la inmejorable batuta del Dr. Francisco García Moreno en el corazón europeo de la investigación en espumas metálicas. Hacer ciencia y tecnología en Alemania te da una visión difícil de alcanzar de otra manera. Catalina Jimenez y Manas Mukherjee hicieron de anfitriones y maestros a su vez. El Helmholtz Zentrum y las personas fueron tan inmejorables que albergué dudas de retornar a España.

Las segunda y tercera estancias de investigación se desarrollaron ya en el ámbito de mi beca FPU. De mediados de Agosto a mediados de Noviembre de 2009 me dediqué a los nanocompuestos poliméricos bajo la supervisión de uno de los popes de la física de polímeros en Europa, el Prof. Dr. Andrzej Galeski. Pude disfrutar de los medios técnicos y del frío ambiente polaco en el Centro de Estudios Moleculares y Moleculares de Lodz en compañía del estudiante de doctorado Marcin Zarod. Ahí realicé mis primeras extrusiones serias. No puedo sino agradecerles todo el conocimiento, vivencias y experiencias que me traje de esa estancia.

De mediados de Julio a mediados de Octubre de 2010 crucé el charco a la Universidad de Washington, al grupo de investigación de una de las figuras más reconocidas y primigenias en el campo de las espumas microcelulares y de las espumas poliméricas en general, el Dr. Vipin Kumar. Él no solo me guió en la parte científica

sino que me dio cobijo en su propia casa, pude convivir y charlar con su encantadora esposa Kumud Kumar y sentirme como uno más de la familia durante el tiempo que viví allí. La confianza que depositaron en mí y la sensación de arropamiento cuando uno está tan lejos de los suyos es algo que no se puede nunca agradecer lo suficiente. Pocas veces uno se encuentra a personas tan buenas en este mundo. En lo técnico, si investigar en Alemania es enriquecedor, verse envuelto en el día a día de una universidad americana es impresionante. No puedo cerrar el capítulo de esta estancia sin recordar al muy inteligente Huimin Guo, compañero del día a día en la UW y a Krishna Nadella de Microgreen Inc. que me permitió presenciar in-situ un novedoso proceso de fabricación de espumas microcelulares.

Del ámbito académico no puedo dejar de mencionar a todos los doctorandos con los que coincidí en el laboratorio CellMat. Desde los "antiguos" Jorge, Rosa Ana, Mónica, Juan o Silvia con la que compartí conferencia en Hamburgo a los más "recientes", algunos de ellos ya doctores, Sergio, Pinto y las prácticas de Estado Sólido, Josías, el rugby y los viajes a Palencia, Belén, Ester las veces que nos hemos reído y el comedor... Samuel, de esas personas que verdaderamente te aportan puntos de vista diferentes sobre las cosas, Natalia, que siempre que hablamos me supo entender, Cesar, con el que tampoco llegué a tener tanto contacto, Cristina y sus excelentes habilidades sociales y disposición. Mención especial para mi merecen Jaime Lázaro con quien compartí años de carrera, estancia en Berlín, comprensión y conexión, Eusebio Solórzano que me llevo de la mano hasta este mundo, me metió el gusanillo de las que a día de hoy son algunas de mis aficiones y que a pesar de haber chocado alguna vez reconozco como una de las personas más dotadas para la investigación que he conocido, Alberto López con el que he compartido muchas horas de laboratorio, juntos supimos sacar adelante proyectos con buenos resultados y del que se puede decir sin miedo a equivocarse que es una buena persona. No puedo cerrar el capítulo de CellMat sin enviar mi agradecimiento a la Dra. Blanca Calvo por su buen hacer experimental, a Laura Izaguirre por la metodología y la voluntariedad, a Puri y por supuesto a Emi Andrés una de las personas más resolutivas y dispuestas a ayudar en cualquier ámbito. Sin duda he de recordar también al Profesor Emérito, Catedrático y responsable de que todos nosotros con el paso de los años nos hayamos visto metidos en este negocio, José Antonio de Saja Saez. A Jesús Medina, Fernando Hidalgo, José Luis Hererro, José Antonio Reglero... a todos ellos también muchas gracias.

Todos somos genotipo y fenotipo. Mi fenotipo se vio influido desde muy pequeño por un grupo de amigos, de los de toda la vida, de esos que conoces desde que tienes 5 años. Cada uno me ha aportado una parte de buena parte de lo que soy hoy. Juan Pascual, con quien me he visto en miles de situaciones, hemos compartido confidencias, sueños, ratos buenos, ratos un poco peores, bodas, bautizos y espero que comuniones... Tiene una visión envidiable de la vida y mejor aún, la lleva a la práctica, eso le ha reportado éxitos merecidos de quien tengo mucho que aprender. El físico e ingeniero Alfonso Santos, conectar desde el principio, charlar y sentirse comprendido como pocos más te comprenden, mi alter ego en muchas cosas. Son muchas las cosas que nos conectan y no es fácil, la física salvó nuestro alma. El Dr. Jorge Muñoz, persigue tus sueños porque nunca te faltarán cualidades para conseguirlos. Hemos crecido juntos y con poca gente me lo he pasado mejor en mi vida que contigo. A veces más cercanos, a veces más lejanos, que la vida no nos separe nunca, está en nuestra mano. Junto a Fernando Mediavilla también he crecido, si alguna vez tuviese que elegir a alguien para llevar a cabo cualquier trabajo de la importancia que fuera sería a él, garantía de éxito. Castellano leal y sincero la sociedad necesitaría más gente así. Y a Roberto de Dios que siempre nos ha ayudado a ver la vida desde otra óptica, desde un punto de vista peculiar, que muchas veces ha servido de nexo de unión entre nosotros. eres una pieza indispensable. No puedo olvidar aquí a Elena Sánchez por la confianza que siempre ha depositado en mí para todo y porque en muchas cosas pensamos parecido y a su hijo, mi ahijado, Juan Pascual Sánchez que hace muy poquito ha nacido a este mundo y a quien deseo acompañar en todo su camino. Quiero mencionar también a Víctor Lafuente con el que caminé muy de cerca durante muchos años importantes de mi vida. Y a Beatriz Moreno, no puedo olvidarte en los agradecimientos

de esta tesis porque siempre me animaste a llegar hasta aquí y siempre confiaste en que lo haría.

A la Cofradía de Ntro. Padre Jesús Nazareno y Ntra. Madre la Virgen de la Amargura y a su Banda de Cornetas y Tambores. Muchos de los mejores momentos que he vivido hasta el día de hoy los he vivido gracias a vosotros. En especial a la "Vieja Guardia", ni os imagináis la cantidad de lecciones de vida que he aprendido con vosotros.

A Danosa, mi actual empresa, por la oportunidad laboral que me brindaron, el respeto y consideración que siempre he sentido por su parte y la cantidad de lecciones no académicas que he aprendido hasta hoy. Hoy soy más, mucho más, gracias a vosotros. En especial a José Luis Alonso, Dr. Miguel Muñoz, Alberto del Rio, Dr. Miguel Ángel Sibila, Ismael González, Oscar Valiente y todos los demás integrantes del departamento de calidad e I+D.

A Leticia Recio, compañera de la última andadura, apoyo silencioso pero constante, siempre al pie del cañón, sin reproches de la vida tan atípica que tengo, me aportas paz y futuro. No es fácil que siempre se me sepa entender. Gracias.

Y a quien todo se lo debo y por quien todo lo soy. El amor puro, verdadero y sincero. De quien no tengo dudas de que siempre, siempre, siempre estarán a mi lado por dura que sea cualquier situación o por feas que se pongan las cosas. Ojalá algún día pueda llegar a una mísera parte de a lo que habéis llegado vosotros en muchos ámbitos de esta vida. A mis padres, que aunque por una cuestión formal su nombre no aparezca en la portada también son merecidos co-autores de esta tesis doctoral. Nunca podré daros lo suficiente las gracias. Os quiero mucho.

RESUMEN EN ESPAÑOL

OBJETIVOS DE LA PRESENTE TESIS

De un modo muy general podemos decir que la presente tesis se centra en el desarrollo de materiales celulares poliméricos con propiedades físicas mejoradas basados en poliolefinas y el correspondiente estudio de estas propiedades físicas. Lo anterior resume todo lo que será presentado en los próximos capítulos. Con este fin se pueden seguir dos posibles aproximaciones. La ecuación que se presenta a continuación modeliza de una manera muy sencilla pero representativa cualquier propiedades física P de un material celular

$$P_{material\ celular} = P_{sólido} \cdot \left(\frac{\rho_{material\ celular}}{\rho_{sólido}}\right)^{n}$$

Esta aproximación empírica establece que el valor de un cierta propiedad P puede ser modelado conociendo el valor de la misma propiedad relativa al material 100% sólido ($P_{sólido}$) su densidad relativa ($\rho_{relativa}$)y un parámetro n que varía entre 1 y 2. A la vista de esta formula está claro que hay dos posibles formas de modificar cualquier propiedad física de un material celular ($P_{material\ celular}$) a una densidad fija : la primera es modificar de alguna manera las propiedades físicas de la matriz sólida y la segunda es modificando la estructura celular de tal manera que el exponente n se acerque lo más posible a 1. En esta tesis ambas aproximaciones han sido empleadas individualmente o combinadas.

Todo el trabajo de investigación presentado en la tesis puede ser estructurado teniendo estas ideas en mente. Los siguientes esquemas están divididos en Modificaciones en la Matriz Polimérica, Modificaciones en la Estructura Celular y Combinación de Modificaciones en la Matriz Polimérica o en la Estructura Celular. En cada caso las técnicas de espumado empleadas se incluyen junto con las propiedades físicas estudiadas y las posibles aplicaciones reales que han motivado la investigación junto con las patentes surgidas del trabajo de investigación.

Modificaciones Matriz Polimérica

- **Adición de Nanoarcillas**
- **Adición de compatibilizantes poliméricos.**
- **Reticulación del polímero.**

Métodos de espumado	Propiedades físicas estudiadas	Aplicaciones Prácticas
- *Disolución de gas en sólido* - *Espumado libre* - *Moldeo a compression en dos etapas*	- *Propiedades mecánicas de sólidos* - *Propiedades barrera/Disolución de gas (sólidos)* - *Reología (sólidos)* - *Interacción del espumante con las nanopartículas (sólidos)*	*No estudiado en el marco de esta tésis*

Relación entre

- *Propiedades Mecánicas (espumas)*
- *Propiedades Barrera/Disolución de gas (espumas)*
- *Interacción agente espumante/ nanopartículas (espumas)*

Modificaciones Estructura Celular

- **Ruta de producción novedosa desarrollada durante la tesis "Moldeo por etapas para espumas estructurales"**

Métodos de espumado	Propiedades físicas estudiadas	Aplicaciones Prácticas
- *Moldeo por etapas para espumas estructurales*	- *Propiedades mecánicas (espumas)* - *Mecanismos físicos involucrados (espumas)*	Patente Española nº 201130271

Combinación modificaciones en matriz polimérica y celular	• Adición de Nanoarcillas • Adición de compatibilizantes poliméricos • Polímeros ramificados • Celdas anisótropas • Estructuras de celda abierta y cerrada.

Métodos de espumado	Propiedades físicas estudiadas	Aplicaciones Prácticas
• *Moldeo a compression mejorado*	• *Propiedades mecánicas (sólidos)* • *Reología (sólidos)*	Patente española nº 201231092

Relación entre

• *Propiedades mecánicas (espumas)*
• *Densidad (espumas)*
• *Estructura celular (espumas)*

Los objetivos generales de la presente tesis son por lo tanto

- Mejorar la morfología celular, rango de densidades alcanzable y propiedades físicas de materiales celulares basados en poliolefinas. Para esta finalidad la matriz polimérica se ha modificado y los parámetros de procesado han sido optimizados. En este sentido se ha desarrollado nuevas rutas de producción y se ha prestado una especial atención a las aplicaciones prácticas.
- La caracterización de la morfología celular y las propiedades físicas y establecer relaciones entre:
  a) Propiedades del sólido precursor y la espumabilidad y propiedades del polímero celular.
  b) Ruta de procesado y parámetros de producción- estructura celular
  c) Estructura celular-propiedades físicas también es una parte importante de los objetivos generales de la presente tesis.

Los objetivos más específicos se podrían resumir en:

- Estudiar el efecto de barrera a gases jugado por las nanoarcillas tipo montmorillonita en diferentes materiales celulares espumados por diferentes procedimientos: disolución de gas en estado sólido, disolución de gas en estado sólido en una matriz polimérica reticulada químicamente, espumado por moldeo a compresión en dos etapas.

- Estudiar la influencia que tiene la presencia de montmorillonitas nanométricas sobre la cinética de espumación, estabilidad y tamaño celular y densidad alcanzable. De especial interés es el efecto nucleante de estas nanoarcillas sobre la estructura de la espuma.

- Correlacionar los efectos de las mencionadas nanoarcillas sobre el comportamiento reológico del polímero con el posterior comportamiento en espumación.

- Estudiar el efecto que tiene la espumación sobre el grado de exfoliación/intercalación de las nanoarcillas. Emplear técnicas in-situ que nos permitan llevar a cabo este estudio durante el propio proceso de espumado.

- Desarrollar un nuevo método de producción para espumas estructurales en base poliolefínica que no tenga nada que ver con los métodos convencionales basados en el moldeo por inyección.

- Realizar un estudio de propiedades mecánicas en espumas estructurales y comparar dichas propiedades con las de espumas convencionales. Estudiar la influencia del tamaño de las pieles sólidas sobre las propiedades mecánicas globales.

- Fabricar espumas con densidades inferiores a 250 kg/m3 de celda cerrada en base polipropileno no reticulado y con propiedades mecánicas mejoradas para aplicaciones estructurales.

- Estudiar la influencia de las nanoarcillas tipo montmorillonita sobre estas matrices de polipropileno en el posterior proceso de espumación.

- Estudiar las propiedades mecánicas en compresión y cizalla para estos materiales celulares basados en polipropilenos no reticulados.

Metodologías empleadas

Para la fabricación de los materiales se han empleado diferentes métodos de espumación a escala de laboratorio que tienen su contrapunto a nivel industrial

- Espumación por disolución de gas en estado sólido. La disolución de gas se realiza dentro de un autoclave en condiciones sub-críticas y posteriormente la muestra se extrae para ser espumada dentro de un baño de silicona a temperaturas superiores a la temperatura de fusión del polímero.

- Espumación por disolución de gas en estado sólido de muestras previamente reticuladas. La reticulación de las muestras se hace químicamente en el interior de una presa de platos calientes. Las muestras ya reticuladas se introducen en el interior de un autoclave el cual se presuriza en condiciones sub-críticas. Posteriormente la muestra se espuma en un baño de aceite de silicona a temperaturas superiores a la de fusión del polímero.

- Espumado libre. La muestra se espuma libremente sin emplear ningún dispositivo que limite su espumación utilizando agentes espumantes químicos.

- Espumado por moldeo por compresión en dos etapas. En una primera etapa las pre-formas sólidas se unen y se reticulan en el interior de una prensa de platos calientes. Cuando la presión se libera se obtiene una pre-espuma que posteriormente se introduce en un molde para conferirla su espumación completa. En la segunda etapa la temperatura de la pre-espuma se eleva por encima de la temperatura de descomposición del espumante.

- Espumado por moldeo a compresión mejorado. La espumación se realiza dentro de un molde el cual se introduce dentro de una prensa de platos calientes. El molde incorpora un sistema de retención del grado de expansión que permite su rápida extracción y enfriado.

- Espumación de espumas estructurales. El método, desarrollado en esta tesis, consiste en recubrir las paredes del molde mediante un material poroso que tenga capacidad de absorber el gas. Esto permite la formación de pieles sólidas en todas las zonas que se encuentran en contacto con este material absorbente.

Para la caracterización de los materiales fabricados y análisis de las diferentes propiedades estudiadas se han empleado los siguientes técnicas experimentales:

- Difracción de rayos X a ángulos grandes (WAXD).
- Calorimetría diferencial de barrido (DSC).
- Termogravimetría (TGA).
- Microscopía electrónica de barrido (SEM).
- Microscopía electrónica de transmisión (TEM).
- Reología extensional.
- Picnometría de gases.
- Máquina de ensayos universal.
- Equipo de fluencia en compresión.
- Difracción de rayos X dispersiva en energía mediante el empleo de radiación sincrotrón. Sincrotrón Bessy.
- Expandómetro óptico.
- Radioscopía de rayos X.

Principales conclusiones y resultados

Es de reseñar que a lo largo de la tesis se han elaborado y patentado dos métodos de fabricación de materiales celulares

- Stages moulding que permite la fabricación de espumas estructurales con el empleo de moldes sencillos y mediante un método de fabricación completamente novedoso. El método permite tener un alto control sobre espesor de pieles sólidas, tamaño y distribución de celdas y densidad final. Estas espumas presentan, a igualdad de densidad, mejores propiedades mecánicas que sus homólogas no estructurales.

- Anicell que permite la fabricación de espumas de baja densidad con matrices no reticuladas. A lo largo de la tesis el método se aplica a polipropileno no reticulado para la fabricación de espumas con densidades en el rango 90-250 kg/m^3 y con dos variantes, celda abierta y celda cerrada. Estas espumas, debido a sus características, presentan unas propiedades mecánicas mejoradas con respecto a otros materiales anteriores y tienen la ventaja de ser reutilizables ya que la matriz no está reticulada.

Además como conclusiones generales de la presente tesis se pueden reseñar

- Se han conseguido nanocompuestos con una estructura intercalada/exfoliada en dos tipos de matrices poliméricas diferentes: polietileno de baja densidad y polipropileno.

- La presencia de nanoarcillas tipo montmorillonita disminuye la difusividad del CO_2 a través de la matriz en un porcentaje del 11%. En este sentido es de reseñar también que la mera adición de un polímero compatibilizante basado en anhídrido maléico produce disminuciones de la difusividad de hasta el 30%. Para mejorar el efecto barrera de estas nanoarcillas habría que conseguir mejores exfoliaciones/compatibilizaciones. Este efecto barrera se ha estudiado mediante un procedimiento gravimétrico aprovechando las técnicas de espumado por disolución de gas.

- Se ha estudiado la espumación por disolución de gas en estado sólido y condiciones sub-críticas de una matriz termoplástica (LDPE). Se ha realizado una intercomparación entre las mismas matrices reticuladas y no reticuladas. La reticulación permite obtener espumas microcelulares de matriz termoplástica por disolución de gas en estado sólido y condiciones sub-críticas y alcanzar densidades del orden de 140 kg/m^3.

- La reticulación por si sola, al influir en la cristalinidad, modifica la solubilidad y difusividad del gas a través del polímero.

- La adición de nanoarcillas tiene un efecto catalítico sobre la descomposición de la azodicarbonamida disminuyendo su temperatura de descomposición y liberando una mayor cantidad de gas.

- El espumado incrementa el grado de exfoliación/intercalación de las nanoarcillas en LDPE. Esto es independiente del agente espumante empleado. Aún así existe una interacción química entre las nanoarcillas y la azodicarbonamida de tal manera que cuando este es el agente espumante empleado los grados de intercalación/exfoliación son mayores antes incluso de que se fabrique el material espumado.

- Se han fabricado bloques de espuma con más de 30 expansiones partiendo de nanocompuestos de polietileno reticulado. La presencia de un agente compatibilizante basado en anhídrido maléico en estos compuestos ayuda a obtener tamaños celulares inferiores y mayores densidades celulares.

● Estos bloques de espuma permiten estudiar los coeficientes de difusión de gas y el papel barrera a gases jugado por las nanoarcillas empleando un método de determinación semi-empírico. Los resultados están en consonancia con los obtenidos por disolución de gas.

● La reología extensional se demuestra como un método muy útil para predecir el posterior comportamiento en espumado de una determinada formulación polimérica basada en polipropileno. Especialmente el parámetro denominado "endurecimiento por deformación" tiene una conexión directa con los posteriores contenidos de celda abierta encontrados en los materiales celulares.

● El empleo de polipropilenos ramificados combinado con una espumación por moldeo a compresión mejorado da como resultado espumas de celda cerrada con densidades inferiores a 250 kg/m^3. Estos materiales presentan unas excelentes propiedades mecánicas. La adición de nanoarcillas modifica la reología del polímero lo cual tiene como consecuencia que los contenidos de celda abierta se incrementen sustancialmente. A pesar de estos altos contenidos de celda abierta en espumas fabricadas partiendo de nanocompuestos las propiedades mecánicas específicas siguen siendo altas. Esto es una consecuencia del refuerzo que las nanoarcillas tienen sobre la matriz polimérica base.

CONCLUSIONES

Modificaciones en la Matriz Polimérica

• La composición química de los materiales celulares basados en polietileno de baja densidad se ha modificado mediante la adición de una carga inorgánica de tamaño nanométrico (nanoarcillas tipo montmorillonita) y un agente compatibilizante basado en polietileno lineal de baja densidad injertado con anhídrido maléico. Los nanocompuestos se han fabricado mediante mezclado en fundido. A través de estos nanocompuestos se han fabricado espumas siguiendo diferentes procesos de espumación lo cual permite realizar comparaciones entre todos ellos.

• La adición de nanoarcillas, a pesar de no estar completamente exfoliadas sino que conservan una estructura intercalada tienen los siguientes efectos sobre la matriz sólida: la estabilidad térmica se incrementa, las propiedades mecánicas en compresión, tracción y flexión también se ven mejoradas, incrementan la cristalinidad de la matriz polimérica y tienen un efecto especialmente marcado

en las propiedades reológicas del polímero. Todas estos efectos se conectan después con las propiedades de la espuma.

- Se presta especial atención a la disolución de gas en los sólidos. Las nanoarcillas disminuyen la difusividad en porcentajes del 11% e incrementan la solubilidad. La presencia de interfaces nanoarcillas-polímero juegan un papel muy importante en este comportamiento. La mera presencia de un polímero compatibilizante injertado con anhídrido maléico reduce la difusividad en un 30% por si mismo.

- La presencia de compatibilizante injertado con anhídrido maléico mejora la estructura celular con ratios de expansión superiores a 2 y tamaños de celda inferiores a 80 μm aun disolviendo CO_2 en estado sub-crítico. Sin embargo la presencia de nanoarcillas empeora manifiestamente la estructura celular como consecuencia de los efectos reológicos que presentan sobre el polímero. Independientemente de esto las nanoarcillas presentan un importante efecto nucleante en el sentido de reducir la cantidad de energía necesaria para nuclear y crecer celdas.

- Cuando la matriz polimérica se reticula empleando peróxido de dicumil se obtienen densidades celulares del orden de $1 \cdot 10^9$ celdas/cm^3 y densidades de 140 kg/m^3 en un polímero semicristalino empleando CO_2 en condiciones sub-críticas. Este comportamiento en espumación se relaciona directamente con las propiedades reológicas medidas para estos polímeros reticulados.

- La presencia de nanoarcillas tiene un efecto catalítico muy importante sobre la descomposición de la azodicarbonamida, acelerando su descomposición y aumentando la cantidad de gas liberada. Sin embargo la estabilidad de los nanocompuestos es inferior, lo que de nuevo está conectado con las propiedades reológicas del polímero. Paralelamente el polímero compatibilizante por si mismo ayuda a alcanzar ratios de expansión mayores.

- El grado de exfoliación de las nanoarcillas se incrementa tras la espumación. Este efecto se estudia mediante radiación sincrotrón en continuo permitiendo obtener la evolución de la exfoliación de las nanoarcillas paralelamente a la espumación. Para ello se emplean agentes espumantes de diferente naturaleza. La especial interacción entre nanoarcillas y azodicarbonamida se pone de Nuevo de manifiesto aquí, cuando se emplea azodicarbonamida el grado de exfoliación de partida de las nanoarcillas es mayor.

- Se consigue la fabricación de espumas con ratios de expansión superiores a 30 y conteniendo nanoarcillas por espumado por moldeo a compresión. Las propiedades mecánicas de estos bloques de espuma se ven mejoradas por la presencia de nanoarcillas.

- Al igual que en la espumación por disolución de gas en estado sólido la reducción en difusividad por la adición de nanoarcillas no es muy grande. La presencia de un polímero compatibilizante injertado con anhídrido maléico tiene por si mismo un efecto mayor de barrera a gases. De nuevo la presencia de interfases nanoarcillas-polímero se postula como la explicación a este fenómeno.

Modificaciones en la estructura celular.

- Se presenta una nueva ruta de fabricación de espumas estructurales que no tiene nada que ver con los métodos de moldeo por inyección habituales. El nuevo método presenta ventajas frente a los métodos convencionales con moldes mucho más sencillos e inversiones iniciales menores.
- El mecanismo físico detrás de este efecto consiste en un proceso de disolución de gas desde la espuma hacia el material amorfo que recubre las paredes del molde de espumado. Se generan pieles sólidas en todas las partes en contacto con el material amorfo que recubre las paredes del molde.
- El método de fabricación permite un control exhaustivo de propiedades de la espuma como grosor de las pieles o densidad final. Esto se consigue variando convenientemente los parámetros de fabricación.
- Las propiedades mecánicas específicas de estas nuevas espumas estructurales son superiores a las de las espumas convencionales, especialmente en flexión.
- Esta nueva tecnología está patentada y la patente se incluye en el marco de esta tesis.

Combinación de modificaciones en la matriz polimérica y en la estructura celular

- Se emplea la técnica de microtomografía de rayos X para caracterizar las espumas de polipropileno de baja densidad. La técnica se emplea para correlacionar parámetros de producción con la posterior morfología celular obtenida.
- La reología del polímero de nuevo juega un papel determinante para la espumabilidad y calidad de la espuma. En especial el denominado "endurecimiento por deformación" o "strain hardening" de la matriz polimérica tiene una importancia vital en parámetros como contenido de celda abierta. La presencia de nanoarcillas, vírgenes u organomodificadas o la presencia de nanotubos de carbono reducen el endurecimiento por deformación de la matriz polimérica e incrementan los contenidos de celda abierta. Estos contenidos de celda abierta tienen una influencia muy marcada sobre propiedades mecánicas de la espuma como módulo elástico

- Puesto que la presencia de nanocargas refuerzan la matriz polimérica esto ayuda a compensar el deterioro que se produce en propiedades mecánicas por los altos contenidos de celda abierta.

- La combinación de polipropilenos ramificados junto con el método de espumación denominado "moldeo por compresión mejorado" permiten obtener espumas en base polipropileno no reticulado con densidades menores de 150 kg/m^3 junto con propiedades mecánicas mejoradas debidas a los altos ratios de anisotropía que presentan estas espumas. Esta combinación de densidades y propiedades mecánicas se puede conseguir tanto en espumas de celda cerrada como en espumas de celda abierta mediante la incorporación de cargas nanométricas. Las propiedades mecánicas obtenidas son similares a las de espumas con matrices sólidas con mejores propiedades mecánicas de partida como el PVC o el SAN. Estas espumas pueden cubrir un rango de aplicaciones prácticas muy amplio que va desde la industria de las palas de aerogeneradores hasta el sector del automóvil o la industria aeronáutica. La tecnología de fabricación de estas espumas se ha patentado y la patente se puede encontrar anexa a esta tesis.

Chapter 1

Introduction

Costs reduction is nowadays one of the main objectives in which many different industries are focused. On the other hand, there are even some applications in which it is mandatory the use of light weight materials and/or obtaining properties that can only be covered by cellular materials, the thermal insulation of cellular polymers for example do not have counterpart in other materials and so, they are essential in thermal insulation applications. Altogether confers cellular materials a fundamental role in technological areas as important as aeronautics, construction, packaging and cushioning, renewable energies, biotechnology or the automotive sector [1,2].

The applications in which cellular polymers are used are each time more and more demanding. Besides this, with time, new applications have appeared with challenging requirements. All these facts have motivated, and motivate every day, a strong research from different points of view, focused in the improvement of the already known cellular materials or in the development of new ones. Even scientifically, there is still a lack of knowledge in several aspects of the science and technology related to these materials.

This thesis work has followed a scientific approach but without losing sight of the industrial requirements and needs. This global approach has allowed to gain new basic knowledge and to contribute to the state of the art but also to the development of novel materials and technologies that can be industrially used.

1.1.- FRAMEWORK AND GENERAL LAYOUT OF THE THESIS

1.1.1 Current research lines in Cellular Polymers

Cellular polymers have undergone a very intense evolution in the last three decades. Modifications both in the polymer matrices as well as in the production processes have given rise to novel and diverse cellular materials with improved properties. Due to these novel properties the industrial sectors and applications in which cellular materials can be used have been extensively broaden lately. Currently, the more outstanding research lines in cellular polymers can be divided into four main areas: microcellular foams, cellular nanocomposites, cellular polymers based on biopolymers and nanocellular foams. Let us introduce briefly each topic:
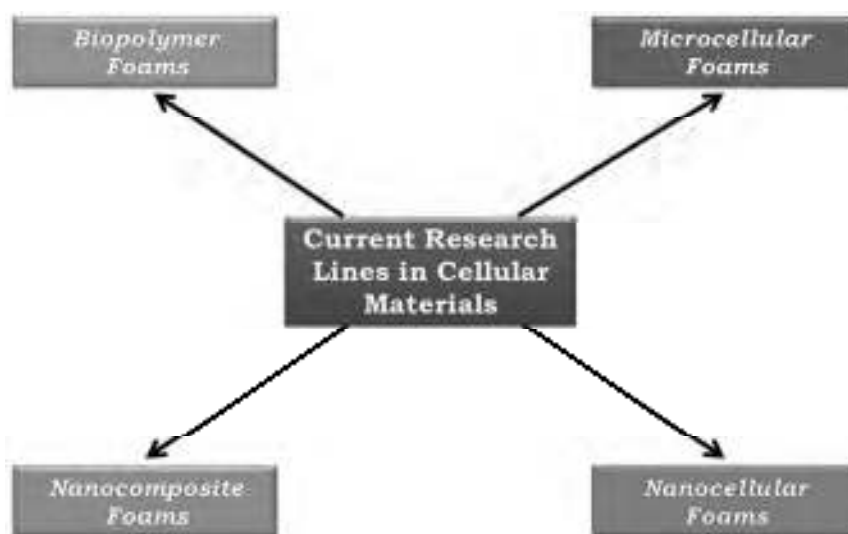
Figure 1.1: Schematic of the current research lines in cellular polymers

1.   *Microcellular Foams*: the research on microcellular foams began in the early eighties in the Massachusetts Institute of Technology in response to a challenge proposed by the photographic film industry. Companies as Kodak were looking for a method aimed at weight reduction with minimal losses in mechanical performance in 1 mm thick sheets. Other industries, as food packaging for example, could take advantage of the development of the materials previously mentioned [9]. Microcellular foams can be defined as those with cell size below 10 µm [5] (below 100 µm in other latter and less restrictive definitions). Theoretically the consecution of such a fine cellular structure would offer an outstanding mechanical performance with linear dependencies with the relative density. These promising expectations motivated the accomplishment of numerous research studies all around the world giving rise to an overwhelming number of scientific publications and patents [4,5]. Nowadays there is still controversy about the real influence of the cell size in the mechanical properties. It seems that at high densities the linear tendencies with the relative density are reached but this situation gets worst when low or medium densities are taken into account. Some properties as fatigue or impact resistance seems to benefit from the smaller cell sizes but some other, like elastic modulus or yield strength, do not show the same dependency and appear insensitive to the cell size [4,5,10]. Altogether still nowadays there is a remarkable interest paid to these materials.

The difficulties associated to the production of microcellular foams have also hindered its industrialization [10]. Only some of the production routes used at lab scale have been finally scaled up. Trexel (http://www.trexel.com) offers the possibility of producing microcellular foams either by extrusion or injection molding. They license the machinery needed and designed by them to other companies all around the world. Together with several advantages other disadvantages are also present and will be mentioned in later chapters. Microgreen must be mentioned also as other company commercializing nowadays microcellular foams. Taking advantage of the patents developed by Prof. V. Kumar in the University of Washington Microgreen (http://www.microgreeninc.com) produces and sells microcellular foams based on recycled PET for very different purposes.

2. *Cellular Nanocomposites*: inevitably developed as result of the huge interest paid to polymer solid nanocomposites, cellular nanocomposites are thought to combine not only the advantages inherent to polymer nanocomposites and cellular polymers, but also to present interesting synergetic effects between both. During the last two decades both industrial and academic institutions have carried out a very intense research on everything related to "nano". The research goes from medicine to electronics passing of course through polymers. In the early 90's Toyota headed the research in polymer nanocomposites developing a formulation based on nylon 6 and nanoclays [11]. The amazing properties published for these composites encouraged a big number of researchers and public institutions to focus their efforts on polymer nanotechnology. The high aspect ratio of the nanofillers employed underlies behind the outstanding performance expected in barrier properties, mechanical behavior or flame retardancy. The interest on cellular nanocomposites has gone parallel to the one on their solid counterparts but it has been less intense and detailed [12,13]. Next chapters contain a further description on this subject so more information can be found later.

3. *Cellular Materials based on Biopolymers*: till some years ago biopolymers were a marginal research field, developed at lab-scale but with no industrial production or application. But due to the more restrictive standards on contamination and to the true need of biodegradable materials as substitutes for traditional non-biodegradable plastics, biopolymers industrialization and research have suffered a remarkable progress in the last few years [14,15]. Nowadays several polymers as polylactic acid (PLA) polyhhydroxybutyrate (PHB) and starch can be disposed for industrial production [14,15]. Again, the

evolution of cellular materials based on biopolymers has taken place parallel to the evolution of solid biopolymers. This is one of the more novel and promising research fields in cellular polymers.

4.   *Nanocellular materials*: ten years ago, when microcellular materials were still on the crest of the wave, scientist decided to go further ¿what happens if we reduce the cell size below the micron. And even more, what properties can we expect if cell sizes in the order of 100 nanometers are achieved? Such a reduction in cell size has not been easy to achieve but in the last four years important progress has been done in the subject. Currently the most relevant companies in cellular materials are putting big efforts on the consecution of a way to produce nanocellular foams at industrial scale. Improvements in mechanical properties and transparency are expected but the more interesting possible applications deal with thermal insulation. From the three thermal conductivity mechanisms present in a material, conduction through the solid, radiation and conduction through the gas phase, this last one is completely suppressed when the cell size is below 100 nm. This is translated into important reductions in thermal conductivity not achievable with any other material [16-20].

The main part of this thesis work can be included in the two first research lines mentioned: microcellular foams and nanocomposite cellular materials. Another research line followed develops a new production route for structural foams and somehow is independent of the rest. Structural foams are cellular materials with a skin-core morphology, that is, two outer solid skins and a foamed core. These light weight materials present higher specific mechanical properties than conventional foams and can be found in numerous applications like aircrafts, sporting goods or vehicles.

Part of the work has been developed in the Centre of Molecular and Macromolecular Studies in Lodz, Poland and part in the Department of Mechanical Engineering of the Univerisity of Washington in Seattle. The largest part of the research was developed in CellMat Laboratoty of the University of Valladolid. The next section briefly describes these laboratories.

1.1.2.- Research Centers

● *Centre of Molecular and Macromolecular Studies (CMMS). Polish Academy of Sciences.*

The Centre of Molecular and Macromolecular Studies in Łódź, Poland, belongs to the network of the Polish Academy of Sciences institutes created to conduct research in selected areas of science.

The research carried out in the Centre covers the range of problems from the area of organic chemistry, bioorganic chemistry and polymer chemistry and physics, with special emphasis on developing methods of making advanced materials, both in the field of low molecular weight and high molecular weight products.

All the polyethylene based nanocomposites included in this thesis were produced and partially characterized in the Polymer Physics Department of the CMMS under the supervision of Prof. Dr. A. Gałęski.

● *Mechanical Engineering Department. University of Washington (UW).*

The University of Washington is one of the oldest and largest public universities in the United States of America. Founded in 1861 its main campus is settled in Seattle but it has campus also in Tacoma or Bothell. More than 12000 bachelors, master, doctoral and professional degrees are conferred in the UW every year.

All the research related to batch gas dissolution foaming was performed in the Mechanical Engineering Department of the UW under the supervision of Dr. V. Kumar. Dr. Kumar is one of the pioneers in the field of microcellular foams. His thesis , ended in 1984, is one of the first ones on the subject. He is co-author of a large number of papers in this field and of several patents, some of them currently used at an industrial scale for the production of microcellular foams based on recycled PET.

● CellMat Laboratory. University of Valladolid.

CellMat Laboratory belongs to the Condensed Matter Physics Department of the University of Valladolid and was founded in 1999 by professors Dr. José Antonio de Saja and Dr. Miguel Ángel Rodríguez Pérez. The main objective of the laboratory can be

summarized as "the production and characterization of cellular materials either based in polymer or metal matrices".

At the beginning, all the efforts were focused on the characterization of the microstructure and physical properties of low density cellular materials based on polyolefins. During this initial phase several papers were published in international journals [28-73] and several theses were based on this work [7,21-27]. With time and with all the knowledge gathered during the previous stage on characterization and physical mechanisms, the laboratory broadened the research fields. Nowadays CellMat not only characterizes the physical properties or microstructure of foams, but also produces their own, in some cases completely novel, materials.

The current research lines followed in CellMat coincide with the areas mentioned in paragraph 1.1.1. The society is demanding each time more and more improved light weight materials with improved properties. CellMat tries to give an answer, both from a technical and scientific point of view. In this sense, since the year 2006, numerous works have been published, together with different theses and patents which give an idea of the kind of work developed during the last years [74-100].

All the work included in this thesis that was performed in CellMat Laboratory has been supervised by Prof. Dr. Miguel Ángel Rodriguez Pérez and goes from the science to possible industrial applications. As already mentioned the research can be framed in the lines of Microcellular Foams and Cellular Nanocomposites.

1.1.3.- General Layout of the Thesis

In a very general way we can say that the thesis is focused on the development of cellular polymers with improved physical properties based on polyolefins and the corresponding study of these physical properties. The previous sentence encompasses pretty well all the research that will be presented in the following chapters. To this end, two different approaches can be followed. Let us take into account equation 1.1, that models in a very simple but representative way any physical property (P) of a cellular material [1].

$$P_{cellular\ material} = P_{solid} \cdot \left(\frac{\rho_{cellular\ material}}{\rho_{solid}} \right)^{n} \qquad Eq.\ 1.1$$

This equation will be introduced in more detail in chapter 2. By now just consider that this empirical approximation states that the value of a certain property ($P_{cellular\ material}$) can be modeled knowing the value of that same property for the fully solid material (P_{solid}), its relative density ($\rho_{relative}$) (density of the cellular material devided by the density of the solid)and a parameter $\boldsymbol{n}$ that varies between 1 and 2. At the sight of this formula it is clear that there are two main ways of improving any physical property of the cellular material (*$P_{cellular\ material}$*) at a fixed density: the first one is modifying, by any means, the physical properties of the solid matrix ($\boldsymbol{P_{solid}}$) the second one is modifying the structure of the cellular material in such a way that the exponent $\boldsymbol{n}$ is as near as 1 as possible. Both approximations have been used independently or even combined.

All the research work presented in this thesis can be structured bearing the previous ideas in mind. The following schemas (figures 1.2 to 1.4) are divided into Modifications in the Polymer Matrix, Modifications in the Cellular Structure and Combination of Modifications of the Polymer Matrix and Cellular Structure. In each case the foaming techniques used are included together with the physical properties studied and the real possible applications that have motivated the research and settlement of patents.

Modifications in the Polymer Matrix

- **Addition of Nanoclays**
- **Addition of Polymeric Coupling Agents.**
- **Polymer Crosslinking.**
- **Polyethylene**

Foaming Methods used	Phisical Properties Studied	Practical Applications

- *Batch Gas Dissolution*
- *Free Foaming*
- *Two-stages Compression Molding*

- *Mechanical Properties (solids)*
- *Barrier Properties/ Gas Dissolution (solids)*
- *Rheology (solids)*
- *Interaction Blowing Agent-Nanoparticles (solids)*

NOT studied in the frame of this thesis work.

Relationship between

- *Mechanical Properties (foams)*
- *Barrier Properties/ Gas Dissolution (foams)*
- *Interaction Blowing Agent-Nanoparticles (foams)*
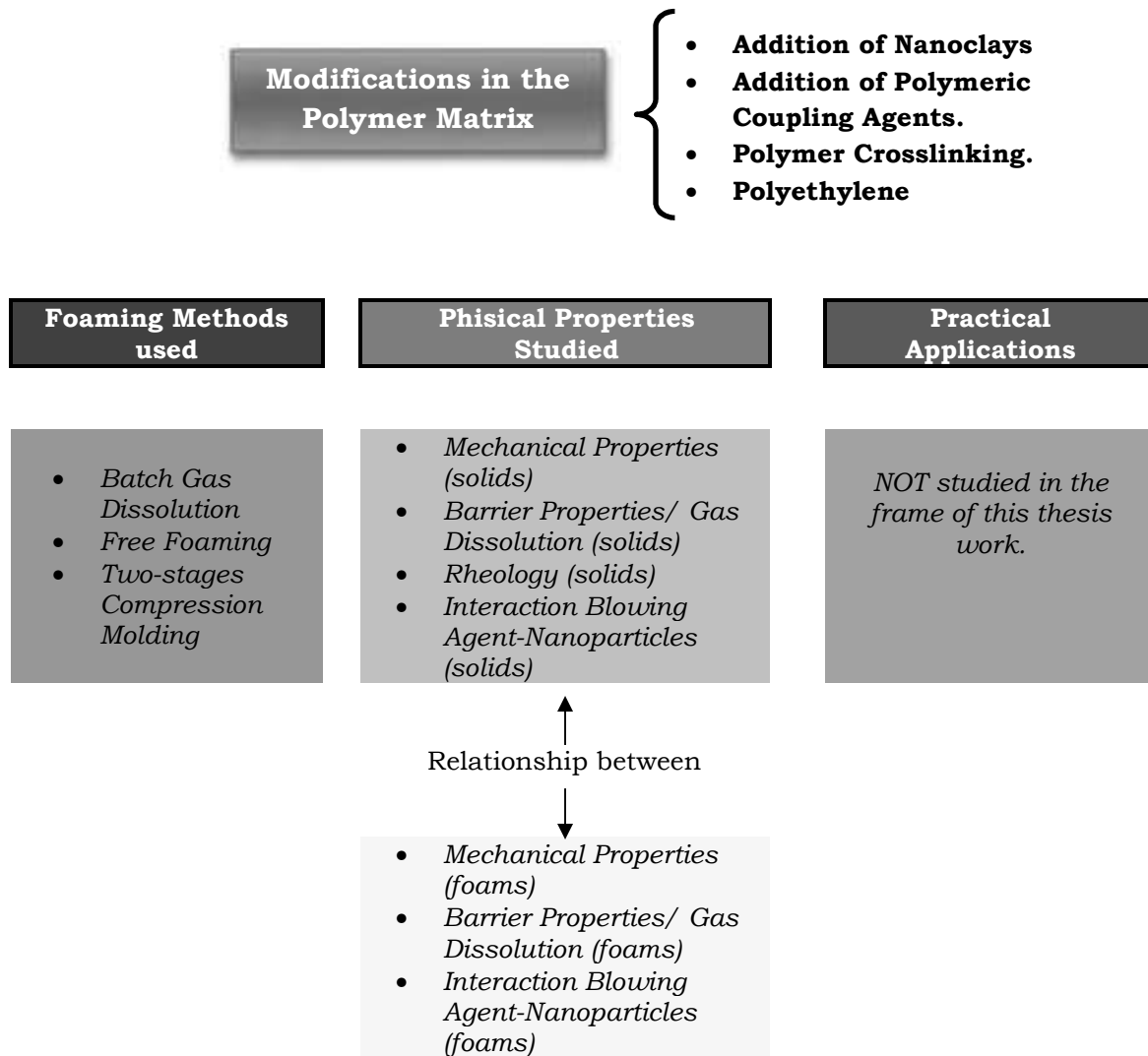
Figure 1.2: Strategies of modification in the polymer matrix followed during the thesis.

Modifications in Cellular Structure

- **Novel production route developed during the thesis "Stages Molding for Structural Foams"**
- **Polyethylene**

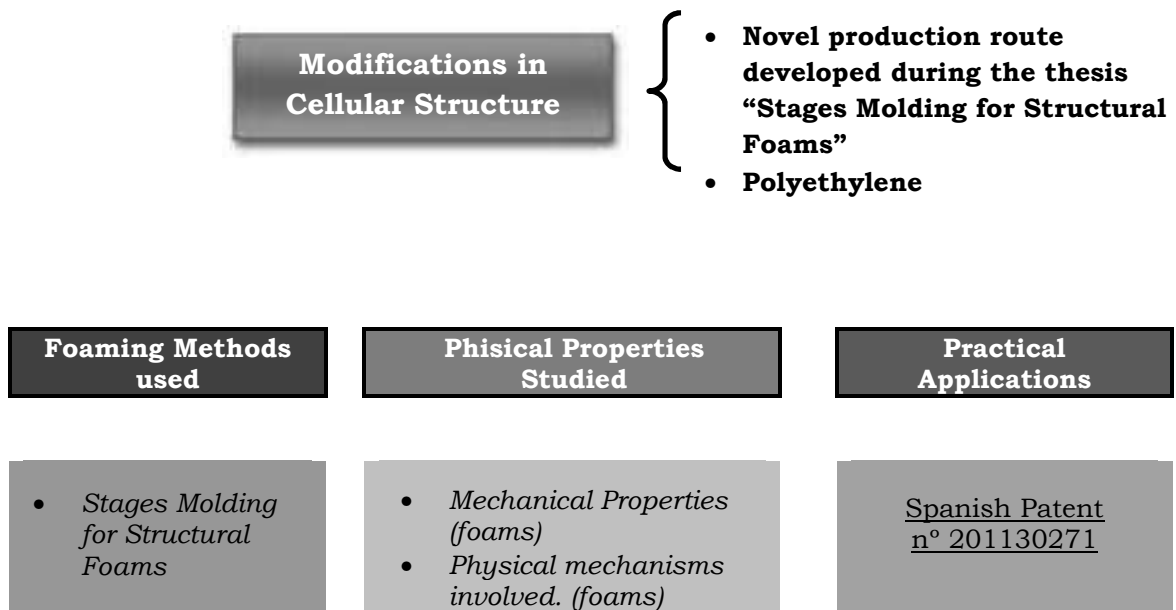| Foaming Methods used	Phisical Properties Studied	Practical Applications
• *Stages Molding for Structural Foams*	• *Mechanical Properties (foams)* • *Physical mechanisms involved. (foams)*	Spanish Patent nº 201130271

Figure 1.3: Strategies of modification of the cellular structure used during the research

Combination of Modifications in the Polymer Matrix and Cellular Structure

- **Addition of Nanoclays**
- **Addition of Polymeric Coupling Agents.**
- **Branched Polymers**
- **Anisotropic Cells**
- **Open and Closed Cell structures.**
- **Polypropylene**

Foaming Methods used	Phisical Properties Studied	Practical Applications
• *Improved Compression Molding*	• *Mechanical Properties (solids)* • *Rheology (solids)*	Spanish patent nº 201231092

Relationship between

- *Mechanical Properties (foams)*
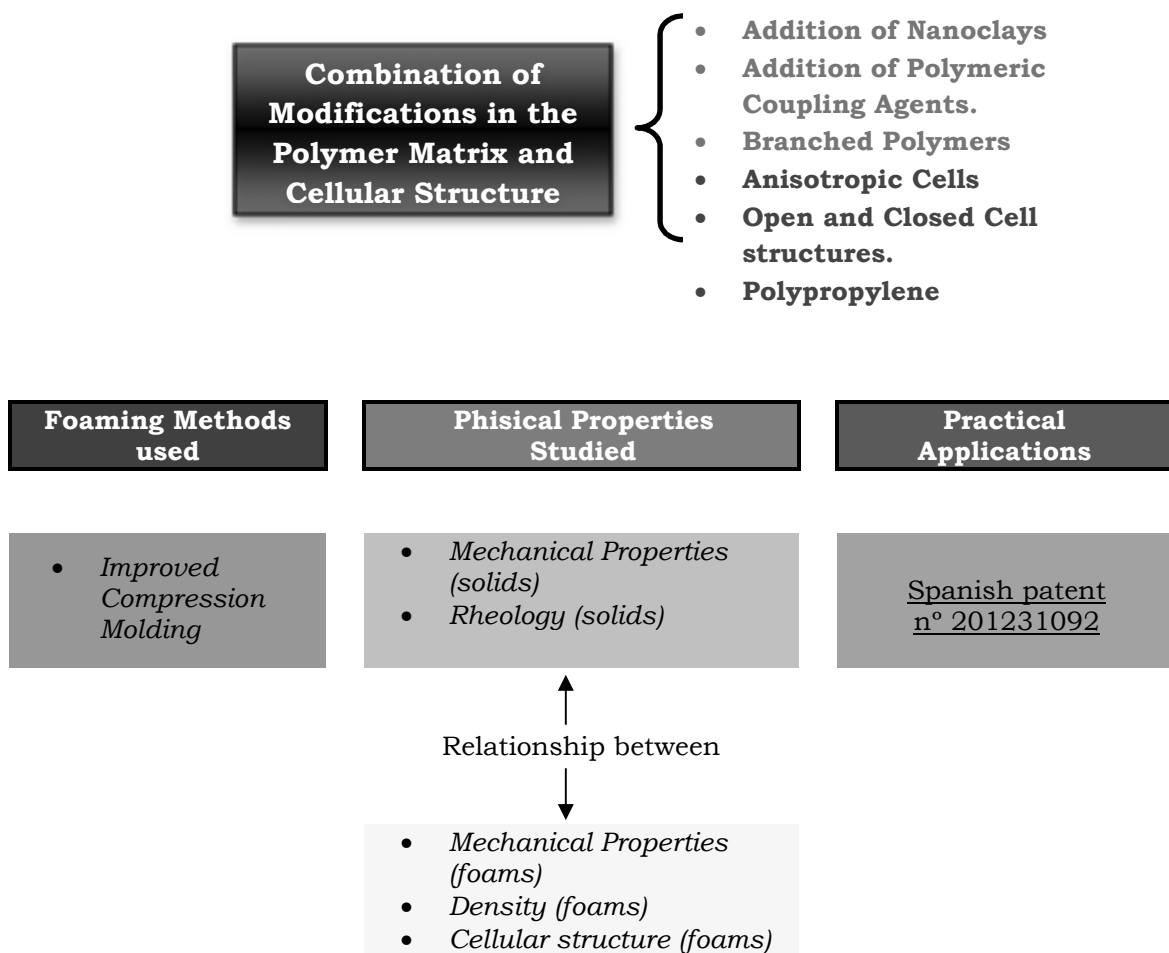- *Density (foams)*
- *Cellular structure (foams)*

Figure 1.4: Combination of modification in polymer matrix and foam structure.

In the previous schemas, when we say "modification in the polymer matrix" or "modification in the cellular structure" we are referring to modifications done purposely. Of course modifications on the polymer matrix have an effect on the foam structure. And the foaming procedures followed to modify the foam structure can induce modifications in the polymer matrix.

The schemas included in figures 1.2, 1.3 and 1.4 give a general view of the strategies, materials used, foaming routes followed, physical properties studied and practical application of the results obtained during the research. These schemas can be considered as a "global map" of the thesis work. In addition, Table 1.1 shows the main projects carried in CellMat during the last years and that have an intimate connection with the research topics of this thesis. All these projects have a marked industrial applicability and have been funded either with private or public funds. Keeping this global map in mind we can define the objectives of the thesis.

Table 1.1: Frame projects of this research work.

MAIN FRAME RESEARCH PROJECTS OF THE THESIS
Título: "Microcellular Nanocomposites for Substitution of Balsa Wood and PVC Core Material"
7th Framework Programme. European Union
From November 2008 to November 2012
Main Researcher: M.A. Rodríguez-Pérez.
Título: "Metals Foaming Under Mechanical Pressure"
Integral Action with the Technical University of Berlin.
From January 2009 to December 2010.
Main Researcher M.A. Rodríguez-Pérez.
Título: "New Developments in Polymer Microcellular Materials: Production, Structure, Properties, Modelling and Applications"
In coordination with the Technical Center Lortek
Funded by the National Program for Materials
From December 2009 to December 2012
Main Researcher: M.A. Rodríguez-Pérez
Título: "New Production Processes of Plastic Parts Based on Microcellular Materials by Self-Injection Molding".
Funded by: FECYT and ABN Pipe Group. Project Innocash.
From January 2010 to December 2011.
Main Researcher: M.A. Rodríguez-Pérez
Título: "Advanced Foams Under Microgravity"
Funded by: European Spatial Agency
From June 2010 to May 2012.
Main Researcher at the University of Valladolid: M.A. Rodríguez-Pérez

1.2.- OBJECTIVES

The main objectives that best summarize the efforts done during the thesis can be stated as

Improving the cellular morphology, density range achievable and physical properties of polyolefin-based cellular materials.

For this purpose, the polymer matrix have been modified and the processing parameters have been optimized. In this sense new production routes have been developed and special attention has been paid to the possible practical applications.

The characterization of the cellular morphology and physical properties and the establishment of relationships between:

a) Properties of the solid precursor – foamability and properties of the cellular polymer.
b) Processing route and production parameters – cellular structure.
c) Cellular structure – physical properties.

According to this, the thesis can be placed in the base of the materials tetrahedral (*Production, Structure, Properties*) but it also touches and pays attention to the upper vertex of *Applications* (figure 1.5).
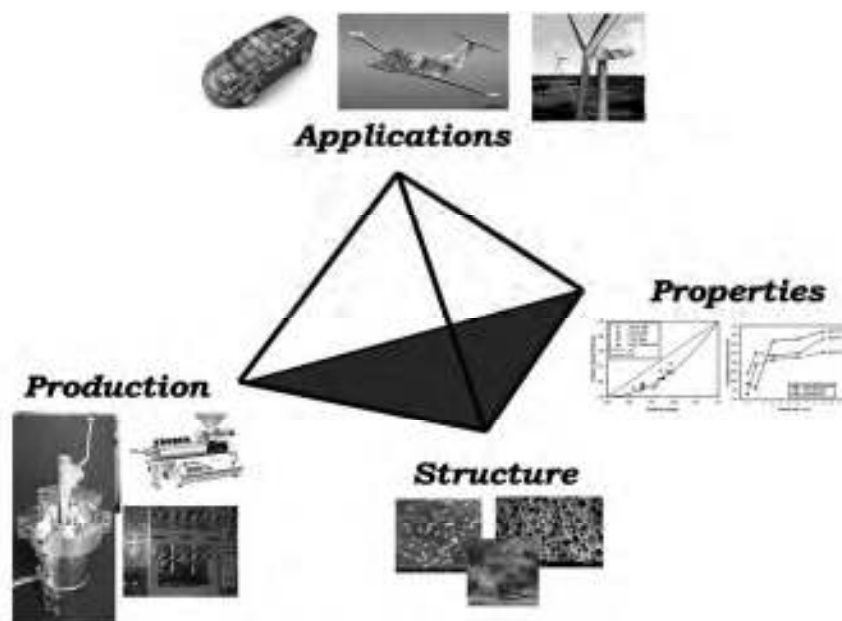
Figure 1.5 : Materials Tetrahedral

This general objective can be divided into some other more specific ones according to schemas 1.2 to 1.4.

> ## **Modifications in the Polymer Matrix**

Producing Medium Density Cellular Materials based on Low Density Polyethylene (LDPE)/Clays Nanocomposites by Batch Gas Dissolution in Sub-critical Conditions.

- Studying the gas barrier role played by the nanoclays in the solid samples. Diffusion coefficient, solubility and permeability. This is done using the same setup used for foaming by gravimetric methods.
- Studying the effect of the different coupling agent additions, independently of the nanoclays, on the gas barrier behavior.
- Characterizing the foamability of LDPE/Clays nanocomposites by batch gas dissolution in sub-critical conditions. Effect of the coupling agent addition, excluding the nanoclays.
- Studying the nucleating effect played by the nanoclays in these systems under these experimental conditions.

Producing Low Density Cellular Materials based on LDPE/Clays Nanocomposites by Batch Gas Dissolution in Sub-critical Conditions

- ➢ Studying the gas barrier behavior of the crosslinked nanocomposites and compare it with the previous non-crosslinked case.
- ➢ Studying the foamability and cellular morphology of these nanocomposites after been crosslinked. Producing foams with low densities.
- ➢ Correlating the rheological behavior of the nanocomposites with the foaming behavior and cellular structures.

Characterizing in detail the foaming behavior of LDPE/Clays nanocomposites in free-foaming and relating it with fundamental properties studied in the solid precursors.

- ◉ Studying fundamental properties of the solid nanocomposite precursors, focusing the attention to the most important properties for foaming.
- ◉ Characterizing in detail, by optical expandometry, the foaming behavior of these nanocomposites. Parameters as for example beginning of the foaming, foaming rate, maximum expansion achievable, stability and collapse rate are studied.
- ◉ Studying the cellular structure and final density of the free-foamed samples.

Studying in-situ the effect of foaming on the exfoliation degree of nanoclays in LDPE based nanocomposites

- ◉ Using a synchrotron radiation source to study the whole foaming process and evolution of the interlamellar spacing of the nanoclays during foaming.
- ◉ Enlighting the physical mechanisms underlying behind this effect. Three different blowing agent with very different nature were used for this purpose.

Producing Low Density Cellular Materials based on LDPE/Clays Nanocomposites with Improved Gas Barrier Properties

- ◉ Producing LDPE/Clays nanocomposite low density foamed blocks (density <30 kg/m^3) by the two steps compression molding.

- Studying the creep behavior of these nano-filled low density foams and comparing it with the non-filled counterparts. Effect of the coupling agent addition and of the nanoclays.

- Studying the effective gas diffusion coefficient of these nanocomposite foams (when subjected to an external long term load). Comparing it to the effective diffusion coefficient of their non-filled counterparts. Again the effect of the coupling agent addition, independently of the nanoclays, is considered.

- Studying the cellular structure of the so produced low density foams with and without nanoclays. Establishing and explaining the observed differences.

- Characterizing the physical properties of the foams (filled and unfilled), paying special attention to the mechanical properties. Comparing them with the properties of the solid precursors.

> **Modifications in the Cellular Structure.**

Producing Medium Density Structural Cellular Materials with Improved Properties by a Novel Route

- Obtaining structural foams by a novel route (Stages Molding), completely different to the current ones based on injection molding.
- Studying the scientific basics underlying behind this route.
- Characterizing the physical properties of the foams.
- Protecting the technology expecting future practical applications

> **Modifications in the Polymer Matrix and Cellular Structure**

Producing Low Density Non-Crosslinked Closed/Open Cell Polypropylene Cellular Materials with High Mechanical Properties

- Developing and optimizing a strategy (formulation + production route) for fabricating polypropylene foams with densities in the range 90-200 kg/m^3 with improved mechanical properties.

 Establishing relationships of the type rheology-open/closed cell content-mechanical properties.

 Studying the effect of different nanoparticles on the rheology of the polymer matrix and therefore on the open cell content and mechanical properties.

 Characterizing the physical properties, specially mechanical properties of these foams and comparing them with current commercial materials.

 Protecting the technology expecting future practical applications.

1.3.- STRUCTURE OF THE THESIS

This thesis consists in a compendium of 10 scientific papers, some of them already published and some other submitted, 2 scientific divulgation papers and 2 patents and is organized in 7 chapters plus 2 annexes. Each chapter contains the following information:

❖ Chapter 2: essential theoretical concepts and the state of the art description not included in the scientific papers.

❖ Chapter 3: detailed description of the production routes used in the thesis, raw materials and experimental techniques.

❖ Chapter 4: includes 6 works focused on the modification of the polymer matrix. In the first two works the materials are produced by gas dissolution, one including the addition of nanoclays and the other one combining polymer crosslinking and nanoclays.. Free foaming is used in the third work and the foamability of the nanocomposites is studied in detail by optical expandometry. Free foaming is also used in the fourth work combined with diffractometry using a synchrotron radiation source. Creep is the main subject of the fifth and sixth works. The fifth introduces the concepts and methodology used in the sixth work. And in the sixth work two steps compression molding is used to produced low density crosslinked LDPE/Clays nanocomposite foams that are characterized in detail.

❖ Chapter 5: includes 2 works related to the tailoring and development of a new production route for the fabrication of structural foams. This chapter covers the part of the thesis dedicated to the modifications of the foam structure. The first work included in this chapter is focused on the description and scientific explanation of the production route and physical

mechanisms involved. The second work describes the structural and mechanical properties shown by these foams.

❖ Chapter 6: includes 2 works that combine modifications in the polymer matrix and in the foam structure. The foams are produced using improved compression molding with a thorough tailoring of the production conditions. The first work describes the production route and characterizes the foams by tomography. The second one is more focused on the rheological and mechanical properties, establishing relations between them.

❖ Chapter 7: summarizes the main conclusions obtained during the whole thesis.

❖ Annex I: comprises two works of scientific divulgation, both written in Spanish.

❖ Annex II: comprises the two patents developed during the thesis.

The papers included in the thesis are summarized in table 1.2

Table 1.2: Publications included in the Thesis

Publications included in this Thesis
J. Escudero, V. Kumar, M. A. Rodriguez-Perez *Sorption Behaviour and Microcellular Foaming in LDPE/Clay Nanocomposites by Batch Gas Dissolution in Sub-Critical Conditions* *Chapter 4*
J. Escudero, E. Laguna, V. Kumar, M. A. Rodriguez-Perez *Microcellular Foaming in Sub-Critical CO_2 of Non-Crosslinked and Crosslinked LDPE and LDPE/Clay Nanocomposites* *Chapter 4*
J. Escudero, B. Notario, J.A. de Saja, M.A. Rodriguez-Perez *Polyethylene Layered Nanocomposites for Foaming Purposes* *Chapter 4*
J. Escudero, B. Notario, C. Jimenez, M.A. Rodriguez-Perez. *In-situ Characterization of Nanoclays Exfoliation During Foaming by Energy Dispersive XRD of Synchrotron Radiation.* Sent to the Journal of Synchrotron Radiation *Chapter 4*
J. Escudero, J. Lazaro, E. Solorzano, M.A. Rodríguez-Pérez, J.A. de Saja. *Gas Diffusion and Re-Diffusion in Polyethylene Foams* *Published. Defect and Diffusion Forum Vols. 283-286 (2009) pp 583-588* *Chapter 4*

J. Escudero, A. Galeski, M.A. Rodríguez-Pérez, J.A. de Saja

Effective Diffusion Coefficient and Mechanical Properties of Low Density Foams Based in Polyethylene/Clays Nanocomposites

Chapter 4

J. Escudero, J. Pinto, M.A. Rodriguez-Perez.

A new technology for the production of polymer structural foams

Chapter 5

J. Escudero, E. Solorzano, M.A. Rodríguez-Pérez, F. Garcia-Moreno J.A. de Saja.

Structural Characterization and Mechanical Behaviour of LDPE Structural Foams. A Comparison with Conventional Foams

Published. Cellular Polymers Vol.28 No 4. (2009) pp 289-302

Chapter 5

Y. Ma, R. Pyrz, M.A. Rodriguez-Perez , J. Escudero, J.Ch. Rauhe, X. Su.

X-ray Microtomographic Study of Nanoclays-Polypropylene Foams

Published. Cellular Polymers Vol. 30. No 3 (2011) pp 95-109.

Chapter 6

J. Escudero, A. Lopez-Gil, E. Laguna, M.A. Rodriguez-Perez, J.A. de Saja.

Low Density Non-Crosslinked Closed/Open Cell Polypropylene Foams with High Mechanical Properties: Rheology, Cellular Morphology and Mechanical Behavior

Accepted. Cellular Polymers

Chapter 6

The work conducted during the thesis was translated into contributions to different international conferences. These contributions are presented in Table 1.3.

Table 1.3: Contributions to International Conferences and Publications in Non-Indexed Journals

Contributions to Conferences and Publications in Non-Indexed Journals
E. Solorzano, J. Escudero, J. Lazaro, M. A. Rodriguez-Perez, J. A. de Saja.
Obtaining Critical Cooling Velocity Maps for Thermal Hardening Treatments in Aluminum Foams: Density Characterization, Finite Elements Analysis, Experimental Validation and Final Results.
Metfoam Conference 2007. Montreal, Canada. September 2007.
J. Escudero, J. Lazaro, E. Solorzano, M.A. Rodríguez-Pérez, J.A. de Saja.
Gas Diffusion and Re-Diffusion in Solid Polyethyelene Foams.
Diffusion in Solids and Liquids, Barcelona, Spain. July 2008.
J. Lazaro, J. Escudero, E. Solorzano, M.A. Rodriguez-Perez, J.A. de Saja.

Heat Transport in Closed Cell Aluminum Foams: Application Notes.

Diffusion in Solids and Liquids, Barcelona, Spain. July 2008.

J. Escudero, M.A. Rodríguez-Pérez, J.A. de Saja.

Mechanical Properties of Structural LDPE Foams Compared with those Conventional Non-Structural LDPE Foams..

Blowing Agents Conference 2009. Hamburg, Germany. May 2009

J. Escudero, J. Pinto, E. Solorzano, M.A. Rodríguez-Pérez, J.A. de Saja.

Structural Foams versus Conventional Foams: Structural Characterization and Mechanical Behavior.

GEP 2009. Valladolid, Spain. September 2009.

E. Solorzano, J. Escudero, J. A. de Saja, M.A. Rodríguez-Pérez.

Pressure Vessels with Optical Windows: New Possibilities in Polymer Gas Dissolution Techniques

Diffusion in Solids and Liquids 2010. Paris, France, July 2010.

E. Solorzano, J. Escudero, J. Pinto, J.A.de Saja, M.A. Rodriguez-Perez.

Gas Diffusion and Other Physical Mechanisms Involved in the Production of Structural Foams..

Diffusion in Solids and Liquids 2010. Paris, France, July 2010

J. Escudero, C. Saiz-Arroyo, M.A. Rodríguez-Pérez, J.A. de Saja.

LDPE Silica Nanocomposites: A System in which Nanoparticles Play a Multifunctional Role.

FOAMS 2010. Seattle, USA. September 2010

E. Laguna, J. Escudero, A. Lopez-Gil, M.A. Rodriguez-Perez, J.A. de Saja.

Caracterización de Nanocompuestos Poliméricos Mediante Reología Extensional.

XII Escuela Nacional de Materiales Moleculares. Castellón (Spain) February 2011.

E. Solorzano, J. Escudero, J. Pinto, M.A. Rodriguez-Perez, J.A. de Saja.

Evolution of Polymers During the Gas Dissolution Process

Diffusion in Solids and Liquids 2011. Algarve, Portugal. June 2011.

M.A. Rodriguez-Perez, J. Escudero, J. Pinto, E. Solorzano

Production of Structural Foams Using Free-Foaming. In-Situ Analysis of the Foaming Process.

FOAMS 2011. Iselin, NJ. USA September 2011.

J. Escudero, E. Laguna. V. Kumar, M.A. Rodriguez-Perez

Gas Diffusion and Foaming in Low Density Polyethylene/Clays Nanocomposites

FOAMS 2011. Iselin, NJ. USA September 2011.

J. Escudero, J. Tirado, M.A. Rodriguez-Perez, J.A. de Saja, D. Rosa, J.A. Vazquez.

Stages Molding: A New Technologie for the Productionf of Plastic Parts.

EUROTEC 2011. Barcelona, Spain. November 2011.

O. Shishkina, Y. Zhu, J. Escudero, A. Lopez-Gil, M.A. Rodriguez-Perez, L. Gorbatikh, S. Lomonov, I. Verpoest.

Multi-level Characterization of the Compressive Behavior of Novel Cellular Nanocomposites

15th European Conference on Composite Materials. Venice, Italy. June 2012

C. Saiz-Arroyo, J. Escudero, A. Lopez-Gil, M.A. Rodriguez-Perez.

Production of Non-Crosslinked Polypropylene Foams with Controlled Density and Tailored Cellular Structure and Physical Properties

FOAMS 2012. Barcelona (Spain) September 2012.

M.A. Rodriguez-Perez, J. Pinto, J. Escudero, A. Lopez-Gil, S. Estravis, C. Saiz-Arroyo, E. Solorzano, S. Pardo.

Nano-Strategies Applied to the Production of Cellular Polymers with Improved Cellular Structure and Properties.

Cellular Materials Conference. Dresden, Germany. November 2012.

J. Escudero, C. Saiz-Arroyo, M.A. Rodríguez-Pérez, J.A. de Saja.

El Efecto Multifuncional de las Nanopartículas en los Materiales Celulares.

Revista de Plásticos Modernos 101 (657) 326-339 (2011). (Appendix I)

J. Escudero, J. Tirado, M. A. Rodriguez-Perez, J.A. de Saja, D. Rosa, J.A. Vazquez.

Stages Molding: Una Nueva Tecnología Para la Fabricación de Piezas de Plástico.

Revista de Plásticos Modernos 102 (659) 32-39 (2011). (Appendix I)

Besides the papers included in the thesis, the autor contributed in other publications in indexed journals that are presented in table 1.4.

Table 1.4: Publications in International Journals not included in this Thesis.

Other Publications in International Journals
J. Lazaro, J. Escudero, E. Solorzano, M.A. Rodriguez-Perez, J.A. de Saja
Heat Transport in Aluminum Foams: Application Notes
Advanced Engineering Materials.(11) 10. pp. 825-831 (2009)
C. Saiz-Arroyo, J. Escudero, M.A. Rodríguez-Pérez, J.A. de Saja.
Improving the Structure and Physical Properties of LDPE Foams Using Silica Nanoparticles as an Additive.
Cellular Polymers (30) 2 pp. 45-60 (2011).
J. Lazaro, E. Solorzano, J. Escudero, M.A. Rodriguez-Perez, J.A. de Saja.
Applicability of Solid Solution Heat Treatments to Aluminum Foams.
Metals (4) 2 pp. 508-528, (2012).

The patents previosuly mentioned are included in Table 1.5 with their corresponding reference.

Table 1.5: Patents published in the frame of the thesis.

Patents
J.A. Vazquez, J.A. de Saja, M.A. Rodriguez-Perez, J. Escudero
System and Method for Moulding Parts Using Free-Standing Moulds.
International Patent Reference:WO/2012/117143. September 2012. (Appendix II)
M.A. Rodriguez-Perez, J.A. de Saja, J. Escudero, A. Lopez-Gil.
Fabricación de Materiales Celulares de Matriz Termoplástica.
Spanish Patent 201231092. July 2012. (Appendix II)

One of the research works developed during the thesis deserved the Foro Ibérico del PVC Award in 2009. This is presented in Table 1.6.

Table 1.6: Research works awarded.

Awards
VI Edition Foro Ibérico del PVC Award.
Microcellular PVC, Fabrication, Mechanical Properties and Advantages Offered by this Materials in Structural Applications.
Supervisors: M.A. Rodriguez-Perez and E. Solorzano.
Centro Catalán del Plástico. Terrasa, Barcelona (Spain). March 2009.

1.4.- BIBLIOGRAPHY

[1]. L.J. Gibson, M.F. Ashby. Cellular Solids: Structure and Properties. 2nd Edition, Cambridge University Press, United Kingdom, (1997).

[2]. D. Klempner, V. Sendijarevic. Handbook of Polymeric Foams and Foam Technology. 2nd Edition. Hanser Publishers, Munich, (2004)

[3]. E. Solórzano. Espumas de Aluminio: Proceso de Espumado, Estructura Celular y Propiedades. Tesis Doctoral, Universidad de Valladolid, (2008).

[4]. D. Eaves. Handbook of Polymer Foams. Rapra Technology, United Kingdom, (2004).

[5]. V. Kumar. Microcellular Polymers: Novel Materials for 21st Century. Progress in Rubber and Plastics Technology 9: 54-70, (1993).

[6]. S.T. Lee. Foam Extrusion: Principles and Practice. Technomic Publishing Company. Lancaster-Pennsylvania, (2000).

[7]. M.A. Rodríguez-Pérez. Propiedades Térmicas y Mecánicas de Espumas de Poliolefinas. Tesis Doctoral, Universidad de Valladolid, (1998)

[8]. R. Gendron (Ed). Thermoplastic Foam Processing. Principles and Development. CRC Press, Boca Raton-Florida, (2005).

[9]. J. Martini-Vvedensky, N.P. Suh, F.A. Waldman. US Patent nº 4.473.665, (1984).

[10]. K.T. Okamoto. Microcellular Processing. Hanser Publishers, Munich, (2008).

[11]. A. Okada, A. Usuki. Chemistry of Polymer-Clay Hybrids. Materials Science and Engineering 3: 109-115, (1995)

[12]. C.C. Ibeh, M. Bubacz. Current Trends in Nanocomposite Foams. Journal of Cellular Plastics 44: 493-515, (2008).

[13]. L.J. Lee, C. Zeng, X. Cao, X. Han, J. Shen, G. Xu. Polymer Nanocomposite Foams. Composites Science and Technology 65: 2344-2636, (2005).

[14]. R. Auras, L.T. Lim, S.E.M. Selke, H. Tsuji (Eds). Poly (lactic acid). Synthesis, Characterization, Properties, Processing and Applications. John Wiley & Sons Inc., Hoboken, New Jersey, (2010).

[15]. S. Chanprateep. Current Trends in Biodegradable Polyhydroxyalkanoates. Journal of Bioscience and Bioengineering 110: 621-632, (2010).

[16]. D. Miller, P. Chatchaisucha, V. Kumar. Microcellular and Nanocellular Solid-State Polyetherimide (PEI) Foams using Sub-Critical Carbon Dioxide I. Processing and Structure. Polymer 50: 5576-5584, (2009)

[17]. D. Miller, V. Kumar. Microcellular and Nanocellular Solid-State Polyetherimide (PEI) Foams using Sub-Critical Carbon Dioxide II. Tensile and Impact Properties. Polymer 52: 2910-2919, (2011).

[18]. J.A. Reglero-Ruiz, J.M. Tallon, M Pedros, M. Dumon. Two Step Microcellular Foaming of Amorphous Polymers in Supercritical CO_2. Journal of Supercritical Fluids 57: 87-94, (2011).

[19]. J.A. Reglero-Ruiz, M. Pedros, J.M. Tallon, M. Dumon. Micro and Nano Cellular Amorphous Polymers (PMMA, PS) in Supercritical CO_2 Assisted Nanostructured CO_2-Philic Block Copolymers-One Step Foaming Process. Journal of Supercritical Fluids 58: 168-176, (2011).

[20]. J.A. Reglero-Ruiz, M. Dumon, J. Pinto, M.A. Rodríguez-Pérez. Low Density Nanocellular Foams Produced by High Pressure Carbon Dioxide. Macromolecular Materials & Engineering 296: 752-759, (2011).

[21]. O. Almanza. Caracterización y Modelización de las Propiedades Térmicas y Mecánicas en Espumas de Poliolefinas. Tesis Doctoral, Universidad de Valladolid, (2000).

[22]. L.O. Arcos y Rábago. Propiedades Térmicas y Mecánicas de Espumas de Poliolefinas Fabricadas en un Proceso de Moldeo por Compresión. Tesis Doctoral, Universidad de Valladolid, (2002).

[23]. J.L. Ruiz-Herrero. Impacto y Fluencia de Espumas con Base Polietileno. Tesis Doctoral, Universidad de Valladolid, (2004).

[24]. J.I. González-Peña. Efecto de los Tratamientos Térmicos en Bloques de Espuma de Polietileno de Baja Densidad Producidos Mediante Moldeo por Compresión. Tesis Doctoral, Universidad de Valladolid, (2006).

[25]. M. Álvarez-Laínez. Propiedades Térmicas, Mecánicas y Acústicas de Espumas de Poliolefina de Celda Abierta. Tesis Doctoral, Universidad de Valladolid, (2007).

[26]. F. Hidalgo-González. Diseño Optimizado de los Parámetros de Proceso de Fabricación de Espuma de Poliolefina Reticulada mediante Moldeo por Compresión. Tesis Doctoral, Universidad de Valladolid, (2008).

[27]. R. Campo-Arnáiz. Aplicación de Técnicas Espectroscópicas al Estudio de la Morfología Polimérica, Propiedades Térmicas y de Emisión de Espumas de Baja Densidad con Base Poliolefina. Tesis Doctoral, Universidad de Valladolid, (2011).

[28]. M.A. Rodríguez-Pérez, S. Rodríguez-Llorente, J.A. de Saja. Dynamic Mechanical Properties of Polyolefin Foams Studied by DMA. Polymer Engineering and Science 37: 959-965, (1997).

[29]. M.A. Rodríguez-Pérez, O. Alonso, J. Souto, J.A. de Saja. Thermal Conductivity of Crosslinked Closed Cell Polyolefin Foams. Polymer Testing 16: 287-298, (1997).

[30]. M.A. Rodríguez-Pérez, S. Díez-Gutierrez, J.A. de Saja. The Recovery Bheaviour of Crosslinked Closed Cell Polyolefin Foams. Polymer Engineering and Science, 38: 831-838, (1998).

[31]. M.A. Rodríguez-Pérez, A. Duijsens, J.A. de Saja. Effect of the Addition of EVA on the Technical Properties of Extruded Foamed Profiles of Low-Density Polyethylene/EVA Blends. Journal of Applied Polymer Science 36: 2587-2596, (1998).

[32]. J.I. Velasco, A.B. Martínez-Benasat, D. Arencón, M.A. Rodríguez-Pérez, J.A. de Saja. Caracterización Mecánica de Espumas Poliolefinicas mediante Impacto por Caída de Dardo Instrumentado. Anales de Ingeniería Mecánica 2: 639-644, (1998).

[33]. J.I. Velasco, A.B. Martínez-Benasat, M.A. Rodríguez-Pérez, J.A. de Saja. Application of Instrumented Falling Dart Impact to the Mechanical Characterization of Thermoplastic Foams. Journal of Materials Science 34: 431-438, (1999).

[34]. M.A. Rodríguez-Pérez, O. Almanza, J.A. de Saja. Anomalous Thickness Increase in Crosslined Closed Cell Polyolefin Foams During Heat Treatments. Journal of Applied Polymer Science 73: 2825-2835, (1999).

[35]. M.A. Rodríguez-Pérez, J.A. de Saja. The Effect of Blending on the Physical Properties of Crosslinked Closed Cell Polyethylene Foams. Cellular Polymers 18: 1-20, (1999).

[36]. M.A. Rodríguez-Pérez, J.A. de Saja. Diseño de Espumas Poliméricas con Base Poliolefïnica (I). Revista de Plásticos Modernos 77: 517-528, (1999).

[37]. M.A. Rodríguez-Pérez, J.A. de Saja. Diseño de Espumas Poliméricas con Base Poliolefïnica (II). Revista de Plásticos Modernos 78: 550-558, (1999).

[38]. M.A. Rodríguez-Pérez, J.A. de Saja. Dynamic Mechanical Analysis Applied to the Characterization of Closed Cell Polyolefin Foams. Polymer Testing 19: 831-848, (1999).

[39]. O. Almanza, M.A. Rodríguez-Pérez, J.A. de Saja. The Thermal Conductivity of Polyethylene Foams Manufactured by a Nitrogen Solution Process. Cellular Polymers 18: 385-401, (1999).

[40]. M.A. Rodríguez-Pérez, J.I. Velasco, D. Arencón, O. Almanza, J.A. de Saja. Mechanical Characterization of Closed-Cell Polyolefin Foams. Journal of Applied Polymer Science 75: 156-166, (2000).

[41]. O. Almanza, M.A. Rodríguez-Pérez, J.A. de Saja. Prediction of the Ratiation Term in the Thermal Conductivity of Crosslinked Closed Cell Polyolefin Foams. Journal of Polymer Science. Part B: Polymer Physics 38: 993-1004, (2000).

[42]. J.I. Velasco, A.B. Martínez, D. Arencón, O. Almanza, M.A. Rodríguez-Pérez, J.A. de Saja. Rigidity Characterization of Flexible Foams by Falling Dart Rebound Tests. Cellular Polymers 19: 155-133, (2000).

[43]. M.A. Rodríguez-Pérez, O. Almanza, J.L del Valle, A. González, J.A. de Saja. Improvement of the Measurement Process Used for the Dynamic Mechanical Characterization of Polyolefin Foams. Polymer Testing 20: 253-267, (2001).

[44]. J.A. Martínez-Díez, M.A. Rodríguez-Pérez, J.A. de Saja, L.O. Arcos y Rábago, O. Almanza. The Thermal Conductivity of a Polyethylene Foam Block Produced by a Compression Molding Process. Journal of Cellular Plastics 37: 21-42, (2001).

[45]. O. Almanza, M.A. Rodríguez-Pérez, J.A. de Saja. The Microstructure of Polethylene Foams Produced by a Nitrogen Solution Process. Polymer 42: 7117-7126, (2001).

[46]. O. Almanza, L.O. Arcos y Rábago, M.A. Rodríguez-Pérez, A. González, J.A. de Saja. Structure-Property Relationships in Polyolefin Foams. Journal of Macromolecular Science, Part B: Physics 40: 603-613, (2001).

[47]. N.J. Mills, M.A. Rodríguez-Pérez. Modelling the Gas-Loss Creep Mechanism in EVA Foam from Running Shoes. Cellular Polymers 20: 79-100, (2001).

[48]. M.A. Rodríguez-Pérez, J.A. de Saja. Morphology of Semicrystalline Foams Based on Polyethylene. Journal of Macromolecular Science, Part B: Physics 41: 761-775, (2002).

[49]. M.A. Rodríguez-Pérez, J.I. González-Peña, N. Witten, J.A. de Saja. The Effect of Cell Size on the Physical Properties of Crosslinked Closed Cell Polyethylene Foams Produced by a High Pressure Nitrogen Solution Process. Cellular Polymers 21: 165-194, (2002).

[50]. M.D. Landete-Ruiz, J.A. Martínez-Díez, M.A. Rodríguez-Pérez, J.A. de Saja, J.M. Martín-Martínez. Improved Adhesion of Low-Density Polyethylene/EVA Foams Using Different Surface Treatments. Journal of Adhesion Science and Technology 16: 1073-1101, (2002).

[51]. M.A. Rodríguez-Pérez. The Effect of Density, Chemical Composition and Cellular Structure on the Dynamic Mechanical Response of Foams. Cellular Polymers 21: 117-136 (2002).

[52]. S. Díez-Gutierrez, M.A. Rodríguez-Pérez, M. Machimbarrena, J. González, J.A. de Saja. Technical Note. Impact Sound Reduction of Crosslinked and Non-Crosslinked Polyethylene Foams as Suspended Floors of Concrete Structures. Journal of Building and Acoustics 10: 261-271, (2003).

[53]. O. Almanza, M.A. Rodríguez-Pérez, J.A. de Saja. Applicability of the Transient Plane Source Method to Measure the Thermal Conductivity of Low Density Polyethylene Foams. Journal of Polymer Science, Part B: Polymer Physics 42: 1226-1234, (2004).

[54]. O. Almanza, Y. Masso-Moreau, N.J. Mills, M.A. Rodríguez-Pérez. Thermal Expansion Coefficient and Bulk Modulus of Polyethylene Closed-Cell Foams. Journal of Polymer Science, Part B: Polymer Physics 42: 3741-3749, (2004).

[55]. O. Almanza, M.A. Rodríguez-Pérez, J.A. de Saja. The Measurement of the Thermal Diffusivity and Heat Capacity of Polyehtylene Foams Using the Transient Plane Source Technique. Polymer International, 53: 2038-2044, (2004).

[56]. J.L. Ruiz-Herrero, M.A. Rodríguez-Pérez, J.A. de Saja. Characterization of Polyethylene Foams under Compressive Impact Loading. Materials Science Forum 480-481: 513-518, (2005).

[57]. O. Almanza, M.A. Rodríguez-Pérez, B. Chernev, J.A. de Saja, P. Zipper. Comparative Study on the Lamellar Structure of Polyethylene Foams. European Polymer Journal 41: 599-609, (2005).

[58]. M.A. Rodríguez-Pérez. Crosslinked Closed Cell Polyolefin Foams: Production, Structure, Properties and Applications. Advances in Polymer Science 184: 87-126, (2005).

[59]. J.L. Ruiz-Herrero, M.A. Rodríguez-Pérez, J.A. de Saja. Effective Diffusion Coefficient for the Gas Contained in Closed Cell Polyethylene-Based Foams Subjected to Compressive Creep Tests. Polymer 46: 3105-3110, (2005).

[60]. R.A. Campo-Arnáiz, M.A. Rodríguez-Pérez, B. Calvo, J.A. de Saja. Extinction Coefficient of Polyolefin Foams. Journal of Polymer Science, Part B: Polymer Physics 43: 1608-1617, (2005).

[61]. J.L. Ruiz-Herrero, M.A. Rodríguez-Pérez, J.A. de Saja. Design and Construction of an Instrumented Falling Weight Impact Tester to Characterize Polymer-Based Foams. Polymer Testing 24: 641-647, (2005).

[62]. J.L. Ruiz-Herrero, M.A. Rodríguez-Pérez, J.A. de Saja. Effect of Sample Size on the Effective Diffusion Coefficients for Gas Contained in Closed Cell Polyethylene-Based Foams Subjected to Compressive Creep Tests. Journal of Applied Polymer Science 99: 2204-2210, (2005).

[63]. J.L. Ruiz-Herrero, M.A. Rodríguez-Pérez, J.A. de Saja. Prediction of Cushion Curves for Closed Cell Polyethylene-Based Foams. Part I: Modelling. Cellular Polymers 24: 329-346, (2005).

[64]. M.A. Rodríguez-Pérez, R.A. Campo-Arnáiz, R. Aroca, J.A. de Saja. Characterization of the Matrix Polymer Morphology of Polyolefin Foams by Raman Spectroscopy. Polymer 46: 12093-12102, (2005).

[65]. M.A. Álvarez-Laínez, M.A. Rodríguez-Pérez, G. Antolín, J. González, J.A. de Saja. Absorción Acústica de Espumas de Poliolefina de Celda Abierta y Cerrada. Revista de Acústica 36: 1-8, (2005).

[66]. J.L. Ruiz-Herrero, M.A. Rodríguez-Pérez, J.A. de Saja. Prediction of Cushion Curves for Closed Cell Polyethylene-Based Foams. Part II: Experimental. Cellular Polymers 25: 156-175, (2006)

[67]. M.A. Rodríguez-Pérez, J.L. Ruiz-Herrero, E. Solórzano, J.A. de Saja. Gas Diffusion in Polyolefin Foams During Creep Tests. Effect on Impact Behaviour and Recovery after Creep. Cellular Polymers 25: 221-236, (2006).

[68]. M.A. Rodríguez-Pérez, J.I. González-Peña, J.A. de Saja. Anisotropic and Heterogenous Thermal Expansion of Polyethylene Foam Blocks: Effect of Thermal Treatments. European Polymer Journal 43: 4474-4485, (2007).

[69]. M. Álvarez-Laínez, M.A. Rodríguez-Pérez, J.A. de Saja. Thermal Conductivity of Open Cell Polyolefin Foams. Advanced Engineering Materials 10: 373-377, (2008).

[70]. M.A. Rodríguez-Pérez, O. Almanza, J.L. Ruiz-Herrero, J.A. de Saja. The Effect of Processing on the Structure and Properties of Crosslinked Closed Cell Polyethylene Foams. Cellular Polymers 27: 179-200, (2008).

[71]. M.A. Rodríguez-Pérez, M. Álvarez-Laínez, J.A. de Saja. Microestructure and Physical Properties of Open Cell Polyolefin Foams. Journal of Applied Polymer Science 114: 1176-1186, (2009).

[72]. M.A. Rodríguez-Pérez, F. Hidalgo, E. Solórzano, J.A. de Saja. Measuring the Time Evolution of the Gas Pressure in Closed Cell Polyolefin Foams Produced by Compression Moulding. Polymer Testing 28: 188-195, (2009).

[73]. M.A. Rodríguez-Pérez, J.I. González-Peña, J.A. de Saja. Modifying the Structure and Properties of Polyethylene Foams using Thermal Treatments. Polymer International 58, 620-629, (2009).

[74]. S. Román Lorza. Formulación y Caracterización de Materiales Celulares Retardantes de Llama Libres de Halógenos basados en Poliolefinas. Tesis Doctoral, Universidad de Valladolid, (2010).

[75]. J.I. Velasco, M. Antunes, O. Ayyad, J.M. López-Cuesta, P. Gaudon, C. Saiz-Arroyo, M.A. Rodríguez-Pérez, J.A. de Saja. Foaming Behaviour and Cellular Structure of LDPE /Hectorite Nanocomposites. Polymer 48: 2098-2108, (2007).

[76]. J.I. Velasco, M. Antunes, O. Ayyad, C. Saiz-Arroyo, M.A. Rodríguez-Pérez, F. Hidalgo, J.A. de Saja. Foams Based on Low Density Polyethylene/Hectorite Nanocomposites: Thermal Stability and Thermo-Mechanical Properties. Journal of Applied Polymer Science 105: 1658-1667, (2007).

[77]. R. Verdejo, F. Barroso-Bujans, M.A. Rodríguez-Pérez, J.A. de Saja, M.A. López-Manchado. Functionalized Graphene Sheets filled Silicona Foam Nanocomposites. Journal of Materials Chemistry 19: 2221-2226, (2008).

[78]. R. Verdejo, C. Saiz-Arroyo, J. Carretero-González, F. Barroso-Bujans, M.A. Rodríguez-Pérez, M.A. López-Manchado. Physical Properties of Silicone Foams filled with Carbon Nanotubes and Functionalized Graphene Sheets. European Polymer Journal 44: 2790-2797, (2008).

[79]. R. Verdejo, F. Barroso-Bujans, M.A. Rodríguez-Pérez, J.A. de Saja, M. Arroyo, M.A. López-Manchado. Carbon Nanotubes Provide Self-Extinguishing Grade to Silicone-Based Foams. Journal of Materials Chemistry 18: 3933-3939, (2008).

[80]. M.A. Rodríguez-Pérez, J. Lobos, C.A. Pérez-Muñoz, J.A. de Saja, L. González, B.M.A. del Carpio. Mechanical Behaviour at Low Strains of LDPE Foams with Cell Sizes in the Microcellular Range: Advantages of using these materials in structural elements. Cellular Polymers 27: 347-362, (2008).

[81]. J. Escudero, E. Solórzano, M.A. Rodríguez-Pérez, F. García-Moreno, J.A. de Saja. Structural Characterization and Mechanical Behaviour of LDPE Structural Foams. A Comparison with Conventional Foams. Cellular Polymers 28: 289-302, (2009).

[82]. M.A. Rodríguez-Pérez, J. Lobos, C.A. Pérez-Muñoz, J.A. de Saja. Mechanical Response of Polyolefin Foams with High Densities and Cell Sizes in the Microcellular Range. Journal of Cellular Plastics 45: 389-403, (2009).

[83]. R. Verdejo, R. Stämpfli, M. Álvarez-Laínez, S. Mourad, M.A. Rodríguez-Pérez, P.A. Brühwiler, M. Shafler. Enhanced Acoustic Damping in Flexible Polyurethane Foams Filled with Carbon Nanotubes. Composites Science and Technology 69: 1564-1569, (2009).

[84]. M. Antunes, V. Realinho, E. Solórzano, M.A. Rodríguez-Pérez, J.A. de Saja, J.I. Velasco. Thermal Conductivity of Carbon Nanofibre-Polypropylene Composite Foams. Defect and Diffusion Forum 297: 996-1001, (2010).

[85]. S. Román-Lorza, M.A. Rodríguez-Pérez, J.A. de Saja. Cellular Structure of Halogen-Free Flame Retardant Foams based on LDPE. Cellular Polymers 28: 249-268, (2009).

[86]. S. Román-Lorza, J. Sabadell, J.J. García-Ruiz, M.A. Rodríguez-Pérez, J.A. de Saja. Fabrication and Characterization of Halogen Free Flame Retardant Polyolefin Foams. Materials Science Forum 636/637: 98-205, (2010)

[87]. S. Román-Lorza, M.A. Rodríguez-Pérez, J.A. de Saja. Cellular Structure of EVA/ATH Halogen-Free Flame Retardant Foams. Journal of Cellular Plastics 10: 1-21, (2010).

[88]. C. Saiz-Arroyo, J. Escudero, M.A. Rodríguez-Pérez, J.A. de Saja. Improving the Strcutre and Physical Properties of LDPE Foams using Silica Nanoparticles as an Additive. Cellular Polymers 30: 63-78, (2011).

[89]. Y. Ma, R. Pyrz, M.A. Rodríguez-Pérez, J. Escudero, J.C. Rauhe, X. Su. X-Ray Microtomographic Study of Nanoclay-Polypropylene Foams. Cellular Polymers 30: 95-110, (2011).

[90]. J.A. Reglero-Ruiz, C. Saiz-Arroyo, M. Dumon, M.A. Rodríguez-Pérez, J.A. de Saja, L. González. Production, Cellular Structure and Thermal Conductivity of Microcellular Methyl Methacrylate-Butyl Acrylate-Methyl Methacrylate Triblock Copolymers. Polymer International 60: 146-152, (2011).

[91]. M.A. Rodríguez-Pérez, R.D. Simoes, C.J.L. Constantino. J.A. de Saja. Structure and Physical Properties of EVA/Starch Precursor Materials for Foaming Applications. Journal of Applied Polymer Science 212: 2324-2330, (2011).

[92]. M. Ardanuy, M.A. Rodríguez-Pérez, J.A. de Saja, J.I. Velasco. Foaming Behaviour, Cellular Structure and Physical Properties of Polybenzoxazine Foams. Polymers for Advanced Technologies DOI 10.1002/pat.1978 (2011).

[93]. M.A. Rodríguez-Pérez, R.D. Simoes, S. Román-Lorza, M. Álvarez-Laínez, C. Montoya-Mesa. C.J.L. Constantino, J.A. de Saja. Foaming of EVA/Starch Blends: Characterization of the Structure, Physical Properties and Biodegradability. Polymer Engineering and Science 52: 62-70, (2012).

[94]. M. Antunes, V. Realinho, J. I. Velasco, E. Solorzano, M. A. Rodriguez-Perez, J. A. de Saja. Thermal Conductivity Anisotropy in Polypropylene Foams Prepared by Supercritical CO2 Dissolution. Materials Chemistry and Physics 136 (1), 268-276 (2012)

[95]. M.M. bernal, I. Molenberg, S. Estravis, M. A. Rodriguez-Perez, I. Huynen, M. A. Lopez-Manchado, R. Verdejo. Comparing the Effect of Carbon-Based Nanofiller on the Physical Properties of Flexible Polyurethane Foams. Journal of Materials Science 47 (15), 5673-5679 (2012).

[96]. C. Saiz-Arroyo, J. A. de Saja, J. I. Velasco, M. A. Rodriguez-Perez. Moulded Polypropylene Foams Produced Using Chemical or Physical Blowing Agents: Structure-Properties Relationship. Journal of Materials Science 47 (15) 5680-5692 (2012).

[97]. E. Solorzano, M. Antunes, C. Saiz-arroyo, M. A. Rodriguez-Perez, J. I. Velasco, J. A. de Saja. Optical Expandometry: A Technique to analyze the Expansion Kinetics of Chemically Blowin Thermoplastic Foams. Journal of Applied Polymer Science 125 (2) 1059-1067 (2012).

[98]. C. Saiz-Arroyo, J. A. de Saja, M. A. Rodriguez-Perez. Production and Characterization of Crosslinked Low-Density Polyethylene Foams Using Waste of Foams With the Same Composition. Polymer Engineering and Science, 52 (4). 751-759 (2012).

[99]. S. Pardo-Alonso, E. Solorzano, S. Estravis, M. A. Rodriguez-Perez, J. A. de Saja. In-situ Evidence of the Nanoparticle Nucleating Effect in Polyurethane Nanoclay Foamed Systems. Soft Matter 8 (44) 11262-11270 (2012).

[100]. J. Pinto, S. Pardo, E. Solorzano, M.A. Rodriguez-Perez, M. Dumon, J. A. de Saja. Diffusion in Solids and Liquids VII 326-328 pp. 434-439 (2012).

Chapter 2

Background and Review of Concepts

2.1.- CELLULAR MATERIALS

The present thesis work is completely focused on the production of polyolefin based cellular materials so a first introduction of some related concepts is made in the chapter. Nowadays cellular materials are broadly extended in very different applications so the available information, both from a scientific and industrial point of view, about these materials is very vast. In this chapter only some selected concepts will be introduced, the more important ones to later properly understand the rest of the work. It is also important to mention that detailed state of the art of the different topic considered is included in the papers included in the chapters 4 to 6.

2.1.1.- Definition of cellular material and initial considerations.

Cellular materials can be found in nature in many different examples. Cork or wood, to name some, have been extensively used during thousands of years. With time the human kind began developing its own cellular materials. The more familiar ones are based on polymers and they can be found in a broad range of applications but nowadays there are production techniques able to produce cellular materials from ceramics, glasses or metals.

A polymer cellular material can be defined as a two-phase structure in which a gaseous phase has been dispersed in a solid polymer matrix. The gaseous phase can be generated using either a chemical or a physical blowing agent and the polymer solid matrix can vary between a huge range of options [1,2].

Several criteria can be used for classifying these materials but namely two main parameters can be considered: open or closed cellular structure and density.

According to the openness of the cells two different classes can be remarked: *Open Cell*, in which the gas can freely travel across the cells since they are interconnected, and *Closed Cell* in which the gas is enclosed inside the cells (see Figure 2.1).
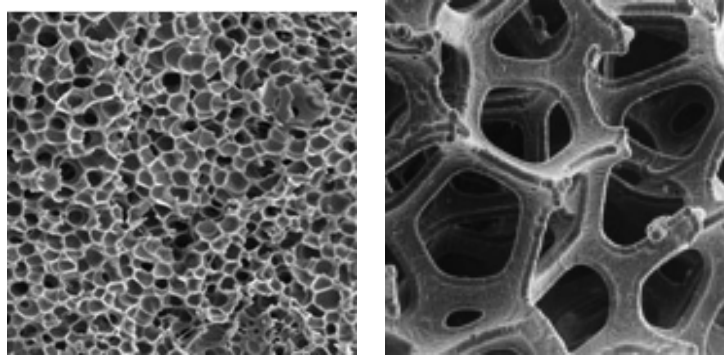
Figure 2.1. Closed cell foam (left) and open cell foam (right).

Density is maybe the parameter that more deeply governs the physical properties of a cellular material and its possible practical applications [1-3]. For the sake of comparison between materials produced form different polymers the concept of relative density is defined. Relative density stands for the quotient between the density of the cellular material and the density of the solid material that forms the solid matrix. Mathematically can be expressed as

Eq. 2.1

$$\rho_{relative} = \frac{\rho_{cellular\ material}}{\rho_{solid}}$$

The concept of Expansion Ratio (ER) is also widely used all along the thesis. It can be defined as the inverse of the relative density and quantifies the number of times that the volume of the solid material has been increased to produce the cellular material.

$$ER = \frac{1}{\rho_{relative}} = \frac{\rho_{solid}}{\rho_{cellular\ material}} \qquad \textit{Eq. 2.2}$$

For relative densities below 0.3 we are talking about *Low Density*. On the other hand, relative densities higher than 0.6 correspond to *High Density* cellular materials. Any value in between can be considered Medium Densities.

Combining the two classifications, openness of the cellular structure and density, we can obtain an interesting map that can be easily related with the industrial applications covered by cellular materials.
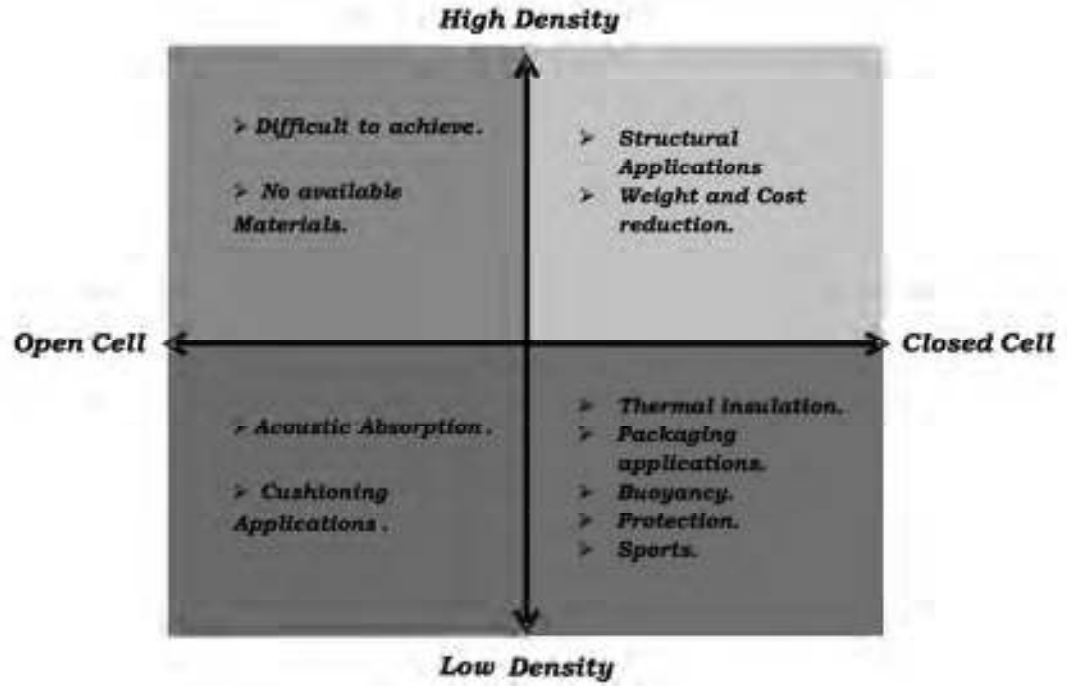
Figure 2.2: Map with a classification of cellular materials taking into account the density and type of cells and its relationships with industrial applications.

The mathematical modeling of any property of these materials can be very complex, considering a lot of influential parameters, but there are also simple formulas that usually give accurate trends. One of this very simple but accurate approximations are referred as *Scale Relationships.* This empirical approximations state that the value of a certain property can be modeled knowing the value of that same property for the fully solid material (Psolid), the relative density ($\rho_{relative}$) of the cellular material and two experimental parameters (C and n) that are typically obtained from experimental data. The relationship is as follows [1]:

$$P_{cellular\ material} = C \cdot P_{solid} \cdot \left(\frac{\rho_{cellular\ material}}{\rho_{solid}}\right)^{n} \qquad Eq.\ 2.3$$

C is a parameter with a value usually near 1 and *n* is an exponent that commonly varies between 1 and 2. Therefore, values of n equal or near 1 mean that the loss of properties compared to the solid is the less strong possible. On the contrary, values of n near or higher than 2 are found in the worst of the cases, when the loss of properties is strong compared to the solid.

Defining a Relative Property as the quotient of a property measured on the cellular polymer to the same property measured on the solid ($P_{cellular\ material}$ / P_{solid}) and considering C=1, equation 1.2 can be expressed as:

$$P_{relative} = (\rho_{relative})^n \qquad Eq.\ 2.4$$

Usually the relative properties of cellular materials are plotted versus the relative density and modeled according to equation 2.3 (figure 2.3). Doing this a value of n can be calculated which gives an idea of the quality of a material in comparison to others or in comparison to the expected results. So has been already mentioned commonly the values of n are between 1 and 2. Values below 1 are not found in most of the cases but, on the contrary, some properties (e.g. strain at break) in certain situations (e.g. heavily filled polymers) present values higher than 2, even near 4.

Achieving values near 1 for the key mechanical properties (stiffness and strength) is not an easy task, especially for medium or lower densities. Since the 1980's several works postulate that the consecution of cells with sizes below 10 µm gives as result behaviors with n very near to 1 [12, 53]. An intense research has been carried out on this hypothesis and controversial results have been obtained [16]. Apparently this fact is true for relative densities higher than 0.6 or for properties as impact resistance or fatigue. In lower ranges of relative densities or for other properties (stiffness and strength) some works state that achieving an homogeneous and closed cell structure are the key features to obtain behaviors with n=1 [57, 79]. The cell size in those cases does not play the critical role.
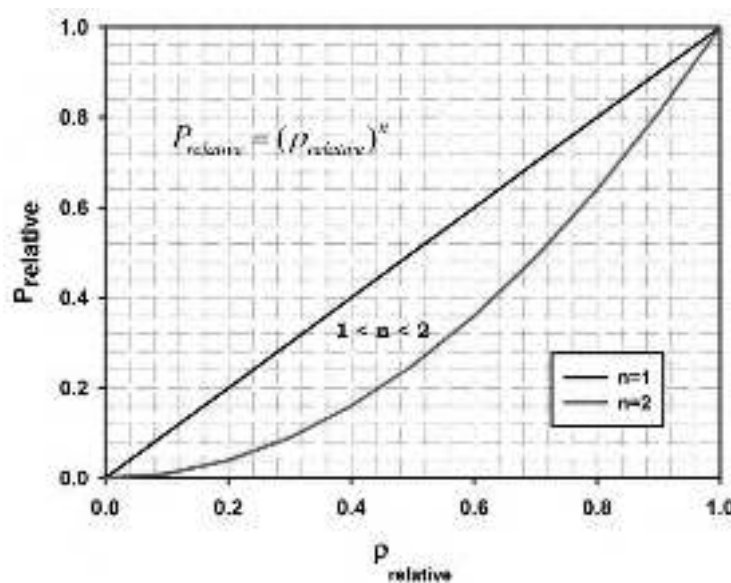

Figure 2.3: Relative properties-relative density relationship for a cellular material

From equation 2.3 it can be easily inferred that the properties of the foam are the result of two different influences: the properties of the solid polymer P_{solid} and the exponent *n* that it is determined by the different features of the cellular structure. It is the aim of this chapter defining and clarifying some concepts related to the cellular structure and the polymer properties. The two following sections deal with these topics

2.1.2.- Cellular Structure

Special attention has been paid all along the thesis to the microstructure of the different foamed materials in terms of their cellular structure morphology. This attention is not gratuitous since several times the macrocopic behavior obtained would not be explainable without first studying and considering the cellular morphology. Moreover, in some occasions during the thesis the cells were externally "forced" to have a certain morphology in order to get desired characteristics and performance. The formulation, production route and production parameters determine the cellular structure and later the cellular structure determines the performance of the foamed materials so properly characterizing and linking these two dependencies is of major importance. In the following paragraphs the typical characteristics of a cellular structure are defined and introduced:

   Mean cell size (ϕ)

Gives a numerical value of the mean diameter of the cells forming the celular structure. The more extended method of determination for this parameter is the *"Method of intersections"* presented in the standard ASTM D3576 [4]. During this thesis work a "home-made" method, based on image processing software using ImageJ, has been used [5]. The wellness of this image processing software has been tested and compared with other determinations finding a high accuracy [5].

Thermal properties of the foam are very influenced by the mean cell size when dealing with low relative densities (lower than 0.15). In this situation the reduction in cell sizes is translated into a reduction in the radiation term that contributes to a decrease of the total thermal conductivity. For higher densities this dependency is not so remarkable [6-9].

As already mentioned the influence of the cell size on the mechanical properties of a foam has generated important controversy in the last decades. Up to date the literature indicates that for relative densities higher than 0.6 or for properties as impact

resistance or fatigue reducing the mean cell size is beneficial. But for densities below 0.6 parameters as cell openness, cell anisotropy and cellular homogeneity gain much more importance than mean cell size in properties such as stiffness and strength [10-12].

⊛ Cell size distribution

It measures the variations in cell size that can be found in a given material. Figure 2.4 shows the cell size distribution of two typical materials.

The influence of the cellular homogeneity on the physical properties of a cellular material is an analyzed topic. In general, it has been found that non-uniform distribution of the cell sizes has in general a detrimental effect on the properties of the material [2,3,13,14]. In this case the solid mass is not homogenously distributed which favors the appearance of cracks in the weaker areas [1].
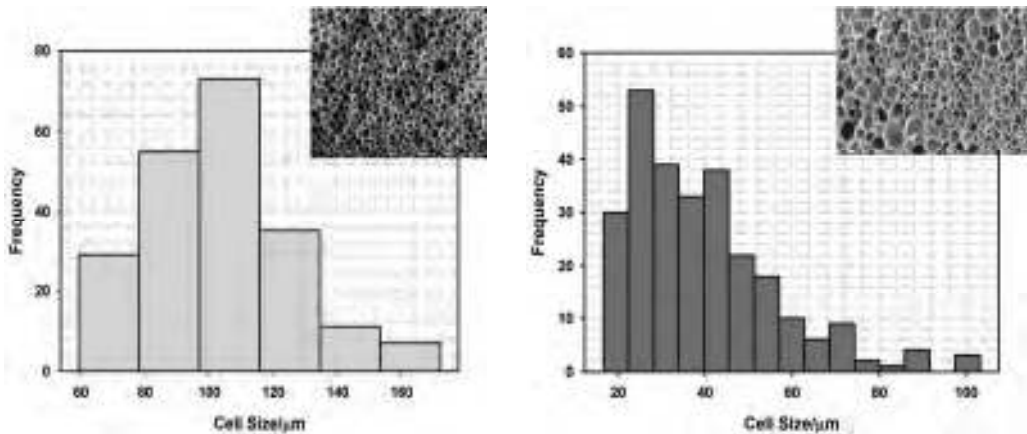
Figure 2.4: Homogeneous (left) and more inhomogeneous cellular structures (right) with their corresponding cell size histograms

The standard deviation (SD) of the cell size distribution is the numerical parameter that should be taken into account when comparing different structures [15,16].

Eq. 2.5

$$SD = \sqrt{\sum_{i=1}^{n} \frac{(\phi_i - \phi)^2}{n}}$$

where n is the total number of cells, ϕ_i is the diameter of each cell , and ϕ is mean cell size. The smaller is the value of SD, the more homogeneous is the cellular structure.

⬤ Open cell content

The open cell content of a foam is in several cases connected with how the mass is distributed between cell walls and edges. When the majority of the mass is placed in the edges, the open cell content is high and, on the contrary, when the mass is preferentially placed on the cell walls the cellular structure tends to be closed cell (low open cell content). Between the completely open and closed cell cellular structures there is a continuous of open cell contents that must be considered. The exact amount of open cell content can be determined using the formula [14]

$$OCC = \frac{Volume\ of\ interconnected\ cells}{Total\ Gas\ Volume}$$

Experimentally, in the frame of the thesis, this parameter has been obtained using a gas pycnometer according to ASTM D6226-10 standard [17].

Since the open cell content is directly connected with the way that mass is distributed in the cells, mechanical properties for example show a strong dependency with it [1,13,14]. The ability of a foam for withstanding a certain applied force is different depending on this mass distribution. In addition the propagation of a sound wave across a foam is completely different depending if the cellular structure is open or closed cell. Open cell foams are optimal for applications in which a good acoustic absorption is aimed. Outgasing or filtration purposes are also benefitted from high open cell contents and the opposite happens for the thermal conductivity. All these aspects gives an idea of the major importance of this feature.

Special attention has been paid to the open cell content in chapter 6 and interesting relationships between rheology of the base polymer-open cell content andmechanical properties have been established.

⬤ Anisotropy Ratio (R)

It is defined as the ratio between the diameter of the cell measured in its maximum elongation direction and the diameter in a perpendicular plane to this direction [1]. According to this definition isotropic cells have a anisotropy ratio equal to 1.Some of the foams produced in chapter 3 presented anisotropy ratio near 3 Figure 2.5 shows examples of an isotropic and an anisotropic cellular structure.

When anisotropy ratios larger than 1 are desired, they can be achieved during the production process. For example constraining the growing of the foam in a preferential direction yields cells oriented in that direction and therefore significant anisotropy

ratios. If the polymer has some preferential molecular orientation (due to the extrusion for example) it may induce also a preferential growing of the cells.

Anisotropy in the cellular structure gives as result anisotropy in the properties of the foam [3]. Large differences can be found between properties measured in the maximum elongation direction and in a perpendicular one. For example the Young Modulus in compression shows a strong dependency wit R. Defining $E_{\parallel}$ as the Young Modulus measured in the direction of higher cell size and $E_{\perp}$ as the modulus in the perpendicular one, the relation between them is given by the equation [18]:

$$\frac{E_{\parallel}}{E_{\perp}} = \frac{2R^2}{1 + \left(\frac{1}{R^3}\right)} \qquad Eq.\ 2.6$$

For an anisotropy ratio of 3, the parallel Young Modulus is almost 18 times higher than the perpendicular one. On the other hand, thermal conductivity is also higher in the direction in which the cells are elongated, reducing therefore the behavior of the material as thermal insulator in this direction [19,20].
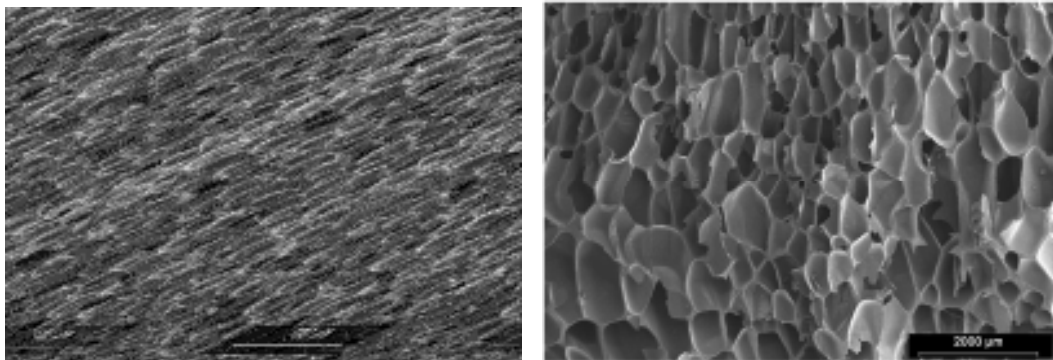
Figure 2.5: Examples of an isotropic cellular structure (R≈1) and ananisotropic cellular structure (R≈3)

2.1.3.- Polymer Matrix

Acting over the solid polymer matrix is the other route for improving the foam properties. This strategy includes also two non-exclusive procedures: modifying the molecular architecture of the polymer matrix or adding fillers in a certain percentage to modify the physical properties [2,3,13,14,21]. Both procedures have been used and combined during the thesis.

In the same way the modification of the polymer matrix and the modification of the cellular structure are not independent. In fact, some modifications of the polymer matrix are deliberately made to obtain certain changes on the cellular morphology.

Briefly, the modification of the polymer matrix can influence the foam properties from the following points of view:

⚫ Improving the foamability of the polymer matrix allows achieving low densities. Depending of the polymer, high expansion ratios require from tuned molecular structures. Otherwise the polymer is not able to retain the gas amount required and the foam collapses. A prior reological study of the polymer matrix really helps to later understand the foamability of the polymer and hence the properties of the foam.

⚫ Using a polymer with a different foamability allows reducing cell size, increasing cell density and improving cellular homogeneity. The modification of the polymer matrix can yield also anisotropy ratios higher than 1.

⚫ Modifying the polymer permits changing the amount of gas that can be dissolved in the polymer matrix and therefore the subsequent cellular structure and expansion ratio expectable. Crystallinity plays a fundamental role in this sense.

⚫ Tuning the physical properties of the foam. Mechanical, thermal, fire resistance and barrier properties to name some are highly dependent on the initial properties of the solid polymer matrix as stated in equation 2.4.

Several examples of all the previous points can be found in the following chapters. The main strategies of modification of the polymer matrix used in this work are briefly described in more detail in the following paragraphs. As already mentioned they can be divided into *modification of the molecular structure* and *use of fillers*.

2.1.3.1.- Modification of the molecular structure

The molecular modifications that will be presented now are aimed at improving the rheological behavior of the polymer for our foaming purposes. These changes in rheology influence the foamability and cellular morphology. But the tailored molecular

architecture not only influences rheology, it also has impact on the mechanical and thermal properties of the polymer. Crystallinity for example is strongly dependent on the molecular conformation of the polymer chains. And even the rate of crystallization is modified (which also influences the foamability of a polymer melt).

The attention is focused on polyolefins, specifically on polyethylene and polypropylene. Taking this into account, the two more extended strategies of molecular modification for these polymers have been studied: *polymer branching* and *polymer crosslinking.*

Polymer branching

During the foaming the polymer matrix is subjected to extensional forces similar to the ones that appear during a blow molding or film blowing process. These extensional forces are due to the gas pressure generated inside the polymer that acts as driving force of the cell growing [13,23].

When high expansion ratios are sought or when the polymer specifically presents a low melt strength the above mentioned extensional force can produce the breakage of the cell walls promoting coalescence and as a consequence larger cell sizes with inhomogeneous cellular structures. In some occasions the polymer is not even able to withstand the gas pressure so the gas escapes and the foam cannot reach the intended expansion ratios [13].

Polypropylene is a significant case of polymer with low melt strength what highly hinders its foamability. Independently of the foaming route chosen (with the exception of bead foaming technology), achieving expansion ratios higher than 2 (densities below 450 kg/m^3) is a difficult task with any common grade of PP. Branching is the common approach when the polymer is intended for foaming purposes. Branched polymers show an improved foaming behavior. In the case of polypropylene there is a need of inducing this branched molecular structure using specific technical methods. For instance the polymer undergoes electron irradiation in an atmosphere poor in oxygen [2,3]. Reactive extrusion is another novel route that can be followed using organic peroxides (peroxydicarbonates) that, after just one extrusion step, yields a highly branched polypropylene without chain scission or degradation [2,3]. In this case, the extrusion process must be done under nitrogen atmosphere. These branched PP's are denoted as "high melt strength" (HMS) indicating their suitability for production process that require from this special rheological behavior.

The rheological extensional behavior of branched polymers is very particular and it is mainly characterized by the presence of "strain hardening". Strain hardening can be defined as a rapid increment in the extensional viscosity of the polymer at high strains [13,14]. This fact is depicted in figure 2.6. The more disordered molecular structure of a branched polymer requires from higher energies imparted to reach high strains. This physical phenomenon is translated into the aforementioned increment in extensional viscosity. In a linear polymer, on the contrary, the molecular chains can slide between each other and therefore the extensional viscosity presents no increment at high strains [24].
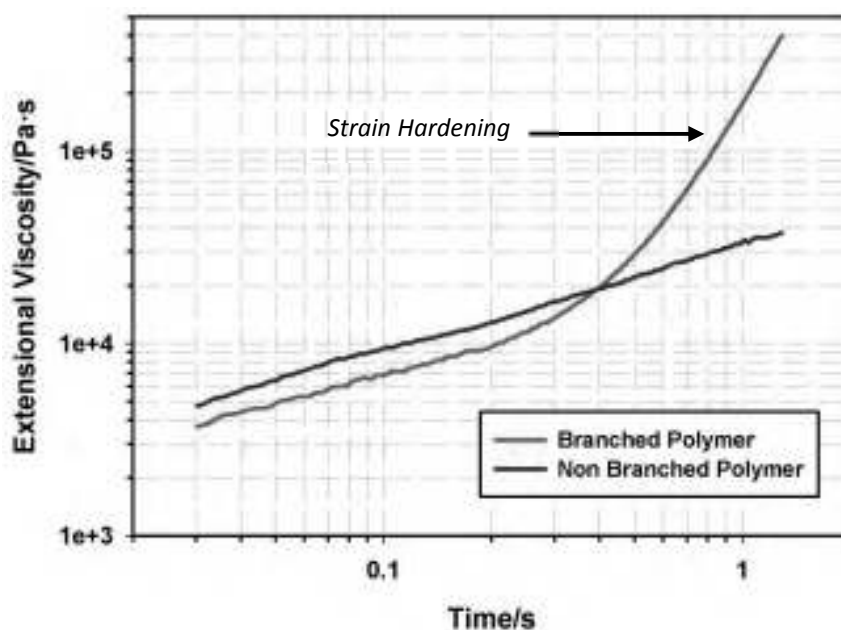
Figure 2.6: Extensional viscosity of two different polypropylenes. The blue line corresponds to a common linear PP, without any branching induced. The red one is for a high melt strength PP, with an induced branched architecture. The appearance of the strain hardening phenomenon is fundamental in the foamability of these polymers.

Low density polyethylene (LDPE) is a polymer that, without any modification, presents a branched molecular structure and therefore strain hardening [21]. Its counterpart, high density polyethylene (HDPE) shows a more ordered linear molecular structure and therefore no strain hardening.

The use of high melt strength polypropylenes is highly extended nowadays and several commercial grades of these materials can be found. Lyonellbasell commercialized an electron beam irradiated polypropylene but this grade cannot be found anymore. Borealis offers the Daploy family of HMS polypropylenes, branched using organic peroxides and unsaturated monomers. AkzoNobel has patented a

reactive extrusion additive based on peroxydicarbonates that can be used for producing "home-made" branched grades under some restrictive conditions. These PP, by itself or blended with certain amounts of linear grades, have been used for producing low density foams with improved cellular structures, reducing the coalescence and the open cell content. They are used both at a lab and industrial scale. The materials are recyclable but their main disadvantage is the price that can double the price of a non-branched counterpart due to the production process and the costs of the used additives [25, 26-30].

Polymer Crosslinking

Crosslinking is a common procedure used when the raw polymer is not able to withstand the biaxial extensional forces that take place during a foaming process [30]. Normally, in foaming processes in which the expansion of the polymer takes place at a high temperature there is usually a need of crosslinking the polymer in order to stabilize the cells during the growing of the foam, specially when low densities are sought [2].

As already mentioned some polymers present a molecular structure with a high ratio of branching. This is the case of low density polyethylene (LDPE). Even this highly branched molecular structure is not enough when the aimed expansion ratio is high and the foaming temperature is also high.

From a rheological point of view it is clarifying studying the effect of crosslinking over the extensional properties of the polymer melt (Figure 2.7)
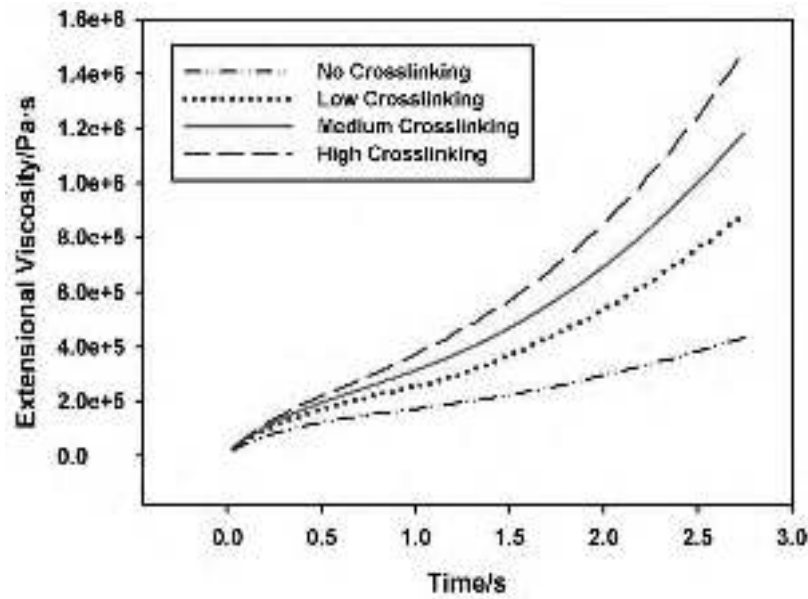
Figure 2.7: Rheological behavior, in terms of extensional viscosity, of a low density polyethylene (LDPE) grade with three different crosslinking degrees. For the sake of comparison the behavior of the raw polymer is also induced.

This figure shows an example of the dependency of extensional viscosity with three different crosslinking degrees in a LDPE matrix (own data). In the crosslinked materials the extensional viscosity is increased with increasing strains (higher times). It is the aforementioned strain hardening effect. This behavior, almost absent in the raw polymer, shows a straight dependency with the crosslinking degree. The increment in extensional viscosity is fundamental for achieving low densities since in these situations the polymer melt suffers strong sagging forces and high strains. The dimensional stability of the foamed part is also improved, benefitting any subsequent thermoforming process [2,3,8,31].

At a molecular level crosslinking a polymer implies the formation of three-dimensional networks (C-C- bond between molecular chains) which at the end are the responsible of the change of properties of the polymer [22]. This three-dimensional structure is graphically depicted in figure 2.8
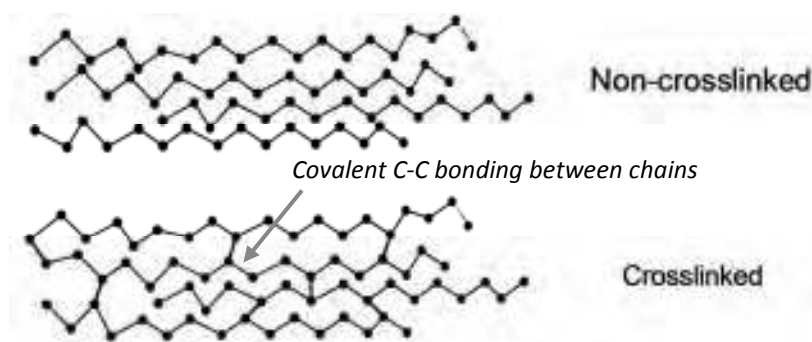
Figure 2.8: Schematic of the molecular architecture in a non-crosslinked polymer and a crosslinked one.

The consecution of this three-dimensional network can be accomplished by two different procedures, physical crosslinking and chemical crosslinking, both of them based on the formation of free radicals in the polyolefin molecule that later on are recombined giving place to covalent bonding between molecular chains [2,22].

1.　　　Physical Crosslinking: the polymer is irradiated with a high energy radiation (β-rays, γ-rays, X-rays or neutrons) in order to produce free radicals. This process involves a complex instrumentation for the irradiation which complicates its applicability. On the other hand, out of the two, is the "cleaner" one since no by-product is left after crosslinking [2,3].

2.　　　Chemical Crosslinking: is the most common one due to its technical simplicity. Two main choices are available in this context: the addition of peroxides or the functionalization of the polyolefins using silanes. Peroxides are chosen according to the melting temperature of the polymer and the decomposition temperature of the blowing agent that will be used for foaming. Dicumyl peroxide is the more extensively used for the crosslinking of LDPE or PVC. Figure 2.9 shows the crosslinking process that typically follows a polyolefin. On the contrary, dicumyl peroxide is not suitable for polypropylene.. In the case of silanes the polyolefin molecule is functionalized with a polifunctional organosilane. The functionalized polymer can be processed like any other thermoplastic and it is only crosslinked in a secondary process by water addition. The process using silanes is suitable both for polyethylene and polypropylene [2,3,22].
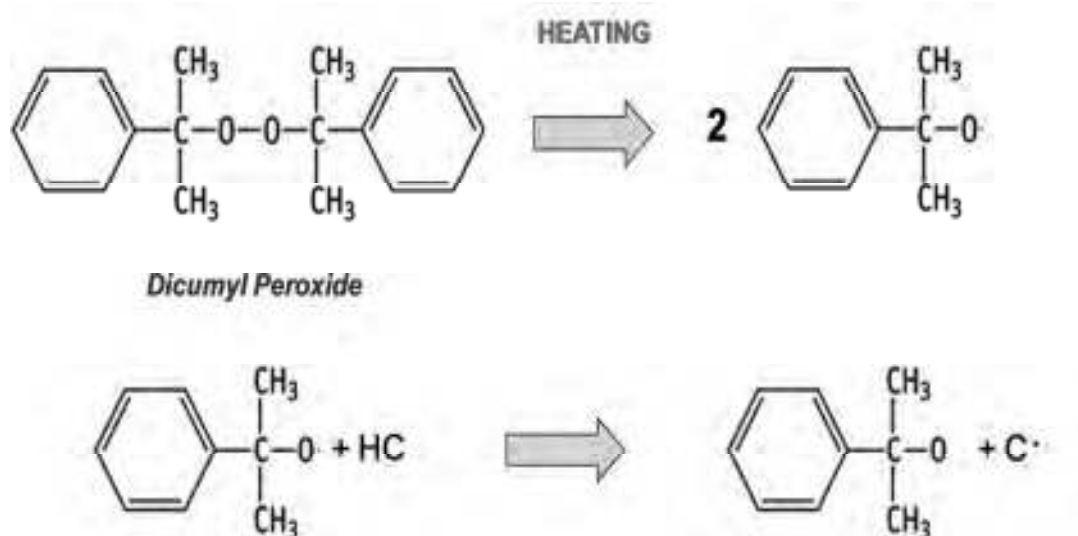
Figure 2.9: How dicumyl peroxide (DCP) acts chemically producing the crosslinking of the polymer matrix.

There is always an optimum crosslinking degree. A too high crosslinking degree can prevent from achieving the expansion ratios needed. On the other hand, a too low crosslinking degree cannot be enough to withstand the foaming process. In the physical crosslinking route the crosslinking degree is controlled by the dose used and in the chemical crosslinking it is controlled by means of the addition of the amount of chemical compound used, temperature and time.

In the market we can find a large number of crosslinked foamed parts. In comparison to branching, crosslinking broadens the window of densities achievable but it stands also an important disadvantage: crosslinked polymers cannot be recycled by conventional procedures (extrusion or injection). This makes these products environmentally harmful.

2.1.3.2.- Use of fillers

The use of fillers as additives in polymers can have very different purposes. The simplest one is reducing the price of the polymer part. Fillers as talc or calcium carbonate are much cheaper than any polymer. But usually they have also a functional purpose. When polymers are used in applications demanding high fire resistance performance, high contents of inorganic fillers are used. Examples can be found in LDPE or EVA filled with aluminum or mgensium hydroxide (40 wt.%, 50 wt.%, 60 wt.%

or even more) to produce halogen-free compounds [34]. They are used as core in sandwich panels in structural applications or as cable jackets.

Large additions of these fillers used together with their inorganic character typically add severe difficulties to the foamability of the polymer blend. These difficulties are sometimes arduous to be overcome and the production of halogen-free flame retardant foamed materials is, even nowadays, one of the handicaps of this research area.

Polymer mechanical properties is another typical field in which fillers play a fundamental role. Traditionally glass or carbon fibers have been used yielding high performance polymer matrices. These fibers show stiffness and strength that can be as high as 20 to 150 times the ones of the raw polymer. When aligned in the desired direction, they impart outstanding properties to the polymer matrix [22].

During the last three decades a new family of inorganic fillers has shown up. The polymer industry has not been indifferent to the big expectations placed on nanotechnology. According to this, big technical and economical efforts have been devoted to what is named *"Polymer Nanocomposites"*. Inorganic fillers have passed from the micro-scale to the nano-scale. Nanoclays, carbon nanotubes, carbon nanofibers, graphene nanoparticles, nanosilicas particles to name some are examples of what could be named as the "polymer fillers of the 21st century" [35,36].

An important part of this thesis deals with these nanofillers and due to this an specific section is needed to introduce them in more detail.

2.2.-POLYMER NANOCOMPOSITES

Traditionally polymers have been filled with micron-sized fillers aimed at improving mechanical behavior, gas barrier properties, flame retardant performance, etc. Sometimes these fillers have been even used with cost reduction purposes exclusively.

Polymer nanocomposites (PNCs) are emerging as a new class of industrially important materials. At loading levels of 2-3 vol.% could offer similar performance to conventional polymeric microcomposites with 30-50 wt% of reinforcing material. Note that high filler loading in the latter materials causes an undesirable increase of density and hence heavy parts, decreased melt flow index and productivity and increased

brittleness. Furthermore, the classical composites are opaque with often a poor surface finish. These problems are absent in PNCs [37-50]. They can be defined as materials that comprise a dispersion of nanometer-size particles in a polymer matrix. These particles have at least one of the dimensions in the nanoscale range. The matrix can be single or multicomponent, containing additional materials that add other functionalities to the system. The nanoparticles can be lamellar, fibrillar, tubular or spherical. The key feature of these nanoparticles is related to the high specific surface characteristic of these fillers. This high specific surface, together with the particle-matrix interactions, deeply determine the final reinforcing effect of the nanoparticles [35,36,43,48].

Far from acting over an isolated property the addition of nanoparticles to a polymer matrix plays a multifunctional role [38-41,44,48]. Figure 2.10 schematizes the different effects that nanoparticles could have over the solid matrix.
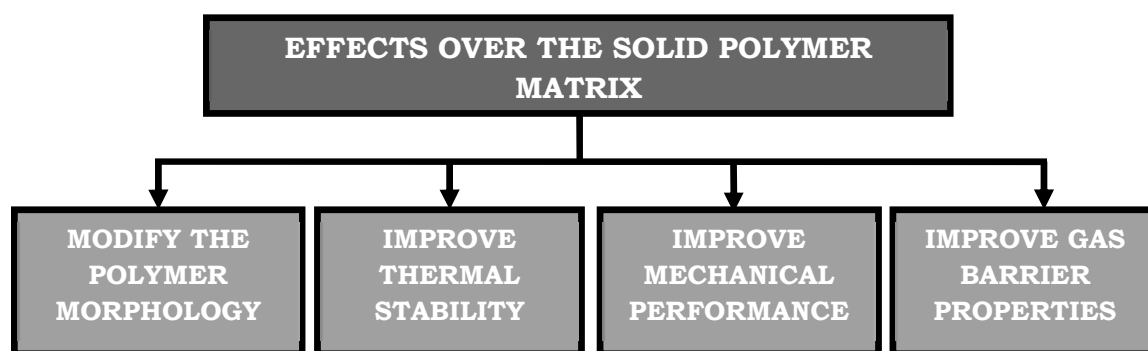
Figure 2.10: Main effects of nanoparticles in solid polymer.

    Modification of the polymer morphology: the high specific surface associated with the nanoparticles could enhance the heterogeneous nucleation during the crystallization therefore the final crystallinity degree in the filled polymer could be higher than in the unfilled one. This influences other properties, improving for example the mechanical properties.

    Improvements in thermal stability: several studies state that the presence of nanoparticles improves the thermal properties of the polymer increasing the thermal degradation temperature and therefore broadens the processing window [35,36]. The loss of properties at high temperatures could be weaker when the polymer matrix is filled with nanoparticles.

    Improvements in mechanical properties: this is one of the most extensively studied fields and also one of the most promising. The experimental determination of mechanical properties of isolated nanoparticles gives incredibly

high values. For example the compressive modulus in the axial direction of carbon nanotubes has a value as high as 1000 GPa. Since the stress is transferred from the polymer matrix to the filler, the high mechanical properties of the latter could be directly translated into high improvements in the nanocomposites, although effects in the interfaces also play key role and the results are not always positive [35,36,41,42].

    Improvements in gas barrier properties: the inclusion of nanoparticles in the polymer matrix hinders the diffusion of gas molecules across the polymer matrix. This strongly depends also on the geometry of the nanoparticles and the interfaces. The lamellar geometry of nanoclays is the most adequate one for these purposes. [35,36,38]

All these improvements are conditional upon a good dispersion and compatibilization of the nanoparticles. A bad dispersion or compatibilization can even deteriorate the properties of the unfilled matrix. The dispersion and compatibilization degree also depend on the polymer matrix and the kind of nanoparticles selected and it is a very complex topic [42,49].

In the frame of this thesis special attention has been paid to the modification of the polymer morphology (chapter 4), improvements in the mechanical performance (chapters 4 and 6) and improvements in the gas barrier properties (chapter 4).

2.2.1.- Polymer/layered silicate nanocomposites

An important part of the work presented in this thesis deals with polymer-layered silicate nanocomposites, their foaming and the performance of the corresponding foams. During the rest of the chapters (chapter 4,5 and 6) a detailed description of the state of the art about the nanocomposites synthesis, properties, their used in cellular materials and the yielded properties and experimental techniques is presented. However there is a lack of general information in those chapters about the layered silicate nanocomposites structure and the typical organic modifications used. The aim of this section is covering that lack of general information that we consider important to well understand the rest of the thesis.

    Layered silicates structure

Layered silicates used in the synthesis of nanocomposites are natural or synthetic minerals consisting of very thin layers that are usually bound together with counter-

ions. Their basic building blocks are tetrahedral sheets in which silicon is surrounded by four oxygen atoms and octahedral sheets in which a metal like aluminum is surrounded by eight oxygen atoms. Therefore in 1:1 layered structures (e.g. kaolinite) a tetrahedral sheet is fused with an octahedral sheet whereby the oxygen atoms are shared [35].

On the other hand the crystal lattice of 2:1 layered silicates (or 2:1 phylosilicates) consists of two-dimensional layers where a central octahedral sheet of alumina is fused to two external silica tetrahedral by the tip, so that the oxygen ions of the octahedral sheet also belong to the tetrahedral sheets (figure 2.10). The layer thickness is around 1 nm and the lateral dimensions may vary from 300 Å to several microns and even larger depending on the particulate silicate, the source of the clay and the method of preparation. Therefore the aspect ratio of these layers (ratio length/thickness) is particularly high with values greater than 1000 [35].

exchangeable cations
nH$_2$O

Key:
○ oxygen   OH hydroxyl   ● aluminum, iron, magnesium

○ ● silicon, occasionally aluminum
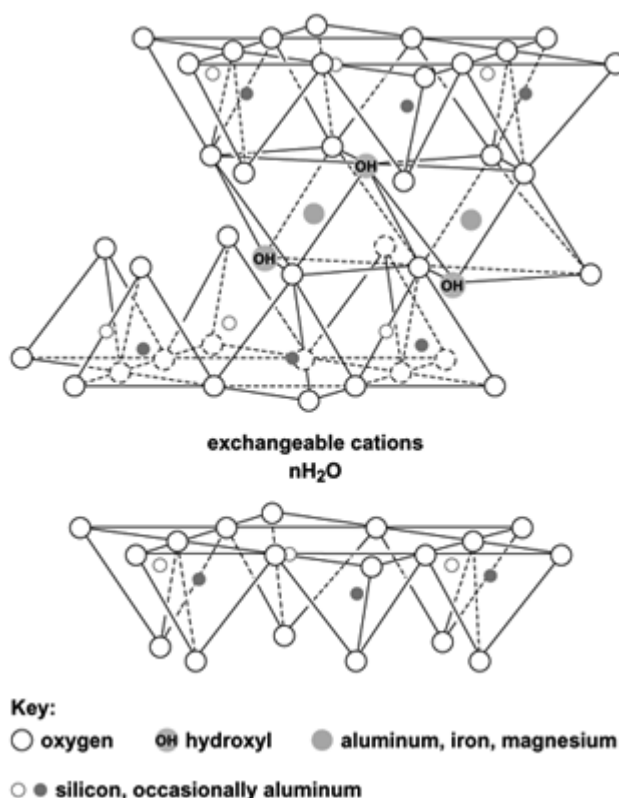
Figure 2.11: Schematic structure of montmorillonite. The functionalized polymer chains bond to the OH groups and delaminate the layered structure of the nanoclay.

The basic 2:1 structure with silicon in the tetrahedral sheets and aluminum in the octahedral sheet, without any substitution of atoms, is called pyrophyllite. Since

the layers do not expand in water pyrophyllite has only an external surface area and essentially no internal one. When silicon in the tetrahedral sheet is substituted by aluminum, the resulting structure is called mica. Due to this substitution the mineral is characterized by a negative surface charge, which is balanced by interlayer potassium cations. However, because the size of the potassium ions matches the hexagonal hole created by the Si/Al tetrahedral layer, it is able to fit very tightly between the layers. Consequently the interlayers collapse and the layers are held together by the electrostatics attraction between the negatively charged tetrahedral layer and the potassium cations. Therefore, micas do not swell in water and, like pyrophylite, have no internal surface area. On the other hand, if in the original pyrophylite structure the trivalent Al-cation in the octahedral layer is partially substituted by the divalent Mg-cation, the structure of montmorillonite is formed, which is the best-known member of a group of clay minerals called smectites. Montmorillonite, the most used nanoclay durint this thesis work, belongs to this group. In this case the overall negative charge is balanced by sodium and calcium ions, which exist hydrated in the interlayer. A particular feature of the resulting structure is that, since these ions do not fit in the tetrahedral layer, as in mica, and the layers are held together by relatively weak forces, water and other polar molecules enter between the unit layers, causing the lattice to expand. This ease for the expansion is the reason why this kind of silicates are the more extended ones in polymer nanocomposites [49].

Along with montmorillonite, hectorite and saponite are oher layered silicates used in nanocomposite materials. Their chemical formula is given in table 2.1

Table 2.1: General formula of the most extended 2:1 phyllosilicates

2:1 Phyllosilicates	General formula
Montmorillonite	$M_x(Al_{4-x}Mg_x)Si_8O_{20}(OH)_4$
Hectorite	$M_x(Mg_{6-x}Li_x)Si_8O_{20}(OH)_4$
Saponite	$M_xMg_6(Si_{8-x}Al_x)O_{20}(OH)_4$

The reason why these materials have received a great deal of attention recently as reinforcing materials for polymers is their potentially high aspect ratio and unique intercalation/exfoliation characteristics [35,36]. In general it is well established that excellent mechanical properties are expected if the dimensions of the reinforcing elements reach molecular levels. Individual clay platelets, being only 1 nm thick, display a perfect crystalline structure. However, the smaller the reinforcing elements

are, the larger is their internal surface and hence their tendency to agglomerate rather than to disperse homogeneously in a matrix. In fact, the silicate layers have the tendency to organize themselves to form stacks with a regular Van der Waals gap between them, called interlayer. The interlayer dimension is determined by the crystal structure of the silicate [41,42]. Micro-aggregates are formed by lateral joining of several primary particles and aggregates are composed of several primary particles and micro-aggregates. Several approaches have been developed to increase the interlayer spacing rendering the nanoclays more adequate for their dispersion and exfoliation in a polymer matrix [35,36, 49,50]. The next section describes the approach followed in the frame of this thesis work that, on the other hand, is also the most extended one:

🌐 *Organic modification of layered silicates*

Since in their pristine state layered silicates are only miscible with hydrophilic polymers, such as poly(ethylene oxide) and poly(vinyl alcohol), in order to render them miscible with other polymers one must exchange the alkali counter- ions with a cationic surfactant. Alkylammonium ions are mostly used, although other onium salts can be used such as sulfonium or phosphonium. This can be readily achieved through ion-exchange reactions that render the clay organophilic. In order to obtain the exchange of the onium ions with the cations in the galleries, water swelling of the silicate is needed [35].

The organic cations lower the surface energy of the silicate and improve wetting with the polymer matrix. Moreover, the long organic chains of such surfactants, with positively charged ends, are tethered to the surface of the negatively charged silicate layers, resulting in an increase of the gallery spacing. It then becomes possible for organic species to diffuse between the layers and eventually separate them. Conclusively the surface modification increases the basal spacing of clays, reducing the van der Waals attraction forces between platelets and allowing for the diffusion of polymer chains which eventually would separate the platelets [35,41-42].

Figure 2.12 depicts the three common aggregation states: inmiscibility, intercalation and exfoliation of nanoclays in a polymer matrix. In the inmiscible state nanoclays appear as micro-sized aggregates of platelets. When intercalated still some of this aggregates can be observed but an important number of individual platelets appear in the micrograph. When completely exfoliated no more micron-size aggregates can be observed, only individual clay nanoparticles. These three delamination states are commonly characterized by x-ray diffraction and the typical diffraction patterns corresponding to each state are also shown in figure 2.12 [48,49].
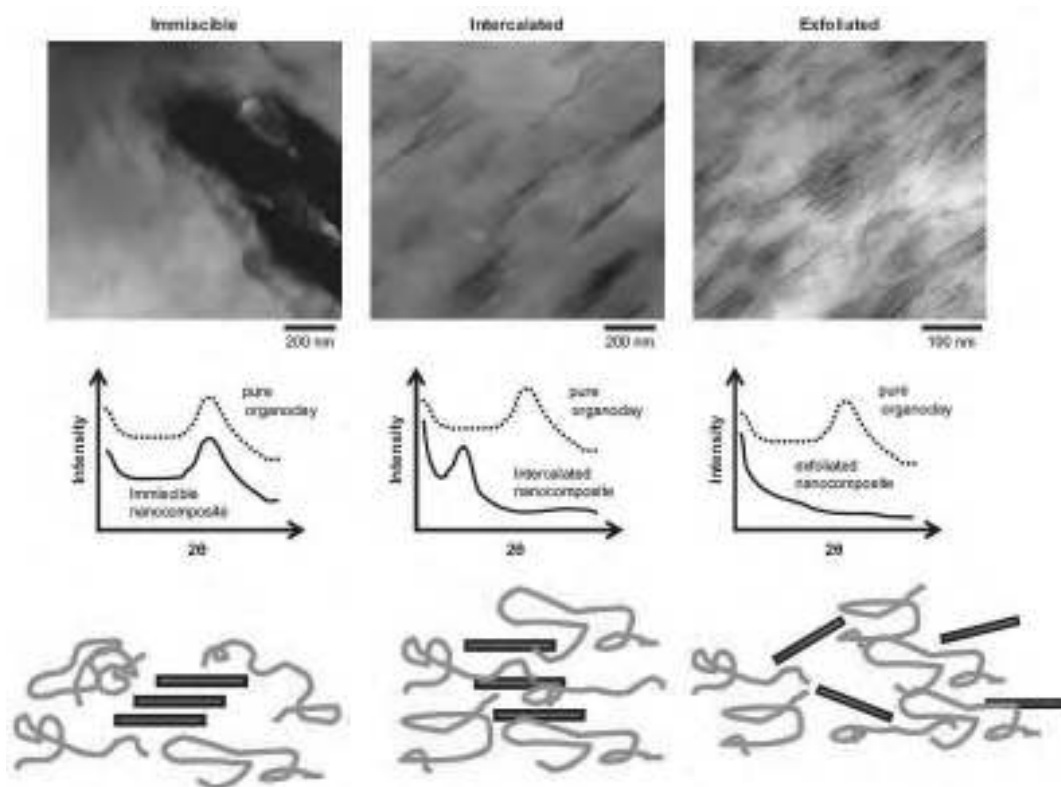
Figure 2.12: Schematic of the three different aggregation states of nanoclays observed by transmission electron microscopy (upper part of the figure) and x-rays diffraction pattern obtained in each case (medium part of the figure) and a graphical schema of the nanoclays platelets and polymer molecular chains (bottom part of the figure).

2.3.- CELLULAR NANOCOMPOSITES

The foaming technologies and processes used with conventional composites have been used in the last years for the production of foamed nanocomposites. The motivation is clear; the excellent properties expected for the solid nanocomposites should be directly transferred to their foamed versions [52,53]. But nanoparticles not only modify the properties of the solid matrix conforming the foam, they have also interesting effects during the foaming process and on the foam itself. Three of them has been chosen as the most remarkable ones: nucleant role over the cellular structure of the foam, modification of the extensional rheology which deeply influences the foaming and finally improvements in the gas barrier properties of the foam (see figure 2.13).
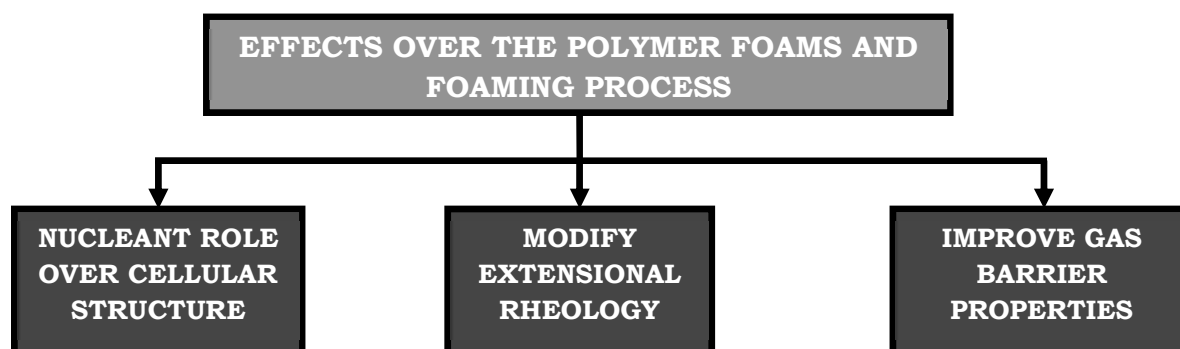
Figure 2.13: Effects of nanoparticles on the foaming process and foamed materials.

⚫ Nucleating role: typically the presence of inorganic particles reduces the energy needed for the formation of a new cell. Therefore cells nucleate preferentially in the interface polymer-filler, enhancing heterogeneous nucleation. The higher is the dispersion and de-agglomeration of the particles and the smaller size, the higher will be nucleation efficiency of the nanoparticles. This benefits the achievement of smaller cell sizes and larger cell densities [52, 54].

⚫ Modification of the extensional rheology: this effect, related with the foaming process, has a atrong influence on the cellular structure and morphology of the foam. During the growing of the cells the polymer undergoes a biaxial extension. This biaxial extension is directly connected with the extensional rheology of the polymer [52,53,55,56]. This has been explained in section 2.1.3.1. Nanoparticles could increase the extensional viscosity of the melt and modifies parameters as important as strain hardening as will be shown in chapter 6.

⚫ Improvements in gas barrier properties: the addition of nanoparticles is expected to reduce the effective gas diffusion coefficient of the gas outside the cells. On the one hand, this gives a better gas efficiency during foaming, reaching low densities. On the other hand foams with a slower ageing should be expected. For this reason nanocomposite foams are attractive materials for packaging or thermal insulation [42,62,63].

From a theoretical point of view the nucleating role together with the modifications in the extensional rheology couldgive as result reduced cell sizes, increased cell densities and more homogeneous cellular structures. The open cell content can be varied also by means of the nanoparticles addition. In any case, all these effects are again influenced by the degree of dispersion and compatibilization of the nanofillers. The better is the dispersion the more pronounced will be the effects over

the cellular structure and gas barrier properties. On the other hand, the extent of coupling polymer-nanoparticle also plays a crucial role. Stronger coupling means smaller interfaces polymer-particle which finally turns into lower nucleation efficiency [52]. But stronger interfaces are fundamental for achieving a good transfer of the stress between the polymer and the filler and therefore for achieving improved mechanical performance. Therefore, the balance between nucleation efficiency and good compatibilization is a critical topic not completely understood.

2.4.- BLOWING AGENTS AND PRODUCTION ROUTES

With time, polymer cellular materials gained more and more importance in the field of polymer materials. The number of practical applications rapidly grew up, more and more industries were dedicated to its production [1-3,65]. Parallel to this the scientific community focused the attention also on these materials, generating basic knowledge for its improvement and modification. Taking all this into account, two different approaches were followed, the study and development of different blowing agents and the use and characterization of various production routes.

An important number of the production routes used are based on the previous experience on production routes for solid polymer materials. This well-known production routes were somehow extended to polymer cellular materials: foaming by compression molding, foaming by injection molding foam, extrusion foaming, foaming during rotational molding. With slight modifications in some cases or more important ones in other,this classical routes were used to produce cellular materials. But the intense research and development on cellular materials gave also rise to new techniques exclusive for foams. A clear example is "reactive foaming", used in the production of polyurethane, the cellular material with the largest market nowadays. And there are some other as batch foaming, pressure quench method, improved compression molding or stages molding. Some of these techniques will be briefly described in the following paragraphs.

Together with the production routes, blowing agents have been a great subject of interest and research. Blowing agents have been developed parallel to production routes, sometimes according to the demands of the later ones, sometimes independently. Depending the way in which the gas is generated, they can be divided into *chemical* of *physical*. As will be seen, the cellular structure and foam properties are strongly dependent upon them so they are subject of major interest [1-3].

The foaming routes used in the research works presented in this thesis (two steps compression moulding, batch foaming, improved compression molding and stages molding) will be introduced in detail in chapter 3. The rest of the foaming routes will be briefly described in the following paragraphs of this chapter. A description of blowing agents, divided into physical and chemical, together with their own characteristics and differences is also presented in this chapter.

2.4.1.- Blowing Agents

A blowing agent can be defined as a substance with the ability of growing a cellular structure in a material. They play a crucial role both in the production process and in the final properties of the polymer foam since the cellular structure or the density or some physical properties such as the thermal conductivity are parameters strongly influenced by them. The selection of the most appropriate blowing agent and the addition of the right amount has an important influence on the performance of the foam and practical applications [2,3].

Blowing agents can be divided into two types, chemical and physical, depending on the mechanism of gas release

2.4.1.1.- Chemical Blowing Agents (CBA)

As a distinctive feature, CBAs release gas as result of a chemical reaction. During the decomposition they release several gases in different amounts. These gases act as driving force for the growing of the foam. Together with the gases a certain amount of solid residues remain after the decomposition [2,3].

Chemical blowing agents show two main advantages. On the one hand they are easily added to the materials that will be later foamed and on the other hand they can be easily processed using conventional equipments.

They can be divided according to the exothermic or endothermic character of the chemical reaction that takes place:

- Endothermic: these blowing agents act as heat sinks and therefore they are used when there exists a need of releasing heat from the polymer. The more common example is sodium bicarbonate that releases CO_2 and water vapor when decomposed. The decomposition window of these materials is very broad (100 ºC to 140 ºC for bicarbonate) and that makes

difficult defining a processing temperature profile. Besides this, the amount of gas released by endothermic blowing agents is much lower (approximately a half) than the one released by exothermic blowing agents. To reach the same expansion ratio higher amounts of endothermic blowing agents than exothermic must be added [2,3,20]. Most of them release water as a byproduct during the decomposition and this hinders their use in water-sensitive polymers as polylactic acid (PLA) or polyethyleneterephtalate (PET). One of the main advantages of typical endothermic CBAs is their health-friendly character, they can be used in foamed parts intended for being in contact with food [13].

⚙   Exothermic: exothermic blowing agents release heat during their decomposition. Besides, the reaction is autocatalytic so the decomposition happens very quickly and in a very narrow temperature range. The more extended exothermic CBA is azodicarbonamide (ADC) [2,6]. It decomposes between 200 °C and 220 °C releasing between 240 and 270 cm^3/g of N_2 (65%) and lower quantities of CO, CO_2 and NH_3 [2, 13, 32]. This material has been used in several of the works presented in chapters 4,5 and 6.

2.4.1.2.- Physical Blowing Agents (PBA)

Physical blowing agents are first dissolved into the polymer. After that a thermodynamic instability is induced in the system polymer+PBA. This thermodynamic instability drastically reduces the solubility of the PBA in the polymer which is finally translated into the nucleation and growing of a cellular structure. Commonly, these PBAs are liquids with a low boiling point or gases. The more common ones are hydrocarbons, halogenated hydrocarbons or inert gases as CO_2 or N_2 [3].

The solubility in the polymer is one of the major features that must be taken into account when choosing a PBA. Other criteria are the environmental impact and the processability. For example CFCs were extensively used for foaming polyurethane or polystyrene due to their high solubility and low thermal conductivity but they were banned due to their detrimental effect on the depletion of the ozone layer. Nowadays butane, pentane or hexane are used in substitution in spite of their dangerous high combustibility [3].

Inert gases as CO_2 or N_2 show several advantages in comparison to the others. They are cheap, abundant and environmentally friendly [2]. Their critical pressure and temperature are also low which makes them very attractive for foaming. When above the critical point the fluid is in the so-called supercritical state. In these conditions the density of the fluid is similar to the fluid state but its ability to flow is much higher. In these conditions the solubility in the polymer is strongly enhanced [66].

CO_2 is the most extensively used PBA in polymer foams. The lower solubility of N_2 makes it less common in the production of foams since higher work pressures should be used in this case [2,66]. CO_2 has been used in some of the works presented in chapter 4.

2.4.2.- Foaming Processes

The development and evolution of the production processes of cellular polymer materials have run parallel to the processes traditionally used for solid polymers. The introduction of a gaseous phase in the system adds complexity to the well developed processes for solids.

The aim of any production process is the consecution of a polymer/gas dissolution the more homogeneous as possible. In this sense three main parameters appears as fundamental in any production route: pressure, temperature and time. These parameters must be conveniently tailored in each process and together with the characteristic of the polymer formulations used will finally determine the morphology and properties of the foam [2,3].

In this chapter we will focus our attention on four of the most extensively used routes for polyolefins: extrusion foaming, injection molding foaming, compression molding foaming and pressure quench method. None of them have been used for the production of the specimens in this thesis. Next chapter will pay attention to the foaming procedures used in the frame of this work: two-steps compression molding, improved compression moulding (variation of the compression moulding), stages moulding (completely new method) and batch gas dissolution.

2.4.2.1.- Extrusion Foaming

The extruders and set-up commonly used for processing solid polymers can be either directly used or modified for foaming. The introduction of a gaseous phase requires a more precise control of parameters as temperature or melt pressure. The blowing agent used can be either chemical or physical although the use of a physical blowing agent requires of special equipment [13,21].

Extrusion foaming comprises different steps:

1.　　　Plasticization of the polymer: the polymer formulation is added to the hopper and melted in the first stages of the extruder machine. The polymer formulation can already contain additives or additives can be added independently. If the foaming is going to be performed using a chemical blowing agent, this material is added also in this step together with the polymer.

2.　　　Dissolution and dispersion of the blowing agent: the shearing forces developed inside the extruder produce the dissolution of the blowing agent in the polymer. The more homogeneous is the dispersion and dissolution of the blowing agent, the better will be the foaming behavior, therefore twin screw extruder are preferred over single screw extruders. The pressure developed by the shearing in this step must be high enough to assure the proper dissolution of the gas in the polymer. In the case of using physical blowing agents they must be added also in this step.

3.　　　Mixing, transport: the polymer/gas system is shear mixed and transported along the extruder during a certain time. As already mentioned this time must be adequate to assure a good homogenization of the polymer/gas system. Temperature profile is also an important parameter that must be adjusted. Temperature must be, of course, high enough to melt and (in the case of CBAs) decompose the blowing agent. But at the time of foaming if the viscosity of the polymer melt is too high or too low (due to the melt temperature) we can obtain an undesired foaming behavior. Besides this, it must be taken into account that the presence of a gas dissolved in the polymer melt has a plasticizing effect, decreasing the glass transition temperature and viscosity of the system. In certain systems the solubility of the gas in the polymer decreases as the temperature increases. Altogether, implies that sometimes the temperature profile is decreased in the last stages of the extruder machine in order to properly adequate the rheological properties of the polymer/gas system for foaming.

4.　　　Pressure drop in the die: when the polymer/gas system flows through the die the pressure drop induces a thermodynamic instability which nucleates and allows cells to nucleate and grow. The gas is no longer dissolved into the polymer. In certain occasions the die has determinate geometries (for the production of a foamed sheet for example). The higher is the pressure drop

and pressure drop rate in this step, the higher will be the cell density obtained and the smaller the cell in the foamed part.

5.   Cooling and stabilization: the cellular structure obtained must be cooled and stabilized. Low cooling rates enhance cells growing and in the worst of the situations the appearance of cell coalescence or coarsening phenomenon. The cooling can be performed by any means, either by immersing the foamed part in water or blowing it with air.

By extrusion foaming either high or low density parts can be produced. For the production of high density parts the selection of the polymer matrix is not so critical and can be performed using linear polymers with adequate melt flow indexes (extrusion grades). Chemical blowing agents are typically used in this case. On the other hand, the production of low density foams by extrusion requires the use of branched polymers and physical blowing agents. Physical blowing agents are used also for the production of high density extruded parts achieving microcellular structures. The Mucell process, patented by Trexel in the 90s is an example of this. Although Mucell is more broadly used for injection foaming, the extrusion version is also found in high density microcellular parts with acceptable surface qualities and with density reductions near 20% [2,33].

Figure 2.14: Examples of foamed parts produced by extrusion foaming

The achievement of microcellular structures in low density parts is more challenging. Park and co-authors, using branched polymers and physical blowing agents with low molecular sizes, have obtained microcellular foams in a wide density range [55,67-72]. Together with the stringent conditions in terms of polymer matrix and blowing agent, high pressure drop rates must be achieved also in the die. This need of

high pressure drop rate strongly limits the diameter of the strand produced (<0.5 mm) and therefore the consecution of parts with a bigger size.

The extrusion foaming procedure presents several advantages and disadvantages. As main advantages we can mention:

⚙   Continuous process: the continuous intrinsic character of extrusion foaming strongly enhances the productivity, rising it as specially suitable for long series. Every kind of polyolefin can be processed following this route.

⚙   Extrusion of solids: the expertise and state of the art gathered by the solid polymers extrusion industry can be more or less directly applied to extrusion foaming. Extruders used for solids can be many times used also for extrusion foaming without changing the screws configuration, etc. and this stands an important benefit for a lot of companies. This is true when foams with high densities are produced. For low density foams special equipments are required.

⚙   Broad density range: as already mentioned the density range achievable is very broad. A prior proper tailoring of the formulation (in terms of polymer and blowing agent), extruder configuration and production parameters must be performed.

Together with these advantages some disadvantages are also present:

⚙   Parts geometry: only simple geometries can be produced. Sheets, profiles, pipes and strands are the more common geometries produced by extrusion. More complex geometries can be produced by thermoforming after extrusion but this adds an additional steps that makes the final product more expensive.

⚙   Extruder modification and set-up: this disadvantage rises when using physical blowing agents to produce low density foams. The conventional extruders must be deeply modified to accommodate a gas at high pressure that will be pumped inside. Extruders already designed for this high pressure gas pumping are expensive which is finally translated in higher market prices of the end-product.

⚙   Extrusion foaming and microcellular structures: when looking for cells in the microcellular range by extrusion several difficulties appear. Only high densities can be reached, if stringent conditions are not used. When looking for a combination of low densities and microcells, the pressure drops

and pressure drop rates at the die must be so high that it limits the size of the final parts produced.

2.4.2.2.- Foaming by injection molding

Injection molding, together with extrusion, is one of the most extended processing techniques for polymers. Therefore, in a natural way, it has been used also for foaming. The first injection system was invented in 1872 by John Hyatt but the really first modern injection machine was patented in 1928 by the German company Cellon Werkw [2]. All the mechanisms involved in these first machines were based on mechanical principles, with manual extraction and without security systems. The first electrical injection molding machines were patented in 1932 [2].

Minimum modifications must be done over a conventional injection molding machine in order to adapt it for foaming using the low pressure injection molding method (see below for a description of this method. Different variations of the conventional injection molding have appeared with time, all of them to solve some of the main disadvantages associated to this process. For example co-injection allows the use of different polymeric materials, one surrounding the other, but moulds and machinery are very expensive [2]. Another example, the Heat & Cool route, is aimed at the improvement of surface quality undergoing different thermal cycles . In the case of the GAIM (Gas Assisted Injection Molding) variant the molding is assisted by the pumping of gas pressure inside the mould, this helps to reduce the amount of material but due to the use of gas high precautions must be taken. MUCELL and Expandable Mould are typical routes in the consecution of structural foamed samples by injection. The already mentioned MUCELL process patented by Trexel in the 90s allows a good control of the cellular structure and implies also a reduction in the initial investments but the size and geometry of the parts are limited. With the use of expandable moulds good surface qualities are achieved but the complexness of the mould and machinery make the process more expensive than the low pressure method [72-74].

Four different steps are common in the low pressure injection molding method that is used to produce foamed parts:

> 1.   Melting and mixing: the polymer formulation is first melted in the barrel of the injection unit. This barrel can usually incorporate a single screw extruder that enhances the mixing of the polymer melt. The blowing agent can be either included in the polymer formulation (CBAs) or pumped in the barrel

(PBAs). The shearing forces developed by the screw allow for an homogeneous dissolution and distribution of the blowing agent. The more homogeneous is the distribution of the blowing agent in the melt, the better will be the foaming behavior.

2.   Mold injection: the mixture polymer/blowing agent is introduced in the mold. Molds can have complex shapes and must be designed in such a way that they can stand the high pressures used during injection. The complexity of these molds is usually very high and they are very expensive. Due to this, injection molding is especially suitable for long series.

3.   Expansion: when the polymer/gas mixture is injected in the mold it suffers a high pressure drop. This pressure drop saturates the polymer/gas mixture and the gas is no longer dissolved in the polymer. Cells nucleate and grow in the polymer melt and the growing of the cells also helps to completely fill the mold cavity. In some variations of injection molding, as for example when expandable molds are used, the polymer/gas mixture is subjected to pressures high enough to keep the gas dissolved in the polymer even after injection. Then the mold is expanded which generates the pressure drop needed for the nucleation and growing of the cells.

4.   Cooling and de-molding: the lower temperature of the mold cools down the polymer melt injected. Once the foamed part is solidified inside the mold cavity is ready for the de-molding. The mold is opened and usually the injection machine comprises some system to enable the expulsion of the foamed part. The mold is closed and the cycle begins.

Figure 2.15: Detail of a structural foams. Two outer solid skins can be observed surrounding a foamed core.

Structural foams, characterized by two solid outer skins (figure 2.15), have been traditionally produced by injection molding in any of its variations. Since the

temperature of the inner walls of the mold cavity is below the melt temperature, the polymer solidifies without foaming as soon as it enters in contact with them. These structural foams present a higher bending stiffness to weight ratio than conventional foams of the same density so they are a good alternative when light materials with improved mechanical properties are sought (figure 2.16). As will be mentioned in the next chapters, in the frame of this thesis a new production route that has nothing to do with injection molding has been developed for the production of structural foams (Stages Molding) (it is described in chapter 3). This new route solves some of the problems associated to injection molding, needs a lower initial investment and it is especially suitable for the production of short series [2,3,66,73-75].

Figure 2.16: Paddleboard and soles produced by injection molding foaming

As main advantages we can distinguish:

⬤ Parts geometry: the complexity of the parts produced can be very high. Together with this, the dimensional accuracy that can be achieved is also high so a wide range of the parts present in the market nowadays have been obtained by injection molding.

⬤ Productivity: a large number of parts can be produced in a certain time space. Parameters as injection pressure, injection speed, temperature or cooling rate are adjusted in order to obtain acceptable surface and shape qualities together with productivities as high as possible. The process is especially suitable for long series.

⬤ Injection of solids: injection molding has been intensively used in the production of solid plastics for years, therefore a large expertise has been gathered in this field. This expertise is more or less directly transferred to injection molding.

Some disadvantages must be also considered. Some of them have been solved in a higher or lower extent in the different variations of the conventional injection molding:

⚙   Density range: relative densities achievable by injection molding are always higher than 0.6. This limits the applicability of the technique for the production of parts when lower densities are required.

⚙   Surface quality and cellular structure: the cell size distribution of this parts is very inhomogeneous, presenting also density gradients in the interior. Besides this, the surface qualities achievable are not always as good as desired. Many of the mentioned variations try to solve this drawback with higher or lower success.

⚙   Set-up and investments: molds usually entail a high complexity and must be able to withstand the high pressures developed during the injection stage. This two facts increase the price of the molds needed. The initial investments are therefore high and sometimes the production of short series is not economically profitable.

2.4.2.3.- One-step Compression Molding

Compression molding, also used for processing solid plastics, has been extended to the production of foamed parts. In this section we will focus our attention in the one-step procedure. The two-steps counterpart will be described in the next chapter since it has been used for producing some of the materials of this thesis. Compression molding foaming, due to its intrinsic characteristics, only allows the use of chemical blowing agents [2].

One-step compression molding comprises four steps:

0.   Mixing and compounding: prior to the compression molding itself the polymer, blowing agent and the rest of the additives are conveniently mixed and compounded using an internal mixer or a twin screw extruder. The compounding temperature must be lower than the decomposition temperature of the CBA and lower also than the activation temperature of the crosslinking additives in the case that these are present.

1.   Temperature/pressure: the previous compound is placed inside a mould and undergoes a certain temperature-pressure program. If a crosslinking agent is present in the compound the temperature is selected above the activation temperature of the crosslinking agent and below the decomposition temperature of the chemical blowing agents. Once the polymer is conveniently

crosslinked the temperature is raised above the decomposition temperature of the blowing agent. The decomposition of the blowing agent is performed under pressure that is applied externally to the compound. The decomposition of the blowing agent generates a certain gas pressure in the polymer melt. The external pressure applied must be always higher than the maximum gas pressure developed in the polymer melt. This way the gas will be dissolved in the polymer. Temperature, pressure and time are the major parameters of this route and must be conveniently adjusted to assure a complete decomposition and good dissolution and dispersion of the blowing agent.

2.   Expansion: when the temperature/pressure stage has finished the external pressure is released, the gas saturates within the polymer and the cell nucleation and growing begins. The foam grows freely out of the mold and reaches a certain density. Typically from blocks or slabs are produced. After the sudden pressure release all the cells (theoretically) nucleate and begin growing at the same time. This prevents cell coarsening and gives as result more homogeneous cellular structures. Altogether enhances the achievement of lower densities with improved cellular structure morphologies.

3.   Cooling and de-molding: after foaming the part must be cooled down to stabilize the cellular structure. This can be done by any mean, immersing it in water, by air blowing, etc. Normally high cooling rates are sought in order to obtain the best properties of the foam. This is specially important if the polymer is not a crosslinked material. Releasing the foamed part from the mold is not easy if the polymer has not been previously crosslinked. That is one of the reasons why compression molding is usually combined with polymer crosslinking.

The density range that can be covered by compression molding is very wide although low densities usually require crosslinking the polymer matrix. The range of applications of compression molded foams is also very wide and goes from thermal insulators to cushioning and packaging purposes. Compression molded foams can be found in toys or shoe soles too [2,3,32].

Figure 2.17: Examples of parts produced by one-step compression molding.

As advantages of the process we can mention:

⚙   Simplicity of the process: both the process and the machinery needed are simple. The investments are low compared to other foaming techniques which makes it very attractive.

⚙   Wide density range covered: high, medium and low density foams can be produced by compression molding. Low density foams require for polymer crosslinking prior to foaming.

⚙   Compression molding of solids: machinery and set-up used for the production of solid parts by compression molding can be directly used for foaming without any modification. There is only a need for specific moulds.

Besides these advantages some disadvantages are also present:

⚙   Crosslinking: usually the production of foams by compression molding requires for crosslinking of the polymer matrix. Crosslinking allows reaching low densities and at the same time enables the releasing of the foamed part from the mold. Crosslinked foams cannot be processed again which prevents from any recycling of the foam by conventional means.

⚙   Density control: the density of the final foamed part can be varied by varying the blowing agent addition but cannot be mechanically controlled. The processing parameters (temperature, pressure and time) deeply influence the amount of blowing agent decomposed so a precise adjustment of the density of the foamed part is only possible after a fine tuning of the process.

⚙   Parts geometry: the process does not allow producing parts with complex geometries. As well as in extrusion complex geometry parts can only be produced adding a subsequent thermoforming stage which reduces the productivity and increases the price of the final foam.

2.4.2.4.- Pressure Quench Method

The pressure quench method can be considered as an alternative to the batch gas dissolution method that will be described in the next chapter. On the contrary to the batch gas dissolution method that is industrially used by Zotefoams or Microgreen, the pressure quench method has not been industrialized due to some of the disadvantages that will be mentioned later. In the case of polyolefins the process comprises the following steps [2,3,77,78].

0.   Compounding and molding: the polymer is compounded with the rest of the additives using a twin screw extruder or an internal mixer. Only physical blowing agents are used in the pressure quench method so no blowing agent is added to the polymer during this step. The compound is later compression molded or extruded into solid precursors with a certain geometry. The thickness of these solid precursors should not be very high in order to assure a later homogeneous gas dissolution within an acceptable time.

1.   Gas dissolution: the solid precursor is placed inside a pressure vessel and undergoes a temperature/pressure program. Temperature is arose above the melting temperature of the polymer. This way the polymer is completely in amorphous state which benefits the homogeneity of the gas dissolution and increases the amount of gas that the polymer can dissolved. CO_2 and N_2 can be used, although CO_2 is been more common due to its high solubility in polymers. The gas pressure inside the vessel and the time that the precursor is subjected to this pressure will determine the total amount of gas dissolved. Normally the time is enough to assure the saturation of the polymer and an homogeneous distribution of the gas. Commonly the gas is at a temperature and pressure above its critical point. In this supercritical state the solubility of the gas is higher which increases the amount of gas that can be dissolved and the dissolution time can be also reduced.

2.   Temperature reduction and pressure release: once the polymer is fully saturated the temperature of the system is reduced. The new temperature is near the melting temperature of the polymer. At this temperature the polymer presents a higher extensional viscosity which helps to stabilize the cellular structure. It must be considered also that the gas dissolved in the polymer melt has a plasticizing effect reducing the melt viscosity. This reduction in temperature will be translated also in a reduction in pressure. At this new

temperature and pressure conditions the pressure is released (ΔP) but not completely. Typically a certain pressure is retained inside the vessel. This remaining pressure will help in the density control and will benefit the growing of the foam. **Δ**P is a fundamental parameter in the control of the final density. Higher expansion ratios require from higher **Δ**P and vice versa.

3.   Cooling and opening: the system is cooled down in order to stabilize the cellular structure and enable the releasing of the foamed part from the interior of the pressure vessel.

All the previously mentioned processing conditions must be correctly adjusted depending on the polymer matrix that is going to be foamed. Some works published lately propose improvements in the pressure quench method procedure. Saiz-Arroyo et al. placed the precursor material inside an aluminum mold [57,79]. The mold has openings that allow the gas to enter inside and comprises also room enough for the growing of the precursor during foaming. This way foamed parts with geometries defined by the mould can be obtained. Mechanical characterization together with other characterizations can be performed over these foams with a defined geometry. These characterizations were unfeasible previously [77-79].

The pressure quench method shows the following advantages:

⬤   Clean route: both CO_2 or N_2 are "green" gases so the production route is not environmentally harmful. No residues remain in the part after foaming (as in the case of many chemical blowing agents) reinforcing the "green" character of the technology.

⬤   Microcellular foams: the pressure quench mthod is a well studied route for the production of microcellular foams even with semi-crystalline polymers. The cellular structures obtained are homogeneous and the cell sizes and cell densities are usually in the microcellular range (<100 or 10 μm)

⬤   Density range: a wide range of densities can be covered, from low to high densities. The polymer matrix can be also crosslinked for reaching much lower densities although this prevents the recyclability of the final foam.

The main disadvantages are as follows:

⬤   Shape: the shape of the parts produced by this method is highly irregular since the geometry of the solid precursor is not kept during foaming. This hinders a proper characterization of the physical properties of the foam. Industrially this is one of the main disadvantages that has prevented the

application of the method at a large scale. As already mentioned previously, some solutions have been proposed to this problem [57,59].

         Control of the final density: following the conventional procedure the final density can be varied but not controlled. The final density can be varied by controlling the saturation pressure, the saturation temperature, the pressure drop and the remaining pressure. An accurate control of the density needs a carefull fine tuning of all these parameters. This problem can be solved by foaming inside a mold as presented by Saiz-Arroyo and co-workers.

         Set-up and industrialization: the use of high rated pressure vessels together with the high cycle times needed are also some of the reasons why the pressure quench method has not been up-scaled. Even though the batch gas dissolution method presents also these two disadvantages and is currently industrially used by at least two companies (Zotefoams and Microgreen).

2.5.- BIBLIOGRAPHY

[1]. L.J. Gibson, M.F. Ashby. Cellular Solids: Structure and Properties. 2nd Edition, Cambridge University Press, United Kingdom, (1997).

[2]. D. Klempner, V. Sendijarevic. Handbook of Polymeric Foams and Foam Technology. 2nd Edition. Hanser Publishers, Munich, (2004)

[3]. D. Eaves. Handbook of Polymer Foams. Rapra Technology, United Kingdom, (2004).

[4]. ASTM D3576-04. Standard test method for cell size of rigid cellular plastics. Annual Book of ASTM Standards, Vol 8.02, (2011).

[5]. J. Pinto, E. Solórzano, M. A. Rodriguez-Perez, J. A. de Saja, Characterization of cellular structure based on user-interactive image analysis procedures; Journal of Cellular Plastics, vol. 49, no. 6, pp. 555-575, (2013).

[6]. O. Almanza. Caracterización y Modelización de las Propiedades Térmicas y Mecánicas en Espumas de Poliolefina. PhD. Thesis, University of Valladolid, (2000).

[7]. L.O. Arcos y Rábago. Propiedades Térmicas y Mecánicas de Espumas de Poliolefina Fabricadas en un Proceso de Moldeo por Compresión. Tesis Doctoral, Universidad de Valladolid, (2002).

[8]. J.I. González-Peña. Efecto de los Tratamientos Térmicos en Bloques de Espuma de Polietileno de Baja Densidad Fabricados mediante Moldeo por Compresión. Tesis Doctoral, Universidad de Valladolid, (2006).

[9]. M. Álvarez-Laínez. Propiedades Térmicas, Mecánicas y Acústicas de Espumas de Poliolefina de Celda Abierta. Tesis Doctoral, Universidad de Valladolid, (2007).

[10]. M.A. Rodríguez-Pérez, J. Lobos, C.A. Pérez-Muñoz, J.A. de Saja. Mechanical Behaviour at Low Strains of LDPE Foams with Cell Sizes in the Microcellular Range: Advantages of Using these Materials in Structural Elements. Cellular Polymers 27: 347-362, (2008).

[11]. M.A. Rodríguez-Pérez, J. Lobos, C.A. Pérez-Muñoz, J.A. de Saja. Mechanical Response of Polyethylene Foams with High Densities and Cell Sizes in the Microcellular Range. Journal of Cellular Plastics 45:389-403, (2009).

[12]. J.E. Weller, V. Kumar. Solid State Microcellular Polycarbonate Foams. II. The Effect of Cell Size on Tensile Properties. Polymer Engineering and Science 50: 2170-2175, (2010).

[13]. S.T. Lee. Foam Extrusion: Principles and Practice. Technomic Publishing Company. Lancaster-Pennsylvania, (2000).

[14]. S. T. Lee, C. B. Park, N. S. Ramesh. Polymeric Foams. Science and Technology. CRC Press, Boca Raton-Florida, (2007).

[15]. M.A. Rodríguez-Pérez, O. Alonso, A. Duijsens, J.A. de Saja. Thermal Expansion of Crosslinked Closed-Cell Polyethylene Foams. Journal of Applied Polymer Science 36: 2587-2596, (1998).

[16]. W. Gong, J. Gao, M. Jiang, L. He, J. Yu, J. Zhu. Influence of Cell Structure Parameters on the Mechanical Properties of Microcellular Polypropylene Materials. Journal of Applied Polymer Science 122: 2907-2914, (2011).

[17]. ASTM D6226-10. Standard Test Method for Open Cell Content of Rigid Cellular Plastics. Annual Book of ASTM Standards, Vol 8.03, (2011).

[18]. A. T. Huber, L. J. Gibson. Anisotropy of Foams. Journal of Materials Science 23: 3031-3040 (1988).

[19]. M. Antunes, J.I. Velasco, V. Realinho, A.B. Martínez, M.A. Rodríguez-Pérez, J.A. de Saja. Heat Transfer in Polypropylene-Based Foams Produced using Different Foaming Processes. Advanced Engineering Materials 11: 811-817, (2009).

[20]. L.R. Glicksman, Heat Transfer in Foams in N.C. Hilyard, A. Cunningham (Eds). Low Density Cellular Plastics-Physics of Basics of Behaviour. Chapman and Hall, London, pp 107-111, (1994).

[21]. J. L. Throne. Thermoplastic Foam Extrusion. An Introduction. Hanser Publishers, Munich, (2004).

[22]. L. Garrido, L. Ibarra, C. Marco. Ciencia y Tecnología de Materiales Poliméricos. Volumen II. Instituto de Ciencia y Tecnología de Polímeros-CSIC, Madrid, (2004).

[23]. L. Garrido, L. Ibarra, C. Marco. Ciencia y Tecnología de Materiales Poliméricos. Volumen I. Instituto de Ciencia y Tecnología de Polímeros-CSIC, Madrid, (2004).

[24]. K.W. Suh, C.P. Park, M.J. Maurer, M.H. Tusim, R. Genova, R. Broos, D.P. Sophiea. Lightweight Cellular Plastics. Advanced Materials 12: 1779-1789, (2000).

[25]. J. Stange, H. Münstedt. Effect of Long-Chain Branching on the Foaming of Polypropylene with Azodicarbonamide. Journal of Cellular Plastics 42: 445-467, (2006).

[26]. H.E. Naguib, C.B. Park. Strategies for Achieving Ultra Low-Density Polypropylene Foams. Polymer Engineering and Science 42:1481-1492, (2002).

[27]. C.B. Park, L.K. Cheung. A Study of Cell Nucleation in the Extrusion of Polypropylene Foams. Polymer Engineering and Science 37:1-10, (1997).

[28]. C. Liu, D. Wei, A. Zheng, Y. Li, H. Xiao. Improving Foamability of Polypropylene by Grafting Modification. Journal of Applied Polymer Science 101: 4114-4123, (2006).

[29]. G.J. Nam, J.H. Yoo, J.W. Lee. Effect of Long-Chain Branches of Polypropylene on Rheological Properties and Foam-Extrusion Performances. Journal of Applied Polymer Science 96: 1793-1800, (2005).

[30]. F. Hidalgo. Diseño Optimizado de los Parámetros de Proceso en la Fabricación de Espumas de Poliolefina Reticulada mediante Moldeo por Compresión. Tesis Doctoral, Universidad de Valladolid, (2008).

[31]. ASTM D2465-11, Standard test methods for determination of gel content and swell ratio of crosslinked ethylene plastics. Annual Book of ASTM Standards, Vol 8.01, (2011).

[32]. C. Saiz-Arroyo, J.A. de Saja, M.A. Rodríguez-Pérez. Production and characterizacion of crosslinked low-density polyethylene foams using waste of foams with the same composition. Journal of Applied Polymer Science, 52, 751-759 (2012).

[33]. S. Roman Lorza. Formulación y Caracterización de Materiales Celulares Retardantes de Llama Libres de Halógenos basados en Poliolefinas. Tesis Doctoral, Universidad de Valladolid, (2010).

[34]. V. Viswanathan, T. Lahe, K. Baloni, A. Agarwal, S. Seal. Challenges and advances in nanocomposite processing techniques. Materials Science & Engineering R54: 121-285, (2006)

[35]. L. A. Utracki. Clay-containing polymeric nanocomposites vol.1. Rapra Technology Limited. United Kingdom (2004).

[36]. L. A. Utracki. Clay-containing polymeric nanocomposites vol.2. Rapra Technology Limited. United Kingdom (2004).

[37]. Y. Du, S.Z. Shen, K. Cai, P.S. Casey. Research progress on polymer-inorganic thermoelectric nanocomposite materials. Progress in Polymer Science, *In press*-DOI 10.1016/j.progpolymsci.2011.11.003, (2011)

[38]. C. Choudalani, A.D. Gotsis. Permeability of polymer/clay nanocomposites. A review. European Polymer Journal 45: 2793-2810, (2010).

[39]. R.F. Gibson. A review of recent research on mechanics of multifunctional composite materials and structures. Composite Materials & Structures 92: 2793-2810, (2010).

[40]. J. Jancar, J.F. Douglas, F.W. Starr, S.K. Kumar, P. Cassagnau, A.J. Lesser, S.S. Sternstein, M.J: Buehler. Current issues in research on structure-property relationship in polymeric nanocomposites. Polymer 51: 3321-3343, (2010).

[41]. S. Pavlidou, C.D. Papaspyrides. A review on polymer layered silicate nanocomposites. Progress in Polymer Science 33: 1119-1198, (2008).

[42]. S.S. Ray, M. Okamoto. Polymer/layered silicate nanocomposites: A review, from preparation to processing. Progress in Polymer Science 28: 1539-1641, (2003).

[43]. S.S. Ray, M. Bousmina. Biodegradable polymers and their layered silicate nanocomposites: In greening the 21st century materials world. Progress in Polymer Science 50: 962-1079, (2005).

[44]. P. Bordes, E. Pollet, L. Avérous. Nano-biocomoposites. Biodegradable polyester/nanoclay systems. Progress in Polymer Science 34: 125-155, (2009).

[45]. T. Kuilla, S. Bhadra, D. Yao, N.H. Kim, S. Bose, J.H. Lee. Recent advances in graphene based polymer composites. Progress in Polymer Science 35: 1350-1375, (2010).

[46]. F. Hussain, M. Hojjati, M. Okamoto, R.E. Gorga. Polymer-matrix nanocomposites, processing, manufacturing and application: An overview. Journal of Composite Materials 40: 1511-1575, (2006).

[47]. Z. Spitalsky, D. Tasis, K. Papagelis, C. Galiotis. Carbon nanotube-polymer composites: Chemistry, processing, mechanical & electrical properties. Progress in Polymer Science 35: 357-401, (2010).

[48]. H. Zou, S. Wu, J. Shen. Polymer/silica nanocomposites: Preparation, characterization, properties and applications. Chemical Reviews 108: 3893-3957, (2008).

[49]. T.J. Pinnavia, G.W. Beall. Polymer-Clay Nanocomposites. John Wiley & Sons, Chichester-England, (2000).

[50]. Fukatani J., Iwasa K., Ueda N., Shibayama K. Polyolefin resin composite, thermoplastic resin composite and process for producing of thermoplastic resin composite. Patent EP 1 193 290 A1.

[51]. C.C. Ibeh, M. Bubacz. Current trends in nanocomposite foams. Journal of Cellular Plastics 44: 493-515, (2008).

[52]. L.J. Lee, C. Zeng, X. Cao, X. Han, J. Shen, G. Xu. Polymer nanocomposite foams. Composites Science and Technology 65: 2344-2636, (2005).

[53]. J.S. Colton, N.P. Suh. Nucleation of microcellular foam: Theory and practice. Polymer Engineering and Science 27: 500-503, (1987).

[54]. W. Zhai, C.B. Park, M. Kontopoulou. Nanosilica addition dramatically improves the cell morphology and expansion ratio of polypropylene heterophasic copolymer foams blown in continuous extrusion. Industral & Engineering Chemistry Research 50: 7282-7289, (2011).

[55]. M. Okamoto, P.H. Nam, P. Maiti, T. Kotaka, T. Nakayama, M. Takada, M. Ohshima, A. Usuki, N. Hasegawa, H. Okamoto. Biaxial flow-induced alignment of silicate layers in polypropylene/clay nanocomposite foam. Nano Letters 1: 503-505, (2001).

[56]. C. Saiz-Arroyo, J. Escudero, M.A. Rodríguez-Pérez, J.A. de Saja. Improving the structure and physical properties of LDPE foams using silica nanoparticles as an additive. Cellular Polymers 30: 63-78, (2011).

[57]. C. Saiz-Arroyo, M.A. Rodríguez-Pérez, J.I. Velasco, J.A. de Saja. LDPE/Silica nanocomposite foams. Relationship between chemical composition, particle dispersión, cellular structure and physical properties. European Polymer Journal, *Submitted.*

[58]. D.N. Bikiaris, G.Z. Papageorgiou, E. Pavlidou, N. Vouroutzis, P. Palatzoglou, G. P. Karayannidis. Preparation by melt mixing and characterization of isotactiv polypropylene/SiO_2 nanocomposites containing untreated and surface-treated nanoparticles. Journal of Applied Polymer Science 100: 2684-2696, (2006).

[59]. S. Jacob, K.K. Suma, J.M. Mendez, K.E. George. Reinforcing effect of nanosilica on polypropylene-nylon fibre composite. Materials Science and Engineering B 168: 245-249, (2010).

[60]. S.M. Lai, C.Y. Huang, S.C. Li, Y.H. Chen, H.C. Hsu, Y.F. Yu, Y.F. Hsiou. Preparation and properties of melt-mixed metallocene polyethylene/silica nanocomposites. Polymer Engineering and Science 51: 434-444, (2010).

[61]. P. Kiliaris, C.D. Papaspyrides. Polymer/layered silicate (clay) nanocomposites: An overview of flame retardancy. Progress in Polymer Science 35: 902-958, (2010).

[62]. F. Yang, G.L. Nelson. Combination effect of nanoparticles with flame retardants on the flammability of nanocomposites. Polymer Degradation and Stability 96: 270-276, (2011).

[63]. S.C. Tjong. Structural and mechanical properties of polymer nanocomposites. Materials Science and Engineering R 53: 73-197, (2006).

[64]. G. Munters, J.G. Tandberg. U. S. Patent nº 2,023,204, (1935).

[65]. K.T. Okamoto. Microcellular Processing. Hanser Publishers, Munich, (2003).

[66]. S. Doroudiani, C.B. Park, M.T. Kortschot. Effect of crystallinity and morphology on the microcellular foam structure of semicrystalline polymers. Polymer Engineering and Science 36: 2645-2662, (1996).

[67]. C.B. Park, L.K. Cheung. A study of cell nucleation in the extrusion of PP foams. Polymer Engineering and Science 37: 1-10, (1997).

[68]. C.B. Park, A.H. Behravesh. Low density microcellular foam processing in extrusion using CO_2. Polymer Engineering and Science 38: 1812-1823, (1998).

[69]. H.E. Naguib, C.B. Park, U. Panzer, N. Reichelt. Strategies for achieving ultra low density polypropylene foams. Polymer Engineering and Science 42: 1481-1492, (2002).

[70]. H.E. Naguib, C.B. Park, N. Reichelt. Fundamental foaming mechanisms governing the volume expansion of extruded polypropylene foams. Journal of Applied Polymer Science 91: 2661-2668, (2004).

[71]. W.G. Zheng, Y.H. Lee, C.B. Park. Use of nanoparticles for improving the foaming behaviour of linear polypropylene. Journal of Applied Polymer Science 117: 2972-2979, (2010).

[72]. T.A. Osswald, L.S. Turng, P.J. Gramann. Injection Molding Handbook. Hanser Publishers, Munich, (2002).

[73]. M.A. Rodriguez-Perez, J.A. de Saja, J. Escudero, D. de Rosa, J. A. Vazquez. Sistema y procedimiento de molde de piezas con moldes autoportantes. Patente española 201130271. (2011)

[74]. J. Escudero, E. Solorzano, M. A. Rodriguez-Perez, F. Garcia-Moreno, J.A. de Saja. Structural characterization and Mechanical Behavior of LDPE Structural Foams. A comparison with Conventional Foams. Cell. Polym. Vol. 28, 4. 289-302 (2009).

[75]. P.R. Hornsby. Thermoplastics structural foams. Part 1 Technology of production. Materials in Engineering 3: 354-362, (1982).

[76]. P.R. Hornsby. Thermoplastics structural foams. Part 2 Properties and applications. Materials in Engineering 3: 443-455, (1982).

[77]. L. Singh, V. Kumar, B.D. Ratner. Generation of porous microcellular 85/15 poly (DL-lactide-co-glycolide) foams for biomedical applications. Biomaterials 25: 2611-2617, (2004).

[78]. M. Antunes, V. Realinho, J.I. Velasco. Study of the influence of the pressure drop rateo on the foaming behaviour and dynamic-mechanical properties of CO_2 dissolution microcellular polypropylene. Journal of Cellular Plastics 46: 551-571, (2010).

[79]. C. Saiz-Arroyo. Fabricación de Materiales Celulares Mejorados Basados en Poliolefinas. Relación Procesado-Composición-Estructura-Propiedades (2012).

Chapter 3

Foaming Processes, Raw Materials and
Experimental Techniques

After the review of general concepts made in the second chapter, this third one goes in detail into the production routes and raw materials specifically used in this research work. Four main methods have been used for producing the studied foam: Stages Molding, Improved Compression Molding, Batch Gas Dissolution and Two-Steps Compression Molding. All of them will be described in detail in this chapter. As polymer matrices all the study has been focused on two polyolefins: low density polyethylene and a high melt strength polypropylene. These polymers have been filled with different nanoparticles: nanoclays (natural and organomodified) and carbon nanotubes. To improve the coupling between the polymer and the nanoclays, a polyethylene and a polypropylene grafted with maleic anhydride have been also used. The aim of the present chapter is presenting further details of all of them. Finally, the experimental techniques are enumerated together with the standards used in each case.

3.1.- FOAMING PROCESSES

Four main foaming methods have been used in the frame of this work:

●   The first one is a completely new process for the production of structural foams. This method has been patented and tries to overcome the difficulties and disadvantages associated to the current industrial production processes of structural foams. The process allows for a deep control of cellular structure, solid skin thickness and final density. The simplicity of the process together with the excellent surface skin and improved mechanical properties make it very interesting both from a scientific and industrial point of view. The patent for this process is enclosed as an appendix at the end of the manuscript.

●   The second method has as main objective the production of low density (<200 kg/m^3) non-crosslinked polypropylene foams with improved mechanical properties. For this purpose a high melt strength polypropylene (described in section 3.2.1) was foamed using a variation of the common compression moulding. This variation is named Improved Compression Moulding and has been completely developed in CellMat Laboratory. A deep optimization of the production conditions and chemical formulation was needed to achieve such low densities with a polypropylene polymer matrix. The combination of HMS polypropylene, nanoparticles and improved compression moulding has been also explored. The whole production process has been also patented and the patent is enclosed as an appendix at the end of the manuscript.

⚫   The third foaming processes is well studied in the literature but not commonly used for foaming semicrystalline polymers. The work conducted in this thesis uses the batch gas dissolution process for foaming a polyethylene matrix with CO_2 in sub-critical conditions. The method allows not only achieving polyethylene or polyehytlene/nanoclays foams but also studying the gas solubility and diffusivity in polyethylene composites and nanocomposites. In a second step the polyethylene matrices were crosslinked and foamed also by batch gas dissolution in subcritical conditions. This scarcely explored research line allowed producing microcelullar foams with expansion ratios as high as 6 (densities around 150 kg/m^3).

⚫   The fourth foaming process is aimed at achieving very high expansion ratios (>30) with a crosslinked polymer. It can be considered as a variation of the conventional compression molding in one stage and it is widely industrially used. The foaming process has been used both with an LDPE unfilled polymer matrix and the same matrix filled with nanoclays.

A detailed description of each process is included in this section. Further details can be found in the corresponding scientific articles as well as in the corresponding patent documents enclosed at the end of the manuscript.

3.1.1.- Stages Molding for the Production of Structural Foams

Sectors as important as aeronautics, automotive or sporting goods are demanding each time more and more cellular materials with improved mechanical properties.

Mechanical properties for conventional foams (i.e. that ones with a constant density across its volume) decrease strongly while reducing density. One way to improve these properties maintaining constant the overall density consists on the production of foams with a sandwich structure, that is to say, presenting two outer solid skins and an inner foamed core. This, usually named skin-core morphology, results in high specific mechanical properties (strength to weight ratio) compared to non structural foams [5].

Commonly, the most usual method to produce structural foams is foaming injection moulding (see section 2.4.2.2) [5]. Some other more sophisticated methods have been developed but based upon this previous one. In all the cases the polymer, blowing agent and other additives are injected inside a mould using high pressures. In the case of the conventional process, the cold walls of the mould enable the polymer

melt to solidify without forming a cellular structure, achieving in this simple way the sandwich structure characteristic of an structural foam. Surface quality is not as good as desired and the density reduction is not very high. In order to correct these disadvantages moulds that can be expanded after the injection of the polymer melt have been designed. These expandable moulds allow a better control of the final cellular structure but in general surface quality is not as good as needed for several industrial applications [1-4]. Other option consists in introducing a gas at elevated pressure inside the mould before the polymer is injected. This gas is then evacuated as the polymer is injected in a process that is commonly known as "gas counter pressure". While doing this much better surface qualities are achieved but skin layers are in general very thin {[1-4]. A relative new patented process known as Smartfoam, tries to obtain a good surface quality with an adequate control of the cellular structure and skin layers thicker than in the previous cases. In a first step solid polymer is injected inside the cavity of the mould forming the solid outer skins. Then, gas is dissolved in the polymer in the injection unit and then this second polymer, with the gas already dissolved, is injected in the mould. This polymer-gas mixture allows forming the cellular core of the foam. In a final step, solid polymer is again injected to end the solid outer skins and as a consequence the structural foam [1].

Injection moulding of solids in all its forms is a quick process. From an industrial point of view, large series of pieces can be produced in short time and the characteristics of these pieces are good enough to fulfill the requirements. But it presents also several disadvantages. Moulds used in any of the processes described above are quite expensive since the pressures used are quite high. At the same time the initial investments necessary are also high and maybe even too high if the production consists in small series. Besides, densities reachable in this process are high, of the order of 700 kg/m^3 for polyolefin based foams with difficulties to obtain lower densities having at the same time a good control of the cellular structure and other parameters.

The production of structural foams by Stages Moulding overcomes several of the mentioned disadvantages. From an industrial point of view, much cheaper moulds and lower initial investments are required to succeed using this new technology. This makes our process very convenient for the production of small series. At the same time lower densities are reachable without sacrificing surface quality. From a scientific point of view we can produce both conventional and structural foams using practically the same process, same composition and with the same density range. This allows us comparing systematically the behavior of both kind of foams. At the same time we have a good control over the cellular structure in terms of cell size and homogeneity. Skin

thickness, density profile and global density are parameters that, together with cellular structure, cannot independently controlled in the injection moulding technique [1-4].

The process comprises three different main steps (figure 3.1):

⚙   Filling of the mould cavity: the first step consists on the feeding of the material inside the "self-bearing" mould. The feeding can be done following different procedures as hoppers, using an extruder machine, or even using injection units. The concept of "self-bearing" moulds is fundamental in this technology and stands for a mould in which the closing system is part of the mould and not an independent part. These "self-bearing" moulds are designed in such a way that they can support the pressures developed during the molding of the sample. In most of the cases the molding material contains a chemical blowing agent that will release gas when heated.

⚙   Molding of the sample: once the mould is filled its temperature is increased somehow in order to decompose the chemical blowing agent and release the gas. The gas pressure produced will act as driving-force allowing the polymer to fill completely the mould cavity. The gas pressures developed are much lower than the pressures developed in any injection moulding process. Therefore the molds are simpler and cheaper than the ones used in injection molding.

⚙   Sample cooling and release: once the thermal cycle needed for the complete filling of the cavity has been completed the mould is cooled and the sample is released.
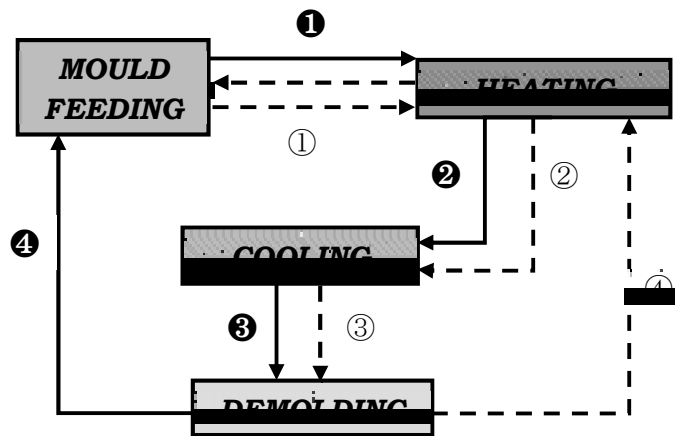
Figure 3.1: Simplified scheme of the Stages Molding process for the production of structural foams. Either the route with the black-filled numbers or the route with the white-filled numbers can be followed.

The key feature for obtaining structural foams using the previous process consists on covering the internal walls of the mould with a material able to dissolve gas (figure 3.2). In the experiments carried out in the laboratory plane sheets of silicone rubber were usually used. Solid skins appear in all the areas in close contact with the silicone rubber sheets. In these areas the gas is dissolved from the polymer into the silicone rubber reducing and even eliminating any porosity in the part skin. Besides this, it has been experimentally proved that any area in close contact with a piece of silicone rubber (even if the piece of silicon rubber is placed in the interior of the foam) develops a solid skin surrounding it. Other materials with the ability to dissolve gas as PTFE has been also tested for example, giving comparable results [4]. Further details can be found in chapter 5.

Mould Walls

Silicone Rubber

Solid skins

Foamed core

Solid skins

Silicone Rubber

Mould Walls
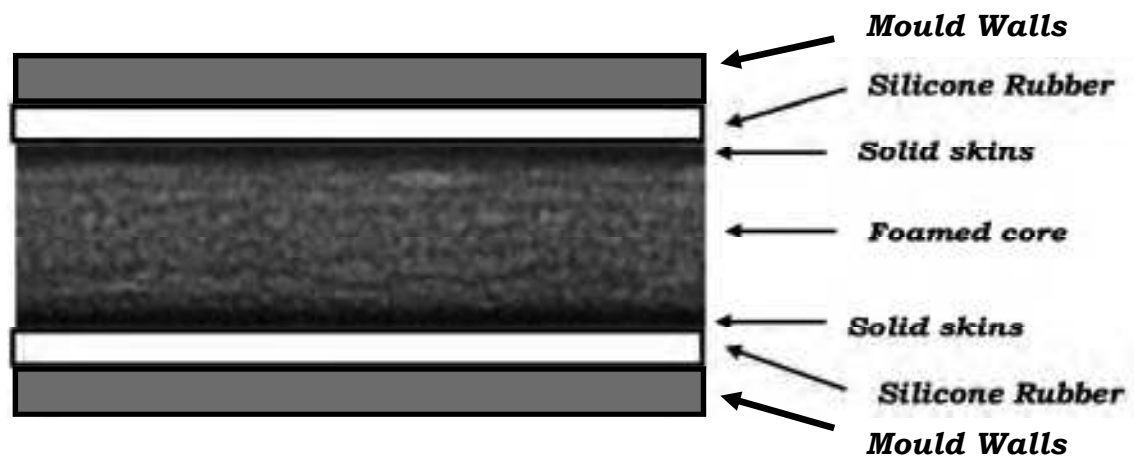
Figure 3.2: Example of the disposition of the silicone rubber sheets in the production of an structural foam by Stages Molding. The solid skins are formed in the areas in close contact with the silicone rubber. The image of the foam has been obtained by X-ray radioscopy.

By controlling the amount of blowing agent, foaming temperature, foaming time and thickness of the silicone rubber a wide variety of parameters of the foam can be controlled and varied: cell size, cell density, skin thickness, density profile. Foams with densities below 450 kg/m^3 and excellent surface qualities have been produced following this procedure [1-4]. Besides this, the bending properties have been significantly improved (see chapter 5). One example of the foams produced by this method is showed in figure 3.3.
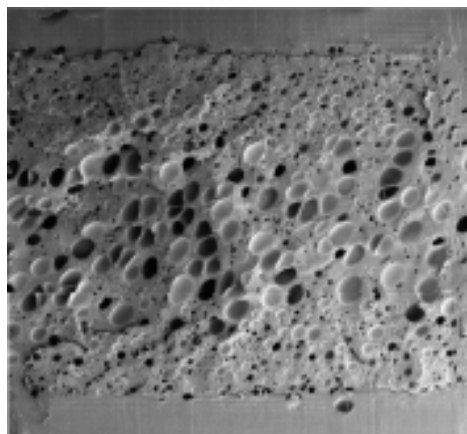
Figure 3.3: Micrograph obtained by electron microscopy of an structural foam obtained by Stages Molding. Two solid skins can be distinguished in the outer parts. A

significant density profile appears in the interior of the foam. These density profiles are typical in structural foams.

3.1.2.- Improved Compression Molding for the production of low density, non-crosslinked PP foams

Compression Molding, in one or two steps, allows obtaining cellular materials based on polyolefins in a simple and economic way and covering a wide range of densities. However two main disadvantages show up: on the one hand it is necessary to crosslink the polymer matrix in order to achieve low densities and on the other hand compression molding in one step offers scarce control of the bulk final density [5]. These two disadvantages completely disagree with our aim of obtaining non-crosslinked low density PP based foams non-crosslinked and with a controlled density.

Improved Compression Molding (ICM) has been entirely developed at CellMat Laboratory and appears as an alternative to the conventional compression molding process. It allows the production of molded parts, non-crosslinked, in a wide range of densities. It is based on a strict control of the chemical composition (specially blowing agent addition) pressure applied and temperature and in the use of specific moulds.

The ICM route comprises different steps. Prior to the ICM all the raw materials (polymer matrix, blowing agent and additives) are mixed using a twin screw extruder or an internal mixer. The different steps followed in the ICM route are schematized in figure 3.4 and explained in the following paragraphs.

⚬ Step A: the mixed materials can be compression molded to form a solid part usually known as "precursor material" (5). For this purpose a mold with the same geometry as the final foamed part is used. The compression molding of the precursor is done using a temperature above the melting temperature (T_m) of the polymer matrix but below the decomposition temperature of the blowing agent to avoid any premature undesired foaming. The pressure applied is enough to properly compacting the precursor.

⚬ Step B: the precursor material (5) is placed inside the ICM mold cavity (11) and the mold is closed. These "self-expandable" molds are comprised by different parts: the body of the mould (1) that in its upper and lower surface shows two slots (2). Two high-temperature rubber gaskets (usually viton) are placed in these slots in order to hermetically close the mold cavity when the

pressure is applied (9) by the T-piston (3). During all the process the T-piston (3) is continuously applying pressure over the polymer melt (10). Part (4) is the lower closure of the mold. The final expansion ratio (density) is controlled using an expansion ring (6). This expansion ring is chosen depending on the final density aimed. During the expansion the T-piston is halted and retained by the retention ring (7).

⚙   Step C: the mold as a whole is placed inside a pre-heated hot-plates press and undergoes a defined temperature-pressure program. Mechanical pressure is applied by means of an external cylindrical piston (8) that serves also as heat conductor from the upper plate of the press to the mold. The temperature is high enough to decompose the blowing agent.

The decomposition of this blowing agent creates a certain gas pressure inside the mold. The external mechanical pressure applied must be always higher than the internal gas pressure created by the blowing agent in such a way that the gas stays dissolved in the polymer melt during the entire temperature-pressure program (C1). Once the blowing agent is decomposed and the generated gas has been dissolved in the polymer the pressure is released at a controlled release rate. The pressure releasing creates a thermodynamic instability. One phase polymer/gas is no present anymore, the gas is no longer dissolved in the polymer melt. This phase separation produces the nucleation an growing of the cells as depicted in (C2). The gas pressure acts as driving force for the cell growing promoting the movement of the piston which is finally halted by the retention ring (C3).

⚙   Step D and E: since the growing of the foam is constrained in one direction cells are preferentially elongated as depicted in (D). Now the mold with the foam inside can be extracted from the hot-plates press and cooled down by any means. Cooling rates as high as possible are beneficial therefore in this thesis work the mold+foam was cooled down by water immersion. After cooling the mold can be opened and the foam released (E).

One of the main differences with the conventional compression molding deals with the fact that pressure is applied to the material during the expansion [6-13]. That difference is later translated in several advantages in comparison with the conventional process:

Fine-tuned control of the final density.

Density is controlled by means of specially designed molds. These "self-expandable" molds are able to apply and retain pressure during the whole process, including the expansion and cellular structure stabilization step. In addition, the design allows controlling the final expansion ratio of the material in a very precise way. Works previous to this thesis have explored the relative density range between 0.3 and 0.6. The work conducted in this thesis explores the relative density range between 0.1 and 0.3.
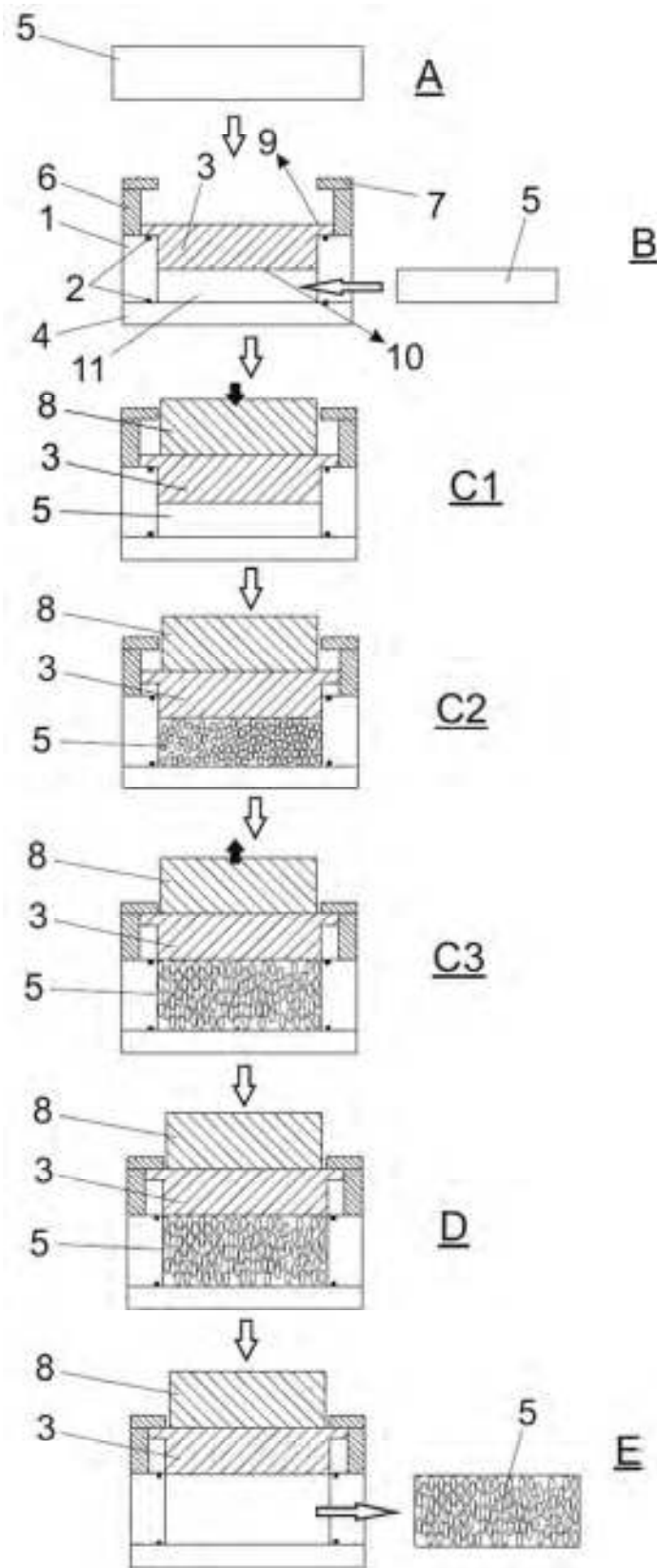
Figure 3.4: schematic of the whole ICM molding route

⬤   Possibility of modifying the microstructure of the cellular material.

ICM allows controlling the cellular structure of the foam independently of the bulk density. This control can be performed by two different procedures: varying the chemical composition (blowing agent addition, present of inorganic fillers,...) or modifying the processing parameters (pressure, temperature, pressure release rate).

Not only the cell size, cell density or homogeneity can be varied, but also the anisotropy ratio of the cellular structure which is a parameter of major importance in this research. Especially important is also the blowing agent addition or the addition of nanoparticles to vary the open cell content of the foam. Foams with improved mechanical properties and different open cell contents can be obtained just by adding a certain amount or inorganic nanofillers as nanoclays for example (see chapter 6).

⬤   Non-crosslinked molded parts.

Parts with diverse geometries can be obtained by ICM which turns the process in very versatile. Although in the frame of this thesis work only polypropylene has been used, in principle any thermoplastic polymer can be foamed by ICM without crosslinking.

Literature contains different examples of previous works that use the ICM route for foaming polymer matrices as diverse as EVA, EVA filled with aluminum or magnesium hydroxide, LDPE, blends of EVA and starch or PP (with relative densities in the range 0.3-0.6) [13-18]. In the frame of this thesis ICM has been used for foaming non-crosslinked PP and PP nanocomposites reaching relative densities in the range (0.1-0.3). Together with the low densities, two main other features of these foams must be emphasized:

1)   The high anisotropy ratios achieved, with values as high as 2.5. These high anisotropy ratios are translated into improved compressive properties (in the direction of maximum anisotropy).

2)   The possibility of obtaining closed cell and open cell cellular structures just by the addition of nanoparticles. Both versions (closed and open cell) present the already mentioned improved mechanical properties. The possibility of combining open cell structures with improved mechanical

properties broadens the range of application of these foams (acoustic absorbers, improved outgasing, filtration purposes,...)

The reproducibility of the process has been analyzed in previous works and is very high [6-13]. Figure 3.5 shows two micrographs of non-crosslinked PP foams produced by ICM. The foam on the left presents a closed cell cellular structure with an anisotropy ratio of 2.2 whereas the one on the right present an open cell cellular structure with an anisotropy ratio of 2.5. The bulk density of both of them is 150 kg/m^3.
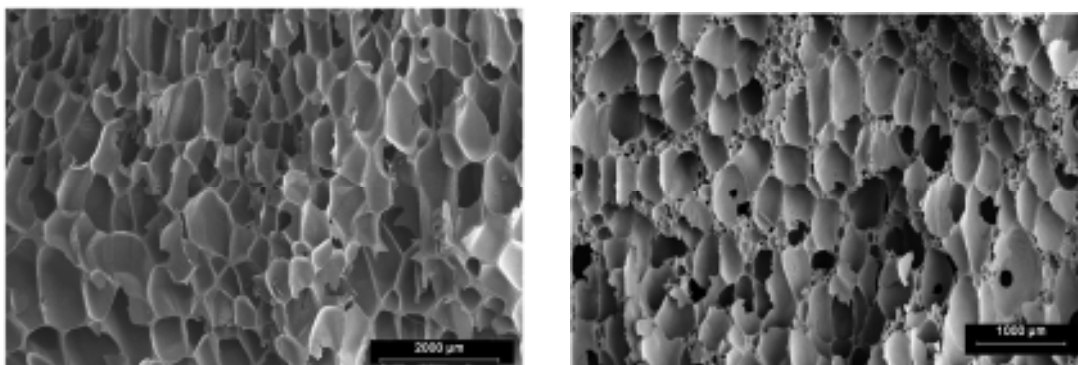
Figure 3.5: Micrographs of non-crosslinked anisotropic foams produced by ICM. Left, closed cell foam. Right, open cell foam. Both of them have a bulk density of 150 kg/m^3

Further details of the process and experimental results obtained are shown in chapter 6. Industrially these foams could have a wide range of application. Industrial niches as important as automotive, railway, wind energy or aeronautic demand foamed materials combining densities below 200 kg/m^3 and outstanding mechanical properties. It has been experimentally demonstrated that the foams produced in the frame of this thesis by ICM have performance comparable than other currently industrially used materials based on PVC or SAN. All these facts will be shown in chapter 6.

3.1.3.- Batch Gas Dissolution in crosslinked and non-crosslinked LDPE nanocomposites

The research in microcellular foams goes back to the early eighties with the work conducted at the MIT in response to a challenge by the packaging and photographic

film companies to reduce the amount of polymer used in their products. Reducing the cell size to the order of 10 μm and increasing the cell density to 10^9 cells/cm^3 would improve the strength to weight ratio of conventional foams giving reasonable values for the intended applications [19,20]. The conducted research allowed the development of the batch gas dissolution technique.

From the basic batch gas dissolution, other different, but more complex, semicontinous [21,22] and continous [23-25] methods have been also developed for the microcellular foaming of polymers. In any of these routes most of the efforts have been focused on amorphous polymers such as polystyrene [19,26,27], polycarbonate [28,29], acrylonitrile-butadiene-styrene (ABS) [30,31], poly(methyl methacrylate) [32] and poly (vinyl-chloride) [33] . In comparison very little work has been conducted on the foaming of semicrystalline polymers, and almost only in continous or with the polymer in the melt state [35-38]. Although the applications of polymers as PE or PP are widely spread their semicrystalline character makes difficult obtaining microcellular foams by the batch gas dissolution technique [39, 44]. Gas is admitted to dissolve only in the amorphous phase as the structure of the crystals hinders the diffusion. The foaming must be conducted also at a temperature near the melting point [46]. In an effort to overcome these difficulties supercritical gases have been used in almost all the studies dealing with microcellular foams from semicrystalline polymers [34, 41-45]. This supercritical state allows for higher solubilities and diffusivities but the more complex set up needed rises as an important disadvantage both at laboratory and industrial scale. When increasing pressure above the CO_2 supercritical range, the cost of the foaming process greatly increases due to the need for gas pumps and high pressure rated vessels.

In the work conducted in this thesis less favorable microcellular foaming conditions have been explored: a semicrystalline polymer has been foamed by batch gas dissolution in sub-critical conditions. Parallel to the foaming analysis the batch gas dissolution method has allowed performing a diffusivity and solubility study in the silicate nanocomposites by gravimetric procedures. Therefore an insight into the gas barrier role played by the nanoclays in the solid matrix has been given.

The batch gas dissolution method followed in this work comprises different steps (figure 3.6):

1.   The composites (polymer+coupling agent) or nanocomposites (polymer+coupling agent+nanoclays) are compression molded into solid slabs. The thickness of these slabs is an important parameter that must be controlled, not too thick in order to favor a quick and homogeneous gas dissolution and not

too thin to a avoid a quicker than desired desorption. Due to this, 1.27 mm thick samples were used in our research work.

2.   Solid slabs of the different materials are wrapped with a porous paper cloth and placed inside a pressure vessel. This paper cloth will ensure a homogeneous dissolution of all the samples even if some of them are in closed contact with each other or in contact with the bottom of the pressure vessel.

3.   The pressure vessel is closed and gas (in this case CO_2) is pumped inside to a pressure of 5 MPa at room temperature. In these temperature-pressure conditions the gas is in sub-critical state. Pressure is kept constant in a value of 5 MPa during the whole dissolution step by means of a digital pressure controller with an error of ± 0.1 MPa.
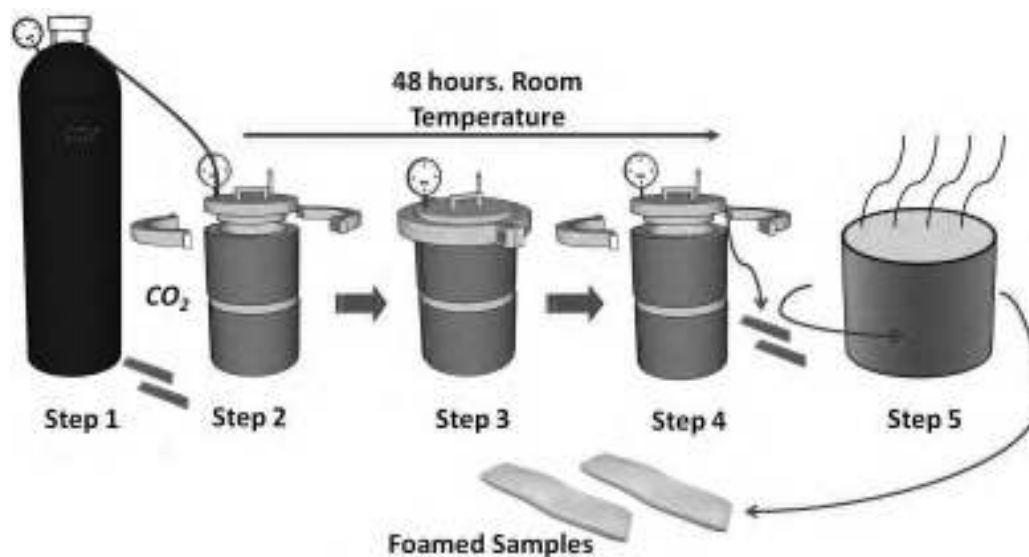
Figure 3.6: Schematic of the batch gas dissolution process

4.   Once the whole saturation of the sample is assured (48 hours at room temperature were used), pressure is released, the pressure vessel is opened and the specimen is removed. Since the gas desorption begins just after the pressure release, the opening of the pressure vessel must be performed as quick as possible trying to keep as much gas as possible dissolved in the sample at the foaming time. The sorption behavior of the samples was also determined by periodically opening the pressure vessel (before complete saturation), removing the specimen, weighting it with a microbalance, placing it again inside the vessel and closing it. All this process was done as quickly as possible. Further details can be found in chapter 4.

5.   In a final step the specimen is immersed in a pre-heated silicone oil bath. Silicone oil assures a very high and homogeneous thermal contact with the whole sample. The immersion temperature is tailored to give the best foaming behavior. For semicrystalline polymers must be slightly above the melting temperature. Density and cellular structure is controlled by varying the immersion time. In addition some specimens of each different material were used for determining the desorption behavior. For this purpose the specimens were placed in a microbalance after saturation instead of being foamed. Weight was recorded periodically and diffusivity was determined from this weight vs. time plots (see chapter 4).

Figure 3.7 shows two micrographs of crosslinked LDPE composites foamed by batch gas dissolution in sub-critical conditions. Different immersion times were used for these samples. In both cases the mean cell size is below 10 μm. Further details for these type of foams will be mentioned in chapter 4.
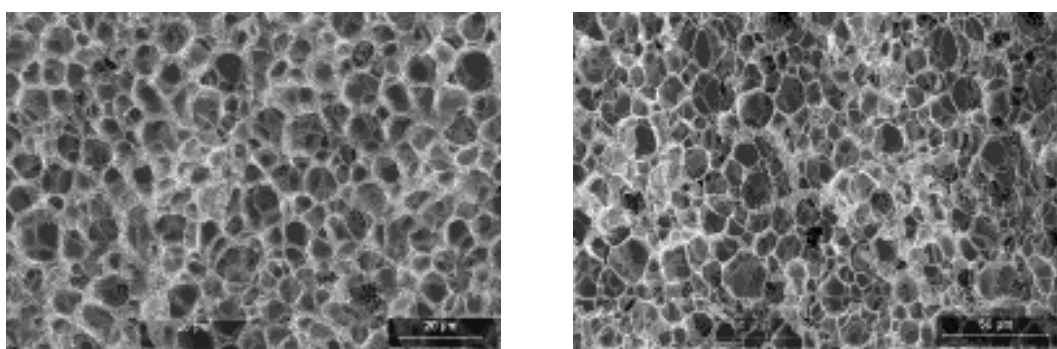
Figure 3.7: Two different micrographs of the same LDPE nanocomposite foamed using different immersion times are produced by batch gas dissolution in sub-critical conditions. The polymer matrix was crosslinked before foaming as will be explained in detail in chapter 4.

3.1.4.- Two-steps Compression Molding for the production of low density crosslinked nanocomposite foams

The so called two stages compression molding is always combined with crosslinked polymers and chemical blowing agents. It is a very suitable process when foamed parts with low densities and not very complex geometries are sought [46,47].

Conventional hot plates presses do not need any modification in order to be used for two-steps compression molding so the initial investments are low. Many aspects of the two-steps compression molding are common with the one-stage counterpart (see section 2.4.2.3). The process can be divided into different steps (figure 3.8):

0.   Mixing and compounding: prior to the compression molding itself the polymer, blowing agent, crosslinking agent and the rest of the additives are conveniently mixed and compounded using an internal mixer or a twin screw extruder. The compounding temperature must be lower than the decomposition temperature of the CBA and lower also than the activation temperature of the crosslinking agent.

1.   Crosslinking and first expansion: The compound (polymer+additives) is placed inside a mold and undergoes a temperature and pressure profile. The temperature is higher than the activation temperature of the crosslinking agent and lower than the decomposition temperature of the blowing agent. The compound is kept under pressure and temperature during a certain time to assure the desired crosslinking degree. When the polymer is conveniently crosslinked the pressure is released and the material suffers a pre-expansion with expansion ratios between 2 and 8.

2.   Second expansion: Just after this pre-expansion the material is placed inside a second mold which has the final dimensions sought. This second mold is heated up above the decomposition temperature of the blowing agent allowing for the full expansion of the foam. This expansion occurs at atmospheric pressure, no pressure is applied. Expansion ratios as high as 40 can be achieved following this procedure.

3.   Cooling and de-molding: Once the material has completely filled the mold it is cooled down by any means and de-molded. On the contrary to other foaming processes, since in this case the material is crosslinked and the foam is by far more stable, the cooling rate is not a parameter as critical as in the other process described.

> **Crosslinking and Pre-Foam:**
> temperature and pressure in a hot press. Material is crosslinked and a pre-foam is obtained. $T_{crosslink.} < T < T_{decomp.}$
> azodicarb

> **Second expansion**: pre-foam is placed inside a mold with the final dimensions and expanded freely inside an oven. $T > T_{decomp. \ azodicarb}$.

> **Cooling and de-molding**: mold cooled down by any means. Foam is de-molded. Total expansion ratio up to 40.

Figure 3.8: Schema of the two steps compression molding foaming route

Rectangular blocks with densities below 30 kg/m^3 have been produced in this thesis work (see chapter 4). Foams present anisotropic cellular structures with cells preferentially elongated in the growing direction (figure 3.9).
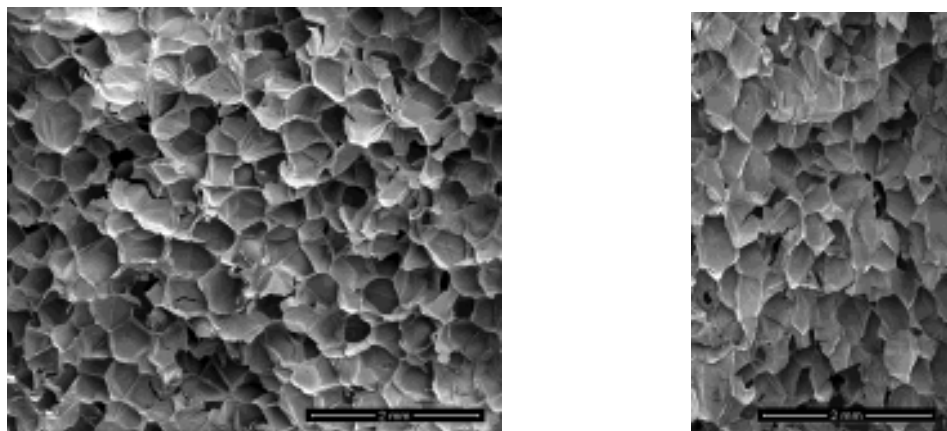
Figure 3.9: cellular structures of samples produce by two-stages compression molding foaming. The image on the left corresponds to a cut perpendicular to the

growing direction and the image on the right corresponds to a cut parallel to the growing direction. A preferential elongation of the cells in the growing direction (thickness of the foam block) can be observed.

A parabolic profile is also found in density. The core of the foamed block has a lower density than the outer solid skins. Several works have studied from a scientific point of view the structure, density, cells geometry and very different issues related with the two-steps compression molding foaming process [6-8]. Further details can be found in chapter 4.

3.2.- RAW MATERIALS

A brief summary of the raw materials used and their main characteristics is presented in this section.

3.2.1.- Polymer matrices

Two different polyolefins were selected as solid matrices for all the foams produced in the frame of this thesis, a low density polyethylene (LDPE) and a high melt strength polypropylene (HMS PP). The LDPE grade selected (table 3.1) has a good extrusion and foaming behaviors and was chosen according to the previous experience of the CellMat Lab. Since one of the aims with the PP was achieving foams with low densities (<200 kg/m^3) a special grade was needed in this case. A branched polypropylene with a high melt strength was the most appropriate for our purposes. These high melt strength polypropylenes are commercially specially designed for foaming purposes. Table 3.1 contains the main features and commercial names of these two polymers

Table 3.1: Main features and commercial names of the two polymer matrices used. (MFI = Melt Flow Index, Tm= melting temperature obtained by DSC, ρ=density).

LOW DENSITY POLYETHYLENE (LDPE)	
Brand Name	*Characteristics*
PE003 Repsol Alcudia	• MFI: 2.4 g/10 min (190 ℃, 2.16 kg) • T_m: 110 ℃ • ρ: 920 kg/m³

HIGH MELT STRENGTH POLYPROPYLENE (HMS PP)	
Brand Name	*Characteristics*
Daploy WB 135 HMS Borealis	• MFI: 2.4 g/10 min (230 ℃, 2.16 kg) • T_m: 165 ℃ • ρ: 890 kg/m³ • Elastic Modulus: 2 GPa

3.2.2.- Nanoparticles

During the last decade the addition of nano-sized particles as fillers to polymer matrices has stimulated much interest within the scientific and industrial communities. As it has been explained in section 2.2 these nanoparticles present a high multifunctionality.

Due to these promising properties, the use of polymer nanocomposites as matrices for foams has focused the attention of researchers in the last years. Foams are not only benefitted from the improvements of the solid matrix but also synergetic effects appear when nanoparticles are present.

Three different types of nanoparticles have been used in the frame of the thesis. A high percentage of the work has been done using organomodified nanoclays as fillers of the polymer matrices. In chapter 6 the work was conducted using also natural nanoclays and multiwall carbon nanotubes. The commercial names as well as the main characteristics of these materials are presented in table 3.2

Table 3.2: Main features and commercial names of the nanoparticles used

MONTMORILLONITE ORGANOMODIFIED NANOCLAYS	
Brand Name	*Characteristics*
Cloisite 20A Southern Clay Products	• Nanoclay organomodified with 2M2HT (Dimethyl dehydrogenated tallow ammonium chloride. • Density: 1.77 g/cm^3 • Basal spacing (d_{001}): 2.42 nm

NATURAL NANOCLAYS	
Brand Name	*Characteristics*
Cloisite Na$^+$ Southern Clay Products	• No organomodification. • Density: 2.86 g/cm^3 • Basal spacing (d_{001}): 1.17 nm

MULTIWALL CARBON NANOTUBES (MWCNT)	
Brand Name	*Characteristics*
Nanocyl NC7000 Nanocyl	• Average diameter: 9.5 nm. • Average length: 1.5 µm • Carbon purity: 90%

For introducing the carbon nanotubes in the formulations a commercial masterbatch was used based on polypropylene. The details concerning this masterbatch are included in table 3.3.

Table 3.3: Commercial masterbatch containing carbon nanotubes used during the research.

MULTIWALL CARBON NANOTUBES (PP MASTERBATCH)	
Brand Name	*Characteristics*
Plasticyl PP2001 Nanocyl	• 20% of MWCNT (Nanocyl NC7000). • MFI: Not measurable. • Tm: 165 ºC • Density: 872 kg/m^3

3.2.3.- Coupling agents

One of the key parameters that deeply determines the properties of a polymer nanocomposite deals with the dispersion and exfoliation of nanoparticles within the polymer matrix and the adhesion between polymer and fillers. Focusing on nanoclays (the most used nanoparticle in the thesis) the delamination of the silicate agglomerates (exfoliation) and the dispersion of the individual platelets is not an easy task. In order

to overcome all the obstacles connected with the dispersion and exfoliation of nanoclays, researchers have followed different approaches [48,49]:

1. Polymerisation in the presence of organoclay.
2. Melt compounding a polymer with a suitable organoclay complex.
3. Other methods as ultrasonic exfoliating of organoclays in a low molecular weight polar liquid or co-precipitation.

Industrially melt compounding is the most attainable approach and it is also the procedure followed in this thesis. Normally grafted polymers are used to improve the coupling between the hydrophilic nanoparticles (nanoclays in our case) and the hydrophobic polymer matrix. In our case the coupling polymers were grafted with maleic anhydride. The main characteristics and commercial names of the selected coupling agents are shown in table 3.4.

Table 3.4: Main features and commercial names of the coupling agents used, one based on polyethylene and the other one based on polypropylene (MFI = Melt Flow Index, Tm= melting temperature obtained by DSC, ρ=density).

COUPLING AGENT BASED ON LLDPE GRAFTED WITH MALEIC ANHYDRIDE	
Brand Name	*Characteristics*
Fusabond MB226DE DuPont	• MFI: 1.5 g/10 min (190 °C, 2.16 kg) • T_m: 115 °C • ρ: 930 kg/m^3 • 0.5% wt. Maleic Anhydride

COUPLING AGENT BASED ON PP GRAFTED WITH MALEIC ANHYDRIDE	
Brand Name	*Characteristics*
Polybond 3200 Chemtura	• MFI: 1.15 g/10 min (190 °C, 2.16 kg) • T_m: 157 °C • ρ: 910 kg/m^3 • 1% wt. Maleic Anhydride

3.2.4.- Blowing Agents

Both physical and chemical blowing agents have been used. An inert gas, CO_2, was used as physical blowing agent. CO_2 was selected because of its higher solubility in a semicrystalline polymer. On the other hand. three different chemical blowing agents were selected for the foaming process: azodicarbonamide, a combination of bicarbonate, citric acid and water and finally microspheres with a volatile hydrocarbon dissolved

inside. The chemical blowing agents were selected according to their suitability for polyolefin matrices. Table 3.5 summarizes the main characteristics of these materials.

Table 3.5: Blowing agents used with their commercial names and main features

PHYSICAL BLOWING AGENT CO_2	
Brand Name	*Characteristics*
CO_2 Airgas Norpac	• Liquid CO_2 • Bottle pressure 50-55 bar • Purity: 99.9%

CHEMICAL BLOWING AGENT: AZODICARBONAMIDE	
Brand Name	*Characteristics*
Porofor ADC M-C1 Lanxess	• Exothermic blowing agent • Decomposition temperature: 210 °C • Average particle size: 3.9 ± 0.6 µm

CHEMICAL BLOWING AGENT: BICARBONATE+CITRIC ACID+H_2O	
Brand Name	*Characteristics*
Hydrocerol BIH40 Clariant	• Endothermic blowing agent • Decomposition temperature: 140 °C • Masterbatch in LDPE, 40% active

CHEMICAL BLOWING AGENT: MICROSPHERES+VOLATILE HYDROCARBON	
Brand Name	*Characteristics*
Expancel 950 DU 80 Akzo Nobel	• Endothermic blowing agent • Expansion temperature: 145°C • Particle size before expansion: 18-24 µm

3.2.5.- Other additives

Other additives in lower additions have been used with different purposes: aiding the extrusion process, improving the foaming, avoiding oxidations, crosslinking the polymer, or lowering the decomposition temperature of the chemical blowing agents. A detailed list of them is presented in table 3.6

Table 3.6: Main features and commercial names of the additives used during the research

OTHER ADDITIVES	
Brand Name	**Characteristics**
Estearic Acid 301 Renichem	• Processing aid.
Irganox 1010 Ciba	• Antioxidant. Used for the formulations with LDPE and PP
Irgafos 168 Ciba	• Antioxidant. Used for the formulations based on PP only
Zinc Oxide (ZnO) Silox Active	• Catalyst of the decomposition reaction of the azodicarbonamide
Luperox DCP40 Arkema	• Crosslinking agent. • 40% of Dicumyl peroxide, 55% of calcium carbonate and 5% of silica gel. • Used for crosslinking LDPE.

3.3.- EXPERIMENTAL TECHNIQUES

Although in all the scientific articles included in this thesis a description of the corresponding experimental techniques is done, table 3.7 includes also a brief compendium of all of them together with the standards and the laboratory equipments used.

Table 3.7: Summary of the experimental techniques used along the work

EXPERIMENTAL TECHNIQUE	CHAPTERS
Density characterization. Archimedes Method Standard UNE-EN 1183/1 Mettler Toledo AT261 scales	4, 5 and 6
Density characterization. Volumetric Method ASTM Standard D1622-08 Mettler Toledo AT261 scales	4, 5 and 6
Scanning Electron Microscopy, (SEM) Electronic Microscope Jeol JSM-820	4, 5 and 6
Transmission electron Microscopy (TEM) Tesla BS 512 with a YAG camera incorporated	4, 5 and 6
Differential Scanning Calorimetry, (DSC) Mettler DSC 822^e	4, 5 and 6
Thermogravimetric Analysis (TGA) Mettler TGA/SDTA 851^e	4, 5 and 6
Extensional Rheology	4 and 6

TA Instruments	
Wide Angle X-rays Scattering (WAXS) Diffractometer Bruker D8	4 and 6
Gas Pycnometry ASTM Standard D6226-10 Micromeritics Accupyc II 1340	4 and 6
Universal testing Machine, (compression, tensile, bending) Standard ISO 527/2 tensile (solids) Standard ISO1926 tensile (foams) Standard ISO 604-2002 compression Standard ISO178 bending	4, 5 and 6
Soxhlet Extraction Standard ASTM D 2765	4
Home-designed compressive creep apparatus Microtest	4
Energy dispersive X-rays diffraction (ED-XRD) EDDi experimental station. BESSY II Synchrotron light source.	4
Optical Expandometer Home-designed equipment	4
X-ray radioscopy Home-designed equipment	5

3.4.- BIBLIOGRAPHY

[1]. M.A. Rodriguez-Perez, J.A. de Saja, J. Escudero, D. de Rosa, J. A. Vazquez. Sistema y procedimiento de molde de piezas con moldes autoportantes. Patente española 201130271. (2011)

[2]. J. Escudero, J. Tirado, M. A. Rodriguez-Perez, J. A. de Saja, D. Rosa, J. A. Vazquez. Stages Molding, a new technology for the production of plastic parts. Technical Paper. EUROTEC 2011.

[3]. J. Escudero, J. Tirado, M. A. Rodriguez-Perez, J. A. de Saja, D. Rosa, J. A. Vazquez. Stages Molding, una nueva tecnología para la producción de piezas de plástico. Revista de Plásticos Modernos, vol. 102, num. 659 (2011).

[4]. J. Escudero, E. Solorzano, M. A. Rodriguez-Perez, F. Garcia-Moreno, J.A. de Saja. Structural characterization and Mechanical Behavior of LDPE Structural Foams. A comparison with Conventional Foams. Cell. Polym. Vol. 28, 4. 289-302 (2009).

[5]. D. Klempner, V. Sendijarevic. Handbook of Polymeric Foams and Foam Technology. 2nd Edition. Hanser Publishers, Munich, (2004)

[6]. J.I. González-Peña. Efecto de los Tratamientos Térmicos en Bloques de Espuma de Polietileno de Baja Densidad fabricados mediante Molde por Compresión. Tesis Doctoral, Universidad de Valladolid, (2006).

[7]. F. Hidalgo. Diseño Optimizado de los Parámetros de Proceso en la Fabricación de Espumas de Poliolefina Reticulada mediante Moldeo por Compresión. Tesis Doctoral, Universidad de Valladolid, (2008).

[8]. C. Saiz-Arroyo, J.A. de Saja, M.A. Rodríguez-Pérez. Production and characterization of crosslinked low-density polyethylene foams using waste of foams with the same composition. Polymer Engineering and Science, *Volume 52, Issue 4*, pp. 751-759, (2012).

[9]. M.A. Rodríguez-Pérez, J. Lobos, C.A. Pérez-Muñoz, J.A. de Saja, L. González, B.M.A. del Carpio. Mechanical behaviour at low strains of LDPE foams with cell sizes in the microcellular range: Advantages of using these materials in structural elements. Cellular Polymers 27: 347-362, (2008).

[10]. M.A. Rodríguez-Pérez, J. Lobos, C.A. Pérez-Muñoz, J.A. de Saja. Mechanical response of polyolefin foams with high densities and cell sizes in the microcellular range. Journal of Cellular Plastics 45: 389-403, (2009).

[11]. M. A. Rodriguez-Perez, J. A. de Saja, J. Escudero, A. Lopez-Gil. Procedimiento de fabricación de materiales celulares de matriz termoplástica. Patente Española 201231092. (2012)

[12]. Y. Ma, R. Pyrz, M. A. Rodriguez-Perez, J. Escudero, J. C. Rauhe, X. Su. X-ray microtomographic study of nanoclay-polypropylene foams. Cell. Polym. Vol. 30, 3, 95-110. (2011)

[13]. S. Román-Lorza. Formulación y Caracterización de Materiales Celulares Retardantes de Llama libres de Halógenos basados en Poliolefinas. Tesis Doctoral, Universidad de Valladolid, (2010).

[14]. S. Román-Lorza, M.A. Rodríguez-Pérez, J.A. de Saja. Cellular structure of halogen-free flame retardant foams based on LDPE. Cellular Polymers 28: 249-268, (2009).

[15]. S. Román-Lorza, M.A. Rodríguez-Pérez, J.A. de Saja, J. Zurro. Cellular structure of EVA/ATH halogen-free flame retardant foams. Journal of Cellular Plastics 10: 1-21, (2010).

[16]. S. Román-Lorza, J. Sabadell, J.J. García-Ruiz, M.A. Rodríguez-Pérez, J.A. de Saja. Fabrication and characterization of halogen free flame retardant polyolefin foams. Materials Science Forum 636/637: 98-205, (2010).

[17]. M.A. Rodríguez-Pérez, R.D. Simoes, C.J.L. Constantino, J.A. de Saja. Structure and physical properties of EVA/Storch precursor materials for foaming applications. Journal of Applied Polymer Science 212: 2324-2330, (2011).

[18]. M.A. Rodríguez-Pérez, R.D. Simoes, S. Román-Lorza, M. Álvarez-Laínez, C. Montoya-Mesa, C.J.L. Constantino, J.A. de Saja. Foaming of EVA/starch blends: Characterization of the structure, physical properties and biodegradability. Polymer Engineering and Science 52: 62-70, (2012).

[19]. Martini J, Suh NP, Waldman FA. Microcellular closed cell foams and their method of manufacture. Patent 4473665 USA. Massachussets Institute of Technology (1984).

[20]. Martini J, Waldman FA and Suh NP. The production and analysis of thermoplastic microcellular foams. SPE ANTEC vol. 28. San Francisco CA; 1982 p. 674.

[21]. V. Kumar, N. P. Suh. A process for making microcelular thermoplastic parts. Polym. Eng. Sci 20, 1323 (1990)

[22]. V. Kumar, G. Schirmer. Semi-continous production of solid-state PET foams. SPE ANTEC Tech. Papers, 41, 2189 (1995)

[23]. C. B. Park and N. P. Suh. A microcellular processing study of Poly(ethylene-terephtalate) in the amorphous and semicrystalline states. Polym. Eng. Sci. 36, 34 (1996)

[24]. Lee, YH ; Kuboki, T ; Park, CB ; Sail, M. The effects of nanoclay on the extrusion foaming of wood fiber/polyethylene nanocomposites. Polym. Eng. Sci. 51, 5, 014-1022 (2011)

[25]. Wong, S ; Lee, JWS; Naguib, HE; Park, CB. Effects of processing parameters on the mechanical properties of injection molded thermoplastic polyolefin (TPO) cellular foams. Macromol. Mat Eng. 293, 7, 605-6013 (2008)

[26]. Otsuka T, Taki K, Ohshima M. Nanocellular foams of PS/PMMA polymer blends. Macromolecular Materials and Engineering 2008 ; 293 (1),78-82.

[27]. Taki K, Waratani Y, Ohshima M. preparation of nanowells on a Ps-b-PMMa thin film by CO_2 treatment. Macromolecular Materials and Engineering 2008; 293 (7), 589-97.

[28]. Kumar V, Weller JE. Production of microcellular polycarbonate using carbon dioxide for bubble nucleation. Journal of Engineering in Industry 1994; 116; 413-20.

[29]. Collias DI, Baird DG, Borggreve RJM. Impact toughening of polycarbonate by microcellular foaming. Polymer 1994; 35; 3978-83.

[30]. Murray RE, Weller J, Kumar V. Solid state microcellular acrylonitrile-butadiene-styrene foams. Cellular Polymers 2000; 19 (6); 413-25

[31]. Nawaby V, Handa P, Fundamental understanding of the ABS-CO_2 interactions, its retrograde behavior and development of nanocellular structures ANTEC vol. 2. Chicago IL. 2004 p. 2532-6.

[32]. S. K. Goel and E. J. Beckman. Generation of microcellular polymeric foams using supercritical carbon dioxide. Polym. Eng. Sci., 34, 1137-48 (1994).

[33]. Kumar V, Weller JE. A process to produce microcelular PVC. International Polymer Processing 1993; VIII (I); 73-80.

[34]. Sauceau, M ; Fages, J; Common, A ; Nikitine, C; Rodier, E. New challenges in polymer foaming : a review on extrusion processes assisted by supercritical carbon dioxide. Prog. Polym. Sci. 36, 6. 749-766.

[35]. Lee J. S. W., Park C.B. Use of nitrogen as blowing agent for the rproduction of fine celled high density HDPE foams. Macromo. Mat. And Eng. 291, 10. 1233-1244 (2006).

[36]. Naguib H. E., Park C.B., Panzer U., Reichelt N. Strategies for achieving ultra low density PP foams. Polym. Eng. And Sci. 2002. 42, 7, 1481-1492.

[37]. Velasco J. I., Antunes M., Realinho V., Ardanuy M. Characterization of polypropylene based microcelular foams produced by batch foaming process. Polym. Eng. And Sci. 2011. 51, 11, 2120-2128

[38]. Park C. B. Cheung L. K. A study of cell nucleation in the extrusion of polypropylene foams. Polym. Eng. And Sci 1997. 37, 1, 1-10.

[39]. D. Miller, V. Kumar. Fabrication of microcellular HDPE foams in a sub-critical CO_2 process. Cell. Polym. 28, 1, (2009)

[40]. Z. Xing, G. Wu, S. Huang, S. Chen, H. Zeng. Preparation of crosslinked polyethylene foams by a radiation and supercritical carbon dioxide approach. J. of Supercritical Fluids 47, 281-289 (2008)

[41]. P. Zhang, N. Q. Zhou, Q. F. Wu, M. Y. Wang, X. F. Peng. Microcellular foaming of PE/PP blends. J. of Applied Polymer Science, 104, 4149-4159 (2007)

[42]. Zhai, W; Wang, H; Yu, J; Dong, JY; He, J. Foaming behavior of isotactic polypropylene in supercritical CO_2. Polymer 49, 13-14, 3146-3156. (2008).

[43]. Yuan, MJ; Winardi, A; Gong,SQ; Turng, LS. Effects of nano- and microfillers and processing parameters on injection molded microcellular composites. Polym. Eng. Sci. 45, 6, 773-788. (2005)

[44]. Jo, C; Naguib, HE. Constitutive modelling of polymer HDPE/clay nanocomposite foams. Polymer, 48, 11, 3349-3360 (2007)

[45]. Taki, K; Tabata, K ; Kihara, S; Ohshima, M. Bubble coalescence in foaming process of polymers. Polym. Eng. Sci. 46,5, 680-690.(2006)

[46]. D. Eaves. Handbook of Polymer Foams. Rapra Technology, United Kingdom, (2004).

[47]. F. Hidalgo. Diseño Optimizado de los Parámetros de Proceso en la Fabricación de Espumas de Poliolefina Reticulada mediante Moldeo por Compresión. Tesis Doctoral, Universidad de Valladolid, (2008).

[48]. L. A. Utracki. Clay-containing polymeric nanocomposites vol.1. Rapra Technology Limited. United Kingdom (2004).

[49]. L. A. Utracki. Clay-containing polymeric nanocomposites vol.2. Rapra Technology Limited. United Kingdom (2004).

Chapter 4

Modifications in the Polymer Matrix

4.1.- INTRODUCTION

The present chapter is focused on the production of polyolefin based cellular materials with improved physical properties by the modification of the polymer matrix, and at the study and characterization of these physical properties. As previously mentioned in chapters 1 and 2, modifications in the polymer matrix can be divided into two different types: modifications in the chemical composition of the polymer matrix and modifications of its molecular architecture.

The chapter is divided according to the kind of blowing agent used: physical or chemical. Only one foaming route has been used with physical blowing agents: solid state batch gas dossilution. On the other hand, two different foaming routes have been followed in the case of chemical blowing agents: free foaming and two-steps compression molding

In the first part of the chapter, dealing with physical blowing agents, two research works are included combining modifications in the chemical composition and modifications in the molecular structure. The second part of the chapter includes four works using chemical blowing agents and combining also modifications in the chemical composition and molecular architecture. The base polymer matrix used in all of them is a low density polyethylene (LDPE).

4.2.- POLYOLEFIN BASED CELLULAR MATERIALS FOAMED BY PHYSICAL BLOWING AGENTS AND IMPROVED BY MODIFICATIONS IN THE POLYMER MATRIX

In this first part of the chapter the modifications in the polymer matrix have been combined with solid state batch gas dissolution (described in chapter 3) that uses CO_2 as physical blowing agent. The modifications in the polymer matrix go in two different ways: addition of nanoclays and coupling agents as modifiers of the chemical composition of the polymer matrix and crosslinking as modification of the molecular architecture.

4.2.1.- Chemical Modifications of the Polymer Matrix

The combination of nanoparticles and physical blowing agents is an interesting system from a scientific and practical point of view. Nanoparticles could act as nucleation sites. The nanometer-size of these particles dramatically increases the number of available nucleation sites together with a consequent decrease in cell size. In the case of nanoclays there are some other interesting effects. The lamellar geometry of this kind of nanoparticles is fundamental in the gas barrier role expected from the addition of these nanoparticles. Nanoclays act as barriers to the gas, increasing the mean free path that a gas molecule must go over in its way to the exterior. Besides this, nanoparticles are known to affect the polymer physical properties. Altogether could contribute to the global improvement of the physical properties of the cellular material: reduced cell size, lower gas diffusion coefficients and improved polymer matrix in the edges.

But obtaining the mentioned improvements is intimately linked to the consecution of a high dispersion degree with high exfoliation of the nanoparticles. With this aim, polymer coupling agents together with chemically modified nanoparticles are used.

The work included in this section is entitled *"Sorption Behaviour and Microcellular Foaming in LDPE/Clay Nanocomposites by Batch Gas Dissolution in Sub-Critical Conditions"*. The main objective of this work is studying the foaming behavior of a semi-crystalline polymer matrix as LDPE filled with montmorillonite-type nanoclays using CO_2 in sub-critical conditions. Prior to the foaming, the diffusivity and solubility of the gas and the influence of nanoclays on these two parameters are studied and correlated with the later foaming. The influence of the coupling agent (MAH-g-LDPE) by itself is also elucidated.

Solubility is increased in samples containing nanoclays due to the existence of interfaces polymer/clays that allow the adsorption and immobilization of gas molecules. Besides, reductions in diffusivity up to 11% are found with additions of 3 wt.% of nanoclays. Interestingly, the higher is the nanoclays content, the lower is the decreased found in diffusivity. This fact is connected with the already mentioned presence of interface polymer/clay that facilitates the diffusion of the gas across them.

When the polymer matrix is chemically modified only with the addition of a coupling agent based on maleic anhydride grafted polyethylene (no nanoclays), reductions in diffusivity up to 30% are found. The more linear character of this

polyethylene together with the polar character of maleic anhydride and its higher affinity with CO_2 justify this result.

The rheology of the polymer is deeply modified when nanoclays are present. In fact this effect on the polymer rheology have a detrimental effect on the foamability of the samples. In any case expansion ratios up to 2 with cell sizes below 80 μm are achieved. It must be taken into account that these expansion ratios and cell sizes are obtained in a semi-crystalline polymer matrix filled with an inorganic filler and using gas in sub-critical conditions. These conditions are not favorable for a foaming process of this nature.

Finally a nucleating effect is observed understood as a reduction in the energy needed for the nucleation and growth of cells. Therefore the foaming is accelerated in the samples containing nanoclays with a cellular structure that that starts growing at lower times.

SORPTION BEHAVIOUR AND MICROCELLULAR FOAMING IN LDPE/CLAY NANOCOMPOSITES BY BATCH GAS DISSOLUTION IN SUB-CRITICAL CONDITIONS

J. Escudero[1], V. Kumar[2], M. A. Rodriguez-Perez[1]

[1]*Cellular Materials Laboratory (CellMat), Condensed Matter Physics Department, University of Valladolid, Paseo de Belén, 47011 Valladolid, Spain. Email: marrod@fmc.uva.es, jabo@fmc.uva.es tel.: +34983423572*

[2]*Department of Mechanical Engineering. University of Washington. Stevens Way, WA 98195. Seattle, Washington, USA.*

ABSTRACT

The batch gas dissolution foaming method has been intensively used for the foaming of amorphous polymers but is not common in the case of semi-crystalline ones, moreover when a nanometer-sized inorganic phase is present in the polymer as in this case. In one step prior to the foaming the solubility and diffusivity of CO_2 have been studied in these samples. The presence of nanoclays increases the gas solubility and slightly reduces the diffusivity. The presence of interfaces polymer-nanoclays justifies these results. In these sub-critical foaming conditions expansion ratios up to 2 with cell sizes of the order of 80 μm were obtained. Finally an interesting nucleation effect of the nanoclays was also observed.

Keywords: gas dissolution, nanoclays, diffusivity, nucleation polyethylene foams.

INTRODUCTION

During the last decade the excellent properties of polymer-clay nanocomposites have stimulated much interest and research within the scientific and industrial communities. With much less inorganic contents of clay than comparable glass- or mineral-reinforced polymers, polymer-clay nanocomposites exhibit physical and mechanical properties significantly different from their more conventional counterparts. They have good thermal stability, high heat distortion temperature, superior barrier properties and high specific stiffness at low concentrations of filler (<5 wt.%) [1-4]. However the highest enhancement in properties improvement can only be realized when the nanoparticles are dispersed uniformly (exfoliated) in the polymer matrix. In the natural state montmorillonite (the most used clays) platelets are held together by van der Waals forces and electrostatic forces to form crystallites (tactoids). Organic cationic surfactants e.g. alkyl ammonium salts are commonly used to modify the negatively charged clay surface through ion exchange, in order to improve wetting and reduce interfacial tension between the polymer and clay that in turn enhances dispersion. Favorable interactions between the polymer matrix and clay surface and the resulting energy reduction

are critical for the formation of exfoliated nanocomposites [1,2, 5-9] . The less desirable but more attainable structure is an intercalated particle dispersion where polymer chains penetrate into the interlayer region of clays to form nanocomposites without totally disrupting crystallites. Particularly barrier properties depend strongly on the extents of intercalation (or exfoliation), orientation and dispersion of nanometer-sized silicate platelets in a polymer matrix. The improvements in barrier properties can be explained by the concept of tortuous paths, that is, when impermeable nanoparticles are incorporated into a polymer the permeating molecules are forced to wiggle around them in a random walk what finally turns to be a tortous pathway. Several theoretical works try to model the expectable reductions in diffusivity from the knowledge of intrinsic parameters of the layered silicates as for example the length, width and the volume fraction of the sheets. The orientation of the sheets together with the state of delamination also play a fundamental role, the permeability is extremely sensitive to the size of the aggregates [3,12]. Experimentally the literature includes several experimental works dealing with different polymer/layered silicate nanocomposite systems characterized by very strong enhancements of their barrier properties. Tortora et al. measured the transport properties of PU/MMT nanocomposites finding changes in the sorption behavior of different hydrophilic and hydrophobic permeants [10]. Ke and Yongping tested the O_2 permeability of intercalated PET nanocomposites. Small amounts of clays effectively reduced the permeability of the PET film [11]. Ogasawara et al. reported also improvements on the helium gas barrier properties of epoxy/MMT nanocomposites finding ten times reductions with the addition of 6 wt.% nanoclays [12]. Even higher reductions are found by Ray et al. in PLA nanocomposites at comparable clay loadings using O_2 as permeant [13]. Literature on the gas barrier properties of nanocomposites based on polyolefins is not so extended. In these systems the highly desirable exfoliation and intercalation are especially challenging and very difficult to obtain. The hydrophobic character of these polymers prevents the development of strong interactions with the aluminosilicate surfaces of the montmorillonites especially the galleries in which the polymer chains need to be inserted for intercalated or exfoliated structures [14-17]. Not only the geometrical morphology of the silicates must be considered but also the kind of organomodification of the particles, the type of coupling agent used and the interfaces formed between the nanoparticle and the polymer matrix are key parameters. These have been proved in polyethylene/nanoclays systems by Picard et al.[18, 19] and Jacquelot et al. [15]. The reductions in diffusivity are much lower than the values theoretically expected and the solubility presents a contradictory behavior. The addition of an inorganic phase should reduce the solubility since gas cannot be dissolved in it, but on the contrary higher values of solubility are found due to the mentioned interfaces formed between the polymer and the nanoclays.

The use of these polymer clay nanocomposites as matrix for foams has been intensively studied also in the last years. The efforts have been focused both in thermoplastic (amorphous and semi-crystalline) and thermoset polymers. The infused nanoparticles have been also very diverse, from carbon nanotubes or nanoclays (mainly montmorillonite) to carbon nanofibers or silica particles [20-26]. Although both physical and chemical blowing agents have been used, the vast majority of the published studies deal with the former ones. Special attention has been paid to the microcellular foamability of these composites [27-30]. Microcellular foams provide improved mechanical and thermal insulation properties over conventional foams but they

require stringent processing conditions such as high pressures, pressure drop rate and a narrow window of processing temperature. The production of microcellular foams is even more difficult in semicrystalline polymers due to the low solubilities of gas in these polymer matrices [31-34]. In an effort to overcome these difficulties supercritical gases have been used in almost all the studies dealing with microcellular foams from semicrystalline polymers [35-39]. This supercritical state allows for higher solubilities and diffusivities but the more complex set up needed rises as an important disadvantage both at laboratory and industrial scale. When increasing pressure above the CO_2 supercritical range, the expense of the foaming process greatly increases due to the need for gas pumps and high pressure rated vessels.

Information regarding foamed polyethylene/nanoparticles systems is scarce though some examples can be found. The semi-crystalline character of polyethylene adds a severe difficulty to the foaming using physical blowing agents. Lee et al. investigated the effect of clay particles on the cell morphology of HDPE/clay nanocomposite foams produced using a batch foaming process [40]. They proved that in comparison with neat HDPE, foamed nanocomposites presented finer and more uniform cellular structures. The influence of clays dispersion on the extrusion foaming by supercritical CO_2 of LDPE was also studied by Lee et al [41]. Few works can also be found using thermally decomposed blowing agents. Riahinezhad studied the correlation between rheology and morphology in blends of PE/EVA containing clays [42], reductions in the cell sizes and increments in the cell density were found with the addition of the layered silicate nanoparticles. Finally Saiz-Arroyo et al. studied the foaming behaviour of a more uncommon system of polyethylene containing nanosilicas. Two foaming routes were used for this purpose, one following the pressure quench method using CO_2 as blowing agent and another one by improved compression moulding using azodicarbonamide [43].

The addition of particles in the nanometer size range has usually a nucleating effect during foaming by microcellular procedures. The combination of nanoparticles with microcellular foaming yields synergetic effects that cannot be understood considering them separately [44]. These synergetic effects turn these foamed nano-filled systems especially interesting both from a scientific and industrial point of view.

In this work a batch gas dissolution foaming technique has been selected for the production of microcellular foams. This technique allows both for the foaming and for a prior study of the permeability of gas in the matrix by the gravimetric method. Not only the influence of the nanoclays on the gas diffusivity has been studied but also the influence of the coupling agent. The data has been correlated with the crystallinity and exfoliation/dispersion morphology of the nanoclays in the composites and later on with the foaming. The foaming has been performed in the less favorable and not intensively studied conditions: semi-crystalline polymer filled with inorganic nanoparticles, gas in sub-critical conditions and by a batch gas dissolution route with saturation at room temperature. An approximation from the rheological behavior of the solid matrices has been followed for understanding the cellular structures. Special attention has been paid to the occurrence of the strain hardening phenomenon This approximation, not commonly followed, finally turns to be indispensable in understanding the obtained results.

EXPERIMENTAL

Materials and Sample preparation

A low density polyethylene PE003 from Repsol Alcudia with 2 g/10min (2.16 kg and 190 ºC) of MFI, density of 920 kg/m^3 and 110 ºC of melting point was used as polymer matrix. For the nanocomposites this polymer matrix was melt blended with montmorillonite-type organomodified nanoclays Cloisite C15A from Southern Clay Products and a coupling agent, maleic anhydride grafted polyethylene Fusabond 226 DE from DuPont (1.5 g/10min of MFI, 120 ºC of melting point). The blending was performed in a twin screw extruder Bühler BTSK 20/40D at 250 rpm with a die temperature of 190 ºC. The proportion of coupling agent to nanoclays was maintained constant in 2:1. In order to clearly distinguish the role played by the nanoclays the PE003 was also melt blended with the coupling agent only. The proportion PE003/coupling agent was maintained equal to the one used in the case of the filled composites. Two different clay contents were used, 3 wt.% and 5 wt.%. The compositions and nomenclature used are summarize in Table 1.

Table 1: Proportion of components for the different kind of samples

Sample	Matrix/parts	Coupling agent/parts	Nanoclays/parts
Unfilled-3%	91	6	0
3% Nanoclays	91	6	3
Unfilled 5%	85	10	0
5% Nanoclays	85	10	5

Solid precursors were produced by compression moulding the raw materials to discs with an uniform thickness of 1.27 mm using two stainless steel plates in a hot press at 190 ºC for 15 minutes and then cooling down with the pressure still applied at a constant cooling rate of 50ºC/min. Then, these discs were cut in pieces of 15 mm x 15 mm for gas dissolution and foaming process

Characterization of solid samples

A Mettler DSC822e differential scanning calorimeter was used for the thermal analysis of the samples a. A heating rate of 10 ^{o}C under N$_2$ environment and a sample weight of 5±0.5 mg were used in all the tests. Crystallinity degree was calculated from the area of the DSC peak, by dividing the heat of fusion by the heat of fusion of a 100% crystalline material, (288 J/g for a 100% crystalline polyethylene [45]). The crystallinities were calculated taking into account the real proportions of polymer deducting the amount of nanoclays.

Rheological behavior was studied by means of a AR2000EX TA Instruments rheometer with an extensional fixture at a temperature of 130 ºC (coinciding with the foaming temperature used as explained later) and a strain rate of 0.5 s^{-1}.

The dispersion and exfoliation of nanoclays were studied by X-ray diffraction (XRD) and transmission electron microscopy (TEM). XRD diffractograms were determined between 1º and

5o by steps of 0.005o by means of a Philips PW 1050/71 using the Cu Kα line. The transmission electron microscope used was a Tesla BS 512 with a YAG camera incorporated. Several images from different areas were analyzed to have representative conclusions.

Foaming procedure

Both the samples with and without nanoclays were microcellular foamed. The batch microcellular foaming procedure is well described in [33,47]. The samples were first saturated in a pressure vessel with an industrial grade CO_2 at room temperature and 5 MPa. Pressure was controlled within ±0.03 MPa by a pressure controller. The saturation time was set to 48 hours, well above the required time for full saturation.

When the pressure was relieved, the samples were immersed in a pre-heated hot glycerin bath for a definite period of time at a certain temperature. They were then quenched in cold water.

Morphology and density of the foams

Density of the samples was measured by Archimedes principle using a Mettler AE240 balance with accuracy of ±10 μg.

The cellular morphology was characterized by scanning electron microscopy (SEM) with a JEOL JSM-820 microscope. Samples were immersed in liquid nitrogen for 5 minutes, fractured and mounted on stubs. The fracture surfaces were sputter coated with gold prior to the microscopy work. The mean cell size and cell density were obtained using image processing software Image J from at least 75 cells in different micrographs from the same specimen [46,47].

Diffusion studies

For characterizing the absorption of gas samples were taken out from the vessel at certain periods of time, weighted using the aforementioned balance and immediately put back inside the vessel at 5 MPa.

Diffusivities of different samples were determined from weight measurements made during the desorption. For this purpose the "Initial Gradient Method" was employed. It states that, for the early stages of desorption the solution of the diffusion equation for a polymer-gas system with a constant diffusivity is given by

$$\frac{M_t}{M_\infty} = \frac{4}{\pi^{1/2}} \left(\frac{Dt}{l^2}\right)^{1/2} \quad (1)$$

Where M_t is the total amount of gas absorbed in the polymer sheet at time t, M_∞ is the equilibrium gas concentration attained theoretically after infinite time, D is the diffusivity and l is the thickness of the polymer sheet. A plot of M_t/ M_∞ as a function of $t^{1/2}/l$ yields essentially a straight line (for the initial period of test) with a slope of $4(D/\pi)^{1/2}$ which is readily solved for D. This value of diffusivity obtained during the desorption stage was afterwards used in the general theoretical equation that models the absorption of gas in an infinite plain sheet [49,50].

$$\frac{M_t}{M_\infty} = 1 - \sum_{n=0}^{\infty} \frac{8}{(2n+1)^2 \pi^2} exp\left[\frac{-D(2n+1)^2 \pi^2 t}{4l^2}\right] \qquad (2)$$

The sum was calculated using the first 40 terms and the theoretical results compared to the experimental values measured during the absorption. The agreement between the theoretical and experimental data will be discussed in the next sections.

RESULTS

Characterization of the solid Nanocomposites

All the composites have been produced by melt blending. As already mentioned in the experimental part a coupling agent was first melt blended with the nanoclays in order to promote the exfoliation of the latter ones. The interlamellar space of the nanocomposites was characterize by XRD and compared with the interlamellar space of the nanoclays as received. From figure 1 the Bragg's Law yields a separation between platelets of 2.45 nm for the organomodified nanoclays as received and this separation is increased to a value of 3.27 nm for the nanocomposites always taking the maximum of the peaks for the calculations. This suggests that the melt blending has promoted the exfoliation degree but there are still agglomerates present in the polymer matrix. An exfoliated/intercalated structure is hypothesized for the nanocomposites.
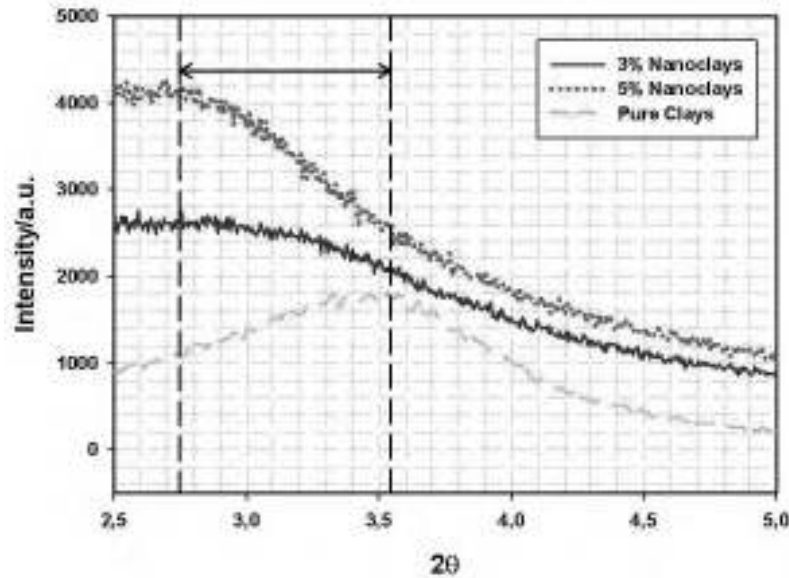
Figure 1: X-ray diffraction curves of the nanocomposites to evaluate the mean interlamellar spacing between platelets.

This structure is confirmed by transmission electron microscopy. Figure 2 a) shows two micrographs for the 5%-Nanoclays samples. On the left individual well exfoliated and dispersed platelets can be distinguished all along the micrograph arranged with a some preferential orientation but in some areas (figure 2 b) still some agglomerates of platelets that have not completely exfoliated can be observed.
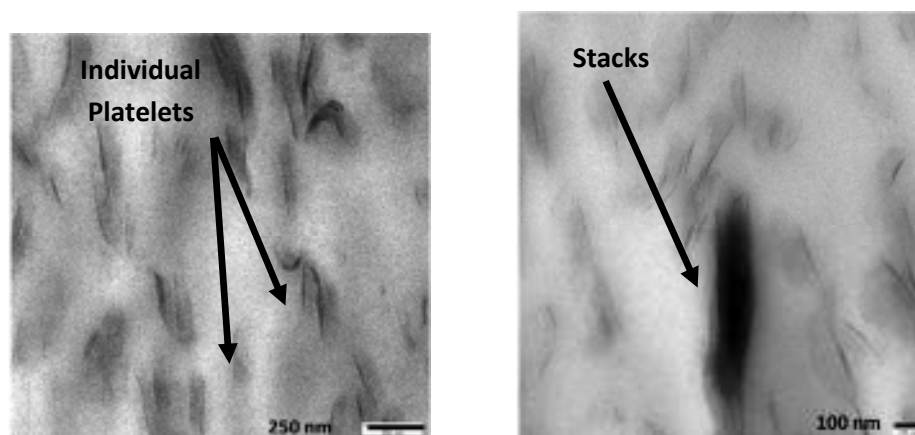
Figure 2: Transmission electron microscopy images obtained

Crystallinity is a parameter of major importance in the study of the sorption behavior of a gas in a polymer. Sometimes nanoparticles are found to play a nucleating role during the crystallization from the melt of several polymers yielding higher degrees of crystallinity [1]. Differential scanning calorimetry provided the results of crystallinity and meting point shown in table 2 for all the formulations

Table 2: Crystallinity and Melting Point for the samples with and without nanoclays

Sample	*Melting Point/ºC*	*Crystallinity/%*
Unfilled-3%	112.07	44.0
3% Nanoclays	111.19	45.4
Unfilled-5%	111.49	45.3
5% Nanoclays	112.52	48.2

The differences in crystallinity between samples are not very large; however a slight nucleating effect of the nanoclays during the crystallization can be inferred for the filled samples. The effect on solubility and diffusivity of this difference in crystallinity will be discussed later.

The rheological behavior is a parameter of major importance that deeply determines the foamability of a polymer matrix. Particularly uniaxial extensional rheology represents well the biaxial flow suffered by the melted polymer during foaming [51,52]. The extensional viscosity of all the samples have been measured at the temperature used later for foaming, this way we will be able to use these data to explain the foaming behavior observed for each formulation. The log-log plot shown in figure 3 depicts the extensional viscosity measurements performed on the samples.
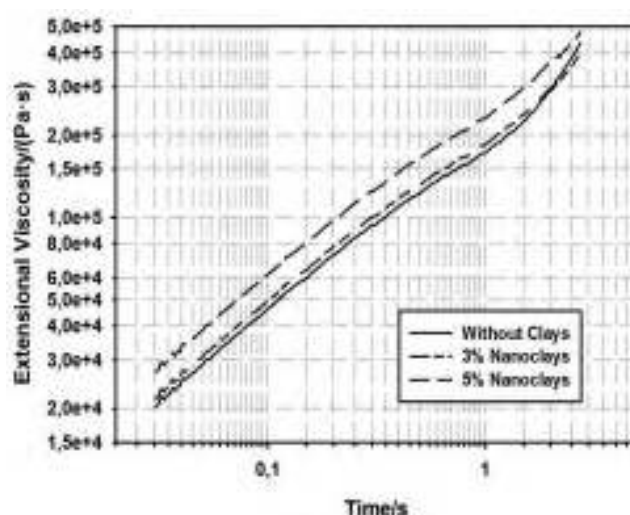
Figure 3: Extensional rheological behavior observed for the unfilled and filled samples at 130 ºC.

The different amounts of coupling agent present in the Unfilled-3% and the Unfilled-5% samples do not influence the extensional viscosity and its behavior is represented by a common plot denoted as "Without Clays". While adding 3 wt.% of nanoclays the extensional viscosity is slightly increased, this increment is much stronger in the case of 5 wt.% nanoclays. This effect of the nanoclays on the viscosity of the polymers was expected. But the strain hardening, defined as an increase of the extensional viscosity with increasing strain at a rate which is higher when compared to the linear viscoleastic limit, is patently reduced for the samples with clays. Table 3 includes the values of the different strain hardening coefficients determined for the different samples at a constant Hencky Strain of 2.5. The reduction in the 5%-Nanoclays samples is even more important than for the 3%-Nanoclays ones. This parameter is directly related with the foamability of any formulation since this enhanced viscosity can reduce the effects of sagging and prevent cell coalescence leading to higher cell concentrations [52]. Lower strain hardenings are commonly translated into poorer foamability. There are several works in the literature that mention also this effect of decreasing in strain hardening with increasing particle concentrations. Particles can partially convert the extensional flow in the surrounding polymer into shear flow and this interferes with the occurrence of strain hardening [53, 54]

Table 3: Strain Hardening coefficients determined for the different sample

Sample	Strain Hardening Coefficient
Without Clays	4.05
3% Nanoclays	3.74
5% Nanoclays	3.18

Sorption Behaviour

One of the beneficial effects expected from the addition of nanoclays to a polymer matrix is the gas barrier role played by these inorganic fillers. Due to its lamellar geometry a good exfoliation and dispersion of nanoclays would increase the mean free path followed by a gas molecule across a polymer.

The batch gas dissolution foaming technique turns to be useful not only for the foaming of the composites but also for the study of the solubility and diffusivity of CO_2 in these polymer/nanoclays composites.

During the gas dissolution at the conditions mentioned in the experimental part the samples were periodically removed from the vessel, weighed and put again inside the vessel at the same temperature and pressure. Samples spent a maximum time of two minutes outside the vessel in each weighing. Table 4 presents the maximum weigh gained by the samples because of the gas dissolved.

Table 4: Maximum gas uptaken at the end of the sorption stage. The values are corrected to the real amount of polymer present in each formulation

Sample	Maximum Gas Uptaken/(mg/g polymer)
Unfilled-3%	28.25
3% Nanoclays	28.55
Unfilled-5%	28.05
5% Nanoclays	30.65

The values for the filled samples have been corrected to the real amount of polymer assuming that the inorganic fillers do not dissolve gas. These corrected values show that the samples with clays absorb more gas than the unfilled counterparts. This difference is especially evident for the 5%-Nanoclays samples with almost a 10% higher amount of gas absorbed. The hypothesis that we set to explain this difference is that there exists an interface polymer-filler in the samples containing clays as a consequence of a non perfect coupling. This interface can be understood as microvoids with the ability of adsorbing gas thus incrementing the total amount of gas dissolved in comparison to the unfilled samples.

The maximum gas uptaken was measured at three different pressures. The case of the Unfilled-5% and 5%-Nanoclays samples represents the behavior found in general for all the samples.. The data obtained is shown in figure 4.
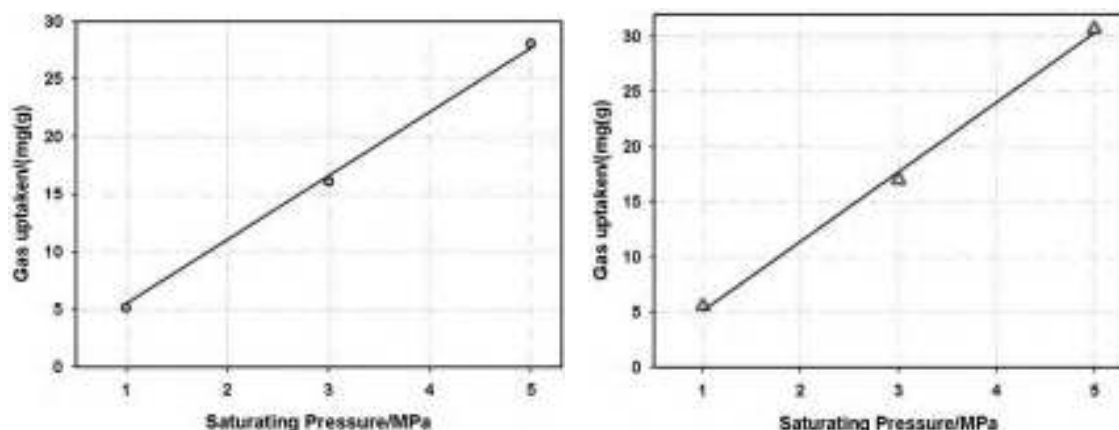
Figure 4: Verification of the Henry's Law for the a) Unfilled-5% and b) 5%-Nanoclays samples

At any pressure the total gas absorbed is higher for the filled composites than for the unfilled but both kind of samples satisfy the Henry's law($C=k_D \cdot P$) in this range of low pressures,

presenting a linear dependency between saturating pressure and total gas absorbed [53]. A dependency according to the Dual Mode Sorption in the case of the 5%-Nanoclays samples would have supported the hypothesis of microvoids in the interface polymer-clays, but is not the case. Assuming a Fickian transport mechanism, the proportionality constant k_D from Henry's law can be identified with the solubility (S) of the composite. Then the solubility for the Unfilled-5% has a value of 5.53 mg/g·MPa in comparison to a value of 6.11 mg/g·MPa for the 5%-Nanoclays. The organophilic clays can give rise to superficial adsorption and to specific interactions with the solvent. It is interesting also that the higher solubilities appear for the samples with slightly higher crystallinity degree. The higher crystallinity reduces the solubility so some adsorption mechanism must be behind the higher solubility values found.

Once the samples were fully saturated were taken out form the vessel for desorption and their weight registered with time. Using the "Initial Gradient Method" the diffusivities (D) were determined from the first stages of the desorption.
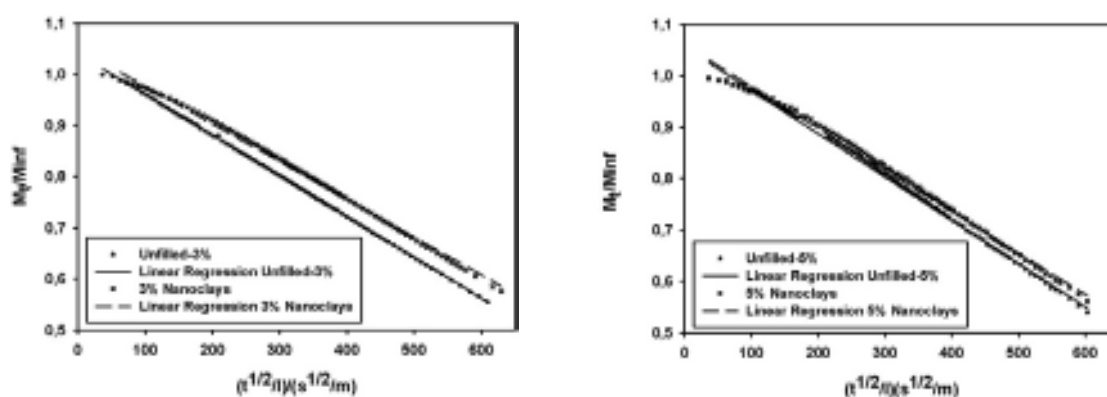
Figure 5: Initial Gradient Method plots. The slope of each plot yields essentially the diffusivities of the samples.

Figure 5 shows the experimental data together with the linear regressions a) for the Unfilled-3% and 3%-Nanoclays and b) for the Unfilled-5% and 5% Nanoclays. From the slope of the linear regressions the diffusivities can be calculated. The values obtained are shown in table 5

Table 5: Diffusivities obtained with the Initial Gradient Method during the desorption.

Sample	*Diffusivity/(cm^2/s)*
Unfilled-3%	$1.21 \cdot 10^{-7}$
3%-Nanoclays	$1.08 \cdot 10^{-7}$
Unfilled-5%	$9.30 \cdot 10^{-8}$
5%-Nanoclays	$8.92 \cdot 10^{-8}$

The addition of 3 wt% nanoclays represent a reduction of 11% in diffusivity. This reduction is lower, near 5% only, in the case of 5 wt.% clays. These moderate reductions in diffusivity can be attributed to the interphase hypothesize between polymer and clays. These interphases would have a detrimental effect on diffusivity allowing gas molecules to find faster ways across the polymer diminishing the gas barrier role played by the platelets. This would justify also that the reduction in diffusivity is lower for the samples with more clays. There are several studies supporting this hypothesis. According to Vankelecom et al.[54] and Picard et al. [18] poor polymer particle interactions lead to an increase of the permeability over the original polymer

because of bypass of gas penetrants around the particles. The interlayer cations used in the clays have also an important influence on the permeability properties of the composite. The slightly higher crystallinity values found for the filled samples should have a negative effect on the diffusivity, with the crystals acting as gas barriers, but the influence of the polymer-clay interphase is higher. It is also interesting to remark that the diffusion coefficient is 30% higher in the samples with lower amounts of coupling agent, hence, lower amounts of maleic anhydride. The polar character of this additive and the high affinity between it and CO_2 can be behind this remarkable difference. This reduction in diffusivity is much higher than the reductions achieved with the addition of lamellar nanoparticles.

The diffusivities obtained from the desorption can be used for modeling the absorption dependency with time. Since the thickness of the samples is much smaller than the other two dimensions we can use equation 2 admitting infinite plain sheets. The agreement between experimental and theoretical data is plotted in figure 6.
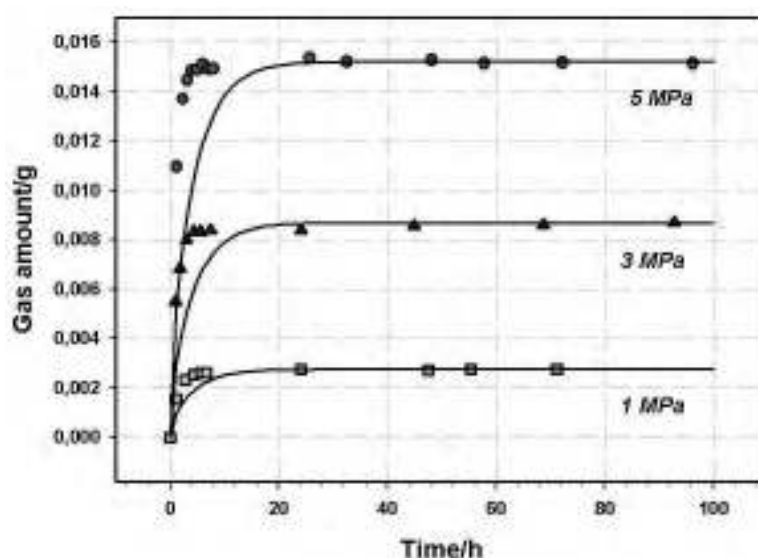
Figure 6: Theoretical and experimental values of the gas uptaken during the sorption stage. The diffusivities obtained previously are used in order to obtain the theoretical solid lines.

Some discrepancies appear at higher pressures between the theoretical (solid line) and experimental (dots) data. The assumption of perfect Fickian transport mechanism with absolute independency between diffusivity and pressure is not completely right but the found discrepancies are low enough to justify this assumption [49]. At the same time the dissolved gas has a plasticizing effect on the amorphous phase of the polymer and so the molecular morphology, which influences the diffusion, is not the same during the sorption as that during the desorption. The found discrepancies are not very big so the implicit assumption of independency between diffusivity and saturating pressure is justified.

Foaming

For foaming, samples were held at a CO_2 pressure of 5 MPa during 48 hours at room temperature. Then, pressure was released and 2 minutes later samples were immersed in a silicon oil bath preheated at 130 ºC. This temperature is around 20 ºC above the melting

temperature of the samples and was selected as the optimum from previous experiences. Upon pressure release no nucleation was visually observed. Immediately after heating the samples are quenched in cold water. These foaming conditions were the same for the samples with and without nanoclays.
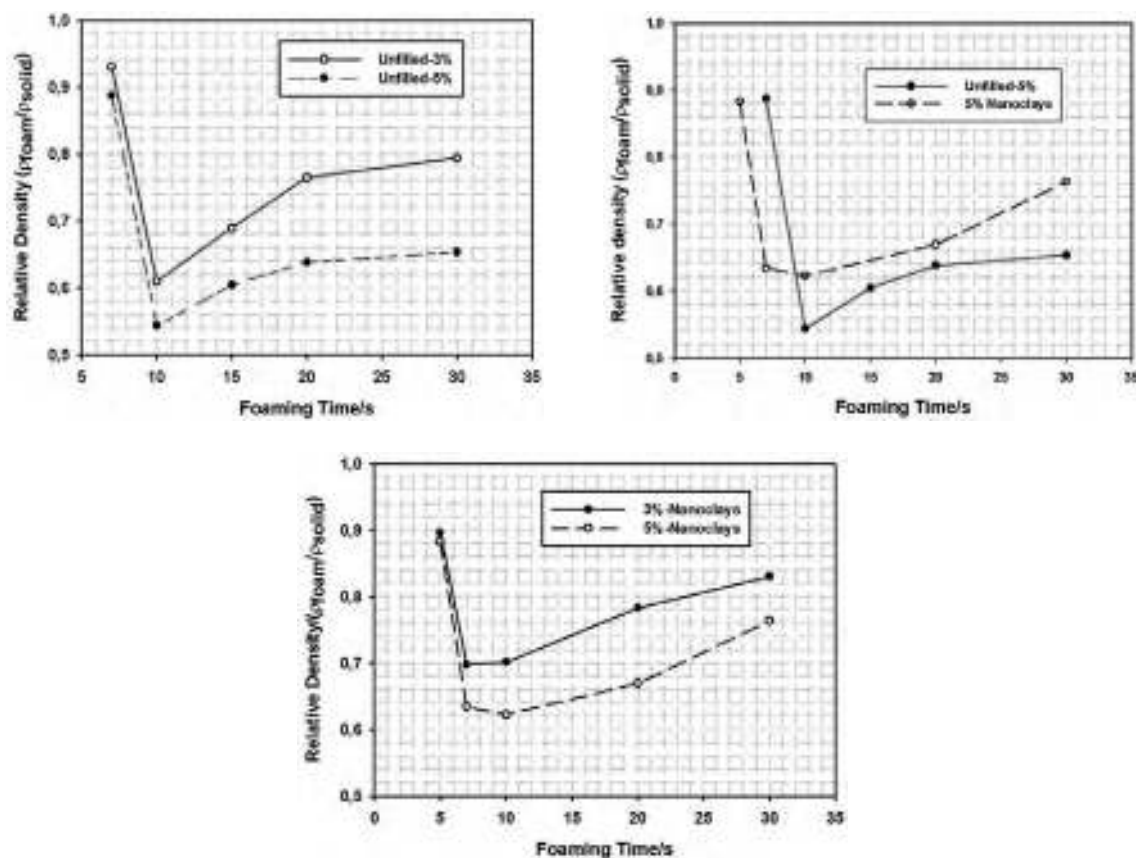
Figure 7: Comparisson of densities for the a) Unfilled-3% and Unfilled-5%, for the b) Unfilled-5% and 5%-Nanoclays and for the c) 3%-Nanoclays and 5%-Nanoclays

There are not large differences between samples of Unfilled-3% and Unfilled-5% in terms of crystallinity, maximum gas uptaken, extensional viscosity or strain hardening but the densities achieved for each of them at different foaming times are remarkably different as shown in figure 7 a). The main difference between samples is the diffusivity, due to the lower diffusivity, at the time of foaming the Unfilled-5% retain more gas than the Unfilled-3% so the ability of withstanding the foaming for these samples is higher. The effect is even clearer for longer foaming times as would be expected. The addition of a coupling agent containing polar molecules of maleic anhydride has a beneficial effect reducing the density. With the gas in subcritical conditions the highest expansion ratio achieved in this semi-crystalline polymer is near 2 (relative density 0.5).

The micrograph on figure 8 shows a general view of the typical morphology common to all the samples foamed following this procedure. Two solid skins appear in the outer parts of the sample because not enough gas remains in these areas at the time of foaming for nucleation. The gas profile across the sample gives also bigger cells in the areas nearer to the skins and the

cell size becomes smaller in the core. The cellular structure homogeneity is much higher in the unfilled samples as it is explained later.
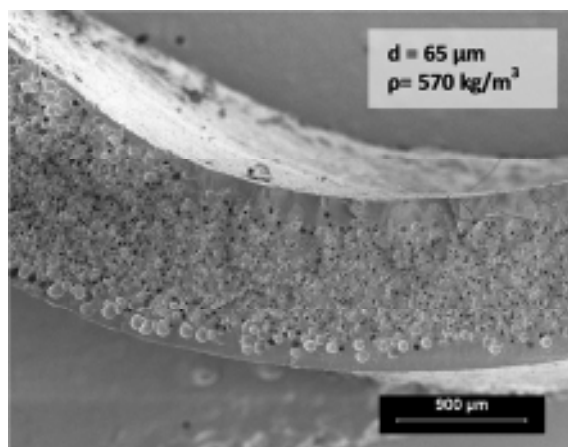
Figure 8: General view of the morphology obtained in the samples by batch gas dissolution in sub-critical conditions. P is the density and d is the average cell size. Unfilled-3% at early stages of foaming.

Although expansion ratios near two with cell sizes below 100 μm have been achieved for this semicrystalline polymer in subcritical conditions the cellular structures are not very stable with foaming time. The instability can be inferred from the density plot in figure 7 and also from the micrographs. Figure 9 depicts an example of the cellular structure of samples foamed at 7 seconds, 10 seconds and 15 seconds of the Unfilled-5%. The not very high population of pores with small cell sizes and high bulk densities shown in figure 9a) at 7 seconds quickly evolves to the one shown in figure 9b) with cell sizes 4 times bigger than in the previous one and bulk densities almost half. 10 seconds foaming time is indeed the one that yields higher reductions in bulk density.
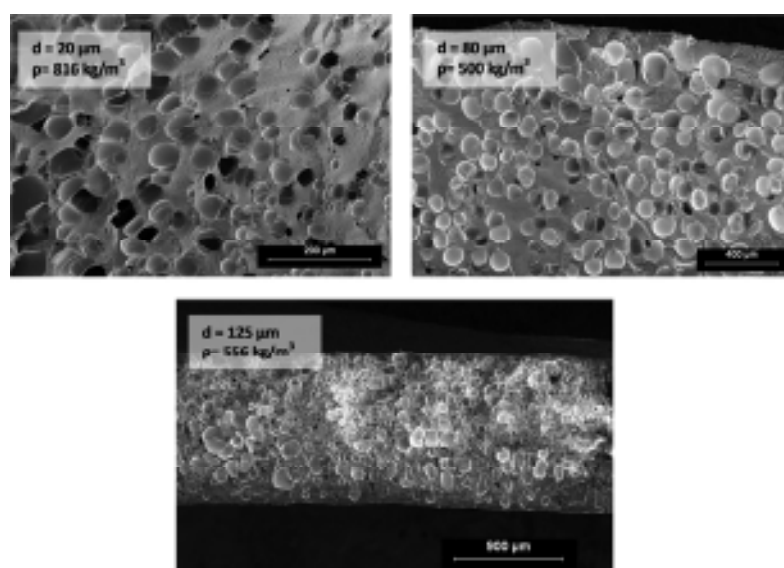
Figure 9: Evolution in the cellular structure for the Unfilled-5% at fixed foaming times of a) 7 seconds, b) 10 seconds and c) 15 seconds.

Further from this point the cell coalescence begins and some big pores appear, mainly in the outer parts of the samples (figure 9c). As a consequence the bulk density increases also. The same trend is observed for the Unfilled-3%. The optimum foams are obtained controlling carefully the foaming conditions used, paying special attention to the foaming time at a fixed temperature.

The addition of nanoclays plays a detrimental role in the foamability of these composites. The reductions in density achievable are lower when nanoclays are present in the formulations as shown in figure 7 b) and 7c) specially in the 3%-Nanoclays case since the proportion coupling agent to polymer is lower. This result is confirmed and supported by the micrographs obtained for the filled foams. In the case of the 5%-nanoclays samples not even a proper cellular structure can be observed. Some small cells seems to have nucleated in the 5 seconds foaming time micrograph shown in figure 10 a). Five seconds later these nucleated cells are translated into cracks and big bubbles in the surface of the foam as shown in figure 10 b). After that the structure is completely collapsed presenting plenty of cracks all across the sample (figure 10 c). The 3%-Nanoclays samples present an intermediate behavior between the Unfilled and the 5%-Nanoclays in terms of cellular structure although the achievable densities are the highest. For those samples, at the early stages of foaming a cellular structure can still be distinguished but it deteriorates extremely quickly.
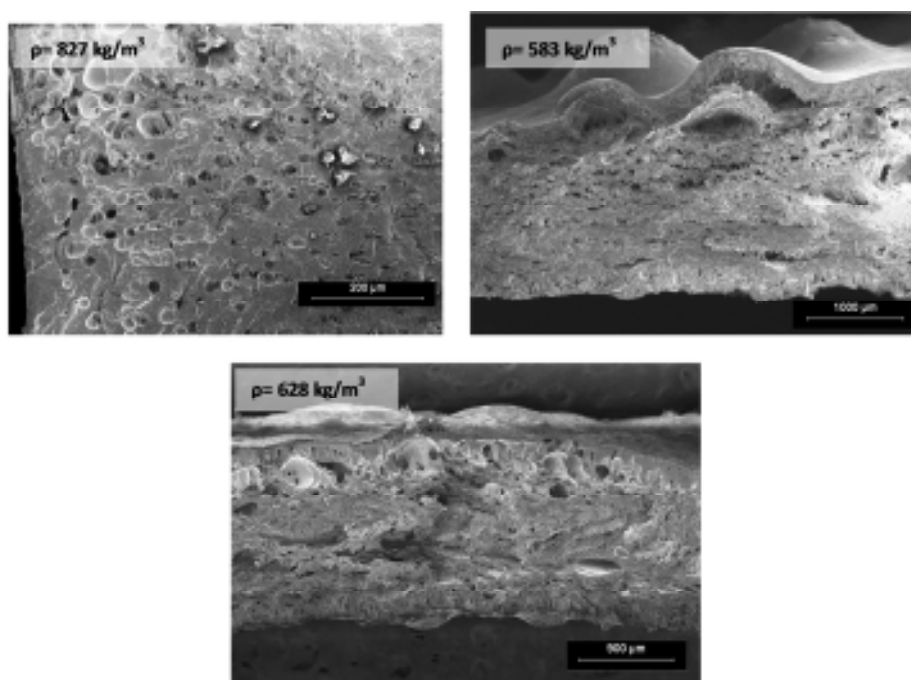
Figure 10: Cellular structure for the 5%-Nanoclays at any foaming time. a) 5 seconds b) 10 seconds and c) 20 seconds.

The reduction in strain hardening observed for the filled samples has a crucial effect on foaming. With the increasing content of clays the polymer melt looses the ability of

withstanding the pressures developed during the cell growth. This justifies the higher densities obtained and the foam morphologies obtained in the case of 3wt.% and 5wt.% clays.

All these results are summarized in figure 11. For a fixed foaming time of 10 seconds micrographs of the Unfilled-5%, 3%-Nanoclays and 5%-Nanoclays are shown. Well developed cells are found for the Unfilled and for the 3 wt.%-Nanoclays but the structure completely collapses when the amount of clays increases up to 5%.
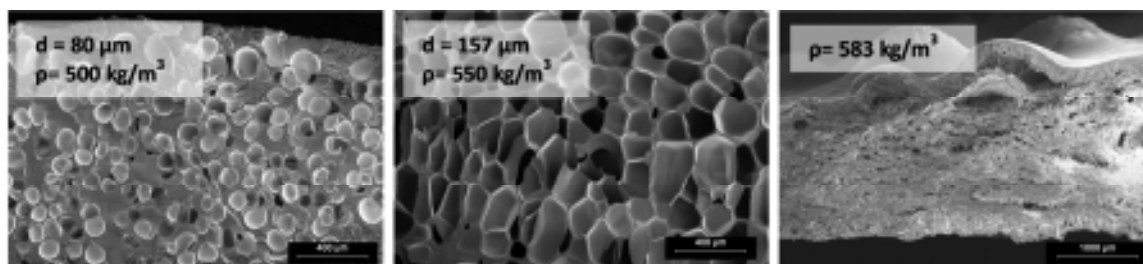
Figure 11:Micrographs at a fixed foaming time of 10 seconds of the a) Unfilled-5% b)3%-Nanoclays and c) 5%-Nanoclays.

It is also interesting the difference in cell density and mean cell size between samples a) and b) in figure 11 taking into account that the foaming time is the same in both cases. The bulk density is approximately the same in both cases but the mean cell size doubles, from a value of 80 μm for the sample without nanoclays to a value of 157 μm for the sample with 3 wt.% of clays and the cell density is reduced in one order of magnitude from $1 \cdot 10^6$ cells/cm^3 to $1 \cdot 10^5$ cells/cm^3. In fact the three micrographs in figure 11 could be understood as three consecutive foaming stages at three different foaming times, from the small cells nucleated in a), growing to a complete and well developed cellular structure in b) and finally collapsing and disappearing in c). These 3 stages are observed at a fixed 10 seconds foaming time simply varying the clay content. This result is explained postulating a nucleating effect of the nanoclays in these nanocomposites. The formation of a new gas phase from a metastable melt phase requires an activation energy barrier to be surmounted to induce the phase separation. In the generally admitted nucleation theory the equations are exponential with respect to this activation energy barrier(ΔG^*) so this parameter is of major importance. The presence of nanoclays lowers this activation energy barrier so nucleation begins at earlier stages. Less energy in the form of heating must be supplied to the sample for the beginning of the nucleation. This hypothesis is supported also from the observation of the densities obtained in figure 7 b). The same relative density is obtained 2 seconds before in the sample containing clays than in the unfilled one (relative densities corresponding to the 5 and 7 seconds foaming time respectively). In fact, the sample containing clays presents a relative density 1.5 times lower at 7 seconds foaming time. This nucleating effect is also the reason for selecting an earlier foaming time of 5 seconds that was not used for the unfilled samples.

Conclusions

In this work the batch gas dissolution method has been used to study, on the one hand the gas diffusivity and solubility and on the other hand the microcellular foamability in sub-critical conditions of well dispersed intercalated/exfoliated LDPE/clays nanocomposites.

In samples containing clays solubility is a 10% higher than in the unfilled samples. These differences in solubility might be due to the existence of interfaces polymer/clays that allow the adsorption and immobilization of gas molecules or to the adsorption of gas on the surfaces of the organophillic matrices and compounds used to modified the clays.

Concerning to diffusivity the addition of 3 wt.% of clays yields reductions up to 11% in this parameter. This reduction in diffusivity is only 5% in the case of samples containing 5 wt.% of nanoclays. The higher amount of interfaces in this later case can be creating more paths for the gas and making easier its escape from the sample increasing therefore the diffusivity. The different amounts of maleic anhydride in unfilled samples give also differences in diffusivity. Samples containing more maleic anhydride present reductions in diffusivity up to 30% in comparison to samples with lower amounts. The polar character of the maleic anhydride and its high affinity with CO_2 justify this result.

The difference in diffusivity between unfilled samples influences their foaming behavior. Samples with lower diffusivities reach also lower densities for any foaming time but this effect is even stronger for long foaming times. Densities near 500 kg/m^3 with mean cell sizes below 80 μm have been obtained for this semicrystalline polymer in sub-critical conditions. The cellular structures obtained are not very stable with time. On the other hand, the addition of nanoclays has a detrimental effect on the foamability of these composites. Densities reachable are always higher in the samples with clays. For 5 wt.% not even a proper cellular structure can be distinguished. The reduction in strain hardening observed in the rheological behavior of the nanocomposites deeply determines the suitability of these samples to be foamed.

Finally a nucleating effect appears with the addition of these nanofillers. This nucleating effect must not be understood as a reduction in cell size for a fixed foaming time in the samples with clays but as a reduction in the energy needed for the nucleation and growth of cells. Therefore the foaming is accelerated in the samples containing nanoclays with cellular structure that begin growing earlier. These means that less heat needs to be supplied to the solid matrix to begin and develop the foaming process.

Bibliography

[1] L.A. Utracki in Clay-containing polymeric nanocomposites. Rapra Technology Limited. United Kingdom (2004).

[2] J. H. Koo in Polymer Nanocomposites. McGraw-Hill. USA (2006).

[3] S. Pavlidou, C.D. Papaspyrides. Prog. Polym. Sci., 33 1119-1198. (2008)

[4] J. Golebiewski, A. Rozanski, J. Dzwonkowski, A Galeski. Europ. Polym, J. 44 270-286 (2008).

[5] P. H. Nam, P Maiti, M. Okamoto, T. Kotaka, N. Hasegawa, A. Usuki. Polymer 42 9633-9640 (2001)

[6] C. E. Corcione, A. Cavallo, E. Pesce, A. Greco, A. Maffezzoli. Polym. Eng. Sci. 51 1281-1285 (2011)

[7] J. Morawiec, A. Pawlak, M. Slouf, A. Galeski, E. Piorkowska, N. Krasnikowa. Europ. Polym. J. 41 1115-1122 (2005)

[8] Y. Teymouri, H. Nazockdast. J. Matter. Sci. 46 6642-6647 (2011).

[9] M. Bousmina. Macromol. 39 4259-4263 (2006).

[10] M. Tortora, G. Gorrasi, V. Vittoria, G. Galli, S. Ritrovati, E. Chiellini. Polym. 43. 6147-6157 (2008)

[11] Z. Ke, B. Yongping. Matter Lett, 59. 3348-3351 (2005)

[12] T. Ogasawara ,Y. Ishida, T. Ishikawa, T. Aoki, T. Ogura. Compos Part A Appl S 37. 2236-2240. (2006)

[13] S.S. Ray, K. Yamada, M. Okamoto, K. Ueda. Polymer 44. 857-866 (2003).

[14] C. Lu, Y. W. Mai. Phys. Rev. Lett. 95, 088303 (2005).

[15] E. Jacquelot, E. Espuche, J. F. Gerard, J. Duchet, P. Mazabraud. J. Polym Sci. 44 431-440 (2006).

[16] R. K. Bharadwaj. Macromol. 34 9189-9192 (2001).

[17] H. R. Dennis, D. L. Hunter, D. Chang, S. Kim, J.L. White, J. W. Cho, D. R. Paul. Polym. 42 9513-9522 (2001).

[18] E. Picard, H. Gauthier, J. F. Gerard, E. Espuche. Colloid and Interface Sci. 307. 364-376 (2007)

[19] E. Picard, A. Vermogen, J. F. Gerard, E. Espuche. J. Poly,. Sci. 46. 2593-2604.

[20]   W. Zhai, C. B. Park, M. Kontopoulou. Ind Eng Chem Res 50, 7282-7289 (2011)

[21]   C. Zeng, X. Han, L. J. Lee, K. W. Koelling, D. L. Tomasko. Adv Mater 15, 1743-1747 (2003).

[22]   Y. H. Lee, K. H. Wang, C. B. Park, M. Sain. J App Polym Sci 103, 2129-2134 (2007).

[23]   S. M. Seraji, M. K. R. Aghjeh, M. Davari, M. S. Hosseini, S. Khelgati. Polym Compos 32, 1095-1105 (2011).

[24]   M. C. Saha, M. E. Kabir, S. Jeelani. Mat Sci Eng A-Struct 479, 213-222 (2008).

[25]   K. Gorem, L. Chen, L. S. Schadler, R. Ozisik. J Supercrit Fluid 51, 420-427 (2010).

[26]   R. Verdejo, C. Saiz-Arroyo, J. Carretero-Gonzalez, F. Barroso-Bujans, M. A. Rodriguez-Perez, M. A.

[27] L. J. Lee, C. Zeng, X. Cao, X. Han, J. Shen, G. Xu. Comp. Sci. Tech. 65 2344-2363 (2005).

[28] C. Zeng, X. Han, L. J. Lee, K. W. Koelling, D. L. Tomasko. Adv. Mater. 15 1743-1747.

[29] J. I. Velasco, M. Antunes, O. Ayyad, C. Saiz-Arroyo, M. A. Rodriguez-Perez, F. Hidalgo, J. A. de Saja. J. Appl. Polym. Sci. 105 1658-1667 (2007).

[30] C. Jo, H. E. Naguib. Polym. 48 3349-3360 (2007).

[31] V. Kumar, N. P. Suh, Polym. Eng. Sci 20, 1323 (1990)

[32] V. Kumar, G. Schirmer, SPE ANTEC Tech. Papers, 41, 2189 (1995)

[33] D. Miller, V. Kumar. Cell. Polym. 28, 1, (2009)

[34] Z. Xing, G. Wu, S. Huang, S. Chen, H. Zeng. J. of Supercritical Fluids 47, 281-289 (2008).

[35] P. Zhang, N. Q. Zhou, Q. F. Wu, M. Y. Wang, X. F. Peng. J. of Applied Polymer Science, 104, 4149-4159 (2007)

[36] Zhai, W; Wang, H; Yu, J; Dong, JY; He, J. Polymer 49, 13-14, 3146-3156. (2008).

[37] Yuan MJ, Winardi A, Gong SQ, Turng LS. Polym. Eng. Sci. 45, 6, 773-788. (2005)

[38] Jo, C; Naguib, HE. Polymer, 48, 11, 3349-3360 (2007)

[39] Taki K, Tabata K, Kihara S, Ohshima M. Polym. Eng. Sci. 46,5, 680-690.(2006)

[40] Y.H. Lee, C.B. Park, K.H. Wang. J. Cell. Plast. 41, 487, (2005).

[41] Y. H. Lee, K. H. Wang, C. B. Park, M. Sain. J. Appl. Polym. Sci. 103, 2129.21-34 (2007).

[42] M. Abbasi, S. N. Khorasani, R. Baheri, J. M. Esfahani. Polym Compos 32, 1718-1725 (2011).

[43]   C. Saiz-Arroyo, M. A. Rodriguez-Perez, J. I. Velasco, J. A. de Saja. Composites part B. Accepted.

[44] C. Saiz-Arroyo, J. Escudero, M.A. Rodriguez-Perez, J. A. de Saja. Cell. Polym. 30, 2, 63-78 (2011).

[45] B. Wunderlich. Macromolecular Physics, 2. Academic Press, New York. 1973-1976.

[46] Paper Pinto

[47] Kumar, V., Suh N.P. Polym. Eng. Sci. 30 (20) 1323-1329 (1990)

[48] Martini J, Suh NP, Waldman FA. Patent 4473665 USA. Massachussets Institute of Technology (1984).

[49] Crank J. In: The mathematics of diffusion. 2nd ed. New York: Oxford Science Press; (1989).

[50] D. L. Tomasko, H. Li, D. Liu, X. Han, M. J. Wingert, L. J. Lee, K. W. Koelling. Ind. Chem. Res. 42 6431-5456 (2003).

[51] Park J. U., Kim J. L., Kim D. H., Ahn K. H., Lee S. J. Macromol Res. 14 (3) 318-323 (2006)

[52] Stange J., Munstedt H. J Cell Plast 42 445-467 (2006)

[53] Le Meins J. F., Moldenaers P., and Mewis J. Ind. Eng. Chem res., 41, 6297-6304. (2002).

[54] Le Meins J. F., Moldenaers P. and Mewis J. Rheologica Acta, 42, 184-190. (2003).

[55] Vieth R. W. in Diffusion in and through polymers: principles and applications. Hanser Publishers, Munich (1990).

[56] I.F.J. Vankelecom, E. Merckx, M. Luts, J.B. Uytterhoeven, J. Phys. Chem 99 13187 (1995).

4.2.2.- Modification of the Polymer Molecular Architecture

In the present section the same materials used in the previous work (filled and unfilled) undergo a crosslinking process using dicumyl peroxide as chemical crosslinking agent. Crosslinking is discussed in chapter 2. Therefore in the work presented in this section the polymer matrix has suffered two different types of changes: chemical modification by the addition of nanoparticles and coupling agents and molecular architecture modification by crosslinking.

The work included in this section is entitled "***Microcellular Foaming in Sub-Critical CO_2 of Non-Crosslinked and Crosslinked LDPE and LDPE/Clay Nanocomposites***". In this work the effects of crosslinking on the gas diffusivity and foamability of filled and unfilled polyethylene nanocomposites are studied.

Crosslinking reduces the crystallinity of the polymer matrix and therefore the gas diffusivity is increased. In spite of this, the foamability of the composites is improved, both in raw samples and in samples containing nanoclays.

Three different crosslinking degrees were induced in each kind of samples. There is an optimum crosslinking degree directly connected with the rheological behavior measured for these samples. Rheology turns to be a key parameter determining the later foamability and properties of the foams.

Finally crosslinking helps to obtain densities below 150 kg/m^3 combined with cell sizes of around 15 µm and cell densities of the order of 10^9 $cells/cm^3$, all this in a semicrystalline matrix and using gas in sub-critical conditions.

MICROCELLULAR FOAMING IN SUB-CRITICAL CO$_2$ OF CROSSLINKED AND NON-CROSSLINKED LDPE/CLAY NANOCOMPOSITES

J. Escudero, E. Laguna, V. Kumar, M. A. Rodriguez-Perez

[1]*Cellular Materials Laboratory (CellMat), Condensed Matter Physics Department, University of Valladolid, Paseo de Belén, 47011 Valladolid, Spain. Email: marrod@fmc.uva.es, jabo@fmc.uva.es tel.: +34983423572*

[2]*Department of Mechanical Engineering. University of Washington. Stevens Way, WA 98195. Seattle, Washington, USA.*

ABSTRACT

The semicrystalline character of low density polyethylene and the inorganic character of nanoclays add severe difficulties to the foamability of these composites by batch gas dissolution in sub-critical conditions. Crosslinking is adopted as a solution that allows achieving high expansion ratios (≈7.5) combined with cell sizes below 10 µm. The rheological properties of the crosslinked composites are connected with their foaming behavior and the stability of the cellular structure. An approach that only takes into account the diffusivities would have been totally insufficient. The presence of nanoclays deteriorate the rheological behavior of the nanocomposites and hence the later foaming behavior. Although this, crosslinking strongly improves the cellular structures and expansion ratios obtained.

Keywords: rheology, crosslinking, nanoclays, gas dissolution, polyethylene foams.

INTRODUCTION

The research in microcellular foams goes back to the early eighties with the work conducted at the MIT in response to a challenge by the packaging and photographic film companies to reduce the amount of polymer used in their products. Reducing the cell size to the order of 10 µm and increasing the cell density to 10^9 cells/cm^3 would improve the strength to weight ratio of conventional foams giving reasonable values for the intended applications [1,2]. This conducted research allowed the development of the batch gas dissolution technique.

From the basic batch gas dissolution, other different, but more complex, semicontinous [3,4] and continous [5-7] methods have been also developed for the microcellular foaming of polymers. In any of these routes most of the efforts have been focused on amorphous polymers such as polystyrene [1,8,9], polycarbonate [10,11], acrylonitrile-butadiene-styrene (ABS) [12,13], poly(methyl methacrylate) [14] and poly (vinyl-chloride) [15] . In comparison very little work has been conducted on the foaming of semicrystalline polymers, and almost only in

continous or with the polymer in the melt state [17-20]. Although the applications of polymers as polyethylene (PE) or polypropylene (PP) are widely spread their semicrystalline character makes difficult obtaining microcellular foams by the batch gas dissolution technique [21, 26]. Gas is admitted to dissolve only in the amorphous phase and the structure of the crystals hinders also its diffusion. The foaming must also be conducted at a temperature near the melting point [28]. In an effort to overcome these difficulties supercritical gases have been used in almost all the studies dealing with microcellular foams from semicrystalline polymers [16, 23-27]. This supercritical state allows for higher solubilities and diffusivities but the more complex setup required is an important disadvantage both at laboratory and industrial scale. When increasing pressure above the CO_2 supercritical range, the expense of the foaming process greatly increases due to the need for gas pumps and high pressure rated vessels.

With the advent of fillers in the nano-range and the incredible properties expected for these innovative additives, the idea of combining nanoparticles and microcellular foaming grew rapidly. Besides the improvements in the solid matrix these nanoparticles act as heterogeneous nucleating sites, reducing the cell size and increasing the cell density [28-34]. The gas dissolution technique would be the perfect candidate for demonstrating all these. Moreover, the combination of microcellular foaming with nanocomposite polymer matrix yields synergetic properties that cannot be inferred considering them separately [29].

Crosslinking is often applied to improve the thermal and mechanical properties of polyethylene due to the formation of a three-dimensional network. It also increases the melt strength which highly improves the foamability of the polymer allowing for important reductions in the reachable density range. The two main methods used for crosslinking polyethylene are electron beam irradiation and peroxide crosslinking. In the irradiation process the crosslinking degree is limited by the depth reached by the electron beam, so the thickness of the materials is restricted [30,31]. The final material has a crosslinking density gradient along its thickness. On the contrary, the use of peroxides, since they are added in the polymer melt, promotes a more uniform distribution of chain interconnections all over the bulk material. Both at an industrial and lab scale the use of peroxide is more affordable with the only disadvantage being the byproducts generated during decomposition [32,33]. The literature dealing with crosslinked foams is very extensive in the case of chemical blowing agents [34,35] and not so broad for physical ones although there are even industrial processes that combine electron irradiation crosslinking with gas dissolution [36,37].

In this study a combination of a semicrystalline polymer with chemical crosslinking, filled with nanoparticles and foamed with sub-critical CO_2 is proposed. Low density polyethylene unfilled and filled with organomodified nanoclays have been microcellular foamed with CO_2 in subcritical conditions and afterwards, both the unfilled and the nano-filled polymers have been chemically crosslinked and microcellular foamed under the same conditions. The foaming of samples with different crosslinking degrees has been studied and connected with their rheological properties. The diffusivities and solubilities for the non-crosslinked unfilled polyethylenes have also been compared with the crosslinked ones. Based on these rheological and diffusive properties an optimum crosslinking degree for foaming has been found. This global approach to understand the foamability of these systems from the rheology and

diffusivity turns to be very useful. Considering only the crosslinking degree would be insufficient to predict foamability. Crosslinking allows also for high density reductions and improvements in the size and homogeneity of the microcellular structures. Expansion ratios up to 7.5 with cell sizes below 10 µm have been reached for this semicrystalline polymer. This combination of low densities with cells in the microcellular range and foaming in sub-critical conditions in semicrystalline polymer makes these materials interesting both from an industrial and scientific point of view. Poorer results were found while foaming the samples containing clays but also in this case crosslinking helps to obtain much more uniform cellular structures.

EXPERIMENTAL

Materials and Sample preparation

A low density polyethylene PE003 from Repsol Alcudia with 2 g/10min of MFI, density of 920 kg/m^3 and melting point of 110 ^{o}C was used as polymer matrix. For producing the nanocomposites this polymer matrix was melt blended with montmorillonite-type organomodified nanoclays Cloisite C15A from Southern Clay Products and a coupling agent, maleic anhydride grafted polyethylene Fusabond 226 DE from DuPont. The proportion of coupling agent to nanoclays was maintained constant at 2:1. In order to clearly distinguish the role played by the nanoclays, the PE003 was also melt blended with the coupling agent only. The proportion PE003/coupling agent was maintained equal to the one used in the case of the filled composites. Table 1 summarizes the compositions used for the two kinds of non-crosslinked (NC) samples.

For chemically crosslinking, Luperox DCP40 dicumyl peroxide from Vigar was used in a proportion of 1.8 phr. All the compositions of the crosslinked samples are also summarized in table 1.

Table 1: Proportion of components for the different kind of samples

Sample	Matrix/parts	Coupling agent/parts	Nanoclays/parts	Dicumyl Peroxide/phr
Unfilled-NC	85	10	0	0
Filled-NC	85	10	5	0
Unfilled-LC	85	10	0	1.8
Unfilled-MC	85	10	0	1.8
Unfilled-HC	85	10	0	1.8
Filled HC	85	10	5	1.8

The blank samples (no crosslinking agent) were made by compression moulding the raw materials to a uniform thickness of 1.27 mm using two stainless steel plates in a hot press at 190 ºC for 15 minutes and then cooling down with the pressure still applied at a constant cooling rate of 50 ^{o}C/min. To achieve different crosslinking degrees the pellets containing the crosslinking agent were compression moulded using three different moulding times of 15 minutes, 30 minutes and 60 minutes in the same conditions as before. These samples will be

denoted as low crosslinking "LC", medium crosslinking "MC" and high crosslinking "HC" respectively. In the case of the samples with nanoclays, only the highest crosslinking degree was studied. Table 2 summarizes the moulding conditions and nomenclature of all the samples.

Table 2: Production conditions for the non-crosslinked and crosslinked samples

Sample	Moulding temperature/ºC	Moulding cooling rate/(ºC/min)	Moulding time/min.
Unfilled-NC	190	50	15
Filled-NC	190	50	15
Unfilled-LC	190	50	15
Unfilled-MC	190	50	30
Unfilled-HC	190	50	60
Filled-HC	190	50	60

Some additional samples crosslinked using the three same moulding times of 15, 30 and 60 minutes but at a temperature of 147 ^{o}C instead of the previous 190 ^{o}C were produced to verify some of the hypothesis postulated later.

Crystallinity, rheology and crosslinking degree characterization

A Mettler DSC822e differential scanning calorimeter was used for the thermal analysis of the samples. A heating rate of 10 ^{o}C under N_2 environment and a sample weight of 5±0.5 mg were used in all the tests. Crystallinity degree was calculated from the area of the DSC peak, by dividing the heat of fusion by the heat of fusion of a 100% crystalline material, (288 J/g for a 100% crystalline polyethylene [45]). The crystallinities were calculated taking into account the real proportions of polymer deducting the amount of nanoclays.

Rheological behavior was studied by means of a AR2000EX TA Instruments rheometer with an extensional fixture at a temperature of 130 ºC (coinciding with the foaming temperature used, as explained later) and a strain rate of 0.5 s^{-1}.

The gel content was determined using a 24 h Soxhlet extraction cycle using xylene as the solvent. Approximately 300 mg of crosslinked grinded polyethylene was placed in a paper bag according to ASTM D 2765. In each experiment, three bags with a different material inside each one were tested simultaneously. This way, absolutely comparable results are obtained in between. After extraction, the solid residue was dried until the weight reached steady state. The gel content can be obtained as the ratio of the final weight of the polymer to its initial weight.

Foaming procedure

Both the non-crosslinked and crosslinked samples were microcellular foamed. The microcellular foaming procedure is well described in [1,17]. The samples were first saturated in a pressure vessel with an industrial grade CO_2 at room temperature and 5 MPa. Pressure was controlled

within ±0.03 MPa by a pressure controller. The saturation time was set to 48 hours, well above the time required for full saturation (7 hours).

When the pressure was relieved, the samples were introduced in a pre-heated hot glycerin bath for a given period of time at a certain temperature. They were then quenched in cold water.

Morphology and density of the foams

Density of the samples was measured by Archimedes principle using a Mettler AE240 balance with accuracy of ±10 µg.

The cellular morphology was characterized by scanning electron microscopy with a JEOL JSM-820 microscope. Samples were immersed in liquid nitrogen for 5 minutes, fractured and mounted on stubs. The fracture surfaces were sputter coated with gold prior to the microscopy work. The mean cell size and cell density were obtained using image processing software Image J from at least 75 cells in different micrographs from the same specimen.

Diffusion studies

For characterizing the absorption of gas, samples were taken out from the vessel at certain periods of time, weighted using the aforementioned balance and replaced inside the vessel at 5 MPa.

To determine diffusivities of the different samples from weight measurements made during the desorption, the "Initial Gradient Method" was employed. It states that, for the early stages of desorption, the solution of the diffusion equation for a polymer-gas system with a constant diffusivity is given by [46]

$$\frac{M_t}{M_\infty} = \frac{4}{\pi^{1/2}}\left(\frac{Dt}{l^2}\right)^{1/2} \qquad (1)$$

where M_t is the total amount of gas absorbed in the polymer sheet at time t, M_∞ is the equilibrium gas concentration attained theoretically after infinite time, D is the diffusivity and l

is the thickness of the polymer sheet. A plot of M_t/M_∞ as a function of $t^{1/2}/l$ yields essentially a straight line (for the initial period of test) with a slope of $4(D/\pi)^{1/2}$ which is readily solved for D.

RESULTS

Crosslinking degree and thermal properties

Figure 1 shows the crosslinking degree achieved versus the time that the samples where held inside the hot press at 190 ºC.
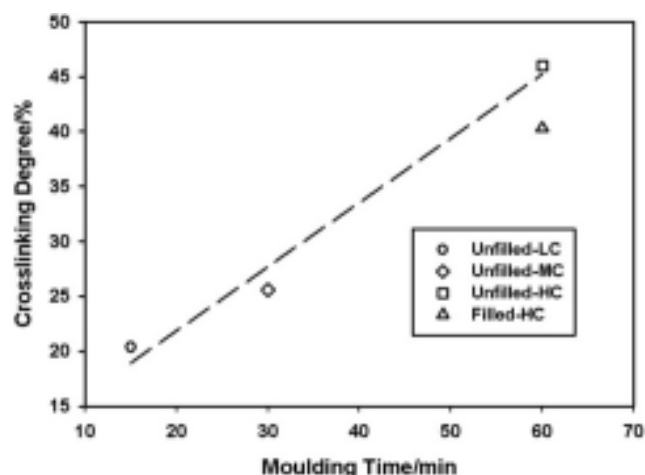
Figure 1: Crosslinking degree as a function of the moulding time. Samples could be further crosslinked since no constant crosslinking degree is reached.

The previous data indicate that the dicumyl peroxide has not been totally decomposed. Higher crosslinking degrees could have been achieved increasing the moulding time above 60 minutes. It is also remarkable that the crosslinking degree for the samples containing nanoclays is considerably lower than for the unfilled one. This could be explained taking into account that for those samples only 95% of the weight introduced inside the bags for extraction corresponds to polymer matrix. Even taking into account this fact in the calculations the value is 3% below the expected, so nanoparticles could be hindering the crosslinking at the interphase.

Differential scanning calorimetry provided the results of crystallinity and melting temperature shown in table 3 for all the samples.

Table 3: Crystallinity and melting point for the unfilled and filled samples.

Sample	Crystallinity/%	Melting Point/ºC
Unfilled-NC	45.3	112.09
Unfilled-LC	44.8	111.89
Unfilled-MC	44.1	112.23
Unfilled-HC	43.1	112.57
Filled-NC	48.2	112.52
Filled-HC	45.8	112.15

Reductions higher than 2% in crystallinity are observed with the increasing crosslinking degree. The chemical crosslinking produces a molecular three-dimensional network with the polymer chains, which reduces the crystalline order, therefore decreasing the crystallinity degree observed in the samples. A similar trend is observed for the samples containing nanoclays. On the contrary, there is no variation in the melting point between the different samples. This suggests that the size of the crystals formed is independent of the crosslinking degree. This interesting behavior of the crystallinity with the crosslinking degree will be used later to explain

the sorption and desorption behavior of these materials. The presence of nanoclays seems to have a nucleating effect for crystals formation increasing slightly the crystallinity degree in the filled samples.

Solubility and Diffusivity

The solubility and diffusivity of CO_2 in the polymers have been evaluated through the sorption experiments. These parameters were studied for non-crosslinked and crosslinked samples choosing the two opposite cases: non-crosslinked and highly crosslinked. Figure 2 a) shows and compares the absorption curves of CO_2 for the non-crosslinked and highly crosslinked samples. The relationship between M_t and $t^{1/2}/l$ is linear as described in equation 1. The mass uptake eventually converged to a steady state value which represented the solubility of gas in the polymer. This solubility is lower in the case of the crosslinked sample than in the raw one as can be seen also in table 4. Solubility of CO_2 in a semicrystalline sample is a strong function of the crystallinity so the differences observed in crystallinity (table 3) between these two samples can explain the higher solubility value obtained for the highly crosslinked sample. In fact, the solubility and crystallinity in both samples correlate perfectly assuming the model in which the relation between these two parameters is expressed as [47]

$$K = K^*(1 - X_c)$$

Where X_c is crystallinity and K^* is the solubility of gas in the completely amorphous matrix of the polymer.
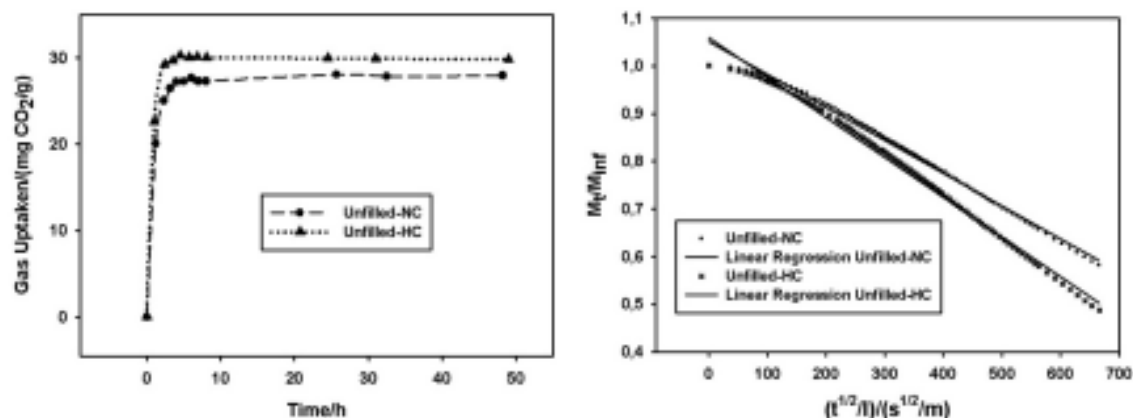
Figure 2: a) Evolution with time of the gas uptaken by the crosslinked and non-crosslinked samples. b) Linear regression at the early stages of desorption. The slope of the plots yields essentially the diffusivity of the samples.

Figure 2 b shows the early stages of the desorption with the calculated linear regressions from which the diffusivity coefficients have been obtained (table 4). Common diffusion models postulate that small gas molecules can diffuse into and pass through the polymers [48]. In amorphous polymers this occurs in the entire bulk of the polymer matrix but in semycristalline ones the presence of crystalline regions complicates the process. This gives rise to a two phase model [43, 44] in which impenetrable crystallites are dispersed in a rubbery amorphous matrix. As a result, diffusivity is higher in the samples with lower crystallinity, the non-crosslinked ones

in this case. The diffusivity for the crosslinked sample almost doubles the one yielded for non-crosslinked one.

Table 4: Solubilities and diffusivities of the crosslinked and non-crosslinked samples

Sample	Solubility/(mg CO_2/g)	Diffusivity/(cm^2/s)
Unfilled-NC	27.94	$9.3 \cdot 10^{-8}$
Unfilled-HC	29.22	$1.8 \cdot 10^{-7}$

The influence of these solubility and diffusivity values on the foaming behavior will be discussed later on.

Rheological behavior

The rheological behavior is a parameter of major importance that deeply determines the foamability of a polymer matrix. Therefore studying the extensional viscosity of the polymer melts will help to later explain the foaming results.
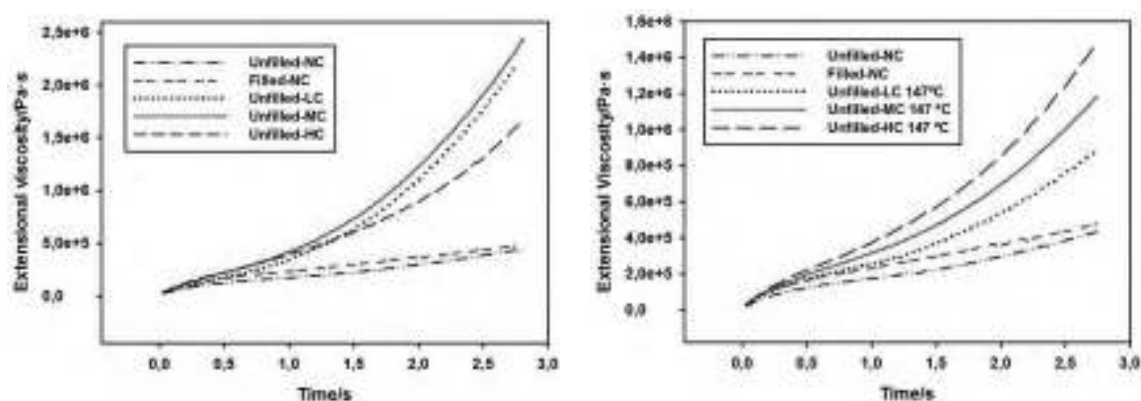
Figure 3: Extensional viscosity measured for a) samples crosslinked at 190 ºC and b) samples crosslinked at 147 ºC.

Figure 3 a) shows the extensional viscosity measured for all the three different crosslinking degrees of unfilled material and compares them also with the non-crosslinked one. The Trouton ratio is defined as the ratio of extensional viscosity to shear viscosity. When this Trouton ratio is measured at high Hencky strains then it gives a direct measurement of the strain hardening. As expected, the viscosity and Trouton ratio (measured at a Hencky strain of 1.4) is much higher for the crosslinked samples than for the non-crosslinked one. But this dependence does not correlate directly with the different gel contents. The highest values are reached for the medium crosslinking instead of the highest one. For the high crosslinking the Trouton ratio is even below the one corresponding to the low crosslinking (Table5).

Table 5: Trouton ratio for the different kinds of specimens crosslinked at 190 ºC. The Trouton ratio was determined at a strain rate of 0.5 s^{-1} and Hencky strain of 1.4.

Sample	Trouton Ratio
Unfilled-NC	4,05
Filled-NC	3,18
Unfilled-LC	8,36
Unfilled-MC	9,79
Unfilled-HC	6,60

The addition of nanoclays also reduces the Trouton ratio. This effect has been observed in previous works. Particles can partially convert the extensional flow in the surrounding polymer into shear flow and this interferes with the occurrence of strain hardening [49, 50]. The experimentally determined Trouton ratios are directly connected with the foam stability as will be seen later.

The samples used in figure 3 b are exactly the same as in figure 3 a but crosslinked at 147 ºC instead of 190 ºC. A more intuitive behavior is found now. In this case the viscosity values are not as high as in figure a) as corresponds to a lower crosslinking temperature, but extensional viscosity and Trouton ratio (Table 6) correlate directly with the crosslinking degree. It is postulated therefore that, although the Unfilled-HC has the highest gel content, its polymer matrix suffers degradation while subjected to 190 ^{o}C during 60 minutes. This degradation deteriorates the rheological properties of these samples which deeply influences the foaming behavior as will be shown later. As mentioned in the experimental part, only the samples crosslinked at 190 ^{o}C has been used in this study, the samples crosslinked at 147 ºC have been used only to sustain the hypothesis of a possible polymer degradation in the Unfilled-HC.

Table 6: Trouton ratio for the different kinds of specimens crosslinked at 147 ºC. The Trouton ratio was determined at a strain rate of 0.5 s^{-1} and Hencky strain of 1.4.

Sample	Trouton Ratio
Unfilled-LC-147 ºC	5,21
Unfilled-MC-147 ºC	5,65
Unfilled-HC-147 ºC	6,10

Foaming

Unfilled samples.

Both kinds of samples, non-crosslinked and crosslinked ones, have been foamed by a batch gas dissolution process in sub-critical conditions. Samples were held at a CO_2 pressure of 5 MPa during 48 hours at room temperature. Then, pressure was released and 2 minutes later samples were immersed in a silicon oil bath preheated at 130 ^{o}C. This temperature is 20 ^{o}C above the melting temperature of the samples. Upon pressure release no nucleation was visually

observed. Figure 4 presents the different densities obtained for foaming times of 10s, 20s, 30s and 60s.
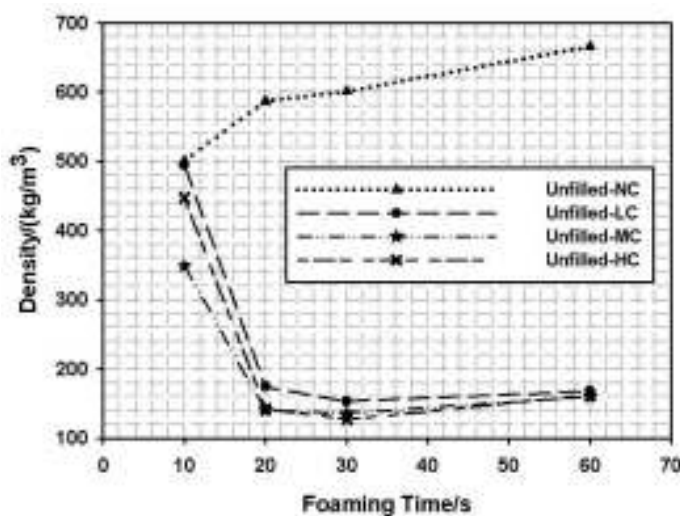
Figure 4: Densities of the crosslinked and non-crosslinked unfilled samples at different foaming times. Expansion ratios as high as 7 with cells in the microcellular range can be reached by crosslinking the polymer.

For the Unfilled-NC samples, the highest expansion ratio (lower than 2) is reached for the lowest foaming time. For these non-crosslinked samples the stability of the cellular structure with foaming time is poor since density presents a rapid increasing trend with time. For example, the expansion ratio has diminish to 1.5 for 20 seconds and it is as low as 1.3 for the longest foaming time of 60 seconds. This is correlated with the low extensional viscosity and Trouton ratio of this system.

On the contrary, the crosslinked samples present a much different behavior. For times above 10 seconds, the densities of the Unfilled-NC, Unfilled-LC and Unfilled-HC are comparable. In spite of this, even with comparable densities, cellular structures are completely different as it is explained in the following paragraphs.
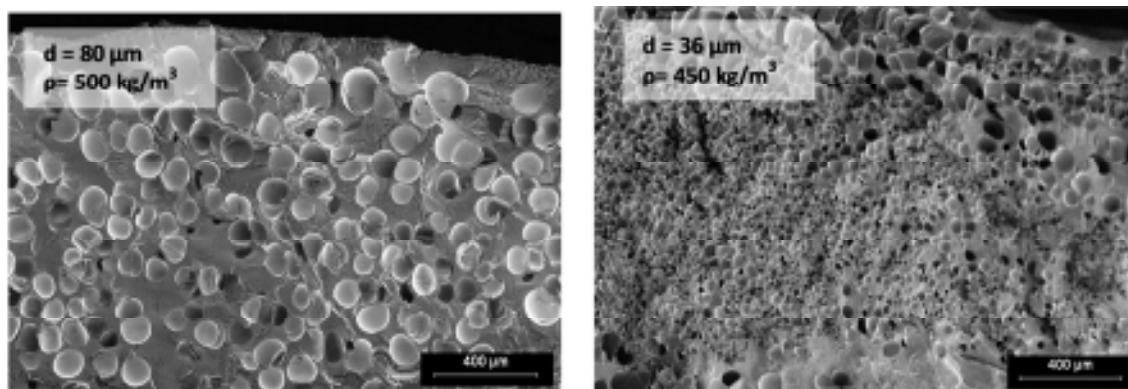
Figure 5 Cellular structures for Unfilled-NC and Unfilled-HC for at 130 ºC and 10s. Bulk densities are comparable in both samples.

Figure 5 shows two micrographs of the Unfilled-NC and the Unfilled-HC. In the first one the cell density is of the order of $5 \cdot 10^5$ cells/cm^3 with a mean cell size of 80 µm while in the crosslinked sample the cell density is of the order of $1.5 \cdot 10^7$ cells/cm^3 with a mean cell size of 36 µm. Crosslinking allows a great reduction in cell size and increase the cell density for the same bulk density range even when the diffusivity of the Unfilled-HC doubles the one obtained for the Unfilled-NC.

Densities around 120 kg/m^3 have been reached for the crosslinked samples which means expansion ratios around 7.5.These samples also have a good stability with foaming time presenting a very smooth increment of density. The three dimensional molecular network formed by crosslinking helps to suppress cell coalescence allowing the cells to grow without rupturing. This suppression effect is stronger even from the early foaming stages for the Unfilled-MC sample. This fact is directly related with the excellent Trouton ratio found for these samples already mentioned and the cellular structure studied next.

Figures 6 to 8 show the mean cell size, bulk density and cellular structure for the low, medium and high gel contents at different foaming times.
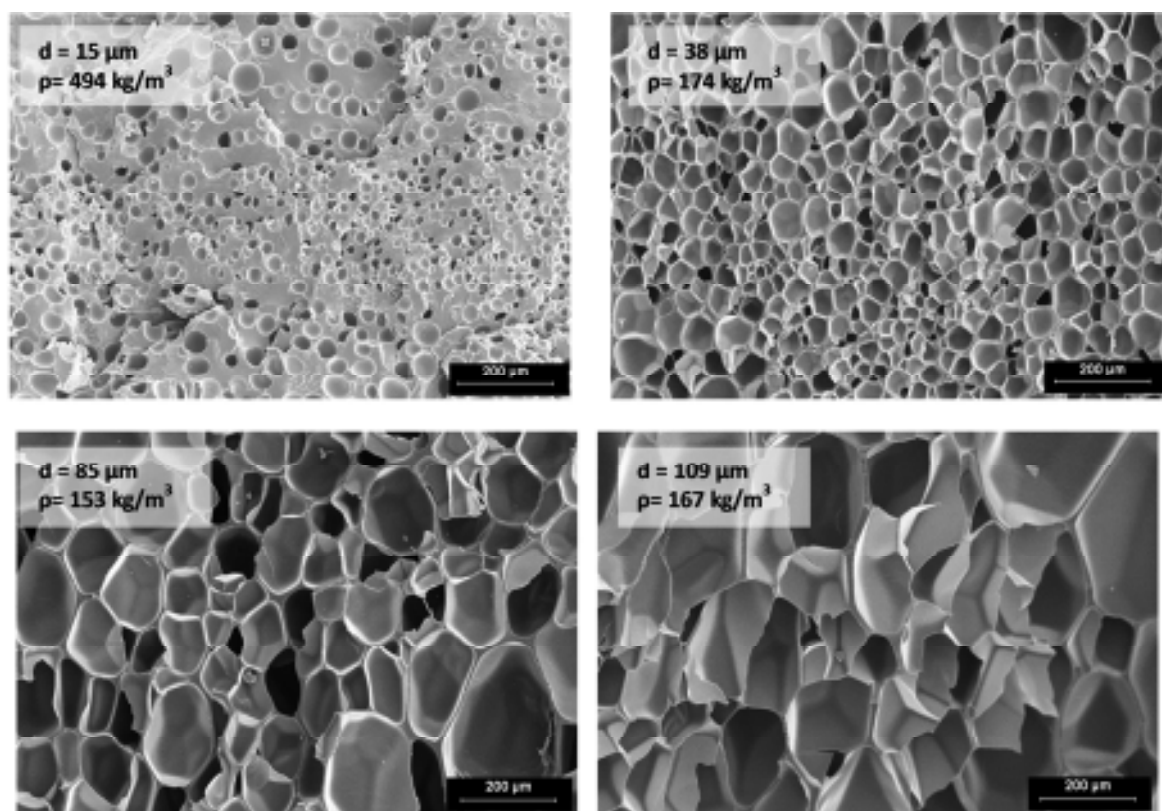
Figure 6: Low crosslinking samples foamed at 10 s, 20s, 30s and 60s with the corresponding mean cell size and sample density. Note that the scale is 200 µm in all cases.
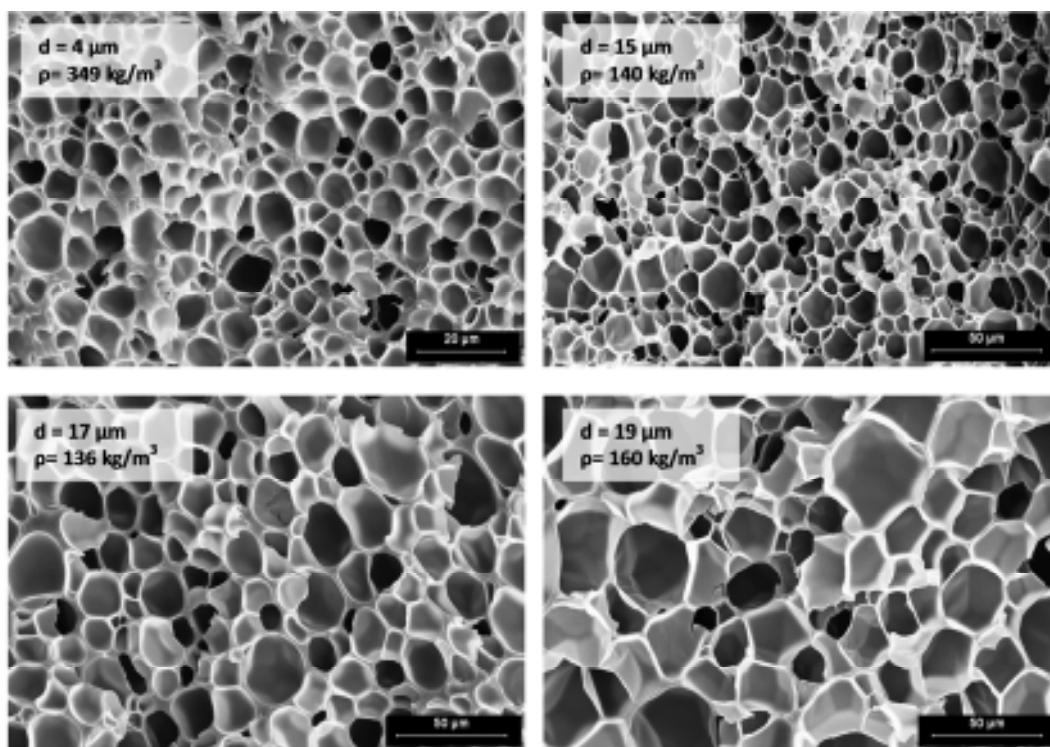
Figure 7: Medium crosslinking samples foamed at 10 s, 20s, 30s and 60s with the corresponding mean cell size and sample density. Note that the scale is 20 µm in the first micrograph and 50 µm in the rest.
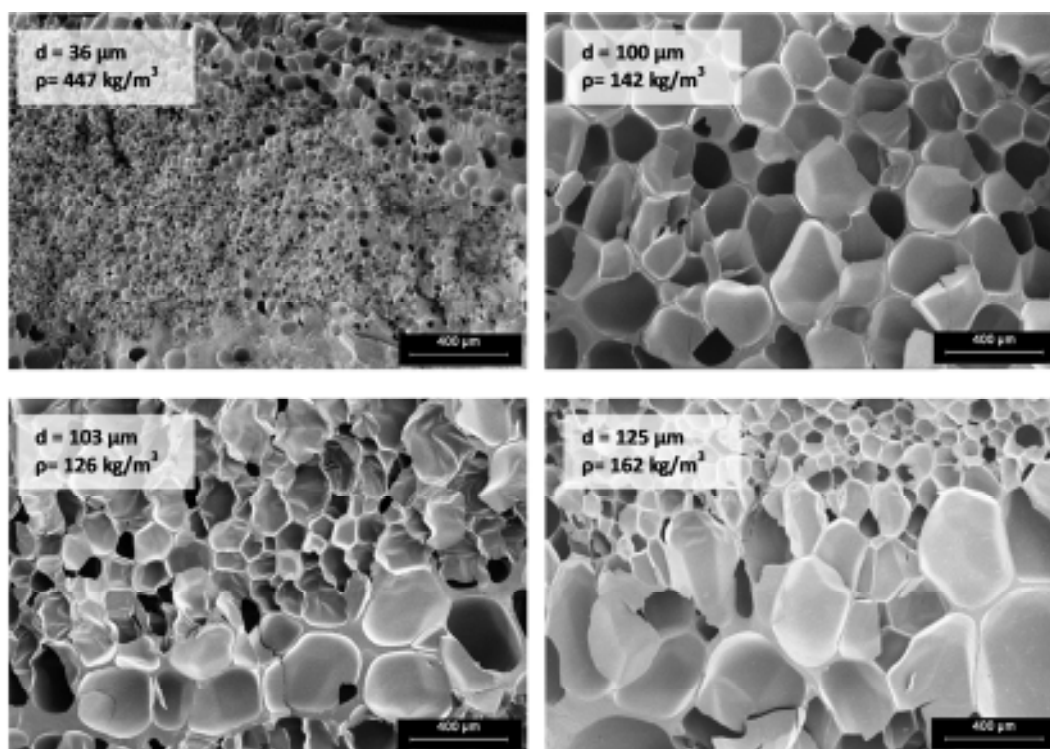
Figure 8: High crosslinking samples foamed at 10 s, 20s, 30s and 60s with the corresponding mean cell size and sample density. Note that the scale is 400 µm in all the micrographs.

In the case of the lower gel content the mean cell size is near or below 100 µm for all the foaming times. Although having the highest gel content, the Unfilled-HC presents the highest cell size values and lowest cell density as a consequence of the lower extensional viscosity and Trouton ratio. An interesting foaming behavior is found for the Unfilled-MC. The combination of a medium gel content with improved extensional viscosity and Trouton ratio yields mean cell size values around 15 µm with cell densities near or above $1 \cdot 10^9$ cells/cm^3 and expansion ratios as high as 7.5. Besides this, the stability of the cell structure is much better than any other case with a mean cell size increasing and a cell density decreasing very smoothly with foaming time as can be seen in figure 9 a) and b)
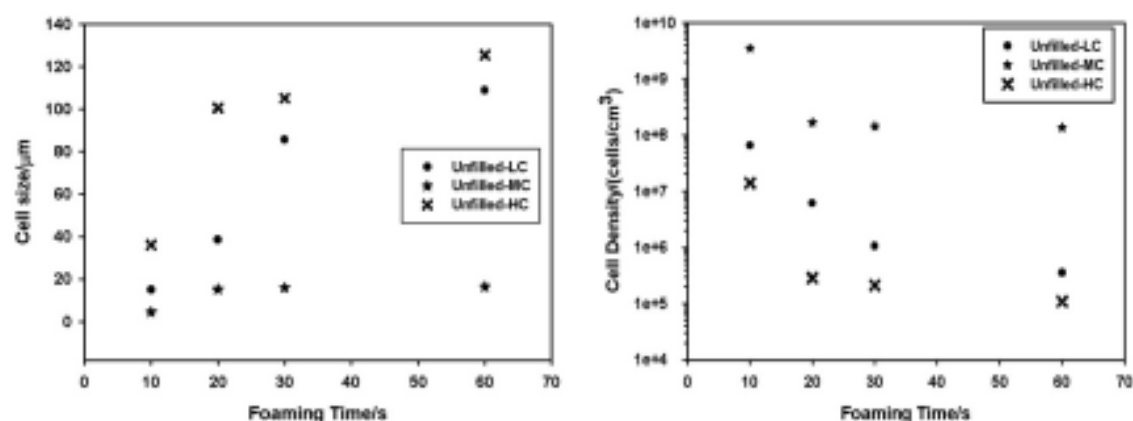
Figure 9 Mean cell size a) and cell density b) dependence with foaming time for the three different gel contents.

Thank to its rheological properties the Unfilled-MC exhibits an improved capacity to withstand cell growth and cell rupture while foaming, yielding an interesting combination of cell density, mean cell size and bulk density for a semycristalline polymer foamed by gas dissolution in sub-critical conditions.
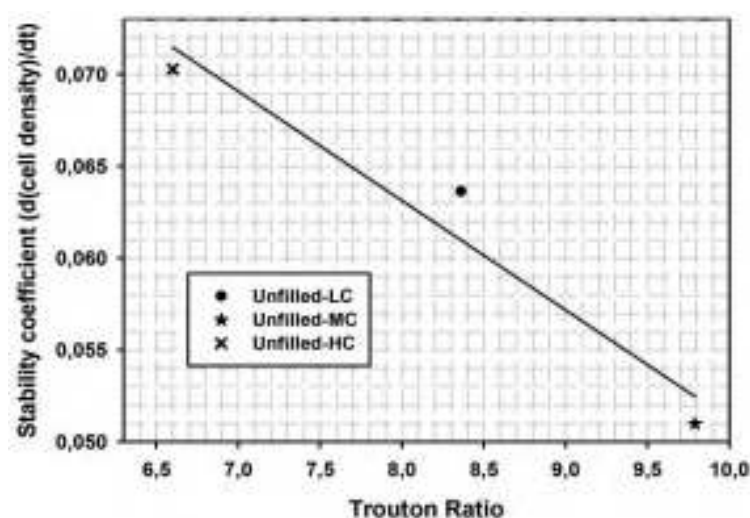
Figure 10: Correlation between the stability parameter calculated and the Trouton ratio for the crosslinked samples.

An idea of the stability of each formulation can be obtained numerically differentiating with time the data contained in the logarithmic plot of the cell density in figure 9. This calculation yields a mean value of the variation with foaming time of the cell density for each sample. Lower values of this calculated parameter mean higher foam stabilities. This stability value correlates directly with the Trouton ratio as it is shown in figure 10. The highest Trouton ratios, obtained for the Unfilled-MC samples, give the higher stabilities of the cellular structure together with the smaller cell sizes and higher density reductions, independently of the crosslinking degree. Rheology turns to be the main parameter governing the foaming behavior in this systems.

As has been seen the fundamental parameter in all the previous discussion is the rheological characteristics of the samples. The solubility and diffusivity do not play a significant role. Although the solubility of the crosslinked samples is higher, indicating that more gas is available for the foaming and lower densities could be reached, this fact is compensated somehow with the higher diffusivity. In the two minutes time elapsed between the pressure release and the foaming, the gas is allowed to diffuse quicker in the crosslinked samples than in the pristine ones.

Stability with temperature

The stability of the cellular structure with the foaming temperature has been also studied for the samples with the higher gel content (Unfilled-HC). This parameter has been found to have less influence on the cellular structure than the foaming time. As can be seen in figure 11, the bulk density of the foam is continuously reduced with increasing foaming temperature. For temperatures of 115 ºC, 130ºC and 145 ºC the cell density is maintained in a narrow range indicating that the cells rupture ratio is low and density diminishes thank to the increment in cell size. At 160 ^{o}C sharply decreases and cell size reaches values near 200 μm while the bulk density remains low.
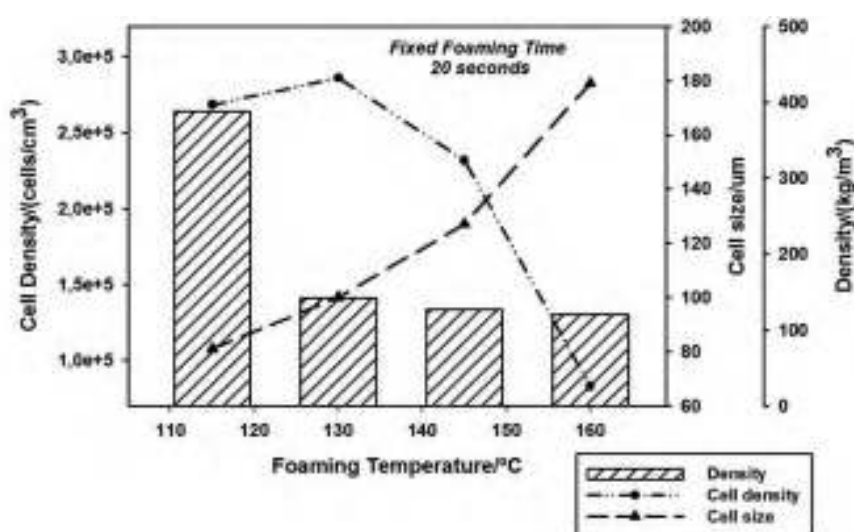
Figure 11: Dependency of the bulk density of the foam, mean cell size and cell density with foaming temperature for the Unfilled-HC samples.

Filled samples

The addition of nanoclay and its influence on the foaming behavior have been also characterized. The nanocomposite samples Filled-NC and Filled-HC mentioned in the experimental part have been foamed following the same procedure as with the unfilled samples. These nanocomposites present an intercalated-exfoliated structure. The compounding procedure, WAXS, rheological and TEM characterization of these materials have been detailed elsewhere [50].
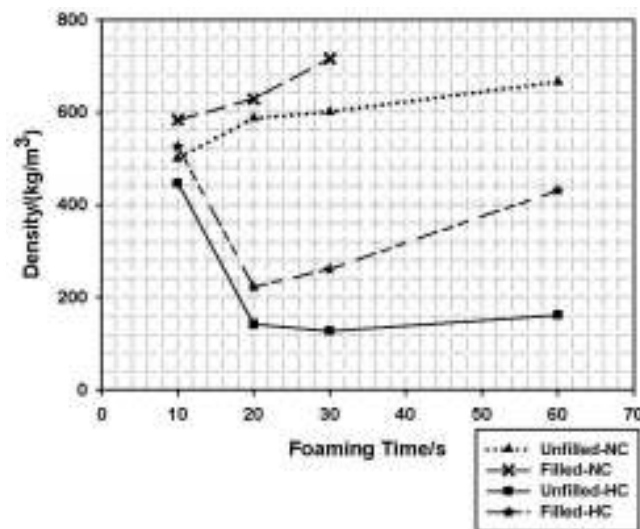
Figure 12 Comparative of densities for filled and unfilled samples and for crosslinked and non-crosslinked filled samples

The addition of 5wt.% of nanoclays deteriorate the cellular structure of the samples foamed in sub-critical conditions. The densities reachable with these samples are around 20% higher than in the absence of nanofillers, and expansion ratios were always below 1.5.
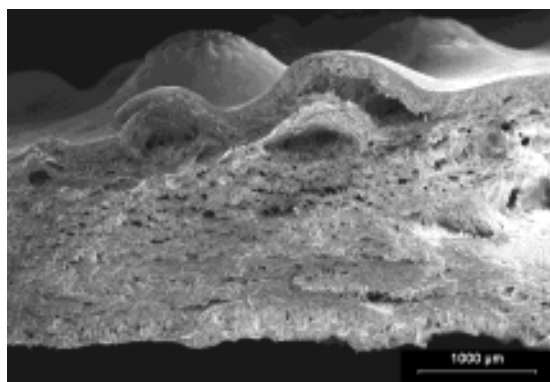
Figure 13 Micrograph of a Filled-NC sample foamed at 10 seconds. A proper cellular structure cannot be distinguished.

A proper cellular structure does not appear, as shown in figure 13 for a sample foamed at 10 seconds. Instead, plenty of cracks and holes with big bubbles in the surfaces are found for these samples. The melted nanocomposite is not able to withstand the cell growth and the gas escapes forming cracks and bubbles. The addition of nanoclays reduces the Trouton ratio of the formulation to values near 3 (table 5), making any strain hardening effect present in the raw polymer disappear, hence the foamability of these composites in sub-critical conditions is greatly hindered.

Crosslinking helps to mitigate this situation, strongly lowering the range of densities with values near 200 kg/m^3 as in the 20 seconds foaming time case (figure 12).
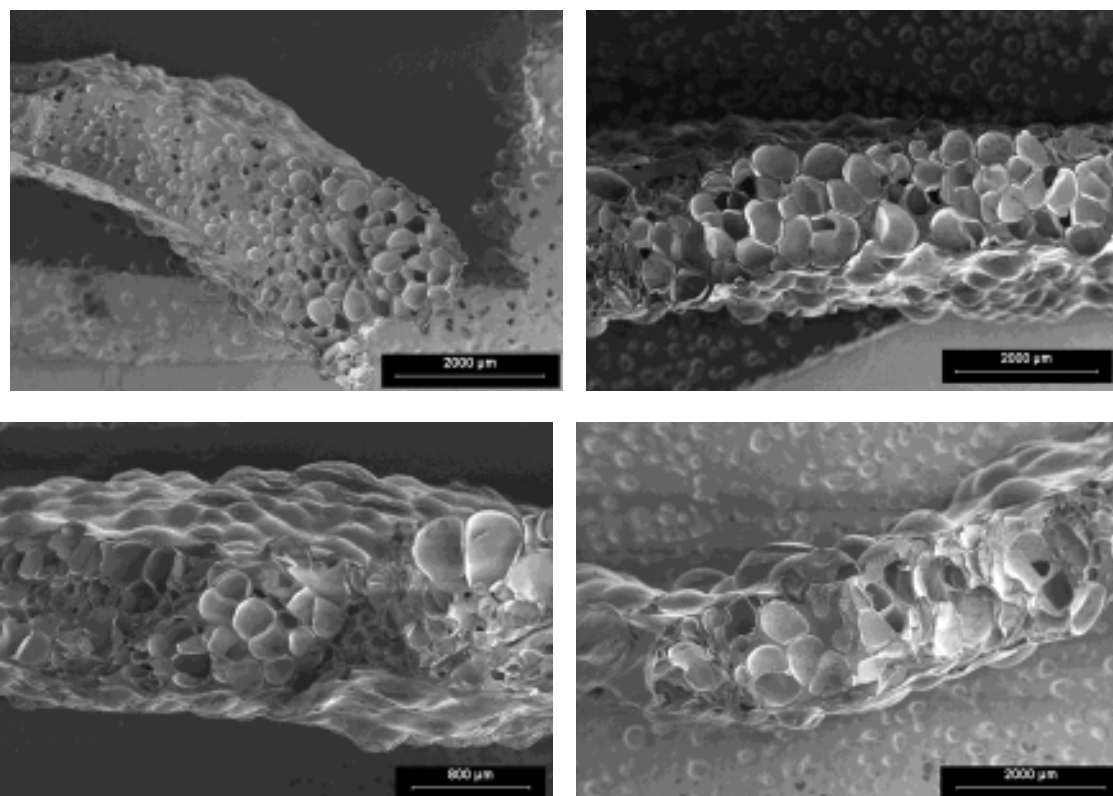
Figure 14: Filled-HC samples at 10s, 20s, 30s and 60 s foaming time.

Developed cellular structures can be perfectly distinguished now although they are very in-homogeneous (figure 14). They can no longer be classified as microcellular since the smallest cell size is 200 μm for the 10 seconds foaming time. The stability with the foaming time is also very poor, cells rapidly collapse and density sharply increases (see figure 12). However crosslinking allows obtaining nanocomposite foams with completely developed cellular structures and moderately low densities using a sub-critical gas dissolution foaming route.

CONCLUSIONS

The sorption behavior and microcellular foaming of a semicrystalline polymer such as LDPE by batch gas dissolution in sub-critical conditions has been studied both in non-crosslinked and crosslinked samples. Crosslinking lowers the crystallinity of the raw LDPE matrix and this is

finally translated in increased solubilities and diffusivities of the gas. The non-crosslinked polymer presents the difficulties already known for this kind of polymers with expansion ratios always lower than 2 and non-homogeneous unstable cellular structures with cell sizes near 100 µm. Crosslinking strongly helps to overcome these difficulties. For the crosslinked samples expansion ratios as high as 7.5 have been reached and the cellular stability both with foaming time and with foaming temperature has been greatly improved. There exists an optimum combination of gel content and processing parameters which yields cell sizes of 15 µm and cell densities of $1·10^9$ cells/cm^3 for a density of 140 kg/m^3. The Trouton ratio of each formulation has a much deeper influence on the foamability than the crosslinking degree and is directly connected with the stability with time of the foams. The rheological characterization turns to be fundamental for understanding the later foaming behaviours. An approach taking into account only the gel content would have been unsuccessful.

The addition of nanoclays to the non-crosslinked samples has been shown to play a deteriorating role on the rheological properties and hence on the cellular structures and microcellular foaming in sub-critical CO_2 of LDPE. The lowest densities reachable are higher and a proper cellular structure cannot be distinguished in this case. Crosslinking again helps to mitigate these detrimental effects allowing for densities near 200 kg/m^3 with well developed cellular structures.

ACKNOWLEDGEMENTS

REFERENCES

[1] Martini J, Suh NP, Waldman FA. Patent 4473665 USA. Massachussets Institute of Technology 1984.

[2] Martini J, Waldman FA and Suh NP. SPE ANTEC vol. 28. San Francisco CA; 1982 p. 674.

[3] V. Kumar, N. P. Suh, Polym. Eng. Sci 20, 1323 (1990)

[4] V. Kumar, G. Schirmer, SPE ANTEC Tech. Papers, 41, 2189 (1995)

[5] C. B. Park and N. P. Suh, Polym. Eng. Sci. 36, 34 (996)

[6] Lee, YH ; Kuboki, т ; Park, CB ; Sail, м Polym. Eng. Sci. 51, 5, 014-1022 (2011)

[7] Wong, S ; Lee, JWS; Naguib, HE; Park, CB. Macromol. Mat Eng. 293, 7, 605-6013 (2008)

[8] Otsuka T, Taki K, Ohshima M, Macromolecular Materials and Engineering 2008 ; 293 (1),78-82.

[9] Taki K, Waratani Y, Ohshima M. Macromolecular Materials and Engineering 2008; 293 (7), 589-97.

[10] Kumar V, Weller JE, Journal of Engineering in Industry 1994; 116; 413-20.

[11] Collias DI, Baird DG, Borggreve RJM. Polymer 1994; 35; 3978-83.

[12] Murray RE, Weller J, Kumar V. Cellular Polymers 2000; 19 (6); 413-25

[13] Nawaby V, Handa P, Fundamental understanding of the ABS-CO2 interactions, its retrograde behavior and development of nanocellular structures ANTEC vol. 2. Chicago IL. 2004 p. 2532-6.

[14] S. K. Geol and E. J. Beckman. Polym. Eng. Sci., 34, 1137-48 (1994).

[15] Kumar V, Weller JE, International Polymer Processing 1993; VIII (I); 73-80.

[16] Sauceau, M ; Fages, J; Common, A ; Nikitine, C; Rodier, E Prog. Polym. Sci. 36, 6. 749-766.

[17] Lee J. S. W., Park C.B. Macromo. Mat. And Eng. 291, 10. 1233-1244.

[18] Naguib H. E., Park C.B., Panzer U., Reichelt N. Polym. Eng. And Sci. 2002. 42, 7, 1481-1492.

[19] Velasco J. I., Antunes M., Realinho V., Ardanuy M. polym. Eng. And Sci. 2011. 51, 11, 2120-2128

[20] Park C. B. Cheung L. K. Polym. Eng. And Sci 1997. 37, 1, 1-10.

[21] D. Miller, V. Kumar. Cell. Polym. 28, 1, (2009)

[22] Z. Xing, G. Wu, S. Huang, S. Chen, H. Zeng. J. of Supercritical Fluids 47, 281-289 (2008)

[23] P. Zhang, N. Q. Zhou, Q. F. Wu, M. Y. Wang, X. F. Peng. J. of Applied Polymer Science, 104, 4149-4159 (2007)

[24] Zhai, W; Wang, H; Yu, J; Dong, JY; He, J. Polymer 49, 13-14, 3146-3156. (2008).

[25] Yuan, MJ; Winardi, A;; Gong, SQ; Turng, LS. Polym. Eng. Sci. 45, 6, 773-788. (2005)

[26] Jo, C; Naguib, HE. Polymer, 48, 11, 3349-3360 (2007)

[27] Taki, K; Tabata, K ; Kihara, S; Ohshima, M. Polym. Eng. Sci. 46,5, 680-690.(2006)

[28] J. S. Colton, Mtls. Manuf. Proc., 4, 253 (1989)

[29] C. Saiz-Arroyo, J. Escudero, M.A. Rodriguez-Perez, J. A. de Saja. Cell. Polym. 30, 2, 63-78 (2011).

[30] J. V. Gulmine, L. Akcelrud. J. Appl. Polym. Sci. 2004. 94, 222-230.

[31] W. Zhai, H. Wang, J. Yu, J. Dong, J. He. Polym. Eng. Sci. 2008 48, 7, 1312-1321.

[32] A.Shojaei, A. behradfar, N. Sheikh. Polym. Adv. Technol. 2011. 22, 2352-2359.

[33] M. Davari, M.K. Razavi, S. M. Seraji. J. Appl. Polym. Sci. 2012. 124, 2789-2797.

[34] C. Saiz-Arroyo, J. A. Saja, M. A. Rodriguez-Perez. Polym. Eng. Sci. 2011. 52, 4, 751-759

[35]M. A. Rodriguez-Perez. Adv. Polym. Sci 2005. 184. 97-126.

[36] Z. Xing, G. Wu, S. Huang, S. Chen, H. Zeng. J. Supercrital Fluids. 2008. 47, 281-289.

[37] Handbook of Polymer Foams. Rapra Technology Limited 2004. UK.

[38] Khorasani, MM; Ghaffarian, SR; Babaie, A; Mohammadi, N. J. Cellular Plastics. 46, 2. 173-190 (2010)

[39] Jiang, XL; Bao, JB; Liu, T; Zhao, L; Xu, ZM; Yuan, WK. J. Cellular Plastics. 45, 6. 515-538 (2009)

[40] Zhai, WT; Yu, J; He, JS. Polymer 49, 10, 2430-2434 (2008)

[41] Lee, LJ; Zeng, CC; Cao, X; Han, XM; Shen, J); Xu, GJ. Composites Science and technology. 65, 15-16. 2344-2363 (2005)

[42] Wee, D; Seong, DG; Youn, JR. Fibers and Polymers. 5, 2, 160-169. (2004)

[43] Doroudiani S, Park CB, Kortschot MT. Polym. Eng. Sci. 36, 21, 2645-2661 (1996)

[44] Kang TK, Chang-Sik H. Polymer Testing 19, 773-783 (2000)

[45] B. Wunderlich. Macromolecular Physics, 2. Academic Press, New York. 1973-1976.

[46] Crank J. In: The mathematics of diffusion. 2nd ed. New York: Oxford Science Press; 1989.

[47] Michaels A.S. and Bixler J., J. Polym. Sci., 50, 393-413 (1961).

[48] Vieth R. W. in Diffusion in and through polymers: principles and applications. Hanser Publishers, Munich (1990).

[49] Le Meins J. F., Moldenaers P., and Mewis J. Ind. Eng. Chem res., 41, 6297-6304. (2002).

[50] Le Meins J. F., Moldenaers P. and Mewis J. Rheologica Acta, 42, 184-190. (2003).

 [51] J. Escudero, E. Laguna-Gutierrez, V. Kumar, M.A. Rodríguez Perez. SPE FOAMS 2011, Iselin.

4.3.- POLYOLEFIN BASED CELLULAR MATERIALS FOAMED BY CHEMICAL BLOWING AGENTS AND IMPROVED BY MODIFICATIONS IN THE POLYMER MATRIX

The second part of the chapter deals with modifications in the polymer matrix combined with chemical blowing agents (described in chapter 3) to produce cellular materials with improved physical properties. The modifications in the polymer matrix, in parallel to the first part of the chapter, go in two different ways: addition of nanoclays and coupling agents as modifiers of the chemical composition of the polymer matrix and crosslinking as modification of the molecular architecture. In this second part two different foaming routes have been used: *free foaming and two stages compression molding.* Both of them were described in chapter 3.

4.3.1.- Chemical Modifications of the Polymer Matrix and Free Foaming

In this section nanoclays together with a coupling agent have been added to the polymer matrix. Nanoclays are montmorillonite type and their surface has been modified using 2M2HT (Dimethyl dehydrogenated tallow ammonium chloride). The coupling agent is a linear low density polyethylene grafted with maleic anhydride.

From a technical point of view free foaming is maybe the simplest foaming method. But in spite of its simplicity valuable information that can be extended to other foaming routes is obtained. An important part of the results observed by free foaming in this section are later observed too in other more complex foaming routes used in the following chapters.

Two works are included in this section. The first one is entitled *"Polyethylene Layered Nanocomposites for Foaming Purposes"*. In this work the foaming of the samples is studied by means of a not very extended technique named *optical expandometry*. Special attention is paid also to the correlation between physical properties of the solid matrix (before foaming), their foamability and the physical properties of the foams obtained from these solid samples.

The addition of nanoparticles improves the mechanical properties of the solids, increases the crystallinity of the polymer matrix and broadens the polymer degradation window increasing the degradation temperature.

Nanoclays have a catalytic effect over azodicarbonamide, which is observed by optical expandometry, reducing the decomposition temperature and increasing the amount of gas released by thin blowing agent at a fixed temperature. Therefore larger maximum expansion ratios are achieved in the presence of nanoclays although the foam stability is lower and the collapse rate is also higher.

A similar catalytic effect is achieved with the only addition of MAH-g-LDPE but in a lower extent. The difference is that in this case the stability and the collapse rate are not harmed since the addition of coupling agent has no substantial influence over the rheology of the polymer.

By x-rays diffraction (XRD) it was observed that the degree of exfoliation of the nanoclays is increased after foaming. The interlamellar spacing of the nanoclays is larger in the foamed samples than in the solid samples prior to the foaming. The foaming, by itself, tends to increase the separation between platelets in the polymer matrix. This result motivates the second work included in this section.

The second work included in this section is entitled *"In-situ Characterization of Nanoclays Exfoliation During Foaming by Energy Dispersive XRD of Synchrotron Radiation"* and is aimed at the study in detail of the mechanisms involved in the previously observed effect of increment in the interlamellar spacing of nanoclays by foaming. Free foaming is the foaming route used but in this case three chemical blowing agents of different nature have been used: azodicarbonamide, Hydrocerol® and Expancel® all of them mentioned and described in chapter 3.

The study was held at the BESSY synchrotron facility of the Helmholtz Zentrum Berlin in Berlin (Germany). The use of energy dispersive synchrotron radiation allows obtaining in-situ diffractograms, that is, diffractograms obtained directly while foaming. This way, the different stages of delamination of the clay particles that take place during foaming can be studied. To elucidate some possible influence of the chemical nature of the gas released, two blowing agents releasing different gases were used : azodicarbonamide and Hydrocerol. To elucidate the influence of the foaming mechanism, microspheres that expand with the gas entrapped inside were also used (Expancel).

The increment in interlamellar spacing is mainly associated with the expansion ratio achieved by the samples. Higher expansion ratios yield higher increments in interlamellar spacing, independently of the nature of the gas released or foaming mechanism. There is an initial increment in the separation between platelets, before foaming, associated with the thermally activated movement of the polymer molecular chains.

The results suggest also a chemical interaction between the azodicarbonamide and nanoclays that is not found with the rest of the blowing agents. This hypothesize chemical interaction supports also the catalytic effects observed in the first work included in this section.

POLYETHYLENE LAYERED SILICATE NANOCOMPOSITES FOR FOAMING PURPOSES

J. Escudero, B. Notario, J. A. de Saja, M. A. Rodriguez-Perez

CellMat Laboratory, Condensed Matter Physics Department, University of Valladolid, Spain

Email: marrod@fmc.uva.es; jabo@fmc.uva.es

ABSTRACT

The more relevant properties for foaming are studied on polyethylene/layered silicate nanocomposites. These polymer nanocomposites are later foamed and their foaming behavior is studied by means of a novel but full of information technique: optical expandometry. The properties and foaming behavior of the different nanocomposite foams are later compared and connected to the properties of the initial solid precursors. Two different clay additions together with two different coupling agent additions are used for these purposes. The nanosilicates improve the mechanical and thermal properties of the polyethylene but are detrimental to the rheological behavior. While foaming, the expansion kinetics are accelerated proportionally to the content of nanoclays. Besides this, the amount of gas released is also higher yielding higher expansion ratios. Interesting results are obtained also with the different additions of coupling agent. The worst rheological behavior of the nanocomposites is later translated in poorer cellular structures.

Keywords: foam, nanoclays, polyethylene.

INTRODUCTION

In the last years the emergence of nanocomposites has resulted in the development of a new group of materials known as foamed nanocomposites. Polymeric nanocomposite foams are currently a subject of attention in both the scientific and industrial communities. The combination of functional nanoparticles and foaming technologies has a high potential to generate a new class of materials that are light weight, high strength and multifunctional [1,2] .

Foams are two phase materials in which a gas has been dispersed in a solid matrix. These lightweight materials are important because of technical, commercial, and environmental issues, representing an important percentage of the nowadays market of plastics. However, the applications of foams are limited by their inferior mechanical strength, poor surface quality and low thermal and dimensional stability in comparison with solid materials [3]. To overcome some of these drawbacks the polymer matrices conforming the solid phase of the foam has been traditionally filled with micron-sized fillers [4-8]. Compared to conventional micro-sized fillers, nanoparticles offer unique advantages for controlling both the foam structures and

properties. Due to the extremely small particle size it is possible to generate a large number of nucleants with a relatively low particle loading. Furthermore, the nanoscaled dimension, the high aspect ratio and the large surface area make these particles desirable as reinforcing elements for the cell walls [9].

As a consequence of these expected outstanding properties the number of works dealing with the production and characterization of polymeric nanocomposite foams has rapidly increased in the last few years. The efforts have been focused both in thermoplastic (amorphous and semi-crystalline) and thermoset polymers. The infused nanoparticles has been also very diverse, from carbon nanotubes or nanoclays (mainly montmorillonite) to carbon nanofibers or silica particles [10-16]. Although both physical and chemical blowing agents have been used, the vast majority of the published studies deal with the former ones. Commonly a gas in supercritical conditions is combined with an amorphous nanofilled polymer for the production in continuous of microcellular foams. The two steps batch foaming route has been also used for the production of nanocomposite foams but not so extensively as the continuous one [17-25]. This foaming route has several advantages, it is very appropriate for example for analyzing the heterogeneous nucleating role played by the nanoinclusions as no other additive are present in the matrix, however it presents also several drawbacks. The experimental set-ups needed are complex and not easily industrially scalable. Together with this, it is not easy to obtain samples with a defined shape or geometry and therefore the possibilities of measuring the macroscopic properties of foamed materials are limited

The use of chemical blowing agents for the production of nanocomposite foams is not so extended in the literature although some examples can be found using injection moulding, extrusion foaming and compression moulding. Guo et al. demonstrated for example that an accurate control of the parameters during injection can lead to the same degree of improvement in several properties that the one obtained with the addition of nanoparticles to the solid polymer [26]. The high pressure drops needed at the die during extrusion foaming to obtain optimum cellular structures is an important limitation in the size and shape of the samples produced. In spite of this, nanoparticles help to enhance the homogeneity of the cellular structure and ultra-low density foams can be obtained by this procedure (20-30 kg/m3) [27-30]. Compression moulding is an industrially extended technique extensively used for the production of foams in big blocks [31-35],. In its two steps version, foams with densities of the order of 30 kg/m3 can be produced from a previously crosslinked polymer matrix. Velasco et al. studied the foaming by this route of polyethylene containing hectorite-type nanoclays. The samples obtained exhibited improved thermal stability and mechanical properties [34]

Information regarding foamed polyethylene/nanoparticles systems is scarce though some examples can be found. The semi-crystalline character of polyethylene adds a severe difficulty to the foaming using physical blowing agents. Lee et al. investigated the effect of clay particles on the cell morphology of HDPE/clay nanocomposite foams produced using a batch foaming process [35]. They proved that in comparison with neat HDPE, foamed nanocomposites presented finer and more uniform cellular structures. The influence of clays dispersion on the extrusion foaming by supercritical CO_2 of LDPE was also studied by Lee et al [36]. Few works can also be found using thermally decomposed blowing agents. Riahinezhad studied the correlation

between rheology and morphology in blends of PE/EVA containing clays [33], reductions in the cell sizes and increments in the cell density were found with the addition of the layered silicate nanoparticles. Finally Saiz-Arroyo et al. studied the foaming behaviour of a more uncommon system of polyethylene containing nanosilicas. Two foaming routes were used for this purpose, one following the pressure quench method using CO_2 as blowing agent and another one using the improved compression moulding route using azodicarbonamide [37].

The properties of the solid nanocomposite matrix deeply influence the foaming behaviour itself and the final properties of the foam. An accurate characterization of the solid polymer containing clays can be used as useful predicting tool of the foamability and performance of a certain formulation in any foaming route. Some of these parameters have been individually characterized by some authors and later related with the foam properties and foaming behaviour but there is a lack of a general overview taking into account several of these parameters all together at the same time and relating them with the foaming process.

In this work special attention has been paid to the relation between the properties of the solid nanocomposite and its influence on the later foaming. Our first objective has been studying the most influencing properties of the solid matrix on foaming in a low density polyethylene/nanoclays system. The aim is establishing clear relationships between these studied properties and the foaming behaviour observed later. The samples undergo a free foaming process using a chemical blowing agent and are studied using a novel and simple but rich in information technique known as optical expandometry. The correlations are established from the numerical data obtained by this technique.

EXPERIMENTAL

Materials and Sample preparation

A low density polyethylene PE003 from Repsol Alcudia with 2 g/10min (2.16 kg and 190 ^{o}C) of MFI, density of 920 kg/m^3 and 110 ^{o}C of melting point was used as polymer matrix. For the nanocomposites production this polymer matrix was melt blended with montmorillonite-type organomodified nanoclays Cloisite C15A from Southern Clay Products and a coupling agent, maleic anhydride grafted polyethylene Fusabond 226 DE from DuPont (1.5 g/10min, 120 ^{o}C of melting point). The blending was performed in a twin screw extruder at 250 rpm with a die temperature of 190 ^{o}C. The proportion of coupling agent to nanoclays was maintained constant in 2:1. In order to clearly distinguish the role played by the nanoclays the PE003 was also melt blended with the coupling agent only. The proportion PE003/coupling agent was maintained equal to the one used in the case of the filled composites. Two different clay contents were used, 3 wt.% and 5 wt.%. The compositions and nomenclature used are summarized in Table 1.

Table 1: Proportion of components for the different samples

Sample	Matrix/parts	Coupling agent/parts	Nanoclays/parts
Raw material	100	0	0
Unfilled-3%	91	6	0
3% Nanoclays	91	6	3
Unfilled 5%	85	10	0
5% Nanoclays	85	10	5

In order to study the foaming behavior the previous formulations were blended with azodicarbonamide (Lanxess Porofor M-C1) in a proportion of 7 wt.%, and antioxidants Irgafos 168 in a proportion of 0.08 wt.% and Irganox 1010 in a proportion of 0.02 wt.% both from CIBA using a twin screw extruder (Collin mod ZK25T) with L/D of 24 at 25 rpm and a temperature profile from 105ºC in the hopper to 125 ºC in the die

 Prior to foaming the formulations containing the blowing agent were compression at 125 ºC and a under a pressure of 2.18 MPa into precursors of 10 mm x 10 mm and 4 mm thickness. These molded precursors were used later for foaming.

Characterization of solid samples

A Mettler DSC822e differential scanning calorimeter was used for the thermal analysis of the samples. A heating rate of 10 ^{o}C under N_2 environment and a sample weight of 5±0.5 mg were used in all the tests. Crystallinity degree was calculated from the area of the DSC peak, by dividing the heat of fusion by the heat of fusion of a 100% crystalline material, (288 J/g for a 100% crystalline polyethylene [38]). The crystallinities were calculated taking into account the real proportions of polymer deducting the amount of nanoclays.

The TGA measurements were performed using a Mettler TGA/SDTA 851e with a temperature program from 50 to 850 ^{o}C at 20 ^{o}C/min in a N_2 atmosphere. TGA was also used to measure the amount of gas released by the decomposition of the azodicarbonamide during foaming in the different samples. For this purpose the temperature profile used was: 50 ^{o}C-185 ^{o}C at 15 ^{o}C/min, isotherm at 185 ^{o}C during 3 minutes, 185 ^{o}C-50 ^{o}C at -6 ^{o}C/min.

Rheological behavior was studied by means of a AR2000EX TA Instruments rheometer with an extensional fixture at a temperature of 190 ^{o}C (coinciding with the foaming temperature used as explained later) and a strain rate of 0.5 s^{-1}.

The dispersion and exfoliation of nanoclays were studied by X-ray diffraction (XRD) and transmission electron microscopy (TEM). XRD diffractograms were determined between 1° and 10° by steps of 0.005° by means of a Philips PW 1050/71 using the Cu Kα line. The transmission electron microscope used was a Tesla BS 512 with a YAG camera incorporated. Several images from different areas were analyzed to have representative conclusions.

Mechanical properties were determined using an universal testing machine Instron model 5500R6025. Three specimens were tested for each kind of sample, all of them at room

temperature. An strain rate of 1 mm/min was used in the tensile tests according to ISO 527/2. The flexural behaviour was determined using a three point bending configuration at a strain rate of 2 mm/min according to ISO 178. All these mechanical tests were performed over the solid materials, non-containing azodicarbonamide.

Optical Expandometry

The expansion of the foams was studied by means of a homemade optical expandometer set-up. The system is based on a rectangular vermiculite furnace with three infrared ceramic heaters placed one on the top and the other two at both lateral sides. To monitor the sample's expansion the furnace has two openings, one at the front and another one at the back, enabling to acquire the shadow image of the free foaming sample by setting a camera and light source one in front of each other at opposed sides. A schematic view of the optical expandometry system is provided in figure 1.
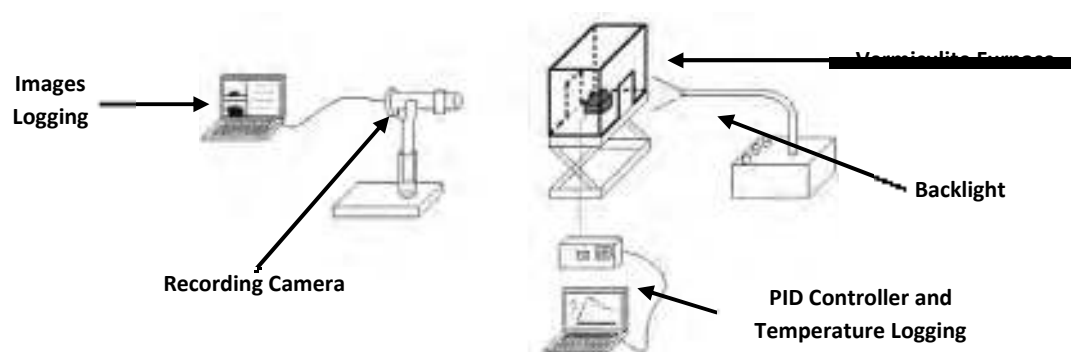
Figure 1: Optical Expandometry set-up used for the foaming characterization

The camera used is a Logitech Mic V-UW 21 and the software used for the acquisition is named SpervisionCam. The light source is a Schott KL-1500T with a diffuser to obtain a planar light field. The temperature is controlled using a PID controller with the input temperature being obtained from a thermocouple slightly introduced inside the sample. Temperature recording is synchronized with image capture. Heating ramps can be adjusted.

After image acquisition an image analysis protocol based on the ImageJ software was carried out to extract quantitative data from the image sequence. The protocol consisted in applying to each image an edge-preserving filtering to homogenize the gray level, a subsequent binarization of the region of interest and a dimensional analysis of the growing binarized foam, all by using ImageJ conventional tools. In this work we measured the projected area (number of pixels). Detailed information about this technique can be found in [39].

Characterization of the foams

The cellular morphology of the foams was characterized by scanning electron microscopy with a JEOL JSM-820 microscope. Samples were immersed in liquid nitrogen for 5 minutes, cut and mounted on stubs. The fracture surfaces were sputter coated with gold prior to the microscopy work. The mean cell size was obtained using image processing software Image J from at least 75 cells in different micrographs from the same specimen [40].

RESULTS AND DISCUSSION

Characterization of the solid nanocomposites

- **Exfoliation and dispersion**

All the composites have been produced by melt blending. As already mentioned in the experimental part a coupling agent was first melt blended with the nanoclays in order to promote the exfoliation of the latter ones. The interlamellar space of the nanocomposites was characterize by XRD and compared with the interlamellar space of the nanoclays as received. From figure 2 the Bragg's Law yields a separation between platelets of 2.45 nm for the organomodified nanoclays as received and this separation is increased to a value of 3.27 nm for the nanocomposites always taking the maximum of the peaks for the calculations. This suggests that the melt blending has promoted some intercalation degree but there are still agglomerates present in the polymer matrix. An exfoliated/intercalated structure is hypothesized for the nanocomposites.
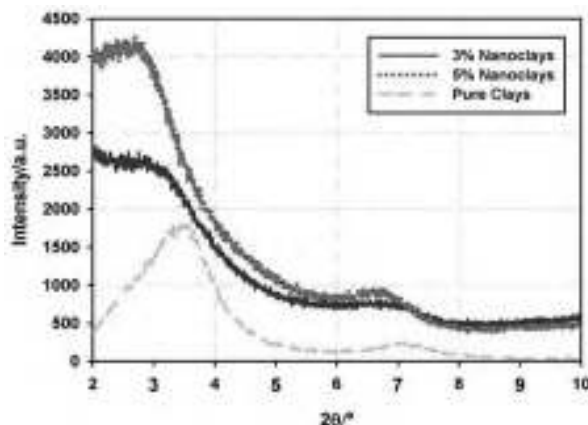
Figure 2: XRD pattern for the pure clays and for the melt blended nanocomposites.

This structure is confirmed by transmission electron microscopy. Figure 3 shows two micrographs for the 5%-Nanoclays samples. On Figure 3 a) individual well exfoliated and dispersed platelets can be distinguished all along the micrograph arranged with a more less preferential orientation but in some areas (figure 3 b)) still some agglomerates of platelets that have not suffered a complete exfoliation can be observed.
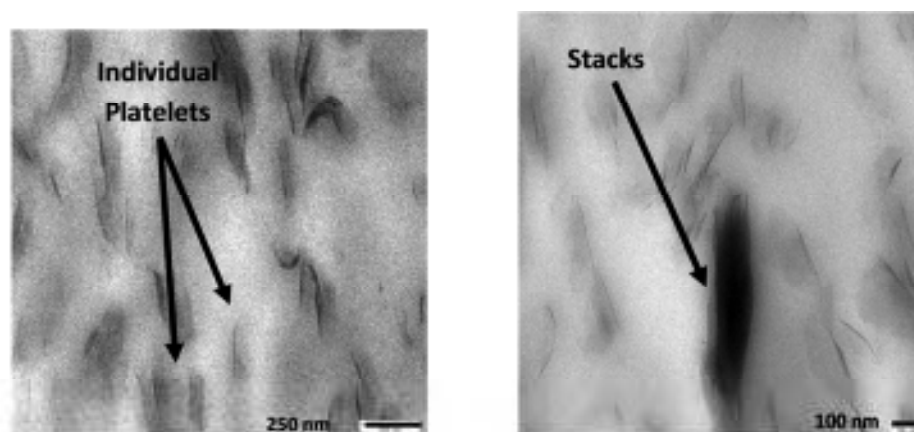
Figure 3: TEM images denoting an intercalated structure for the nanoclays. Individual platelets can be distinguished along the polymer (left) but some agglomerates are still present.

The exfoliation degree influences not only the properties of the solid matrix but it has also a deep influence on the foams themselves. A high exfoliation degree and a good dispersion of the platelets influences the cellular structure from several points of view. Single platelets can act as nucleation sites for the cells formation, reducing the cell size and increasing the cell density. Well exfoliated clays can play also an stabilizing role of the polymer melt while foaming reducing cell coarsening and collapse and allowing therefore to higher expansion ratios. High reductions in the gas diffusivity, which is a parameter of major importance for foams intended for insulation, cushioning or packaging, are expected only in the case of exfoliated morphologies [34-36]. As will be seen later the foaming by itself has also a beneficial effect on the nanoclays exfoliation. Higher exfoliation degrees are found for the foams than for the solids.

- **Thermal properties**

Differential scanning calorimetry provided the results of crystallinity and meting point shown in table 2 for all the formulations

Table 2: Thermal properties of the samples in terms of melting temperature and crystallinity percentage

Sample	*Melting Point/°C*	*Crystallinity/%*
Raw Polymer	112.66	44.0
Unfilled-3%	112.07	44.0
3% Nanoclays	111.19	45.4
Unfilled-5%	111.49	45.3
5% Nanoclays	112.52	48.2

The differences in crystallinity between samples are not large, however an slight nucleating effect of the nanoclays during the crystallization can be inferred for the filled samples. This higher crystallinity by itself can have an improving effect on the mechanical properties of the solid matrix which can be transferred later to the foams. Crystallinity would have a more patent

effect on foaming routes using physical blowing agents, modifying the solubility and diffusivity of gases and affecting therefore the final cellular structure [41], but its influence on foaming in the case of using chemical blowing agents is not so remarkable. The addition of the coupling agent increases also the crystallinity of the final formulation as can be observed in Unfilled-5% samples. The linear character of the LLDPE in which the coupling agent is based, gives as a result a higher crystalline order which is translated in higher crystallinities.

- **Polymer stability**

The thermal stability of the samples and the influence of the nanoclays on this parameter were studied performing thermogravimetric analysis. Although the experiments were performed in the range of 50 $^{\circ}$C to 850 $^{\circ}$C, for the sake of simplicity figure 4 only contains the interval 350 $^{\circ}$C-600 $^{\circ}$C. No additional weight loss was found before 350 $^{\circ}$C or after 600 $^{\circ}$C.
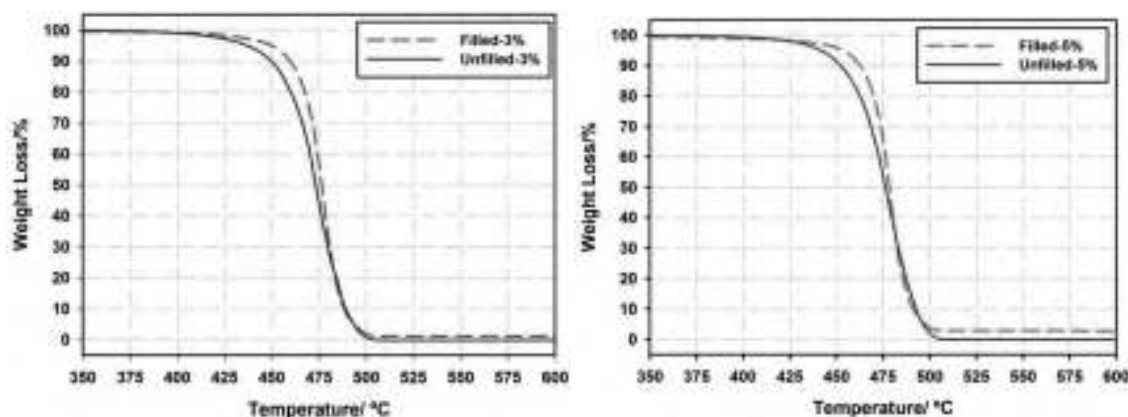
Figure 4: polymer stability characterized by thermogravimetrical analysis (TGA). The nanoclays delay the degradation temperature of the polymer.

The addition of nanoclays increases the onset of the degradation temperature in 9 $^{\circ}$C for the 3 wt.% and in 10 $^{\circ}$C for the 5 wt.% (Table 3). The presence of compatibilizer does not have a significant influence in the thermal degradation of the polymer matrix. These results suggest that clays act as a gas barrier during the polymer pyrolysis delaying the onset of decomposition of the polymer.

Table 3: Onset temperature for the degradation of the polymer obtained from TGA.

Sample	Onset Temperature/ $^{\circ}$C
Unfilled-3%	460.80
Filled-3%	468.54
Unfilled-5%	460.35
Filled-5%	470.76

- **Rheology: extensional viscosity**

The rheological behavior is a parameter of major importance that deeply determines the foamability of a polymer matrix. Particularly the uniaxial extensional rheology represents well

the biaxial flow suffered by the melted polymer during foaming. The extensional viscosity of all the samples have been measured at the temperature used later for foaming, this way we will be able to use these data to explain the foaming behavior observed for each formulation. The log-log plot shown in figure 5 depicts the extensional viscosity measurements performed on the samples.
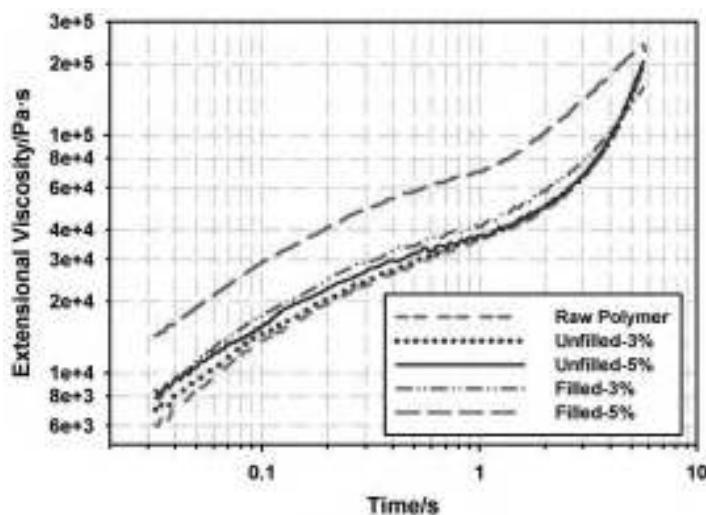
Figure 5: Extensional viscosity for the different samples. Special attention is paid to the occurrence of strain hardening phenomenon.

The different amounts of coupling agent present in the Unfilled-3% and the Unfilled-5% samples slightly influence the extensional viscosity as can be observed in figure 5. While adding 3 wt.% of nanoclays the extensional viscosity is moderately increased, this increment is much stronger in the case of 5 wt.% nanoclays. This effect of the nanoclays on the viscosity of the polymers was expected from the beginning. But the strain hardening, defined as an increase of the extensional viscosity with increasing strain at a rate which is higher when compared to the linear viscoleastic limit, is patently reduced for the samples with clays. The reduction in the 5 wt.%-Nanoclays samples is even more important than for the 3 wt.%-Nanoclays ones. This parameter is directly related with the stability of the foam of any formulation since this enhanced viscosity can reduce the effects of sagging and prevent cell coalescence leading to higher stabilities. Lower strain hardenings are commonly translated into poorer foamability and stability. There are several works in the literature that mention also this effect of decrease in strain hardening with increasing particle concentrations. Particles can partially convert the extensional flow in the surrounding polymer into shear flow and this interferes with the occurrence of strain hardening [42, 43].

Table 4: Trouton ratio calculated from the extensional viscosity plots at a Hencky strain equal to 2.5. This parameter numerically quantifies the strain hardening present in the samples.

Sample	Trouton Ratio
Raw Polymer	9.62
Unfilled-3%	9.54
Filled-3%	5.64
Unfilled-5%	9.21
Filled-5%	4.81

The Trouton ratio is defined as the ratio of extensional viscosity to shear viscosity. When this Trouton ratio is measured at high Hencky strains then it gives a direct measurement of the strain hardening. Table 4 contains the Trouton ratio for each formulation measured at a Hencky strain of 3. A reduction of 41% in strain hardening is found with the addition of 3% of nanoclays and this reduction goes up to 48% in the case of 5% nanoclays. This reductions in strain hardening are directly related with the poorer stabilities found for these foams later.

- **Mechanical Properties**

The mechanical properties of a foam are the result of two main contributions. On the one hand the morphology of the cellular structure in terms of cell size, cell density, homogeneity, anisotropy ratio and fraction of mass in the struts can have a deep impact on the final mechanical behavior of the foam. But on the other hand, an important contribution comes from the performance of the solid matrix that forms the foam. From this point of view improving the mechanical behavior of the solid matrix is a good starting point for improving the final mechanical properties of the foam. Figure 6 contains the mechanical characterization data in tensile and three point bending tests performed for the different kinds of samples.
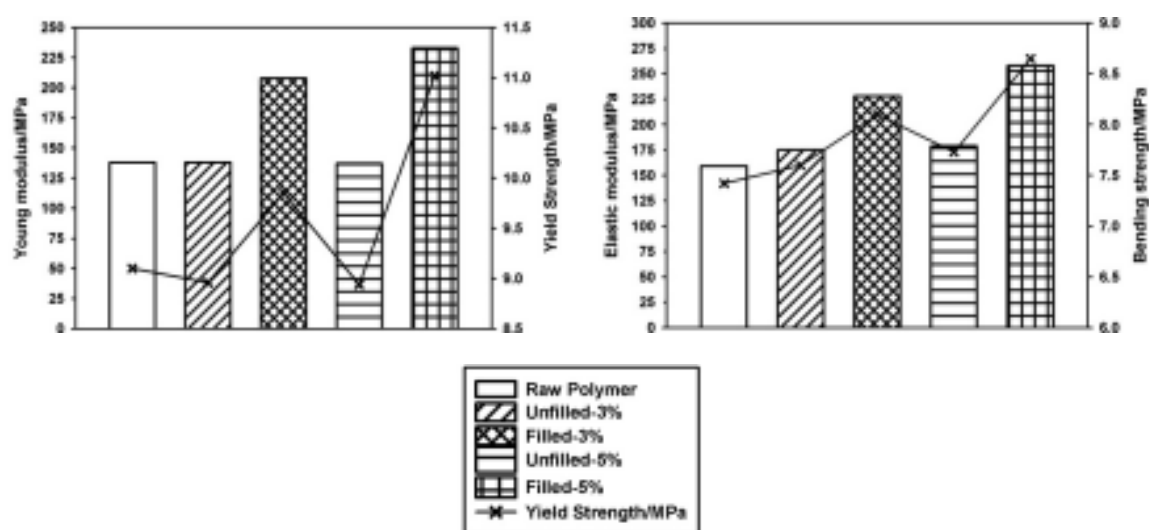
Figure 6: Mechanical properties in a) tension and b) bending. Both the elastic modulus and the yield strength have been studied.

Figure 6 a) depicts the improvements in tensile properties achieved with the addition of nanoclays. The Young modulus is increased in a 51% with the addition of 3% of clays and this increment reaches a value of 69% with 5% of clays going from a value of 138 MPa to a value of 233 MPa for the nano-reinforced sample. On the contrary the coupling agent does not influence the elastic properties in tension as can be inferred by comparing the Young modulus of the unfilled samples with the performance of the raw polymer. The yield strength is also improved with the addition of nanoparticles but the coupling agent addition does not have any remarkable effect.

Figure 6 b) depicts also the improvements in bending achieved with the nano-reinforcement. Isolating the beneficial effects of the nanoclays (that is, comparing Filled samples to Unfilled samples) the increments are up to 30% for the 3 wt.% clays and up to 44% for the 5 wt.% clays. These increments are higher, 43% and 62% respectively, if we make the comparison with the raw polymer. Interestingly in this case the only addition of coupling agent improves the bending elastic properties in 10% and 12% respectively. The bending strength is also improved for the filled samples. The addition of coupling agent slightly improves also this mechanical property.

Theoretically these improvements in properties should be directly translated in improvements in the performance of the foams. The equation $P_f = P_s \cdot \left(\frac{\rho_f}{\rho_s}\right)^n$ constitutes a very simple but accurate modeling of the elastic properties of foams [44]. The properties of the foam (P_f) are directly proportional to the properties of the solid matrix (P_s). ρ_f and ρ_s stand for the density of the foam and density of the polymer matrix respectively and n is an exponential parameter varying usually between 1 and 2 that fundamentally depends on the morphology of the cellular structure. This equation can be applied to both elastic modulus and strength.

Foaming of Nanocomposites

Optical Expandometry

Although the experimental technique is very simple, a lot of practical information about the foaming behavior of the samples can be obtained. The conclusions, obtained for a free foaming process, give a good guidance about the foaming behavior expectable following other foaming routes as compression moulding, improved compression moulding, foaming by extrusion or by injection, etc. The following are some of the parameters that can be studied:

- Expansion kinetics: related with the expansion rate, onset temperature and time to maximum expansion. Since in our case all the systems contain a thermally activated decomposing chemical blowing agent the expansion behavior can depend on the heating rate, maximum temperature and blowing agent content. Any catalytic effect of the fillers on the azodicarbonamide is affecting this expansion kinetics.

- Maximum expansion: the material will reach a maximum expansion that will depend on the heating rate, blowing agent content and polymer rheology during foaming. A preliminary study by optical expandometry helps to precisely adjust the processing

parameters and formulation prior to the foaming of any polymer in order to achieve the higher possible expansions.

- Stability time: after reaching the maximum expansion, if the sample is maintained at a constant temperature it will eventually collapse. The collapse rate of the material will be influenced by the rheology, presence of fillers, temperature, etc. The stability time is defined as the time interval since the foam reaches 95% of its maximum expansion till the foam crosses this value again during the collapse.

All these parameters are visually depicted in figure 7 on a typical plot obtained using this technique. From these plots all the previous parameters can be numerically quantified.
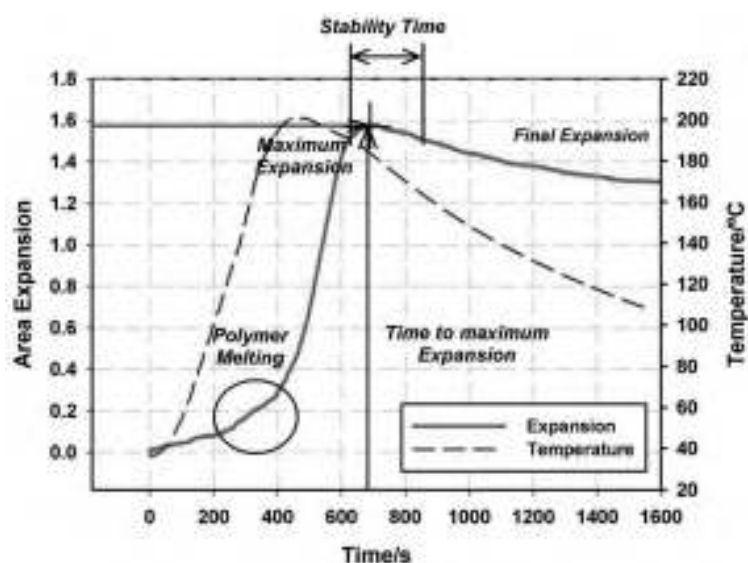
Figure 7: Schematic of the different parameters that can be quantified from a typical plot obtained by optical expandometry.

Consecutive images of the expansion of the Unfilled-5% (up) and Filled-5% (down) are shown in figure 8. A feature that can be inferred   just from visual observation is the more inhomogeneous expansion found in general in the filled samples. This in-homogeneity in the expansion is linked to the dispersion of the nanoclays. Homogenous expansions are found in every case for the unfilled specimens
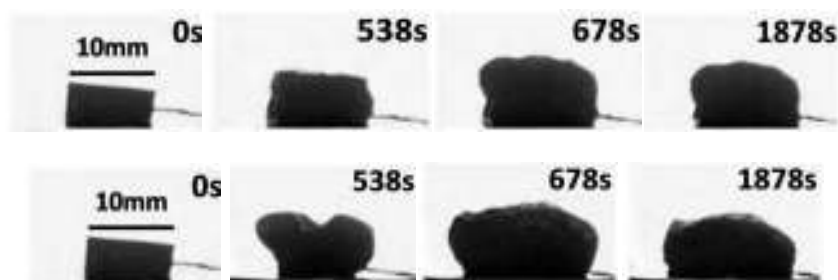
Figure 8: Images obtained by optical expandometry a) Unfilled 5%. b) Filled-5%. After image processing numerical data can be obtained,

- Effects of the nanoclays content

Figure 9 shows the foaming behavior characterized by expandometry for the four different kinds of samples at 185 ^{o}C and 190 ^{o}C respectively. The first effect observed is related with the expansion kinetics. The foaming begins earlier in the samples containing clays independently of the temperature (foaming onset, table 6) And it is also sensitive to the content of clays. This behavior is due to a catalytic effect of the nanoclays over the azodicarbonamide, accelerating its decomposition. Figure 10 shows the thermogravimetric experiments performed using precursors of the different materials. An equivalent temperature profile to the one used for foaming in the furnace was used. The catalytic effect of the nanoclays is also observed from the thermogravimetry experiments. The decomposition of the azodicarbonamide starts before in the filled samples and depends also on the amount of filler present.

At 190 ^{o}C, as a consequence of a higher foaming temperature and the catalytic effect of the nanoclays, the lower melt strength of the polymer at this temperature is not able to withstand completely the higher gas yield obtained. That is the reason why the expansion rate and maximum expansion reached for the Filled-3% and Filled-5% is lower at this temperature than at 185 ^{o}C. For the Unfilled samples the trends followed are more logical. The maximum expansions and expansion rates are found at the higher foaming temperature (tables 5 and 6). No catalytic effect is present in this case and at the same time the higher strain hardenings found for the unfilled samples help to withstand better the gas pressure developed inside the cells at 190 ^{o}C. As a conclusion valid for future foaming by any route of these samples, lower foaming temperatures should be used for the filled samples than for the unfilled ones.

At both foaming temperatures the maximum expansions reached are significantly higher in the filled samples, especially for the Filled-5%. From figure 10 it is clear that the amount of gas released by the samples containing clays is higher than for the unfilled ones. The weight loss associated with the decomposition of the azodicarbonamide has a direct dependency with the addition of clays present in the precursor material. As a consequence of the catalytic effect of the nanoclays over the azodicarbonamide the gas yield is also higher with nanoclays. Higher amounts of gas released yield higher expansion ratios. Besides this, nanoclays could be also playing a gas barrier role, hindering the gas escape from the cells allowing for more gas available and benefiting also the consecution of higher expansions. The differences in maximum expansion reached are up to 105%. If one is able to stop the foaming (by cooling by any means) at the right time the use of nanoclays is strongly recommended in order to achieve significantly higher maximum expansions.
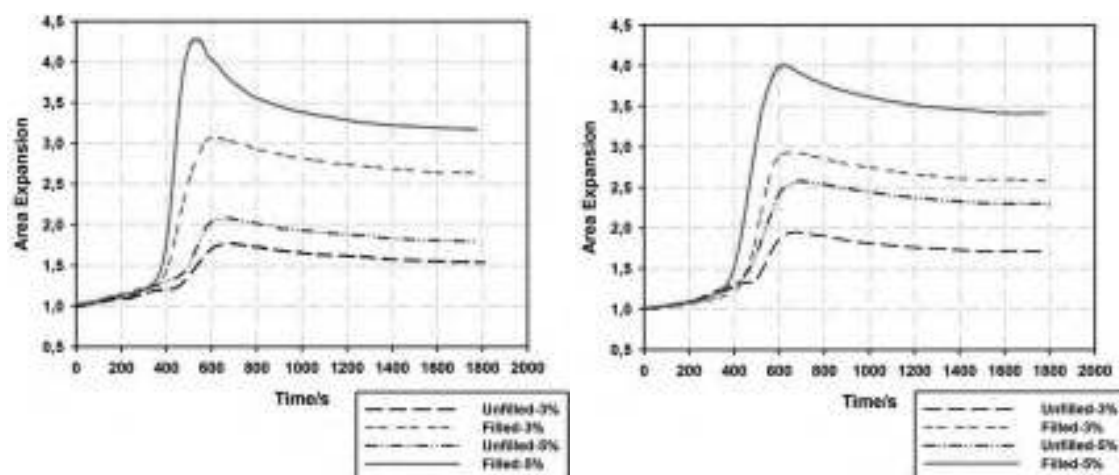
Figure 9: Area expansion measured while foaming for all the samples at a foaming temperature of a) 185 ^{o}C and b) 190 ^{o}C.

The stability time is defined as the time period since the foam reaches 95% of its maximum expansion while growing until it crosses again this 95% maximum expansion when collapsing. It gives an idea of the time window available to stop the foaming process in order to have the best foaming in terms of expansion ratio. The stability time is always decreased in the samples containing clays. It goes from 176 seconds for the Unfilled-5% to only 80 seconds for the Filled-5%. The strain hardening is playing a fundamental role in this property. The high strains reached at the maximum expansion for the samples with clays together with the low ability at this high strains to withstand the pressure reduces strongly the stability times in the filled samples in comparison to the unfilled ones. Numerical data for all this discussion is provided in Table 5. The stability times for the filled samples are higher at 190 ^{o}C. This could be expected taking into account that the maximum expansion reached is lower at this temperature together with a lower pressure remaining inside the cells. The collapse rate is directly dependent with the maximum expansion reach. Higher maximum expansions are translated into higher collapse rates. Samples containing nanoclays therefore present higher collapse rates than the corresponding unfilled ones. Numerical data about collapse rates are provided in table 6.
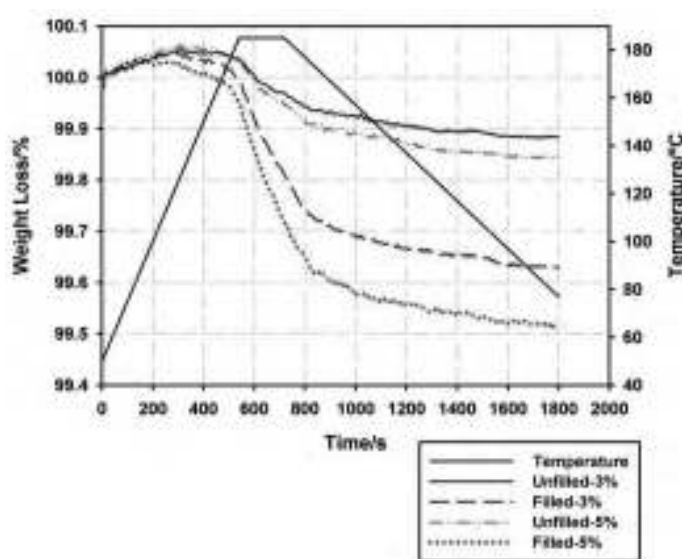
Figure 10: Decomposition behavior of the azodicarbonamide determined by thermogravimetry. The temperature profile used is equivalent to the one used for foaming in the furnace.

Table 5: numerical data obtained at the two different temperatures for the main parameters studied.

Sample	Temperature /°C	Time to Maximum Expansion /s	Stability /s	Maximum Expansion	Difference/ %	Final Expansion	Difference/ %
Unfilled-3%	185	692	170	1.78	73	1.54	71
Filled-3%	185	618	112	3.08		2.64	
Unfilled-5%	185	700	176	2.09	105	1.79	77
Filled-5%	185	532	80	4.29		3.17	
Unfilled-3%	190	686	177	1.95	51	1.71	51
Filled-3%	190	664	150	2.94		2.59	
Unfilled-5%	190	700	182	2.58	55	2.30	49
Filled-5%	190	602	110	4.01		3.42	

The differences in maximum expansion, that were as high as 105% between filled and unfilled samples are patently lower at the final time (77%). This is related with the collapse kinetics,

samples containing nanoclays collapse much faster than the unfilled ones although the "final" expansion is still higher for the samples with clays.

- Effects of the coupling agent content

The two different coupling agent contents allow studying the possible effect on foaming. It is experimentally demonstrated that a slightly higher amount of gas is released for the samples containing more coupling agent (Unfilled-5%) (figure 10) and this is finally translated in terms of the maximum expansion reached. The difference in maximum expansion is 32% higher at 190 ^{o}C for the Unfilled-5% than for the Unfilled-3%. The linear character of the polymer together with the maleic anhydride helps to reach lower densities. It plays also a fundamental role in the expansion rates. Samples containing more coupling agent also present higher expansion rates (table 6). As a conclusion the addition of higher amounts of coupling agent help to reach lower densities and higher expansion rates. The stability time is very similar independently of the coupling agent content. The Trouton ratio for the Unfilled-3% and Unfilled-5% was very similar, therefore no big differences could be expected in stability while foaming. Collapse rate and foaming onset time are not influenced by the different additions of coupling agent. In addition, no difference in foaming onset are found by thermogravimetry (figure 10). As a general conclusion of this paragraph, that can be extended also to other foaming processes, the addition of a small amount of a LLDPE grafted with maleic anhydride helps to improve the foaming behavior in terms of maximum expansion and expansion rate without compromising the stability of the foam.

Table 6: expansion rate, foaming onset and collapse rate calculated from the optical expandometry for all the samples.

Sample	Temperature /^{o}C	Expansion rate/(exp. area/s)	Foaming onset/s	Collapse rate/|exp. area/s|
Unfilled-3%	185	$3.61 \cdot 10^{-3}$	446	$4.97 \cdot 10^{-4}$
Filled-3%	185	$11.00 \cdot 10^{-3}$	340	$7.79 \cdot 10^{-4}$
Unfilled-5%	185	$6.15 \cdot 10^{-3}$	452	$4.95 \cdot 10^{-4}$
Filled-5%	185	$28.10 \cdot 10^{-3}$	304	$26.90 \cdot 10^{-4}$
Unfilled-3%	190	$5.32 \cdot 10^{-3}$	448	$4.78 \cdot 10^{-4}$
Filled-3%	190	$11.90 \cdot 10^{-3}$	359	$6.53 \cdot 10^{-4}$
Unfilled-5%	190	$7.65 \cdot 10^{-3}$	423	$4.60 \cdot 10^{-4}$
Filled-5%	190	$16.60 \cdot 10^{-3}$	308	$15.10 \cdot 10^{-4}$

Exfoliation after Foaming

After foaming the samples containing clays were again tested by XRD in order to study any possible effect of the foaming on the structure of the nanoclays. XRD of the solid precursor prior to the foaming was also performed. The results are shown in figure 11. In the foamed samples the peaks associated with the interlamellar spacing of the ordered nanoclays are strongly shifted to lower angles, below 2°. In the range of angles studied only smooth shoulders can be observed now, indicating that the foaming has increased the spacing between platelets. The

exfoliation always desired has been strongly promoted just by foaming, so the exfoliation degree is higher in the foamed samples than in the solids. The shoulder found is even smoother in the Filled-5% sample which is the one that has reach a higher expansion suggesting that higher expansion ratios promote better exfoliations, at least to some extent.
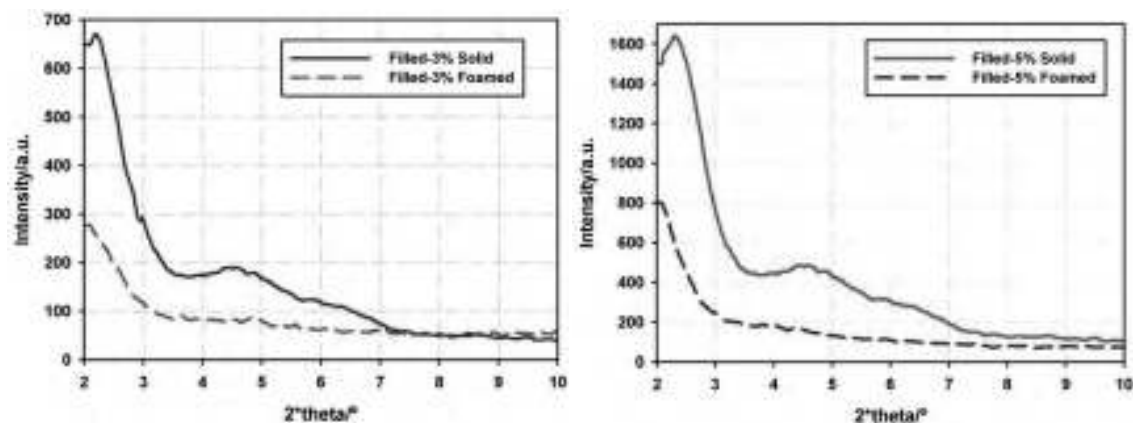

Figure 11: XRD patterns obtained for a) the solid precursors prior to the foaming and b) samples after being foamed. An important improvement in exfoliation is found.

The polymer molecular chains chemically bonded to the edges of the nanoclays platelets suffer a re-organization during foaming. This re-organization helps to increase the interlamellar separation improving the nanoclays exfoliation. This improvement in the exfoliation degree after foaming has been observed also by other authors using polyolefin nanocomposites [30]

Cellular structure

The foams in their final state, after optical expandometry tests, were analyzed in terms of their cellular structure. Figure 12 shows the micrographs obtained for the Unfilled-5% and Filled-5% at 185 ºC and 190 ºC respectively.
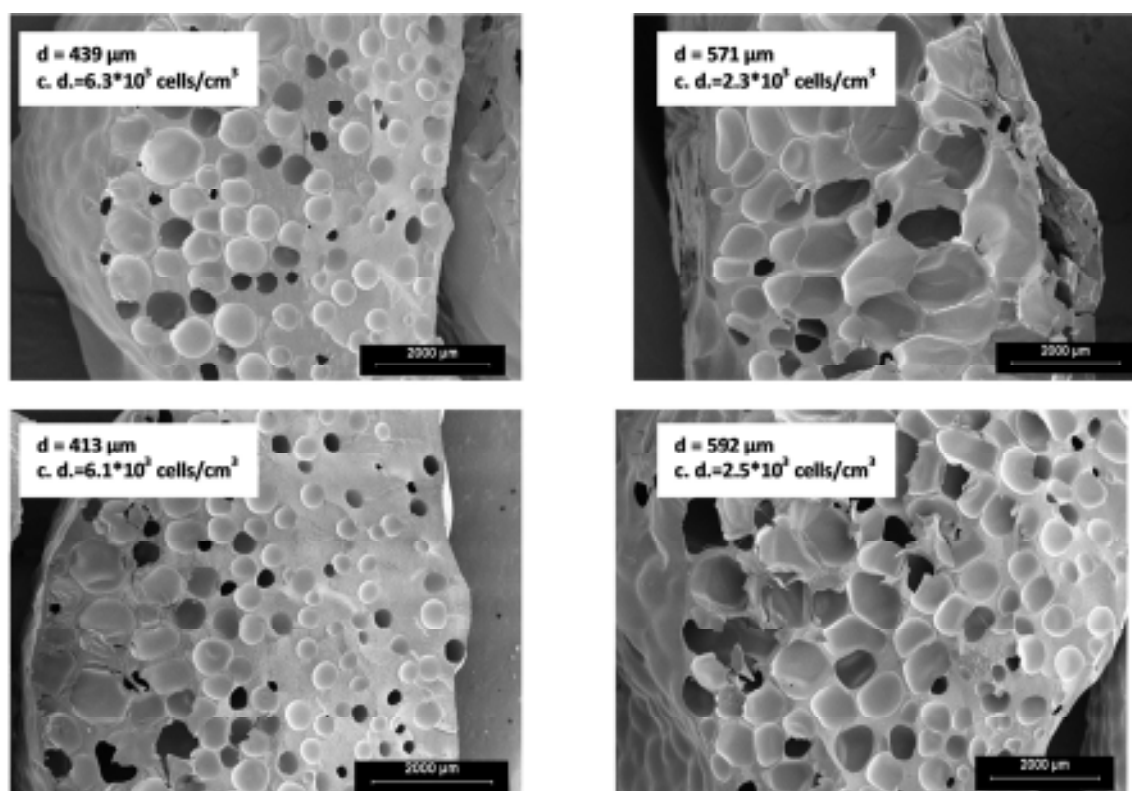
Figure 12: Micrographs showing the cellular structure of the foamed samples in their final state. "d" stands for mean diameter of the cells (cell size) and "c.d." stands for cell density.

The free foaming process yield non-homogeneous cellular structures. The higher expansion ratios, achieved with the filled samples, are translated into larger cell sizes in the foams. Together with this, the lower cell densities found for the samples filled with nanoclays suggest that a more intense cell rupture and coalescence have taken place in comparison to the unfilled ones. The same behavior is observed for the samples containing 3% of nanoclays (Unfilled-3% and Filled-3%). This is coherent with the lower strain hardening in these materials.

Conclusions

Solid polyethylene layered silicate nanocomposites have been characterized in terms of exfoliation and dispersion of the clays, thermal properties, polymer degradation, rheology and mechanical properties, all of them important features for the later production of foams having as solid matrix these materials. An intercalated structure with a good dispersion of the clays has been found in all the cases. This well dispersed intercalated/exfoliated morphology slightly increases the crystallinity of the corresponding unfilled matrix. The nanoclays also broaden the polymer degradation window moving the onset temperature 10 ^{o}C further. This result favors the performance of the filled foams at high temperatures. The rheology has been studied in terms of polymer extensional viscosity, paying special attention to the strain hardening phenomenon occurrence. The presence of nanoclays strongly reduces the strain hardening. Strain hardening is of major importance while foaming so a decrement of this parameter has a strong detrimental effect on foam stability as it is confirmed later. On the contrary, the addition of

nanoclays improves patently the mechanical properties in tension and bending for these materials. As has been demonstrated theoretically, the mechanical properties of any foam produced from these materials will benefit from this fact.

A study about the foaming behavior of these materials has been performed by optical expandometry. An interesting catalytic effect of the nanoclays over the azodicarbonamide is found, accelerating the foaming. The amount of gas released by the azodicarbonamide in the filled samples is also higher, therefore higher expansion ratios (lower densities) are reached in the filled specimens together with higher expansion rates. A gas barrier effect of the clays could be playing also a role here, allowing for more gas available for foaming. On the other hand, the stability of the nanocomposite foams is poorer as expected from the strong reductions in strain hardening found previously. Lower processing temperatures are recommended for the filled samples together with a more strict control of the foaming time in order to maximize the expansion ratio. The collapse rates found are directly proportional to the maximum expansions reached, therefore samples containing nanoclays collapse more quickly than the unfilled ones. The addition of a linear low density polyethylene grafted with maleic anhydride helps to achieve higher expansion ratios and also higher maximum expansion ratios (as a consequence of a higher amount of gas released too) but has no influence on the onset temperature or collapse rate. The stability time, since directly connected with the strain hardening appearance, is not compromised in the unfilled samples by the addition of the LLDPE containing maleic anhydride .

Finally, an interesting effect of the foaming over the nanoclays morphology has been found. Higher exfoliation degrees, always pursued by any means, have been accomplished just by foaming the polymer. A remarkable improvement in exfoliation has been achieved, directly connected with the expansion ratio of the samples. The beneficial effects expected from the high exfoliation degrees would be more present in the foams than in the solids.

ACKNOWLEDGEMENTS

BIBLIOGRAPHY

[1]   C. C. Ibeh, M. Bubacz: Current trends in nanocomposite foams *J. Cell. Plast.* **44**, 493-515 (2008)

[2]   L.A. Utracki in Clay-containing polymeric nanocomposites. *Rapra Technology Limited.* United Kingdom (2004).

[3]   R.A. Vaia, E.P. Giannelis: Polymer nanocomposites: status and oportunities. *MRS Bull.*, **26,** 394, (2001).

[4]   H. E. Naguib, C. B. Park, P. C. Lee: Effect of the talc content on the volume expansion ratio of extruded PP foam. *J. Cell. Plast.* **39**, 499-511 (2003).

[5]   H. H. Yang, C. D. Han: The effect of nucleating agents on the foam extrusion characteristics. *J. Appl. Polym. Sci.* **29,** 4465-4470 (2003).

[6]   H. X. Huang, J. K. Wang : Improving polypropylene microcellular foaming through blending and the addition of nano-calcium carbonate. *J. Appl. Polym. Sci.* **106**, 505-513 (2007).

[7]   F. Saint-Michel, L. Chazeau, J. Y. Cavaille : Mechanical properties of high density polyurethane foams : II Effect of the filler size. *Comp. Sci and Tech.* **66,** 2709-2718 (2006).

[8]   S. Roman-Lorza, M. A. Rodriguez-Perez, J. A. de Saja, J. Zurro: Cellular structure of EVA/ATH halogen free flame retardant foams. *J. Cell. Plast.* **0** 1-21 (2010).

[9]   L.J. Lee, C. Zeng, X. Cao, X. Han, J. Shen, G. Xu: Polymer nanocomposite foams. *Compos. Sci. Technol.*, **65**, 2344, (2005).

[10]   W. Zhai, C. B. Park, M. Kontopoulou: Nanosilica addition dramatically improves the cell morphology and expansion ratio of polypropylene heterophasic copolymer foams blown in continous extrusion *Ind Eng Chem Res* **50**, 7282-7289 (2011).

[11]   C. Zeng, X. Han, L. J. Lee, K. W. Koelling, D. L. Tomasko: Polymer-clay nanocomposite foams prepared using carbon dioxide. *Adv Mater* **15**, 1743-1747 (2003).

[12]   Y. H. Lee, K. H. Wang, C. B. Park, M. Sain: Effects of clay dispersion on the foam morphology of LDPE/clay nanocomposites. *J App Polym Sci* **103**, 2129-2134 (2007).

[13]   S. M. Seraji, M. K. R. Aghjeh, M. Davari, M. S. Hosseini, S. Khelgati: Effects of clay dispersion on the cell structure of LDPE/clay nanocomposites *Polym Compos* **32**, 1095-1105 (2011).

[14]   M. C. Saha, M. E. Kabir, S. Jeelani: Enhancement of the thermal and mechanical properties of polyurethane foam infused with nanoparticles. *Mat Sci Eng A-Struct* **479**, 213-222 (2008).

[15]   K. Gorem, L. Chen, L. S. Schadler, R. Ozisik: Influence of nanoparticle surface chemistry and size on supercritical carbon dioxide processed nanocomposite foam morphology. *J Supercrit Fluid* **51**, 420-427 (2010).

[16]   R. Verdejo, C. Saiz-Arroyo, J. Carretero-Gonzalez, F. Barroso-Bujans, M. A. Rodriguez-Perez, M. A. Lopez-Manchado: Physical properties of silicone foams filled with carbón nanotubes and functionalized graphene sheets. *Europ. Polym.* J.**44**, 2790-2797 (2008).

[17]   V. Kumar, N. P. Suh: A process for making microcellular thermoplastic parts. *Polym. Eng. Sci* **20**, 1323 (1990)

[18]   V. Kumar, G. Schirmer, *SPE ANTEC Tech. Papers*, **41**, 2189 (1995)

[19]   D. Miller, V. Kumar: Fabrication of microcellular hdpe foams in a sub-criticl CO_2 process. *Cell. Polym*. **28**, 1, (2009)

[20]   Z. Xing, G. Wu, S. Huang, S. Chen, H. Zeng: Preparation of microcellular cross-linked polyethylene foams by a radiation and supercritical carbon dioxide approach. *J. of Supercritical Fluids* **47**, 281-289 (2008).

[21]   P. Zhang, N. Q. Zhou, Q. F. Wu, M. Y. Wang, X. F. Peng: Microcellular foaming of PE/PP blends. *J. of Applied Polymer Science*, **104**, 4149-4159 (2007)

[22]   Zhai, W; Wang, H; Yu, J; Dong, JY; He, J: Foaming behavior of iotactic polypropylene in supercritical CO_2 influenced by phase morphology via chan grafting. *Polymer* **49**, 3146-3156. (2008).

[23]   Yuan MJ, Winardi A, Gong SQ, Turng LS_ Effects of nano- and micro-fillers and processing parameters on injection molded microcellular composites. *Polym. Eng. Sci*. **45**, (6), 773-788. (2005)

[24]   Jo, C; Naguib, HE. Polymer: Constitutive modelling of HDPE polymer/clay nanocomposite foams. *Polym.* **48**, (11), 3349-3360 (2007)

[25]   Taki K, Tabata K, Kihara S, Ohshima M: Bubble coalescence in foaming process of polymers. *Polym. Eng. Sci*. **46**,(5), 680-690.(2006)

[26]   M. C. Guo, M. C. Heuzev, P. J. Carreau : Cell structure and dynamic properties of injection molded polypropylene foams. *Polym Eng Sci* **47**, 1070-1081 (2007).

[27]   A. K. Chaudhary,K. Jayaraman: Extrusion of linear polypropylene-clay foams. *Polym Eng Sci* **51,** 1749-1756 (2011).

[28]   W. Zhai, C. B. Park. Effect of nanoclay addition on the foaming behavior of linear polypropylene-based soft thermoplastic polyolefin foam blown in continous extrusion. *Polym Eng Sci.* **51**, 2387-2397 (2011).

[29]   G. Guo, K. H. Wang, C. B. Park, Y. S. Kim, G. Li: Effects of nanoparticles on the density reduction and cell morphology of extruded metallocene polyethylen/wood fiber nanocomposites. *J App Polym Sci.* **104,** 1058-1063. (2007).

[30]   J. I. Velasco, M. Antunes, O. Ayyad, J. M. Lopez-Cuesta, P. Gaudon, C. Saiz-Arroyo, M. A. Rodríguez-Pérez, J. A. de Saja: Foaming behavior and cellular tructure of LDPE/hectorite nanocomposites. *Polym.* **18**, 2098-2108 (2007).

[31]   M. Antunes, J. I. Velasco, V. Realinho, E. Solórzano: Study of the cellular structure heterogeneity and anisotropy of polypropylene and polypropylene nanocompoite foams. *Polym Eng Sci* **49**, 2400-2413 (2009).

[32]   M. Riahinezhad, I. Ghasemi, M. Karrabi, H. Azizi: Morphology and tensile properties of crosslinked nanocomposite foams of low density polyethylene and poly(ethylene-co-vinyl acetate) blends J Vinyl *Addit Technol* **16**, 229-237 (2010).

[33]   M. Abbasi, S. N. Khorasani, R. Baheri, J. M. Esfahani: Microcellular foaming of low density polyethylene using $CaCO_3$ as a nucleating agent. *Polym Compos* **32**, 1718-1725 (2011).

[34]   M.A. Rodríguez-Pérez, Crosslinked closed cell polyolefin foams: Production, structure, properties and applications. *Advances in Polymer Science,* **184**: 87-126. (2005);

[35]   J.A.Martínez-Díez, M.A.Rodríguez-Pérez, J.A. de Saja, L.O. Arcos y Rábago, O.A. Almanza, "The Thermal conductivity of a Polyethylene Foam Block produced by a Compression Molding Process", *Journal of Cellular Plastics* **37**, 21-42 (2001)

[36]   J. I. Velasco, M. Antunes, O. Ayyad, C. Saiz-Arroyo, M. A. Rodríguez-Pérez. F. Hidalgo, J. A. de Saja: Foams base don low density polyethylene/hectorite nanocomposites: termal stability and thermo-mechanical properties. *J App Polym Sci* **105**, 1658-1667 (2007).

[37]   Y.H. Lee, C.B. Park, K.H. Wang. HDPE/Clay nanocomposite foams blown with supercritical CO_2 *J. Cell. Plast*. **41**, 487, (2005).

[38]   Y. H. lee, K. H. Wang, C. B. Park, M. Sain. Effects of clay dispersion on the foam morphology of LDPE/Clay nanocomposites. *J. Appl. Polym. Sci*. **103**, (2129)21-34 (2007).

[39]   C. Saiz-Arroyo, M. A. Rodriguez-Perez, J. I. Velasco, J. A. de Saja: Influence of foaming process on the structure properties relationship of foamed LDPE/Silica nanocomposites. *Composites part B*. Accepted.

[40]   B. Wunderlich. Macromolecular Physics, 2. *Academic Press, New York.* 1973-1976.

[41]   E. Solorzano, M. Antunes, C. Saiz-Arroyo, M. A. Rodriguez-Perez, J. I. Velasco, J. A. de Saja: Optical expandometry a technique to analyze the expansión kinetics of chemically blown thermoplastic foams. *J. Appl. Polym. Sci.* **125**, 1059-1067 (2012).

[42]   J. Pinto, E. Solórzano, M. A. Rodriguez-Perez, J. A. de Saja, Characterization of cellular structure based on user-interactive image analysis procedures; *Journal of Cellular Plastics*, submitted, 2013

[43]   Doroudiani S, Park CB, Kortschot MT. Effect of crystallinity and morphology on the microcellular foam structure of semicrystalline polymers. *Polym. Eng. Sci*. **36**, (21), 2645-2661 (1996).

[44]   P. Spitael and C. W. Macosko, Strain hardening in polypropylenes and its role in extrusion foaming, *Polym. Eng. Sci.*, **44** 2090–2100 (2004)

[45]   Le Meins J. F., Moldenaers P., and Mewis J: Suspensions in polymer melts. Effect of particle size on the shear flow behavior *Ind. Eng. Chem res*., **41**, 6297-6304. (2002).

[46]   Le Meins J. F., Moldenaers P. and Mewis J: Suspensions of monodisperse spheres in polymer melts: particle size effects in extensional flow. *Rheologica Acta,* **42**, 184-190. (2003).

[47]   L. J. Gibson, m. F. Ashby. *Cellular Solids.* Cambridge University Press. United Kingdom (1999).

IN SITU CHARACTERIZATION OF NANOCLAYS EXFOLIATION DURING FOAMING BY ENERGY DISPERSIVE XRD OF SYNCHROTRON RADIATION

J. Escudero1, B. Notario1, C. Jimenez2, M.A. Rodriguez-Perez1

1. Cellular Materials Laboratory (CellMat), Condensed Matter Physics Department, University of Valladolid, Valladolid, Spain. Email: marrod@fmc.uva.es

2. Helmhotz-Zentrum Berlin, Albert-Einstein-Straße 15, 12489 Berlin, Germany

ABSTRACT

Outstanding physical properties are expected from poymer nanocomposites based on nanoclays but several theoretical and experimental studies have shown that these outstanding behavior is only achieved when nanoclays are well dispersed and exfoliated. Foaming, by itself, increases the dispersion and exfoliation of nanoclays in a polymer matrix. The present study uses energy dispersive x-ray diffraction using synchrotron radiation for the in-situ study of the exfoliation of nanoclays during the foaming process. This technique gives an insight into the physical mechanisms underlying behind the exfoliation promoted by the foaming in an LDPE/CLays system. Besides, a methodology has been established for studying in-situ, using synchrotron radiation, the exfoliation during foaming of nanoclays added to a polymer matrix.

INTRODUCTION

During the last decade the excellent properties of clay-polymer nanocomposites (CPNC) have stimulated much interest and research within the scientific and industrial communities. The high surface to volume ratio of nanoclays leads to a high reinforcement efficiency. Thus, clay polymer nanocomposites with well dispersed platelets at a low clay loading show highly increased modulus, yield strength as well as reduced flame propagation and permeability. In crystallizable polymer matrices the clay platelets can promote faster crystallization and higher levels of crystallinity which improves solvent and moisture resistance but reduces impact strength [1-4].

There are three basic structures for polymer/clay mixtures: conventional clay-filled composites with micron-sized aggregates of clay particles, nanocomposites with intercalated clay with locally ordered structure and exfoliated nanocomposites with disordered structure. Not all performance characteristics depend to the same degree on exfoliation, however the benefits increase with the degree of exfoliation and dispersion between platelets. Thus, the goal of clay/polymer nanocomposite technology is to achieve the highest possible degree of clay exfoliation, i. e., the best dispersion and distribution in a polymeric matrix. Currently three main methods for achieving it can be distinguished [1,2], being the first and second the most extended ones:

1. Polymerisation in the presence of organoclay.
2. Melt compounding a polymer with a suitable organoclay complex.
3. Other methods as ultrasonic exfoliating of organoclays in a low molecular weight polar liquid or co-precipitation [5-7].

Numerous examples of nanocomposites based on very different polymers and produced by any of the three previously mentioned routes can be found in the literature. This work and the corresponding revision of the state of the art will focus the attention on nanocomposites produced from polyethylene (PE). The non-polar character of PE makes difficult the consecution of an exfoliated structure. Polymerisation in the presence of organoclays consists on the intercalation of the clay with a compound that subsequently enters the polymerisation reaction (either polycondensation or radical polymerisation). Jin et al reported full exfoliation of polyethylene/montmorillonite system prepared by Ziegler-Natta polymerisation of ethylene in the presence of organoclay [8]. Although after the polymerisation the degree of exfoliation was high a partial re-aggregation of montmorillonite (MMT) platelets resulted after processing by compression moulding. Alexandre et al. polymerized polyethylene in the presence of either montmorillonite or hectorite [9]. Clay exfoliation in the reaction products was confirmed by XRD and TEM but the tensile properties of the resulting nanocomposites were poor and essentially independent of the nature and content of the silicate. Moreover, during melt processing of the CPNC the interlayer spacing partially collapsed. This suggests that the previous systems are thermodynamically unstable and the strong-solid interaction between clay platelets drives the phase separation. Melt blending overcomes these difficulties and is the industrially preferred method for preparing clay/polymer nanocomposites with thermoplastic polymer matrices. Typically, the polymer is melted and combined with the desired amount of the intercalated clay in an extruder, internal mixer or continuous mixer. The process is more economic, closer to the ultimate product manufacturer and more versatile. Literature on this topic is really broad. Wang et al. produced polyethylene/clay nanocomposites by melt blending and determined their flammable properties [10]. The heat release rate is reduced by 32% for the nanocomposites in comparison to the raw polyethylene. Microstructure and mechanical properties of PE/clay melt blended nanocomposites were determined by Liang and co-workers [11]. In order to improve the nanoclays exfoliation a coupling agent based on maleic anhydride grafted polyethylene was used. Important improvements were found in tensile and impact strength at low clay loadings (6 wt.%). Thermodynamically the melt blended nanocomposites are stable but the achievement of fully exfoliated morphologies is not easy. Commonly these nanocomposites exhibit the more attainable intercalated/exfoliated structures, with higher or lower degrees of exfoliation in each case.

Cellular nanocomposites are currently subject of attention in both scientific and industrial communities. The combination of functional nanoparticles and foaming technologies has a high potential to generate a new class of materials that are light weight, high strength and multifunctional [12]. As a consequence of these expected outstanding properties the number of works dealing with the production and characterization of polymeric nanocomposite foams has rapidly increased in the last few years. The efforts have been focused both in thermoplastic (amorphous and semi-crystalline) and thermoset polymers. The infused nanoparticles has been

also very diverse, from carbon nanotubes to carbon nanofibers or silica particles, to nanoclays which represent a very important number of the works published [13-22]. Most of the works relate the observed properties of the foam (thermal, mechanical, fire resistant, barrier to gases) to the state of aggregation and dispersion of the nanoparticles in the solid matrix prior to foaming. But the foaming process itself influences the dispersion and aggregation of the particles in the final foam.

An interesting result was found by Velasco et al. a few years ago. This paper shows that the degree of exfoliation was enhanced after foaming [23,24]. The foams were produced from a melt blended nanocomposite based on polyethylene and hectorite. The solid matrix prior to foaming presented an intercalated/exfoliated structure. Improvements in thermal or mechanical properties appear only when the exfoliation is complete (after foaming). The same result has been observed by the authors of this work several times in the lab. The state of delamination of the nanoclays was characterized by determining the XRD pattern before and after foaming and comparing them. This conventional technique will be referred as ex-situ XRD from now on. Although very useful, it does not give insight into the mechanisms involved in the exfoliation during foaming.

In this work an energy dispersive x-ray diffraction (ED-XRD) technique using synchrotron radiation has been used to follow in-situ the evolution of the interlamellar spacing during foaming in LDPE/MMT systems. The in-situ technique has been combined with blowing agents of different nature, different additions of a same blowing agent and different additions of nanoclays to gain knowledge on the mechanisms underlying behind the exfoliation during foaming. The whole behavior has been characterized, from the diffraction pattern of the solid precursor passing through all the intermediate states to the final solidified foam.

MOTIVATION

From our previous experience the interlamellar spacing of the MMT nanoclays present in polymer nanocomposites is increased after foaming. Figure 1 shows the ex-situ diffractograms of the precursor (solid composite (a LDPE containing MMT) + azodicarbonamide as blowing agent) and of the foam produced from that precursor. In this first case the expansion ratio achieved is equal to four (density of the foam 250 kg/m^3). The peak corresponding to the nanoclays is clearly distinguished for the solid precursors with a value around 2.3º both for samples filled with 3 wt.% and 5 wt.% of nanoclays. This peak is shifted to angles below 2º after foaming. In the range of angles studied only smooth shoulders can be observed now, indicating that the foaming has increased the spacing between platelets. The beneficial exfoliation always desired has been strongly promoted just by foaming, so the exfoliation degree is higher in the foamed samples than in the solid precursors.
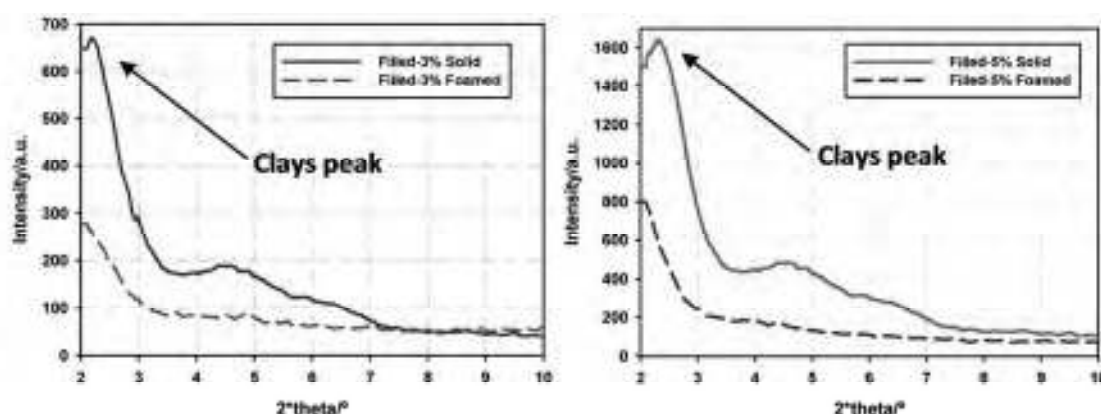
Figure 1: ex-situ XRD before and after foaming. The foaming shifts the main peak of the nanoclays to lower angles denoting an increment in the exfoliation degree.

Figure 2 shows this same effect but for foams with an expansion ratio equal to 30 (approximately densities of 30 kg/m^3). Now the effect is even more patent, the peak is strongly shifted to lower angles and the intensity is decreased. Only very smooth shoulders can be found for the foamed samples in the studied 2-theta range.
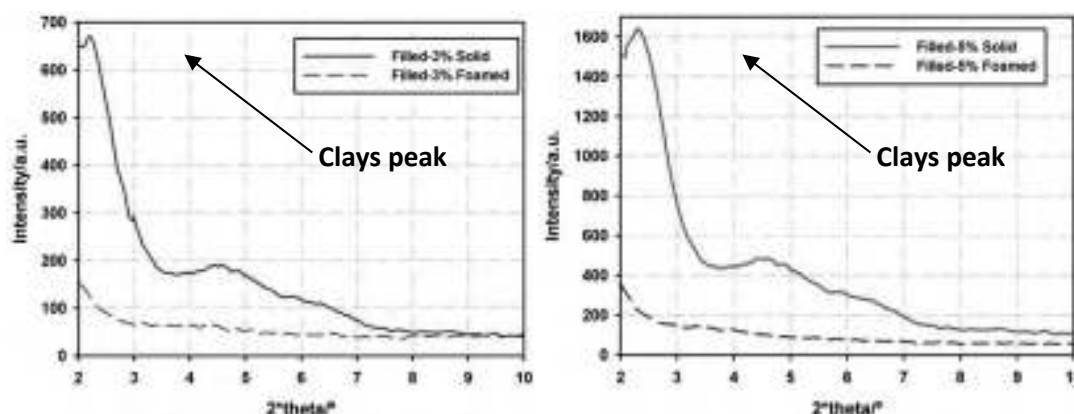

Figure 2: ex-situ XRD before and after foaming. The expansion ratio achieved is 30, much higher than in figure 1. The increment in exfoliation degree is proportional to the expansion ratio reached.

These results suggest not only an increment of the exfoliation degree after foaming in these polymer nanocomposites but also a dependency with the expansion ratio achieved. The higher is the expansion ratio the higher is also the increment in the interlamellar spacing and rupture of the ordered structure of the organomodified nanoclays.

This ex-situ study of the samples before and after foaming shows interesting results about exfoliation, a parameter of major importance in silicate layered nanocomposites but gives no insight into the mechanisms involved. From the previous presented data several questions rise up:

- Up to date all the previous observed effects have been obtained using azodicarbonamide as blowing agent but we do not know if there exists any influence of the blowing agent nature on the increment of exfoliation during foaming or it only depends on the foaming process
- We do not know if foaming is the only factor that produces the increment of interlamellar spacing or the polymer melting has also an effect.
- It is not clear if the exfoliation degree observed after foaming and solidification of the foam is the maximum reached or there is a higher value during some intermediate state.
- We do not know if the foam collapse and solidification have an effect on the exfoliation degree.
- There is a lack of knowledge about the influence of the blowing agent amount and hence of the expansion ratio achieved on the interlamellar spacing.
- The amount of nanoclays could be playing also some role.

In order to answer all these questions and gain knowledge on the mechanisms underlying behind this interesting effect an in-situ study using synchrotron radiation has been performed.

MATERIALS

A low density polyethylene PE003 from Repsol Alcudia with a melt flow index of 2 g/10min (measured at 190ºC and 2.16Kg), density 920 kg/m^3 and a melting temperature of 110 ^{o}C was used as polymer matrix. For the nanocomposites this polymer matrix was melt blended with montmorillonite-type organomodified nanoclays Cloisite C15A from Southern Clay Products and a coupling agent, maleic anhydride grafted polyethylene Fusabond 226 DE from DuPont (melt flow index of 1.5 g/10min at 190ºC and a melting temperature of 120 ^{o}C). The blending was performed in a twin screw extruder Bühler BTSK 20/40D at 250 rpm with a die temperature of 190 ^{o}C. The proportion of coupling agent to nanoclays was maintained constant in 2:1.

In order to study the foaming behavior the previous nanocomposites were blended with three different blowing agents (4, 7 and 10 wt.% of Azodicarbonamide, 3 wt% of Hydrocerol and 4 wt% of Expancel) and antioxidants Irgafos 168 (from Ciba) in a proportion of 0.08 wt.% and Irganox 1010 (from Ciba) in a proportion of 0.02 wt.% to prevent thermal oxidation of the polymer. The amounts of the different blowing agents were selected according to previous experiences. The blending was performed in a twin screw extruder (Collin mod ZK25T) L/D. To avoid any difference in the exfoliation of the platelets during the blending, a constant shear mixing energy was imparted to all the samples. A screw speed of 50 rpm was used in all the formulations with a constant feeding speed and a temperature profile identical for all the compositions. This was varied from 105ºC in the hopper to 125ºC in the die, in steps of 5ºC. Such profile was chosen in order to avoid premature decomposition of the blowing agents during the compounding steps. The material was water cooled and pelletized.

The three blowing agents that were used are:

- Azodicarbonamide (Porofor ADC/M-C1 from Lanxess). An exothermic chemical foaming agent presented as a yellow powder which has an average particle size of 3.9 ± 0.6 μm

and an onset of decomposition around 210ºC. The main released gases are N_2 (62%), CO (35%) and NH_3 (less than 3%) [25, 26]. In the following it will be denoted as AZO.

- Hydrocerol (BIH 40 E from Clariant). An endothermic chemical foaming agent masterbatch in form of white pellets with a 60% of active compound which has an onset of decomposition of 140ºC. These blowing agents are mainly compounds of alkali carbonate, citric acid and citric acid esters in a carrier based on LDPE. The carrier in this case was LPDE. The main products released in the decomposition are CO_2 and H_2O [27-29]. In the following it will be denoted as HY.

- Expancel (950 DU 80 from AkzoNobel). Microspheres with a particle size comprised between 18 and 24 µm, a density ≤ 12 kg/m³ (once expanded) that are characterized by having a dissolved gas, typically a hydrocarbon, inside of them. The onset of activation is around 140 ºC. Unlike the others two blowing agents mentioned above where once the temperature of decomposition is reached the gas is released, in this case when the activation temperature is reached the microspheres start to expand maintaining most of the gas confined within [30-32]. In the following it will be denoted as EXP.

Prior to foaming, the formulations containing the different blowing agents were compression molded into precursors disks of 100 mm diameter by 4 mm thickness using a two-hot plates press. In all the formulations the temperature of the press was fixed at 125ºC (below the decomposition point of all blowing agents). The material is first molten without pressure for 15minutes, then pressed under a constant pressure of 2.18 MPa for another 15 minutes and finally cooled down under the same pressure. These molded precursors were cut into samples of $10 \times 10 \times 4$ mm³ for foaming.

Two different clay contents were used, 3 wt.% and 5 wt.%. For the samples containing azodicarbonamide three different additions of the blowing agent were studied, 4 wt%, 7 wt.% and 10 wt.%. Two different foaming temperatures were also used for all the samples, 185 ºC and 190 ºC. Compositions and nomenclature are summarized in Table 1.

Table 1: Proportion of components for the different kind of samples and foaming temperature

Sample	Matrix/parts	Coupling agent/parts	Nanoclays /parts	wt.% Blowing Agent	Temperature /ºC
5% Nanoclays_AZO4_185	85	10	5	4	185
5% Nanoclays_AZO4_190	85	10	5	4	190
3% Nanoclays_AZO7_185	91	6	3	7	185
3% Nanoclays_AZO7_190	91	6	3	7	190
5% Nanoclays_AZO7_185	85	10	5	7	185

5% Nanoclays_AZO7_190	85	10	5	7	190
5% Nanoclays_AZO10_185	85	10	5	10	185
5% Nanoclays_AZO10_190	85	10	5	10	190
5% Nanoclays_HY_185	85	10	5	3	185
5% Nanoclays_HY_190	85	10	5	3	190
5% Nanoclays_EXP_185	85	10	5	4	185
5% Nanoclays_EXP_190	85	10	5	4	190

EXPERIMENTAL

An ex-situ study of the solid precursors (already containing the different blowing agents) was performed using a conventional XRD equipment (Philips PW 1050/71 using the Cu Kα line between 1º and 10º by steps of 0.005º) prior to the in-situ foaming in the synchrotron beamline.

The exfoliation of nanoclays during foaming was followed in-situ by ED-XRD at the EDDi experimental station hosted at the BESSY II synchrotron light source of the Helmholtz Centre Berlin (figure 3). Samples were illuminated by a white X-ray beam of 2×1 mm^2 (height $\times$ width) cross-section. Peaks of intensity were detected at particular energies, E_{hkl}, in transmission geometry at the angle $2\theta = 1.7°$ by a Ge multichannel analysing detector, since the diffracted photon energies obey Bragg's law, which reads in its energy-dispersive form as:

$$E_{hkl} = hc/2d_{hkl} \sin\theta$$

where h is Planck's constant and c the speed of light (see reference [1, 33] for a detail description of EDDi).

A self-designed X-ray transparent furnace equipped with infrared lamps and Kapton windows was mounted on a positioning table attached to the goniometer. The sample size was 20×10×4 mm^3. The 10 mm side was placed parallel to the beam direction and the 4 mm side indicates the compaction direction during the production of the precursor material. A thermocouple was inserted into the sample parallel to the 20 mm side and beside the beam path for recording and controlling the temperature program using a CAL3300 controller and a self-develop program that runs under LabView. The temperature was increased from 30ºC up to the foaming temperatures 185 or 190 °C at about 10 K·min^{-1} and held there for an isothermal step. After 600 s, the IR- lamps were turned off and cooling took place. ED-XRD data acquisition and positioning table was computer controlled by the software package Spec. Acquisition started when the sample temperature was 100 °C on heating. The counting time per spectrum was 30 s, after which a lateral sample displacement of 1 mm was programed in order to detect each time diffracted photon-energies from a volume which was previously not irradiated by the X-rays.

Complementary spectra were also acquired for 30 s at ambient temperature, before heating and after cooling.
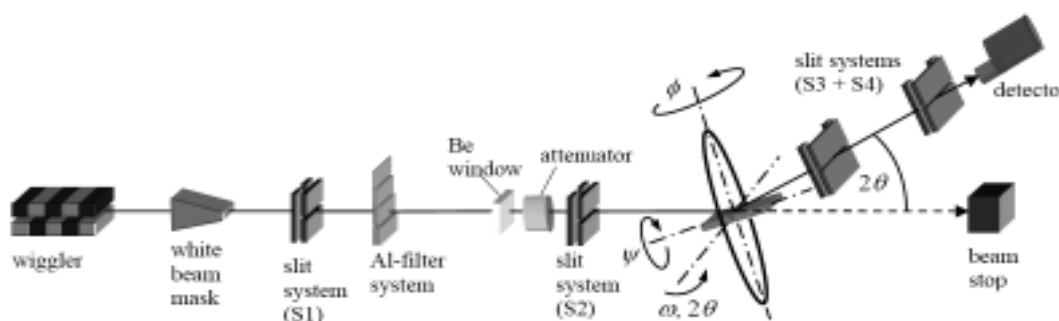
Figure 3: EDDi experimental station hosted at the BESSY II synchrotron light source. The beam crosses a system of slits, filters and attenuators before hitting the sample [33].

For each spectrum the energy corresponding to the maximum of the nanoclays peak was calculated and converted into interlamellar spacing according to the formula $d_{hkl} = hc/2E_{hkl}\sin\theta$. The obtained interlamellar spacing was plotted as a function of the foaming time. Since the acquisition of each spectrum lasts 30 seconds the midpoint was selected as representative. The correlation between interlamellar spacing and time allows for analyzing also the correlation with sample temperature.

Density of the foamed samples was measured using the Archimedes' principle.

 The TGA measurements were performed using a Mettler TGA/SDTA 851e used to measure the amount of gas released by the decomposition of the azodicarbonamide during foaming in the different samples. For this purpose the temperature profile used was: 50 ^{o}C-185 ^{o}C at 15 ^{o}C/min, isotherm at 185 ^{o}C during 3 minutes, 185 ^{o}C-50 ^{o}C at -6 ^{o}C/min.

RESULTS AND DISCUSSION

Ex-situ study

This prior ex-situ study is aimed at characterizing the initial exfoliated/intercalated state of the nanoclays before foaming and comparing the results with the corresponding ones obtained later in the synchrotron. Figure 4 shows the diffraction patterns obtained for nanocomposites containing 5 wt.% nanoclays, different blowing agents and without blowing agent. Since the processing conditions of all the composites have been the same the differences found in the aggregation state of the clays can be only attributed to the different nature of the blowing agents employed.
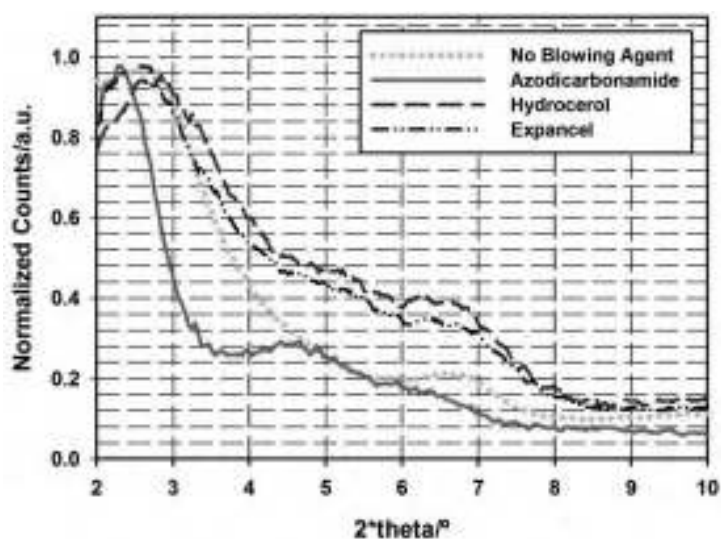
Figure 4: Ex-situ XRD in the solid precursors already containing a given blowing agent. The diffraction patterns are compared with the solid matrix without blowing agent. Blending with azodicarbonamide promotes the separation between platelets, on the contrary to the two other blowing agents.

In the samples that combine azodicarbonamide with nanoclays the main diffraction peak is more shifted to lower angles than the rest of the samples. Indeed, in the samples blended with Hydrocerol or Expancel, the peak coincides with the one of the samples without blowing agent. This suggests that there exists some kind of chemical interaction between the azodicarbonamide and the nanoclays that promotes some degree of exfoliation during blending. On the contrary, the state of aggregation of the nanocomposite remains unaltered after blending with Hydrocerol or Expancel.

In-situ study

- **Effects related to the nature of the blowing agent**

Table 2: Final densities achieved with the different blowing agents at 185 ºC and 190 ºC. The maximum expansion ratios achievable with Expancel or Hydrocerol are lower than with azodicarbonamide. This is later translated in lower increments in the separation between platelets.

Sample	Density/(kg/m^3)
5% Nanoclays_AZO7_185	250.3
5% Nanoclays_HY_185	648.0
5% Nanoclays_EXP_185	609.5
5% Nanoclays_AZO7_190	237.8
5% Nanoclays_HY_190	639.8
5% Nanoclays_EXP_190	616.8

The evolution of interlamellar spacing obtained from the in-situ diffractograms during foaming is presented in figure 5 as a function of the foaming time and sample temperature. The point corresponding to time 0 seconds corresponds to the in-situ diffractogram of the solid precursor material before foaming. The point corresponding to time 4500 seconds corresponds to the in-situ diffractogram of the solidified foam.
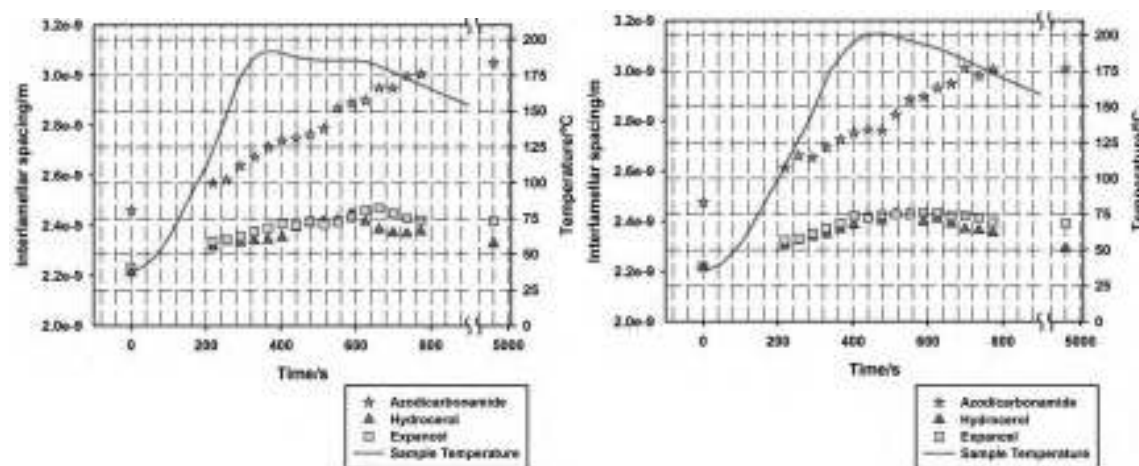
Figure 5: evolution during foaming of the interlamellar spacing as a function of time and sample temperature. The increment in exfoliation degree occurs, in a higher or lower extent, independently of the nature of the blowing agent used. a) Foaming temperature 185ºC, b) Foaming temperature 190ºC.

Initially, at t=0 seconds, the separation between platelets in the samples blended with azodicarbonamide is 10% larger than the one in samples blended with Hydrocerol or Expancel. This behavior follows the same trend found ex-situ (see Figure 4). Azodicarbonamide helps to increase the interlamellar spacing during blending.

The thermally activated higher mobility of the polymer molecular chains helps to separate the nanoclays platelets. This can be stated from the interlamellar spacing value found at t≈200 seconds which corresponds to a temperature of 110 ºC and is 5% larger than at t=0 seconds. This increment is the same for all blowing agents.

In the samples containing azodicarbonamide, from 540-560 seconds the rate of increment in the interlamellar spacing is higher than for Expancell and Hydrocerol. At that time the sample temperature coincides with the decomposition temperature of the azodicarbonamide. The foaming begins and hence the interlamellar spacing is increased stronger than previously. This effect is not observed with Hydrocerol or Expancel since the decomposition temperature window is broader. In any case the foaming using these last two blowing agents also helps to increase the exfoliation of the clays independently of the different foaming mechanisms involved. In the case of the Expancel the gas is confined inside the microspheres in every moment, therefore the increment in exfoliation is attributed to a separation due to the stretching of the polymer chains chemically bonded to the nanoclay platelets. The nature of the gas released or the releasing of gas itself do not influence the exfoliation during foaming for this particular case.

The expansion ratios achievable with the azodicarbonamide are higher than the ones achievable with Hydrocerol or Expancel. Final expansion ratios reached in each sample are shown in table 2. This is the reason behind the lower increments in interlamellar spacing found for the samples containing Hydrocerol and Expancel in comparison to samples foamed with azodicarbonamide. Thus, there is a direct relationship between expansion ratio and degree of exfoliation. Moreover, for the HY and EXP, the interlamellar spacing reaches a maximum and then decays to a lower value as the foam collapses and solidifies. On the contrary, with azodicarbonamide, the collapse and solidification of the foam do not change the interlamellar spacing reached. Our hypothesis is that the proposed chemical interaction between nanoclays and azodicarbonamide also helps to retain the maximum separation achieved between platelets. The platelets are hooked to their new positions. Since Hydrocerol and Expancel do not show any interaction with the layered silicates, the foam collapse and solidification produce also some collapse on the lamellar structure.

- **Effects related to the blowing agent content**

Three different amounts of the blowing agent that presents the most interesting results (azodicarbonamide) were used for this study. Two different temperatures were used, 185º C and 190º C.

Table 3: final densities in samples with different azodicarbonamide additions.

Sample	Density/(kg/m^3)
5% Nanoclays_AZO4_185	293.7
5% Nanoclays_AZO7_185	250.3
5% Nanoclays_AZO10_185	287.7
5% Nanoclays_AZO4_190	294.9
5% Nanoclays_AZO7_190	237.8
5% Nanoclays_AZO10_190	261.3

The results are shown in figure 6. The first remarkable result is that at t=0 seconds, the interlamellar spacing becomes larger with increasing azodicarbonamide content, but not proportionally. The difference between 7 and 10 wt.% is small. This result supports the hypothesized chemical interaction azodicarbonamide-nanoclays. At high blowing agent additions (above 7 wt.%) all the clay nanoparticles are interacting with the azodicarbonamide as if a saturation in the interaction nanoclays-azodicarbonamide is reached.

The effect of the melting of the polymer on accelerating the growth of the interlamellar spacing is observed again for these samples. The sample containing 4 wt.% azodicarbonamide reaches the maximum expansion before the other two samples (all the available gas has been already released) and so does the interlamellar spacing.

At both foaming temperatures the highest expansion ratios (lowest densities) are achieved with the samples containing 7 wt.% of azodicarbonamide as can be seen in table 3. This is translated again in the highest increments in interlamellar spacing. The amount of gas that can be released

in the 5% Nanoclays_AZO4 samples is lower and hence the foaming ends earlier. Therefore the maximum value of interlamellar spacing is reached before than in the samples containing 7 wt.% and 10 wt.% of azodicarbonamide. The maximum degree of exfoliation reached is maintained after solidification of the foam. The hypothesis again is that the presence of azodicarbonamide helps to keep the nanoclay platelets in their new positions after foaming.
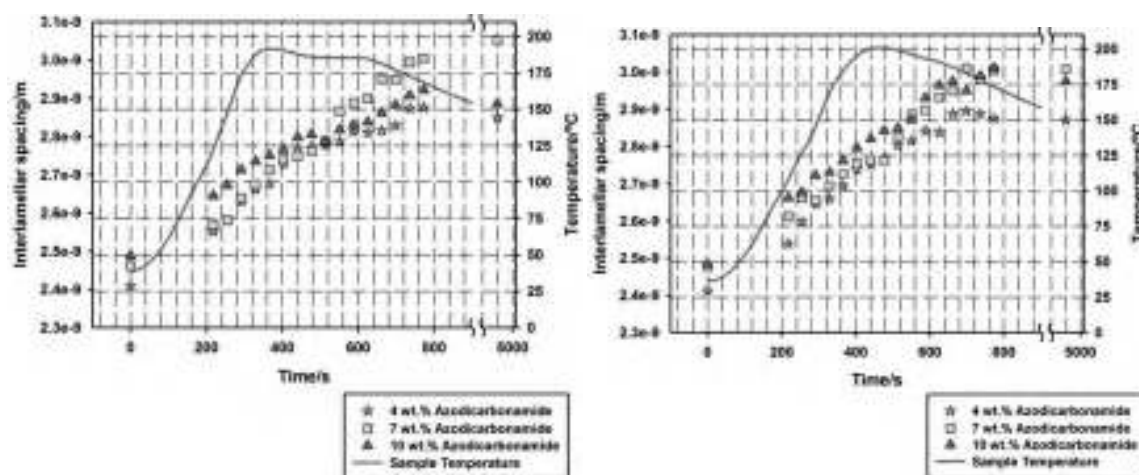

Figure 6: evolution during foaming of the separation between platelets characterized in-situ using different additions of azodicarbonamide. a) Foaming temperature 185ºC, b) Foaming Temperature 190ºC.

- **Effects related to the nanoclay addition**

As already mentioned two different additions of nanoclays were studied, fixing the kind and amount of blowing agent. Table 4 shows the final densities achieved for the different samples. The bigger addition of nanoclays yields also higher expansion ratios. Several reasons lie behind this. One first reason deals with the catalytic effect of the nanoclays over the azodicarbonamide which finally yields a higher amount of gas released. This catalytic effect is demonstrated by thermogravimetry shown in figure 6. The weight loss measured by thermogravimetry is due to the decomposition of the azodicarbonamide, therefore to the gas released. "Blank for 3%" and "Blank for 5%" are samples without nanoclays but maintaining the same ratio coupling agent/polymer matrix as in the samples with clays. As can be inferred from figure 7 the higher is the addition of clays, the higher is the amount of gas released at a given temperature and therefore higher expansion ratios can be achieved. Not only the amount of gas released is higher in the samples with clays but also the decomposition begins earlier in these samples. The nanoclays could be also helping to increase the stability of the polymer melt during the foaming. This allows retaining more gas which is finally translated into lower densities. The presence of nanoclays can also play a role as gas barrier limiting the gas escape and increasing the amount of gas available during the foam expansion.

Table 4: final densities achieved in samples with different additions of nanoclays. Higher amounts of nanoclays are beneficial for reaching lower densities.

Sample	Density/(kg/m³)
3% Nanoclays_AZO7_185	324.2
5% Nanoclays_AZO7_185	250.3
3% Nanoclays_AZO7_190	313.1
5% Nanoclays_AZO7_190	237.8

In any case the samples containing 5 wt.% of nanoparticles reach larger expansions. And, as it is shown in figure 8, the direct correlation between increment in interlamellar spacing and expansion ratio appears again in this case. The final exfoliation degree is always higher for the 5% Nanoclays_AZO samples.
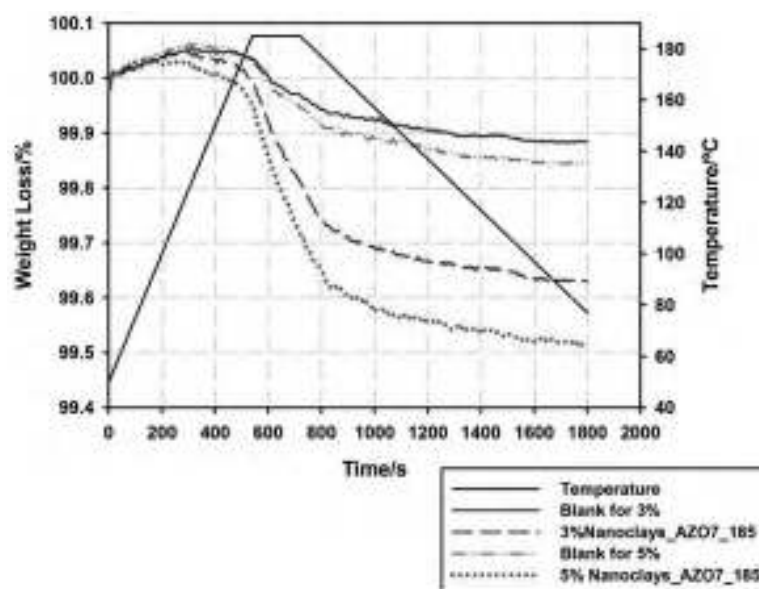
Figure 7: Weight loss measured by thermogravimetry due to the decomposition and gas release of the azodicarbonamide in samples containing different amounts of nanoclays and its corresponding blank samples. The experiments were performed using a similar temperature program to the one used in the diffraction tests.

The increment in interlamellar spacing attributed to the thermally activated mobility of the molecular chains is observed again independently of the nanoclays addition for temperatures below the decomposition of the blowing agent. For higher temperatures, the material containing more clays produces a larger interlamellar spacing.
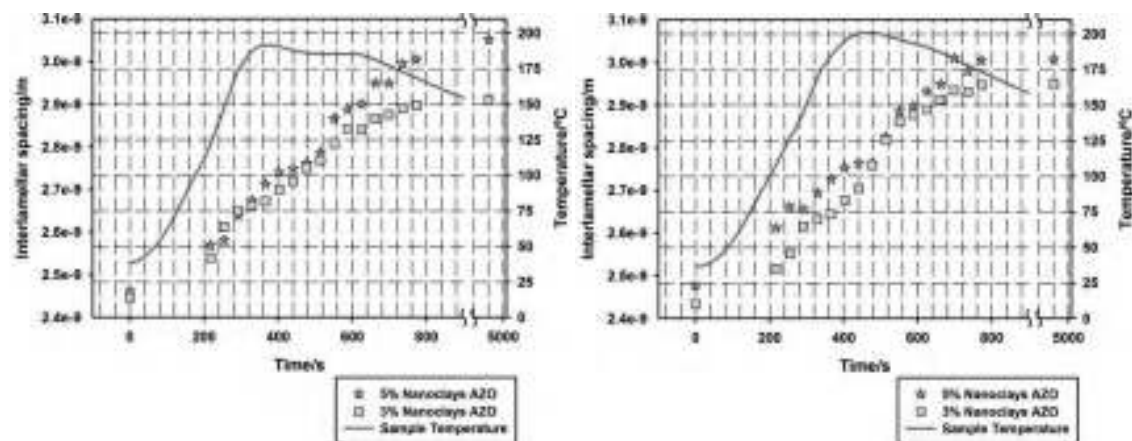
Figure 8: evolution of the interlamellar spacing during foaming in samples containing different additions of nanoparticles. The differences found in expansion ratio are correlated with the differences found in interlamellar spacing.

Summary: Correlation Expansion Ratio-Increment in Interlamellar Spacing

Almost all the samples studied fit well to a linear regression between expansion ratio and increment in the interlamellar spacing (see figure 9). Independently of the kind of blowing agent used or gas released during the foaming, an increment in the interlamellar spacing associated with foaming occurs. The higher is the expansion ratio reached, the higher the exfoliation degree of the nanoclays is. This increment in the interlamellar spacing can be as high as 24% for samples expanding more than 3.5 times.
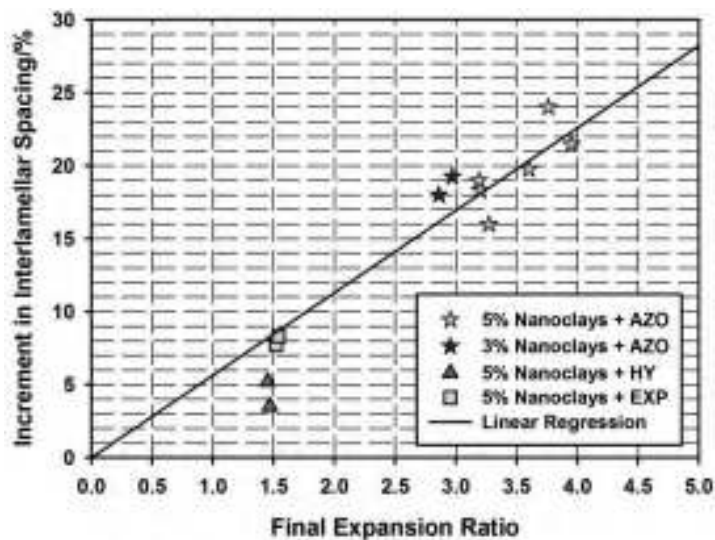
Figure 9: Correlation between expansion ratio and increment in interlamellar spacing for the different blowing agents and different materials.

Samples containing Hydrocerol (triangles in figure 9) lie below the linear regression. As was studied previously, in these samples the lamellar structure of the nanoclays presents the

stronger collapse coinciding with the collapse of the foam. Although the samples containing Expancel also present some collapse after reaching the maximum separation between platelets, this collapse is not so strong. On the other hand, samples containing azodicarbonamide maintain the maximum separation between platelets even though the collapse of the foam. That is the reason why almost all samples containing azodicarbonamide lie near or above the linear regression. The fundamental reason explaining these differences are still unknown and further research of this topic is needed.

6.Conclusions

Energy dispersive diffraction of synchrotron radiation is a useful technique to take an insight into the mechanisms involved in the increment of the exfoliation degree of LDPE/clay nanocomposites during foaming using chemical blowing agents. The whole evolution of the process has been characterized in-situ for the first time and all questions that motivated the study have been answered.

Three blowing agents of very different nature were selected. The increment of interlamellar spacing while foaming occurs, in a higher or lower extent, independently of the blowing agent used. Therefore the phenomenon is mainly associated with the foaming itself and not with the kind of gas or foaming procedure used.

The mixture of nanoclays with azodicarbonamide yields higher exfoliation degrees during blending. than Hydrocerol or Expancel, does not have any effect on the exfoliation. Therefore a chemical interaction between azodicarbonamide and organomodified nanoclays is postulated. This chemical interaction helps to the clays delamination during blending and it seems to be connected with the catalytic effect of the used nanoclays in the decomposition temperature of azodicarbonamide.

The increment in the exfoliation degree is not only promoted by the foaming but also by the thermal mobility of the polymer molecular chains. When the samples temperature increases, an increment in the interlamellar spacing is also observed. This effect is observed independently of the blowing agent nature, blowing agent addition or nanoclays content.

There exists a direct correlation between expansion ratio and increment in interlamellar spacing. The higher increments in exfoliation degree are found in the samples with lower densities. In the case of the azodicarbonamide samples the maximum interlamellar spacing is conserved after foam collapse and solidification. On the contrary, in the samples containing Expancel and Hydrocerol the exfoliation degree found after collapse and solidification is lower than the maximum observed. The postulated interaction azodicarbonamide-nanoclays may help to keep the nanoclays platelets hooked to their new positions reached during the foaming.

This scientific work has shown a new experimental methodology that allows following in-situ the exfoliation process of nanoclays. Foaming, by itself, promotes the separation degree between platelets in a nanoclay-filled composite. In any application involving nanoclays the highest as possible exfoliation degree is sought. From this point of view cellular materials are

benefitted, presenting a higher exfoliation degree than their initial solid matrices. This can be considered as an interesting synergetic effect between the use of nanoclays and foaming.

Acknowledgements

References

[1]   L.A. Utracki in Clay-containing polymeric nanocomposites. Rapra Technology Limited. United Kingdom (2004).

[2]   J. H. Koo in Polymer Nanocomposites. McGraw-Hill. USA (2006).

[3]   S. Pavlidou, C.D. Papaspyrides. Prog. Polym. Sci., 33 1119-1198. (2008)

[4]   J. Golebiewski, A. Rozanski, J. Dzwonkowski, A Galeski. Europ. Polym, J. 44 270-286 (2008).

[5]   E.C. Lee, D.F. Mielewski, R. J. Baird, Polym. Eng. Sci., 44 (9) 1773-1782 (2004)

[6]   C. Lam, K. Lau, H. Cheung, H. Ling. Mat. Lett. 59 (11) 1369-1372 (2005).

[7]   J. Li, G. Jiang, S. Y. Guo, L. J. Zhao. Plast. Rubb. Compos. 36 (7) 308-313 (2007).

[8]   Y. H. Jin, H. J. Park, S. S. Im, S. Y. Kwak, S. Kwak. Macromol. Rapid. Commun. 23, 135-140 (2002).

[9]   M. Alexandre, P. Dubois, T. Sun, J. M. garces, R. Jerome. Polymer 43 2123-2132 (2002).

[10]   S. Wang, Y. hu, Q. Zhongkai, Z. Wang, Z. Chen, W. Fan. Mat Lett. 57 (18) 2675-2678 (2003)

[11]   G. Liang, J. Xu, S. Bao, W. Xu. J. Appl. Plym. Sci 91, 3974-3980 (2004).

[12]   C. C. Ibeh, M. Bubacz. J. Cell. Plast. 44, 493-515 (2008).

[13]   W. Zhai, C. B. Park, M. Kontopoulou. Ind Eng Chem Res 50, 7282-7289 (2011)

[14]   C. Zeng, X. Han, L. J. Lee, K. W. Koelling, D. L. Tomasko. Adv Mater 15, 1743-1747 (2003).

[15]   Y. H. Lee, K. H. Wang, C. B. Park, M. Sain. J App Polym Sci 103, 2129-2134 (2007).

[16]   S. M. Seraji, M. K. R. Aghjeh, M. Davari, M. S. Hosseini, S. Khelgati. Polym Compos 32, 1095-1105 (2011).

[17]   M. C. Saha, M. E. Kabir, S. Jeelani. Mat Sci Eng A-Struct 479, 213-222 (2008).

[18]   K. Gorem, L. Chen, L. S. Schadler, R. Ozisik. J Supercrit Fluid 51, 420-427 (2010).

[19]   R. Verdejo, C. Saiz-Arroyo, J. Carretero-Gonzalez, F. Barroso-Bujans, M. A. Rodriguez-Perez, M. A. Lopez-Manchado. Europ. Polym. J.44, 2790-2797 (2008).

[20]   M.M. Bernal, I. Molenberg, S. Estravis, M. A. Rodriguez-Perez, I. Huynen, M. A. Lopez-Manchado, R. Verdejo. J. of Mat. Sci. 47 (15), 5673-5679 (2012).

[21]   C. Saiz-Arroyo, J. Escudero, M.A. Rodríguez-Pérez, J.A. de Saja. Cell. Polym. 30: 63-78, (2011).

[22]   C. Saiz-Arroyo, M. A. Rodriguez-Perez, J. I. Velasco, J. A. de Saja. Composites B 48. 40-50 (2013).

[23]   J. I. Velasco, M. Antunes, O. Ayyad, C. Saiz-Arroyo, M. A. Rodríguez-Pérez. F. Hidalgo, J. A. de Saja. J App Polym Sci 105, 1658-1667 (2007).

[24]   C. Zeng, X. Ha, L. J. Lee, K. W. Koeling, D. L. Tomasco. Adv. Mater. 20, 1743-1747 (2003)

[25]   J. A. Reyes-Labarta, A. Marcilla. J. Appl. Polym Sci. 107, 339-346 (2008).

[26]   A. S. Bhatti, D. Dollimore. Thermoch. Acta, 76, 63-77 (1984).

[27]   M. E. Gomes, J. S. Godinho, D. Tchalamov,A. M. Cunha, R. L. Reis. J. Appl. Med. Polym. 6, 75-80 (2002).

[28]   X. Qin, M. R. Thompson, A. N. Hrymak. Polym. Eng. Sci. 47. 522-529 (2007).

[29]   A. K. Bledzki, O. Faruk. J. Cell. Plast. 41. 539-550 (2005).

[30]   H. Andersson, P. Griss, G. Stemme.Sens. Act. 84, 290-295 (2002).

[31]   J. Yao, M. R. Barzegari, D. Rodrigue. Cell. Polym 20. 5-19 (2010).

[32]   T. Ohji, T. Sekino, K. Niihara. Key Eng. Mat. 317-318. 899-904. (2006).

[33]   Genzel Ch, Denks I, Gibmeier J, Klaus M, Wagener G. Nucl Instr and Meth in Phys Res A 578 23-33 (2007).

4.3.2.- Modification of the Molecular Architecture and Two-Stages Compression Molding

The materials containing nanoclays and a coupling agent studied in the previous section are now crosslinked (using dicumyl peroxide) and foamed by two-stages compression molding to obtain low density cellular materials. Crosslinking, as a modification of the molecular architecture of the polymer, is essential in order to achieve such low densities.

Low density cellular materials based on polyolefins show several advantages since they can be used as impact absorbers or thermal insulators. Nevertheless they show also drawbacks: the mechanical behavior of the materials is poor and present also a poor creep behavior due to the gas diffusion taking place during these creep tests. The addition of nanoparticles try to solve these drawbacks acting as nanometric reinforcements in the micrometric cell walls of the foam to improve the mechanical behavious and reduce the gas diffusion coefficient.

The present section presents two works. The first one is entitled *"Gas Diffusion and Re-Diffusion in Polyethylene Foams"*. This works uses a semi-empirical method to determine experiemtnally the effective diffusion coefficient (under load) of the gas entrapped in the interior of the cells of low density polyethylene foams. A direct correlation is established between this coefficient and the bulk density of the foam. When the load is released and takes place the recovery of the foam sample, the re-diffusion of the gas is also studied. This first study serves as an introduction for the second work presented in the thesis that uses the aforementioned semi-empirical method to determine the effective diffusion coefficient in low density foams filled with nanoclays.

The second work presented is entitled *"Effective Diffusion Coefficient and Mechanical Properties of Low Density Foams Based in Polyethylene/Clays Nanocomposites"*. Apart from determining the effective diffusion coefficient in low density nanocomposite foams and comparing it with unfilled foams this work pays special attention to the mechanical properties of these low density samples and to the production process itself.

The production method used allows obtaining low density foams (densities below 30 kg/m^3) filled with nanoclays (in additions up to 5 wt.%). Foamed blocks up to 8000 cm^3 have been produced.

A microstructural characterization of the cellular structure is also carried out. The cells morphology is later correlated with the diffusive and mechanical properties of the samples. Nanoclays improve the mechanical properties in tension, compression and improve also the energy absorption capability of these low density samples.

The effective diffusion coefficient has been experimentally measured elucidating the gas barrier role played by the nanoclays in these materials and the effect of the coupling agent over this coefficient.

Finally, the delamination state of the nanoclays before and after foaming is characterized. The results obtained are in good agreement with the conclusions obtained by synchrotron radiation in section 4.3.1.

Gas diffusion and re-diffusion in polyethylene foams

J. Escudero[1,a], J. Lázaro[1], E. Solorzano[1], M.A. Rodríguez-Perez[1],
J.A. de Saja[1]

[1]Cellular Materials Group (CellMat), Condensed Matter Physics Department, Faculty of Sciences,
University of Valladolid, 47011 Valladolid, Spain.

[a]jabo@fmc.uva.es

Keywords: Polyethylene foams; Diffusion coefficient; Creep testing; Recovery testing.

Abstract. In this work, the effective diffusion coefficient of the gas contained in closed cell polyethylene foams under static loading is measured. To do this, compressive creep experiments were performed on low density polyethylene foams produced under a gas diffusion process. Density dependence of this coefficient has been analysed as well as the variation of pressure with time inside the cells. Finally, immediately after compressive creep, the recovery behaviour of the foams was also characterised. Different abilities for recovering were observed depending on the density of the foam and the absolute recovery resulted independent of the initial stress applied.

Introduction

Closed cell polymeric foams have a wide range of applications due to its unique combination of properties. One of the most extended applications of these foams is in packaging and cushioning [1,2]. In these applications, foams are subjected to static loads which can produce a significant foam deformation. These deformations involve a decrease of the mechanical performance of the foam due to both the plastic deformation of the polymeric matrix and gas diffusion from the cells. Therefore, understanding and modelling the creep response and the closely related degassing behaviour under static loads is an important issue from a practical point of view and an interesting topic from a fundamental point of view due to the complicated structure of polymer foams.

There have been some attempts to relate the creep behaviour of the cellular solid to its cellular structure and the base material properties. Some authors, assuming that the main mechanisms involving creep are related to the deformation of the solid matrix, have predicted a creep rate proportional to $(\rho_f / \rho_s)^{-n}$ where n is an empirical constant [3]. However, in these flexible closed-cell polymeric foams the contribution of the gas escape is non-negligible so more realistic models should include the gas diffusion.

Some studies have been made in this sense considering the cellular solid both as a discrete and continuous media. Briscoe [4] studied experimentally and theoretically the degassing behaviour of LDPE foams during storage, been able to obtain numerical gas diffusion coefficients. Mills [1] obtained also an analytical equation for this diffusion coefficient using a discrete model. This equation is as follows:

$$D_{eff} = \frac{6 P p_a}{f_f R}$$ (1)

where P is the polymer permeability, p_a the initial pressure in the cells, f_f the fraction of polymer in the foam cell faces and R the foam relative density [5,6]. Nevertheless, several additional characteristics that should have an influence, such as foam size, were not considered in this study.

Ruiz-Herrero [7,8] presented a simple method based on both creep experimental data and on the assumption on an isothermal compression process to determine the diffusion coefficient of low density polyethylene foams produced by a compression moulding technique. Gas diffusion coefficients obtained this way were in concordance with the ones found in literature and the model also allows analysing the effect of sample size on the gas diffusion. This model, developed in part

by Ruiz-Herrero [7,8], is the one used in this study and it will be further explained in the following sections.

Some experimental results were also obtained from the analysis of the recovery behaviour. Plots of deformation to time from the recovery after creep could be obtained using image processing techniques [9].

In our work, the diffusion coefficient for foams produced by a gas dissolution process is obtained. These foams are excellent from a scientific point of view because of its homogeneity. The diffusion coefficient for these foams has been never studied before. The use of a cylindrical geometry as a way of optimizing the process is something new also in the characterization of the diffusion coefficients for polyethylene foams.

On the other hand, an attempt to obtain re-diffusion coefficients during the recovery has been also made. In this case, the deformation of the samples has been directly monitored instead of using image processing techniques.

Materials

Six foams with different densities and based on a crosslinked polyethylene matrix were analysed during this work. Zotefoams Plc. kindly provided these sheets produced using their autoclave process. First step of this process consists in mixing and extruding the base polymer (polyethylene in this case) with the crosslinking agent and other additives. After that, the sheets obtained in the first step are chemically crosslinked in an oven at a temperature of about 135 ℃. Slabs cut from the extruded sheet are introduced in an autoclave in order to dissolve nitrogen gas. Both temperature and pressure are controlled inside this autoclave. Pressure values range between 200 and 1000 bars of nitrogen and temperature is near to the melting point of the polymer [10]. With the gas already dissolved, a second low pressure autoclave is used to produce the expansion of the material. Pressure now is lower than in the previous step but high enough to retain the internal pressure of the material while heating. The solid sheets are heated over the melting point of the polymer and when the temperature profile is homogeneous, pressure is released obtaining the final expansion of the foam. Finally foams are cooled at room temperature [10]. The whole process is outlined in Fig. 1
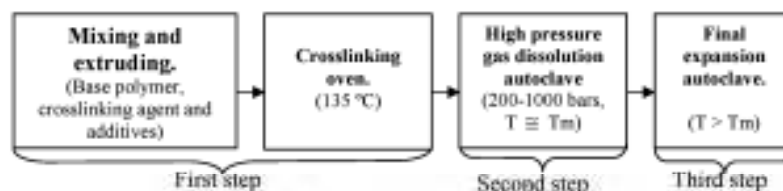
Fig. 1: Fabrication process of the samples

Some important characteristics of the analysed foams such as density, mean cell size, collapse stress, mean cell wall thickness and gel content are showed in Table 1 [9].

Table 1: Characteristics of the foams under study.

Foam	Density /(Kg/m^3)	Mean cell size/μm	Mean wall thickness/μm	Collapse stress /Pa	Cristalinity	Gel content
LD15	18,2	313	1,4	13690		
LD24	22,1	312	1,9	19610		
LD33	31,9	424	3,6	36000	41,6 ± 3,0 %	45 ± 3%
LD45	43,5	397	2,5	67520		
LD60	56,5	773	10,3	95550		
LD70	71,5	528	6,0	140410		

The density values cover a range wide enough, between approximately 15 and 70 kg/m3. The mean cell size is between 300 and 700 μm while the mean wall thickness is in the range of 1 and 10 μm. The cristalinity and gel content are constant for all the samples

During the production process, final density is controlled by the amount of gas dissolved during the high pressure step. Temperature and time are the fundamental parameters to achieve this. On the other hand, the cellular structure (mean cell size and mean cell wall thickness) is controlled by means of the pressure drop rate at the end of the second step. One of the most important parameters in the gas diffusion is the foams gel content [9]. In this case the gel content was approximately the same for all the samples with differences not higher than a 2%.

Foams obtained in this production process have all a very homogeneous cellular structure and similar chemical compositions for different densities what makes them optimal to be studied from a scientific point of view [9].

Experimental

A lab-designed compressive creep apparatus was used to measure the response of the foams to an applied constant stress over a 7 days period. Two creep rigs are shown in Figure 2. In each of them, the thickness of the foam is monitored with a linear variable displacement transducer (LVDT) which is connected to a computer. Immediately after creep, the recovery behaviour of these foams was also measured. To this end, the increasing thickness of the samples is monitored also using another LVDT. The recovery of the foams occurs between two plates of a very low weight (<10 g).
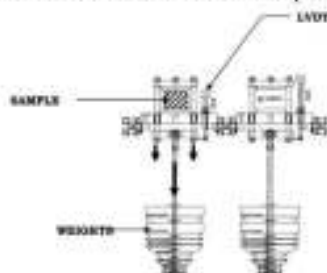
Fig. 2: Scheme of the home-made creep apparatus

The recovery is faster in the outer parts of the foams since gas diffusion is improved there. This fact makes the recovery an inhomogeneous process. Samples were cut off with a cylindrical geometry to favour a more homogeneous behaviour all along the sample. The diameter of the cylinders was 30 mm in all cases. For each foam, experiments at five different stresses were carried out at a mean temperature of 23 °C. These five stresses are all higher than the collapse stress of the foam in percentages of 15%, 24%, 33%, 44% and 55% (see Figure 3). Both creep and recovery were measured during seven days acquiring a sample each ten seconds.

Analysis and results

a) Creep

Assuming isothermal conditions during the compression of the gas and a null Poisson ratio ($v=0$), the uniaxial compressive stress for these foams loaded in the post-collapse region can be obtained using the Eq. (2), as present Gibson and Ashby [2].

$$\sigma = \sigma_c + \frac{P_0 \varepsilon}{1 - \varepsilon - \rho_f / \rho_s}.$$ (2)

where ε is the deformation, P_0 is the initial pressure inside the cells and $R = \rho_f / \rho_s$ is the relative density of the foam.

According to Eq. (2), if the compressive stress is plotted as a function of the gas volumetric strain $\varepsilon/(1- \varepsilon\text{-}R)$ for a fixed creep time, the slope of the curve would represent the pressure of the gas contained in the cells, Figure 4. Proceeding like this for different creep times, it is possible to obtain the evolution of pressure inside the cells for each density. As it can be observed in Figure 5, pressure decays with time as an exponential function for each foam. Svanström *et al.* [11] proposed a solution of the diffusion equation for a cylindrical geometry as it is in our case. According to this analytical solution, the diffusion coefficient can be obtained from the pressure decay curve using the following equation

$$D_{\text{eff}} = -\frac{1}{2,4048^2}\frac{d}{dt}\left\{\ln\left[\frac{P(t)}{P_0}\frac{(\beta_{01}a)^2}{4}\right]\right\}. \tag{3}$$

where $P(t)$ is the pressure inside the cells at a time t, P_0 is the pressure in the cells for the unloaded foam, a is the radius of the cylinder and β_{01} is the first order root of the Bessel's function of 0th order. The term $\ln\left[\frac{P(t)}{P_0}\frac{(\beta_{01}a)^2}{4}\right]$ is well fitted to a linear function with time so it was possible to obtain a numerical non time depending diffusion coefficient in all cases.
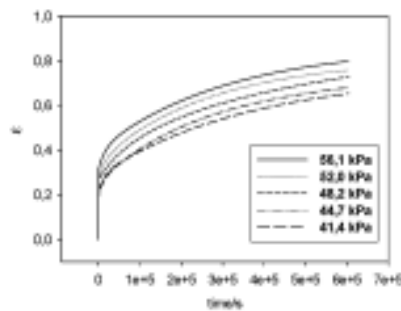
Fig. 3: Creep response for the LD33 at five different stresses   Fig. 4: Isochronous curves for the LD33
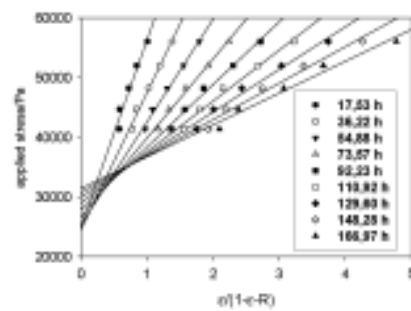
Table 2: Diffusion coefficients for each foam

Foam	LD15	LD24	LD33	LD45	LD60	LD70
$D_{\text{eff}}(m^2/s)$	$8,16\times10^{-7}$	$8,07\times10^{-7}$	$6,17\times10^{-7}$	$4,71\times10^{-7}$	$3,30\times10^{-7}$	$2,66\times10^{-7}$

According to Eq. (3), diffusion coefficients were obtained for all the densities. In Table 2 there is a relation of the coefficients for each density

There exists an inverse linear dependency with density in agreement with the analytical equation of Mills [1], see Figure 6.
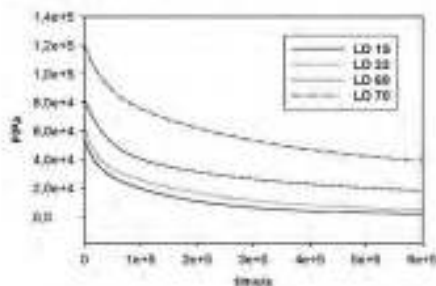
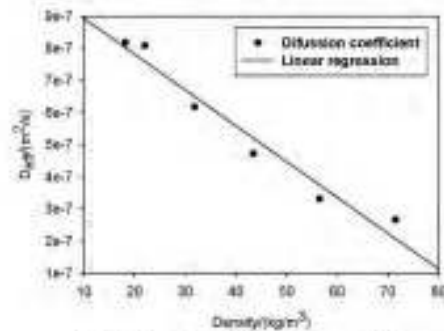Fig. 5: Pressure evolution for four different samples   Fig 6: Diffusion coefficients versus density

As it can be seen in Figure 5 the final pressures inside the cells are well below the atmospheric one. This effect is even greater for the lowest density foams.

The final unitary deformations are approximately the same for all samples when tested at high stresses but differs for lower ones. So the effect of the different diffusion coefficients is more evident for stresses near the collapse. This fact is schematized in Figure 7.
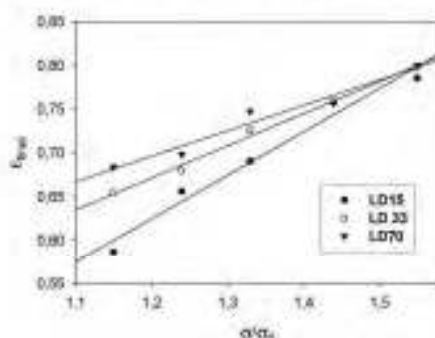

Fig. 7: Final unitary deformations for three samples

b) Recovery

At the beginning, the recovery is very fast [10,12,13]. This first recovery can not be ascribed to the re-diffusion of the gas inside the foam, it should be due to the viscoelastic behaviour of the polymer matrix. This effect is practically instantaneous and no gas diffuses inside the foam during it. Once this effect has taken place, the recovery of the foam is much slower. Gas re-diffuses inside the cells at a rate apparently slower than the rate observed during creep. During creep there is an external applied pressure that helps the gas to escape, this external force does no exist during recovery. We might be tempted to apply the same model as in creep to obtain numerical re-diffusion coefficients, but it seems to be hardly applicable in the recovery case. Even so, if we follow the same steps as in creep, obtained data suggest that re-diffusion coefficient for recovery would be more a time-dependent function than just a constant. Calculating a mean value, the re-diffusion coefficients would be at least one order of magnitude lower than those for creep. This fact will be deeply studied in the future to obtain reliable coefficients during recovery.
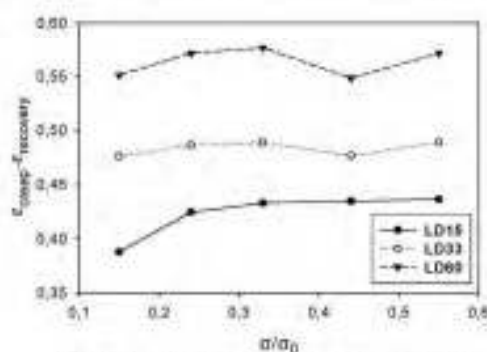
Fig. 8: Absolute recovery for three of the samples

In Figure 8 it can be observed that the higher is the density of the foam, the greater is its ability for recovering. To understand it, it is necessary to take into account that the gas loss is lower for the high density samples. The remaining pressure inside the cells is higher in this case. This ability for recovering also seems to be independent of the initial stress applied during creep.

Conclusions

Creep tests have allowed us to determine the gas diffusion coefficient for foams produced using a gas dissolution process. The dependency of this property with density is clear. As it was expected, a reduction in the gas loss is obtained increasing the density. The final deformations are the same when high stresses are considered but differ when lower stresses are applied during creep.

Recovery presents a non homogeneous behaviour so the cylindrical geometry chosen results more adequate to study it [10]. It is also a process much slower than creep. Data obtained suggests that de re-diffusion coefficient is a time dependent function. This topic should be studied with more detail. We can estimate that the re-diffusion coefficient would be an order of magnitude slower than the diffusion one. A better ability for recovering has been found for foams with a higher density. This can be explained taking into account the lower final gas loss for these foams.

Acknowledgements

References

[1] N.J. Mills and M.A. Rodriguez-Perez: Cell. Polym. Vol. 20 (2001), p. 79

[2] L.J. Gibson and M.F. Ashby: *Cellular solids: Structure and Properties* (Pergamon Press, Oxford, England, 1997).

[3] A.G. Ostrogorsky, L.R. Glicksman and D.W.I. Reitz: J. Heat Mass Tran. Vol. 29, 1986, p. 1169

[4] B.J. Briscoe and T. Savvas: Adv. Polym. Tech. Vol. 17 (1998), p. 87

[5] N.J. Mills and A. Gilchrist: J. Cell. Plast. Vol. 33 (1997), p. 264

[6] C.P Park: *Polyolefin Foam* (in Handbook of Polymeric Foams and Foam Technology, D. Klempner and K.C. Frisch Eds., Carl Hanser Verlag, Munich, 1991).

[7] J.L. Ruiz-Herreo, M.A. Rodriguez-Perez and J.A. de Saja: Polymer vol. 46 (2005), p. 3105

[8] J.L. Ruiz-Herreo, M.A. Rodriguez-Perez and J.A. de Saja: J. Appl. Polym. Sci. Vol. 99 (2005), p. 2204

[9] O. Almanza: *Characterization and modelled of the thermal and mechanical properties of polyethylene based foams* (Ph.D Thesis, University of Valladolid, 2000).

[10] M.A. Rodriguez-Perez, J.L. Ruiz-Herrero, E. Solórzano and J.A. de Saja: Cell. Polym. Vol. 25 (2006), p. 221

[11] M.A. Rodriguez-Perez, S. Diez-Gutierrez and J.A. de Saja: Polym. Eng. Sci. Vol. 38 (1998), p. 24

[12] M. Svanström, O. Ramnäs, M. Olsson and U. Jarfelt: J. Cell. Polym. Vol. 16 (1997), p. 182

[13] M.A. Rodriguez-Perez, O. Alamanza, J.L. Ruiz-Herrero and J.A. de Saja: Cell. Polym. Vol. 27 (2008), p. 147

EFFECTIVE DIFFUSION COEFFICIENT AND MECHANICAL PROPERTIES OF LOW DENSITY FOAMS BASED IN POLYETHYLENE/CLAYS NANOCOMPOSITES

J. Escudero[1], M. A. Rodriguez-Perez[1], A. Galeski[2]

[1]CellMat Laboratory, Condensed Matter Physics Department, University of Valladolid, Spain

[2]Centre for Molecular and Macromolecular Studies. Polish Academy of Science. Lodz, Poland.

Email: marrod@fmc.uva.es; jabo@fmc.uva.es

ABSTRACT

In this paper the effective diffusion coefficient, under static creep loading, of low density foams filled with nanoclays is compared with the same coefficient of non-filled samples. This way, the gas barrier role played by the nanoclays present in the cell walls and struts is elucidated. Together with this, thermal and mechanical properties besides cellular structure are studied for these nano-filled low density foams. Thermal and mechanical properties are largely improved by the addition of clays. On the contrary the reductions in effective diffusivity are not significant. These diffusivities are correlated with the ones found for the filled polymer matrix, prior to foaming. Finally an interesting increment in the interlamellar space of the nanoclays after foaming is observed. Foaming by itself induces exfoliation.

INTRODUCTION

Polymeric foams are widely spread nowadays in several daily applications from sporting goods to leisure toys. In other fields as cushioning or packaging, polymeric foams are currently indispensable materials. When used for these cushioning or packaging purposes, as well as when considering structural applications, foams are subjected to long-term static loadings that could affect their mechanical properties due to, on the one hand, the plastic deformation of the matrix and on the other hand, the gas diffusion from the cells [1]. Together with this, the gas escape, often called ageing, deeply influences the thermal insulation capability of these materials [2-4]. Therefore the reduction and minimization of the degassing behavior of polymeric foams is a subject of major importance.

During the last decade the excellent properties of polymer-clay nanocomposites have stimulated much interest and research within the scientific and industrial communities. With

much less inorganic contents of clay than comparable glass- or mineral-reinforced polymers, polymer-clay nanocomposites exhibit physical and mechanical properties significantly different from their more conventional counterparts. They could have good thermal stability, high heat distortion temperature and high specific stiffness at low concentrations of filler (<5 wt.%) [5-8]. Nevertheless some of the most promising possible applications of these silicate-layered nanocomposites come from the superior barrier properties expected for these novel materials. The improvements in barrier properties can be explained by the concept of tortuous paths, that is, when impermeable nanoparticles are incorporated into a polymer, the permeating molecules are forced to wiggle around them in a random walk what finally turns to be a tortuous pathway. Several theoretical works try to model the expectable reductions in diffusivity from the knowledge of intrinsic parameters of the layered silicates as for example the length, width and the volume fraction of the sheets. The orientation of the sheets together with the state of delaminating also play a fundamental role, the permeability for example is extremely sensitive to the size of the aggregates [7,9]. Therefore the higher improvements in barrier properties are mainly expected in the case that the nanoclays are highly exfoliated and well dispersed within the polymer matrix.

The diffussion coefficient in solid polymer/clay nanocomposites has been widely studied. A lot of works claim important reductions in diffusivity when nanoclays are well exfoliated in the polymer matrix [10-14]. When this reduction in diffusion is not so remarkable it is attributed to the type of coupling agent and to the interfaces formed between nanoparticle and polymer matrix. All these factors are studied in the works of Jacquelot et al. [15] and Picard et al. [43,44]. The determination of the effective diffusion coefficient in polymer foamed nanocomposites when the foam is subjected to a creep loading is not straightforward. Ippalapalli et al. [16] have presented recently a theoretical study modeling the diffusion in polymer nanocomposites and correlating the theoretical data with thermal conductivity measurements.

Due to all these promising properties the use of these polymer clay nanocomposites as matrix for foams has been intensively studied also in the last years. The efforts have been focused both in thermoplastic (amorphous and semi-crystalline) and thermoset polymers. In principle several different properties of the foam would benefit from the addition of nano-scaled particles [17-23]. Particularly, the addition of nanosilicates, because of their lamellar geometry, would reduce the effective diffusion coefficient of gas from the cells, reducing and minimizing the degassing. The mechanical properties are also improved. This way foams produced from polymer matrices reinforced with nanoclays could be excellent materials for cushioning and packaging purposes or structural applications [24-27]. Although the number of papers dealing with foamed nanocomposites is high, most of them are focused in mechanical properties such as stiffness, strength, toughness, etc. with no papers dealing with the diffusion of gas for a foam produced under creep loading.

There have been several studies and attempts to model the effective diffusion coefficient in polymeric foams. Pilon et al. reviewed the diffusion models in closed-cell polymeric foams [28] and Briscoe studied experimentally and theoretically the degassing behavior of LDPE high

density foams during storage, obtaining effective diffusion coefficients varying between 10^{-10} and 10^{-11} m^2/s [29]. Mills, using a discrete model, predicted a diffusion coefficient for the undeformed foam given by $D_{eff} = \frac{6Pp_a}{f_f R}$ where P is the polymer permeability, p_a the initial pressure in the cells, f_f the fraction of polymer in the foam cell faces and R the foam relative density. The values for the effective diffusion coefficients of gas contained in the cells for LDPE (densities 66 and 22 kg/m^3) and EVA (density 34 kg/m^3) foams have been predicted theoretically by Mills and Gilchrist [30]. All the previous literature review follows a theoretical approach modeling the foam behavior. Ruiz-Herrero et al. developed an empirical procedure based both in creep experimental data and a mathematical solution of the diffusion equation to evaluate the effective diffusion coefficient of polymeric foam. The authors found experimentally the linear dependency with density predicted theoretically in other works and the gas diffusion coefficients obtained are in concordance with the ones found in the literature. The simplicity of the method together with the possibility of obtaining numerical values measured experimentally makes it very interesting from a scientific point of view [31-34]. It turns to be very convenient for experimentally determining the effective diffusion coefficients of polymeric foams filled with nanosized layered silicates and comparing the obtained values with the ones of unfilled foams [31,32].

The present work sheds light on the effective diffusion coefficient of the gas outside the cells under creep loading in crosslinked low density LDPE foams filled with montmorillonite-type nanoclays from an empirical point of view. To cover this main objective several steps have been followed. A first step consisted in obtaining large blocks of low density foams ($\approx$30 kg/m^3) from a solid polyethylene matrix reinforced with nanoclays. The effect of these high expansion ratios on the exfoliation of the nanoclays is studied and related with the rest of the measured properties. A second step was characterizing the cellular structure and mechanical properties. Finally the effective diffusion coefficients are correlated with the diffusivities measured experimentally for their correspondent solid matrices.

EXPERIMENTAL

Materials and Sample preparation

A low density polyethylene PE003 from Repsol Alcudia with 2 g/10min (2.16 kg and 190 ^{o}C) of MFI, density of 920 kg/m^3 and 110 ^{o}C of melting point was used as polymer matrix. For the nanocomposites this polymer matrix was melt blended with montmorillonite-type organomodified nanoclays Cloisite C15A from Southern Clay Products and a coupling agent, maleic anhydride grafted polyethylene Fusabond 226 DE from DuPont (1.5 g/10min, 120 ^{o}C of melting point). The blending was performed in a twin screw extruder Bühler BTSK 20/40D at 250 rpm with a die temperature of 190 ^{o}C. The proportion of coupling agent to nanoclays was maintained constant in 2:1. In order to clearly distinguish the role played by the nanoclays the PE003 was also melt blended with the coupling agent only. The proportion PE003/coupling agent was maintained equal to the one used in the case of the filled composites. Two different

clay contents were used, 3 wt.% and 5 wt.%. The compositions and nomenclature used are summarized in Table 1.

Table 1: Proportion of components for the different kind of samples

Sample	Matrix/parts	Coupling agent/parts	Nanoclays/parts
Unfilled-3%	91	6	0
3% Nanoclays	91	6	3
Unfilled 5%	85	10	0
5% Nanoclays	85	10	5

The previous formulations (100 phr) were initially melt blended in another twin screw extruder (Collin mod ZK25T) with L/D of 24 at 25 rpm and 125 ºC in the die incorporating the following materials:

- Azodicarbonamide Lanxess Porofor M-C1 (19.3 phr) with particle size of 3.9 μm, used as chemical blowing agent.
- Stearic acid 301 Renichen (0.1 phr) used as lubricant.
- Zinc oxide Silox Active, Safic Alcan, (0.06 phr) used as azodicarbonamide activator
- Dicumyl peroxide DCP40 Luperox (1.8 phr) used as crosslinking agent.

The previous formulation gives good foaming results for the samples containing clays but not for the unfilled samples. This is due to the differences in the decomposition kinetics of the azodicarbonamide in the presence of nanoclays and due also to the differences in the rheology with the addition of nanoclays. Therefore a different formulation was used for the unfilled samples as follows:

- Azodicarbonamide Lanxess Porofor M-C1 (18.85 phr) used as chemical blowing agent.
- Stearic acid 301 Renichen (0.1 phr) used as lubricant.
- Zinc oxide Silox Active, Safic Alcan, (0.03 phr) used as azodicarbonamide activator
- Dicumyl peroxide DCP40 Luperox (1.8 phr) used as crosslinking agent.

The lower melt viscosity observed in the unfilled samples in comparison to the filled ones allows reducing the blowing agent and blowing agent activator amounts. The gas pressures developed when trying to foam the unfilled polymer matrices with the first formulation were so high that the polymer melt was unable to withstand them. Both formulations were adjusted to give the best foaming behavior in each case. As will be shown later, the differences in the formulations do not produce differences in gel content, cellular structure or open cell content.

Foaming Procedure

The pellets already containing all the previous materials were placed inside a steel mould of dimensions 153 mm long, 71 mm width and 4 mm thick and compression molded at 120 ºC and 9 MPa during 15 minutes. The resulting solid non-crosslinked precursors are cooled under pressure using re-circulating water.

A two step compression moulding foaming process was used for the foams production all the specimens [36]. In the first step (pre-foaming) seven solid precursors are placed inside a rectangular mould and subjected to a temperature of 147 ºC at a constant pressure of 18 MPa during 55 minutes. During this step the dicumyl peroxide is decomposed and the crosslinking reaction takes place, a partial decomposition of the blowing agent is also produced. When the pressure is released the material partially expands reaching expansion ratios of around 2. In a second step, the already crosslinked pre-expanded foam is placed inside a rectangular pre-heated mould at 190 ºC and maintained at this temperature for 60 minutes inside a pre-heated furnace. The pre-foam is free to expand inside the mould and finally reaches an expansion ratio of around 30. The dimensions of the final foamed block are 400 mm long, 200 mm width and 100 mm height.

These blocks were machined into five sheets of different thicknesses as it is depicted in figure 1.
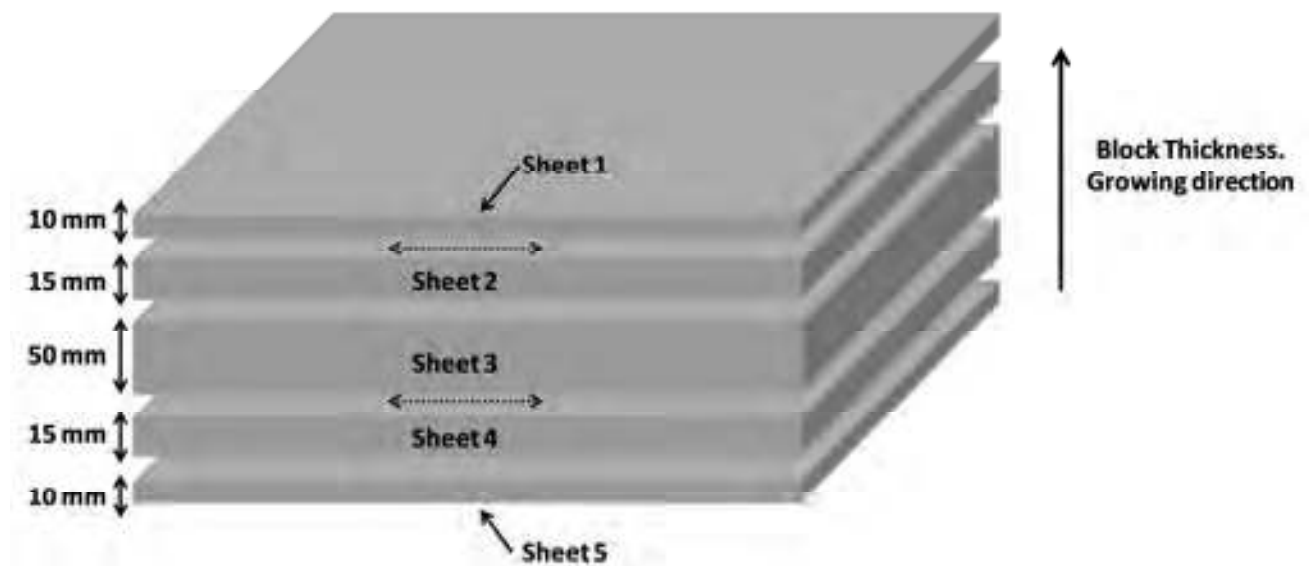
Figure 1: Slicing scheme of the foamed blocks.

As will be seen later all the specimens for the different characterizations were obtained from sheet 3 except specimens for tensile measurements which were obtained from sheets 2 and 4, this samples were obtained in the direction of the dotted arrows. Due to the foaming process these two sheets can be considered equal in terms of density, cell size, cell shape, homogeneity, etc. In order to avoid any effect related to the higher density of the outer skins(typical for this type of processing method), sheets 1 and 5 were not used in any characterization.

Table 2 shows the average density of the different materials measured in sheet 3. As it can be observed the foams density was almost the same for the analyzed materials

Table 2: Densities measured for the different blocks

Sample	Density/(kg/m^3)
Unfilled-3%	25.48
3% Nanoclays	25.55
Unfilled 5%	25.88
5% Nanoclays	26.00

Characterization of solid and foamed samples

A Mettler DSC822e differential scanning calorimeter was used for the thermal analysis of the samples. A heating rate of 10 ^{o}C under N$_2$ environment and a sample weight of 5±0.5 mg were used in all the tests. Crystallinity degree was calculated from the area of the DSC peak, by dividing the heat of fusion by the heat of fusion of a 100% crystalline material, (288 J/g for a 100% crystalline polyethylene [35]). The crystallinities were calculated taking into account the real proportions of polymer deducting the amount of nanoclays.

The TGA measurements were performed using a Mettler TGA/SDTA 851e with a temperature program from 50 to 850 ^{o}C at 20 ^{o}C/min in a N$_2$ atmosphere.

Density measurements were performed by Archimedes principle using the density determination kit for the AT261 Mettler balance. The results were compared with the determination of density by geometrical means.

The dispersion and exfoliation of nanoclays were studied by X-ray diffraction (XRD) and transmission electron microscopy (TEM). XRD diffractograms were determined between 1° and 10° by steps of 0.005° by means of a Philips PW 1050/71 using the Cu Kα line. The transmission electron microscope used was a Tesla BS 512 with a YAG camera incorporated.

The gel content was determined using a 24 h Soxhlet extraction cycle using xylene as the solvent. Approximately 300 mg of crosslinked grinded polyethylene foam was placed in a paper bag according to ASTM D 2765. In each experiment, four bags with a different material inside each one were tested simultaneously. This way, absolutely comparable results are obtained. After extraction, the solid residue was dried until a constant weight was obtained. The gel content obtained as the percentage ratio of the final weight (solid residue) to the initial weight for each sample.

Open cell content of foamed materials was determined according with ASTM Standard D6226-10 using a gas pycnometer Accupyc II 1340 from Micromeritics.

The cellular morphology was characterized by scanning electron microscopy with a JEOL JSM-820 microscope. Samples were immersed in liquid nitrogen for 5 minutes, fractured and mounted on stubs. The fracture surfaces were sputter coated with gold prior to the microscopy work. The mean cell size, cell wall thickness, anisotropy and cell density were obtained using image processing software Image J from at least 75 cells in different micrographs from the same specimen [37].

Mechanical properties were determined using an universal testing machine Instron model 5500R6025. Three specimens were tested for each kind of sample, all of them at room temperature. Solid materials were characterized in tension at a strain rate of 1 mm/min according to ISO 527/2. For the foams the tensile tests were performed with a strain rate of 5 mm/min according to ISO 1926. The compressive behaviour in the foams was determined using a strain rate of 180 mm/min till the 75% of deformation was reached. Five continuous cycles without recovery between cycles were tested in each sample.

A lab-designed compressive creep apparatus was used to measure the response of the foams to an applied constant stress over a 7 days period. Two creep rigs are shown in figure 2. In each of them, the thickness of the foam is monitored with a linear variable displacement transducer (LVDT) which is connected to a computer. The diameter of the cylinders was 30 mm and 50 mm thichness in all cases. Experiments at five different stresses were carried out at a mean temperature of 23 ºC. These five stresses are all higher than the collapse stress of the foam. Further details of this set-up can be found in [31-34]
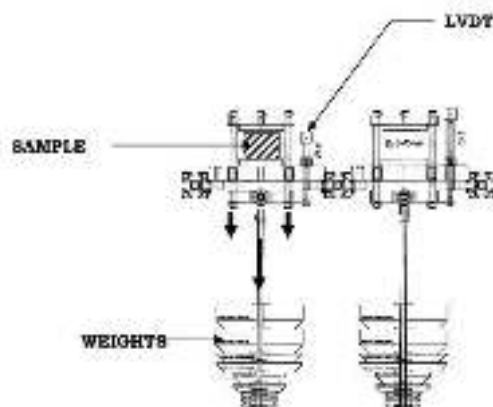
Figure 2: Scheme of the lab-designed creep apparatus.

RESULTS

X-rays diffraction, calorimetric parameters and thermogravimetric behaviour.

The exfoliation degree deeply determines the properties both of the solids and of the foams so the first step consisted in determining the separation between platelets of the nanoclays by x-ray diffraction. The continuous line in figure 3 represents the diffraction pattern obtained for the solid precursors before foaming. The (100) peak of the nanoclays can be clearly distinguished. Bragg's law for this peak yields a separation between platelet of 3.8 nm, what is higher than the 2.45 nm separation found for the as-received organomodified clays. This suggests that the melt blending has promoted some exfoliation degree but there are still agglomerates present in the polymer matrix. The same conclusion can be obtained from the observation of the TEM images. Figure 4 shows two micrographs for the 5%-Nanoclays samples. On the left, individual well exfoliated and dispersed platelets can be distinguished all along the micrograph arranged with a some preferential orientation but in some areas (figure 4 right)) still some agglomerates of platelets that have not suffered a complete exfoliation can be observed.

Therefore the solid nanocomposites present an intercalated/exfoliated structure with ordered agglomerates still present.

After foaming with an expansion ratio of 30 times the diffraction pattern is patently changed. In the solids the main peak associated with the nanoclays corresponds to a separation between platelets of 3.8 nm. After foaming the peak is changed into a smooth and less intense shoulder indicating a much higher degree of exfoliation. The still ordered structure of the nanoclays present in the solid precursors is almost completely destroyed by the foaming process. The always desired high exfoliation degree is achieved by foaming.
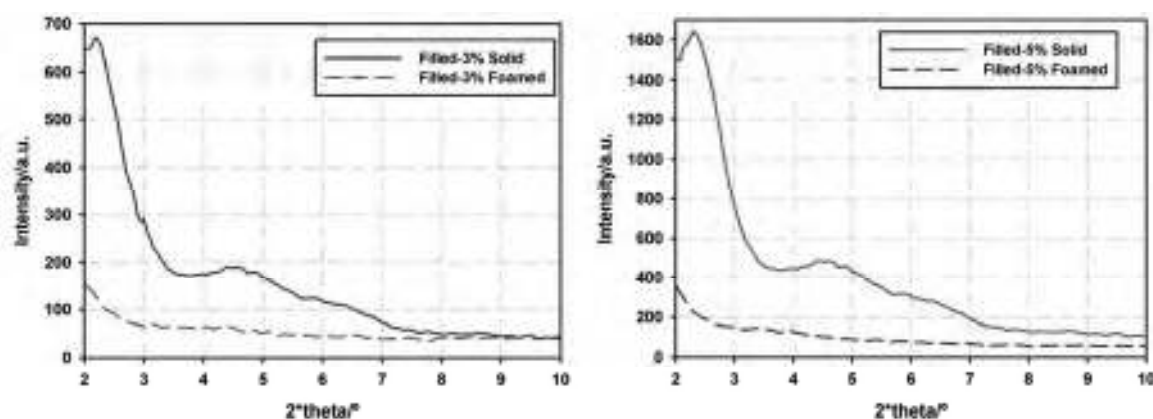
Figure 3: X-ray diffraction patterns for the solids and for the foams. The foaming strongly increases the interlamellar separation and destroys the lamellar ordered structure of the nanoparticles.
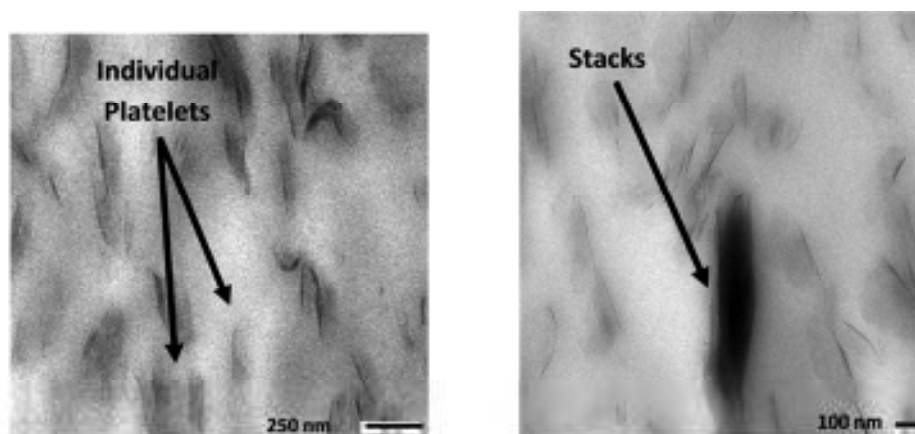
Figure 4: Transmission electron microscopy images obtained in the solid material containing 5 wt.% of nanoclays.

Table 2 shows characteristic parameters obtained from the differential scanning calorimetry. The crystallinity of the polymer matrix is reduced in the foams compared to the solid. On the

contrary to the solids in the foams the polymer matrix is already crosslinked. The chemical crosslinking produces a molecular three-dimensional molecular network, which reduces the crystalline order decreasing therefore the crystallinity degree observed in the samples. There is also a reduction of the melting point between the solids and the foamed samples. This suggests that the size of the crystals formed is different in the foams than in the solids, due again to the chemical crosslinking of the polymer [38]. In any case, the addition of nanoclays has a nucleating effect increasing the crystallinity degree both in the solids and in the foams. This enhancement in crystallinity produced by the addition of clays is slightly higher in the foams which, could be related with the higher exfoliation achieved in the foams.

Table 2: Calorimetric characterization of the samples before been foamed (solids) and after been foamed (foamed).

Sample	Melting Point (solids)/°C	Crystallinity (solids)/%	Melting Point (foamed)/°C	Crystallinity (foamed)/%
Unfilled-3%	112.07	44.0	109.28	41,6
3% Nanoclays	111.19	45.4	109.78	43.0
Unfilled-5%	111.49	45.3	109.97	42.1
5% Nanoclays	112.52	48.2	109.46	45.4

The higher exfoliation of the silicates in the foams helps in the nucleating role played by the nanoparticles during the crystallization in comparison to the unfilled samples.

The thermal stability and degradation of the polymer and the influence of the nanoclays on this parameter was studied and compared between solids and foams. Figure 5 shows the weight loss obtained by thermogravimetric analysis in the range of temperatures between 350 ºC and 600 ºC. No changes were observed outside this range. The addition of nanoclays increases the onset of the degradation temperature in 9 ^{o}C for the 3 wt.% and in 10 ^{o}C for the 5 wt.% (Table 3). The presence of compatibilizer does not have a significant influence in the thermal degradation of the polymer matrix. These results suggest that the addition of clays has an stabilizing effect on the molecular structure of the polymer when subjected to high temperatures.
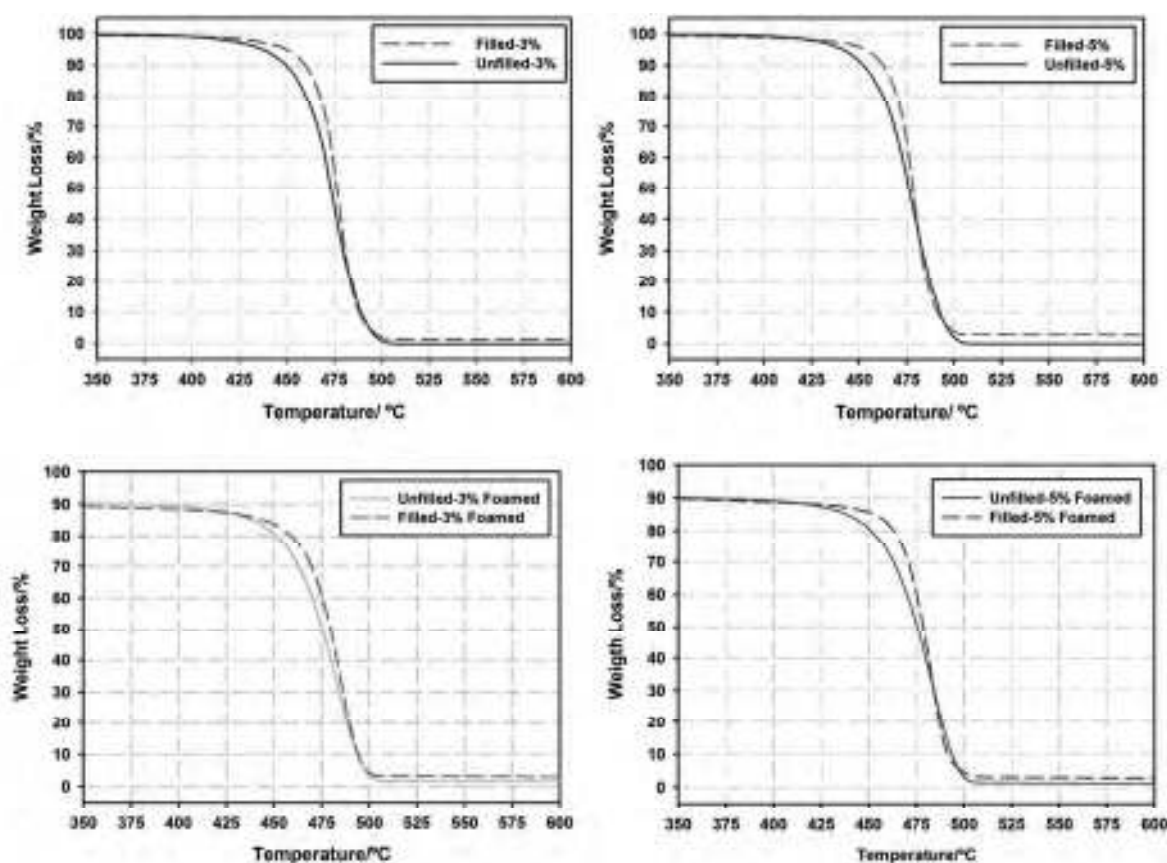
Figure 5: Weight Loss versus temperature determined by thermogravimetry. a) and b) correspond to the materials before been foamed and c) and d) correspond to the materials after been foamed. The addition of nanoclays delays the polymer degradation to higher temperatures and this effect is more pronounced in the foamed materials.

This increment on the onset of the degradation temperature is higher for the foams. The differences are up to 15 ºC for the foamed Filled-5% samples (table 3). Nanoclays have a barrier effect during the pyrolysis of the material and as a consequence the degradation occurs at higher temperatures. Higher exfoliation degrees and better dispersion of the nanoclays aggregates favours the occurrence of this shift in the degradation and that explains the improved results found in the foams compared to the solids. Besides this, the onset temperature values are always higher for the foams than for the solids. Since the polymer in the foams is already crosslinked, the molecular three-dimensional network formed helps to increase the degradation temperature.

Table 3: Onset degradation temperature determined experimentally by thermogravimetry for the material before been foamed and after been foamed.

Sample	Onset Temperature/°C	Onset Temperature (After Foaming)/°C
Unfilled-3%	460.80	461.32
3% Nanoclays	468.54	471.57
Unfilled-5%	460.35	461.23
5% Nanoclays	470.76	475.87

Gel content and cellular morphology

The low densities reached require high crosslinking degrees. Table 4 summarizes the gel contents of the different samples. The differences between the samples are within the error of the measurement technique. The addition of nanoclays does not have an influence on this parameter, at least at this high crosslinking values. These comparable values of crosslinking between samples make easier the later study of cellular structure, mechanical properties and diffusion behaviour. No influence of the crosslinking degree can be expected between different samples in the rest of the properties.

Table 4: Crosslinking degree achieved in the different samples. The differences are within the error of the determination technique.

Sample	Gel Content/%
Unfilled-3%	56.39 ± 1%
3% Nanoclays	58.19 ± 1%
Unfilled-5%	58.68 ± 1%
5% Nanoclays	60.88 ± 1%

The cellular structure of the foams has been studied in terms of cell size, cell density, cell wall thickness and anisotropy ratio. Samples from sheet 3 were obtained for this purpose (see figure 1). In this case it is interesting not only comparing samples with and without nanoclays but also samples with different amounts of compatibilizer, i.e. different amounts of linear low density polyethylene grafted with maleic anhydride. Figure 6 depicts the cellular structure of the four different kinds of samples in two complimentary views, one in a plain perpendicular to the growing direction (thickness of the block, figure 1) and the other one in a plain parallel to the growing direction. Cell sizes are between 200 µm and 300 µm. No nucleating effect of the nanoclays is observed comparing unfilled and filled samples at a fixed filler percentage, cell sizes are even slightly higher in the filled samples. Instead of this, a more than 10% reduction in cell size is found for the samples containing higher percentages of coupling agent. This linear low density polyethylene grafted with maleic anhydride is helping to reduce the cell size together with an increase in the cell density up to a 53%. Again, no difference in cell density is found between samples with or without nanoclays, no nucleating effect has been observed in the

frame of this work. This result could be expected because it is known that the main nucleating agents for the cells in this type of processing route are the residues of the blowing agent
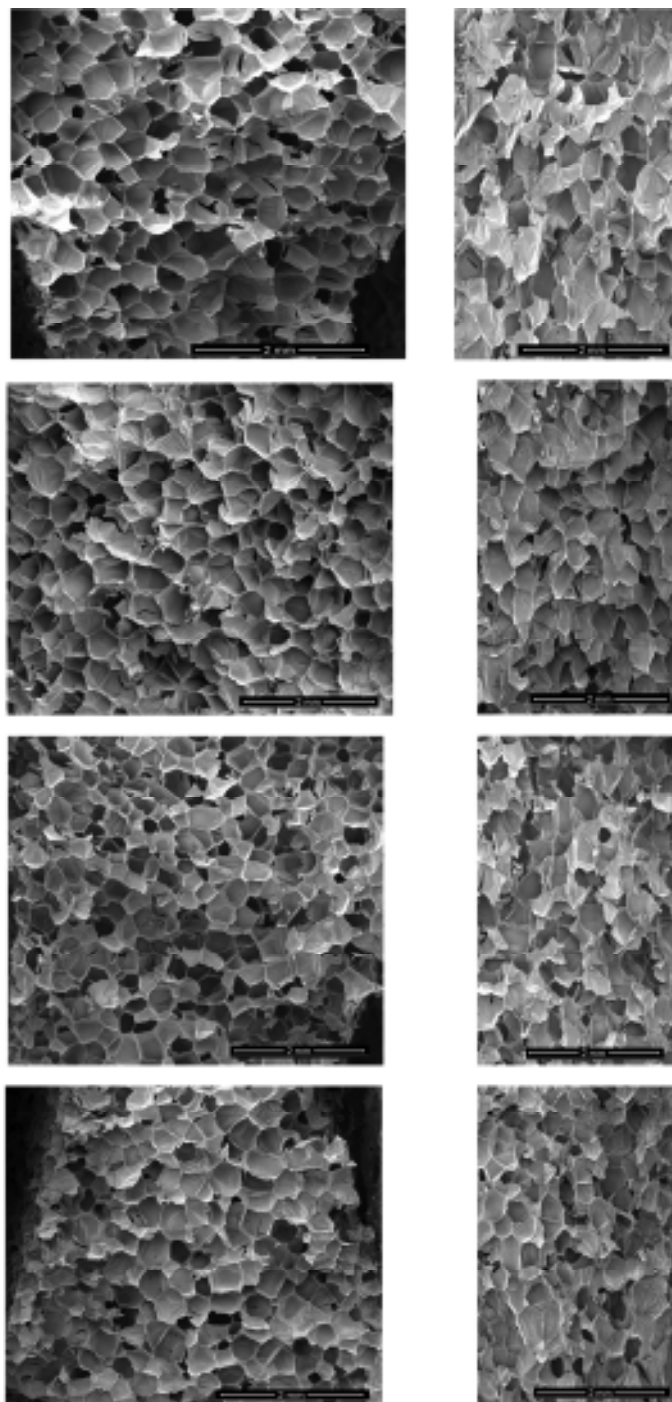

Figure 6: SEM micrographs for the a)Unfilled-3%, b) Filled-3% c) Unfilled-5% d) Filled-5%. In every case the micrograph on the left corresponds to a plain perpendicular to the growing direction and the one on the right corresponds to a plain parallel to the growing direction. The samples were taken from sheet 3.

Cell walls are slightly thicker in the samples containing clays. This higher thickness should be beneficial for the effective diffusivity of the foam, reducing the effective diffusion coefficient. The addition of the coupling agent has no effect on the cell wall thickness.

The anisotropy ratio of a foam can be defined as the ratio between the diameter of the cells in the direction of higher elongation and the diameter in the perpendicular direction. For isotropic cells the anisotropy ratio is equal to 1 and higher than one for anisotropic foams. The two steps production process employed, with the growing of the foam preferentially constrained in one direction, yields oriented cells when studied in a plain parallel to this growing direction. This anisotropy is clear when observing the micrographs on the right for each sample obtained from specimens from sheet 3. The anisotropy ratio has been quantified and included in table 5. This value is almost constant, with no trend with the nanoclays content or the coupling agent content. Anisotropy has a fundamental role when studying the mechanical behaviour of the foam. When the sample is subjected to a compressive stress in a direction coinciding with the growing direction of the foam, the elastic modulus is significantly higher than if it was compressed in a perpendicular direction [39]. As it is observed in figure 6 cells are completely isotropic in a plain perpendicular to the growing direction.

Table 5: morphological parameter characterizing each kind of sample

Sample	Cell Size/μm	Cell Density/(cells/cm^3)	Cell Wall Thickness/ μm	Anisotropy
Unfilled-3%	296	3.4·10^4	12.8	1.55
3% Nanoclays	302	3.3·10^4	13.3	1.55
Unfilled-5%	260	5.2·10^4	12.7	1.43
5% Nanoclays	267	4.9·10^4	13.6	1.48

The open cell content is of major importance when studying the mechanical and diffusive properties of these low density foams. Mechanical properties for example are directly dependent with the proportion of mass in the cell walls, parameter which is finally connected with the open cell content [40]. On the other hand it makes no sense studying the diffusivity of the gas outside the cells in open cell foams. A right characterization of the interconnectivity of the cells is mandatory prior to the study of the effective gas diffusion coefficient or the study of the mechanical properties. Table 6 contains the open cell contents obtained for the different foams.

Table 6: Open cell content of the different foams. Since the values are very low all the samples can be considered as closed cell.

Sample	Open Cell Content/%
Unfilled-3% foam	6.02
3% Nanoclays foam	6.25
Unfilled-5% foam	6.53
5% Nanoclays foam	5.64

From these low values can be concluded that the interconnectivity of the cells in the foams is almost negligible, therefore all the samples can be considered as closed cell. No remarkable differences can be observed between samples with different clay contents or coupling agent contents. The closed cell morphology of the foams justifies the later study of the effective diffusion coefficient. On the other hand a closed cell structure means a more homogeneous mass distribution along the cell walls which at the end benefits the mechanical properties. The production route followed turns to be adequate for the fabrication of large blocks of closed cell low density foams nanoreinforced with clays. Once we have studied the morphology of the foams and their solid matrices the next steps consist in the determination of the mechanical properties and the effective diffusion coefficient.

Mechanical Properties

The mechanical properties in tension were characterized and compared with those of the solid matrix. The tensile properties of the foams were measured in a direction perpendicular to the anisotropy direction of the cells (figure 1).

In the solids (figure 7 left) the addition of 3 wt.% of nanoclays improves the elastic modulus in 51%. This improvement goes up to 69% when 5% wt.% nanoclays are added to the composites. As can be inferred also from figure 7 the different amounts of coupling agent do not influence the elastic modulus. A similar trend is followed by the tensile strength, no influence of the coupling agent content and improvements up to 11% for the 3% Nanoclays and 24% for the 5% Nanoclays.

Considering the foams, the addition of nanoclays also helps to improve the elastic modulus in tension but to a lower extent than in the case of the solids. With 3 wt.% nanoclays the foams have a modulus 8% higher than the solid. The foams filled with 5 wt.% show an improvement of 40 %. Improvements are found also for the tensile strength. For this mechanical property the improvement goes up to 9% for the 3% Nanoclays and up to 14% for the 5% Nanoclays. These improvements are also lower than in the case of the solids.
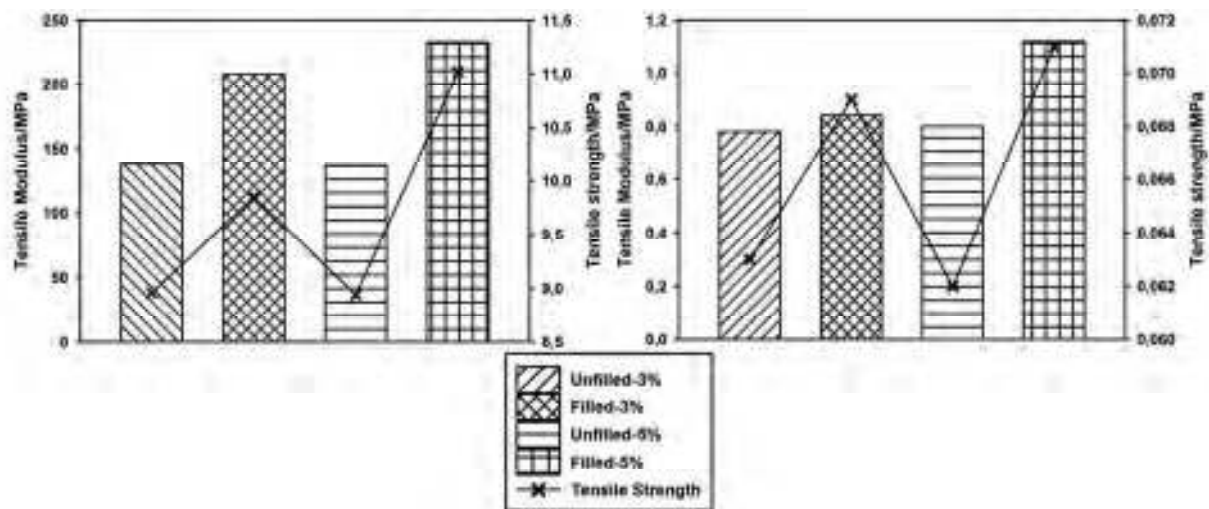
Figure 7: Mechanical properties in tension for the solids (left) and for the foams (right). Both the tensile modulus and the tensile strength are included.

At the sight of the previous values the properties of the foams will be related to the properties of the solids. The equation $E_f = E_s \cdot \left(\frac{\rho_f}{\rho_s}\right)^n$ constitutes a very simple but accurate modeling of the elastic properties in tension of foams [40]. The elastic modulus of the foam (E_f) is directly proportional to the same property of the solid matrix (E_s). ρ_f and ρ_s stand for the density of the foam and density of the polymer matrix respectively and *n* is an exponential parameter varying usually between 1 and 2 and fundamentally dependent on the morphology of the cellular structure. Fitting the previous experimental data measured for the four kinds of foams yields a constant exponential parameter "n" of 1.55, equal in all the cases. This exponent, significantly lower than 2, denotes a good mechanical performance in tension for these foams. The fact that the value of the exponent is the same in all the cases was expectable taking into account that the anisotropy of the cells and open cell content is the same in all the foams. The slight differences found in cell size varying the coupling agent content do not seem to have an influence on the tensile behavior. The improvements in tension properties found with the addition of nanoclays are only due to the reinforcement that the nanoparticles produce on the solids. No synergetic effect of the nanoclays is found in the foams, as in other works because in this case the cellular structure is not improved by the incorporation of clay particles[41].

Focusing now the attention in the compressive behavior and according to the experimental and theoretical model used later to obtain the effective diffusion coefficient the foams must be loaded in the post-collapse region. So, prior to the experimental determination of the effective diffusivity it is necessary to correctly determine the collapse strength in compression for the foamed materials. Together with the collapse strength, the elastic modulus in compression was also studied. Numerical data for these two properties are plotted in figure 8.
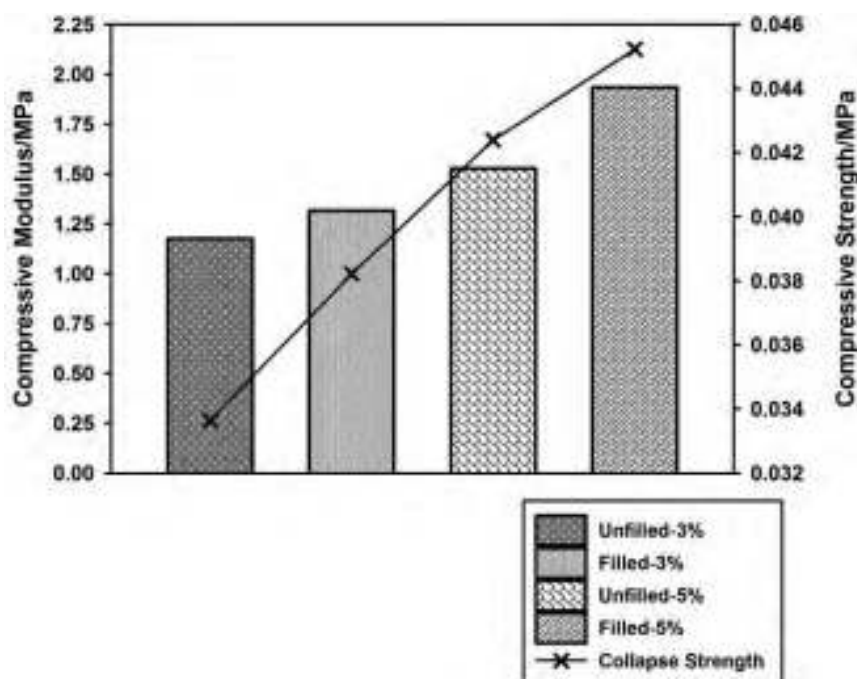
Figure 8: Collapse strength and elastic modulus in compression for the four kinds of samples.

Unlike tension, higher amounts of maleic anhydride grafted linear low density polyethylene increase both the compressive modulus and the collapse strength of the foams. The increments in modulus ascribable exclusively to the nanoclays are of 12% for the foamed Filled-3% and up to 27% for the foamed Filled-5%. In compression the modulus are patently higher than in tension since the anisotropy of the cells coinciding with the compressive direction helps to withstand the stresses applied conferring excellent compressive properties to the foam. Since anisotropy and open cell content are comparable in all the samples, the differences observed in the mechanical performance are mainly attributable to the different coupling agent contents or different nanoclays percentages in each case.

As previously described in the experimental section the foams were subjected to five continuous different cycles in compression. This way we can determine and compare the energy absorbed in each cycle. This property is fundamental when thinking in possible cushioning or packaging applications for these materials. Figure 9 shows the dependency with the cycle number of the energy absorbed for the different kinds of samples. The data are numerically fitted to exponential decay mathematical functions.
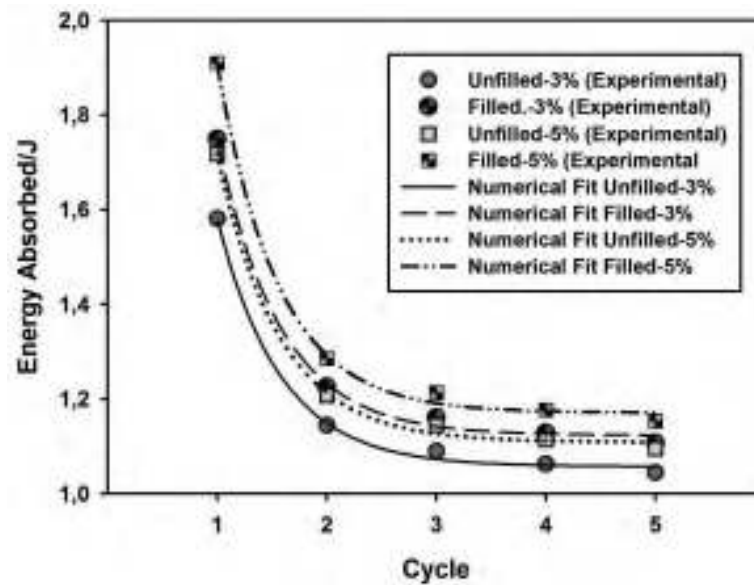
Figure 9: Variation in the energy absorbed with the number of cycles. The presence of nanoclays increases the energy that the foam is able to absorbe in the different compressive cycles.

The shape of the plots is parallel in all the samples, only shifted in energy, which indicates that the loss of properties is not affected by the different compositions. The differences appear when considering the energy that is capable to absorb each sample. The addition of nanoclays allows absorbing more energy and this behaviour is maintained during all the cycles, this happens both for the foamed Filled-3% and foamed Filled-5%, especially for this last one. Once again the presence of a higher amount of coupling agent benefits the behaviour of the foam. A similar effect is obtained adding 3% of nanoclays or increasing the coupling agent proportion from 6 wt.% to 10 wt.%. Thinking in a possible cushioning or packaging application of these materials the samples containing clays would have superior properties in this sense.

The significant improvement in the mechanical properties of the foams containing clays should be due first to the reinforcement of the cell walls and second to the higher crystallinity of the polymer matrix induced by the clays presence.

Diffusion

A lab-designed compressive apparatus was used to measure the response of the foams to an applied constant stress over a 7 days period [31-34]. From the characterization of the creep behaviour of a foam over a long time period we can also determine the effective diffusion coefficient (D_{eff}) of the gas outside the cells. Assuming isothermal conditions during the compression of the gas and a null Poisson coefficient (v=0), the uniaxial compressive stress for these foams loaded in the post-collapse region can be obtained using the formula (1)

$$\sigma = \sigma_0 + \frac{P_0 \varepsilon}{1 - \varepsilon - \rho_f / \rho_s} \qquad (1)$$

where σ is the collapse strength, ε is the deformation, P_0 is the initial pressure inside the cells and R=ρ_f / ρ_s is the relative density of the foam. According to formula 1 plotting the compressive

stress as a function of the gas volumetric strain ε/(1- ε-R) for a fixed creep time "t" yields a slope of the curve that represents the pressure of the gas contained in the cells at time "t" (figure 10, right).
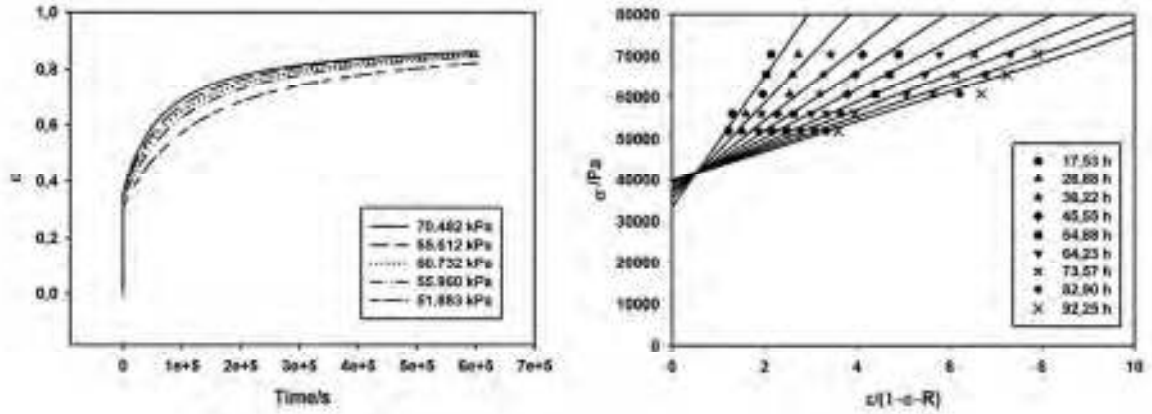

Figure 10: Left, strain evolution with time at five constant stresses higher than the collapse strength of the foam. Right, isochronous stress-strain curves at nine different times. The data corresponds to the 5% Nanoclays sample

Using this method for different creep times we can obtain the evolution of the pressure inside the cells for each sample. From the evolution of pressure with time and using the diffusion equation of the gas inside the cells we can obtain the diffusion coefficient. Svanström et al. proposed a solution of the diffusion equation for a cylindrical geometry as it is in our case [42]. According to this analytical solution, the effective diffusion coefficient can be obtained using the equation (2):

$$D_{eff} = -\frac{1}{2.4048^2}\frac{d}{dt}\left\{ln\left[\frac{P(t)}{P_0}\frac{(\beta_{01}a)^2}{4}\right]\right\} \qquad (2)$$

Where P(t) is the pressure inside the cells at a time t, P_0 is the pressure in the cells for the unloaded foam, a is the radius of the cylinder and β_{01} is the first order root of the Bessel's function of 0th order.
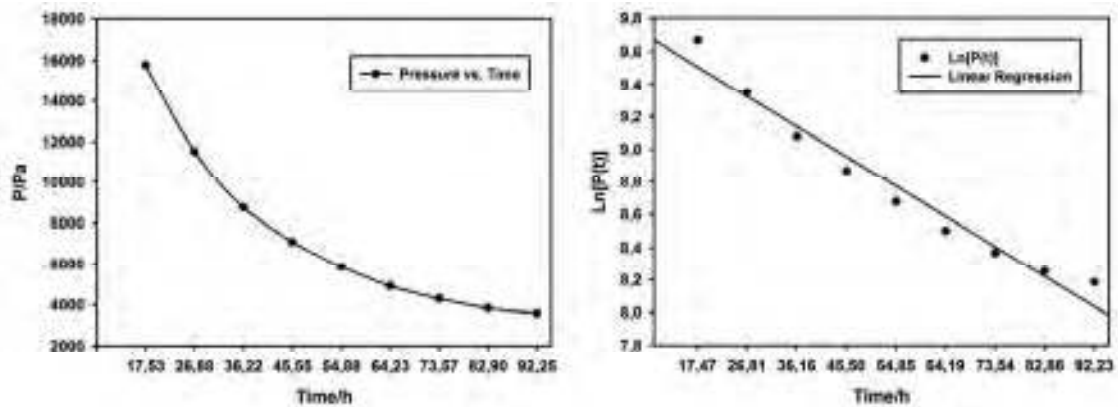
Figure11: Left, pressure evolution with time obtained using equation 1. The neper logarithm of the pressure is plotted on the right. The slope of the plot yields the effective diffusion coefficient. The data corresponds to the 5% Nanoclays sample.

The term $ln\left[\frac{P(t)}{P_0}\frac{(\beta_{01}a)^2}{4}\right]$ is well fitted to a linear function with time so it is possible to obtain a numerical non-time depending diffusion coefficient in all cases. For the sake of simplicity only the figures corresponding to the 5%-Nanoclays sample are included. The diffusion coefficients obtained using this method for the different samples are shown in table 7.

Table 7: Effective diffusion coefficients obtained for the different kinds of samples using equation 2 and the experimental data measured.

Sample	$D_{eff}/(m^2/s)$
Unfilled-3%	$10.98 \cdot 10^{-7}$
3% Nanoclays	$10.88 \cdot 10^{-7}$
Uniflled-5%	$9.92 \cdot 10^{-7}$
5% Nanoclays	$9.34 \cdot 10^{-7}$

Parameters as gel content or open cell content have comparable values for all the samples so no influence can be expected from them on diffusivity. Gas solubility and diffusivity are strongly dependent upon the crystallinity of the polymer matrix. Higher crystallinities reduce the gas solubility and hinder the diffusion through the polymer matrix [40]. As previously studied the samples containing clays exhibit higher crystallinity values and therefore lower effective gas diffusivity values should be expected for these samples. Besides this, thicker cell wall thicknesses are found also for the filled samples which should also make more difficult the gas escape from the interior of the cells. The nanoclay platelets, by themselves, should play a gas barrier role increasing the mean free pathway that a gas molecule must follow in its way to the exterior across the polymer matrix. Altogether, an strong reduction in the effective gas diffusivity is expected for he nanoclay-filled low density foams in comparison to the unfilled ones but the experimental results do not confirm these expectations. The addition of 3 wt.% gives as result a negligible 1% reduction in the effective diffusion coefficient even when the nanoclays in the cell walls are presumed to be quite well exfoliated. Comparing the values of the Unfilled-5% and Filled-5% the reduction is more appreciable, up to a value of 6%. Theoretically with the addition of 3wt.% and 5 wt.% well dispersed and exfoliated nanoclays, increments in the crystallinity and thickening of the cell walls the effective diffusion coefficients should have been more patently reduced. On the contrary, experimentally, the highest reduction is found varying the coupling agent content with an improvement in the gas barrier properties up to 10%. The linear character of the coupling polymer together with the grafted maleic anhydride helps to reduce the effective diffusivity of the foam.

A prior study using CO_2 and a gravimetric method for the determination of the diffusivities was performed over solid specimens of the four mentioned samples. The obtained values are included in table 8.

Table 8: Diffusivities for the solid materials obtained in a previous work and using CO_2 as permeant. Although the gas is different the trends are the same as in the foams.

Sample	*Diffusivity/(m^2/s)*
Unfilled-3% (solids)	$12.1 \cdot 10^{-12}$
3%-Nanoclays (solids)	$10.8 \cdot 10^{-12}$
Unfilled-5% (solids)	$9.30 \cdot 10^{-12}$
5%-Nanoclays (solids)	$8.92 \cdot 10^{-12}$

According to Alsoy theoretically the effective diffusion coefficient of a closed cell foam is directly proportional to the diffusivity corresponding to the solid matrix [4]. The reductions in diffusivity found for CO_2 in the solid samples are in general higher than the ones found for the effective diffusion coefficient of the foams, but the general trends are maintained. It is especially remarkable that the highest reductions are found not with the addition of sheet-like nanoparticles but adding a certain amount of linear polyethylene grafted with maleic anhydride and this fact is found both in the diffusivities of the solids as well as in the effective diffusion coefficients of the foams.

In the case of the solids the lower than expected reductions in diffusivity found were attributed to some extent to the not perfect exfoliation achieved. But in the foams this exfoliation degree is much improved but still the reductions in the effective diffusion coefficient are low. The hypothesis of a bad coupling between the nanoclays and the polymer rises as a possible explanation to the observed results. The presence of interfaces between the exfoliated platelets and the polymer matrix is increasing the possible paths that the gas can follow in its way to the exterior [44, 45]. On the contrary the linearity of the coupling agent polymer and the high affinity of the maleic anhydride to the gas act as barriers to the gas escape patently reducing the diffusion.

Conclusions

A method for the production of big blocks of low density closed cell polyethylene foams filled with montmorillonite-type nanoclays is presented. The thirty expansions reached improve the exfoliation of the nanoclays. The XRD demonstrates that the lamellar order has been ruptured to a high extent just by foaming, so we can consider that the foams present a highly exfoliated nanoscaled morphology. This highly exfoliated morphology broadens the polymer degradation window and helps to the nucleation during the crystallization from the melt but does not have any influence on the gel content, open cell content, cell size, cell density or anisotropy ratio. On the other hand the addition of higher amounts of linear low density polyethylene grafted with maleic anhydride helps to reduce the cell size and increase the cell density maintaining constant the other parameters.

Tension mechanical properties, both the elastic modulus and tensile strength, are highly improved with the addition of nanoclays in the solids as well as in the foams. Percentage-wise in comparison to the unfilled materials, the improvements in the solids are higher than in the foams. Using the potential law yields an exponent n equal to 1.55 what denotes an outstanding

behavior for the foams with this characteristic cellular structure. This exponent is the same both for the filled and for the unfilled materials so no synergetic effect of the nanoparticles with the foaming has been found.

The compressive properties are higher than the properties measured in tension. The preferential orientation of the cells coinciding with the compressive direction helps to this fact. Again in this case, the addition of nanoclays improves both the elastic modulus and the compressive strength. What it is interesting now is that the mere addition of a higher amount of coupling agent patently improves both mechanical properties in compression. Nanoclays and higher amounts of coupling agent increase also the energy absorbed, the improvement is maintained along different compressive cycles. This property is of particular importance when considering cushioning or packaging applications, benefiting the damping behavior of the foam.

The effective diffusion coefficients of the gas outside the cells have been experimentally determined allowing elucidating empirically the barrier role effect of the nanoclays. Even with the high degrees of exfoliation observed, the reductions in diffusion are lower than expected. Higher amounts of clays mean higher reduction in the diffusion coefficient but, what is surprising, is that the highest reductions are found when passing from 6 wt.% to 10 wt.% of coupling agent. This same trend was observed when studying the diffusivities of the solid matrices with CO_2 by gravimetric methods. The linear character of the coupling polymer and the high affinity of the maleic anhydride could be behind these results. The low reductions in diffusion found in the foams with the addition of clays are explained bearing in mind the interfaces formed between the clays and the polymer matrices. These interfaces can act as rapid pathways to the exterior for the gas in detriment of the diffusion coefficients.

Acknowledgements

Bibliography

[1]   Mills NJ, Rodriguez-Perez MA. Cell Polym 20 (2) 79–100 (2011)

[2]   Hoogendorn. Thermal ageing. In: Hilyard NC, Cunninham A, editors. Low density cellular plastics; physical basis of behaviour. New York: Chapman & Hall; (1994)

[3]   Bart GCJ, Du Cauze de Nazelle GMR. J Cell Plast 29, 29–42 (1993).

[4]   Alsoy S. J Cell Plast 35, 247-271 (1999)

[5]   L.A. Utracki in Clay-containing polymeric nanocomposites. Rapra Technology Limited. United Kingdom (2004).

[6]   J. H. Koo in Polymer Nanocomposites. McGraw-Hill. USA (2006).

[7]   S. Pavlidou, C.D. Papaspyrides. Prog. Polym. Sci., 33 1119-1198. (2008)

[8]   J. Golebiewski, A. Rozanski, J. Dzwonkowski, A Galeski. Europ. Polym, J. 44 270-286 (2008).

[9]   T. Ogasawara ,Y. Ishida, T. Ishikawa, T. Aoki, T. Ogura. Compos Part A Appl S 37. 2236-2240. (2006)

[10]   M. Tortora, G. Gorrasi, V. Vittoria, G. Galli, S. Ritrovati, E. Chiellini. Polym. 43. 6147-6157 (2008)

[11]   Z. Ke, B. Yongping. Matter Lett, 59. 3348-3351 (2005)

[12]   T. Ogasawara ,Y. Ishida, T. Ishikawa, T. Aoki, T. Ogura. Compos Part A Appl S 37. 2236-2240. (2006)

[13]   S.S. Ray, K. Yamada, M. Okamoto, K. Ueda. Polymer 44. 857-866 (2003).

[14]   C. Lu, Y. W. Mai. Phys. Rev. Lett. 95, 088303 (2005).

[15]   E. Jacquelot, E. Espuche, J. F. Gerard, J. Duchet, P. Mazabraud. J. Polym Sci. 44 431-440 (2006).

[16]   S. Ippalapalli, A. D. Ranaprathapan, S. N. Singh, G. Harikrishnan. ChemPhysChem doi: 10.1002/cphc.201200977(2013)

[17]   W. Zhai, C. B. Park, M. Kontopoulou. Ind Eng Chem Res 50, 7282-7289 (2011)

[18]   C. Zeng, X. Han, L. J. Lee, K. W. Koelling, D. L. Tomasko. Adv Mater 15, 1743-1747 (2003).

[19]   Y. H. Lee, K. H. Wang, C. B. Park, M. Sain. J App Polym Sci 103, 2129-2134 (2007).

[20]   S. M. Seraji, M. K. R. Aghjeh, M. Davari, M. S. Hosseini, S. Khelgati. Polym Compos 32, 1095-1105 (2011).

[21]   M. C. Saha, M. E. Kabir, S. Jeelani. Mat Sci Eng A-Struct 479, 213-222 (2008).

[22]   K. Gorem, L. Chen, L. S. Schadler, R. Ozisik. J Supercrit Fluid 51, 420-427 (2010).

[23]   R. Verdejo, C. Saiz-Arroyo, J. Carretero-Gonzalez, F. Barroso-Bujans, M. A. Rodriguez-Perez, M. A. Lopez-Manchado. Europ. Polym. J.44, 2790-2797 (2008).

[24]   M. Tortora, G. Gorrasi, V. Vittoria, G. Galli, S. Ritrovati, E. Chiellini. Polym. 43. 6147-6157 (2008)

[25]   Z. Ke, B. Yongping. Matter Lett, 59. 3348-3351 (2005)

[26]   T. Ogasawara ,Y. Ishida, T. Ishikawa, T. Aoki, T. Ogura. Compos Part A Appl S 37. 2236-2240. (2006)

[27]   S.S. Ray, K. Yamada, M. Okamoto, K. Ueda. Polymer 44. 857-866 (2003).

[28]   Pilon L, Fedorov AG, Viskanta R. J Cell Plast 36, 451–74 (2000).

[29]   Briscoe BJ, Savvas T. Adv Polym Technol 17 (2), 87–106 (1998)

[30]   Mills NJ, Gilchrist A. J Cell Plast 33 (3), 264–92 (1997).

[31]   J.L. Ruiz-Herreo, M.A. Rodriguez-Perez and J.A. de Saja: Polymer 46, 3105-3110 (2005)

[32]   J.L. Ruiz-Herrero, M.A. Rodriguez-Perez and J.A. de Saja: J. Appl. Polym. Sci. 99, 2204-2210 (2005)

[33]   M. A. Rodriguez-Perez, J.L. Ruiz-Herrero, E. Solorzano, J. A. de Saja. Cell Polym 25 (4) 221-236 (2006)

[34]   J. Escudero, J. Lazaro, E. Solorzano, M. A. Rodriguez-Perez, J. A. de Saja. Def. and Diff. Forum 283-286, 583-588 (2009)

 [35]   B. Wunderlich. Macromolecular Physics, 2. Academic Press, New York. 1973-1976.

[36]   D. Klempner, V. Sendijarevic. Handbook of Polymeric Foams and Foam Technology. 2nd Edition. Hanser Publishers, Munich, (2004)

[37]   J. Pinto, E. Solórzano, M. A. Rodriguez-Perez, J. A. de Saja, Characterization of cellular structure based on user-interactive image analysis procedures; *Journal of Cellular Plastics*, submitted, 2013

[38]   Kang TK, Chang-Sik H. Polymer Testing 19, 773-783 (2000)

[39]   A. T. Huber, L. J. Gibson. J. Mat. Sci 23. 3031-3040 (1988)

[40]   L. J. Gibson, m. F. Ashby. Cellular Solids. Cambridge University Press. United Kingdom (1999).

[41]   C. Saiz-Arroyo, J. Escudero, M.A. Rodriguez-Perez, J. A. de Saja. Cell. Polym. 30, 2, 63-78 (2011).

[42]   M. Svanstrom, O. Ramnas, M. Olsson and U. Jarfelt: J. Cell. Polym. 16, 182-193 (1997)

[43]   Doroudiani S, Park CB, Kortschot MT. Polym. Eng. Sci. 36, 21, 2645-2661 (1996)

[44]   E. Picard, H. Gauthier, J. F. Gerard, E. Espuche. Colloid and Interface Sci. 307. 364-376 (2007)

[45]   E. Picard, A. Vermogen, J. F. Gerard, E. Espuche. J. Poly,. Sci. 46. 2593-2604.

Chapter 5

Modifications in the Cellular Structure

5.1.- INTRODUCTION

The other strategy exposed in chapter 2 to improve the physical properties of a cellular material consists in modifying the cellular structure. The approach followed for this purpose has been elaborating novel production routes that yield modified cellular structures in order to improve physical properties.

This chapter is focused on the production of structural foams by a novel production route entirely developed during the thesis. This production route is named *Stages Molding* and it has been patented. The patent document can be found in Annex II, at the end of the manuscript.

All the work presented in this thesis dealing with Stages Molding has been developed based on low density polyethylene (LDPE) although the production route can be extended to other polymer matrices. Besides, only chemical blowing agents (azodicarbonamide) have been used.

5.2.- MODIFICATIONS OF THE CELLULAR STRUCTURE: STAGES MOLDING

5.2.1- Description of the Production Route

In this first part of the chapter structural foams production route is described.

Structural foams are commonly produced by injection molding, in any of its several variants. But this production route present several undesirable drawbacks. The initial investments are high, the surface quality of the parts produced is not always as good as desired, parts have always high densities and in general the control over the final cellular structure is poor (see chapter 2, section 2.4.2.1).

The work presented in this section is entitled *"A new technology for the production of polymer structural foams"*. The work presents the fundamentals, from a scientific and technical point of view, of a new technology developed for the production of structural foams. This technology covers some of the drawbacks previously mentioned:

- The initial investments are low. The molds are cheaper than in injection molding and the technology used is simple.
- The surface quality is good, comparable to the one obtained in solid parts.
- A higher control is achieved in morphological parameters as cell size, thickness of the outer solid skins or bulk density.
- A lower range of densities is achievable compared to injection molding.

These mentioned characteristics together with the main features of this novel route make it specially suitable for the production of small series.

The paper is focused on experimenting the physical mechanisms that allow producing structural foams using a free foaming approach.

A new technology for the production of polymer structural foams

J. Escudero[1], J. Pinto[2], M.A. Rodriguez-Perez[1]

1. Cellular Materials Laboratory (CellMat), Condensed Matter Physics Department, University of Valladolid, Valladolid, Spain. Email: marrod@fmc.uva.es

2. Italian Institute of Technology, Geneve, Italy.

INTRODUCTION

Industrial sectors as important as aeronautics, sporting goods, or the automotive sector are demanding each time more and more foams with improved mechanical properties.

It is well known that conventional foams (foams with constant relative density along the volume) have relative low stiffness and strength when the density is reduced. One way to improve these properties maintaining constant the bulk density consists in producing foams with a sandwich structure, that is to say, presenting two outer solid skins and an inner foamed core. This, usually named skin-core morphology, results in high specific mechanical properties (strength to weight ratio) compared to non-structural foams [1].

Commonly, the most usual method to produce structural foams is conventional injection moulding. Some other more sophisticated methods have been developed but based upon this previous one [2]. In all the cases the polymer, blowing agent and other additives are injected inside a mould using high pressures. In the case of the conventional process, the cold walls of the mould enable the polymer melt to solidify without forming a cellular structure, achieving in this simple way the sandwich structure characteristic of structural foams. Surface quality is not as good as desired and the density reduction is not very high. In order to overcome these disadvantages moulds that can be expanded after the injection of the polymer melt have been designed. These expandable moulds allow a better control of the final cellular structure but in general surface quality is not as good as needed for several industrial applications. Other option consists in introducing a gas at elevated pressure inside the mould before the polymer is injected. The gas is then evacuated as the polymer is injected in a process that is commonly known as "gas counter pressure". While doing this, much better surface qualities are achieved but skin layers are in general very thin [3,4]. Even a commercial route has been patented to achieve structural foams. Smartfoam®, as it is commercially named, try to obtain a good surface quality with an

adequate control of the cellular structure and skin layers thicker than in the previous cases. In a first step solid polymer is injected inside the cavity of the mould forming the solid outer skins. Then, gas is dissolved in the polymer in the injection unit and then this polymer, with the gas already dissolved, is injected in the mould. This polymer-gas mixture allows forming the cellular core of the foam. In a final step, solid polymer is again injected to end the solid outer skins and as a consequence the structural foam [5].

Injection moulding in all its forms is a quick process. From an industrial point of view, large series of pieces can be produced in short time gaps and the characteristics of these pieces are good enough to fulfill the requirements. But it presents also several disadvantages. Moulds used in any of the processes described above are quite expensive since the pressures used are quite high. At the same time the initial investments necessary are also high and maybe even too high if the production consists in small series. Besides, densities reachable in this process are high, in the order of 700 kg/m3, with difficulties to obtain lower densities combined with a good control of the cellular structure and other parameters [6-10].

In this work we want to present an alternative route to the production of structural foams that has nothing to do with injection moulding. From an industrial point of view, much cheaper moulds and lower initial investments are required. This makes the process very convenient specially for the production of small series. At the same time, lower densities are reachable without sacrifying surface quality. From a scientific point of view it is possible to produce both conventional and structural foams using practically the same process, same composition and in the same density range which allow us to compare systematically the behavior of both kind of foams. Good control over the cellular structure from the point of view of cell size and homogeneity is achieved. Skin thickness, density profile and global density can be controlled independently following the procedure presented in this work. The structural characterization of the foams produced under this new route has been also made showing at the end the improvement in mechanical properties that these new structural foams present.

EXPERIMENTAL

Materials

Polyethylene-based structural foams have been produced in this work. The polymer selected is a low density polyethylene (LDPE) PE003 from Repsol Alcudia with

a density of 920 kg/m3 and a melt flow index of 4.2 g/10 min (190 °C and 2.16 kg). The chemical blowing agent used is commercial azodicarbonamide Lanxess Porofor with a particle size of 20 µm. The percentage of azodicarbonamide used in all the cases was 7 wt.%. This percentage was found to be optimum for the purpose of this work in a preliminary study. In order to promote the activation of azodicarbonamide a 0.06% of ZnO was added as kicker. To prevent oxidation, Irganox 1010 was mixed in a percentage of 0.1% together with a 1% of stearic acid as processing aid.

Samples Production

Foam discs of 150 mm in diameter were produced following a process of free-foaming inside a mould at a temperature of 180 °C. To do this, solid sheets of precursor material, which already contain the blowing agent and the rest of the additives, were introduced inside a steel mould. After that, the mould is closed and put inside a pre-heated furnace to undergo the free expansion process previously mentioned.

The aforementioned procedure is the one used in the production of conventional foams, that is, those with a constant density along its profile. In the case of structural foams, the only difference is that the inner surfaces of the steel mould walls were covered with 1.5 mm sheet of silicone rubber AVSM141 from Avon Group Manufacturing. This silicone rubber has a hardness of 60 and its operating temperature conditions are between -40 °C and 200 °C. Solid skins are developed everywhere where exists contact between the polymer and the silicone rubber during foaming. The key parameter in the selection of silicone rubber as covering material is its amorphous character and therefore its high capacity of dissolving gas as will be shown later on.

The foaming process is the same for both kinds of structures (conventional and structural foams), the only difference is the presence of silicone rubber covering the walls of the mould in the case of structural materials. Chemical compositions and bulk densities are the same what, from a scientific point of view is ideal to compare between both kinds of materials.

Structural foams have a thickness of 12 mm and cover a range of densities between 500 kg/m3 and 800 kg/m3. Density is controlled by the amount of precursor material introduced in the mould and measured by geometrical procedures. To study the dependency of skin thickness with time a unique density was chosen and samples were produced with different foaming times at the same temperature of 180 °C. Foaming time is an important parameter for these structural foams as will be seen later.

Morphology Analysis

Foam morphology characterization was made via scanning electron microscopy with a microscope model JEOL JSM-S20. Micrographs were analyzed by means of the image processing software ImageJ. Skin thickness was calculated as the average distance between the sample surface and the closest cells to the skin.

RESULTS AND DISCUSSION

Structural Foams Production

As can be inferred from the experimental part, the only difference between the production of conventional foams and structural foams in our case is the addition of a silicone rubber sheet covering the internal walls of the mould. It has been experimentally proved that all the parts of the sample that are in close contact with the silicone rubber during foaming develop solid skins. These solid skins have a density very near the one of LDPE as will be shown later. An example of the experimental set-up used and the materials obtained is shown in figure 1.
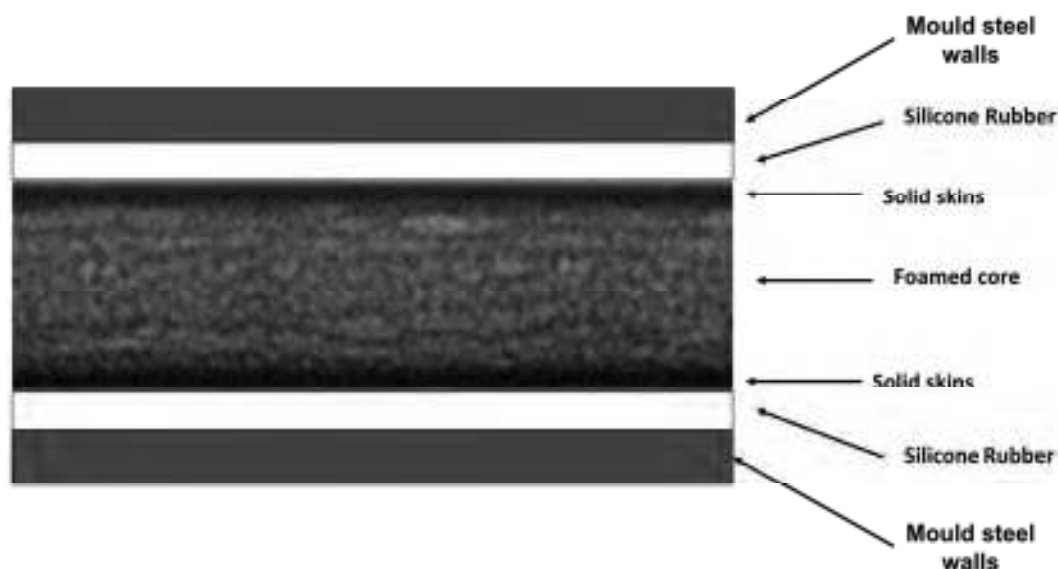
Figure 1: Scheme of the disposition of the silicone rubber according to the sample.

Solid skins appear where the sample is in close contact with the rubber.

The formation of solid skins in the areas in close contact with this silicone rubber is due to a process of gas diffusion from the polymer to the rubber [12,13,14,15]. The

main gas released during the decomposition process of the azodicarbonamide is nitrogen. At the foaming temperature and pressure developed inside the mould for a 7 % of blowing agent, nitrogen is in supercritical conditions. This, together with the amorphous character of the silicone rubber, would improve the dissolution of gas in this material.

To confirm this hypothesis a very simple experiment was carried out. Silicone rubber was covered with conventional 50 µm aluminum foil in such a way that this aluminum foil was in between the foam and the silicone. The idea is to avoid the diffusion of gas from the polymer to the silicone maintaining intact the elastic and other properties of the rubber. Foams produce following this procedure present no solid skin as we expected. An example of this experiment is presented in figure 2.
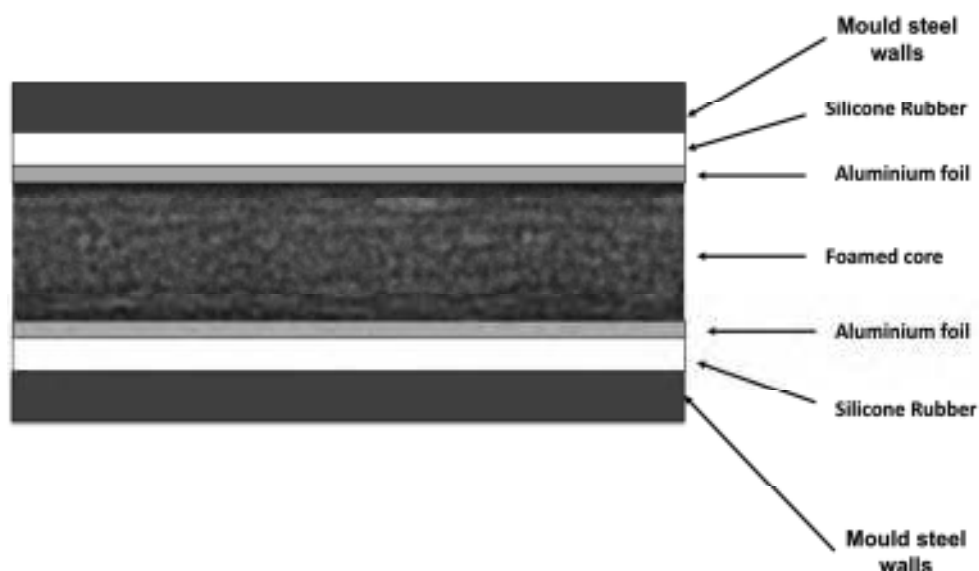
Figure 2: Scheme of the disposition of the silicone rubber and aluminum foil according to the sample. In this case no solid skins appear in the material.

Once the foaming has ended and the silicone covering is extracted outside the mould, it would lose weight slowly as a consequence of re-diffusion of the gas to the atmosphere. In the case that no gas would have dissolved, no weight loss would be expected. Taking this into account the weight of the silicone covering was registered continuously during the first 12 hours after the extraction from the mould. The silicone piece was put inside the scales just after extracting it from the mould and weight was registered recording 1 sample per second for about 12 hours. The results are presented in figure 3.
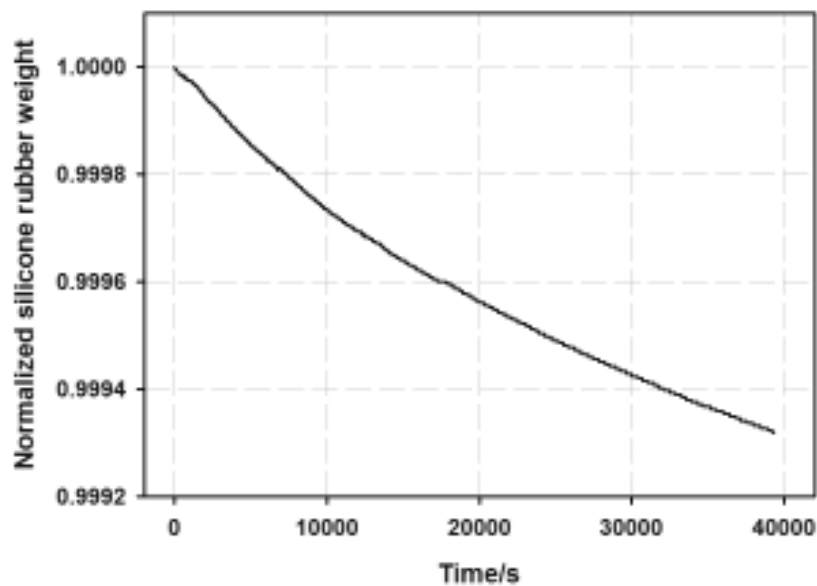
Figure 3: Weight loss of naked silicone rubber. This weight loss is due to the re-diffusion of gas to the atmosphere

There is a clear weight loss reaching a total value of 0.07 % after 12 hours. Previously a piece of silicone of the same dimensions and characteristics was undergone the same temperature profile inside the furnace and weighted during the same number of hours to exclude possible effects of contractions or heating of the air inside the scales. No weight variation was found in this case.

In a second experiment the same procedure was followed with the piece of silicone rubber covered with the aluminum foil. Since in this case the gas dissolution has been almost completely avoided, a minimum weight loss is expected. A comparison between the naked silicone rubber and the one covered with aluminum is presented in figure number 4. According to our hypothesis the loss in this case is minimum and much smaller than the one of the naked silicone with a total value of 0.018 % after 12 hours.
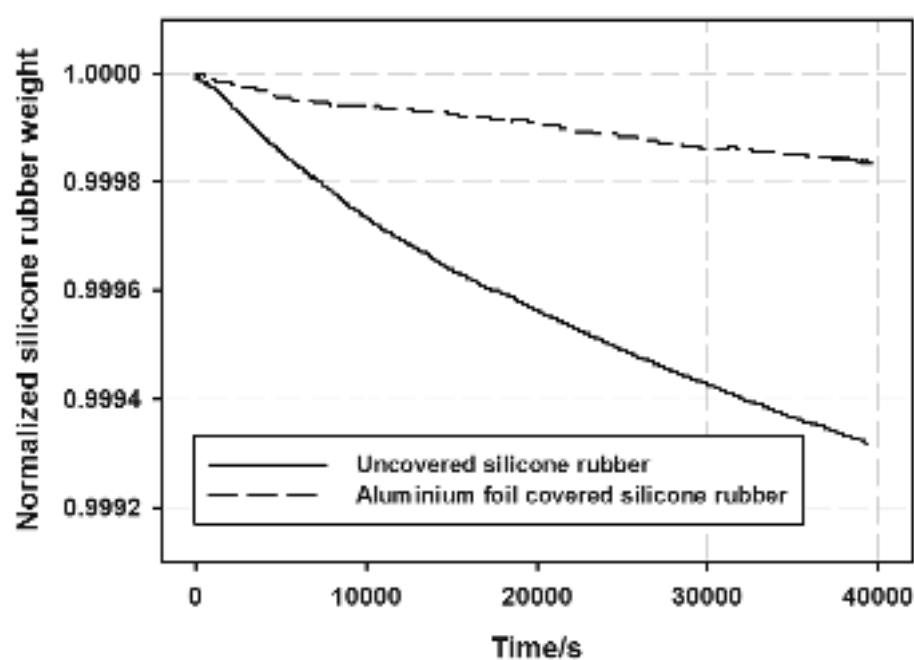
Figure 4: Comparison with the silicone covered with aluminum foil. The weight loss is much smaller in this case.

Altogether supports the idea that the gas from the outer parts of the foam dissolves in the silicone rubber that is in contact with them and form the solid skins typical of an structural foam.

Foam Morphology

In figure number 5 a micrograph of a foam produced under this new process is presented
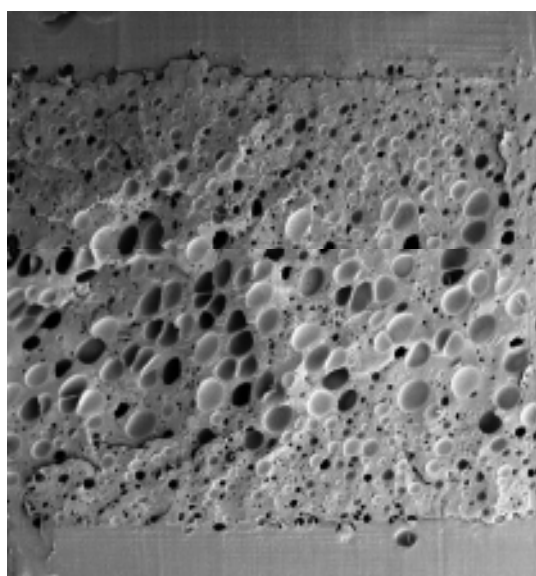
Figure 5: Micrograph of a structural foam produce under this new process.

Two solid skins can be observed, each of them with a thickness that represents approximately 10 % of the total thickness of the foam. In the central part the structure of a conventional foam is observed, with cell sizes typical of a free foaming process. And in between the solid skins and the central part, there exist two transition areas with smaller cell sizes: this transition areas play a crucial role while determining the mechanical properties of each sample. The structure is not essentially different from the one of structural foams fabricated under an injection molding process.

Cell size and the vertical density profiles have been studied in a parallel work [11]. Since the formation of the solid skins is due to the dissolution of gas in the silicone rubber, the final morphology is very dependent with processing parameters such as temperature or pressure developed inside the mould. Pressure depends mainly on the amount of blowing agent decompose, that is to say, on foaming time to a limit. At a constant temperature and fixed density, different samples were produced at different foaming times (30 min., 60 min., 90 min., 120 min. and 150 min.) to study the variation of skin thickness. The corresponding micrographs are shown in figure 6.
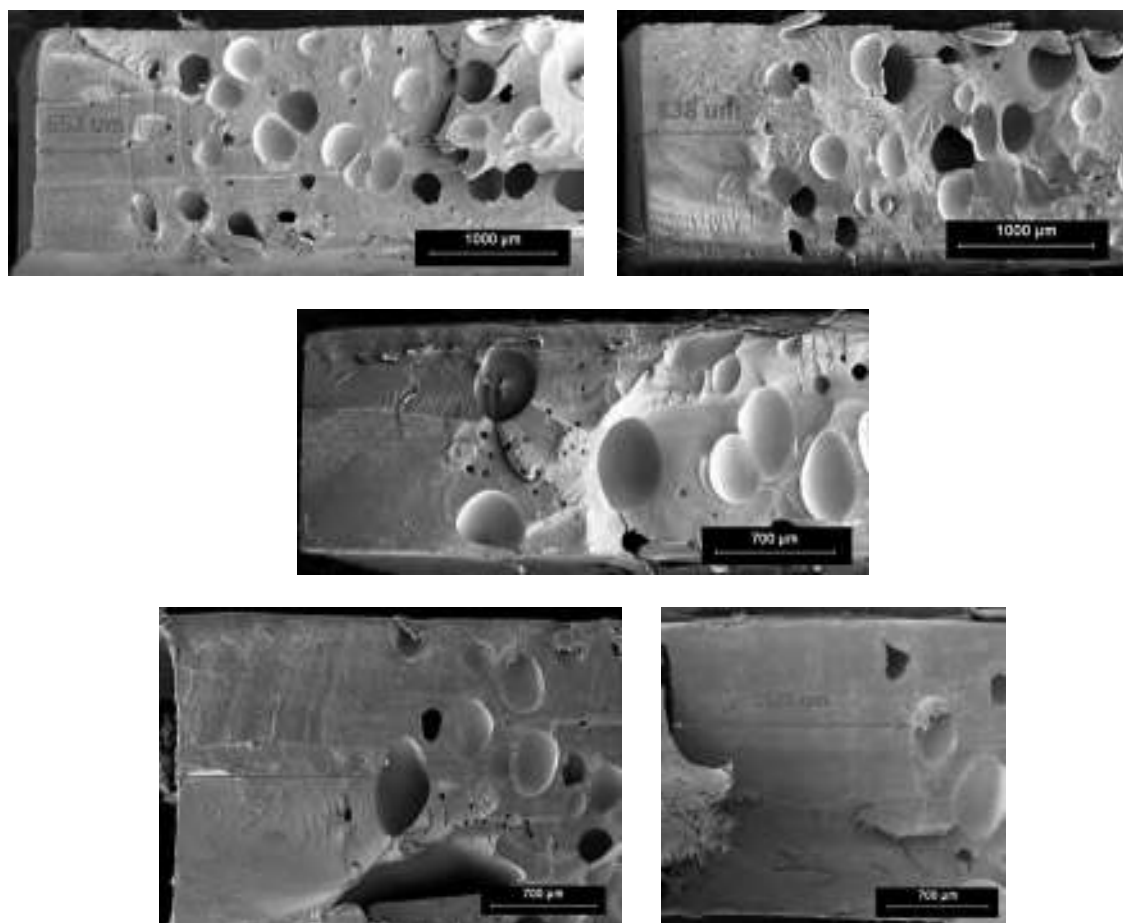
Figure 6: Structural foams produced at five different foaming times of 30 min., 60 min., 90 min., 120 min. And 150 min. Solid skin thickness is presented in each case.

The skin thickness that can be achieved for a constat bulk density increases with the foaming time. The dependency solid skin thickness versus foaming time is presented in figure 7.
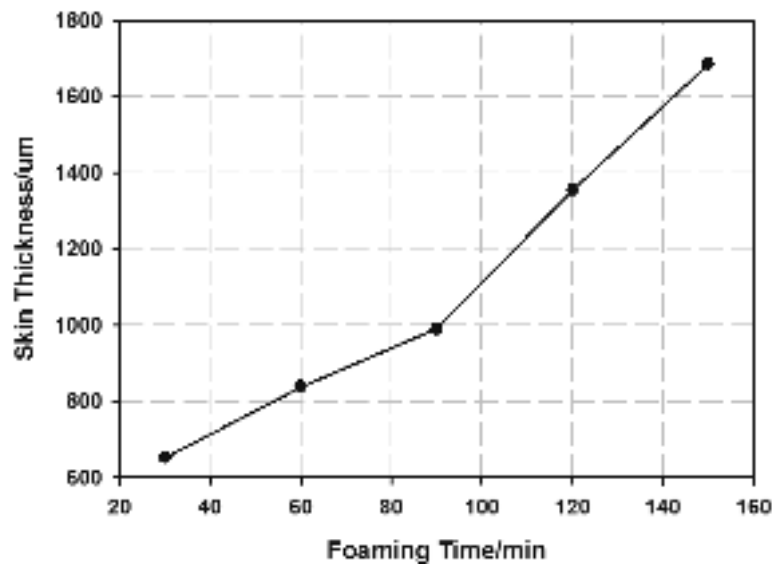

Figure 7: Dependency of skin thickness with foaming time for a constant bulk density.

The decomposition with time of the azodicarbonamide is not a linear process [16] and this fact would explain the non-linearity observed in figure 7. At higher pressures inside the mould, the skin thickness that we can achieve is higher also, in concordance with the hypothesis of gas dissolution presented. More foaming time means also longer time to promote the gas dissolution from inner parts of the foam, therefore thicker solid skins.

Both from a scientific and technical point of view, the availability of achieving thicker solid skins for a fixed bulk density just varying the foaming time opens a broad range of possibilities.

CONCLUSIONS

A new method is presented to produce structural foams in a very simple way. Moulds are much cheaper and initial investments are much lower than in the case of injection moulding which makes this new route very suitable, specially for small series. Final foam structure and morphology is analogous to structural foams produced by

injection moulding. Besides, the new route presented in this work yield samples with improved surface quality.

The physical mechanism behind consists in a process of gas dissolution in an amorphous material such as silicone rubber. The gas yielded by the decomposition of azodicarbonamide from the outer parts of the foam migrates from the polymer to the rubber, resulting in solid skins in all the areas in close contact with the amorphous material.

Parameters such as skin thickness can be controlled independently of the bulk density of the foam just varying the foaming time.

Since both conventional and structural foams are produced with the same chemical composition, density and experimental conditions, we can make a proper comparison of properties between materials produce under the same process.

ACKNOWLEDGEMENTS

REFERENCES

[1]   D. Klempner and V.Sendijarevic, Polymeric Foams and Foam Technology, Hanser Publisher, Munich (2004).

[2]   Barzegari, M.R. and Rodrigue, D. Polym. Eng. Sci., 47 (9), 1459-1468, (2007)

[3]   Bledzki A. K., Rohleder M., Kirschling H., Chate A. Cell. Polym. 2008, vol. 27, no 6, pp. 327-345

[4]   Zhang, Y.; Rodrigue, D.; Ait-Kadi, A. J Appl Polym Sci, Vol. 90, 2139-2149 (2003)

[5]   U. Stieler. Proceedings Blowing Agents and Foaming Processes 2008. Paper 12.

[6]   Barzegari, M. R. and Rodrigue D. Cell. Polym. 27(5); 285-301.

[7]   Bikhu, S. S. and Founas, M. SAE Technical Paper Series 930434, International Cong. And Exposition, Detroit, M.I, 1993.

[8]   Hobbs, S. Y. Journal of Cellular Plastics, Vol. 12, No. 5, 258-263 (1976)

[9]   Wu, J. S. and Yeh, T. M. Journal of Polymer Research. vol. 1 nº 1 pp. 61-68.

[10]   Avalle, M, Belingardi, G. and Montanini, R. International Journal of Impact Engineering vol. 25 (2001) pp. 455-472.

[11]   J. Escudero, E. Solorzano, M.A. Rodríguez-Perez, F. Garcia-Moreno, J.A. de Saja. Journal. Cellular Polymers, Vol. 28, nº 4 p. 289-302.

[12]   R. M. Barrer, J. A. Barrie, N. K. Raman. Polymer 1962, Vol.3, p. 595-603

[13]   R. M. Barrer, J. A. Barrie, N. K. Raman. Polymer 1962, Vol.3, p. 605-614

[14]   G. K. Fleming and W. J. Koros. Macromolecules, 1986, Vol.19, p. 2285-2291

[15]   M. A. Kykin, V. I. Bondar, YU. M. Kukharsky, A. V. Tarasov. Journal of Polymer Science B: Polymer Physics 1997, Vol. 35, p. 1339–1348.

[16]   Sims, G. L. A. and Sirithongtaworn, W. Cellular Polymers 1997, vol 16, nº 4, pp 271-283.

[17]   Blanchet, J. F. and Rodrigue D. Cellular Polymers 2004, vol. 23, nº 4, pp. 193-210.

[18]   Timoshenko S. P. and Goodier J. N., "Theory of Elasticity", Mc Graw-Hill, Singapore (1982).

[19]   Hartsock, J.A. In design of Foam-Filled structures, Technomic. Stamford, CT, 1969; Chapter 1.

5.3.- Physical Properties of the Developed Structural Foams

241

The production of structural foams is highly motivated by the need in the market of cellular materials with high specific mechanical properties. Several application demand a combination of low densities with high mechanical properties that conventional foams cannot cover.

This section presents a work entitled *"Structural Characterization and Mechanical Behaviour of LDPE Structural Foams. A Comparison with Conventional Foams"*. This work characterizes the main mechanical properties in terms of tension, bending and compression of structural foams produced by Stages Molding in a varied range of densities and compares them with their conventional counterparts. Due to the nature of the production process, both structural and conventional foams are produced in a very similar manner with slight differences in between. This fact makes the properties comparison more accurate and reliable.

The density profiles of the foams have been characterized by x-rays radioscopy. The structure found is similar to the ones obtained in structural foams produced by injection molding.

The results have shown that bending properties are the ones more benefitted by the skin-core morphology of the samples produced.

Structural Characterization and Mechanical Behaviour of LDPE Structural Foams. A Comparison with Conventional Foams

J. Escudero[1], E. Solórzano[2], M.A. Rodriguez-Perez[1*], F. Garcia-Moreno[3,3], and J.A. de Saja[1].

[1]Cellular Materials Laboratory (CellMat). Condensed Matter Physics Department, University of Valladolid, 47011 Valladolid, Spain
[2]Helmholtz-Zentrum Berlin Hahn-Meitner Platz, D-14190, Berlin, Germany
[3]Technische Universität Berlin, Hardenbergstrasse 36, 10623 Berlin, Germany

ABSTRACT

Structural foams are composed of two solid layers enclosing a foamed core. The application of sandwich structural foams has rapidly increased in the last decade. Injection moulding is currently used to produce these foams, being not common to produce conventional foams of similar densities and chemical compositions in a similar process. In this paper an alternative route to produce structural foams has been used. This method allows fabricating conventional foams with the same chemical composition and density than the structural foams, so comparisons between properties of both kinds of materials can be made in a proper way, i.e. avoiding effects of different chemical compositions and/or different densities. The structural and mechanical properties in tension, compression and bending have been characterized both for structural and conventional foams based on a low density polyethylene. The results have showed that the sandwich structure of structural foams improves a 50% the mechanical behaviour in bending, however no improvements in compression or tension have been found.

INTRODUCTION

The demand of foams with improved mechanical properties has rapidly increased in the last decade. It is well known that conventional foams (foams with constant relative density along the volume) have relatively low stiffness

---

O.J. Escudero, E. Solórzano, M.A. Rodríguez-Pérez, F. García-Moreno, and J.A. de Saja

and strength when the density is reduced. To improve these properties at a constant overall density the structure of usual foams can be modified by producing structural foams having a skin-core morphology. It is known, that this sandwich structure results in high specific mechanical properties (strength to weight ratio) compared with non structural foams[1]. Nowadays structural foams can be found in many different applications like aircrafts, sporting goods or vehicles[1].

The production of structural foams is mainly based on injection moulding. Cold walls of the mould enable the polymer melt to solidify without forming a cellular structure achieving structural foams in a conventional injection moulding process. Although, it is possible to obtain a skin-core morphology in the conventional injection moulding process, some other more sophisticated routes have been developed to improve surface quality and to increase density reduction[2]. One of this processes consist in designing moulds that can be expanded after the injection of the polymer melt. These expandable moulds allow a better control of the final cellular structure but in general surface quality is not as good as needed for several industrial applications[4]. To improve this surface quality a gas at elevated pressure is introduced in the mould before injecting the polymer. As long as the polymer is injected, the gas is evacuated in a process that is usually known as gas counter pressure. Using this procedure, better surface qualities are achieved but skin layers are in general very thin[3,4]. A commercial production process named Smartfoam® is also used in order to eliminate the disadvantages of the other processes. In a first step solid polymer is injected inside the cavity of the mould forming the solid outer skins. In a second step, the gas is dissolved in the polymer in the injection unit and then is injected in the mould. This polymer-gas mixture allows forming the cellular core of the foam. In a final step, solid polymer is again injected to produce the second solid sheet and as consequence the structural foam[5].

Several authors have investigated the relationships between mechanical properties and skin-core morphology of structural foams. Different analytical models have been proposed to predict the mechanical behaviour of these foams taking into account the skin thickness, core density and density distribution along the samples[7,8]. All these investigations were conducted on injection moulded samples. On the other hand and as far as we know the real improvement obtained by producing structural foams as an alternative to conventional foams have not been studied in detail for foams produced using the same composition and with the same density range. The reason for this is that the structural control during injection moulding is far from being perfect. In fact, skin thickness, density profile, global density, cell size and homogeneity are parameters that can not be independently well controlled

in the injection moulding technique, and due to this reason it is not easy to perform a systematic study of the properties of injection moulded foams in comparison with that of conventional foams[7-10].

In this paper the structural foams were produced using an alternative route that is not based on injection moulding. From a scientific point of view, this method allows producing structural and conventional foams using similar processes and using the same chemical composition. This fact will allow comparing the behaviour of both materials, gaining knowledge on the advantages offered by structural foams.

Bearing the previous ideas in mind, this paper presents a comparative study of the mechanical properties of structural and conventional foams of the same density and chemical composition. Using an universal testing machine, mechanical properties in tension, compression and bending have been characterized and compared.

EXPERIMENTAL

Materials

The polymer used in this study was a low density polyethylene (LDPE). This polymer has a density of 920 kg/m3 with a melt flow index of 4.2 g/10 min. The azodicarbonamide used is a commercial one with a particle size of 20 µm. The blowing agent concentration was 7 wt.% for the produced materials.

Samples

Foam discs of 150 mm in diameter were produced at a temperature of 180 °C. Several solid sheets of the precursor material, which contains the blowing agent, with a thickness of 1 mm were introduced inside the mould and the mould inside a furnace at the previous temperature. Free expansion took place inside this mould. In the case of conventional foams, steel moulds were used. On the other hand, structural foams were produced inside expandable moulds. The foaming process is the same for both kinds of structures, only changing the type of mould used in each case, so from a scientific point of view comparison between properties can be made between them because chemical compositions and densities are the same. Conventional foam samples had a thickness of 12 mm and structural foams samples had a thickness of 9 mm. Five different densities were chosen, ranging from 500 kg/m³ to 800 kg/m³. Density was controlled by the amount of precursor material introduced in

O.J. Escudero, F. Saldrzano, M.A. Rodriguez Perez, E. Garcia-Moreno, and J.A. de Saja

the mould and measured by geometrical procedures. In order to study the dependency of the skin thickness with the processing parameters, a unique density was chosen and samples were produced with different foaming times at the same temperature of 180 °C.

Morphology Analysis

Foam morphology characterization was made using micrographs obtained with a SEM microscope JEOL JSM-820. Skin thickness and cell diameter were determined using the image processing software Image J. Using these micrographs, skin thickness was calculated by the average distance between the sample surface and the closest cells.

In order to calculate the cell diameter, the diameter of about 50 cells was measured for each sample.

X-rays transmission images were obtained using a Hamamatsu microfocus X-ray tube operating at 100 kV and 100 µA and a 120 x 120 flat panel also from Hamamatsu[11]. Image resolution according to the image magnification employed was 50 µm per pixel. Density profiles were obtained by using special programmed functions that implement the Burger-Lambert[12] absorption equation in ImageJ software[13].

Mechanical Properties

All the mechanical properties were measured using an universal testing machine Instron model 5500R6025. For compression tests additional cylindrical samples were produced with a diameter of 32 mm and 32 mm in height. Samples were compressed at a rate of 1 mm/min. Rectangular samples with dimensions of 15 mm width, 100 mm length and heights of 9 and 12 mm were cut from the original discs to carry out three-point bending tests at a rate of 10 mm/min with an span of 100 mm following the standard UNE53204-1. Tensile tests were carried out at a speed of 50 mm/min at room temperature using standard test specimens according to UNE53510.

A detailed description of these characterisation techniques has been previously published[14-18].

Structural Characterization and Mechanical Behaviour of LGPE Structural Foams. A Comparison with Conventional Foams

RESULTS AND DISCUSSION

Cell size

The average cell size of the inner part of the structural foam was measured for all the densities under study. The results are showed in **Figure 1**; it can be observed that there exist a linear relationship between density and cell size. Cell sizes can vary in a wide range that goes from 600 μm to approximately 1400 μm. Cell sizes for the foamed core of the structural foam are in the typical range obtained for foams produced under a conventional free expansion process.

Foam Morphology

The morphology of these foams is not very different to the one of structural foams produced under an injection moulding process[2]. In **Figure 2** a micrograph of a foam produced under this new process is presented. At the top and at the bottom of the image two solid skins are observed. Two transition areas are detected immediately after these solid skins. In these areas the cellular size is smaller than in the foamed core. These transition areas play a crucial role while studying the mechanical behaviour of a structural foam[17]. At the centre of the image we find the typical foamed core with cell sizes in the range studied above.
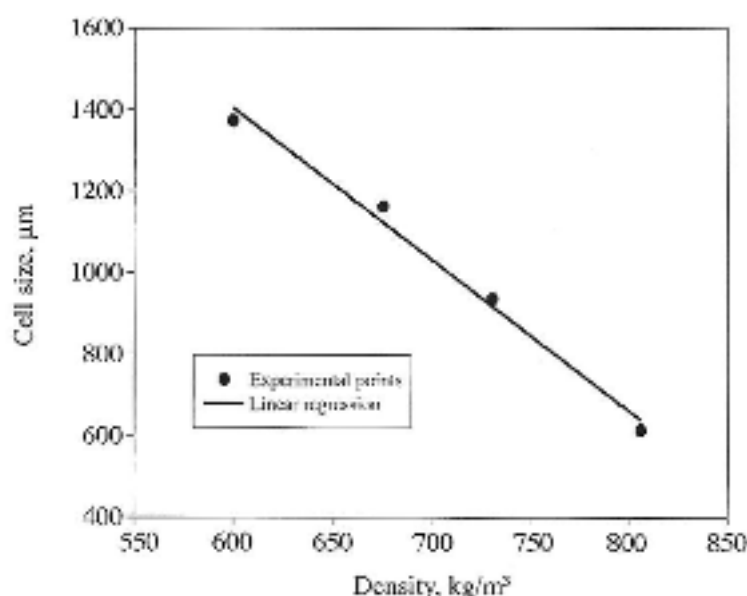

Figure 1. Cell size *versus* density for the foamed core of the structural foams

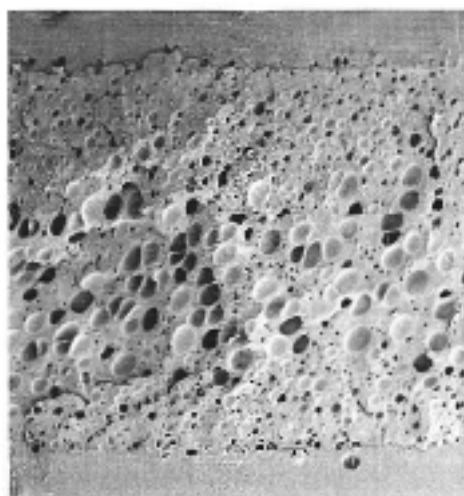O.J. Escudero, E. Solórzano, M.A. Rodríguez-Perez, F. García-Moreno, and J.A. de Saja

Figure 2. Micrograph of an structural foam produced under this new process

Height: 9mm

Figure 3. X-ray image of one typical structural foam. In grey is represented the analyzed area for vertical density profiles calculation

Figure 3 shows an example of the images obtained using x-rays. The density gradient trough the sample thickness in clearly observed. In addition, it seems clear the high homogeneity of the foamed materials.

Analysing these images, numerical vertical density profiles were obtained for all the structural samples. Average densities calculated by integration were in good accordance with the average densities measured geometrically from the samples with an error not larger than a 3%.

Figure 4 corresponds with the numerical vertical density profiles for the structural foams with densities of 630 kg/m³ and 731 kg/m³. Again we can observe the solid skins and transition areas considered before. The foamed

Structural Characterization and Mechanical Behaviour of LDPE Structural Foams. A Comparison with Conventional Foams
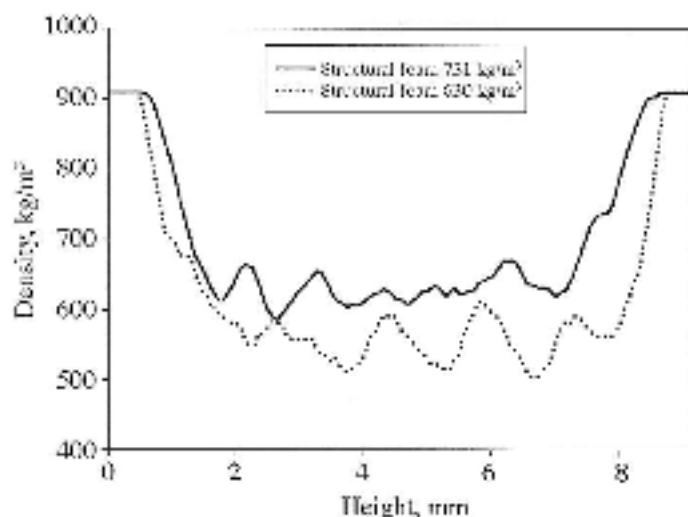

Figure 4. Numerical vertical profiles for two different structural foams with densities of 630 kg/m³ and 731 kg/m³

core has a density well below the average density of the structural foam. There is still a remaining influence of the solid sheets of the precursor introduced inside the mould as can be deduced from the peaks observed in the zone of the foamed core.

From these density profiles, we can make a characterization of the dependency of the skin thickness with the density of the sample. For a fixed amount of blowing agent and for samples foamed at the same temperature and foaming time, a linear dependency is found between density and skin thickness as it can be seen in **Figure 5**.

MECHANICAL PROPERTIES

Compression

Figure 6 shows the Young modulus in compression measured both for conventional and structural foams.

The experimental data were fitted to an analytical function of the form[15]:

O.J. Escudero, E. Solórzano, M.A. Rodríguez-Perez, F. García-Moreno, and J.A. de Saja
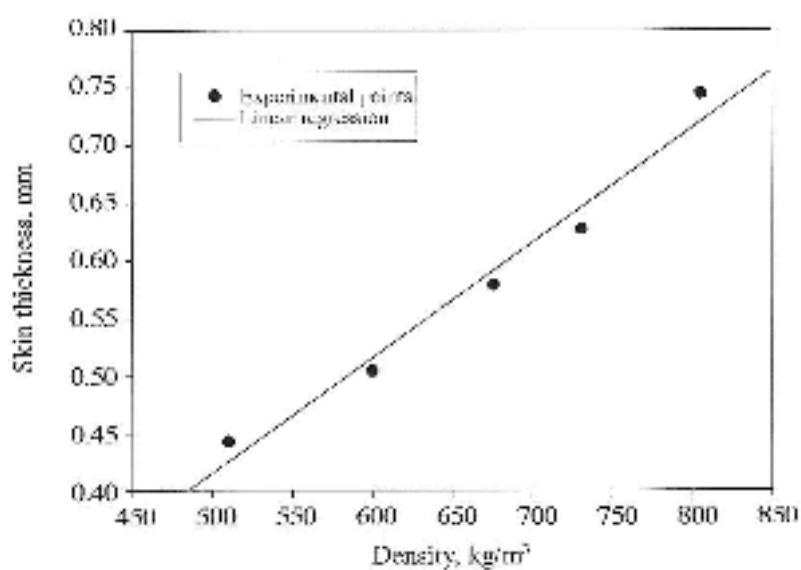
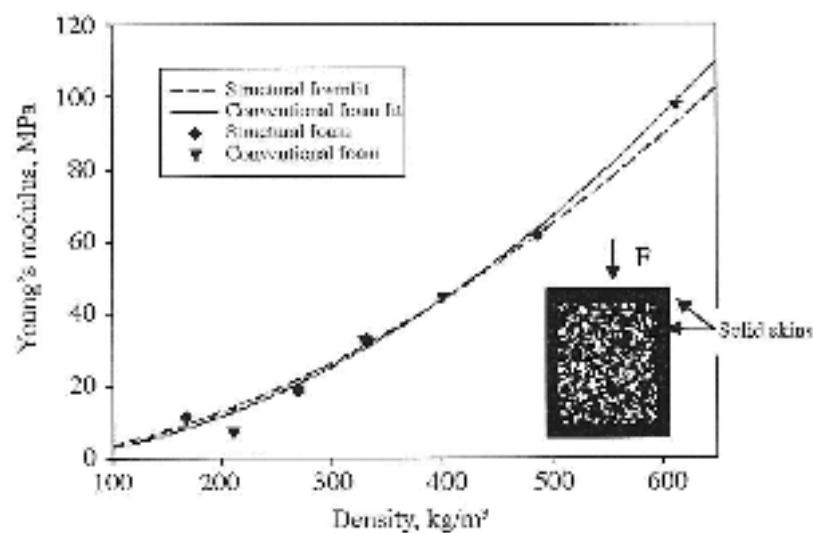**Figure 5. Dependency of solid skin thickness with density**

Figure 6. Young's modulus for structural and conventional foams. An almost parabolic behaviour is observed and no difference is found with the structural foams with solid skins

$$E = C \cdot \left(\frac{\rho}{\rho_s} \right)^n$$

where C is a constant and (ρ/ρs) is the relative density of the foam. The value for the exponent n in this case is approximately 1.85 and C takes a value of 250 MPa. The cylindrical samples used in this mechanical characterization had solid lateral outer skins as well as solid skins in the superior and inferior taps.

As it can be observed in **Figure 6**, there are not important differences for foams with solid skins and foams without solid skins. Values of Young modulus are practically the same for all densities. The same fact happens for the yield strength (**Figure 7**) and the energy absorbed. Young modulus, yield strength and energy absorbed depend only on density and not on the sample structure in this case.

Solid skins represent an important amount of the total density of the foam. As a consequence, the foamed core has a much lower density than the average one as have been observed above with the numerical density profiles. This combination of solid skins with a core of a density well below the average yields response similar to a conventional foam.
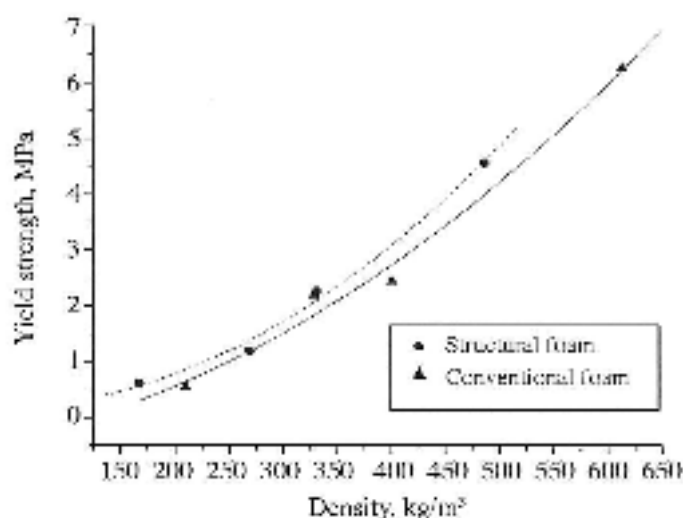

Figure 7. Yield strength both for conventional and structural foams. No main differences are observed also in this case

O.J. Recalera, E. Solórzano, M.A. Rodríguez-Pérez, F. García-Moreno, and J.A. de Saja.

Tension

In this case the force was applied parallel to the direction of the solid outer layers of the structural foams. A graphical sketch of this disposal is shown in **Figure 8**.

Young modulus was measured also in tension. Again, no difference between structural and conventional foams is found as can be observed in **Figure 8**. The behaviour is the same for both kinds of structures having a dependency only with density. Solid outer skins do not seem to play any role. The explanation for this fact is the same as in the case of compression.

The strain at break for both kinds of foams was also considered, its dependency with density is plotted in **Figure 9**. In this case, high differences were found. For structural foams this value is at least a 20% lower than in the case of conventional foams. The lower density core in the case of the structural foams acts as an area that enables the failure of the sample at lower strains than in the case of the conventional ones.

Bending

It does not exist a complete dependency between stress and strain in the curve of the bending behaviour, so in order to have comparable values for the flexural
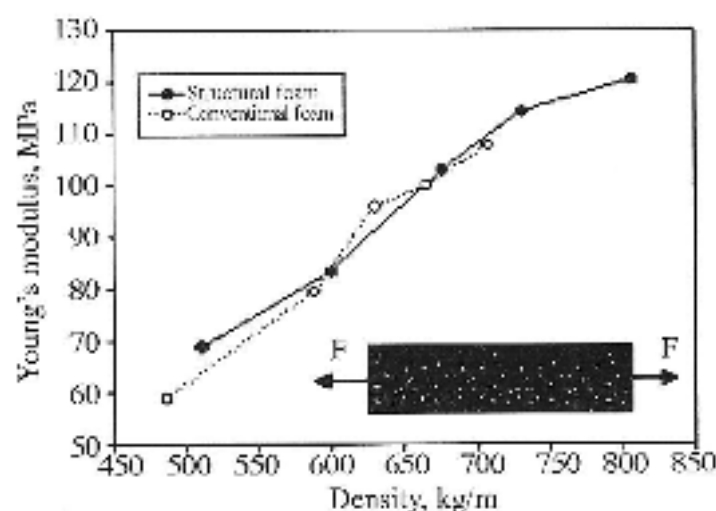

Figure 8. Young's modulus in tension. Comparison for both kinds of structures
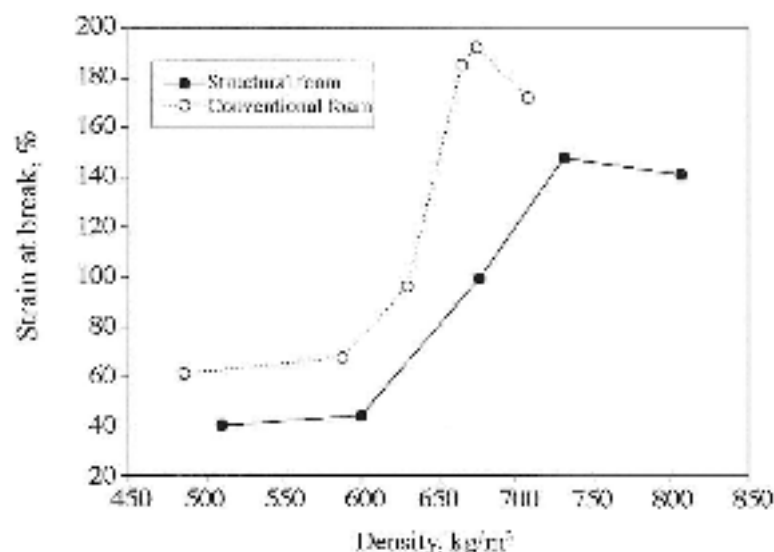
Figure 9. Strain at break for the different densities studied

modulus, a constant deformation of 1% was chosen. To calculate a thickness-independent deformation the following formula was used[19].

$$\varepsilon = \frac{600 \cdot S \cdot H}{L^2} \%$$

where S is the perpendicular distance to the neutral axis, H is the thickness of the beam and L is the distance between rods during the test (span).

At this constant deformation, the flexural modulus was calculated using the formula:

$$E = \frac{S^3}{4BW^3}\left[1 + 2,85\left(\frac{W}{S}\right)^2 - 0,84\left(\frac{W}{S}\right)^3\right]\frac{\Delta P}{\Delta y}$$

where ΔP is the load applied, Δy is the distance to the neutral axis and S, B and W are geometrical parameters of the beam as depicted in **Figure 10**.

In this case, the force is applied perpendicular to the solid skins. The flexural modulus calculated this way is plotted in **Figure 11**. As was expected, the top and bottom solid skins play a very important role increasing the mechanical

O.J. Escudero, E. Solórzano, M.A. Rodríguez-Pérez, F. García-Moreno, and J.A. de Saja
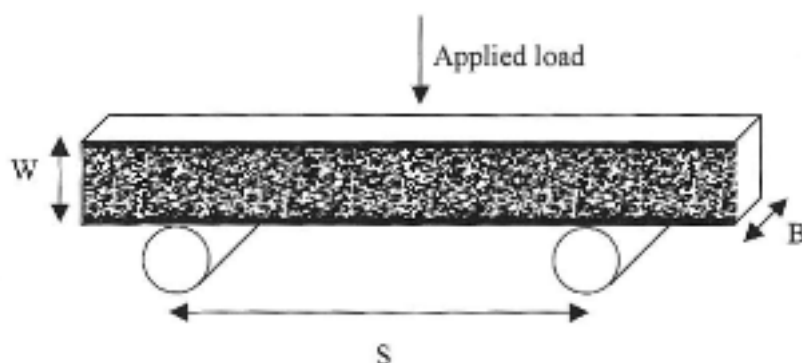

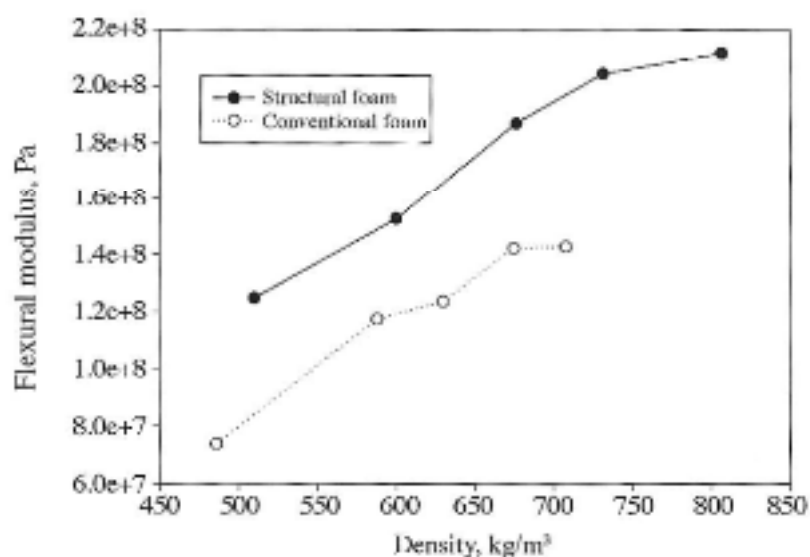**Figure 10. Scheme of the three point bending test**

Figure 11. Flexural modulus for structural and conventional foams

properties in bending for structural foams. In **Figure 11**, it can be seen that flexural modulus values are more than a 50% higher than in the case of conventional foams. Solid skins are supporting most of the applied load. This result is supported by the work of Hartsock that assumes that the stiffness of a sandwich structure is only related to the contribution of the skin layers[20].

CONCLUSIONS

From a scientific point of view, we can produce structural and conventional foams in a very similar process. Therefore we can make a comparison of properties between materials produce under the same process.

Numerical vertical density profiles have been calculated using x-ray images for all the foams. The typical structure of solid skins followed by a transition area and a foamed core with a density well below the average of the sample is found. This structure is not different to the one found in a structural foam produced under an injection moulding process.

In order to compare the mechanical properties, conventional and structural foams have been produced by this new method with similar densities. For the Young modulus in compression there are no differences between conventional and structural foams as for the yield strength and energy absorbed, depending these values only of the average density of the sample. The same result is found while measuring the Young modulus in tension. On the contrary the strain at break in tension is at least a 20% lower in the case of structural foams.

Flexural modulus presents important differences in the case of the structural foams. Structural foams increment their bending properties in at least a 50% in comparison with conventional foams with the same average density.

ACKNOWLEDGEMENTS

REFERENCES

1. Klempner D. and Sendijarevic V., *Polymeric Foams and Foam Technology*, Hanser Publisher, Munich (2004).

2. Barzegari M.R. and Rodrigue D., *Polym. Eng. Sci.*, **47(9)**, (2007) 1459-1468.

O.J. Escudero, E. Solórzano, M.A. Rodríguez-Pérez, F. García-Moreno, and J.A. de Saja

3. Bledzki A.K., Rohleder M., Kirschling H., and Chate A., *Cell. Polym.*, 2008, vol. 27, no 6, pp. 327-345.

4. Zhang Y., Rodrigue D., and Ait-Kadi A., *J. Appl. Polym. Sci.*, **90** (2003) 2139-2149.

5. Stieler U., Proceedings *Blowing Agents and Foaming Processes 2008*. Paper 12.

6. Barzegari M.R. and Rodrigue D., *Cell. Polym.*, **27(5)** 285-301.

7. Bikhu S.S. and Founas M., SAE Technical Paper Series 930434, *International Cong. And Exposition*, Detroit, M.I, 1993.

8. Hobbs S.Y., *Journal of Cellular Plastics*, **12(5)** (1976) 258-263.

9. Wu J.S. and Yeh T.M., *Journal of Polymer Research*, vol. 1 n° 1 pp. 61-68.

10. Avalle M, Belingardi G. and Montanini R. *International Journal of Impact Engineering*, **25** (2001) 455-472.

11. García Moreno F., Fromme M., and Banhart J., *Advanced Engineering Materials*, **6** (2004) 416–420.

12. Vinod Kumar G.S., García-Moreno F., Bahcsán N., Brothers A.H., Murty B.S. and Banhart J., *Phys. Chem. Chem. Phys.*, **9** (2007) 6415 - 6425.

13. Abramoff M.D., Magelhaes P.J., and Ram S.J., *Biophotonics International*, volume 11, issue 7, pp. 36-42, 2004.

14. Rodriguez-Perez M.A and de Saja J.A., *Cellular Polymers*, **18** (1999), 1-20.

15. Ruiz-Herrero J.L., Rodriguez-Perez M.A, and de Saja J.A., *Polymer*, **46** (2005) 3105.

16. Martínez-Díez J.A., Rodríguez-Pérez M.A, de Saja J.A., Arcos y Rábago L.O., and Almanza O.A., *Journal of Cellular Plastics*, **37** (2001) 21-42.

17. Blanchet J.F. and Rodrigue D., *Cellular Polymers*, **23(4)** (2004) 193-210.

18. Gibson I.J. and Ashby M.F., *Cellular Solids*, Cambridge University Press, 1997.

19. Timoshenko S.P. and Goodier J.N., "Theory of Elasticity", Mc Graw-Hill, Singapore (1982).

20. Hartsock J.A. In; *Design of Foam-Filled Structures*, Technomic. Stamford C.T., 1969, Chapter 1.

Chapter 6

Combination of Modifications in the Polymer Matrix and in the Cellular Structure

6.1.- INTRODUCTION

The present chapter combines both types of strategies to improve the physical properties of cellular materials: modifications in the polymer matrix and modifications in the cellular structure.

On the contrary to the previous chapters, the polymer matrix selected in this section is polypropylene.

The modifications in the polymer matrix follow the same approaches used in chapter 4: addition of montmorillonite-type nanoclays together with a coupling agent, in this case based on maleic anhydride grafted polypropylene (MAH-g-PP). Together with this, branched polypropylenes with high melt strength (HMS) are used.

The modifications in the cellular structure are obtained using Improved Compression Molding (see chapter 3) as foaming method. A tailored control of the foaming parameters yields cellular morphologies with high specific mechanical properties as will be seen.

Altogether it allows obtaining two different versions of low density polypropylene foams, open cell and closed cell, with high specific mechanical properties in both cases. Since the polymer matrix has suffered no crosslinking, the cellular materials produced are recyclable. The physical properties of these materials have been compared with those of commercial materials of the same densities.

The foaming technology presented in this chapter has been named AniCell and it has been patented. The patent document can be found in Annex I at the end of the manuscript.

All the research that is encompassed in this chapter was developed in the frame of the European Project ***Nancore: Microcellular Nanocomposites for Substitution of Balsa Wood and PVC Core Material.*** The objective of this project was the substitution of balsa wood and PVC foams as core materials for lightweight composite sandwich structures. The material is intended to be applicable for widespread industrial use, as for example in the windpower industry, rail, ship building or the automotive sector.

6.2.- MODIFICATIONS OF THE CHEMISTRY OF THE POLYMER MATRIX COMBINED WITH MODIFICATIONS OF THE CELLULAR STRUCTURE: ANICELL

6.2.1- Description of the Production Route

In this section a brief description of the production route and foaming parameters are presented. Further details about the production route can be found in the corresponding patent document and the second scientific work enclosed. The morphology of the cellular structure is also studied using x-ray microtomography.

The work presented in this section is entitled ***"X-ray Microtomographic Study of Nanoclays-Polypropylene Foams"*** and is published in the Journal of Cellular Polymers Vol. 30, nº 3 pp. 95-109 (2011). As already mentioned, mechanical properties have a strong dependency with the global cellular morphology of the foam: cell size, homogeneity, cell density and specially with the anisotropy ratio of the cells. This work characterizes, by x-ray microtomography, the cellular structure of polypropylene foams produced by improved compression molding using different foaming parameters.

Microtomography is a non-destructive technique so it allows making mechanical tests on the same specimens that have been characterize by microtomography, establishing a direct correlation.

The work establishes a relationship between cell volume distribution, sphericity of the cells (anisotropy ratio) and processing parameters. This relationship helps to later tailor the foaming parameters to obtain the best mechanical behavior (section 6.4.2).

X-ray Microtomographic Study of Nanoclay-Polypropylene Foams

Y. Ma[2], R. Pyrz[*1], M.A. Rodriguez-Perez[3], J. Escudero[3], J.Ch. Rauhe[1] and X. Su[2]

[1]Department of Mechanical and Manufacturing Engineering, Aalborg University, 9220 Aalborg East, Denmark

[2]LTCS and Department of Mechanics & Aerospace Engineering, College of Engineering, Peking University, Beijing 100871, P.R. China

[3]Cellular Materials Laboratory (CellMat), Condensed Matter Physics Department, University of Valladolid, 47011 Valladolid, Spain

SUMMARY

In the present paper X-ray microtomography technique has been applied to investigate internal, three dimensional structure of clay/polypropylene nanocomposite foams. Several sets of foam samples were prepared using the improved compression moulding technique that allows controlling independently the cells' size, cells' shape and density of foams. Then the X-ray images were acquired followed by an application of image processing steps and final reconstruction of foams microstructure. Volume distribution of cells has been extracted from three dimensional images and related to processing parameters. Since not only the size but also the shape of cells influences a load bearing capacity of foams, the sphericity parameter has been selected as a relative quantifier of cells shape. The sphericity parameter has been also related to different processing parameters.

INTRODUCTION

Mechanical performance of cellular foams depends on properties of a building material and geometrical morphology of cells i.e. their density, size and orientation distribution, their shape and wall thickness distribution. Mechanical modelling of cellular foams usually idealizes the foam structure as being described by a polygonal network in two dimensions [1, 2] or three

---

*corresponding author, email: rp@m-tech.aau.dk

Y. Ma, R. Pyrz, M.A. Rodriguez-Perez, J. Escudero, J.Ch. Rauhe1 and X. Su

dimensional polyhedral structure [3-5]. These kinds of analyses provided many useful information relating geometrical features of the microstructure to the overall properties. The geometrical descriptors of idealized cells such as cell edge length, number of junctions per wall, wall thickness and shape, and anisotropy and randomness issues can be easily identified in these models and subject to alteration for parametric studies. Furthermore, different morphological descriptors can be derived based upon well defined geometrical features of cells. However, in many practical instances morphology of cells does not reveal any geometrical regularity [6-10] and addressing quantification of size and shape of cells needs other approaches. This is also true for the present work. Furthermore, a common problem in morphological analysis of non-homogeneous materials is that three-dimensional information of microstructure is required but its images are two-dimensional. Monitoring materials' microstructure using X-ray microtomography allows us to begin to bridge this gap since a three-dimensional image of the specimen can be reconstructed from non-destructive, serial sections and can be processed to show and measure three-dimensional features.

Most X-ray microtomography developments have so far been made using large synchrotron sources. This has limited X-ray microtomography to a research tool available only at the major synchrotron facilities. The use of X-ray tubes with a very small focus together with a very sensitive recording devices enable the design of a bench-top X-ray microtomography with a spatial resolution less than 3 micrometers. This technique has been subject to significant improvements during recent years and is used in the present work to reconstruct and analyse foam microstructure of clay/polypropylene nanocomposite materials.

The material samples were prepared using improved compression moulding technique [11] and several sets of foam specimens have been processed altering processing parameters. Three dimensional reconstructed images of foams have been created from X-ray scans after an appropriate image processing procedure was developed and implemented to X-ray scans. The volume distribution of cells has been extracted from reconstructed images and related to some processing parameters and mechanical properties. As the shape of cells does not appear to exhibit geometrical regularity, the sphericity parameter has been used to characterize the shape of cells.

MATERIALS PREPARATION

Foams were produced using the improved compression moulding technology. Pellets containing the formulation based on a high melt strength polypropylene, nanoclays (5 wt%) and a chemical blowing agent were inserted into a cylindrical

mould. The pellets were heated up to the decomposition temperature of the blowing agent and during this stage the pellets were constrained to expand by the application of external pressure exerted through a piston placed inside the mould. After the whole blowing agent had decomposed the piston was moved in a controlled manner to release the pressure. The foaming took place during movement of the piston. This procedure allows controlling independently the density and cell sizes of foams and the details of the technique are described elsewhere [11, 12].

Two sets of samples have been prepared with processing parameters and resulting mechanical properties listed in **Table 1**. The first series of samples with four specimen families were manufactured with variable foaming pressure keeping other parameters constant. These specimens were used for a basic morphological analysis. In the second series of samples three specimens' families were prepared with single changes of temperature and pressure keeping the blowing agent content at half amount as applied in the first set of samples. The purpose of the second set of samples has been to give only indicative information how the microstructure will change under alteration of a singled out processing parameter.

Table 1. Processing parameters and mechanical properties of samples

Sample	Blowing agent content [%]	Foaming temperature [°C]	Foaming pressure [MPa]	Density [kg/m³]	Young's modulus [MPa]	Compressive strength [MPa]
Series 1						
1.1	5	190	8.33	175.7	42.1	0.54
1.2	5	190	3.89	174.5	46.6	0.61
1.3	5	190	1.67	183.6	58.0	0.90
1.4	5	190	0.67	184.3	76.5	0.98
Series 2						
2.1	2.5	190	1.67	182.5	115.0	2.0
2.2	2.5	180	0.67	173.7	48.8	1.11
2.3	2.5	190	0.67	158.2	77.9	1.14

X-RAY MICROTOMOGRAPHY

In X-ray microtomography, the object is rotated to obtain radiographic projections from different viewing angles. The projections are the measured values of the overall attenuation that X-rays undergo when they travel through

Y. Ma, R. Pyrz, M.A. Rodriguez-Perez, J. Escudero, J.Ch. Rauhe I and X. Su

the object, **Figure 1**. The object can be moved up and down depending on the axial position of the volume element to be irradiated. An image magnification is achieved by moving the object horizontally between the source-detector set. The attenuation of each ray in a beam results from interactions between the radiation used for imaging and the substance of which the object is composed. X-rays passing through material are absorbed according to a linear attenuation coefficient that has some spatial variation depending on the local composition and density. These differences in the linear attenuation coefficient provide the contrast necessary to form an image. In an idealized case of parallel X-ray illumination a profile of the attenuation through the sample is obtained. Practically, the attenuation measurement is averaged over a finite-sized volume element in the sample since the detector has finite spatial resolution to discriminate between closely spaced ray paths. By rotating the sample in discrete angular increments through 180° and collecting every time projection images, sufficient data are obtained to reconstruct slices of the three-dimensional object. A reconstruction procedure is usually based on the back-projection principle. The attenuation recorded in each projection is due to the microstructure of the object along the individual lines. It is not possible to know from one projection where along the line the attenuation occurs. However, it is possible to distribute the measured attenuation evenly along the line. If this is done along projections from several angular views, the superposition of the attenuation values should correspond to the features present in the microstructure, **Figure 2**.
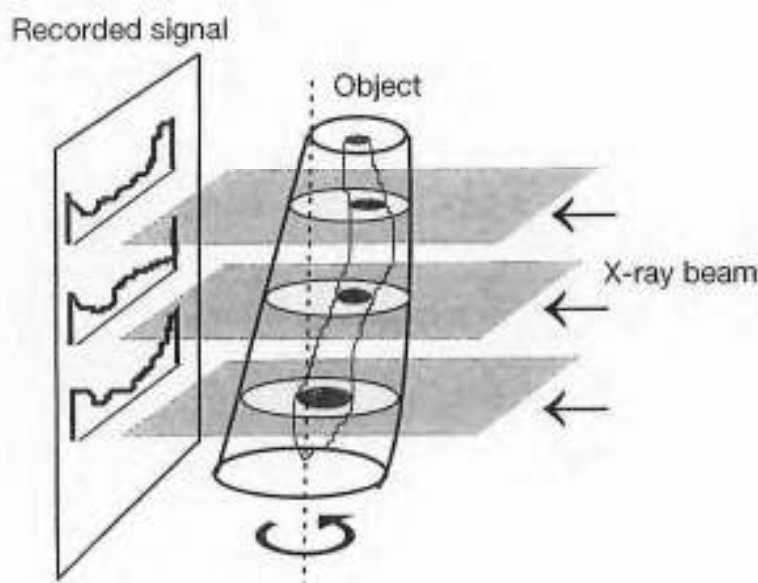

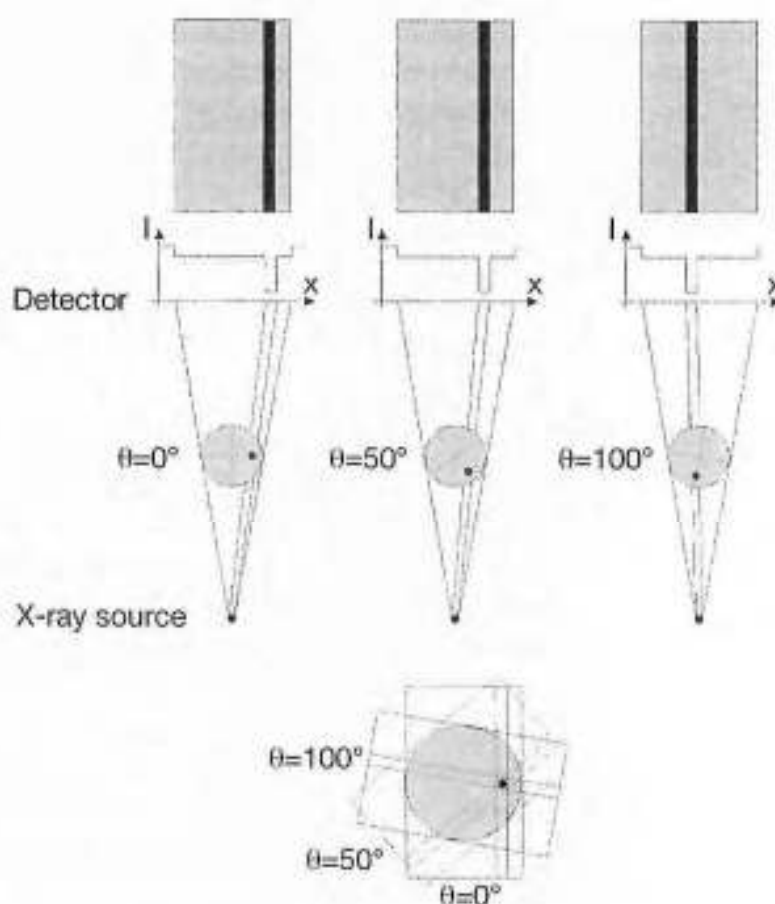**Figure 1.** *Projection profiles through an object*

Figure 2. *Reconstruction procedure for plane cross sections*

All these projections are used in a reconstruction algorithm, which calculates a set of serial non-destructive sections where the interpretation of the image, i.e. cross section, can be done in terms of attenuation of the X-rays in the object. Then, a three-dimensional image of the specimen can be reconstructed from serial sections and can be processed to show and measure three-dimensional features. A presence of noise in reconstructed images is inherent to the X-ray technique and therefore it is important to select an analysis method that would solve a problem of image deblurring in an efficient way.

In the present work the Skyscan 1072 X-ray scanner was used with the resolution 3 µm. The three dimensional reconstructed images have been subjected to image processing procedure using Aphelion image processing package. For illustrative purposes, the major steps in the procedure are shown in **Figure 3** for reconstructed plane cross sections. The three dimensional image analysis follows the same steps. **Figure 3a** shows a gray image of the reconstructed

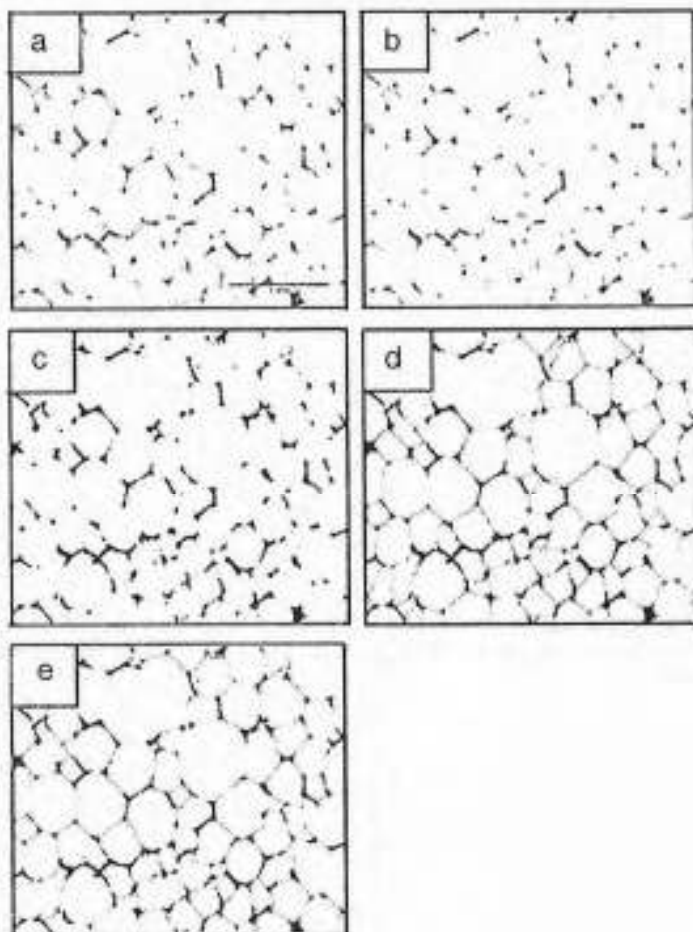Y. Ma, R. Pyrz, M.A. Rodriguez-Perez, J. Escudero, J.Ch. Rauhe1 and X. Su

Figure 3. Original grey scale image from the X-ray scanner (a); image after median filter application (b); binary image after thresholding (c); binary image after the unconstrained watershed segmentation (d); binary image after the constrained segmentation (e)

cross section obtained from the scanner followed by the application of a median filter in **Figure 3b**. The median filtering does not introduce new gray values to the feature and preserves the edges. Then a binary thresholding is applied to the image (**Figure 3c**) converting the image into the set of black and white pixels. This step removes the noise however thin walls, that only weakly attenuate X-rays and have a light grey appearance, may be also removed from the image. Rebuilding thin walls can be done using so called watershed segmentation procedure which in many instances leads to oversegmentation i.e. creation of new artificial walls not present in the structure (**Figure 3d**). This can be avoided by the application of constrained watershed segmentation which is more comprehensive and removes deficiencies of the standard

watershed segmentation [13]. The final image, **Figure 3e**, is used for creation of three-dimensional structure and for measurements.

The left column in **Figure 4** shows the plane section arbitrarily selected from the stack of reconstructed cross sections for each sample belonging
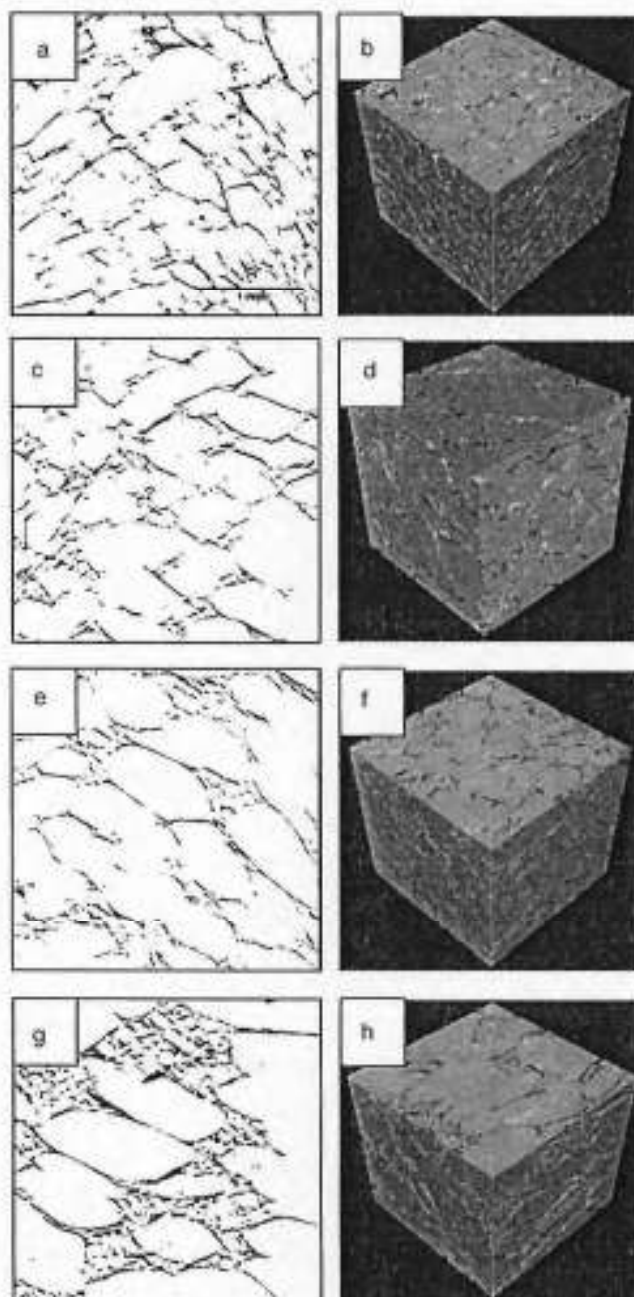

Figure 4. Reconstructed cross sections (left column) and corresponding three-dimensional images (right column) of samples from the first series of experimental specimens 1.1-1.4 (from top to bottom)

Y. Ma, R. Pyrz, M.A. Rodriguez-Perez, J. Escudero, J.Ch. Rauhe1 and X. Su

to the first series of experimental specimens whereas the right column illustrates corresponding three dimensional structures. In the similar way **Figure 5** illustrates internal structure of samples from the second series of experimental specimens. For comparative purposes a SEM image of sample 2.1 is shown in **Figure 6**. An appearance of small cell clusters surrounded by larger cells is clearly seen on SEM and reconstructed cross section from
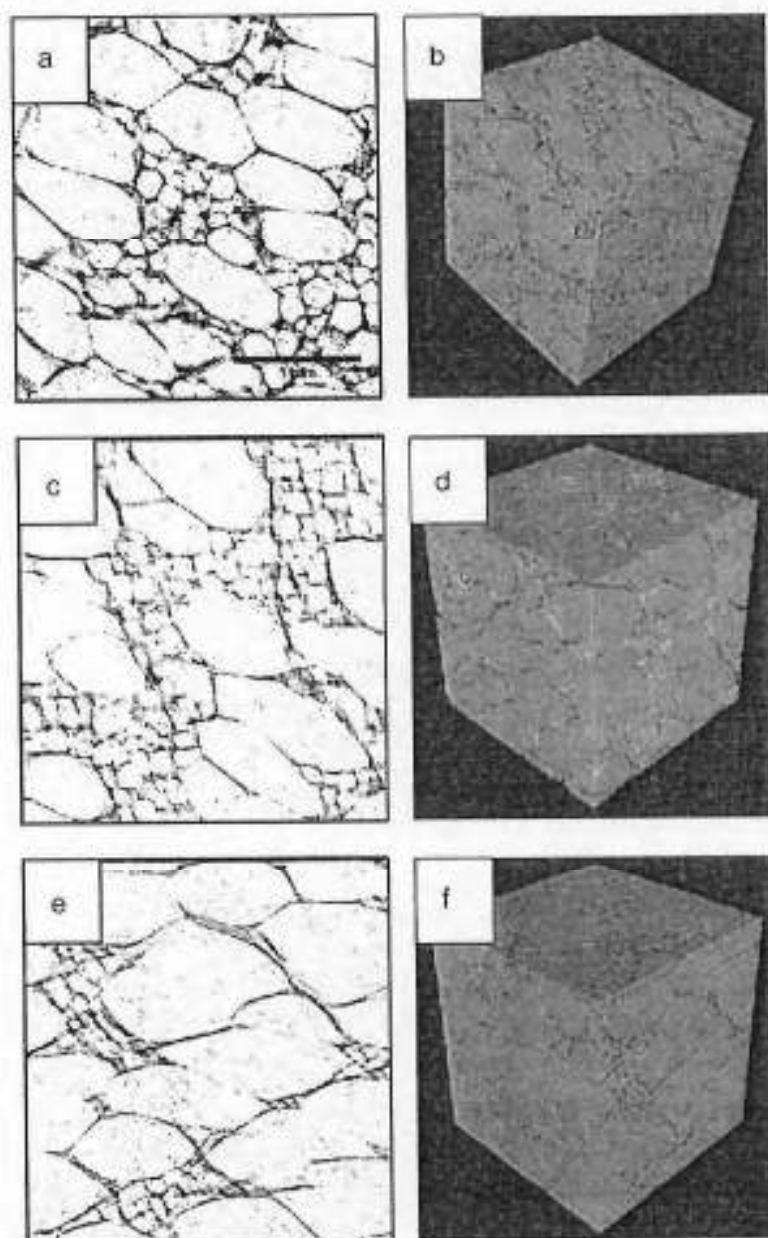

Figure 5. *Reconstructed cross sections (left column) and corresponding three-dimensional images (right column) of samples from the first series of experimental specimens 2.1-2.3 (from top to bottom)*
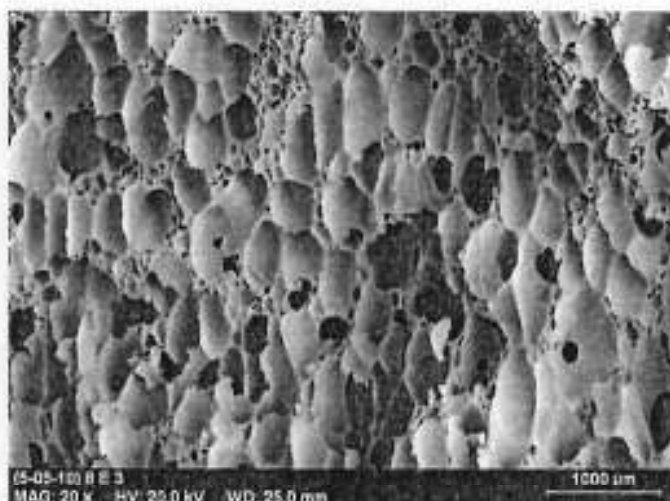
Figure 6. *SEM image of foam structure for 2.1 specimen*

Figure 5a. Apart from being visually very informative the reconstructed three dimensional images provide quantitative data regarding the microstructure build up. Each voxel i.e. three dimensional pixel of the image, belongs either to the substance or to the pore and Cartesian coordinates are assigned to all voxels in the reconstructed image allowing to perform spacial measurements of volume, surface and line geometrical entities. It should be pointed out that for a better clarity of three dimensional images the assignment of voxels has been inverted in **Figures 4** and **5** i.e. the pores are seen as solid features whereas the cell walls are indicated as porous skeleton.

ANALYSIS AND DISCUSSION

The total porosity of the foams has been calculated as a volume fraction of voxels belonging to the pore. In the similar manner, the distribution of cells volume has been calculated as an overall volume of voxels contained within single cells. The frequency distribution of cell volumes for all samples is shown in **Figure 7**. The logarithmic horizontal axis indicates that all samples contain a broad range of cell volumes. The variation of the mean cell volume and the specific Young's modulus with the applied foaming pressure is shown in **Figure 8** for the first series of samples. It is clear that decreasing the foaming pressure results in larger mean cell volumes and improved stiffness. However this conclusion should be supplemented with further observation extracted from X-ray images. For each experimental sample an x quantile of Y quantity has been calculated. If the selected quantity corresponds to cell volume than

Y. Mo, R. Pyrz, M.A. Rodriguez-Perez, J. Escudero, J.Ch. Rauhe¹ and X. Su

Table 2. Morphological parameters of samples

Sample	Porosity [%]	Cell volume [mm³] E-03				Mean sphericity Φ_{mean}
		mean	0.25 quantile	0.5 quantile	0.75 quantile	
Series 1						
1.1	88	8.08	1.01	2.76	9.06	0.709
1.2	89	10.30	0.64	1.88	7.19	0.704
1.3	85	15.40	0.87	2.53	14.80	0.688
1.4	86	20.30	0.82	2.08	5.57	0.649
Series 2						
2.1	80	8.62	0.97	2.01	4.15	0.761
2.2	83	10.60	1.41	2.88	5.86	0.742
2.3	85	14.30	0.56	1.75	5.47	0.697

0.25 quantile of cell volume population Y means that 25% of cells in the population have volume less than Y. The data is presented in **Table 2**. Now looking at the 0.75 quantile from samples 1.4 of the first series it follows that 75% of cell volumes is less than 5.57 mm³ E-03. Thus a majority of cells have relatively small volumes and the large value for the mean cell volume comes from less populated by large cells.

In the second series of samples the content of the blowing agent has been reduced to 2.5 wt% and only single changes in temperature (specimens 2.2) and foaming pressure (specimens 2.1 and 2.3) have been made. The material data from **Table 1** indicate that specimens 2.1 exhibit significantly improved mechanical properties. Furthermore, the mean volume of cells is small and quantile values indicate that 75% of cells have mean volume smaller than 4.15 mm³ E-03 which is well below the value for the best 1.4 sample from the first series. It also appears that lowering the foaming temperature deteriorates mechanical properties of foams.

It is apparent from X-ray and SEM images that cell shapes cannot be approximated by polyhedral network and characterized in topological terms, and therefore other shape descriptors would be useful. A sphericity parameter, Φ, is a compactness measure of a shape. It is defined [14] as the ratio of the surface area of a sphere (with the same volume as the given particle) to the surface area of the particle. In the present setting a particle represents the cell. The expression for the sphericity reads:

$$\Phi = \frac{A_s}{A_p} = \frac{\sqrt[3]{36\pi V_2^P}}{A_p}$$
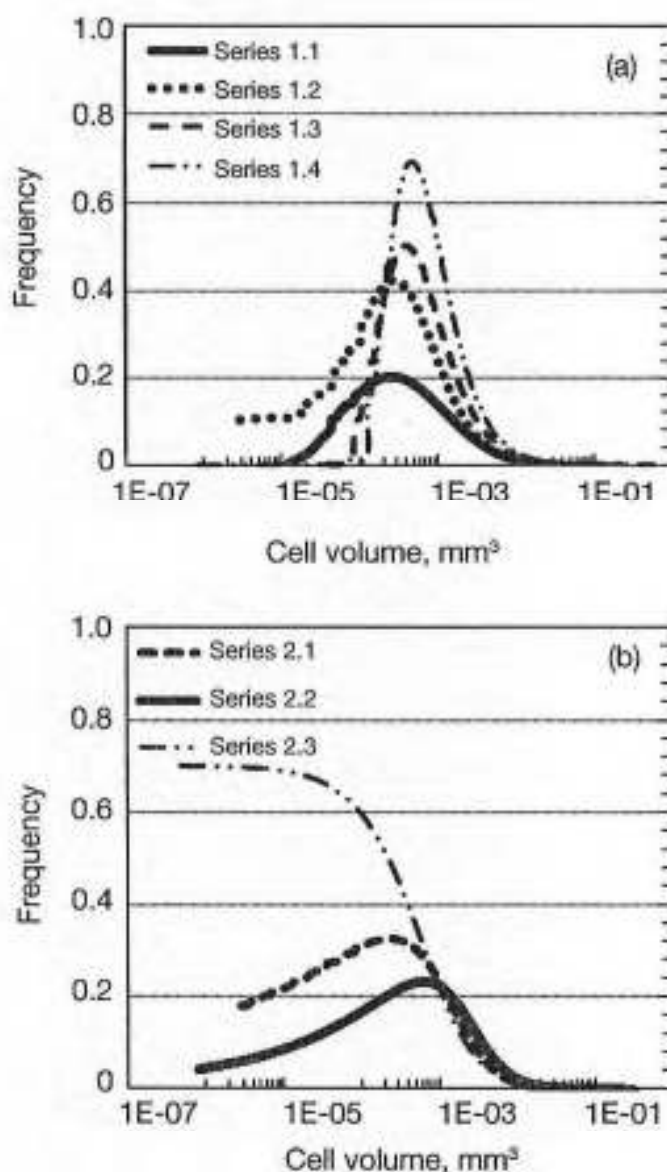
Figure 7. *Frequency distribution of cell volumes for samples from the first series (a) and for samples from the second series (b)*

where V_p is volume of the cell and A_p is the surface area of the cell. The surface area can be also calculated from image voxels. The sphericity parameters for all samples are included in **Table 2**. The frequency distribution of the sphericity for the sample 2.1 having the best mechanical characteristics is shown in **Figure 9**. The solid line represents the β distribution function which approximates the discrete frequency distribution of the sphericity. Increasing sphericity of cells

Y. Ma, R. Pyrz, M.A. Rodriguez-Perez, J. Escudero, J.Ch. Rauhe l and X. Su
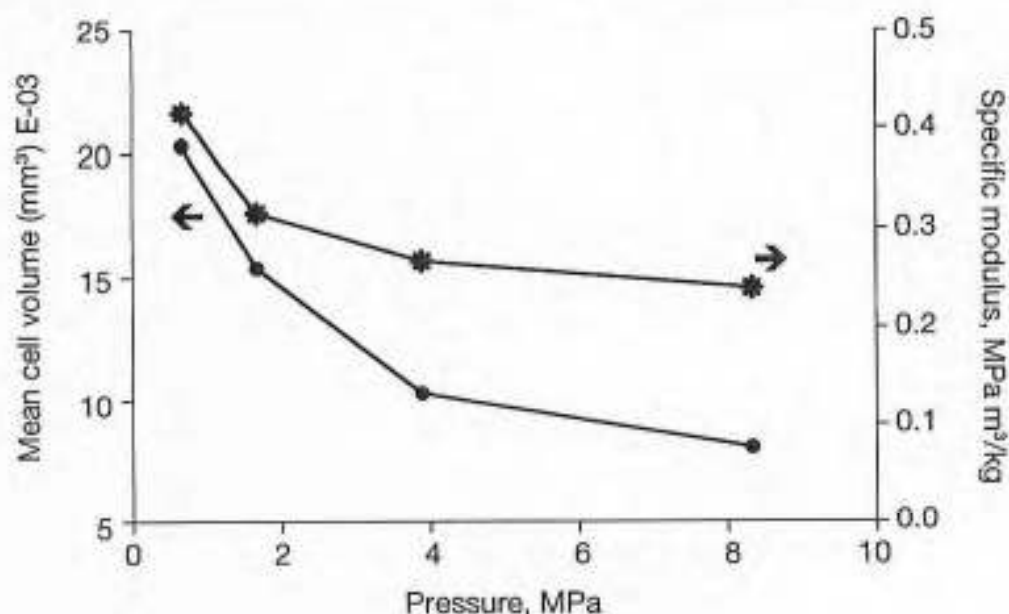
Figure 8. *Variation of the mean cell volumes and specific Young's modulus with foaming pressure for experimental specimens from the first series of samples*
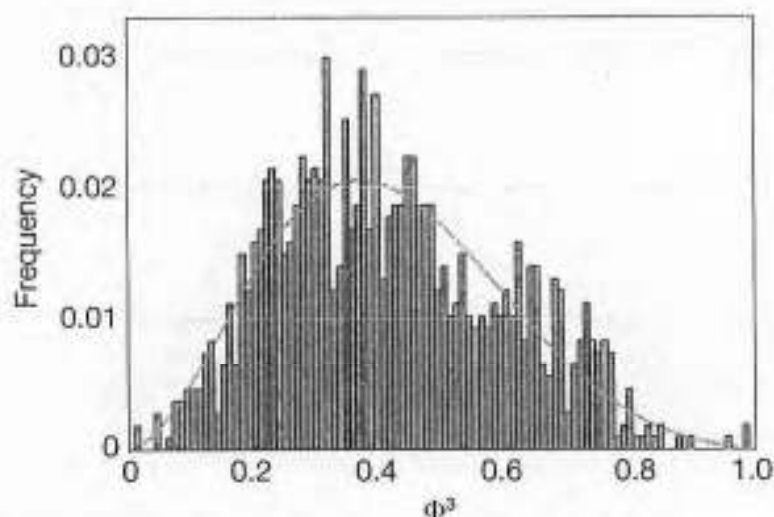
Figure 9. *Frequency distribution of sphericity for the specimen 2.1*

from the first series of experiments follows with the increasing foaming pressure, **Figure 10**. However, the changes in some of the processing parameters (samples 2.1 and 2.3) result in shifting sphericity values to other intervals as indicated in **Figure 10** by two outliers. It is however expected that the monotonic relation between foaming pressure and sphericity will be maintained.
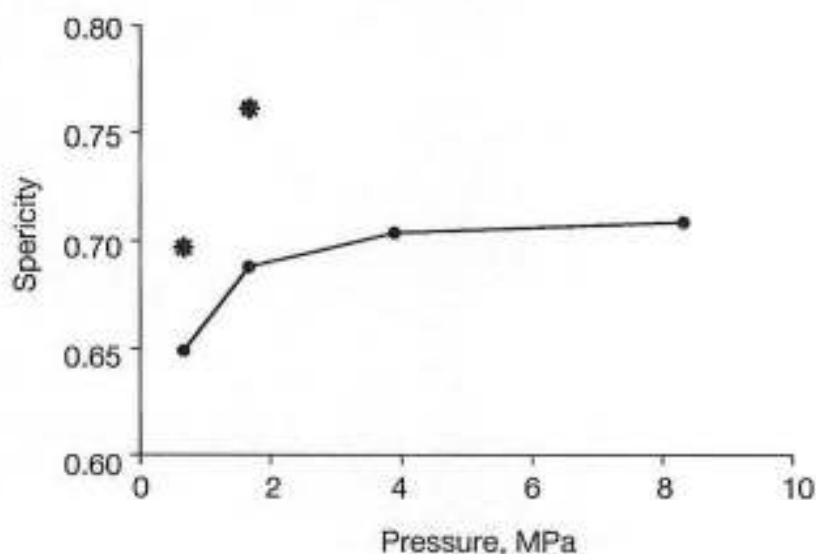
Figure 10. *Variation of the sphericity parameter with foaming pressure*

The present analysis indicates that a monotonic relation between processing parameters and/ or mechanical characteristics of foams and representative morphological descriptors of foams may exist. The challenge is to select adequate parameters that can be assessed and measured on real three-dimensional microstructure and are related to processing conditions and mechanical properties. For instance, from parametric studies of Voronoi polyhedral foams [3] it follows that nodal connectivity of cells significantly influences mechanical response of foams and the connectivity increase enhances the mechanical properties through the shift from the bending deformation modes toward stretching deformation modes. However, by no means it is the only parameter that is related to mechanical properties and more importantly, for most traditional foaming technologies nodal connectivity cannot be controlled and usually appears to have a low averaged value around 3. The degree of irregularity of cells, cell wall shapes, spacial distribution of cell volumes and clustering tendency are other factors that are related to processing parameters and deformation mechanisms that determine the mechanical response.

CONCLUSION

The most important aspect of X-ray microtomography is that the method is non-destructive and provides the microstructure of foams as it is not as it

Y. Ma, R. Pyrz, M.A. Rodriguez-Perez, J. Escudero, J.Ch. Rouhe T and X. Su

is described by some mathematical model. As a consequence, geometrical features of the microstructure that characterize its morphology can be assessed and measured. This has been done in the present work for the cell volume distribution and sphericity parameter. Both entities appear to be related to processing parameters and mechanical properties of foams processed using the improved compression moulding technique. In order to predict the relations that might exist between morphological descriptors and mechanical and processing parameters it is necessary to determine deformation mechanisms operative in the microstructure under loading. This can be done by performing in situ loading experiments on foam samples mounted in the loading device that is placed inside the X-ray scanner chamber. The investigation is actually in the progress.

ACKNOWLEDGEMENTS

REFERENCES

1. James Ren X. and Silberschmidt V.V., *Comput. Mat. Sci.*, **43** (2008), 65-74.

2. Harders H., Hupfer K. and Rösler J., *Acta Materialia*, **53** (2005), 1335-1345.

3. Alkhader M. and Vural M., *Int. J. Engng. Sci.*, **46** (2008), 1035-1051.

4. Redenbach C., *Comput. Mat. Sci.*, **44** (2009), 1397-1407.

5. Tekoglu C., Gibson L.J., Pardoen T. and Onck P.R., *Prog. Mat. Sci.*, **56** (2011), 109-138.

6. Viot P. and Bernard D., *J. Mater. Sci.*, **41** (2006), 1277-1279.

7. Viot P., Plougonven E. and Bernard D., *Composites A*, **39** (2008), 1266-1281.

8. Youssef S., Maire E. and Gaertner R., *Acta Materialia*, **53** (2005), 719-730.

9. Elmoutaouakkil A., Fuchs G., Bergounhon P., Péres P. and Peyrin F., *J. Phys. D: Appl. Phys.*, **36** (2003), A37-A43.

10. Van den Bulcke J., Boone M., Van Acker J. and Van HoorebekL., *Microsc. Microanal.*, **15** (2009), 395-402.

11. Rodriguez-Perez M.A., Lobos J., Perez-Muñoz C.A., de Saja J.A. and del Carpio B.M.A., *Cellular Polymers*, **27** (2008), 347-362.

12. Román-Lorza S., Rodriguez-Perez M.A. and de Saja J.A., *Cellular Polymers*, **28** (2009), 249-268.

13. Soille P., *Morphological Image Analysis: Principles and Applications*, Springer-Verlag, Berlin/Heidelberg/New York, (2003).

14. Wadell H., *J. Geology*, **43** (1935), 250-280.

275

6.3.- Physical Properties of the Developed Structural Foams

Polypropylene has a low cost, high stiffness for static load bearing purposes and higher service temperature than other polymer matrices, which make it a very interesting material for several different applications. But, in spite of all the previous advantages, the foamability of polypropylene is not good. It presents a low melt strength, so achieving high expansion ratios (higher than 2) is not easy. Due to this, achieving low densities with closed cell structures showing high mechanical properties with a non-crosslinked polypropylene matrix is the aim of this research.

This section presents a work entitled ***"Low Density Non-Crosslinked Closed/Open Cell Polypropylene Foams with High Mechanical Properties: Rheology, Cellular Morphology and Mechanical Behavior"***.

Rheology plays a fundamental role in the consecution of closed or open cell polypropylene foams. The work establishes a relation between rheological behavior, open cell content and mechanical performance, so an initial characterization of the rheological properties of the polypropylene matrix is fundamental for the prediction of the later properties that can be expected in the foams. In the same line of previous chapters, nanoclays have a detrimental effect on the rheological properties of the polymer matrix and therefore the cellular structures obtained have a higher open cell content.

On the one hand close cell foams with densities in the range 90-200 kg/m^3 are obtained. These samples present high specific mechanical properties, comparable or even better than commercial PVC or SAN foams. On the other hand the addition of nanoclays prevents from achieving closed cell foams but in spite of this, the reinforcing role played by the nanoclays help to obtain open cell foams with high specific mechanical properties too. This combination open cell/high mechanical properties covers a range of properties not typically reached by other materials.

Therefore, two different versions of foams are presented in this work, closed and open cell, with physical properties comparable or better to other commercial materials, recyclable and in an interesting density range (90-200 kg/m^3). These materials has been named Anicell and in principle they could be good substitutes of current materials in several applications as it is summarized in figure 6.1.
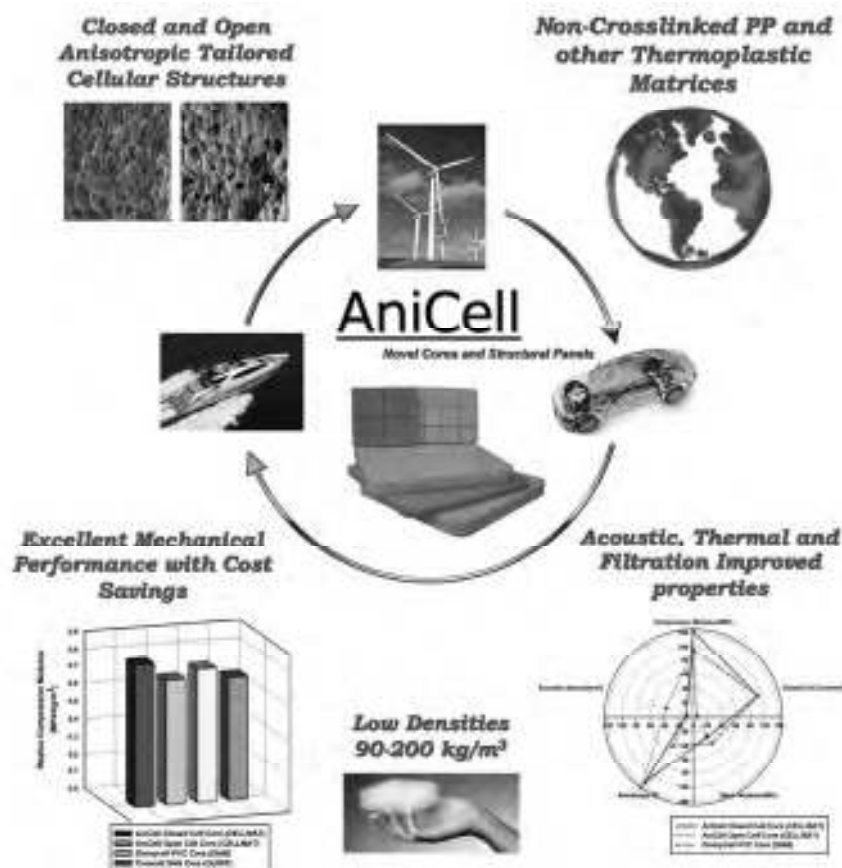
Figure 6.1: Schematic summary of the potential applications and principal advantages offered by AniCell.

LOW DENSITY NON-CROSSLINKED CLOSED/OPEN CELL POLYPROPYLENE FOAMS WITH HIGH MECHANICAL PROPERTIES.

J. Escudero [1], A. Lopez-Gil [2], E. Laguna-Gutiérrez[1], M.A. Rodriguez-Perez[1]

[1]Cellular Materials Laboratory, (CellMat). Condensed Matter Physics Department, University of Valladolid, Paseo de Belén 7, 47011, Valladolid, Spain.

[2]CellMat Technologies S.L. CTTA, Paseo de Belén 9A, 47011 Valladolid, Spain

Corresponding author: M.A. Rodriguez-Perez. Tel: +34 983184035. Fax: +34 983423192. E-mail address: marrod@fmc.uva.es

ABSTRACT

Low density polypropylene based foams with different cellular structures have been produced by the improved compression molding route using a high melt strength polypropylene as matrix polymer. In addition, different type of nanoparticles has been introduced in the formulation (multi-wall carbon nanotubes, organomodifed nanoclays and natural nanoclays) to modify the structure and properties. The results have showed a clear correlation between the open cell content of the foams and the mechanical properties in compression. In the unfilled polypropylene high specific mechanical properties are only achievable with low values of open cell content. In comparison, for an equal value of the interconnectivity between cells, the samples containing nanoclays present much higher specific properties. This result is attributed to the reinforcement of these nanoparticles in the solid matrix, due to an improved exfoliation during the foaming process and the presence of a bimodal cellular structure. The produced foams have interesting properties with stiffness similar to those of commercial polymer foams used for the core of sandwich panels.

Key-words: PP foams, nanocomposites, nanoclays, carbon nanotubes, open cell content

INTRODUCTION

Polymeric foams can be defined as two-phase materials in which a gas is dispersed in a continuous macromolecular phase [1,2]. These materials have wide applications in insulation and packaging as well as in the automotive and construction industries because of their excellent properties: they are light-weight and exhibit a high stiffness and strength to weight ratio, superior insulating qualities and excellent energy absorption. PE and PS are two of the most commonly used materials for thermoplastic foam production [3] but, due to its outstanding functional characteristics, PP has been considered industrially as substitute for these materials. PP has a low material cost like PE but on the contrary it presents a much better stiffness for static load bearing purposes. Since at room temperature PP is in rubbery state its impact resistance is higher than the one of PS. PE and PS foams are not suitable in applications that require high service temperatures, the heat deflection temperature of PP in comparison is higher. Finally PP foams have a comparable chemical resistance to PE but better than PS [1-4].

It is well known that for foams the loss of mechanical properties at low relative densities is very strong, with normally a square dependency with density [1,2,6]. The most common approaches followed to solve this problem consist on the one hand on reinforcing the polymer matrix trying to increase its stiffness and on the other hand on modifying the cellular structure of the foam somehow to improve the mechanical behavior [5,6].

Dealing with the first approach, in the last years a lot of efforts have been focused in the production of polymer composite foams reinforced with particles in the nano-scale dimension. Several nanoparticles have been used for this purpose, namely carbon nanotubes, carbon nanofibers or silica particles but one of the most extended and promising ones is the reinforcement using nanoclays. The addition of these silicate layered nanoparticles imparts to the polymer good thermal stability, high heat distortion temperature and high specific stiffness at low concentrations of filler. Several works in the literature have studied nanoclays-filled polypropylene foams using different foaming methods and diverse blowing agents. Chaudary et al. found that the addition of nanoclays to a linear PP promotes the strain hardening phenomenon. The foams were produced by extrusion foaming using a chemical blowing agent [7]. Due to the appearance of the strain hardening they obtained much better foams with the nanofilled samples than with the raw linear PP. A similar discussion is done by Zhai et al. in terms of cell nucleation and cell coalescence. The addition of nanoclays (5 wt.%) dramatically improves the cell morphology of extruded foams using CO_2 as physical blowing agent [8].Antunes et al. compared the effect of different fillers in polypropylene based foams. Together with nanoclays the study includes the effect of other fillers such as cellulose fibers or carbon nanofibers [9]. Although the semicrystalline character of polypropylene makes difficult its foaming using a batch gas dissolution foaming technique Velasco et al. accomplished an study using this procedure. The study compares the microcellular foamability of raw polypropylene with two filled polypropylenes, one reinforced with cellulosic fibers and the other one using organomodifiednanoclays. The cellular structure found was finer in the case of

the nanoclays-filled formulations. This fact together with the inherent reinforcement over the solid matrix yielded foams with improved stiffness [10].

Concerning the second approach the influence of the cellular structure and morphology on the mechanical properties of a foam is a broadly studied topic in the literature. Several parameters can be distinguished as the most influencing ones, namely cell size, cellular homogeneity, anisotropy ratio and open cell content.

The influence of the cell size on the mechanical performance is not a well-established subject with different controversial studies. Gong et al. found an enhancement in mechanical properties of chemically foamed PP microcellular samples with the reduction of the cell size [11]. Similar results were found by Rachtanapunp and co-workers in PP/PE blends. Smaller and more uniform cells resulted in improvements of the compressive properties [12,13]. The beneficial effects of cell uniformity were studied also by Saiz-Arroyo et al. using either physical or chemical blowing agents in PP based foams. Each type of blowing agent produces better foams in a certain density range and it is found that the measured mechanical properties are deeply influenced by the cell size homogeneity achieved in each case [14]. Miller and co-workers found important improvements in the tensile and impact properties of PEI foams when passing from the microcellular to the nanocellular range but no improvement was observed when passing from the conventional to the microcellular range [15,16]. No improvement was neither found with the reduction of cell size in the tensile properties of polycarbonate foams produced using sub-critical CO_2 by Weller et al [17,18].

The effect of anisotropy ratio of the cells has been deeply studied both from a theoretical [6,19] and experimental [20-23] point of view in diverse polymer systems. Compression properties are the most benefitted ones from the anisotropy when measured in a direction coinciding with the direction of higher elongation of the cells. Theoretically, the quotient between the elastic modulus measured in the anisotropy direction and the same property measured in a perpendicular direction can be modeled by the formula $\frac{E_3}{E_1} = \frac{2R^2}{1+(\frac{1}{R^3})}$ where E_3 and E_1 are the elastic modulus in the anisotropy direction and in a perpendicular one respectively and R represents the anisotropy ratio of the foam [19]. As can be observed, the dependency with R is very strong for the compressive properties. There are several industrial foam production processes that try to take advantage of this fact too [24-26]. The present work pays special attention to the open cell content of the produced foams. They are classified as open cell foams when OC is higher than 80% while on the contrary, they are classified as closed cell foams when OC is lower than 20%. This parameter is related with how the mass is distributed in the foam structure. The preferential distribution of mass in the cell walls yields closed cell morphologies and on the contrary, when the mass is preferentially distributed in the struts open cell structures are obtained. This mass distribution is directly connected with the observed mechanical properties of the foam [6].

In the particular case of PP obtaining closed cell structures is not a simple task and this fact has limited the applicability of PP foams. The low melt strength exhibited by the linear polypropyelenes leads to rupture of the cell walls under the elongational forces occurring

during cell growth; as a result final foam has a high amount of coalesced and open cells which harms mechanical properties. This low melt strength hinders also the production of low density PP based foams [14, 27]. Literature contains numerous and very different attempts to surmount these problems. Ahmadi and Hornsby tried to improve the foamability of PP just by modifying the foaming conditions during injection molding [28]. As it was mentioned in previous paragraphs, the addition of certain types of particles to linear polypropylenes increases the melt strength and imparts typical features of branched polymers [7,8]. A less desirable solution goes through the crosslinking of the PP matrix. It turns the polymer non-recyclable and at the same time the crosslinking process can involve a certain degree of dangerousness [29-31]. A simple and extended solution consist in using special grades of PP known as high melt strength on which, by promoting a high degree of branching, the melt strength is significantly increased. Although the price of these branched grades can double the price of the normal ones the simplicity of the processing techniques makes the global production economically affordable [32-34].

The aim of this work is to present a procedure for the production of low density non-crosslinked closed/open cell polypropylene foams with high specific mechanical properties. These novel materials are based on a branched polymer and produced using the improved compression molding technique [35-38]. The variation of the processing conditions and polymer formulation yields a broad range of different cell openness which therefore permits an experimental study of the dependency between mechanical properties and open cell content. The almost unexplored possibility of combining high open cell contents with high specific mechanical properties is also studied and achieved by the reinforcement of the polymer matrix with organomodified and natural nanoclays together with carbon nanotubes.

EXPERIMENTAL

- **Materials**

A branched high melt strength homopolymer polypropylene (Daploy WB 130 HMS from Borealis) was used as main polymer matrix in all the cases. The density of this polymer is 910 kg/cm^3. The melt flow index for this polymer is 2.4 g/10 min (230 ºC/2.16 kg) and the melting temperature is 163 ºC. Several different kinds of nanoparticles were used as additives: montmorillonite-type nanoclays organomodified with quaternary ammonium salts Cloisite 20 A from Southern Clay Products, multiwall carbon nanotubes (MWCNT) in masterbatch form (Plasticyl PP2001 with 20 wt.% of carbon nanotubes Nanocyl NC7000 from Nanocyl, MFI=0.3 g/10 min) and natural nanoclays Cloisite Na$^+$ from Southern Clay Products. In order to improve the dispersion and exfoliation of the organomodified nanoclays a coupling agent was also used. This coupling agent is a 1 wt.% maleic grafted polypropylene Polybond 3200 from Chemtura. The proportion between coupling agent and nanoclays was maintained constant based on previous experience in a value of 2:1 respectively.

The foaming was performed using a chemical blowing agent, azodicarbonamide Lanxess Porofor M-C1 with an average particle size of 3.9 ± 0.6 µm. The proportion of blowing agent was kept constant in a value of 2 wt.% both in the unfilled samples and in the samples filled with different kinds of nanoparticles. Antioxidants Irgafos 168 (from Ciba) in a proportion of 0.08 wt.% and Irganox 1010 in a proportion of 0.02 wt.% (from Ciba) were also used to avoid thermal degradation of the polymer.

The mixing was always done using a twin screw extruder Collin ZK 25T with and L/D of 24. In the case of the organomodified nanoclays the as received clays were first melt blended with the coupling agent in the mentioned proportion (2 parts coupling agent per 1 part nanoclays) at an average speed of 50 rpm and a die temperature of 195 ºC. Afterwards the masterbatch coupling agent-nanoclays was diluted with the high melt strength polypropylene using the same extrusion conditions in order to finally get 5 wt.% of nanoclays. The MWCNT masterbatch was melt blended also in the same extrusion conditions with the branched polypropylene seeking a final proportion of 1 wt.% of carbon nanotubes. 5 wt.% of the natural nanoclays were directly blended with the branched polymer using the same temperature profile in the extruder and same processing speed. Table 1 summarizes the different samples studied.

Table 1: Different nanocomposites produced with the different proportions of each component

Sample	Branched PP/wt.%	Coupling Agent/wt.%	Masterbatch MWCNT/wt.%	Organomodified Nanoclays/wt.%	Natural Nanoclays/wt.%
Pure PP	100	0	0	0	0
PP+MWCNT	95	0	5	0	0
PP+NC	85	10	0	5	0
PP+NNC	95	0	0	0	5

The previously mentioned composites together with the unfilled polypropylene are afterwards blended with the azodicarbonamide (2 wt.%) and the antioxidants (0.08 wt.% Irgafos 168 and 0.02 wt.% Irganox 1010). The same extruder is used for this purpose at an speed of 120 rpm and a die temperature of 155 ºC to avoid the premature decomposition of the blowing agent.

- **Samples Foaming**

These foams are intended for lightweight industrial applications so the densities of these materials should be lower than 200 kg/m^3. Achieving such low density foams with a non-crosslinked polypropylene matrix is not a simple task. For this reason, a branched high melt strength polypropylene was selected as base material. In addition the foaming method selected, improved compression molding (ICM), plays also a fundamental role in the achievement of such low densities. The ICM foaming route comprises three different steps:

1. Mold filling: pellets of the previous formulations already containing the blowing agent and the rest of the additives are introduced inside a disc-shape stainless steel mold.

Once the mold is correctly filled it is closed using a piston and placed inside a pre-heated hot plates press.

2. Temperature and pressure: the temperature of the press plates is always higher than the decomposition temperature of the chemical blowing agent used. In our case a temperature of 200 ºC was used for the pure PP and for the formulation containing nanotubes. In the case of the formulations containing clays a temperature of 190 ºC was used instead. The decomposition of the blowing agent generates a certain gas pressure (P_{ADC}) inside the mold. The mechanical pressure (P_0) applied externally is always higher than the gas pressure inside the mold. In the working conditions used the gas generated is dissolved into the polymer and no foaming occurs while this external pressure is applied. In our case pressures of 35 bar for the pure and MWCNT formulations and of 7 bar for the clay-containing formulations were applied during 15 minutes. These processing parameters were optimized through experimental testing and we selected the ones giving better properties for each material.

3. Pressure release and cooling: once the blowing agent is totally decomposed and completely dissolved in the polymer the pressure is released at a controlled rate. The whole foaming occurs inside the mold and the foam growing is constrained in the direction coinciding with the pressure release one. The density is controlled by retaining the piston displacement (d) at a certain point (ER Control Part in figure 1) and afterwards the mold with the foam inside can be freely extracted from the hot press and cooled, in our case immersing it in cool water.
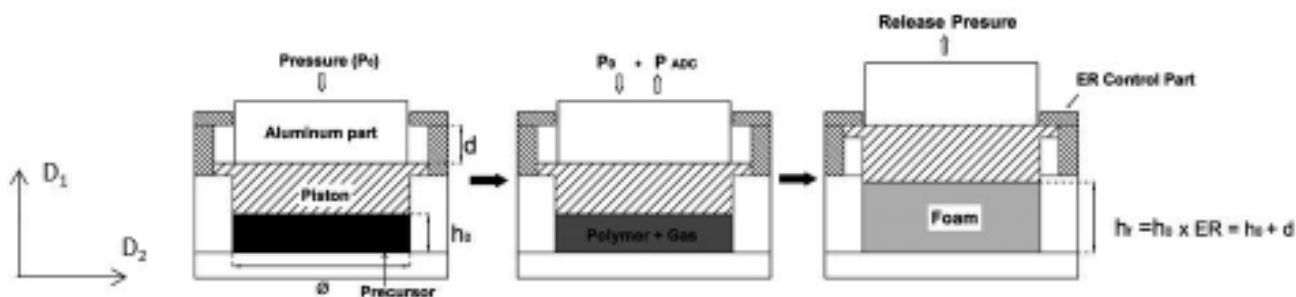
Figure 1: Schematic in the expansion plane (D_1/D_2) showing the different steps followed in the Improve Compression Molding Route

The ICM foaming route has several advantages in comparison to other conventional routes. On one hand the possibility of achieving an accurate control of foam density and on the other hand the possibility of modifying the microstructure of the foamed part, (in terms of cell size, cell type and cell shape) by acting on both foaming parameters and chemical composition. Further details of the ICM foaming route can be found elsewhere [35-39].

The foams produced in this paper had densities of 150 kg/m^3 and 180 kg/m^3.The samples were disks with 150 mm in diameter and 12 mm and 10 mm thickness (h_f) respectively.

- **Samples Characterization**

The density of the samples was measured by the geometric method, that is, dividing the mass of the samples between their corresponding volume (ASTM Standard D1622-08).

Cellular structure of the whole collection of foams was analyzed using scanning electron microscopy, (SEM). In order not to distort their microstructure, samples were frozen in liquid nitrogen and afterwards fractured. Surface fracture was made conductive by sputtering deposition of a thin layer of gold and observed using a Jeol JSM-820 scanning electron microscope.

Cell size as well as anisotropy ratio, were measured using an image processing tool based on the software ImageJ [39]. At least 75 cells per image and at least three different images were analyzed.

Open cell content of foamed materials was determined according with ASTM Standard D6226-10 using a gas pycnometer Accupyc II 1340 from Micromeritics.

Compression tests were carried out in a universal testing machine, (Instron model 5500R6025). Samples of 20x20 mm^{2}cut from the 150 mm diameter discs were tested at an strain rate of $1.67x10^{-3}$ s^{-1} where h is the height of the specimen. The maximum static strain was 75% for all the experiments. The maximum standard deviation (in percentage) obtained for the foams measured in compression was $\pm$ 5%. Tensile tests for the solids were performed according to ASTM D638 using an strain rate of 6.67x10-4 s-1. The solids were produced by compression molding. In this particular case, the maximum standard deviation obtained for the solid samples was $\pm$ 2%.

RESULTS

- **Cellular Structure of the foams**

Micrographs taken along the plane parallel to the expansion direction (D_1/D_2) corresponding to the different foams are presented in figure 2. Morphological parameters in terms of cell size and anisotropy ratio are collected in table 2
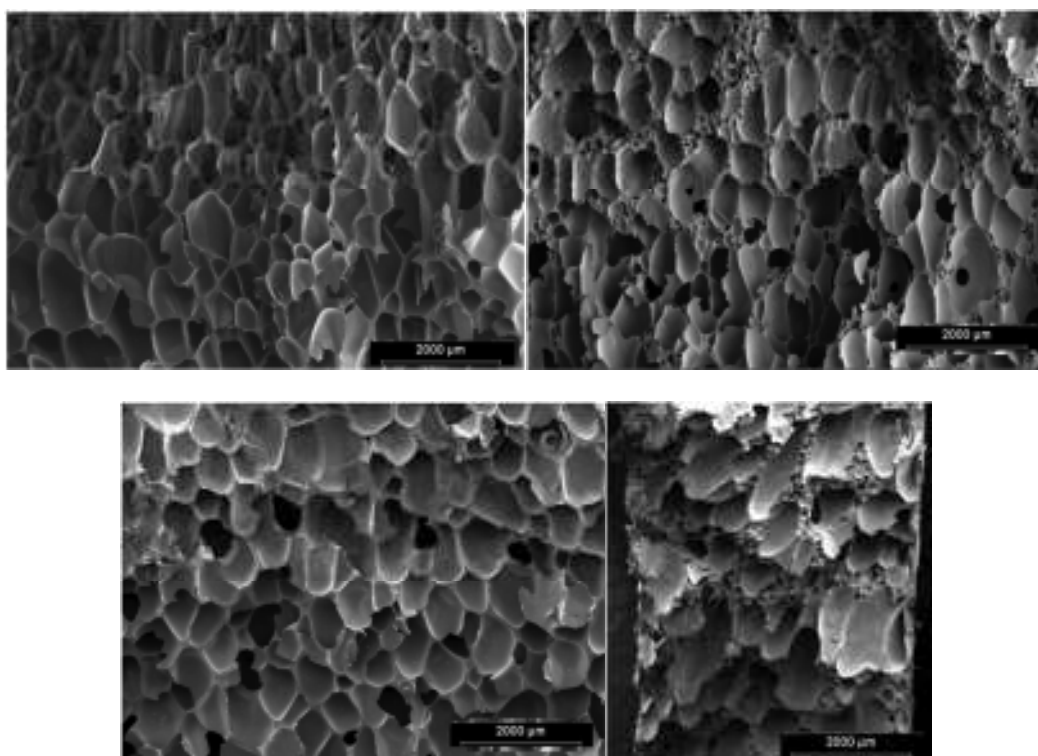
Figure 2: Micrographs corresponding to a) pure PP b) PP+5 wt.%Nanoclays c) PP+1 wt.% MWCNT and d) PP+5 wt.% Natural Nanoclays.

The mean cell size presents comparable values between samples with no large differences. The solid residues left after the decomposition of the azodicarbonamide is a competing nucleation mechanism that is present both in the samples with and without nanoclays. The presence of a bi-modal cell distribution is characteristic of the foams containing clays. This bi-modal distribution, that can be visually observed in micrographs of figure 2, doubles the standard deviation value calculated for the different samples. On the contrary the samples containing multi wall carbon nanotubes present the more homogeneous cellular structure with the lowest standard deviation. Due to the bi-modal distribution, the cell density is also strongly increased in the samples containing clays, with values almost eight times higher than in the rest of the samples (table 2). The appearance of two different populations of cells is the only fact that can be attributed to a nucleation role played by the nanoclays. Although the mean cell size is bigger for the samples containing clays and the open cell content is also remarkably higher, denoting coalescence and cell coarsening phenomenon, the presence of a significant population of cells, placed preferentially on the cell walls of the bigger cells and with cell sizes below 100 μm can be connected to the nucleation of the exfoliated/intercalated nanoclays.

The preferential growth of the cells in the pressure release direction gives as result anisotropy values higher than 1. All the samples have anisotropy ratios near 2.5 except the one containing carbon nanotubes. Although the production conditions are the same in all cases, this last sample has an anisotropy patently lower, with a value of 1.6

Table 2: Quantification of morphological parameters corresponding to the cellular structure of the different samples

Sample	Density /(kg/m³)	Mean Cell Size/μm	Standard Deviation/ μm	Cell Density /(cells/cm³)	Anisotropy Ratio	OC (%)
Pure PP	179	300	105	$1.4 \cdot 10^4$	2.2	18
PP+MWCNT	181	315	96	$1.1 \cdot 10^4$	1.6	52
PP+NC	180	321	262	$8.3 \cdot 10^4$	2.6	94
PP+NNC	182	343	203	$8.6 \cdot 10^4$	2.5	78

These high anisotropy values could benefit several properties of the foams. For example, theoretically, for an anisotropy of 2.5, the elastic modulus in compression measured in the direction of maximum elongation of the cells would be 11.75 times higher than the one measured in a perpendicular direction [19].

- **Mechanical properties of unfilled polypropylene foams**

One key morphological parameter of major importance influencing the mechanical properties of foams is the open cell content. The open cell content is mainly connected with how the mass is distributed in the foam. When the mass is mainly placed in the cell walls we are dealing with closed cell foams. And, on the contrary, open cell foams are obtained when the mass is mainly placed in the edges. This mass distribution is strongly connected with how the foam withstands the external stresses applied, therefore strongly influences the mechanical properties. Homogenous mass distributions (mass placed in the cell walls) yield stiffer foams so in general, for structural applications, closed cell foams are required [6, 19]. A study of the dependency of the elastic modulus in compression with the open cell content has been also performed. The study was carried out using exclusively the pure HMS PP. Varying the azodicarbonamide content between 2 wt.% and 5 wt.% and fixing the rest of the foaming conditions, different open cell contents were achieved maintaining constant the anisotropy ratio, cell size and homogeneity [14]. Seven different specimens were produced with seven different open cell contents. The specific elastic modulus and collapse strength (property divided by the foam density) in compression was measured for all of them and correlated with the corresponding open cell contents in figure 3.
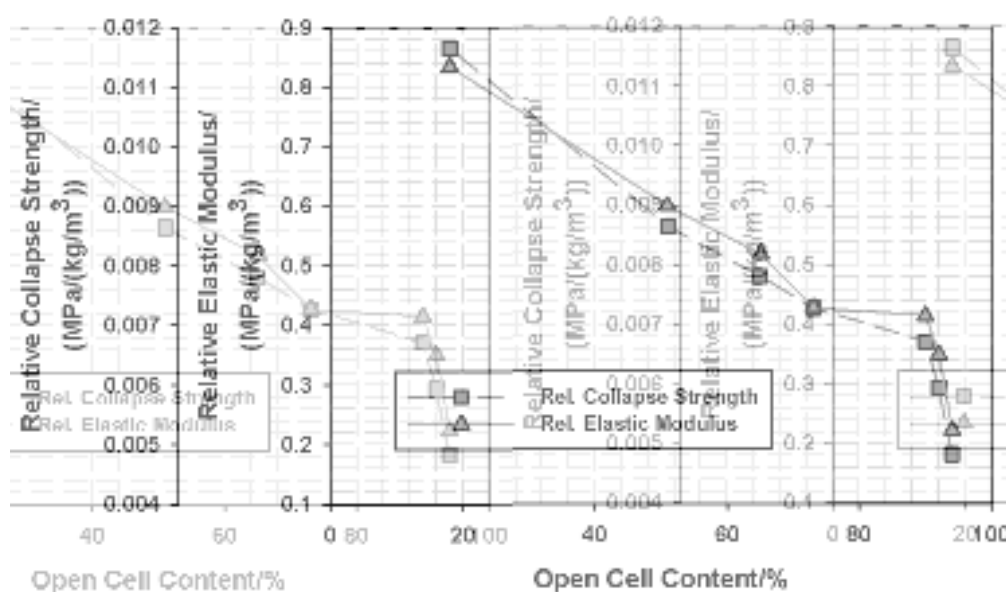
Figure 3: Correlation between open cell content, compressive modulus and collapse strength for the pure PP foams.

The mechanical properties are drastically reduced when the cells in the foam are interconnected. At high open cell contents slight variations in the interconnectivity produce important differences in the mechanical performance. Both the elastic modulus in compression and the collapse strength follow the same tendency. With this unreinforced polymer matrix, good specific mechanical properties are only reached with closed cell cellular structures.

- **Mechanical properties of filled polypropylene foams**

The tensile modulus of the solid specimens was also measured in order to quantify the improvements produced by the addition of the nanofillers. The pure HMS PP presents a 1.98GPa modulus that is increased to a value of 2.20GPa for the samples containing nanoclays. Surprisingly the addition of 1 wt.% of carbon nanotubes negligibly improves the elastic modulus (Table 3). A poor coupling between the polymer matrix and the carbon nanotubes and/or the presence of bundles of nanotubes could justify the negligible reinforcement found.

Table 3: Elastic Modulus of the solid samples filled with different kinds of nanoparticles

Solid Sample	Elastic Modulus/GPa
Pure PP HMS	1.98
PP + MWCNT	2.02
PP + NC	2.21
PP + NNC	2.18

At equal open cell contents, the elastic modulus of the foams produced from the nanocomposites containing clays are remarkably higher than the unfilled ones. The same behavior is found for the collapse strength. These interesting results are depicted in figure 4
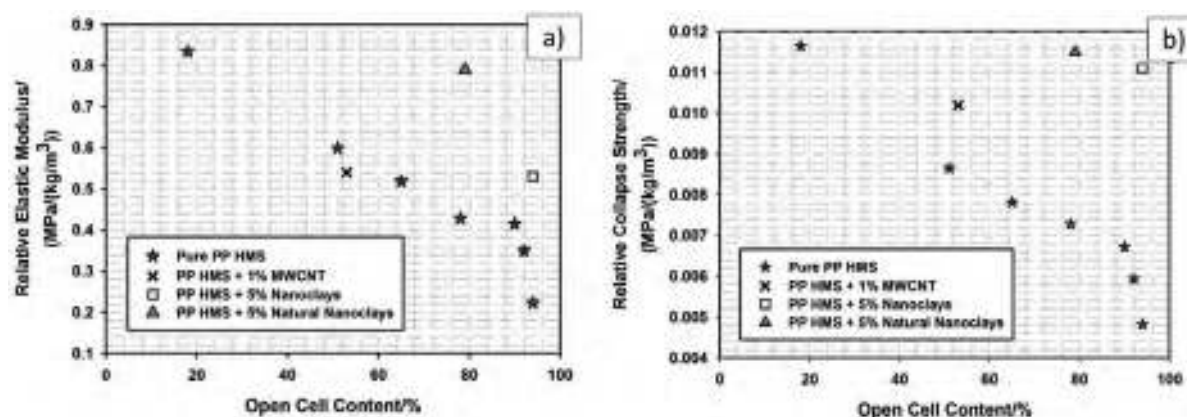

Figure 4: Comparison between the elastic modulus and collapse strength of filled and unfilled polypropylene at certain open cell contents.

At equal open cell contents the specific elastic modulus of the samples containing natural nanoclays almost doubles the value of the unfilled one and the addition of organomodified nanoclays multiplies by 2.5 the specific elastic modulus in compression of the unfilled samples at a open cell content higher than 90%. The anisotropy ratio of unfilled and of nanoclays-filled samples is practically the same so the improvements found in elastic properties at fixed open cell values could be attributed, partly, to the reinforcement of the nanoparticles over the solid matrix. When the interconnectivity of the cells is high, the solid matrix acquires a more relevant role withstanding the external applied stresses. But this is not the only reason behind. The reinforcements over the solid matrix showed in table 3 do not justify the improvements found on the foams. Two other reasons are proposed to support these results. In the case of the nanoclays it has been demonstrated in previous works that the foaming by itself promotes the exfoliation of the nanoparticles yielding higher mechanical properties [40]. Besides this, the presence of nanoclays gives rise to a bimodal cell size distribution, with two main different populations of cells, some bigger ones and some smaller ones. The smaller cells, only present in the samples with clays, can be acting as reinforcement points conferring the foams an improved compressive behavior. In the case of the MWCNT the specific mechanical properties are slightly lower. As previously mentioned the reinforcement over the solid matrix does not exists. This fact, together with the lower anisotropy values achieved in these foams, diminish the mechanical performance of these samples.

Collapse strength of the foams depends more strongly on the properties of the solid matrix than on other structural parameters as the anisotropy ratio. This result can be inferred from figure 4b). At comparable open cell contents the filled samples present improvements in collapse strength in all the cases (18% improvement for MWCNT, 58% improvement for Natural Nanoclays and 130% improvement for Organomodified Nanoclays). Even for the samples containing carbon nanotubes, that present a smaller anisotropy ratio, the collapse strength is increased. The case of the organomodified clays is interesting. At a higher open cell content

than the natural nanoclays (94% to 78%) they present a similar collapse strength due to the higher reinforcement of the organomodified nanoclays on the solid matrix.

GENERAL OVERVIEW AND COMPARISSON WITH OTHER STIFF FOAMS USED IN STRUCTURAL APPLICATIONS

For the sake of comparison the elastic modulus in compression was measured also in two commercial materials, one based in a PVC solid matrix and the other one based on a SAN solid matrix. The PVC based foams are cross-linked, losing any recyclability. Both the PVC and the SAN based materials are used as cores and structural panels for applications such as yachts, wind power blades, automotive sector or aircraft construction. All these applications seek a high stiffness-to-weight ratio in their core materials. The PVC foams (produced by DIAB) are closed cell with an homogeneous and isotropic cellular structure. The SAN foams, commercially named Corecell, are produced by Gurit and share properties with their counterparts: closed cell structure, homogeneity in the cell size distribution and isotropy.

Although the solid PVC or SAN are stiffer matrices than the polypropylene (typical elastic modulus are 3 GPa for PVC, 3.75GPa for SAN and 2 GPa for PP) the compressive modulus of the PP-based foams are comparable or higher in the two studied densities of 150 kg/m^3 and 180 kg/m^3. The high anisotropy ratios achieved compensate for the lower stiffness of the polypropylene matrix, yielding high specific mechanical properties for the developed foams. Even the >90% open cell organomodified nanoclays filled foams have acceptable properties compared to the commercial materials. The theoretical estimation with n=1.5 included in figure 5 is made using an elastic modulus of 2 GPa for the solid according to the formula $E_f = E_S \left(\frac{\rho_f}{\rho_s}\right)^n$ where E_f and E_s represent the elastic modulus of the foam and of the solid respectively, ρ_f and ρ_s represent the density of the foam and of the solid and n is a variable exponent between 1 and 2 [6]. Conventional foams have a value of n near 2 so the value of n=1.5 found in our samples gives an idea of the improved mechanical behavior achieved in our samples.

A different trend is found for the collapse strength. This property is more influenced by the modulus of the solid matrix than the compressive modulus and this fact is reflected in figure 5 right. The commercial foams based in PVC or in SAN present, at any density, much higher collapse strength values since they are based in stiffer matrices. The reinforcement produced by the nanoclays over the solid matrix yield comparable or higher collapse strength values even when these foams have open cells. The lower values are found for the MWCNT according to their non-reinforcement and lower anisotropy ratios.

As a final conclusion low density foams have been produced based on a non cross-linked polypropylene matrix with high specific compressive properties in two different versions: open and closed cell. It is not so common finding open cell foams with good mechanical behavior so these are novel materials. The openness of the cells confers these foams improved properties as sound absorbers and filtration capabilities.
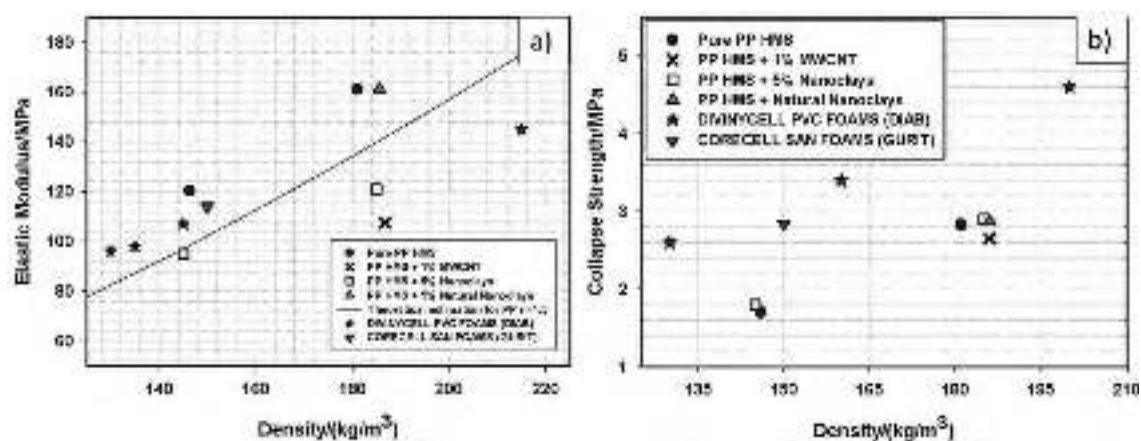
Figure 5: General map of compressive modulus (left) and collapse strength (right) for the different nanocomposites. Two commercial materials have been included for comparison.

CONCLUSIONS

A direct correlation has been established between the cellular morphologies obtained in terms of open cell content and the mechanical properties in compression for several pure and nanoreinforced PP based foams. Slight variations in the interconnectivity (at high interconnectivities) of the cells have a high impact on the measured mechanical properties. In the unfilled polypropylene high specific mechanical properties are only achievable with low values of open cell content. In comparison, for an equal value of interconnection between cells, the samples containing nanoclays present much higher specific properties. This result is attributed to the reinforcement of these nanoparticles on the solid matrix, due to an improved exfoliation during the foaming process and the presence of a bimodal cellular structure.

The combination of a branched high melt strength polypropylene with the improved compression molding foaming route allows obtaining non-cross-linked polypropylene foams with densities as low as 150 kg/m³ and below. Because of the inherent anisotropy ratio obtained due to the foaming route these foams present also high specific mechanical properties, comparable to commercial foams produced from cross-linked stiffer solid matrices. Two different types of materials can be distinguished, both with high specific properties. The first one based on unfilled polypropylene can be considered as closed cell (values <20%). The second one corresponds to foams that combine good mechanical performance with high open cell contents (>80%). These later foams are obtained with the addition of nanoparticles, mainly nanoclays, to the branched polypropylene.

BIBLIOGRAPHY

[1]   Klempner D., Sendijarevic V. handbook of polymeric foams and foam technology. 2ndedn. Hanser Publisher. Munich. (2004)

[2]   Eaves D. Handbook of polymeric foams. Rapra Technology, Shawbury (2004).

[3]   Leaversuch R. D. Mod.Plast73, 52 (1996).

[4]   Park C. B., Cheung L. K. PolymEngSci 37 (1) 1-10 (1997)

[5]   Lee S. T., Foam Extrusion Principles and Practice. CRC Lancaster (2000).

[6]   L. J. Gibson, m. F. Ashby. Cellular Solids. Cambridge University Press.United Kingdom (1999).

[7]   Chaudhary A. K., Jayaraman. Polym. Eng. Sci. 51 (9) 1749-1756 (2011)

[8]   Zhai W., Kuboki T., Wang L., park C.B. Ind. Eng. Chem. Res. 49 (20) 9834-9845 (2010).

[9]   Antunes M., Realinho V., Ardanuy M., Maspoch M. Ll., Velasco J. I. Cell. Polym. 30 (4) 187-200 (2011)

[10]   Velasco J. I., Antunes M., Realinho V., Ardanuy M. Polym. Eng. AndSci. 51 2120-2128 (2011)

[11]   Gong W., Gao J., Jiang M., He L., Yu J., Zhu J. Polymer 122, 2907-2914 (2011)

[12]   Rachtanapunp P., Matuana L. M., Selke S. E. M. SocPlastEngAnnu tech Conf 2003, 61, 1762.

[13]   Rachtanapunp P., Selke S. E. M., Matuana l. M. PolymEngSci 44, 1551-1565 (2004).

[14]   Saiz-Arroyo C., de Saja J. A., Velasco J. I., Rodriguez-Perez M. A. J. Matter Sci 47 (15) 5680-5692 (2012)

[15]   Miller D., Chatchaisucha P., Kumar V. Polymer 50 (23) 5576-5584 (2009).

[16]   Miller D., Kumar V. Polymer 52 (13)2910-2919 (2011).

[17]   Weller J., Kumar V. PolymEngSci 50 (11) 2160-2169 (2010).

[18]   Weller J., Kumar V. PolymEngSci 50 (11) 2170-2175 (2010).

[19]   A. T. Huber, L. J. Gibson. J. Mat. Sci 23. 3031-3040 (1988).

[20]   Jang W. Y., Kraynik A. M., Kyriakides S. Int. J. Solid. Struct. 45 (7-8) 1845-1875 (2008)

[21]   Rodriguez-Perez M. A. Adv. PolymSci. 185 55-56 (2005)

[22]   Rodriguez-Perez M. A., Velasco J. I., Arencon O., de Saja J. A. J. ApplPolym Sic 75 (1) 156-166 (2000)

[23]   Lee T., Lakes R. S. J Mat Sci 32 (9) 2397-2401 (1997).

[24]   Simard Y., Lalancette E., Jones D. T. U. S. patent 0104478 (2011)

[25]   Alderson A., Alderson K. L., Davies P. J., Smart G. M. U. S. patent 0029796 (2010).

[26]   Duwenhorst J., Ruellmann M., Prissok F., Lasai S., Mayer S., Harms M., Gabriel C. U. S. patent 0038579 (2010).

[27]   Zheng W. G., Lee Y. H., park C. B. J. Appl. Polym. Sci. 117 2972-2979 (2010).

[28]   Ahmadi A. A., Hornsby P. R: Plas Rubber proc Appl. 5 (35) (1985).

[29]   Nojiri A., Sawasaki T., Koreeda T. U.S. Patent 4424293 (1984).

[30]   Nojiri A., Sawazaki T., Konishi T., Kudo S., Onobori S. Furukawa rev. 2 (34) (1982).

[31]   Lee Y.D. Wang L. F. J. Appl. Polym. Sci. 32 4639-4647 (1986).

[32]   Naguib He., park C. B., Panzer u. Polym. Eng. Sci 42 1481-1492 (2002).

[33]   Zhai W., Kuboki T., Wang l., Park C. B., Lee E. K., Naguib H. E. Ind. Eng. Chem. Res. 49 9834-9845(2010).

[34]   Bhattacharya S., Gupta R. K., Jollands M., Bhattacharya S. N. Polym. Eng. Sci. 49 2070-2084 (2009)

[35]   Rodriguez-Perez M. A., Lobos J., Perez-Muñoz C. A., de Saja j. A. CellPolym 27 327-342 (2008)

[36]   Rodriguez-PerezM. A., Lobos J.,Perez-Muñoz C. A., de Saja j. A. J. CellPlast 45 389-403 (2009)

[37]   Rodriguez-Perez M. A., Simoes R. D., Roman-Lorza S., Alvarez-Lainez M., Montoya-Mesa C., Constantino C.J.L., de Saja J. A. PolymEngSci 52 62-70 (2011).

[38]   Y. Ma, Pyrz R., Rodriguez-Perez M. A., Escudero J., Rauhe J. Ch., Su X. CellPolym 30 (3) 95-109 (2011).

[39]   Pinto J., Rodriguez-Perez MA., de Saja JA in XI Reunión del Grupo Especializado de Polímeros (GEP) 10-14 September 2009, Valladolid. Spain.

[40]   J. I. Velasco, M. Antunes, O. Ayyad, C. Saiz-Arroyo, M. A. Rodríguez-Pérez. F. Hidalgo, J. A. de Saja. J App PolymSci 105, 1658-1667 (2007).

Chapter 7

Conclusions and Future Lines

This chapter summarizes the main conclusions yielded from the different research lines followed along the work. In second place future research lines connected with the thesis are suggested.

7.1.- CONCLUSIONS

Modifications in the Polymer Matrix

- The chemical composition of polyolefin-based cellular materials (low density polyethylene LDPE) has been modified by the addition of an inorganic nanometer-sized phase (organomodified montmorillonite nanoclays) and a maleic grafted polyethylene (LLDPE-g-MA) acting as coupling agent. The nanocomposites have been produced by melt blending and foamed using two different routes: batch gas dissolution and free foaming. It allows to make comparisons between the structures and properties of the foams obtained in each different route.

- The dispersion and delamination of the nanoclays in the polymer matrix have been analyzed. The use of a coupling agent and the shear forces developed during the melt blending promote the intercalation and dispersion of the nanoparticles but the exfoliation is not complete. All the nanocomposites present an intercalated/exfoliated morphology. Despite this uncompleted exfoliation the effect of the nanoclays over the solid composites is clear. The thermal stability is increased proportionally to the clays addition. The tensile, compressive and bending properties are also improved. The nanoparticles also have a nucleating effect increasing the crystallinity of the polymer matrix. Especially remarkable is the influence of the nanofillers over the rheological behavior. The Trouton ratio of the polymer matrix is patently lowered in the presence of nanoclays. All these properties are later connected with the properties and structure of the foams.

- As a prior step to the foaming by batch gas dissolution, the solubility and diffusivity of the composites is studied by gravimetric techniques. Nanoclays reduce diffusivity in percentages below 11%. This small reductions in diffusivity can be attributed to the interface polymer-clays which also justifies the higher solubilities found in the samples containing clays. The presence of a coupling agent by itself (excluding the effect of the nanoclays) yields reductions in diffusivity up to 30%. The polar character of the maleic anhydride and its high affinity with CO_2 justify this result.

- The addition of a maleic anhydride grafted polyethylene (excluding nanoclays) helps to improve the cellular structures (smaller cell size, higher homogeneity, lower bulk density) when the composites are foamed by batch gas dissolution. This same conclusion is obtained using other foaming routes. Expansion ratios up to 2 and cell sizes below 80 μm have been obtained dissolving CO_2 in sub-critical conditions in a semi-crystalline polymer matrix. The addition of nanoclays strongly deteriorates the cellular morphologies and prevent from reaching densities below 600 kg/m^3. This is connected with reductions in Trouton ratio already mentioned, which turns to be a fundamental parameter influencing foamability. Although this detrimental role played during foaming, nanoclays have an interesting nucleating effect, not in the sense of reducing cell size but lowering the amount of energy needed for the nucleation and growth of cells. Foaming is accelerated in samples containing nanoclays, with cellular structures that begin growing earlier.

- The chemical composition of the previously mentioned nanocomposites has been modified with a crosslinking agent, dicumyl peroxide (DCP), that, when thermally decomposed, modifies the molecular architecture of the polymer matrix generating a three-dimensional network. These crosslinked composites have been foamed by batch gas dissolution using CO_2 in sub-critical conditions.

- Crosslinking reduces the crystallinity and hence increases the gas solubility and diffusivity of the polymer matrix. This has been measured using gravimetric techniques prior to the foaming step.

- Crosslinking greatly improves the foamability of the nano-filled samples, allowing obtaining a proper cellular structure which was not possible in the non-crosslinked samples as has been already mentioned.

- There is an optimum degree of crosslinking that yields cell sizes below 15 μm, cell densities of $1 \cdot 10^9$ cells/cm^3 and bulk densities around 140 kg/m^3 using a semi-crystalline polymer and CO_2 in sub-critical conditions. This optimum crosslinking degree is connected with the optimum rheological behavior in terms of extensional viscosity and Trouton ratio. Rheological behavior is a key parameter, even more important than crosslinking degree, for the foamability of the samples.

- Optical expandometry has turned to be a very appropriate method for studying the free foaming behavior of these nanocomposites. It gives a lot of valuable information in an easy way.

- Nanoclays have a catalytic effect over azodicarbonamide, accelerating its decomposition and increasing the amount of gas released in their presence. Therefore higher maximum expansion ratios are reached in the filled samples together with higher expansion rates. On the other hand the stability of the nanocomposites is poorer, once again connected with the lower Trouton ratio value measured for them.

- Again, the addition of a coupling agent (without nanoclays) helps to reach higher expansion ratio but has no influence on the foaming onset temperature or collapse rate. The stability time remains the same too.

- The degree of exfoliation of the nanoclays, measured by x-rays diffraction, is higher after foaming. This is a first indication that the foaming, by itself, promotes an increase in interlamellar spacing between clay platelets. This result motivates the study of this phenomenon by energy dispersive synchrotron radiation.

- Synchrotron radiation allows us to obtain continuous diffraction patterns during the whole foaming time of the samples. This way we can characterize and relate the evolution of the exfoliation of the clays with the evolution of the foam. Three different blowing agents (azodicarbonamide, Hydrocerol and Expancel (expandable microspheres)) of different nature and with the different foaming mechanisms has been used to discard any effect of the foaming gas used or foaming mechanism.

- The increment of interlamellar spacing while foaming occurs, in a higher or lower extent, independently of the blowing agent used. Therefore the phenomenon is mainly associated with the foaming itself and not with the kind of gas or foaming procedure used.

- Melt blending azodicarbonamide with the nanocomposites containing clays gives as result an initial increase in the interlamellar spacing of these nanoparticles. This does not happens with the other two blowing agents. A chemical interaction between azodicarbonamide and organomodified nanoclays is postulated. This chemical interaction helps to the clays delamination during

blending and it seems to be connected with the catalytic effect of the used nanoclays in the decomposition temperature of azodicarbonamide.

🌑 The thermally activated higher mobility of the polymer molecular chains is also connected with increments in the interlamellar spacing of the nanoclays.

🌑 The maximum increments in interlamellar spacing are found for the samples with higher expansion ratios. More indeed, the increase in interlamellar spacing is proportional to the expansion ratio achieved, independently of the blowing agent used.

🌑 A methodology for following in-situ the exfoliation of nanoclays during foaming has been established. Since the beneficial effects of nanoclays can only be expected when high exfoliation degrees are achieved, foaming is demonstrated to help in this purpose.

🌑 Once again the chemical composition of the previously mentioned nanocomposites has been modified with a crosslinking agent, dicumyl peroxide (DCP), that, when thermally decomposed, modifies the molecular architecture of the polymer matrix generating a three-dimensional network. These crosslinked composites have been foamed by compression molding using a chemical blowing agent (azodicarbonamide)

🌑 A method to produce big blocks of low density (more than 30 expansions) closed cell polyethylene foams filled with montmorillonite-type nanoclays is presented. This high expansion ratio is demonstrated to patently improve the exfoliation degree of the nanocomposites, supporting the conclusions obtained in previous works.

🌑 The addition of a linear low density polyethylene grafted with maleic anhydride (coupling agent), in composites without nanoclays, reduces the mean cell size and increase the cell density at the same bulk density. This result is in the same line as the ones obtained by batch gas dissolution and free foaming.

🌑 The presence of nanoclays in these foams helps to improve mechanical properties in tension and compression but in a lower extent than the improvement obtained in the solids. There is no synergetic effect between the nanoparticles and the foaming procedure. Mechanical properties in compression are higher than in tension. This is due to the preferential orientation of the cells

coinciding with the compression direction, induced by the expansion during foaming.

🔘 Nanoclays and maleic grafted polyethylene increase the energy absorbed in compression and this improvement is maintained along consecutive compressive cycles.

🔘 The effective diffusion coefficient (under static loading) has been experimentally determined for the filled and unfilled composites allowing elucidating the gas barrier role played by the nanoclays. In spite of the high exfoliation degree measured by x-rays diffraction, the reductions in diffusivity are not very remarkable when nanoclays are present. On the contrary, in the samples containing coupling agent (without clays) the reductions in diffusivity are more significant thanks to the linear character of the coupling agent and the high affinity of CO_2 with maleic anhydride. These results coincide with the results obtained previously by batch gas dissolution using gravimetric methods and the same hypothesis (presence of interfaces polymer-nanoclays) is postulated.

Modifications in the cellular structure

🔘 A new foaming route is presented for the production of structural foams, that is, foams with skin-core morphology as described in chapter 5. This new foaming route has nothing to do with injection molding, showing several advantages in comparison to this latter one. The pressures developed during the production are much lower than by injection, so cheaper molds can be used. The initial investments required are also lower and the surface quality of the parts is good.

🔘 The physical mechanism behind the consecution of these structural foams consists in a process of gas dissolution in an amorphous material. The mold inner walls are covered with an amorphous material. During foaming, the gas from the outer parts of the foam migrates to the amorphous material covering the mold walls. This results in solid skins in all the areas in close contact with the amorphous material.

🔘 The final morphology of the structural foam is influenced by the foaming parameters and the amount of blowing agent. Foaming time affects the outer solid skins so the skin thickness can be independently controlled from the bulk density of the foam just varying the foaming time.

- The skin-core morphology of structural foams produced following this new technology is equivalent to the one of foams produced by injection molding. Two solid outer skins are found with a cell size profile incrementing from the outer parts to the center.

- Chemical composition, proportions and foaming procedure for structural foams is the same as for conventional foams (excluding the coverage of the mold walls with a amorphous material). Therefore, the properties of structural and conventional foams can be scientifically compared using this foaming technique independently of other variables.

- Specific mechanical properties of these structural foams are higher than conventional foams. Especially in bending properties, with increments above 50%.

- This novel technology for the production of structural foams is enclosed in a more general one named Stages Molding and is currenty patented. The corresponding patent can be found at the end of the manuscript. This fact withstands the industrial applicability of the technology developed.

Combination of modifications in the polymer matrix and in the cellular structure

- Low density polypropylene foams produced by improved compression molding from high melt strength polypropylene matrices were characterized by x-rays microtomography. This technique is very useful in the characterization of relevant parameters as three-dimensional anisotropy, sphericity, cell volume distribution or connectivity of the cells.

- In a first step relationships between the processing parameters and the geometrical features of the foams are established. The influence of foaming time and amount of blowing agent over structural characteristics as connectivity of the cells or homogeneity of the cellular structure is evaluated.

- The previous process-structure relations are very useful for, later on, establishing relationships structure-mechanical-properties.

- The rheology of the selected polymer matrix is fundamental for the foamability and foam quality. The strain hardening coefficient of the formulation directly determines the amount of interconnected cells in the foam.

- The addition of nanoparticles such as organomodified nanoclays, natural nanoclays or carbon nanotubes prevent the occurrence of strain hardening. Therefore the cellular structures of foams containing nanoparticles are

characterized by high open cell contents. Different open cell contents can be achieved also in the non-filled foams varying the blowing agent content and selecting the right processing parameters.

🌑 The open cell contents affects remarkably to the elastic modulus of the foams, measured in compression. The elastic modulus decreases strongly when the open cell content of the foam increases. The highest mechanical properties are found when the foams are completely closed cell.

🌑 Nano-filled foams always present high open cell contents. In comparison to non-filled foams, in spite of having high open cell contents nano-filled foams present higher mechanical properties. This comes as a result of the reinforcement role played by nanoparticles and thanks also to the double population of cells found in the filled foams.

🌑 The combination of a branched high melt strength polypropylene with the improved compression moulding foaming route allows obtaining non-crosslinked polypropylene foams with densities as low as 150 kg/m^3 and below. Because of the inherent anisotropy ratio obtained due to the foaming route these foams present also high specific mechanical properties both with open and close cell morphologies. These mechanical properties are comparable or higher than those of commercial foams based on stiffer matrices as PVC or SAN. Nevertheless other mechanical properties as collapse strength depend more on the properties of the solid matrix than in the cellular structure of the foam.

🌑 These foams based on non-crosslinked polypropylene with low densities and high specific mechanical properties can cover a wide range of industrial applications such as cores for wind power blades or panels for the yachts industry, the automotive sector or the aeronautical industry. The technology is currently patented and the patent can be found in Annex I of this manuscript.

7.2.- FUTURE LINES

Modifications in the Polymer Matrix

🌑 Produce foams with different kinds of nanoclays as for example sepiolites. Use different coupling methods and study their nucleating effect in terms of coupling degree and geometry.

- Crosslinking the LDPE with electrons irradiation. Achieve the same crosslinking degrees with this procedure and compare the foaming behavior with the samples chemically crosslinked.

- Add lower contents of azodicarbonamide and repeat the optical expandometry study. Study the influence of the azodicarbonamide content over all the parameters studied by optical expandometry.

- Combine the synchrotron radiation study with optical expandometry or radioscopy to correlate in the same experiment the exfoliation degree with the expansion ratio.

- Study the interaction between modified nanoclays-coupling agent-azodicarbonamide from a chemical point of view, Explain chemically the catalytic effect of the nanoclays over the azodicarbonamide and the other effects exposed in this work.

- Improve the dispersion, exfoliation and coupling of nanoclays added to LDPE. Use the same semi-empirical method to study the gas diffusion on this LDPE matrices with improved dispersion, exfoliation and coupling of nanoclays.

- Reduce the nanoclays content to values of 1 wt.% or lower and repeat the diffusion study with the semi-empirical method.

- Open cell content is a parameter useful to be considered to correlate with or explain the diffusion coefficients obtained. This parameter can be measured with air pycnometry and added to the rest of the study.

Modifications in the cellular structure

- Extend the same structural foams production route to other polymers such as polypropylene. Use, as well, other foaming agents that generate comparable gas pressures.

- Study by x-rays radioscopy the evolution of the solid skins and skin thickness and correlate with the expansion kinetics.

- Obtain different skin thicknesses for the same bulk density. Model the mechanical properties theoretically an compare with the data obtained experimentally.

Combination of modifications in the polymer matrix and in the cellular structure

- Study other properties as acoustic behavior, filtration of thermal properties in the low density non-crosslinked high mechanical properties polypropylene foams.
- Extend the production route to stiffer polymer matrices.

Annex I

Patents

I.1.- INTRODUCTION

As already mentioned in previous chapters part of the work conducted during this doctoral thesis gave rise to two different novel technologies for the production of cellular materials. These two technologies were officially patented and registered and the two corresponding patents are presented in this chapter.

I.2.- PATENT 1. SYSTEM AND METHOD FOR MOULDING PARTS USING FREESTANDING MOULDS

The first patent has the international publication number WO/2012/117143 and corresponds to the technology mentioned as "Stages Molding" during the rest of the thesis. The title of the patent is "System and method for moulding parts using freestanding moulds". This patent encloses, as a particular case, the production of structural foams using the procedures described in Chapter 5. It is presented as an alternative to the conventional injection moulding based routes for the production of cellular materials in a wide range of relative densities that go from 0.5 to 1. Cheaper moulds are employed and the machinery used shows a higher simplicity than injection moulding. Altogether, Stages Moulding allows for the production of complex shaped parts from a wide variety of polymers with excellent surface quality and reduced thermal and mechanical stresses.

1

SISTEMA Y PROCEDIMIENTO DE MOLDEO DE PIEZAS CON MOLDES
AUTOPORTANTES

Campo de la invención

5   La invención se engloba dentro del campo de los sistemas de fabricación de piezas de diversos materiales poliméricos y otros aditivos con diferentes características como piezas compactas, piezas estructurales de densidad reducida o piezas de densidad reducida.

Antecedentes de la invención

10   La mayor parte de los precedentes de esta invención están relacionados con el moldeo por inyección, que es la tecnología más extendida para la fabricación de piezas de productos plásticos.

John Hyatt patentó en 1872 el primer sistema de inyección, compuesto por un pistón que contenía derivados de la celulosa fundidos en una cámara. Sin embargo, no

15   es hasta 1928 cuando se atribuye a la compañía alemana Cellon-Werkw, la primera patente de una máquina de inyección moderna. Paralelamente, Beard y Delafield desarrollaron la técnica en Inglaterra, con los derechos de la patente inglesa para la compañía F.A. Hughes Ltd. Los sistemas anteriores funcionaban con aire comprimido, la extracción y parte de los controles eran manuales y carecían de sistemas de

20   seguridad.

En 1932 se patentó la primera máquina de inyección operada por sistemas eléctricos (Eckert & Ziegler). Es en esta década cuando el polietileno (PE) y el policloruro de vinilo (PVC), materiales de alta producción y bajo coste, provocaron una revolución en el desarrollo de la maquinaria. Ya en 1956 se patentó el primer sistema

25   de inyección mediante husillo en EEUU, esta aportación supone el cambio de mayor relevancia en el desarrollo de los sistemas inyectores. A partir de la década de los 80, las mejoras se enfocan a la automatización de los diseños, la eficacia y el control de los procesos.

Un sistema de moldeo por inyección tradicional está formado por tres módulos

30   principales: la unidad de inyección o plastificación del polímero fundido, la unidad de cierre, que soporta el molde y el sistema de apertura, cierre y expulsión de la pieza; y por último, la unidad de control de todos los parámetros involucrados en el proceso. Es importante resaltar que en esta tecnología se usan moldes que no son autoportantes y que las temperaturas del molde son en general claramente inferiores a la temperatura

35   de reblandecimiento de las materias primas utilizadas.

2

El proceso de obtención de una pieza de plástico inyectada sigue un orden de operaciones que se repite en cada una de las piezas. Este proceso recibe el nombre de ciclo de inyección, y está formado por las siguientes etapas: cierre del molde, fase de plastificación o dosificación, inyección del plástico (llenado y mantenimiento),

5 enfriamiento, y por último apertura del molde y expulsión de la pieza. De todas las etapas anteriores es la etapa de enfriamiento la que ocupa el mayor tiempo dentro del ciclo.

Los diseños actuales de un sistema de moldeo por inyección están condicionados por las necesidades geométricas de las piezas y los diferentes

10 polímeros involucrados. Generalmente se trata de disponer de sistemas rápidos de inyección, bajas temperaturas y un ciclo de moldeo corto que asegure menores costos de producción.

En resumen, el moldeo por inyección es una técnica completamente desarrollada de ventajas suficientemente conocidas, si bien presenta algunos

15 inconvenientes desde el punto de vista del proceso y la realización de ciertos tipos de piezas. Se discuten a continuación dichas desventajas.

Para comenzar la fabricación de un tipo de pieza es necesario realizar un complicado montaje del molde en el equipo de inyección. Posteriormente, es necesario, preparar el sistema y calibrarlo, para comenzar la tirada de una sola serie

20 de piezas. Dicha tirada debe ser lo suficientemente numerosa para que todo el proceso sea rentable. Adicionalmente, debido a las altas presiones de trabajo, los moldes utilizados son muy costosos, por lo que la inversión, en máquina y moldes, es muy elevada.

En segundo lugar, las piezas obtenidas mediante moldeo por inyección suelen

25 presentar baja calidad superficial, presentan líneas de soldadura, rechupes y están sometidas a elevadas contracciones térmicas, lo que se debe a que la pieza ha sido sometida a estrés térmico y mecánico. Además el volumen máximo de las piezas fabricables mediante esta tecnología está limitado a unos 10 litros por las elevadas presiones necesarias para llenar los moldes. Por último, existen ciertas limitaciones en

30 las materias primas que se usan. Por ejemplo, es necesario usar polímeros de baja viscosidad (elevado índice de fluidez) y no es posible emplear formulaciones con elevados cantidades de refuerzos o cargas (en la práctica no se suelen usar cantidades de refuerzo superiores al 30% en peso) por el incremento de viscosidad que producen estos materiales y que dificulta el llenado del molde.

35 Podemos por tanto concluir que mediante el moldeo por inyección, es posible

3

obtener piezas compactas de volúmenes inferiores a 10 litros asumiendo una elevada inversión inicial y un acabado superficial mejorable. El proceso sólo resulta rentable cuando el número de piezas fabricadas es muy elevado.

Durante las últimas décadas han surgido algunas tecnologías que introducen variantes importantes en el proceso tradicional de moldeo por inyección, con el objetivo de mejorar algunos de los inconvenientes de está técnica. A continuación se revisan los avances más destacados:

- Coinyección: El sistema de coinyección (US2009152768(A1), US200301283(A1)) posee sistemas de inyección independientes, permitiendo el uso simultáneo de materiales poliméricos estéticos y reciclados. Se diseñó como alternativa al proceso estructural de espumado. A diferencia de otros procesos multicomponente, en la coinyección uno de los materiales puede encapsular al otro. Este proceso proporciona buenos acabados superficiales, reducción de coste y en algunos casos piezas estructurales celulares. La viscosidad y temperatura de fusión de ambos componentes es el parámetro de control fundamental para que el proceso sea eficaz. Como inconvenientes, referentes al equipamiento, supone una gran inversión y amortización de moldes, y está restringido a tiradas masivas.

- Heat & Cool: El sistema Heat and Cool (JP 60 111335 A, US4963312, US6451403) se basa en un control exhaustivo de la temperatura del molde, realizando un ciclado térmico del molde que se calienta y enfría en cada ciclo para proporcionar un mejor acabado superficial, Las piezas obtenidas presentan elevado brillo y resistencia, menores tensiones internas, y reducidas líneas de unión y de flujo. Nuevamente, este sistema requiere de una gran inversión en moldes por las altas prestaciones mecánicas requeridas, además de la incorporación de un sistema de calentamiento y enfriamiento al molde y de un incremento de los tiempos de ciclo respecto al proceso convencional. En la actualidad este proceso suele estar restringido a la fabricación de piezas para los sectores de automoción y electrónico.

- GAIM: La Inyección asistida por Gas (ES 2253281T3, WO03091007A1, DE4435012 (C1)) moldea piezas plásticas con secciones huecas en su interior, consiguiendo así reducción en la cantidad de materia prima, ciclos más cortos y reducción del estrés térmico, mejorando el acabado superficial y reduciendo las fuerzas de cierre del sistema. Este sistema no es válido para la fabricación

4

de todo tipo de piezas inyectadas y supone una gran inversión inicial, precauciones por el trabajo con gas inerte a presión, mayor especialización y mayor número de variables en el proceso de difícil control. Además, el espesor de la pieza con sección hueca no es predecible ni uniforme, aunque si es

5   reproducible.

- WIT o WAIM: Una variante del sistema anterior es la Inyección asistida por Agua (WIT) (DE 19518963 A, US 6896844, WO2007036037), en la que se sutituye las funciones realizadas por el gas en el sistema previo por agua a presión con el objetivo de reducir el tiempo de enfriamiento. Este sistema

10   mejora las propiedades de la pieza obtenida, el tiempo de ciclo y el control del espesor, comparando con el sistema GAIM, si bien no da solución al elevado coste del sistema y los moldes, su posible corrosión por la introducción en el sistema de agua y el difícil control de los parámetros del proceso.

- MUCELL: Por último, la tecnología Mucell (US6169122, US6231942,

15   US6235380, etc) implementa un sistema propio de control de la estructura celular de la pieza con ventajas en el proceso de fabricación y en el coste del equipamiento, pero sólo está disponible para la fabricación de piezas celulares de diferentes materiales plásticos y de dimensiones limitadas, con reducciones de peso bajas (no suelen superar el 25% de reducción de peso) y pobres

20   acabados superficiales.

En cuanto a otras tecnologías de fabricación independientes del moldeo por inyección, como pueden ser el moldeo por soplado, el termoconformado, etc, no proporcionan la versatilidad suficiente para fabricar cualquier tipo de pieza, siendo sólo

25   aplicables a algunas geometrías, tamaños y materiales.

Descripción de la invención

La invención se refiere a un sistema de moldeo con moldes autoportantes que comprende:

30   - un equipo alimentador de material de moldeo en un molde autoportante, que comprende una pluralidad de medios de alimentación de diferentes compuestos para su introducción en los moldes autoportantes como tolvas, unidades de extrusión o unidades de inyección.

- un equipo accionador de un elemento calefactor del molde autoportante,

35   situado junto al propio accionador o en el propio molde autoportante,

5

configurado para el atemperado inicial de un molde autoportante, y para alcanzar el ciclo térmico necesario para conseguir el llenado del molde autoportante. El elemento calefactor puede ser un sistema de hornos fijo a diferentes temperaturas situado en el propio módulo de calentamiento, que proporcione las condiciones de fabricación apropiadas para cualquier pieza del sistema, y se accione por el equipo accionador del elemento calefactor, o puede ser un elemento calefactor móvil situado en el propio molde autoportante que es accionado por el equipo accionador situado en el módulo de calentamiento.

- un equipo enfriador del molde autoportante lleno de material configurado para enfriar el molde autoportante, mediante aire, agua u otros medios, hasta disminuir la temperatura del molde autoportante a valores que permitan la apertura del molde sin deterioro de la forma y calidad superficial de la pieza, y

- un equipo de desmoldeo de la pieza moldeada en el molde autoportante,

siendo todos ellos equipos independientes instalados en módulos de trabajo por los que transita el molde autoportante por medios de desplazamiento seleccionados entre manuales y automáticos, entendiéndose por módulo de trabajo al equipo o conjunto de equipos agrupados en un mismo lugar para la realización de un trabajo específico sobre el molde portante, como calentamiento (módulo de calentamiento), alimentación (módulo de alimentación), calentamiento y alimentación (módulo de calentamiento y alimentación) , enfriamiento (módulos de enfriamiento), (módulo de desmoldeo) desmoldeo....

Ciertos materiales pueden requerir de un mezclado y procesado previo que podría realizarse en una línea de compounding, en un mezclador interno, en equipos para mezclado en frio (dry blending), etc. La alimentación de los moldes puede realizarse con la materia prima a temperaturas por encima de la de reblandecimiento o con las materias primas en estado sólido.

Se entiende por densidad relativa, la densidad de la pieza final obtenida dividida por la densidad del material de partida en el proceso. Es una medida de la porosidad de la pieza fabricada y por tanto es también una medida de la reducción de peso lograda frente a una pieza compacta.

Se entiende por molde autoportante al sistema acoplado de molde y sistema de cierre del mismo. El molde y su sistema de cierre se diseñan de forma que son capaces de soportar las presiones internas y las temperaturas a la que les somete durante todo el proceso de fabricación. Los moldes autoportantes usados en esta

6

invención pueden transitar por los distintos módulos del proceso, en los que tiene lugar las distintas etapas de fabricación, siendo estos moldes estancos al polímero fundido. El molde de esta invención tiene una cavidad interna en la cual se va a fabricar la pieza.

5   En algunas de las variantes de esta invención el molde autoportante tiene una cavidad previa a la cavidad interna del molde que denominaremos colector. Ambos, molde autoportante y colector, mediante un sistema de cierre adecuado forman una unidad autoportante que pueden transitar por las distintas etapas del proceso de fabricación siendo estancos al polímero fundido. La finalidad del colector es facilitar el

10   llenado del molde.

Todas las piezas obtenidas de manera simultánea se han de clasificar por tipos, siendo posible una vez realizado este proceso su adecuado embalado y almacenamiento.

Opcionalmente el sistema puede comprender:

15   - un módulo de almacenamiento de moldes,

como punto de partida del proceso, en el que los moldes se encuentran almacenados en esta estación ya cerrados y listos para comenzar el proceso,

- un módulo de acondicionado del molde o vacío:

20   En algunas variantes de la invención puede ser necesario hacer vacío en el molde, antes de la fase de alimentación, durante dicha fase o tras la misma,

- un módulo para el recubrimiento interno del molde.

En algunas variantes de esta invención puede ser necesario el

25   recubrimiento interno del molde con materiales con capacidad para absorber gases (compuestos siliconados, polisulfonas, politetrafluoroetileno (PTFE), entre otros), este proceso podría llevarse a cabo en una fase anterior a la de alimentación del molde o bien el molde podría haber sido fabricado incorporando dichos recubrimientos.

30   El procedimiento moldeo de piezas con moldes autoportantes que utiliza el sistema anteriormente descrito comprende:

- una etapa de llenado de un molde autoportante que comprende alimentación del molde con material de moldeo de la pieza y calentamiento del molde autoportante, pudiéndose realizar primero el calentamiento del

35   molde y luego la alimentación o primero la alimentación y luego el

7

calentamiento del molde,

- una etapa de enfriamiento del molde autoportante lleno y

- una etapa de desmoldeo de la pieza moldeada en el molde autoportante, una vez alcanzada la temperatura de desmoldeo,

5 realizándose cada etapa en módulos independientes por los que transita el molde autoportante.

El llenado del interior del molde autoportante se puede realizar mediante la alimentación en el molde de un material polimérico mezclado con un agente espumante químico capaz de generar una fase gaseosa, y el calentamiento se realiza

10 por elevación de la temperatura por encima de la temperatura de descomposición de dicho agente espumante, que expande el material que rellena el molde.

Opcionalmente se puede utilizar un molde autoportante con colector, de manera que en la etapa de llenado la alimentación puede realizarse por introducción de material polimérico en el molde autoportante y posterior aplicación de presión en el

15 interior del molde autoportante a través del colector mediante un agente espumante que expande al elevar su temperatura, o mediante otros medios como con pistones hidráulicos o introduciendo vapor, aceite u agua.

Las familias de piezas obtenidas mediante la presente invención pueden clasificarse en tres categorías principales en función de su densidad (ρ) y estructura

20 interna:

Piezas compactas (ρ pieza= ρ material de partida) con densidad relativa 1.

Piezas estructurales de densidad reducida (ρ pieza < ρ material de partida) con densidades relativas entre 0.02 y 0.99 y en las que el material es compacto (denso) en las superficies y poroso en las zonas internas formando lo que se suele denominar una

25 estructura piel sólida - núcleo espumado.

Piezas de densidad reducida (ρ pieza << ρ material de partida) con densidades relativas entre 0.02 y 0.99

Con este novedoso sistema se consiguen solucionar los problemas anteriormente expuestos, permitiendo así:

30 - Fabricar piezas de cualquier forma, tamaño y composición, con la posibilidad de lograr piezas de densidad reducida.

- Lograr piezas con excelentes calidades superficiales y con tensiones internas reducidas.

- Reducir los costes en moldes y maquinaria

35 - Hacer la rentabilidad del proceso menos dependiente del tiempo de ciclo.

8

- Lograr un proceso de fabricación más versátil y que permita la fabricación de varios tipos de piezas de forma simultanea.

El sistema fabricación de piezas por etapas mediante moldes autoportantes, supone un proceso versátil para la fabricación de piezas de muy diferentes tamaños, formas, y composiciones químicas con excelente calidad superficial, bajas tensiones internas, con la posibilidad de fabricar piezas de densidad reducida usando moldes y maquinaría de bajo coste. La tecnología permite fabricar varios tipos de piezas de forma simultánea y elimina la necesidad de montaje de molde y calibración del mismo inherente a los procesos de moldeo por inyección tradicionales.

Una descripción más detallada de los aspectos más destacados de esta tecnología es la siguiente:

▪ Desde el punto de vista de la maquinaria utilizada:

El sistema objeto de la invención es sostenible, no es predecible el fin de su vida útil pues los elementos formadores son independientes y reemplazables.

Permite una elevada reducción de costes, comparado con cualquier sistema de inyección, tanto en maquinaria como en los moldes utilizados.

El proceso es automatizado, estando los moldes codificados de forma que la lectura del código de cada uno permita la aplicación directa de los parámetros de proceso y la fabricación autónoma de cada una de las piezas.

Los moldes son autónomos, sencillos y autoportantes, suponiendo una menor inversión en el proceso y un acceso a mayor número de piezas a fabricar.

La producción de diferentes piezas en distintos moldes es simultánea, de modo que el proceso global pueda ser considerado continuo, para unas mismas o diferentes piezas. Esta característica proporciona versatilidad a todo el sistema, pudiendo coincidir varios moldes a lo largo de todo el proceso en las distintas estaciones.

El sistema requiere de presiones de trabajo muy inferiores a las de la inyección convencional. Las presiones de llenado de los moldes autoportantes están siempre por debajo de los 160 bares siendo típicamente inferiores a los 50 bares.

Es posible trabajar con varios materiales plásticos simultáneamente

▪ Desde el punto de vista de las características de la pieza:

La pieza obtenida presenta ausencia de rechupes y de líneas de soldadura

Tiene un acabado superficial mejorado

El material que compone la pieza sufre menor estrés térmico, las presiones de trabajo son menores que las del proceso tradicional y las contracciones térmicas están mejor controladas.

9

Se reduce la densidad de la pieza fabricada hasta el 98% en peso.

No existen limitaciones en cuanto a la composición química de las piezas, es decir se pueden usar todo tipo de polímeros (de alta y baja viscosidad) y todo tipo de aditivos incluidos, cargas, nanocargas, refuerzos, ayudantes de proceso, ignifugantes, etc. Estos aditivos se pueden incorporar en las formulaciones en proporciones muy elevadas (hasta un 80% en peso) y superiores a las que se pueden usar en el moldeo por inyección.

Las piezas pueden tener regiones macroscópicas (de varias decenas de cm^3 en volumen) con diferentes composiciones químicas y densidades. Es decir, por ejemplo, una misma pieza podría estar constituida por dos o más zonas fabricadas en distintos polímeros o distintas formulaciones y además con densidades claramente diferentes en dos o más zonas de la pieza.

Se pueden fabricar piezas con estructura piel sólida-núcleo espumado.

▪ Desde el punto de vista del sistema global:

El sistema global se encuentra dividido en diferentes estaciones para realizar cada una de las etapas, el tránsito entre ellas se puede realizar por medio de un autómata.

Permite la fabricación de tiradas de piezas sin importar la cantidad a fabricar para amortizar la puesta a punto del molde y máquina. El sistema es muy versátil y el parámetro amortización del molde no es restrictivo.

Las condiciones de fabricación son reproducibles.

Permite fabricar en función de las necesidades diarias generadas (metodología Just in time), sin necesidad de previsión y es adaptable a la producción.

Es posible fabricar piezas de gran tamaño.

Breve descripción de los dibujos

A continuación se pasa a describir de manera muy breve una serie de dibujos que ayudan a comprender mejor la invención y que se relacionan expresamente con una realización de dicha invención que se presenta como un ejemplo no limitativo de ésta.

La Figura 1 muestra esquema del sistema de la invención.

La Figura 2 muestra una vista en perspectiva de un molde autoportante con colector.

La figura 3 muestra un esquema de una opción del sistema en la que el procedimiento es cíclico.

En las figuras anteriormente citadas se identifican una serie de referencias que

10

corresponden a los elementos indicados a continuación, sin que ello suponga carácter limitativo alguno:

      1.- Equipo de alimentación

      2.- Equipo accionador del elemento calentador

5   3.- Equipo de enfriamiento

      4.- Equipo de desmoldeo

      5.- Molde autoportante

      6.- Cavidad interior del molde autoportante

      7.- Colector del molde autoportante

10   8.- Entrada de alimentación

      9.- Sistema de cierre

      10.- módulo de alimentación

      11.-Módulo de calentamiento

      12.- Módulo de enfriamiento

15   13.- Módulo de desmoldeo

      14.- Elemento calefactor

<u>Descripción detallada de un modo de realización</u>

El sistema de la invención de una realización preferida, tal y como se muestra en la figura 1 comprende:

20   - un módulo de alimentación (10) que comprende un equipo de alimentación (1) de material de moldeo en un molde autoportante, que comprende al menos una estación de alimentación con medios de alimentación de diferentes compuestos para su introducción en los moldes autoportantes,

      - un módulo de calentamiento (11) que comprende un equipo calentador (14) y

25   un equipo accionador (2) de un elemento calefactor (14) del molde autoportante,

      - un módulo de enfriamiento (12) que comprende un equipo de enfriamiento (3) del molde autoportante lleno de material, y

      - un módulo de desmoldeo (13) que comprende un equipo de desmoldeo (4)

30   de la pieza moldeada en el molde autoportante,

por los que transita el molde autoportante (5).

La fase de llenado del molde autoportante del procedimiento de moldeo de la invención y el tipo de molde autoportante a utilizar varía según el tipo de pieza a fabricar. Determinadas piezas, como las piezas compactas y las piezas estructurales

35   de densidad reducida, se fabrican utilizando moldes autoportantes que comprenden

11

varias piezas que dan lugar a una cavidad en su interior (6), un colector (7) y un sistema de cierre (9) que asegura la estanqueidad al polímero durante el proceso de llenado del molde. En la fabricación de las piezas de densidad reducida el colector (7) no es necesario estando el molde formado por un conjunto de piezas que dan lugar a una cavidad interior (6) y un sistema de cierre (9) que asegura que el molde es estando al polímero durante todo el proceso.

5

La figura 3 muestra una alternativa a la Figura 1, que muestra dos posibles caminos para el molde en la que el circuito completo del procedimiento se cierra permitiendo que sea un proceso cíclico.

10 A continuación se describe en detalle la forma de fabricar piezas compactas, piezas estructurales de densidad reducida y piezas de densidad reducida utilizando el sistema y procedimiento de la invención:

Como nota aclaratoria al término "agente espumante" utilizado a continuación, indicar que se entiende por material espumante aquel material que cuando alcanza una temperatura crítica, que denominaremos temperatura de descomposición, genera una fase gaseosa. Dicha fase gaseosa puede permitir la expansión de un segundo material en el que se haya introducido previamente el agente espumante.

15

1) Piezas Compactas

El proceso de fabricación de piezas compactas mediante el sistema de fabricación de la invención utiliza un molde autoportante (5) con sistema colector que es sometido al siguiente proceso:

20

- Una primera etapa de llenado de un molde autoportante (5), que comprende un sistema colector (7), que comprende el calentamiento del molde autoportante, y la alimentación, pudiéndose realizar a la inversa, primero alimentar el molde y luego calentarlo,

25

El llenado del molde se realiza por introducción en el molde autoportante de un material polimérico a temperaturas por encima de la de reblandecimiento del material o en estado sólido y la aplicación de presión en el interior del

12

para rellenar el molde. La cantidad (volumen) de material que contiene agente espumante y la cantidad (volumen) de espumante se seleccionan de forma que el material celular queda en el interior del colector.

5 ▪ Mediante pistones hidráulicos o mecánicos con accionamiento mecánico. Los pistones son externos al colector y se introducen en este para hacer la presión. Preferentemente habiéndose calentado el molde previamente aunque se puede calentar con posterioridad a la aplicación de la presión.

10 ▪ Mediante vapor, aire comprimido, agua, aceite o cualquier otro fluido que pueda utilizarse a tal fin, calentándose el molde previamente o posteriormente.

- Una segunda etapa de enfriamiento

- Una tercera etapa de desmoldeo de la pieza interior al molde

15 De forma adicional puede ser necesaria la extracción de gases internos al molde mediante un proceso de vacío utilizando un equipo generador de vacío. Dicho proceso se realizaría previo a la fase de alimentación del molde, durante dicha fase o una vez que el molde haya sido alimentado.

Las piezas obtenidas mediante este proceso son compactas y por tanto no 20 presentan porosidad. Su densidad relativa es igual a 1.

2) Piezas estructurales de densidad reducida.

El proceso de fabricación de piezas estructurales de densidad reducida mediante el sistema de fabricación de la invención, utiliza un molde autoportante con sistema colector que es sometido al siguiente proceso:

25 - Una primera etapa de llenado de un molde autoportante que comprende un colector, que comprende el calentamiento del molde autoportante y la alimentación del mismo, pudiéndose realizar primero la alimentación del molde y luego el calentamiento o a la inversa,

El llenado se consigue por alimentación en el molde de un material 30 polimérico a temperaturas por encima de la de reblandecimiento del material o en estado sólido y mediante la alimentación a través del colector de un material mezclado con un agente espumante o de un agente espumante.

El agente espumante permite que, una vez es calentado por encima de 35 su temperatura de descomposición, genere la presión necesaria para

13

rellenar el molde.

La aplicación de presión en el interior del molde autoportante a través del colector permite que el material polimérico introducido en el molde sea capaz de rellenar el volumen interno del mismo.. La cantidad de material que contiene agente espumante y la cantidad de espumante se seleccionan de forma que el material celular generado en el colector sea capaz de introducirse en la pieza dando lugar a una pieza con estructura celular interna y por tanto con una porosidad controlable. Estas piezas presentan densidades relativas en el rango 0.02 a 0.99.

- una segunda etapa de enfriamiento

- una tercera etapa de desmoldeo de la pieza interior al molde

De forma adicional puede ser necesaria la extracción de gases internos al molde mediante un proceso de vacío. Dicho proceso se realizaría previo a la fase de alimentación del molde con un generador de vacio, durante dicha fase o una vez que el molde haya sido alimentado

3) Piezas de densidad reducida

El proceso de fabricación de piezas de densidad reducida mediante el sistema de fabricación de la invención, utiliza un molde autoportante sin sistema colector que es sometido al siguiente proceso:

- Una primera etapa de llenado del molde por calentamiento del molde y alimentación pudiéndose realizar a la inversa, primero alimentar el molde y luego calentarlo.

El llenado del molde se realiza por introducción de un material polimérico a temperaturas por encima de la de reblandecimiento del material o en estado sólido en el molde y de un agente espumante químico que es capaz de generar una fase gaseosa cuando la temperatura se eleva por encima de la temperatura de descomposición de dicho agente. Dicho gas expande el material que rellena el molde.

Las piezas obtenidas mediante este proceso son celulares y por tanto presentan porosidad. El rango de densidad relativa alcanzable mediante este proceso está entre 0.02 y 0.99.

- Una segunda etapa de enfriamiento, y

- Una etapa final de desmoldeo de la pieza interior al molde

De forma adicional puede ser necesaria la extracción de gases internos al molde mediante un proceso de vacío. Dicho proceso se realizaría previo a la fase de

14

alimentación del molde, durante dicha fase o una vez que el molde haya sido alimentado.

Dentro del campo de la fabricación de piezas de densidad reducida existen aspectos que permitan lograr estructuras específicas en las piezas como por ejemplo calidades superficiales mejoradas o pieles internas. Así por ejemplo si se desea obtener una estructura piel-núcleo se pueden recubrir la zonas internas de la cavidad del molde en las que se desea obtener dicha estructura con un material capaz de disolver gas y estable térmicamente a temperaturas superiores a la de espumación. Algunos ejemplos de estos materiales son siliconas, polisulfonas o poitetrafluoroetileno (PTFE). Mediante este procedimiento se fabrican piezas celulares con estructura piel-núcleo y densidades relativas en el rango 0.02-0.99.

Si además se desean lograr zonas sólidas no espumadas en el interior del núcleo interno espumado, esto se puede lograr introduciendo partículas sólidas de un material capaz de disolver gas y estables a temperaturas superiores a la de descomposición del agente espumante en la mezcla de materias primas usadas para alimentar el molde.

Para los tres tipos de piezas mencionadas previamente (compactas, estructurales de densidad reducida y de densidad reducida) existe la posibilidad de fabricar piezas con composiciones químicas y/o densidades variables a lo largo de la pieza. Para ello en la fase de alimentación el molde se alimentaría con diversos materiales cada uno de ellos con distintas composiciones químicas y/ o cantidades o tipo de agentes espumantes. Durante la fase de llenado la pieza quedaría constituida por regiones macroscópicas de composiciones químicas diversas y/o densidades que podrían variar de forma significativa de unas zonas a otras.

Una aplicación práctica de la invención sería la fabricación de piezas estructurales con pieles densas y cores celulares para lo que en la etapa de llenado del molde se realiza una alimentación del molde autoportante en el módulo de alimentación, en tres subetapas:

- inicialmente se introduce material que no incorpora agente espumante que se sitúa en la parte inferior del molde,

- a continuación se introduce material que incorpora un agente espumante o que se mezcla con un agente espumante, de manera que este material se sitúa en la zona intermedia del molde.

- finalmente se vuelve a incorporar un material que no incorpore agente espumante y que se sitúa en la parte superior del molde.

15

Una vez que el molde ha pasado por los módulos de alimentación, calentamiento y enfriamiento, para lograr el llenado del mismo y la conformación de la pieza, se obtiene una pieza con pieles densas y cores celulares dado que la estructura celular se genera fundamentalmente en las zonas en las que se incorporó un agente espumante.

5

16

REIVINDICACIONES

1.- Sistema de moldeo de piezas con moldes autoportantes (5) caracterizado por que comprende:

- un equipo alimentador (1) de material de moldeo en un molde autoportante, que comprende una pluralidad de medios de alimentación de diferentes compuestos,

- un equipo accionador (2) de un elemento calefactor (14) del molde autoportante,

- un equipo enfriador (3) del molde autoportante lleno de material, y

- un equipo desmoldeador (4) de la pieza moldeada en el molde autoportante, siendo todos ellos equipos independientes instalados en módulos de trabajo por los que transita el molde autoportante (5).

2.- Sistema de moldeo según reivindicación 1 caracterizado por que comprende un equipo generador de vacío en el molde.

3.- Sistema de moldeo según reivindicaciones 1-2 caracterizado por que comprende un equipo generador de presión seleccionado entre pistones hidráulicos o mecánicos.

4.- Sistema de moldeo de piezas con moldes autoportantes según reivindicación 1 caracterizado por que comprende:

- un módulo de alimentación (10) que comprende el equipo alimentador (1),

- un módulo de calentamiento (11) que comprende el equipo accionador (2) de un elemento calefactor (14),

- un módulo de enfriamiento (12) que comprende un equipo de enfriamiento (3) y

- un módulo de desmoldeo (13) que comprende un equipo de desmoldeo (4).

5.- Sistema de moldeo de piezas con moldes autoportantes según reivindicación 1 caracterizado por que comprende:

- un módulo de calentamiento y alimentación que comprende el equipo alimentador (1) y el equipo accionador (2) de un elemento calefactor (14),

- un módulo de enfriamiento (12) que comprende un equipo de enfriamiento (3) y

- un módulo de desmoldeo (13) que comprende un equipo de desmoldeo (4).

6.- Sistema de moldeo según reivindicaciones 4 y 5 caracterizado por que comprende un módulo de acondicionamiento del molde autoportante que comprende un equipo generador de vacío que se utiliza para hacer vacío en el interior del molde.

7.- Sistema de moldeo según reivindicaciones anteriores caracterizado por que

17

comprende medios de desplazamiento automáticos que conectan los módulos (10, 11, 12, 13) por los que transita el molde autoportante (5).

8.- Sistema de moldeo de piezas con moldes autoportantes según reivindicaciones 1-7 caracterizado por que el elemento calefactor (14) es al menos un horno fijo accionable por el equipo accionador (2) junto al que se sitúa.

9.- Sistema de moldeo de piezas con moldes autoportantes según reivindicaciones 1-7 caracterizado por que el elemento calefactor (14) accionable por el equipo accionador (2) está situado en el propio molde autoportante (5).

10.- Sistema de moldeo de piezas con moldes autoportantes según reivindicación 1 caracterizado por que el molde autoportante (5) comprende un conjunto de piezas con una cavidad en su cara interior (6), un sistema de cierre (9) y un colector (7)

11.- Sistema de moldeo de piezas con moldes autoportantes según reivindicación 2 caracterizado por que el módulo de calentamiento (11) comprende al menos un pistón seleccionado entre hidráulico o mecánico de aplicación de presión en el interior del molde autoportante (5)

12.- Procedimiento de moldeo de piezas con moldes autoportantes (5) caracterizado por comprender:

- una etapa de llenado de un molde autoportante que comprende alimentación del molde y calentamiento del molde autoportante (5),
- una etapa de enfriamiento del molde autoportante (5) lleno y
- una etapa de desmoldeo de la pieza moldeada en el molde autoportante (5), una vez alcanzada la temperatura de desmoldeo,

realizándose cada etapa en módulos independientes (10, 11, 12, 13) por los que transita el molde autoportante (5).

13.- Procedimiento de moldeo de piezas según reivindicación 12 caracterizado por que el llenado del molde autoportante se realiza por alimentación del molde y posterior calentamiento del molde autoportante.

14.- Procedimiento de moldeo de piezas según reivindicación 12 caracterizado por que el llenado del molde autoportante se realiza por calentamiento previo del molde autoportante y posterior alimentación del molde.

15.- Procedimiento de moldeo de piezas según reivindicación 12-14 caracterizado por que el llenado del interior del molde autoportante se realiza mediante la introducción en el molde (5) de un material polimérico mezclado con un agente espumante químico capaz de generar una fase gaseosa, y el calentamiento se realiza por elevación de la temperatura del molde por encima de la temperatura de descomposición de dicho

agente espumante, que expande el material que rellena el molde.

16.- Procedimiento de moldeo de piezas según reivindicaciones 12-14 caracterizado por que se utiliza un molde autoportante (5) que comprende un colector (7), de manera que en la etapa de llenado del molde autoportante (5), la alimentación del molde (5) se

5   realiza por alimentación del molde autoportante (5) con material polimérico (7) y posterior aplicación de presión en el interior del molde autoportante (5) a través del colector (7).

17.- Procedimiento de moldeo según reivindicación 16 caracterizado por que la presión se aplica mediante la introducción en el colector (7) de un material mezclado con

10   agente espumante o de un agente espumante.

18.- Procedimiento de moldeo según reivindicación 17 caracterizado por que el volumen de material que contiene agente espumante y el volumen de espumante se seleccionan de forma que el material celular generado en el colector (7) limita su volumen a dicho colector (7).

15   19.- Procedimiento de moldeo por inyección según reivindicación 17 caracterizado por que el volumen de material que contiene agente espumante y el volumen de espumante se seleccionan de forma que el material celular generado en el colector (7) se introduce en la cavidad interior (6) del molde autoportante (5)

20.- Procedimiento de moldeo según reivindicación 16 caracterizado por que la presión

20   se aplica mediante pistones hidráulicos o mecánicos con accionamiento mecánico.

21.- Procedimiento de moldeo según reivindicación 16 caracterizado por que la presión se aplica mediante la introducción en el colector de un fluido seleccionado entre vapor, aire comprimido, agua y aceite.

22.- Procedimiento de moldeo según reivindicaciones 12-21 caracterizado por que

25   comprende una etapa adicional de extracción de gases internos al molde autoportante mediante un proceso de vacío.

23.- Procedimiento de moldeo según reivindicaciones 12-21 caracterizado por que comprende una etapa inicial de recubrimiento interno del molde autoportante con materiales con capacidad para absorber gases.

30   24. Procedimiento de moldeo según reivindicaciones 12 a 23 caracterizado porque en la etapa de llenado, se realiza una alimentación del molde autoportante en tres subetapas:

    - inicialmente se introduce material que no incorpora agente espumante que se sitúa en la parte inferior del molde,

35   - a continuación se introduce material que incorpora un agente espumante o
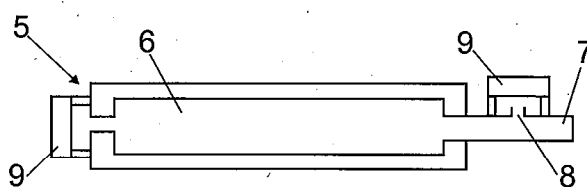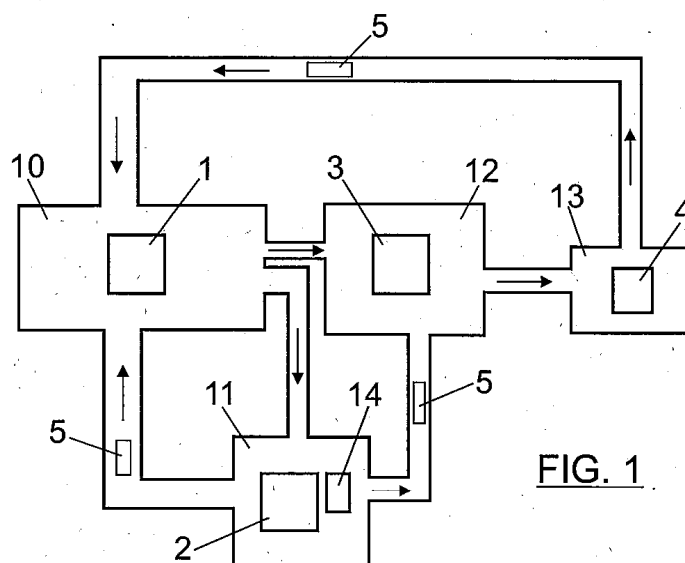
19

que se mezcla con un agente espumante, de manera que este material se sitúa en la zona intermedia del molde.

- finalmente se vuelve a incorporar un material que no incorpore agente espumante y que se sitúa en la parte superior del molde.
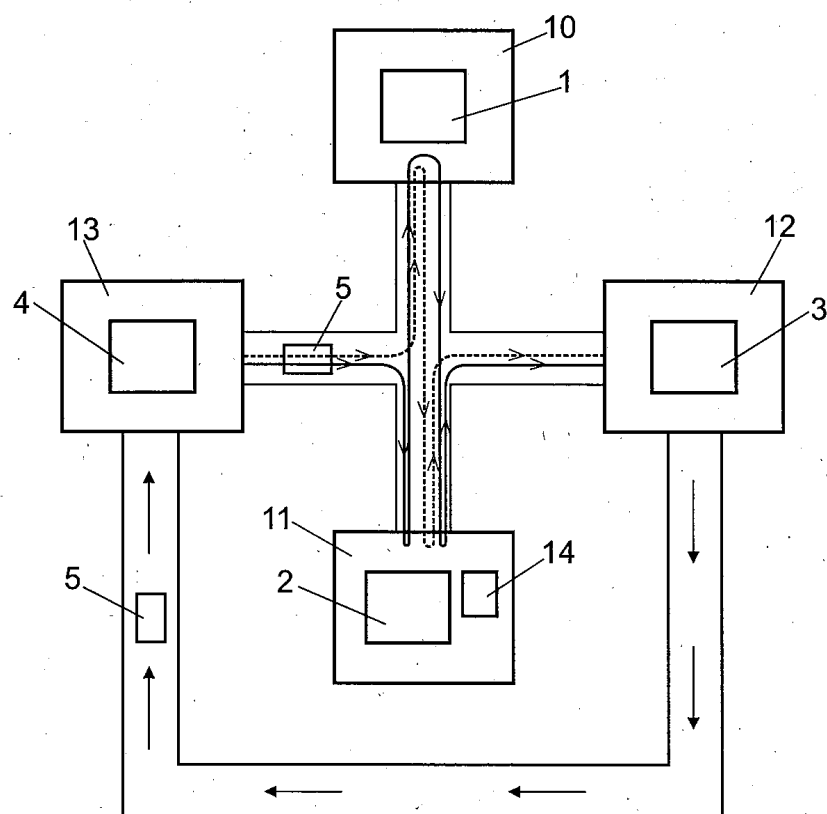
5

- 00 -

FIG. 1

FIG. 2

- 00 -

FIG. 3

I.3.- PATENT 2. PRODUCTION PROCEDURE FOR THERMOPLASTIC CELLULAR MATERIALS

The second patent was developed in the frame of the European Project Nancore and is entitled "Production procedure for thermoplastic cellular materials". This patent presents a novel technology for the production of non-crosslinked anisotropic low-density thermoplastic foams with outstanding mechanical properties and is the result of the experimental work presented mainly in Chapter 6. Almost all the experimental work concerning this patent has been done using polypropylene as the thermoplastic solid matrix of the foams. The production of low density foams from non-crosslinked polypropylene is a challenging task, furthermore when high relative mechanical properties are sought. The relatively low stiffness of polypropylene (in comparison with other polymers as PVC) is compensated by the anisotropic cellular structure of the foams that is the main distinguishing characteristic of the patent, together with the low relative densities that can be reached (as low as 0.1, that is to say expansion rates up to 10). Besides this the patent also encloses the possibility of achieving open cell structures with the same properties as before (same density range and comparable mechanical properties). Since both open and closed cell structures are achieved these foams cover a wide range of technical niches where recyclable (non-crosslinked) materials with high mechanical properties are mandatory.

- 1 -

PROCEDIMIENTO DE FABRICACIÓN MATERIALES CELULARES DE MATRIZ
TERMOPLÁSTICA

<u>Campo de la invención</u>

5   La presente invención se engloba dentro del campo de la industria relativa a la producción de paneles celulares de baja densidad no reticulados con matriz termoplástica, altas prestaciones mecánicas y buen acabado superficial.

<u>Antecedentes</u>

          Las propiedades mecánicas de un material celular dependen
10   fundamentalmente de la densidad del material, de las propiedades del polímero de partida que conforma la matriz y de la microestructura celular. Así, cuando la densidad del material disminuye, las propiedades mecánicas sufren una disminución muy acusada. Mediante la modificación de la microestructura, para una densidad fija y una matriz de partida dada, se pueden mejorar las propiedades mecánicas de una manera
15   muy significativa.

          La modificación de la microestructura para dar lugar a una estructura celular anisotrópica en el material celular es un método conocido para compensar la disminución de propiedades mecánicas que se produce con la densidad.

          Por otro lado, la proporción de masa en las paredes celulares es otro
20   parámetro microestructural que está fuertemente relacionado con las propiedades mecánicas específicas del material celular. Un alto contenido de celda cerrada es indicativo de una alta proporción de masa en las paredes y da lugar a propiedades mecánicas específicas óptimas. Bajos contenidos de celda cerrada van normalmente asociados a bajas proporciones de masa en las paredes de las celdas y esto da lugar
25   a propiedades mecánicas específicas bajas.

     Varios de los parámetros mencionados en los párrafos previos y otros conceptos importantes que aparecen en este documento se definen de la siguiente manera.

- Propiedades mecánicas específicas: se define como el valor de una cierta propiedad mecánica dividido entre la densidad del material sobre el que se
30   mide dicha propiedad. De esta manera se independiza la propiedad de la densidad, dando un valor más fácilmente comparable.

- Contenido de celda cerrada: es directamente proporcional a la fracción en volumen de celdas que no están interconectadas. Una mayor presencia de masa en las paredes disminuye las interconexiones entre celdas y aumenta
35   el contenido de celda cerrada. Una estructura de celda abierta se

- 2 -

caracteriza porque el volumen de las celdas interconectadas es idéntico al volumen de la fase gaseosa. Una estructura parcialmente interconectada se caracteriza porque una fracción del volumen de fase gaseosa está interconectada.

5

- Densidad relativa: es el cociente entre la densidad del material celular y la del sólido del cual se parte. Es una medida de la fracción volumétrica de fase sólida presente en el material.

- Grado de expansión: es el cociente entre el volumen del material celular y el volumen del material sólido de partida. Mide por tanto el incremento de

10

volumen que sufre el material durante el proceso de espumado

- Índice de anisotropía: cociente entre la dimensión de una celda en una dirección determinada y la dimensión medida en otra dirección.

- Tortuosidad: Es el cociente entre la distancia que debe recorrer el gas para atravesar el material y el espesor de ese material. Es por tanto una medida

15

de lo intrincada que es la estructura celular del material, es un parámetro que tiene importancia para estructuras celulares con elevados contenidos de celdas abiertas.

- Módulo elástico relativo, esfuerzo de colapso relativo, módulo de cizalla relativo: se refiere al valor de cualquiera de estas propiedades mecánicas

20

dividido entre la densidad de la pieza sobre la que se está midiendo. Es una manera de independizar de la densidad el valor de la propiedad mecánica. De esta manera se obtiene un valor mucho más comparable sin necesidad de especificar la densidad.

- Agente espumante: aquel material que cuando alcanza una temperatura

25

crítica, que denominaremos temperatura de descomposición, genera una fase gaseosa. Dicha fase gaseosa puede permitir la expansión de un segundo material en el que se haya introducido previamente el agente espumante.

- Nanopartículas. Son partículas que tienen al menos una de sus

30

dimensiones (largo, ancho, espesor-diametro) en la escala nanométrica, es decir alguna de sus dimensiones tiene tamaños inferiores a unos 200 nanométricos. Hay nanopartículas con forma laminar, con forma de fibra e isotrópicas. Ejemplos de este tipo de partículas son nanoarcillas, nanotubos de carbono, nanofibras de carbono, sílices nanométrica,

35

grafenos, organo titanatos, organo zirconatos, etc.

- 3 -

Cuando el índice de anisotropía es igual a 1, el crecimiento de las celdas es el mismo en todas las direcciones y su forma es completamente isotrópica. De ahora en adelante, en el supuesto caso de una lámina de material celular con dos superficies planas opuestas, un índice de anisotropía mayor que 1 indicará que las celdas están elongadas en la dirección del grosor de la lámina que en cualquier dirección contenida en un plano paralelo a las dos superficies planas. De hecho, normalmente las celdas serán altamente isótropas en un plano paralelo a las dos superficies planas opuestas. Esta configuración de anisotropía incrementará las propiedades mecánicas en compresión medidas en la dirección del grosor de la lámina.

La producción de láminas de material celular a partir de un proceso de extrusión da lugar a índices de anisotropía inferiores a la unidad respecto a la definición anterior puesto que el propio proceso de extrusión tiende a producir un alineamiento de las celdas en la dirección de extrusión la cual es perpendicular a la dirección de grosor de la lámina.

Obviando la anisotropía, la mera producción de materiales celulares de celda cerrada de baja densidad relativa (<0.2) a partir de una matriz polimérica termoplástica no reticulada es un proceso complicado y por ello en muchas tecnologías se recurre a la reticulación de la matriz. Esto da lugar a que el producto final no pueda ser reciclado, sea más frágil y presente peor comportamiento en fatiga o impacto. Además los procesos de producción son extremadamente caros, elevando el precio del producto final.

Diversas patentes buscan la consecución de una estructura anisotrópica por diferentes procedimientos y con distintas finalidades:

US 2010 0029796 A1 divulga un procedimiento en el que las espumas, una vez que han sido fabricadas, se someten a un ciclo de temperatura y deformación mecánica para inducir celdas anisotrópicas.

En US 4 053 341 el procedimiento se centra en espumas de polietileno que en este caso están reticuladas. Se consiguen celdas anisotrópicas únicamente en ciertas láminas interiores pero no en la totalidad de la espuma. Las láminas exteriores tienen celdas completamente isótropas.

En US 4 673 695 el polímero se disuelve en un solvente como método de consecución de la estructura anisotrópica. No se menciona si el método permite obtención de celdas abiertas o cerradas.

- 4 -

La patente US 2010 0038579 A1 se centra en la producción de estructuras anisotrópicas en elastómeros mediante la introducción de partículas magnetizables en la matriz que al aplicar un campo magnético facilitan la orientación de la matriz.

El método de procesado de EP 0 411 437 B1 consigue ratios de anisotropía altos
5   con valores entre 5 y 12 pero restringe a su aplicación a polyethersulfonas. En US 2005 0112356 A1 la anisotropía se consigue mediante la introducción en la matriz de nanofibras orientadas, aunque la producción se centra en un polímero concreto, un alkenyl aromático.

En GB 1 007 411 el método de producción constriñe el crecimiento de la pieza
10   espumada a una única dirección pero la patente se restringe a policloruro de vinilo, el material es reticulado y además se limita a espumas de celda cerrada.

La patente US 2011 0104478 presenta un método de conseguir espumas anisotrópicas pero en el cual los ratios de anisotropía en ningún caso superan un valor de 1,7. En este proceso la anisotropía se consigue por depresurización durante el
15   enfriamiento.

Ninguno de los antecedentes anteriores presenta la posibilidad de controlar el contenido de celda abierta o celda cerrada manteniendo unas buenas propiedades mecánicas específicas así como la posibilidad de variar tamaño de celda, ratio de anisotropía o tortuosidad todo ello combinado con un control preciso de la densidad de
20   la pieza final y el uso de un polímero no reticulado como matriz para el material celular.

Descripción de la invención

La invención se refiere a un procedimiento de obtención de materiales celulares de matriz termoplástica no reticulada con densidades relativas menores a 0.2 en los cuales se consiguen índices de anisotropía superiores a 2, porcentajes variables del
25   contenido de celda abierta, y altas propiedades mecánicas específicas, comparables a las obtenidas comercialmente con otros materiales en base PVC o SAN, con buena calidad superficial y con un coste de producción más económico frente a los actuales del mercado. Cuando se habla de altas propiedades mecánicas se hace referencia a un valor del módulo elástico relativo en compresión superior a 0,6 MPa/(kg/m^3) un
30   módulo de cizalla relativo superior a 0,18 MPa/(kg/m^3) y un esfuerzo de colapso superior a 0,010 MPa/(kg/m^3).

El procedimiento comprende principalmente las siguientes etapas:

1) MEZCLA Y GRANCEADO PARA FABRICACIÓN DEL MATERIAL
35   PRECURSOR

- 5 -

El primer paso consiste en la mezcla en una mezcladora o extrusora de las materias primas que se van a emplear en la fabricación de la lámina siendo estas al menos un polímero termoplástico, un agente espumante químico, y aditivos en unas condiciones de temperatura y cizalla en las cuales el polímero esté fundido pero por debajo de las condiciones de descomposición del agente espumante. Una alternativa a esta ruta es la utilización de un proceso de mezclado en frío usando polvos para los componentes de la mezcla.

▪ Las materias primas a emplear son las siguientes:

a.- el elemento básico es un polímero termoplástico, como puede ser polietileno, polipropileno, policloruro de vinilo, polietilen tereftalato, poliestireno, poliamida, almidón, poliacido láctico, etc. o también mezclas de los mismos en las cantidades adecuadas para la obtención del producto final deseado.

b.- un agente espumante químico. Dentro de la amplia variedad de estos productos podemos utilizar entre otros la azodicarbonamida, oxibis (hidracina de bencensulfonil), 5-feniltetrazol, bicarbonato, ácido cítrico o mezclas de los mismos, etc.

La cantidad de agente espumante es un parámetro crítico que debe ser ajustado con precisión en función del grado de expansión (densidad relativa) y estructura celular (tamaño de celda, anisotropía, tortuosidad, contenido de celda abierta, etc.) que se quiere alcanzar en el producto final. El agente espumante se introduce de forma que se logre una buena dispersión del mismo.

c.- otros aditivos como cargas (talco, carbonato cálcio, nanoarcillas, nanosílicas, nanotubos de carbono, nanofibras de carbono, grafenos), refuerzos (fibras de vidrio, fibras de carbono), ayudantes de proceso (ceras, ácido esteárico), agentes nucleantes (talco, nanopartículas tipo arcillas, silicas), antioxidantes, pigmentos, activadores de la reacción del agente espumante (óxido de zinc), agentes repolimerizantes como neoalkoxy organotitanatos u organozirconatos, etc. Una de las novedades y aspecto beneficioso de la presente invención es la no necesidad recurrir a matrices reticuladas (es decir en las que existen enlace carbono-carbono entre cadenas) y por lo tanto en ningún caso contendrá agentes reticulantes. Es conveniente señalar aquí que la introducción de cargas de tamaño nanométrico será determinante en la obtención de estructuras celulares anisotrópicas de celda abierta de elevadas prestaciones mecánicas.

- 6 -

d.- en el caso de emplear ciertas cargas de tamaño nanométrico como nanoarcillas organomodificadas   puede ser necesario emplear en la formulación de partida un polímero compatibilizante injertado con anhídrido maléico o cualquier otro tipo de agente compatibilizante con el fin de producir la buena dispersión/exfoliación de dichas partículas de tamaño nanométrico.

Los aditivos se introducen de forma que exista una buena dispersión de todos ellos en la matriz polimérica.

La mezcla, una vez solidificada, se grancea a la salida de la extrusora o mezcladora a un tamaño suficientemente pequeño para permitir su introducción posterior en los moldes de fabricación.

- Esta mezcla también podrá ser extruida en forma de lámina u otra forma de tal manera que dicho material se introduzca en el molde posteriormente actuando como precursor.

- La granza fabricada podría también sufrir posteriormente un proceso de compactación para darle una cierta geometría que posteriormente sería introducido en el molde para la producción de la lámina celular.

2) <u>INTRODUCCIÓN EN MOLDE ESPECÍFICO DEL MATERIAL PRECURSOR</u>

La formulación previamente generada y en cualquiera de las formas citadas en la etapa de mezcla y granceo, que será el material precursor, se introduce en un molde que comprende una pieza desplazable unidireccionalmente y de control de la densidad, para su espumación.

El molde comprende :

- Un cuerpo (1) que será la cavidad principal de formación de la lámina, que comprende:
    - en todo su perímetro superior e inferior un alojamiento donde van colocadas juntas (2) de material elástico resistente a la temperatura como por ejemplo vitón, teflón, etc.
    - atornillada a su parte inferior una tapa (4) de la misma área que el área externa de este,
- Un pistón en forma de T (3), como elemento desplazable unidireccionalmente, cuyo cuerpo encaja con baja tolerancia en el seno del cuerpo del molde (1). La parte inferior del pistón (10), una vez que este está introducido en el seno del molde, dejará un

espacio libre entre este y la base interna del cuerpo del molde, cavidad interna (11), donde irá alojado el material precursor (5). La parte superior del pistón en forma de T (9) entrará en contacto en un momento determinado con la junta elástica (2) del cuerpo del molde

5

(1) ejerciendo presión sobre ella y dejando la cavidad interna del molde (11) completamente estanca a gases y al escape del material fundido,

- Una pieza expansora (6) unida al cuerpo del molde (1) y cuya altura es variable en función del grado de expansión buscado y/o al grosor

10

final de la lámina que se quiere producir, cuya área interna coincide con baja tolerancia con el área externa de la parte superior del pistón en forma de T (9), de tal manera que actúa como guía de este durante su ascenso, y

- Un pieza de de retención unidad (7) tanto a la pieza expansora (6)

15

como al cuerpo del molde (1) con área externa igual a la de estos dos y área interna inferior a la de la parte superior del pistón (9) y al área interna de la pieza expansora (6) de tal manera que el pistón en forma de T (3), una vez alcanzada la expansión deseada, vea detenido su ascenso por la pieza de retención (7), permitiendo

20

mantener controlada la densidad final de la pieza.

El material del cual esté fabricado el molde puede ser cualquiera con tal de que soporte las condiciones de presión y temperaturas desarrolladas durante el proceso.

La introducción del material en el molde se puede hacer por diferentes

25

métodos. El más sencillo sería introducir el material en forma de granza, polvo o en forma de material precursor antes de colocar el pintón. Otra manera sería hacerlo a través de una abertura en el cuerpo (1) o en la tapa inferior (4). En este caso se podría introducir tanto en estado sólido (en forma de granza o polvo) como en estado fundido usando un equipo de

30

extrusión o mediante técnicas de vacío. Una vez introducido el material la abertura usada para dicha introducción debería ser sellada adecuadamente para impedir pérdidas de material.

La cantidad de material a introducir será tal que si estuviera totalmente compacto en estado fundido rellenaría completamente, al menos, el

35

espacio libre entre pistón y base inferior del molde (11) mencionado

- 8 -

anteriormente de tal manera que el pistón (3) en cualquier estado previo a la descomposición del agente espumante ya realiza presión sobre el material precursor (5). La cantidad de material a introducir está relacionada con la densidad relativa final de la pieza que se quiera alcanzar y con el la

5
pieza de expansión utilizada en cada caso. Las densidades relativas alcanzables por este proceso pueden alcanzar valores tan bajos como 0.05 y cualquier valor superior aunque el proceso esté preferentemente enfocado al rango de bajas densidades (densidades relativas inferiores a 0.2)

10

3) <u>ESPUMACIÓN Y FORMACIÓN DE LA LÁMINA EN EL MOLDE</u>

El molde completamente montado, cerrado y con el material precursor en su interior es sometido a un ciclo que combina conjuntamente presión y temperatura, durante el tiempo suficiente para que se produzca una cantidad suficiente de gas que

15
permita lograr la expansión deseada (etapas 3.1, 3.2 y 3.3). Como norma general el tiempo bajo el cual el molde permanece bajo condiciones de presión y/o temperatura debe ser el mínimo necesario para que se descomponga la totalidad del agente espumante con el fin de optimizar las propiedades mecánicas específicas de la pieza final.

20
3.1) Por efecto de la presión aplicada el gas queda disuelto dentro del polímero sin producir ningún tipo de espumación mientras la presión continúe ejerciéndose.

▪ La presión puede ser ejercida de forma mecánica mediante una prensa situando un segundo pistón cilíndrico (8) sobre el pistón en forma de T (3) para transmitir la presión hasta el material o de cualquiera otra forma

25
siempre y cuando esta presión sea superior a la presión de gas generada por el agente espumante al descomponer, de tal manera que este gas generado quede disuelto en el polímero precursor fundido sin producir ningún tipo de espumación mientras la presión continúe aplicada. La presión puede mantenerse constante durante todo el proceso o puede

30
variarse siempre y cuando sea superior a la presión de gas generada por la descomposición del agente espumante.

▪ La temperatura puede ser aplicada calefactando los platos superior e inferior de la prensa, mediante camisas laterales calefactoras externas, mediante calefactores infrarrojos, mediante resistencias eléctricas

35
insertadas en el cuerpo del molde, mediante circuitos para aceite

termostando en el cuerpo del molde   o mediante cualquier otro procedimiento. La temperatura ha de ser tal que produzca la fusión de la matriz polimérica si el polímero es semicristalino o permita alcanzar la temperatura de transición vítrea si el polímero es amorfo y la descomposición del agente espumante. El proceso de calentamiento se puede realizar mediante diferentes escalones de temperatura si, por ejemplo, primero se quiere producir la fusión del polímero y posteriormente la descomposición del agente espumante.

En el caso de que la formulación de partida no contenga cargas de tamaño nanométrico como nanoarcillas, nanotubos de carbono, nanofibras de carbono, etc. las presiones recomendables a ejercer para optimizar las propiedades mecánicas específicas son medias (35 bar). En el caso de que la formulación de partida contenga cargas de tamaño nanométrico como nanoarcillas, nanotubos de carbono, nanofibras de carbono etc. las presiones recomendables a ejercer para optimizar las propiedades mecánicas son bajas (7 bar). El parámetro de presión debe ser ajustado con precisión para conseguir una pieza final óptima. Además, mediante la variación de la presión aplicada se pueden controlar y variar parámetros como el ratio de anisotropía, el tamaño celular o la tortuosidad de la estructura. En general presiones mayores dan lugar a valores menores de anisotropía y tamaños de celda reducidos.

3.2) Transcurrido el tiempo tras el cual el agente espumante se ha descompuesto hasta el punto deseado la presión se libera. El gas generado deja de estar disuelto y produce el crecimiento de la lámina solo en grosor.

3.3) La presión generada por el gas anteriormente disuelto en el polímero produce el ascenso del pistón en forma de T hasta que este ascenso se ve limitado por la pieza de retención.

La presión de gas generada como consecuencia de la descomposición del agente espumante actuará como fuerza de empuje del crecimiento de la matriz polimérica en la dirección de liberación de la presión generando una estructura celular anisotrópica con máxima anisotropía en esta dirección.

El crecimiento (etapas 3.2 y 3.3) se restringe a la dirección de liberación de la presión siendo esta la dirección de máxima anisotropía. Velocidades de liberación de presión altas (1000 mm/min) dan lugar a acabados superficiales rugosos y de peor apariencia visual. Velocidades de liberación de presión bajas (10 mm/min) dan lugar a acabados superficiales suaves con buena apariencia visual. De esta manera el

-10-

parámetro de calidad superficial puede ser controlado y variado en función a las necesidades.

4) ENFRIAMIENTO DEL MOLDE

5   Una vez transcurrido el tiempo estrictamente necesario para que el agente espumante haya descompuesto en su totalidad el molde ha de ser enfriado.

El enfriamiento se puede producir de diferentes modos, mediante circulación de aire, sumergiendo el molde en un baño de agua u otro líquido para un enfriamiento rápido, introduciendo circuitos por los que se puede producir la entrada y salida de
10   agua o aceite en el cuerpo del molde, etc.

La estructura celular anisotrópica conseguida durante la etapa 3 puede continuar evolucionando una vez liberada la presión y/o el calentamiento hacia una estructura celular isótropa por lo cual la velocidad de enfriamiento ha de ser lo más rápida posible y el tiempo que transcurre hasta que este enfriamiento comienza debe
15   ser el menor posible.

En el caso de que el cuerpo del molde pueda ser enfriado in-situ mediante la re-circulación de agua por el interior de ese cuerpo o mediante cualquier otro procedimiento se podrá prescindir de la pieza de retención (7) actuando el plato superior de la prensa, o cualquier otro procedimiento que se haya empleado para
20   aplicar presión sobre el pistón en forma de T, como mecanismo limitante del ascenso de dicho pistón y por tanto del crecimiento de la espuma. Sin embargo puesto que se busca una velocidad de enfriamiento lo más alta posible es muy conveniente tener la capacidad de extraer el molde de la prensa. Desde este punto de vista, el la pieza de expansión y la de retención son piezas imprescindibles que permiten mantener
25   controlada la densidad final de la pieza mientras el molde es extraído de la prensa para proceder a su enfriamiento por inmersión en agua o cualquier otro procedimiento, dejando además la prensa libre para que comience la fabricación de otra pieza.

5) DESMOLDEO

30   El momento en el que la totalidad del molde y la de la lámina en él contenida se encuentra a una temperatura inferior a la temperatura de cristalización (si es semicristalino) o de transición vítrea (si es amorfo) del material termoplástico que la conforma, el molde puede ser desmontado y la lámina ya conformada y sólida extraída de su interior sin presentar mayor dificultad.

35

- 11 -

Como nota general la presente invención permite la fabricación de materiales celulares anisotrópicos tanto de celda cerrada como de celda abierta y manteniendo altas propiedades mecánicas específicas en ambos casos. En el caso del material con estructura celular anisotrópica de celda abierta la formulación de partida deberá

5   contener un cierto porcentaje de partículas de tamaño nanométrico como nanoarcillas tanto organomodificadas como naturales, nanotubos de carbono, nanofibras de carbono, etc. Estas partículas de tamaño nanométrico fomentan la presencia de una estructura de celda abierta manteniendo o incrementando el ratio de anisotropía de la estructura celular y reforzando la matriz polimérica de tal manera que las propiedades

10   mecánicas específicas alcanzadas son del mismo orden de magnitud que las del correspondiente material celular de celda cerrada sin nanopartículas. Esta combinación de paneles con altas propiedades mecánicas específicas y altos contenidos de celda abierta es muy útil en aplicaciones en las que se busquen paneles estructurales con un buen comportamiento como absorbente acústico.

15   Según este procedimiento cuanto mayor es el grado de expansión alcanzado (menor densidad relativa) se alcanzan mayores valores del índice de anisotropía. Puesto que la disminución de la densidad produce una fuerte disminución de las propiedades mecánicas el hecho de que el grado de anisotropía también aumente al disminuir la densidad compensa dicha fuerte disminución de propiedades mecánicas.

20   Descrita suficientemente la naturaleza de la invención, así como la manera de llevarse a la práctica, debe hacerse constar que las disposiciones anteriormente indicadas y representadas en los dibujos adjuntos son susceptibles de modificaciones de detalle en cuanto no alteren sus principios fundamentales, establecidos en los párrafos anteriores y resumidos en las reivindicaciones que se exponen

25   posteriormente.

Su aplicación está enfocada fundamentalmente a la industria de los generadores eólicos, a la industria aeronáutica, al sector de la automoción y al sector náutico entre otros. Además la posibilidad de variar la estructura celular manteniendo un excelente comportamiento mecánico y bajas densidades permite encontrar aplicaciones desde el

30   punto de vista del acondicionamiento acústico o del aislamiento térmico entre otros.

Las espumas poliméricas de baja densidad, además de las dificultades asociadas a su proceso de producción, en el caso de partir de una matriz polimérica no reticulada, presentan una importante disminución de propiedades mecánicas con la densidad. La consecución de una estructura celular anisotrópica compensa esta

35   disminución dotándolas de unas altas propiedades mecánicas específicas.

-12-

Existen numerosas investigaciones y patentes conducentes por un lado a la fabricación de espumas poliméricas de baja densidad y por otro de estructuras celulares con alta anisotropía pero ninguna supone una combinación de ambas partiendo de una matriz polimérica termoplástica no reticulada y consiguiendo además

5   contenidos de celda abierta variables. Unido a esto, la invención permite la variación y el control preciso de la densidad y la estructura celular en términos de ratio de anisotropía y tamaño de celda mediante el propio proceso de producción.

La presente invención presenta materiales celulares que combinan baja densidad partiendo de matrices poliméricas no reticuladas con estructuras celulares altamente

10   anisótropas y con contenidos de celda abierta variables y que por su morfología están dotados de unas altas propiedades mecánicas específicas y una excelente calidad superficial.

El grado de anisotropía aumenta a medida que disminuye la densidad relativa de la pieza fabricada, este hecho es ideal para compensar convenientemente la pérdida de

15   propiedades mecánicas que se produce en estas bajas densidades. El proceso de fabricación permite el control preciso y la variación de la densidad, del índice de anisotropía de la estructura celular y del tamaño de celda de la pieza.

La invención permire obtener altos contenidos de celda abierta manteniendo constante la alta anisotropía, la baja densidad y las altas propiedades mecánicas

20   específicas mediante la introducción de cargas de tamaño nanométrico.

El material celular conseguido resulta además competitivo en cuanto a costes respecto a otros competidores del mercado a igualdad de propiedades mecánicas específicas. El precio final del producto presenta un ahorro aproximado del 30% respecto a otros productos del mercado de similares prestaciones.

25

Breve descripción de los dibujos

A continuación se pasa a describir de manera muy breve una serie de dibujos que ayudan a comprender mejor la invención y que se relacionan expresamente con una realización de dicha invención que se presenta como un ejemplo no limitativo de

30   ésta.

La Figura 1 muestra las diferentes etapas de producción del material

La Figura 2 muestra esquemáticamente la evolución de la estructura celular durante el proceso de espumado en la que se observan las modificaciones en densidades y anisotropía.

35   La figura 3a muestra una imágen de la estructura celular anisotrópica con alto contenido de celda abierta correspondiente a una material celular en base

polipropileno que contiene nanopartículas de tipo nanoarcillas. (ejemplo 1) fabricada mediante el procedimiento de la invención.

La Figura 3b muestra una imagen de la estructura celular anisótropica para un material fabricado en base un polipropileno de alta resistencia en el fundido (ejemplo 2) fabricada mediante el procedimiento de la invención..

La Figura 3c muestra una imagen de la estructura celular con menor grado de anisotropía fabricada en base un polipropileno de alta resistencia en el fundido (ejemplo 3)

En las figuras anteriormente citadas se identifican una serie de referencias que corresponden a los elementos indicados a continuación, sin que ello suponga carácter limitativo alguno:

1.- cuerpo del molde

2.- junta elástica

3.- pistón en T

4.-tapa inferior

5.- material precursor

6.- pieza expansora

7.- pieza de retención

8.- pistón cilíndrico

9.- sector superior del pistón en T

10.- base del pistón

11.- cavidad interior

Descripción detallada de un modo de realización

Tal y como se muestra en la figura 1 el procedimiento de fabricación de materiales celulares de matriz termoplástica no reticulada con densidades relativas inferiores a 0.2, con índices de anisotropía superiores a 1.5 tanto en celda abierta como en celda parcialmente interconectada y un módulo elástico relativo en compresión superior a 0,6 MPa/(kg/m^3) un módulo de cizalla relativo superior a 0,18 MPa/(kg/m^3) y un esfuerzo de colapso superior a 0,010 MPa/(kg/m^3), comprende:

- Una etapa inicial (A) de mezcla y granceado de al menos un polímero termoplástico con un agente espumante químico y al menos una nanopartícula del tipo nanoarcilla, nanotubo de carbono, nanofibra de carbono, sílice, grafeno, organotitanatos y organizirconatos, etc. formando

-14-

un material precursor (5),

- Posteriormente introducir el material precursor (5) obtenido, en un molde que comprende una pieza (3) de expansión unidireccional del material precursor (5) y otra de control de la densidad (6 y 7), (B)

5 - tras introducir la mezcla en el molde se eleva la temperatura del molde por encima de la temperatura de descomposición del agente espumante hasta obtener la fusión de la matriz polimérica y la descomposición del agente espumante (C1), aplicando simultáneamente una presión a la pieza de expansión unidireccional (3) del molde con unos valores por encima de la

10 presión generada por el agente espumante, hasta que el polímero funda y descomponga el agente espumante,

- se libera la presión (C2) para que se produzca la expansión (C3), mostrado en la figura 2, estando el valor final de la misma controlado por la pieza de retención de la expansión (7),

15 - se enfría el molde (D), y

- finalmente se desmoldea (E) la lámina obtenida cuando la totalidad del molde y la de la lámina en él contenida se encuentra a una temperatura inferior a la temperatura de cristalización si el polímero es semicristalino o a la de transición vítrea si el polímero es amorfo.

20 A continuación se detallan una serie de ejemplos prácticos de aplicación del procedimiento descrito con el molde de la invención:

Ejemplo 1

Fabricación de lámina de baja densidad con estructura celular anisotrópica y alto contenido de celdas abiertas en base polipropileno no reticulado y empleando

25 como carga nanoarcillas que presenta altas propiedades mecánicas específicas.

En un primer paso se mezclan en una extrusora doble husillo co-rotatorio polipropileno de alta resistencia al fundido (Daploy WB 135 HMS, Borealis), un polipropileno injertado con anhídrido maléico (Polybond 3150, Chemtura) nanoarcillas de tipo montmorillonita organomodificadas con sales cuaternarias de amonio (Cloisite

30 20 A, Southern Clay Products), un agente espumante, en este caso azodicarbonamida (Porofor M-C1, Lanxess) y antioxidantes Irgafos 168 e Irganox 1010 (Ciba) en proporciones de 81,9 %, 10%, 5 %, 3 %, 0,08% y 0,02 % respectivamente.

La mezcla se grancea y se introduce en el interior del cuerpo de un molde de acero inoxidable.

35 Dicho cuerpo del molde comprende:

-15-

- Un cuerpo (1) que comprende una cavidad interior (11) principal de formación de la lámina, que comprende:

  - en todo su perímetro superior e inferior una junta de material elástico resistente a la temperatura (2) como por ejemplo vitón y

  - atornillada a su parte inferior una tapa (4) fabricada en el mismo material que el cuerpo del molde y de la misma área que el área externa de este,

- un pistón (3) con sección transversal en forma de T. La parte más sobresaliente del pistón, esto es el sector superior (9), presiona contra la junta elástica (2) dejando el compartimento interno (11) del cuerpo (1) estanco a gases y al escape del material. Entre la base del cuerpo del pistón (10) y la base la cavidad (4) quedará un espacio (11) de 2 mm de altura. La cantidad de material (5) a introducir se calcula para que, una vez compactado, el material ocupe completamente este espacio entre base del molde (4) y pistón (3). De esta manera el pistón permanecerá constantemente realizando presión sobre la totalidad del material fundido,

- una pieza expansora (6) unida al cuerpo del molde, dicha pieza expansora con una altura variable según el espesor final (densidad final) de la lámina que se quiera fabricar, y

- una pieza de retención (7) unida al cuerpo del molde y que por sus dimensiones actuará como limitador de la expansión durante el ascenso del pistón durante la relajación de la presión.

El conjunto completo se introduce en una prensa de platos calientes precalentada a la temperatura de trabajo. Sobre el pistón en forma de T se coloca un segundo pistón cilíndrico de aluminio que transmitirá la presión y el calor al material. Los platos de la prensa están precalentados a 190 ºC y se ejerce una presión de 5 bar. Las nanoarcillas presentan un efecto catalizante sobre la azodicarbonamida reduciendo la temperatura de descomposición, por lo que la temperatura óptima de proceso es 190ºC.

El conjunto del molde permanece bajo estas condiciones durante el tiempo necesario para que el polímero funda y descomponga el agente espumante. Por efecto de la presión aplicada sobre el material el gas descompuesto queda disuelto dentro del polímero sin producir espumación.

-16-

Transcurrido dicho tiempo la presión se libera lentamente a una velocidad de 10 mm/min dejando crecer el material en una única dirección. El pistón en forma de T se ve detenido por la pieza de retención alcanzándose así la expansión deseada.

El conjunto del molde se extrae de la prensa y se sumerge en agua para proceder a su enfriamiento. Una vez que la temperatura ha descendido por debajo de la temperatura de solidificación del polímero el conjunto puede extraerse del agua y desmontarse para proceder a la extracción de la lámina.

En estas condiciones se obtiene una pieza, tal y como se muestra en la figura 3a, de densidad 150 kg/m^3 con un 85% de contenido de celda abierta y un valor de anisotropía celular cercano a 3 (figura 3a). Las propiedades mecánicas en compresión dan un módulo de Young de 100 MPa, modulo de cizalla de 33 MPa y un esfuerzo de colapso de 1,8 MPa. La pieza presenta un excelente acabado superficial.

Ejemplo 2

Fabricación de lámina de baja densidad con estructura celular anisotrópica y celda cerrada en base polipropileno no reticulado que presenta altas propiedades mecánicas específicas.

En un primer paso se mezclan en una extrusora doble husillo co-rotatorio polipropileno de alta resistencia al fundido (Daploy WB 135 HMS, Borealis), un agente espumante, en este caso azodicarbonamida (Porofor M-C1, Lanxess) y antioxidantes Irgafos 168 e Irganox 1010 (Ciba) en proporciones de 96,9 %, 3 %, 0,08% y 0,02 % respectivamente.

La mezcla se grancea y se introduce en el interior del cuerpo de un molde de acero inoxidable.

Dicho cuerpo del molde comprende:

- Un cuerpo (1) que comprende una cavidad interior (11) principal de formación de la lámina, que comprende:

   ▪ en todo su perímetro superior e inferior una junta de material elástico resistente a la temperatura (2) como por ejemplo vitón y

   ▪ atornillada a su parte inferior una tapa (4) fabricada en el mismo material que el cuerpo del molde y de la misma área que el área externa de este,

- un pistón (3) con sección transversal en forma de T (Figura 1) cuyo sector superior (9) del pistón presiona contra la junta elástica (2) dejando el compartimento interno del cuerpo estanco a gases y al escape del material.

-17-

Entre la base inferior (10) del cuerpo del pistón (3) y la base interior de la cavidad (4) queda un espacio (11) de 2 mm de altura. La cantidad de material a introducir se calcula para que, una vez compactado y fundido, el material (5) ocupe completamente este espacio entre base de la cavidad (10) y base (10) del pistón (3) . De esta manera el pistón permanecerá constantemente realizando presión sobre la totalidad del material fundido,

- una pieza expansora (6) atornillada unida al cuerpo del molde, con una altura variable según el espesor final (densidad final) de la lámina que se quiera fabricar, y

- una pieza de retención (7) unidad al cuerpo del molde y que por sus dimensiones actuará como limitador de la expansión durante el ascenso del pistón durante la relajación de la presión.

El conjunto completo se introduce en una prensa de platos calientes precalentada a la temperatura de trabajo. Sobre el pistón (3) en forma de T se coloca un segundo pistón cilíndrico (8) de aluminio que transmitirá la presión y el calor al material. Los platos de la prensa están precalentados a 200 ºC y se ejerce una presión de 35 bar. El conjunto del molde permanece bajo estas condiciones durante el tiempo necesario para que el polímero funda y descomponga el agente espumante.

Por efecto de la presión aplicada sobre el material (5) el gas descompuesto queda disuelto dentro del polímero sin producir espumación.

Transcurrido dicho tiempo la presión se libera lentamente a una velocidad de 10 mm/min dejando crecer el material en una única dirección. El pistón (3) en forma de T se ve detenido por la pieza de retención alcanzándose así la expansión deseada.

El conjunto del molde se extrae de la prensa y se sumerge en agua para proceder a su enfriamiento.

Una vez que la temperatura ha descendido por debajo de la temperatura de solidificación del polímero el conjunto puede extraerse del agua y desmontarse para proceder a la extracción de la lámina.

En estas condiciones se obtiene una pieza de densidad 150 kg/m^3 con un 5% de celda abierta y un valor de anisotropía celular cercano a 3 (figura 3b). Las propiedades mecánicas en compresión dan un módulo de Young de 120 MPa un módulo de cizalla de 35 MPa y un esfuerzo de colapso de 1.8 MPa. La pieza presenta un excelente acabado superficial.

Tal y como se ve en la figura 3b, Una menor densidad (mayor expansión) da lugar a estructuras más anisotrópicas.

-18-

Ejemplo 3

Fabricación de lámina de baja densidad con estructura celular anisotrópica y celda cerrada en base polipropileno no reticulado que presenta altas propiedades mecánicas específicas y que además presenta una reducción en el tamaño de celda.

5   Las condiciones de fabricación en este caso son exactamente iguales a las empleadas en el ejemplo 2 a excepción de la presión empleada que pasa de 35 bar a una presión de 85 bar. Este aumento de presión tiene como consecuencia una disminución en el ratio de anisotropía y una disminución también en el tamaño medio de celda que presenta la pieza final. La anisotropía pasa de un valor cercano a 3 en el

10   ejemplo 2 a un valor de 1.5 en este caso y el tamaño celular pasa de las 300 µm obtenidas en el ejemplo 1 a una media de 150 µm (figura 3c).

Como consecuencia de la disminución en el ratio de anisotropía que presenta esta muestra, sus propiedades mecánicas también se ven disminuidas hasta un valor del módulo de Young en compresión de 90 MPa para la misma densidad de 150

15   kg/m^3.

A pesar de esta disminución el módulo de Young específico sigue siendo alto y la disminución de tamaño de poro tiene un efecto positivo en las propiedades aislantes térmicas del panel pudiendo ser empleado en aplicaciones estructurales donde el aislamiento térmico sea importante.

20   En conclusión se puede decir que:

- Cuando la cantidad de agente espumante es la mínima necesaria para alcanzar el grado de expansión deseado entonces las propiedades mecánicas específicas son óptimas.

- Mediante la variación de la presión externa aplicada se puede variar y controlar la

25   estructura celular final en términos de grado de anisotropía, tamaño de celda y tortuosidad.

- Mayores presiones externas dan lugar a menores ratios de anisotropía y menores tamaño de celda.

- Liberaciones lentas (< 10 mm/min) de la presión dan lugar a una mejor calidad

30   externa de la pieza y velocidades de liberación rápidas (> 1000 mm/min) dan lugar a una peor calidad externa de la pieza.

- En el caso de incluir expresamente la presencia de cargas de tamaño nanométrico del tipo nanoarcillas organomodificadas, nanotubos de carbono, nanofibras de carbono, etc. se dan lugar a estructuras celulares con contenidos de celda cerrada

35   inferiores al 90% y propiedades mecánicas específicas similares a las obtenidas en el

-19-

caso de contenidos de celda cerrada superiores al 90%.

- En el caso de incluir expresamente la presencia de nanoarcillas naturales (no organomodificadas) da lugar a estructuras celulares con contenidos de celda cerrada inferiores al 90% y propiedades mecánicas específicas similares a las obtenidas en el

5　　caso de contenidos de celda cerrada superiores al 90% sin la necesidad de añadir polímeros compatibilizantes con las ventajas inherentes a este hecho.

- En el caso de incluir expresamente la presencia de nanoarcillas, tanto organomodificadas como naturales, en combinación con el agente espumante azodicarbonamida se produce un efecto catalítico de activación de la descomposición

10　　de dicha azodicarbonamida lo cual permite reducir las temperaturas de proceso para conseguir la misma liberación de gas.

- El grado de anisotropía aumenta a medida aumenta el grado de expansión (disminuye la densidad relativa) de tal manera que se produce una compensación de la disminución de propiedades mecánicas a bajas densidades.

15

-20-

REIVINDICACIONES

1- Procedimiento de fabricación de materiales celulares de matriz termoplástica no reticulada con densidades relativas inferiores a 0.2, con índices de anisotropía superiores a 1.5 tanto en celda abierta como en celda parcialmente interconectada y un módulo elástico relativo en compresión superior a 0,6 MPa/(kg/m^3) un módulo de cizalla relativo superior a 0,18 MPa/(kg/m^3) y un esfuerzo de colapso superior a 0,010 MPa/(kg/m^3), caracterizado por que comprende las etapas de:

- Una etapa inicial (A) de mezcla y granceado de al menos un polímero termoplástico con un agente espumante químico y al menos una nanopartícula, formando un material precursor (5),

- Posteriormente introducir el material precursor (5) obtenido, en un molde (B) que comprende una pieza (3) de expansión unidireccional del material precursor (5) y otra de control de la densidad (6 y 7),

- tras introducir la mezcla en el molde se eleva la temperatura del molde por encima de la temperatura de descomposición del agente espumante hasta obtener la fusión de la matriz polimérica y la descomposición del agente espumante, aplicando simultáneamente una presión a la pieza de expansión unidireccional (3) del molde con unos valores por encima de la presión generada por el agente espumante, hasta que el polímero funda y descomponga el agente espumante, (C1)

- se libera la presión (C2) para que se produzca la expansión (C3), estando el valor final de la misma controlado por la pieza de retención de la expansión (7),

- se enfría el molde (D), y

- finalmente se desmoldea (E) la lámina obtenida cuando la totalidad del molde y la de la lámina en él contenida se encuentra a una temperatura inferior a la temperatura de cristalización si el polímero es semicristalino o a la de transición vítrea si el polímero es amorfo.

2- Procedimiento de fabricación de materiales celulares según reivindicación 1 caracterizado por que el molde en el que se introduce el material precursor (5) es un molde que comprende:

○ Un cuerpo (1) que comprende una cavidad interior (11) principal de formación de la lámina en la que se introduce la mezcla (5) y que comprende:

-21-

- ▪ en todo su perímetro superior e inferior una junta de material elástico resistente a la temperatura (2) y
- ▪ atornillada a su parte inferior una tapa (4) de la misma área que el área externa de este,

5

- o un pistón (3) con sección transversal en forma de T cuyo sector superior (9) presiona contra la junta elástica (2) dejando la cavidad (11) del cuerpo (1) estanco a gases y al escape del material (5), de manera que entre la base inferior (10) del cuerpo del pistón (3) y la base interior de la cavidad (4) queda un espacio (11) en el que se

10

  introduce el material precursor (5),

- o una pieza expansora (6) unida al cuerpo del molde, con una altura variable según el espesor final (densidad final) de la lámina que se quiera fabricar, y
- o una pieza de retención (7) limitadora de la expansión unida al

15

  cuerpo del molde

3-. Procedimiento según reivindicaciones 1 o 2 caracterizado por que en la etapa inicial (A) se mezcla y grancea con el al menos un polímero termoplástico con un agente espumante químico, al menos una nanopartícula seleccionada entre nanoarcilla, nanotubo de carbono, nanofibra de carbono, sílice, grafeno,

20

organotitanatos u organozirconatos

4.- Procedimiento según reivindicaciones anteriores caracterizado por que la mezcla comprende como polímero termoplástico polietileno de baja densidad, polietileno de de alta densidad, polietileno lineal de densidad, polipropilenos homopolímeros o copolímeros lineales o ramificados, PVC, PET, PS, PA, etc o mezclas de los mismos.

25

5.- Procedimiento según reivindicaciones anteriores caracterizado por que la mezcla comprende como agente espumante un compuesto seleccionado entre azodicarbonamida, Oxibis (hidracina de bencensulfonil), 5-feniltetrazol, bicarbonato, ácido cítrico, etc. o mezclas de los mismos.

6.-Procedimiento para la fabricación de piezas termoplásticas espumadas de acuerdo

30

a la reivindicaciones anteriores caracterizado por que la cantidad de agente espumante introducido en la formulación se ajusta de tal manera que el gas generado en su descomposición sea igual o mayor al necesario para conseguir el grado de expansión deseado.

7.- Procedimiento según reivindicaciones anteriores caracterizado por que la mezcla

35

de la etapa inicial (A) incluye aditivos seleccionados entre:

-22-

- cargas seleccionadas entre talco, carbonato cálcico, nanoarcillas, nanosílicas, nanotubos de carbono, nanofibras de carbono o grafenos,

- refuerzos seleccionados entre fibras de vidrio o fibras de carbono,

- ayudantes de proceso seleccionados entre ceras o ácido esteárico,

5   - agentes nucleantes seleccionados entre talco, nanopartículas o silicas,

- antioxidantes,

- pigmentos,

- activadores de la reacción del agente espumante,

- espumante y/o

10   - agentes repolimerizantes seleccionado entre neoalkoxy organotitanatos u organozirconatos.

8.- Procedimiento según reivindicación 7 caracterizado por que la mezcla de la etapa inicial (A) incorpora nanoarcillas organomodificadas como cargas de tamaño nanométrico y un polímero compatibilizante que promueve la dispersión y exfoliación

15   de dichas partículas de tamaño nanométrico.

9.- Procedimiento según reivindicaciones anteriores caracterizado por que la mezcla es prensada o extruida previa a la introducción en el molde dando lugar a un material precursor sólido.

10.- Procedimiento según reivindicaciones 2-9 caracterizado por que la presión sobre

20   el material precursor en el molde (B) es ejercida de forma mecánica mediante una prensa situando un segundo pistón cilíndrico (8) sobre el pistón (3) en forma de T para transmitir la presión hasta el material (5) de tal manera que el gas generado quede disuelto en el polímero fundido precursor sin producir ningún tipo de espumación mientras la presión continúe aplicada.

25   11.- Procedimiento según reivindicación 10 caracterizado por que la temperatura aplicada en el material precursor situado en el molde (B) se aplica calefactando los platos superior e inferior de la prensa, mediante elementos emisores de calor seleccionados entre camisas laterales calefactoras externas, infrarrojos o resistencias eléctricas insertadas en el cuerpo del molde, circuitos internos al molde en los que se

30   introducen líquidos para calentar..

12.- Procedimiento según reivindicaciones anteriores caracterizado por que el enfriamiento del molde se produce por un método seleccionado entre circulación de aire, sumergiendo el molde en un baño de agua u otro líquido para un enfriamiento rápido o introduciendo circuitos por los que se puede producir la entrada y salida de
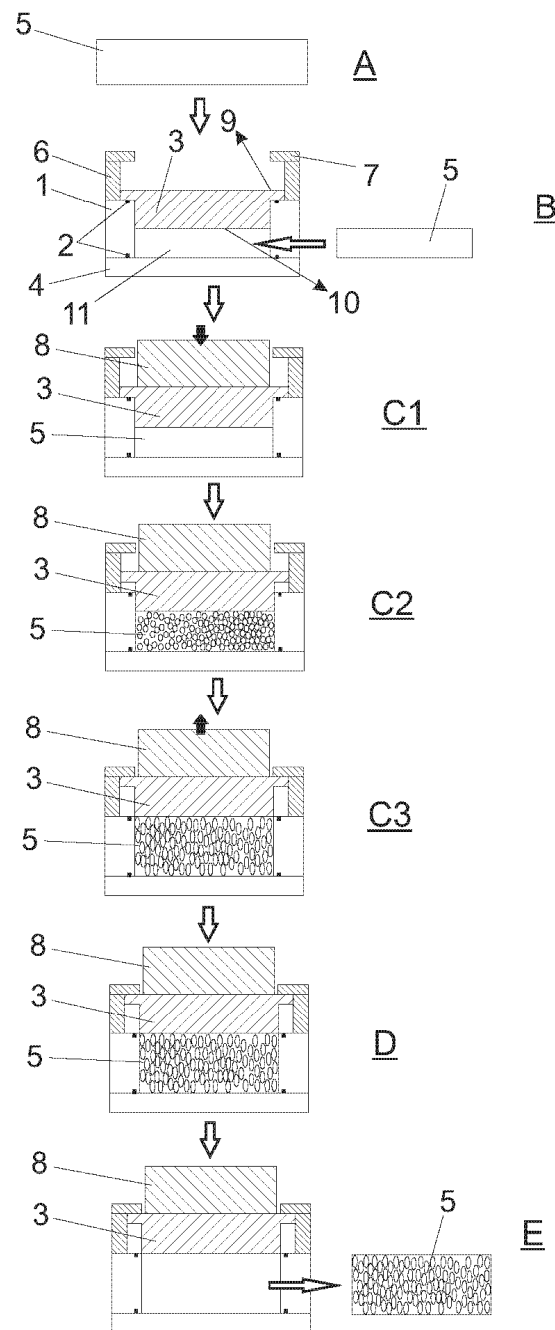
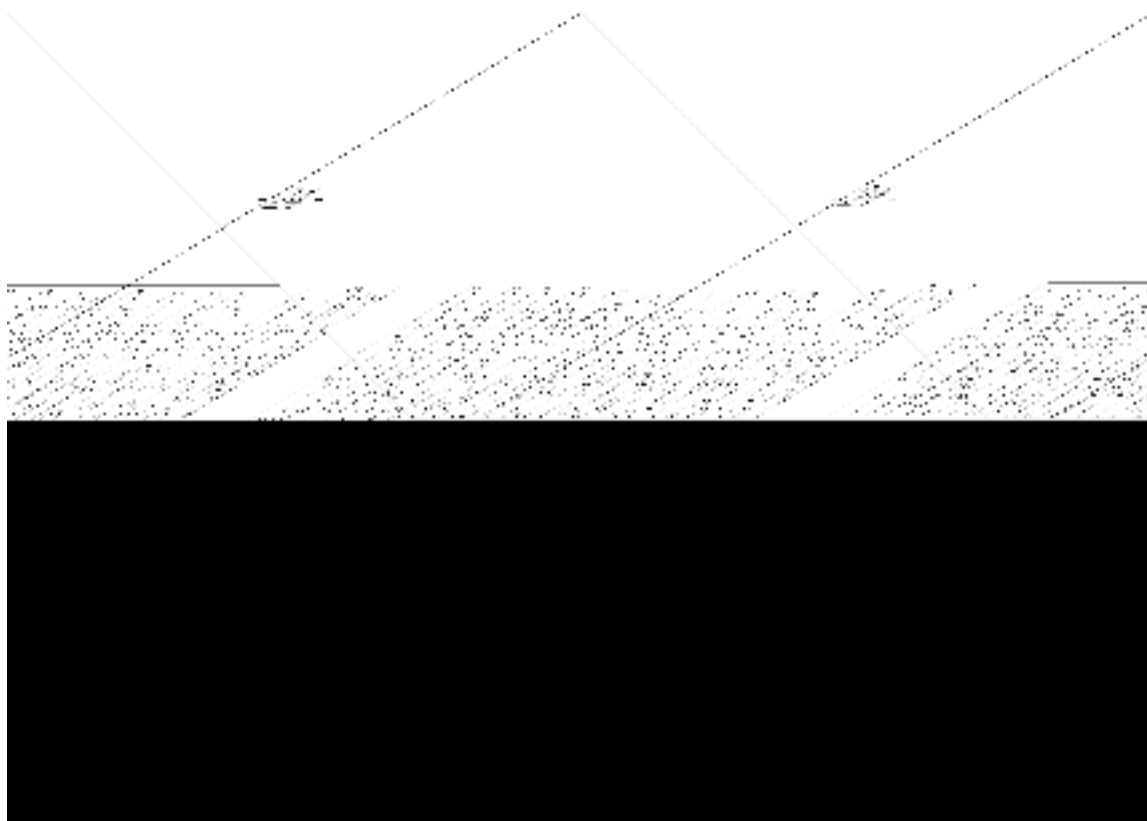35   agua u otros líquidos en el cuerpo del molde.

- 23 -

FIG. 1
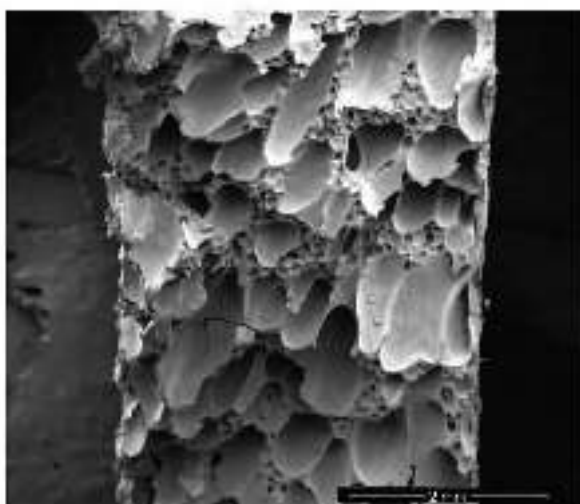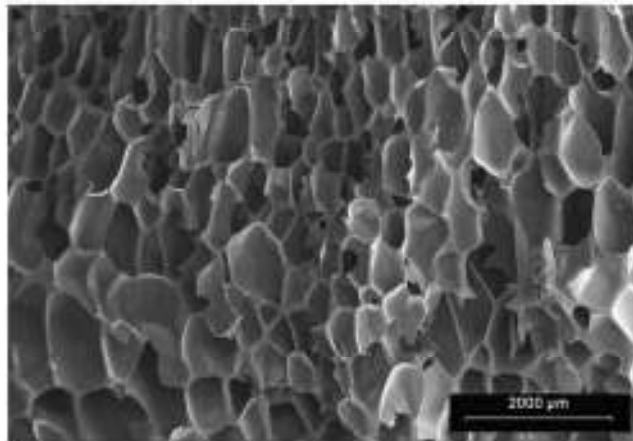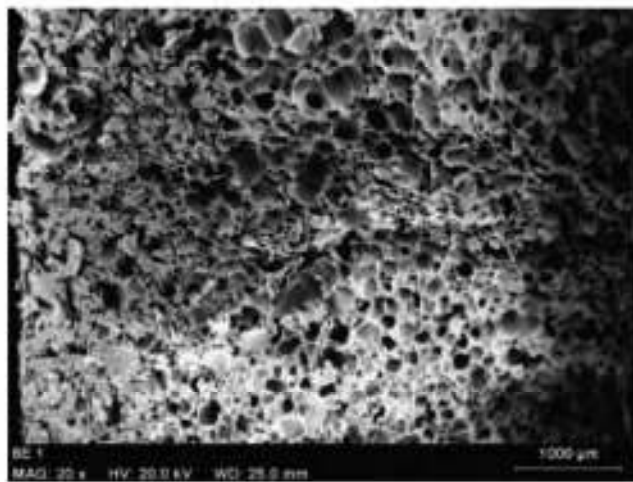
FIG. 2

FIG. 3A

- 25 -

FIG. 3B

FIG. 3C

Annex II

Non-indexed Publications

II.1.- INTRODUCTION

Annex II present two works published in the spanish journal "Revista de Plásticos Modernos" (Journal of Modern Plastics) which is a publication with high dissemination in the spanish plastic industry. Both publications have dissemination purposes but without losing the scientific focus, both of them include experimental data and a scientific approach.

II.2.- NON-INDEXED PUBLICATION 1. THE MULTIFUNCTIONAL ROLE OF NANOPARTICLES IN CELLULAR MATERIALS

During the previous chapters we have discussed, at great length, the influence of nanoparticles over very different properties of cellular materials. As already studied, properties are not modified independently, the addition of nanoparticles always affect several different properties at the same time. The first publication presented in this annex II pretends to give a general overview about the multifunctional role of nanoparticles found in cellular material based on nanocomposites. Futhermore, interesting synergetic effects effects were found in diverse systems as nanosilica particles in LDPE-based foams or carbon nanotubes in polypropylene-based cellular materials.

Artículos

El efecto multifuncional de las nanopartículas en los materiales celulares

Autores:
J. Escudero, C.
Saiz-Arroyo, M. A.
Rodríguez-Pérez, J.
A. de Saja

Laboratorio de Materiales Celulares CellMat
Departamento de Física de la Materia Condensada, Universidad de Valladolid
Prado de la Magdalena s/n 47011 Valladolid
jdss@fmc.uva.es

Resumen

La adición de partículas de tamaño nanométrico a materiales poliméricos representa uno de los campos más prometedores dentro del mundo de los plásticos. La amplia multifuncionalidad que presentan estas nanopartículas las convierten en atractivos candidatos para la mejora de propiedades en múltiples sectores industriales. Si además se recurre a estas nanopartículas para fabricar materiales celulares hemos comprobado que aparecen efectos sinérgicos muy interesantes.

El Laboratorio de Materiales Celulares CellMat de la Universidad de Valladolid trabaja en la actualidad en diferentes tesis doctorales y proyectos, tanto con financiación pública como privada, basadas en este tema. El presente artículo pretende dar una visión general así como mostrar desde una perspectiva tanto científica como tecnológica las diversas aplicaciones de estos materiales compuestos

Palabras clave: nanocompuestos poliméricos, materiales celulares, sílices nanométricas, nanoarcillas.

THE MULTIFUNCTIONAL EFFECT OF NANOPARTICLES IN CELLULAR MATERIALS

Abstract

The addition of particles in the nano-scale to polymeric materials represents nowadays one of the most promising areas in the world of plastics. The great multifunctionality that these nanoparticles present makes them interesting candidates for the improvement of properties in several areas. At the same time when a cellular material is produced having as solid matrix one of this nanocomposites synergetic effects appear.

The Cellular Materials Laboratoty CellMat of the University of Valladolid is currently working in different PhD. Thesis and projects, with both private and public funding, dealing with this area. This paper pretends to give a general overview as well as show, from both a scientific and technical point of view, the different applications of these materials.

Key words: polymer nanocomposites, cellular solids, nanosilicas, nanoclays.

326
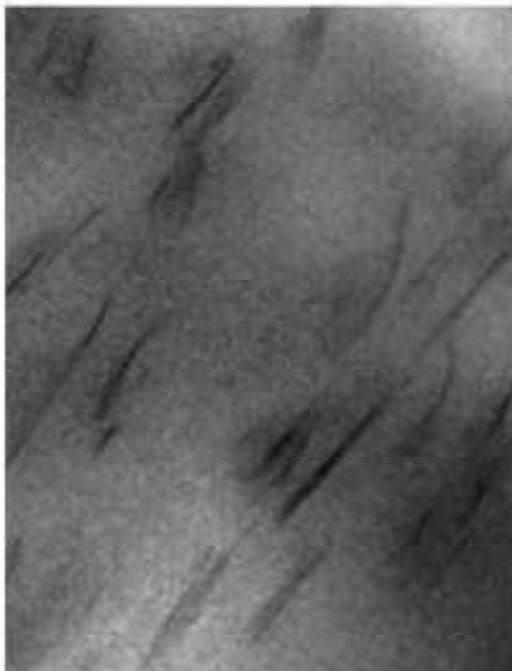
Introducción

En los últimos años la denominada nanotecnología es una de las disciplinas que más interés ha suscitado tanto entre la comunidad científica como en el ámbito industrial. Son tales las expectativas generadas que aún a día de hoy cualquier cosa a la que anteceda el prefijo "nano" despierta una atención casi mágica.

La ciencia de materiales y el mundo de los plásticos en particular, no se han quedado en absoluto atrás en la carrera de exploración de las nuevas y prometedoras posibilidades que se esperan en el mundo nanométrico. Así, la nanociencia se aplica a día de hoy en sectores como la electrónica, materiales magnéticos, biomateriales, materiales conductores eléctricos, conductores térmicos, materiales de construcción, etc [1,2].

En el caso de los plásticos encontraríamos los denominados nanocompuestos poliméricos. Estos nuevos materiales consisten en la dispersión de cargas de tamaño nanométrico dentro de una matriz polimérica. En principio, estos nanocompuestos podrían ser fabricados fundamentalmente empleando métodos de fabricación convencionales o incluso empleando métodos de fabricación ya desarrollados para nanocom-

puestos cerámicos o metálicos. Los nanocompuestos poliméricos deberían tener unas propiedades sobresalientes en comparación a los plásticos habituales a costa de un pequeño incremento en precio [3].

Científicamente es conocido que en la escala nanométrica propiedades como la temperatura de fusión, el campo remanente en un material magnético o el gap de un semiconductor dependen del tamaño del cristal que se esté considerando. Incluso se ha demostrado que las propiedades mecánicas de algunas aleaciones metálicas se incrementan hiperbólicamente cuando reducimos el tamaño del dominio bajo estudio [1, 2].

Para poder aplicar el término de nanocompuesto al menos una de las dimensiones de las cargas que se adicionan al material debe ser inferior a 10 nm. La relación de aspecto de estas partículas (cociente del área superficial frente al volumen) juega un papel fundamental. Por ejemplo el caso de la arcilla montmorillonita, una de las nanocargas más habitualmente empleadas, el 40% de sus átomos se encuentra sobre la superficie de cada una de las láminas que la conforman. Este hecho, que en principio podría parecer accesorio, determina propiedades tan importantes como la procesabilidad, la adhesión matriz-nanocarga o la orientación dentro del material.

Tradicionalmente los materiales poliméricos han sido aditivados con cargas de tamaño micrométrico con el fin de incrementar su comportamiento mecánico, mejorar su efecto como barrera a gases, dotarles de una capacidad retardante de llama, etc. Estos aditivos micrométricos permiten mejorar muy diversas propiedades del plástico sin suponer un detrimento considerable en su bajo peso y su ductilidad. Los avances en nanotecnología han permitido disminuir el tamaño de las cargas introducidas en el polímero hasta la nanoescala. Centrándonos por ejemplo en las propiedades mecánicas, las teorías micromecánicas aceptadas para explicar el comportamiento de un determinado material cargado consideraban como posibles variables de influencia las propiedades de los constituyentes, su fracción en volumen, su forma y aglomeración o la adhesión matriz-carga pero mostraban independencia del tamaño de la carga. En general esto es cierto en la escala micrométrica, sin embargo pueden perder toda validez cuando nos vamos a escalas del orden del nanómetro. Diversos estudios, tanto experimentales como teóricos, muestran que pequeños porcentajes de estos aditivos pueden suponer incrementos enormes en todas las propiedades mencionadas anteriormente [3].

Todas estas mejoras en propiedades que aparecen en los nanocompuestos poliméricos sólidos tendrían su extensión en el mundo de los materiales celulares de matriz polimérica. Lo interesante es que las mejoras encontradas en los materiales celulares no son consecuencia únicamente de la matriz base sino que estas

Artículos

nanocargas juegan también un papel importante en el proceso de espumación. Este efecto sinérgico de las nanopartículas nos lleva a encontrar incrementos aún mayores en diversas propiedades en el material celular con respecto a los de la matriz polimérica sólida [4].

En este artículo pondremos de manifiesto el efecto sinérgico y el papel multifuncional que las cargas de tamaño nanométrico tienen en los materiales celulares a través de la experiencia que el laboratorio CellMat de la Universidad de Valladolid tiene en este campo.

Plásticos y nanopartículas

Las nanocargas dentro del sector de los plásticos no tienen un único efecto aislado sobre una única determinada propiedad sino que aun a bajas proporciones juegan un papel importante en la modificación y mejora de las propiedades y aplicaciones más importantes de los polímeros.
En la figura 1 se esquematizan los principales efectos que las nanopartículas tienen sobre la matriz polimérica sólida.

- Modificar la morfología del polímero: la presencia de nanopartículas puede incluso modificar el hábito cristalino en el cual cristaliza un determinado polímero o puede inducir cristalizaciones preferenciales en ciertas direcciones cristalográficas. Sin embargo el principal efecto sobre la morfología del polímero consiste en actuar como agentes nucleantes durante la cristalización. En el proceso de cristalización las cargas favorecen la nucleación heterogénea frente la homogénea convencional que seguiría el polímero en ausencia de éstas. Puesto que el proceso de nucleación implica la adsorción de macromoléculas sobre la superficie del nucleante, cuanto mayor sea le energía super-

ficial de la carga y más parecida sea su estructura cristalográfica a la estructura de la matriz polimérica mayor será el efecto nucleante desempeñado. Como ya se comentó en la introducción, debido a la enorme relación de aspecto que presentan las cargas de tamaño nanométrico y por tanto su gran energía superficial, estas nanopartículas deberían tener un gran efecto como agentes nucleantes incrementando el grado de cristalinidad del polímero y por lo tanto mejorando propiedades tales como las mecánicas de la matriz de partida [5,6].

- Mejorar la estabilidad térmica: diversos estudios indican que la presencia de nanopartículas incrementan el comportamiento térmico del polímero inhibiendo la degradación por temperatura. Esto amplía la ventana de procesado de determinados polímeros en cuanto a temperatura se refiere, entre otras muchas ventajas. En ciertas aplicaciones ello puede traducirse en solventar problemas surgidos como consecuencia de la pérdida de propiedades del polímero asociados a la temperatura [7,8,9].

- Mejorar el rendimiento mecánico: una de las principales razones por las que los nanocompuestos poliméricos han atraído tanta atención radica en las prometedoras propiedades mecánicas que presentarían. Por ejemplo, los nanotubos de carbono en la dirección axial presentarían un módulo de Young en compresión de 1000 GPa, mucho más alto que cualquier carga de tamaño micrométrico convencional. Debido a ello, para obtener unas propiedades mecánicas sobresalientes se requeriría únicamente la adición de bajos porcentajes de estas nanopartículas. Puesto que los esfuerzos mecánicos se transfieren hasta la nanocarga a través de la matriz, la buena dispersión y desaglome-

Figura 1: Principales mejoras que presentan los nanocompuestos poliméricos frente a los plásticos convencionales.

Artículos

ración así como la obtención de una buena compatibilización entre la nanopartícula y la matriz del polímero son fundamentales para sacar el mayor partido de estas propiedades [10,11].

· Mejorar la resistencia a la llama: las mejores propiedades vinculadas a la resistencia a la llama están también relacionadas con la mayor estabilidad térmica de los nanocompuestos. Por ejemplo, en nanocompuestos cargados con un 2% a un 8% de nanoarcillas tipo montmorillonita, se encuentran disminuciones en la inflamabilidad que van desde el 50% hasta el 80%. En este caso por ejemplo la carbonización de la arcilla actúa como aislante favoreciendo el comportamiento retardante. A su vez, debido a las propiedades de barrera a gases que comúnmente presentan estas nanocargas, la penetración de oxígeno hacia el interior del plástico se ve disminuida considerablemente reduciendo el poder de combustión [12,13].

A la hora de fabricar un material celular a partir de un nanocompuesto polimérico todas las propiedades aportadas por las nanocargas a la matriz se transmitirán a la muestra espumada. Pero lo que resulta realmente interesante es que, a la hora de emplear nanopartículas en un material celular aparecerán nuevas mejoras añadidas a las del material sólido [9]. En la figura 2 se detallan esquemáticamente los beneficios que las nanopartículas aportan inherentemente al plástico espumado.

· Papel como nucleantes: la presencia de cargas dentro de la matriz polimérica disminuye la energía superficial que una celda necesita para nuclear y formarse durante el proceso de espumación. Por

Figura 2: Efectos de las nanopartículas inherentes a los materiales celulares.

lo tanto las cargas constituyen localizaciones preferentes para la nucleación celular. En el caso de emplear nanocargas, si se ha conseguido una dispersión alta y homogénea, el número de centros nucleantes por unidad de volumen será mucho mayor que en el caso de cargas convencionales. Esto dará lugar a estructuras celulares muy homogéneas, con una alta densidad celular y una reducción en el tamaño de poro, redundando en una mejora de las propiedades globales de la espuma [14, 15].

· Modificación de la viscosidad extensional: el principal mecanismo de deformación que tiene lugar durante el crecimiento celular es una extensión biaxial, por lo tanto la viscosidad extensional de la matriz tiene una importancia radical durante el proceso de espumado. Las nanopartículas suelen suponer un incremento de esta viscosidad lo cual a la larga se traduce en una mayor capacidad del polímero para retener el gas durante la formación

de la espuma permitiéndonos obtener expansiones más altas con tamaños de poro inferiores [15].

· Mejora en las propiedades de barrera: las nanocargas aumentarían el recorrido libre medio que una molécula de gas debería seguir al atravesar una determinada porción de matriz polimérica. Esta disminución en la permeabilidad a gases es muy importante a la hora de considerar un material celular. En aplicaciones de embalaje, campo en el cual las espumas poliméricas tienen una gran presencia, las espumas soportan cargas durante largos periodos de tiempo sufriendo un proceso de fluencia. Evitar el escape hacia el exterior del gas contenido en las celdas es fundamental para conservar el rendimiento mecánico de estos materiales.

Los esquemas anteriores nos dan una idea de la multifuncionalidad que aporta la nanotecnología aplicada al campo de los plásticos y los plásticos celulares. Sin

embargo, para tener una idea más precisa, a continuación se detalla una experiencia práctica llevada a cabo en nuestro laboratorio.

Nanocompuestos de polietileno cargado con nanosílicas: un ejemplo de multifuncionalidad

Dentro de la experiencia del laboratorio CellMat en el campo de los nanocompuestos celulares una línea de investigación importante consiste en el estudio de las sílices nanométricas como carga en diversos plásticos, tanto en su vertiente sólido continuo como celular.

Aunque no tan famosas como las nanoarcillas o los nanotubos de carbono, las sílices nanométricas representan un sistema de estudio ideal desde un punto de vista científico y con prometedoras posibles aplicaciones industriales. Debido a su abundancia en la naturaleza presentan un bajo coste. Poseen una alta resistencia térmica y una alta capacidad de ser funcionalizadas confiriéndolas un carácter hidrófobo que facilite su compatibilización y dispersión dentro de una matriz polimérica. Además, debido a su simetría esférica la interpretación de los resultados experimentales obtenidos se ve libre de posibles efectos debidos a otras geometrías más complejas.

Existen diversos estudios en los que estas nanopartículas han sido añadidas a diferentes polímeros como poliuretano, policarbonato, poliestireno, EVA o PMMA. En nuestro caso el estudio se ha realizado sobre una matriz de polietileno. En primer lugar se caracterizaron las matrices sólidas cargadas y en segundo lugar estos sólidos fueron espumados y sus propiedades fueron estudiadas y comparadas con las del sólido.

En el estudio se utilizó un polietileno de baja densidad PE003 con un MFI de 2 g/10 min y una densidad de 920 kg/m³ al cual se añaden diferentes porcentajes de sílices R974, 1%, 3%, 6%, y 9% producidas por Evonik y sus propiedades se comparan con las del material sin cargar (0%). Empleando estos mismos materiales se fabricaron espumas mediante un proceso de moldeo por compresión mejorado, empleando como agente espumante azodicarbonamida Lanxess Porofor M-C1 con un tamaño de partícula de 3 µm. Todas las espumas fabricadas tienen la misma densidad relativa.

En la figura 3 se muestran dos micrografías correspondientes a los materiales celulares sin carga (izquierda) y con un 6% de sílices nanométricas (derecha). Se observa claramente una disminución en el tamaño celular medio pasando de 75 µm en el caso del material puro a 55 µm en el caso de añadir un 6% de nanopartículas. Además la distribución en el tamaño de celda es mucho más estrecha en el caso del material cargado indicando una mayor homogeneidad celular.
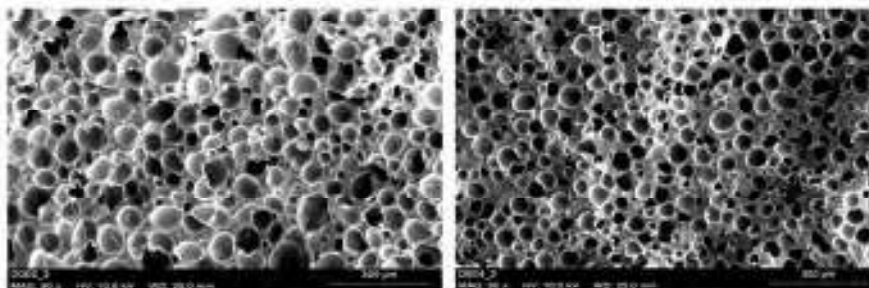
Artículos

Figura 3: Micrografías correspondientes a espumas no cargadas (izquierda) y cargadas con un 6% de nanosílicas derecha. Se observa la disminución en el tamaño de poro.

Este hecho ejemplifica el efecto nucleante que juegan las nanocargas durante el proceso de espumado del cual se había hablado durante la introducción.

Como ya se puso de manifiesto, en el campo de los materiales celulares el estudio de la viscosidad elongacional del polímero es fundamental para entender posteriormente la morfología de la espumación que van a sufrir estos materiales. La idea de estos ensayos en laboratorio consiste en mantener fija una velocidad de deformación determinada y medir la resistencia que opone el polímero a dicha deformación. Para realizar estas medidas en nuestro caso se empleó un reómetro ARES de la casa TA instruments.

En la figura 4 se muestran los resultados obtenidos para estos materiales. En el eje de ordenadas se representa la viscosidad elongacional en Pa+s frente al tiempo durante el que se deforma la muestra en segundos (eje de abscisas).

Se observa que la viscosidad elongacional del polímero aumenta considerablemente a medida que aumenta el porcentaje de carga agregada. Estas diferencias son aún más palpables en el caso de someter al polímero a altas deformaciones (tiempos altos). Este hecho permitiría obtener espumas de menor densidad con una mejor estructura celular usando sílices nanométricas como aditivo a la matriz del material.

Centrándonos en el estudio de las propiedades mecánicas de estos materiales se realiza un estudio del comportamiento a compresión tanto para los materiales sólidos como para los celulares. En la figura 5 se representa el módulo de Young tanto para sólidos como para espumas a los diferentes porcentajes de nanosílicas añadidos.

En el caso de los sólidos la mejora en propiedades mecánicas puede llegar hasta un 18% cuando añadimos un 6% de nanocargas. Sin embargo, si prestamos aten-
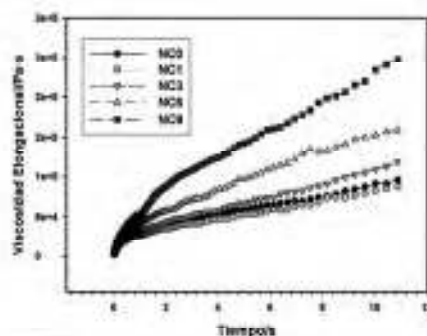

Figura 4: Viscosidad elongacional para los diferentes porcentajes de nanosílicas.

ción al caso de las espumas la mejora puede llegar a tomar valores superiores al 86%. Además una superior mejora se produce para un porcentaje de nanosílicas de un 3%. El incremento en propiedades mecánicas es mucho más alto en el caso de las espumas lo cual pone de manifiesto el efecto sinérgico que las nanoarcillas tienen en este tipo de nanocompuestos celulares de matriz polimérica.

En la figura 6 se representa el módulo de Young relativo a la densidad para espumas con diferentes porcentajes de carga. Este cálculo nos dará una idea de la influencia que tiene la estructura celular sobre las propiedades mecánicas de estos materiales, independizando el resultado de las propiedades mecánicas de la matriz.

Se observa que el mejor valor se obtiene para un porcentaje de 6%. Este porcentaje de nanocargas daba lugar a la estructura celular con el menor tamaño de
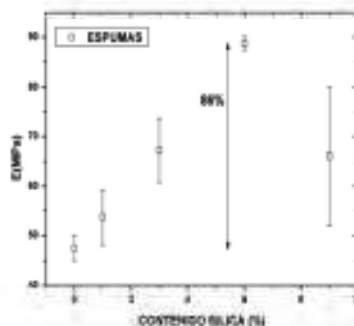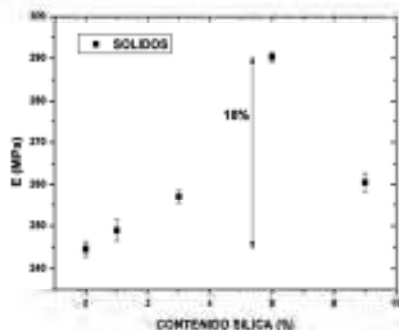
Artículos

Figura 5: Módulo de Young en compresión tanto para sólidos (izquierda) como para espumas (derecha) a los diferentes porcentajes de nanosílicas añadidos.
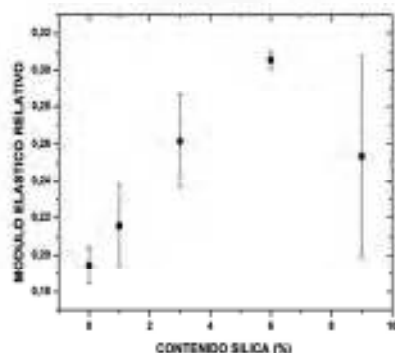

Figura 6: Módulo de Young relativo de los materiales celulares para los diferentes porcentajes de sílices nanométricas.

Figura 7: Esfuerzo de colapso para los materiales celulares a los diferentes porcentajes sílices.

celda. El hecho de tener una estructura celular más homogénea y con un menor tamaño de poro es beneficioso en cuanto lo que a propiedades mecánicas en compresión se refiere. Luego las nanosílicas no solo incrementan las propiedades mecánicas del sólido y esta mejora se transfiere posteriormente a la espuma, sino que, como consecuencia de su efecto nucleante este crecimiento es aún mayor en el caso del material espumado.

La figura 7 ilustra el esfuerzo de colapso obtenido en las espumas para los diferentes porcentajes de carga añadidos. De nuevo la tendencia es la misma, los mejores valores se obtienen para un porcentaje de 6%. Para el sistema considerado este porcentaje sería el óptimo a añadir para conseguir una mejora tanto en propiedades mecánicas como para conseguir estructuras celulares más homogéneas y de menor tamaño de celda.
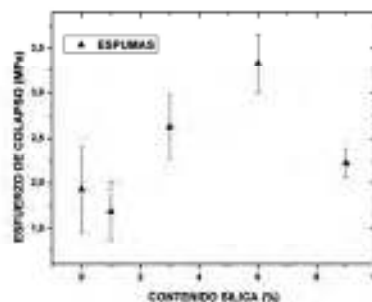
Algunos casos prácticos

En la actualidad son numerosos los esfuerzos realizados tanto desde la industria privada como desde diferentes grupos de investigación académica internacionales para aplicar la gran multifuncionalidad de estos nanocompuestos en diferentes casos prácticos. A continuación se detallan, clasificados por la aplicación buscada, algunos de los proyectos más importantes en los que se encuentra involucrado en la actualidad en Laboratorio de Materiales Celulares CellMat relacionados con este campo.

334

Artículos

- Requerimientos mecánicos y materiales ligeros. NANCORE es uno de los proyectos de mayor envergadura en los que el laboratorio CellMat está trabajando en la actualidad. Financiado por la Unión Europea y liderado por la multinacional danesa LM Glasfiber, NANCORE busca como objetivo principal la consecución de un novedoso material de relleno para las palas de aerogeneradores. En la actualidad los materiales más habitualmente empleados para esta aplicación son la madera de Balsa, con los condicionamientos medioambientales que ello conlleva así como una espuma de PVC con una complicada ruta de producción. El consorcio, formado por 13 socios de toda Europa entre grupos de investigación y empresas pretende desarrollar un material celular de relleno en base polipropileno o poliuretano a los que se les ha añadido un determinado porcentaje de nanocargas. Como posibles cargas se consideran nanoarcillas, nanotubos o nanofibras de carbono. El nuevo material debería ser capaz de soportar los requeri-

mientos mecánicos a los que se encuentran sometidas estas enormes palas, tanto en cizalla como en compresión además de tener una densidad por debajo de 200 kg/m³. Por otra parte deberá tener un precio mucho menor que la espuma de PVC (debido a un proceso de fabricación más sencillo) y liberaría a las empresas consumidoras de su dependencia de la madera de Balsa.

- Fabricación de piezas aligeradas. La consecución de piezas aligeradas es uno de los objetivos de diversas empresas del mundo de los plásticos. Lo que se busca es tener una pieza de menor densidad, tanto para aplicaciones en las cuales el peso es importante como para conseguir un ahorro de material, sin comprometer las solicitaciones mecánicas requeridas del material. Para ello es necesario conseguir una estructura celular con bajos tamaños de celda y una alta homogeneidad. Dentro del marco del programa "Innocash" el laboratorio CellMat y la empresa ABN Pipe desarrollan
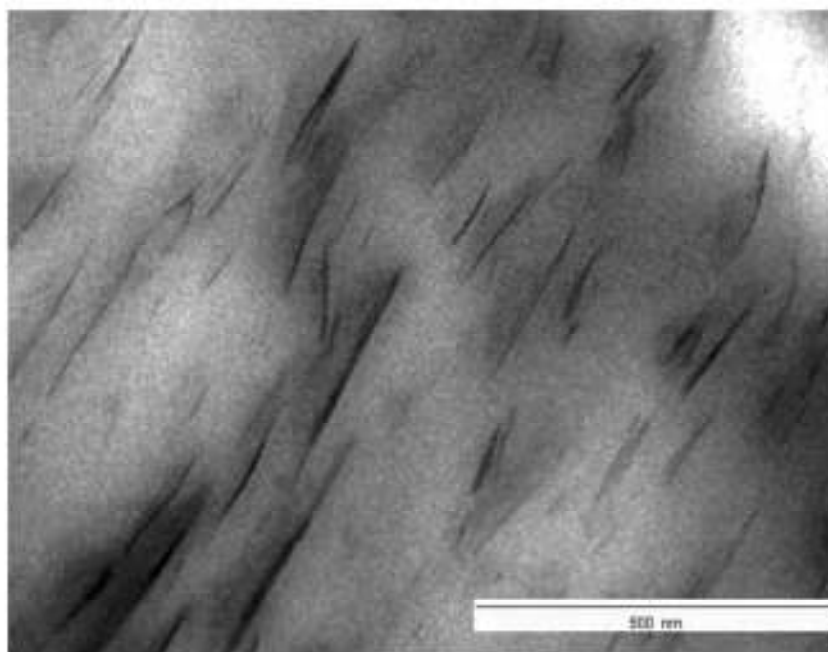

500 nm

Figura 8: Imagen TEM donde se aprecia la buena dispersión y exfoliación de nanoarcillas en polipropileno lograda en el marco del proyecto Nancore.

un proyecto conjunto para fabricar piezas aligeradas basadas en plástico mediante la tecnología "Stages Moulding" desarrollada conjuntamente. En este nuevo proceso de producción se usan nanopartículas como agentes nucleantes para reducir el tamaño de celda y aumentar el número y la homogeneidad de las celdas formadas. Estas partículas permiten además incrementar la viscosidad extensional o las propiedades mecánicas del material. La combinación de la tecnología "Stages Moulding" con la adición de nanocargas da lugar a un método barato de fabricación de piezas ligeras con propiedades mecánicas optimizadas y una excelente apariencia externa. Esta tecnología, debido al uso de moldes de bajo coste y a la reducción de materias primas necesarias, es un método ventajoso frente a la tecnología de inyección cuando se quieren fabricar series cortas y/o piezas de gran tamaño [16, 17].

Figura 8: Ejemplo de piezas fabricadas mediante la tecnología "Stages Moulding".
Arriba, piezas aligeradas empleadas en la unión de tuberías. Abajo, espuma estructural con morfología skin-core fabricada según el nuevo procedimiento.

Artículos

- Fabricación de aislantes térmicos optimizados: la conductividad térmica de un material celular polimérico depende de una manera importante de su tamaño de poro. Reducciones en el tamaño de celda aumentan la capacidad como aislantes térmico de estas espumas. Como ya se ha comentado anteriormente, la adición de nanopartículas facilitan este proceso. En la actualidad CellMat trabaja en el desarrollo de materiales, tanto con matrices termoplásticas como termoestables, que hacen uso de este concepto.

- Propiedades de barrera: en el marco de una tesis doctoral desarrollada en el departamento se lleva a cabo el estudio de la permeabilidad a gases de nanocompuestos cargados con nanoarcillas en base polietileno. Partiendo de matrices de polietileno con porcentajes de 3% y 5% de carga se llevan a cabo procesos de espumación empleando agentes espumantes tanto físicos como químicos. Durante la disolución de gas previa a la espumación física se lleva a cabo un estudio de desorción de gas empleando una balanza de alta precisión. Las muestras espumadas durante procedimientos químicos se someten posteriormente a un proceso de fluencia. Mediante el estudio de la variación longitudinal de la muestra al aplicar cargas por encima del esfuerzo de colapso del material se puede llegar a determinar el coeficiente de difusión efectivo y distinguir el efecto barrera de las nanoarcillas.

- Estudio de los mecanismos de espumación: desde un punto de vista más básico, el estudio de los mecanismos de formación de celdas en presencia de nanopartículas es fundamental para la consecución de un determinado objetivo. En este sentido se lleva a cabo el proyecto "Advanced foams under microgravity" en colaboración con la Agencia Espacial Europea (ESA) para estudiar la influencia de las nanopartículas en la espumación en condiciones de gravedad variable.

Conclusiones

El mundo del plástico no ha sido ajeno en absoluto a la potencial revolución que representa la nanotecnología tanto desde un punto de vista científico como industrial. En la actualidad es muy grande el esfuerzo volcado en el mundo de los polímeros cargados con nanopartículas, tanto en la investigación básica como en la búsqueda de concretas aplicaciones prácticas.

El papel que juegan estas nanopartículas cuando son aditivadas a una matriz polimérica no se limita a la mejora de una única propiedad. Al contrario, existe una asombrosa multifuncionalidad que abarca propiedades del plástico tales como su estabilidad térmica, rendimiento mecánico, resistencia a la llama, barrera a gases o incluso desde el punto de vista de la propia morfología a nivel molecular. Pero si empleamos además estas matrices poliméricas nanocargadas en la producción de materiales celulares encontramos efectos sinérgicos muy interesantes.

Estos efectos sinérgicos se han puesto de manifiesto en un caso muy concreto y poco convencional: materiales celulares basados en polietileno de baja densidad cargado con sílices nanométricas. Se ha estudiado el efecto que tienen estas nanopartículas en la reología del polímero, en la estructura celular que se obtiene y en la mejora de sus propiedades mecánicas. Las mejoras encontradas en el material celular al emplear nanocargas son mucho mayores que las correspondientes al material sólido.

El Laboratorio de Materiales Celulares CellMat de la Universidad de Valladolid ha tenido ocasión además de comprobar el alto interés que el mundo "nano" ha despertado en los materiales poliméricos tanto en el sector público como en el sector privado. Además de proyectos financiados con fondos de la Unión Europea o la Agencia Espacial Europea son múltiples las empresas privadas que buscan beneficiarse de esta multifuncionalidad. Debido a ello los proyectos en los que se participa actualmente tienen vertientes muy diversas, desde la mejora de las propiedades mecánicas hasta el incremento de las propiedades aislantes térmicas pasando por sus efectos como barrera a gases, su positiva incidencia en la estructura celular en piezas aligeradas o la riqueza conceptual que aportan en el estudio de los mecanismos básicos de espumación en presencia de nanocargas.

Bibliografía

1. A. Utracki. Clay-containing polymeric nano-composites United Kingdom. Rapra Technology Limited.2004. ISBN 1-85957-437-8.

2. Bharat Bhusan. Handbook of nanotechnology. Germany, Springer Verlag 2003 ISBN 3-540-01218-4.

3. Joseph H. Koo. Polymer Nanocomposites. USA. McGraw-Hill 2006. ISBN 0-07-145821-2.

4. C. Saiz-Arroyo, J. Escudero, M.A. Rodríguez-Perez, J. A. de Saja. LDPE Silica Nanocomposites: A System in which Nanoparticles Play a Multifunctional Role. FOAMS2010. Seattle, USA.

5. Vesely, D. The development of spherulite morphology in polymers. Journal of Macromolecular Science-Physics 1996, v. B35, pp.411-425.

6. Kojima Y., Usuki A., Kawasumi M. Fine structure of nylon 6-clay hybrid. Journal of Polymer Science Part B Polymer Physics. 1994 v. 32 pp. 625-630.

7. Tanoue S, Utracki LA, Garcia-Rejon A Melt compounding of differenet grades of polystyrene with organoclay. Part 1: Compounding and characterization. Polymer Engineering and Science 2004 v. 44 pp. 1046-1060.

8. Delozier DM, Orwoll RA, Cahoon JF. Preparation and characterization of polyimide/organoclay nanocomposites. Polymer 2002 v. 43 pp. 813-822.

9. J.I. Velasco, M. Antunes, O. Ayyad, C. Saiz-Arroyo, M.A. Rodríguez-Pérez, F. Hidalgo, J.A. de Saja. Foams Base don Low density Polyethylene /Hectorite Nanocomposites: Thermal Stability and Thermomechanical Properties. Journal of Applied Polymer Science. 2007. v. 105 pp. 1658-1667.

10. Tjong SC, Meng YZ, Xu Y. Preparation and properties of polyamide 6/polypropylene-vermiculite nanocomposite/polyamide 6 alloys Journal of Applied Polymer Science. 2002. v.86 pp.2330-2337.

11. Uribe-Arocha P, Mehler C, Puskas JE. Effect of sample thickness on the mechanical properties of injection-molded polyamide-6 and polyamide-6 clay nanocomposites Polymer 2003 v.44 pp. 2441-2446.

12. Gilman JW, Kashiwagi T, Brown JET, Lomakin S, Giannelis EP, Manias E Flammability studies of polymer layered silicate nanocomposites 43rd International Sampe Symposium and Exhibition on Materials and Process Affordability Keys to the Future 1998 v. 43 pp. 1053-1066.

13. Gilman JW, VanderHart D, Asano A Recent advances in characterization and processing of flame retardant polymer nanocomposites. Abstracts of Papers of the American Chemical Society. 2001 v.28 pp. 612-615.

14. M. A. Rodriguez-Perez, P. García de Aciluu Laa, J. Arevalo-Gutierrez, C. Saiz-Arroyo, E. Solorzano, J.A. de Saja. Foaming of LDPE/silica nanocomposites: improving the cellular structure and mechanical properties. ANTEC 2009.

15. C. Saiz-Arroyo, J. Escudero, M.A. Rodríguez-Perez, J.A. de Saja. improving the Structure and Physical Properties of LDPE Foams Using Silica Nanoparticles as an Additive. Cellular Polymers 2011. v. 30 pp. 45-60 (in press)

16. J. Escudero, E. Solorzano, M.A. Rodríguez-Perez, F. García-Moreno, J.A. de Saja. Structural Characterization and Mechanical Behaviour of LDPE Structural Foams. A Comparison with Conventional Foams. Cellular Polymers 2009 v. 28 nº 4 pp. 289-302.

17. M.A. Rodriguez-Perez, J.A. de Saja, J. Escudero, J.A. Vazquez, "Sistema y procedimiento de moldeo de piezas con moldes autoportantes". Patente española número 201130271

II.3.- NON-INDEXED PUBLICATION 2. STAGES MOULDING, A NEW TECHNOLOGY FOR THE PRODUCTION OF PLASTIC PARTS

The stages moulding technology has been already described in previos chapters, the specific part of structural foams was widely described in chapter 5 and other aspects of the technology were presented in the corresponding patent in Annex I.

The industrial dissemination character of "Revista de Plásticos Modernos" is ideal to promote a new technology as Stages Moulding in the spanish plastics industry. Therefore the second publication included in Annex II gives a technical vision, mainly focused to the industrial applications of the technology. The paper summarizes the main characteristics of the technology and present some examples of real parts produced.

Artículos

STAGES MOULDING:
Una nueva tecnología para la fabricación de piezas de plástico

Autores: J. Escudero[1], J. Tirado[1], M.A. Rodriguez-Perez[1], J.A. de Saja[1], D. Rosa[2], J.A. Vazquez[1]

RESUMEN:

En este artículo se describe una nueva tecnología para la producción de piezas moldeadas de plástico denominada "Stages Moulding". Esta tecnología patentada permite fabricar piezas con formas complejas utilizando una elevada variedad de polímeros, con excelente calidad superficial, tensiones térmicas y mecánicas reducidas y tiene la posibilidad de dar lugar a piezas de densidad reducida entre otras ventajas interesantes. Además, este nuevo proceso usa moldes y máquinas más baratos que los usados en el moldeo por inyección tradicional. Las características mencionadas hacen de esta tecnología un método con un futuro muy prometedor para la producción de piezas de plástico. Este artículo resume las principales características del proceso "Stages Moulding" presentando algunos ejemplos de piezas reales producidas.

PALABRAS CLAVE: Stages Moulding, moldeo por inyección, calidad superficial, espuma estructural, materiales celulares, densidad reducida.

ABSTRACT:

This paper presents a novel technology to produce plastic parts called "Stages Moulding". The patented technology allows producing plastic parts with complex shapes, from a wide variety of polymers, with excellent surface quality, reduced thermal and mechanical stresses and the possibility to produce parts with reduced weights among other interesting advantages. Moreover, this novel process uses much cheaper moulds and machinery than those used in injection moulding. The specific characteristics previously mentioned make this technology very promising for the production of moulded plastic parts. The paper summarises the main characteristics of this technology presenting some real examples of parts produced.

KEYWORDS: Stages Moulding, injection moulding, surface quality, structural foams, cellular materials, reduced density.

INTRODUCCIÓN

El moldeo por inyección es una de las tecnologías más extendidas en la fabricación de piezas de plástico. Si hacemos una revisión histórica de esta técnica nos tenemos que remontar a 1872 año en el cual John Hyatt patenta el primer sistema de inyección compuesto por un pistón que contenía derivados de la celulosa fundidos en una cámara. Sin embargo no es

1. Cellular Materials Laboratory (CellMat), Condensed Matter Physics Department, University of Valladolid, 47011 Valladolid, Spain. marrod@fmc.uva.es

2. Grupo ABN Pipe, Carretera Baños de Arteixo 48, Parque Empresarial Agrela, 15008, A Coruña.

hasta 1928 cuando se atribuye a la compañía alemana Cellon-Werke la primera patente de una máquina de inyección moderna. Paralelamente Beard y Delafield desarrollaron la técnica en Inglaterra, con los derechos de la patente inglesa para la compañía F.A. Hughes Ltd. Los sistemas anteriores funcionaban con aire comprimido, la extracción y parte de los controles eran manuales y carecían de sistemas de seguridad. En 1932 se patenta la primera máquina de inyección operada por sistemas eléctricos y no es hasta 1956 cuando se empiezan a emplear husillos en los equipos de inyección. A partir de ese momento las mejoras se centran en los sistemas de automatización, en la eficacia y control de los procesos. Con el fin también de solucionar algunos de los problemas presentados por el moldeo por inyección convencional surgen variantes tomando como base este último. A continuación se reseñan las más importantes:

- Coinyección: posee sistemas de inyección independientes permitiendo el uso simultáneo de materiales poliméricos diferentes de tal manera que un material encapsula al otro. Se puede emplear también para la fabricación de piezas estructurales celulares. Como inconvenientes, el equipamiento supone una gran inversión y amortización de moldes por lo cual está restringido a tiradas masivas [1].
- Heat & Cool: se realiza un ciclado térmico del molde que se calienta y enfría en cada ciclo para proporcionar un mejor acabado superficial. El sistema requiere de una alta inversión en moldes y además los tiempos de ciclo se incrementan con respecto al proceso convencional [2].
- GAIM: en este método se realiza inyección asistida por gas para moldear piezas plásticas con secciones huecas en su interior reduciendo la materia prima necesaria. El sistema no es válido para la fabricación de todo tipo de piezas aparte de las precauciones necesarias por trabajar con un gas inerte [3].
- WIT o WAIM: se corresponde con una variante del método anterior en la cual en lugar de emplear gas se emplea agua. Esto ayuda a reducir el tiempo de ciclo, sin embargo el sistema presenta un coste elevado y pude existir corrosión por la introducción de agua en el sistema [3].
- MUCELL: esta tecnología implementa un sistema propio de control de la estructura celular de la pieza lo cual implica ventajas en el proceso de fabricación y en el coste del equipamiento. Tan sólo está disponible para la fabricación de piezas celulares de dimensiones limitadas con reducciones de peso bajas y pobres acabados superficiales [4].
- Moldes expandibles: este método implementa moldes que son capaces de expandirse durante el proceso de inyección. De esta manera se pueden fabricar también piezas estructurales celulares con mejores acabados superficiales sin embargo,

de nuevo, la complejidad de los moldes entraña una alta inversión [5].

Aparte de los inconvenientes asociados a cada uno de estos métodos existen una serie de desventajas comunes a cualquier proceso de moldeo por inyección. Debido a las altas presiones de trabajo, en cualquiera de los casos los moldes empleados son muy costosos, así la inversión en maquinaria y moldes es muy elevada. Para la fabricación de un tipo de pieza es necesario realizar un complicado montaje, preparar el sistema y calibrarlo para comenzar la tirada de una sola serie de piezas. La tirada debe ser suficientemente numerosa para que el proceso sea rentable. Las piezas obtenidas suelen presentar baja calidad superficial con líneas de soldadura y rechupes. El volumen máximo fabricable está limitado a unos 10 litros por las elevadas presiones necesarias para llenar los moldes. Existen además ciertas limitaciones en las materias primas que se pueden usar, así es necesario polímeros de baja viscosidad y no es posible emplear formulaciones con elevadas cantidades de refuerzos o cargas [6-10].

- La tecnología Stages Moulding surge como alternativa al moldeo por inyección tradicional y soluciona buena parte de las desventajas de este. Con este novedoso sistema se consiguen solucionar los problemas anteriormente expuestos permitiendo reducir costes en moldes y maquinaria, fabricar piezas de diversas geometrías y composición que tengan además una buena calidad superficial y fabricar piezas de densidad reducida y estructurales celulares entre otras. El proceso es mucho más versátil y permite la fabricación de varios tipos de piezas de forma simultánea [11].

LA TECNOLOGÍA STAGES MOULDING

Introducción

La tecnología Stages Moulding surge fruto de las investigaciones conjuntas entre el Laboratorio de Materiales Celulares CellMat de la Universidad de Valladolid y el Grupo ABN Pipe Systems realizada en los últimos cinco años. Actualmente la tecnología está patentada [11].

Describiremos a continuación los principios básicos en los que se basa.

Descripción del proceso

La tecnología Stages Moulding permite la fabricación de piezas tanto sólidas como con densidad reducida. El proceso de fabricación de una pieza siguiendo esta tecnología comprende tres etapas fundamentalmente (figura 1):
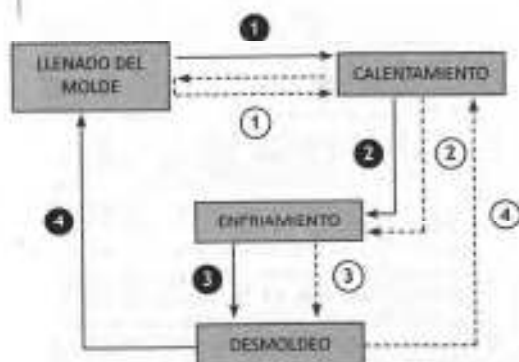
Artículos

Figura 1: Esquema simplificado del proceso de producción de piezas por Stages Moulding.
En la figura 1 Se muestra esquemáticamente el proceso que se sigue en la fabricación de una pieza. La doble línea punteada del paso 1 indica una ruta alternativa en la cual el molde puede ser precalentado previo a su llenado y calentado de nuevo tras éste.

- Llenado del molde: la primera etapa consiste en la alimentación del material del moldeo en el molde autoportante. Esta alimentación puede realizarse siguiendo diversos procedimientos, como tolvas, unidades de extrusión o incluso unidades de inyección. Con el concepto de molde autoportante, inherente a esta tecnología, nos referimos a un molde en el cual el sistema de cierre es una parte intrínseca del molde. Estos moldes autoportantes están diseñados de tal manera que serán capaces de soportar las presiones generadas durante la etapa de moldeo.
- En la mayor parte de los casos el material de moldeo contiene como aditivo un agente espumante que liberará gas al descomponerse por efecto de la temperatura.
- Moldeo de la pieza: una vez introducido el material de moldeo dentro del molde se eleva la temperatura de ésta de tal manera que se produzca la descomposición del agente espumante dentro del polímero fundido liberando gas. La presión generada como consecuencia de la liberación de gas actuará como fuerza impulsora permitiendo al polímero rellenar todas las partes del molde a reproducir. Mediante esta metodología se obtendrán piezas moldeadas con densidades relativas inferiores a la unidad cuya porosidad podemos controlar. En el caso de querer conseguir piezas completamente sólidas el molde incorpora además un colector. Tras la incorporación del polímero en el molde se le aplica una cierta presión

a través del colector haciendo uso de pistones hidráulicos, introduciendo vapor, aceite u agua o de nuevo empleando un agente espumante que expande al elevar su temperatura.

- Enfriamiento y desmoldeo de la pieza: una vez realizado el ciclo térmico necesario para el correcto rellenado del molde éste ha de ser enfriado mediante algún procedimiento como por ejemplo enfriamiento en agua, aceite, usando gases, etc. Cuando se ha enfriado hasta una temperatura tal que la pieza se puede extraer fácilmente sin producir ningún deterioro sobre su superficie o estructura de la misma se procede a su desmoldeo tras el cual el proceso habría finalizado.

En el caso de querer obtener piezas con estructura piel sólida-núcleo espumado los pasos a seguir son completamente análogos a los especificados en los puntos anteriores salvo que las paredes del molde en las cuales se quieren obtener estas pieles sólidas deben ser recubiertas mediante un material capaz de absorber gas tal como silicona sólida o PTFE.

Ventajas:

El sistema de fabricación de piezas por etapas mediante moldes autoportantes "Stages Moulding" supone un proceso versátil para la fabricación de piezas de muy diferentes tamaños, formas y composiciones químicas con excelente calidad superficial, bajas tensiones internas, con la posibilidad de fabricar piezas de densidad reducida usando moldes y maquinaria de bajo coste. La tecnología permite fabricar varios tipos de piezas de forma simultánea y elimina la necesidad de montaje del molde y calibración del mismo inherente a los procesos de moldeo por inyección tradicionales. Las ventajas inherentes a este método de fabricación pueden ser divididas en tres grupos diferentes:

- Desde el punto de vista de la maquinaria empleada: la introducción del concepto de "moldes autoportantes" dota al proceso de una mayor autonomía y sencillez lo cual supone una menor inversión en el proceso así como un mayor acceso al número de piezas a fabricar. A su vez la mayor simplicidad de la maquinaria utilizada frente a la inyección convencional permite una elevada reducción de costes (ver más adelante).
- La producción de diferentes piezas en diferentes moldes es simultánea, de modo que el proceso global puede ser considerado como continuo para unas mismas o diferentes piezas. A lo largo del proceso pueden coincidir diferentes moldes en distintas estaciones.
- El sistema requiere de presiones de trabajo muy inferiores a las de la inyección convencional. Las presiones de llenado de los moldes autoportantes están siempre por debajo de los 100 bar, siendo típicamente inferiores a los 15 bar.

- Desde el punto de vista de las características de la pieza: las piezas presentan ausencia de rechupes y líneas de soldadura. Su acabado superficial es mejor que en el caso del moldeo por inyección. Se pueden conseguir reducciones de peso de hasta el 98% así como conseguir también piezas estructurales con estructura piel sólida- núcleo espumado.
- No existen limitaciones en cuanto a la composición química de las piezas, es decir, se pueden usar todo tipo de polímeros tanto de alta como de baja viscosidad y todo tipo de aditivos en porcentajes de hasta un 80% en peso.
- Desde el punto de vista del sistema global: el proceso puede ser automatizado. Puesto que el sistema global se encuentra dividido en diferentes estaciones para realizar cada una de las etapas esto permite fabricar en función de las necesidades diarias generadas (metodología "Just in time"), sin importar la cantidad a fabricar para amortizar la puesta a punto del molde y máquina. Además también es posible fabricar piezas de gran tamaño.

La tabla 1 resume las principales características de la tecnología.

Ejemplos prácticos

Moldeo de piezas poliméricas de densidad reducida
Industrialmente son múltiples las ocasiones en las que se presenta la necesidad de fabricar un número no demasiado alto de un cierto de tipo de piezas moldeadas por inyección. Para cada una de estas denominadas "series cortas" es necesario realizar un determinado molde de inyección, calibrar molde y maquinaria, encontrar los parámetros óptimos de inyección, etc. Al final, tanto el esfuerzo económico como en tiempo de trabajo no compensa en relación al pequeño número de piezas que se desea fabricar de una única serie. Para estas series cortas la tecnología Stages Moulding presenta unas características óptimas. A continuación se muestran dos casos prácticos de piezas producidas industrialmente.

En la figura 2 se muestra una pieza con forma de rueda fabricada mediante la tecnología Stages Moulding y la

Tabla 1: Resumen de las principales características del proceso	
Rango de densidades	Tres tipo de piezas a) Piezas sólidas b) Piezas de densidad reducida c) Piezas estructurales (piel sólida-núcleo espumada) d) Piezas de densidad reducida anisotrópicas
Polímeros utilizables y alta densidad, polipropileno, poliestireno, PVC, poliuretano, etc.	El rango es muy amplio: polietileno de baja
Cargas/fillers y contenido máximo	Ejemplos de ellas serían talco, fibra de vidrio, hidróxido de aluminio, nanoarcillas, nanotubos de carbono. El porcentaje máximo estaría en un 80%
Presiones de cierre	Típicamente inferiores a 15 bar
Tiempos de ciclo	Controlables según el número de piezas fabricadas simultáneamente.
Tamaño de las piezas	Tamaño y geometría variable en un rango mucho más amplio que el moldeo convencional debido a las presiones generadas y a las bajas densidades. Hasta 2000 mm x 1500 mm con espesores desde 0.25 mm a 60 mm. En desarrollo, piezas hasta 3000 mm x 2000 mm con espesores desde 0.25 mm a 120 mm.

estructura interna correspondiente a ella. En el caso mostrado, en el que la pieza está fabricada en base polipropileno, se ha conseguido una reducción de peso superior al 50% con una excelente calidad superficial como se puede observar en la imagen y una presión de cierre inferior a 15 bar. Una curva típica de presión durante la fase de llenado del molde se muestra en la figura 3. Este tipo de piezas presenta todas las ventajas ya comentadas inherentes a esta tecnología.

Las piezas de unión empleadas en conducciones hidráulicas mostradas en la figura 4 se fabrican siguiendo el mismo procedimiento también en base polipropileno. En este caso, además, el método de rellenado del molde autoportante es más sencillo aún empleándose únicamente una tolva para la introducción del polímero más agente espumante. La reducción de densidad es superior al 50 % y la presión de cierre menor de 10 bar.

Moldeo de materiales celulares estructurales
Industrialmente sectores tan importantes como el aeronáutico, el sector de la automoción o el de materiales deportivos demandan cada vez más materiales celulares con propiedades mecánicas mejoradas.

Figura 3: Curva de presión típica para la fabricación de una pieza

Figura 2: Pieza industrial moldeada mediante la tecnología Stages Moulding y su estructura interna. Reducción de densidad mayor del 50% y presión de cierre inferior a 15 bar
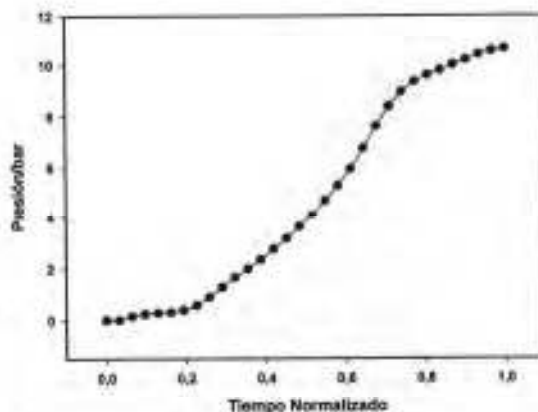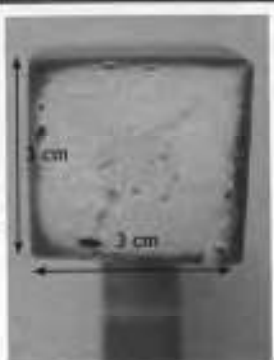
59 cm.

3 cm

3 cm

Puesto que las espumas convencionales (entendidas como aquellas que tienen una densidad constante a lo largo de todo su volumen) presentan unas propiedades mecánicas que disminuyen de una manera muy importante al reducir la densidad. Una manera de mejorar estas propiedades mecánicas manteniendo la densidad global constante consiste en generar una estructura tipo sándwich con pieles externas sólidas y un núcleo interno espumado. De esta manera las propiedades mecánicas específicas se ven incrementadas respecto a la espuma convencional.

La tecnología Stages Moulding, tal y como se ha comentado en apartados previos, presenta también la posibilidad de fabricar este tipo de materiales celulares estructurales de una manera sencilla.

En la figura 5 se muestra una micrografía correspondiente a una pieza estructural fabricada por Stages Moulding. Debido a la piel sólida que se forma en las partes externas la calidad superficial de estas piezas es óptima mejorando notablemente las producidas mediante otros métodos de inyección. La densidad de esta pieza es aproximadamente la mitad que la del polímero original y la presión de cierre ejercida durante el proceso es de aproximadamente 20 bar.

Como ya se indicó en la descripción del proceso para la fabricación de estas piezas las paredes externas del molde se recubren con un material capaz de absorber gas. De esta manera se fabrican discos de las mismas dimensiones pero de espuma convencional en la cual el perfil de densidad es constante a lo largo del volumen. Para ambos tipos de materiales se extraen
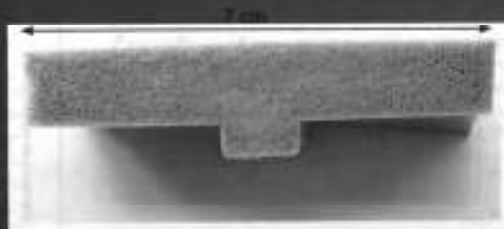
Figura 4: Piezas de unión empleadas en conducciones hidráulicas fabricadas por Stages Moulding y su correspondiente estructura celular interna. Densidad inferior a la mitad de la del polímero de partida y presión de cierre inferior a 10 bar.

Figura 5 : Pieza estructural celular obtenida por Stages Moulding y una micrografía de su estructura interna. Se observa las dos pieles externas sólidas encerrando un núcleo espumado.
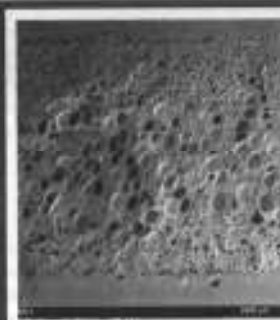
probetas para ensayos mecánicos y comparan las propiedades en flexión tanto para estructurales como para convencionales.

En la figura 6 se presentan los datos numéricos obtenidos para estos materiales. Se observa que en el caso de la espuma estructural fabricada mediante
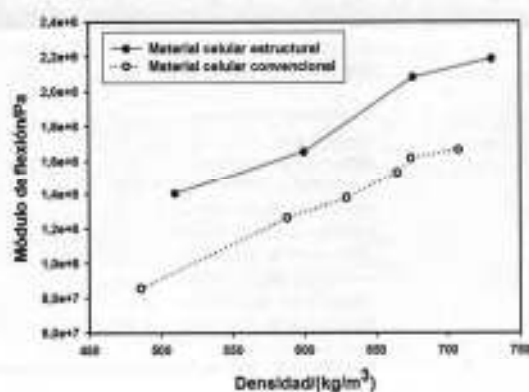

Figura 6: Módulo de flexión comparado para materiales celulares estructurales y convencionales producidos según la tecnología Stages Moulding.
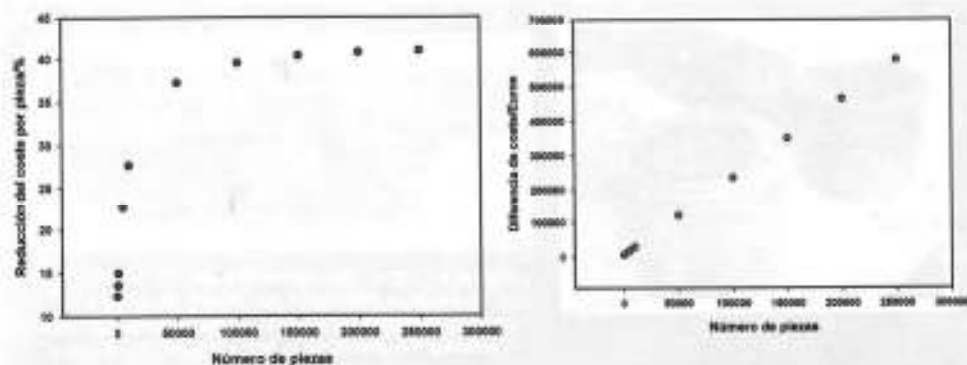
Artículos

Figura 7. a) % de diferencia en el coste de fabricación de la pieza mediante el moldeo por inyección tradicional y la tecnología stages moulding en función del número de piezas fabricadasg, b) diferencia de coste (en euros) en función del número de piezas fabricadas.

Stages Moulding el módulo en flexión se incrementa hasta en un 50% [12].

Análisis de costes

Las figura 7 muestran la diferencia entre los costes de fabricación de las piezas de la figura 2 fabricadas mediante moldeo por inyección tradicional y Stages Moulding en función del número de piezas fabricadas. Se puede observar que las reducciones de coste mediante el uso de la tecnología Stages Moulding son muy importantes, llegando a ser del 40%, lo que para una serie de 250000 euros puede dar lugar a ahorros en los costes de fabricación superiores a los 500.000

euros. Las principales fuentes de ahorro de costes por orden de importancia están en la reducción de la materia prima necesaria para fabricar la pieza, en el menor coste de los moldes y en el menor coste/hora asociado al uso de esta tecnología.

Conclusiones

El moldeo por inyección convencional es una tecnología cuyas ventajas han sido ampliamente establecidas a lo largo de muchos años de uso de esta técnica. Sin embargo presenta también múltiples desventajas. A lo largo del tiempo han surgido diversas aproximaciones que ha tratado de solventar parte de estos inconve-

Tabla 2. Ventajas de la tecnología Stages Moulding frente al moldeo por inyección convencional

Económicas	Técnicas
	Sin líneas de soldadura
	Sin rechupes
	Sin tensiones internas
Moldes más económicos.	Excelentes acabados superficiales
	Posibilidad de co-inyección.
	Bajas presiones de llenado
	Posibilidad de realizar piezas no realizables
Hasta un 50% más baratos	en moldeo por inyección.
	Metodología Just In Time
Maquinaria más económica. Hasta un 50%	Posibilidad de usar cargas y materiales recuperados
Reducción de costes en materias primas. Hasta un 50%	Posibilidad de usar varios polímeros en el mismo molde

nientes. Estas diversas aproximaciones han sido satisfactorias en algunos puntos pero insuficientes o incluso perjudiciales en otros muchos.

La tecnología Stages Moulding surge como alternativa completamente diferente a cualquiera de los procesos de moldeo por inyección. Esta nueva técnica resuelve buena parte de los problemas existentes. Supone unas menores inversiones iniciales empleando moldes más sencillos y económicos y permite la producción de piezas de muy diferentes y complejas geometrías con buena calidad superficial y menores tensiones internas con ausencia de rechupes o líneas de soldadura.

Además de permitir la fabricación de piezas sólidas se pueden obtener también piezas de densidad reducida y excelente apariencia externa. Una de las variantes del proceso permite también la fabricación de piezas celulares con estructura piel-sólida núcleo espumado y piezas anisotrópicas. Estas piezas celulares estructurales presentan unas propiedades mecánicas específicas muy superiores en comparación a los materiales celulares convencionales.

La aplicabilidad de esta técnica ya ha sido demostrada mediante su uso en varias aplicaciones industriales reales. Las tablas 2 y 3 muestran las principales ventajas de la tecnología.

Tabla 3. Nuevas posibilidades que se abren con esta tecnología	
Fabricación de nuevas estructuras	Piezas de gran dimensión y elevados espesores Piezas de densidad reducida Piezas estructurales Piezas anisotrópicas

Agradecimientos.

Bibliografía

1. U. Stieler. Proceedings Blowing Agents and Foaming Processes 2008. Paper 12.
2. Jeng MC, Chen SC, Minh PS, et al. International Comunications in Heat and Mass Transfer Vol. 37 nº 9 pp. 1295-1304.
3. Zhang, Y.; Rodrigue, D.; Ait-Kadi, A. J Appl Polym Sci, Vol. 90, 2139-2149 (2003).
4. Suh NP. Macromolecular Symposia Vol. 201 pp. 187-201.
5. Bledzki A. K., Rohleder M., Kirschling H., Chate A. Cell. Polym. 2008, vol. 27, no 6, pp. 327-345.
6. Barzegari, M. R. and Rodrigue D. Cell. Polym. 27(5): 285-301.
7. Bikhu, S. S. and Founas, M. SAE Technical Paper Series 930434, International Cong. And Exposition. Detroit, M.I, 1993.
8. Hobbs, S. Y. Journal of Cellular Plastics, Vol. 12, No. 5, 258-263 (1976).
9. Wu, J. S. and Yeh, T. M. Journal of Polymer Research. vol. 1 nº 1 pp. 61-68.
10. Avalle. M. Belingardi, G. and Montanini, R. International Journal of Impact Engineering vol. 25 (2001) pp. 455-472.
11. M.A. Rodríguez-Pérez, J.A. de Saja, J. Escudero, J.A. Vázquez, "Sistema y procedimiento de moldeo de piezas con moldes autoportantes". Patente española número 201130271.
12. J. Escudero, E. Solorzano, M.A. Rodríguez-Pérez, F. García-Moreno, J.A. de Saja. Journal. Cellular Polymers, Vol. 28, nº 4 p. 289-302.